*L.A. Artsimovich*

# CONTROLLED THERMONUCLEAR REACTIONS

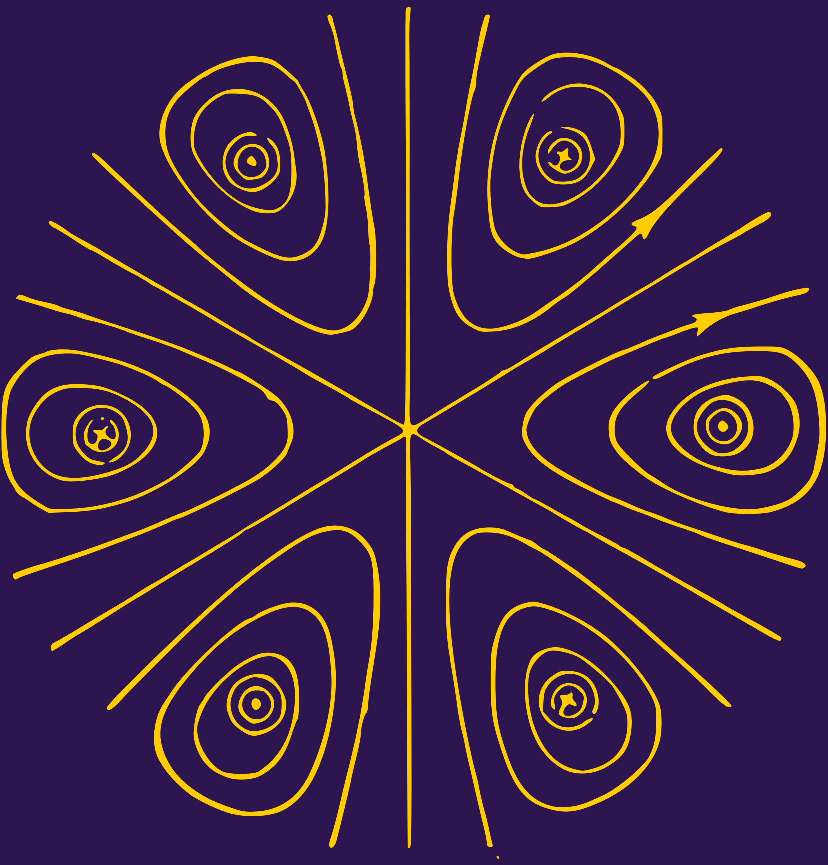

# CONTROLLED
THERMONUCLEAR
REACTIONS

# CONTROLLED THERMONUCLEAR REACTIONS

L. A. ARTSIMOVICH

Edited by
A. C. KOLB and R. S. PEASE

Translated by
P. KELLY and A. PEIPERL

OLIVER & BOYD
EDINBURGH & LONDON

OLIVER AND BOYD LTD

Tweeddale Court
Edinburgh 1

39a Welbeck Street
London, W. 1

This is a translation from L. A. Artsimovich: Управляемые Термоядерные Реакции published by Gosudarstvennoe Izdatel'stvo Fiziko-Matematicheskoi Literatury, Moscow 1961, second edition 1963

ENGLISH EDITION
First published . . . . 1964

© Translation 1964, Oliver & Boyd Ltd and Gordon & Breach

Printed in Great Britain by
Hazell Watson & Viney Ltd, Aylesbury, Bucks

# FOREWORD TO THE RUSSIAN EDITION

Amongst the various purposes which the foreword to a book is intended to serve, the main one is commonly that of giving the author an opportunity to mitigate, by means of a properly devised defence, the forthcoming assault of the critics, the elements of this defence being on the one hand a frank admission of the book's defects and, on the other, an irrefutable demonstration that such defects are absolutely unavoidable. Such a form of literary self-defence is particularly necessary when the subject being expounded is a rapidly expanding field of science or technology in the initial phase of its development. This is precisely the present state of research into controlled thermonuclear reactions. The author must therefore begin this book with self-criticism.

At the very outset, the reader must be warned that the title of the book is not a wholly accurate reflection of its contents. The title represents the goal towards which we are striving, but for the present this goal only glimmers in the distance, and a long and difficult road has to be traversed before we get there. What the book describes is the small fraction of the road which has been travelled so far, together with an outline of the sort of obstacles which have yet to be overcome in order to solve the problem before us. The reader should not look here for the numerical and technological details of industrial thermonuclear reactors because at this time there are no such reactors. We find ourselves now at an earlier stage when our primary task is to determine the scientific principles which will underlie the thermonuclear technology of the future.

Thermonuclear reactions occur in a form of matter which is comparatively novel in the laboratory—high-temperature plasma. The studies which have been carried out on the properties of high-temperature plasma constitute the main subject of this book. An account is given of the principal theoretical concepts of the various processes which take place in plasma; methods of heating and of thermally insulating plasma are examined; devices built for carrying out experiments with high-temperature plasma are described, and the results of these experiments are evaluated. Plasma physics is the subject of the first four chapters; the remaining four are devoted to the main trends of experimental research on the problem of producing controlled thermonuclear reactions.

The choice and arrangement of the material have been governed by the belief that a clear understanding of the problems can be obtained without draping the meagre skeleton of experimental facts in a voluminous garment of mathematical elaboration; a rational balance must be maintained between theoretical and experimental information. For this reason the book in general includes only that minimum of theoretical knowledge needed to guide the reader through the physics of high-temperature plasma. Lengthy derivations of formulae have been omitted; and in all cases where either clarity or pedantry had to be chosen, preference is given to the first.

With rare exceptions the book does not take account of research carried out after the end of 1960. The Gaussian c.g.s. system of units is used unless otherwise stated.

The author expresses deep gratitude to the large staff of the Plasma Research Department at the 'I.V. Kurchatov' Atomic Energy Institute of the U.S.S.R. Academy of Sciences, for the very valuable and friendly help they gave in preparing the book by making available experimental data, calculations, graphs and photographs, and by providing much valuable advice and comment.

Special mention must be made of the help given by R. Z. Sagdeev: § **4.7** of the book is basically his work, and also the greater part of § **7.7**. The author is indebted to V. M. Glagolev for the analysis of the main methods of high-frequency confinement of plasma (§ **8.17** and § **8.18**). Without the help of E. V. Artyushkov the publication of this book would probably have been delayed for a long time. It was he who did the very laborious work of preparing the manuscript for printing, and did it with great conscientiousness and skill. In addition he made numerous difficult and detailed calculations, and prepared a large number of the graphs used in the book.

L. A. ARTSIMOVICH

*June 1961*

# FOREWORD TO THE ENGLISH EDITION

The problem of controlled thermonuclear fusion belongs to the border region between science and technology which can be called 'scientific invention'. When we survey the work on nuclear fusion as a whole we find that new ideas born of the creative imagination of inventors are intermingled with the results of theoretical and experimental research on plasma physics, and that usually these ideas have flowed directly from the research. The tremendous importance of the ultimate goal and the enormous difficulties that lie in the way combine to stamp the problem of thermonuclear fusion with a quite distinctive character. For the time being we find ourselves as it were on the dividing line between dream and reality. It is this that brings an element of emotionalism into the study of this problem—the succession of hope and despair, the searching doubts followed by assurance of success.

It is natural that everything should be in motion in such a living field of study and therefore any book on controlled thermonuclear reactions can at best represent only a snapshot photograph which shows the situation as it is for a very short period of time. The present work was published in the U.S.S.R. in the summer of 1961 and the author has therefore introduced a number of amendments and additions to the original Russian text. Major alterations have been made to passages bearing on systems of the theta-pinch type; the sections dealing with toroidal discharges have been supplemented with fresh data; and in respect of plasma stability in magnetic traps, a series of new results is given which has been derived from recent theoretical and experimental studies. These additions do not, of course, cover all the recent developments in this new scientific field, but if this book in its English edition proves useful to young scientists and, in particular, if it can show them that the problem of thermonuclear fusion is not as easy to solve as it sometimes seems at first glance, then the author will consider his task accomplished.

I regard it as my pleasant obligation to thank P. Kelly and A. Peiperl for translating this book, and Drs. R. S. Pease and A. C. Kolb for editing the translation and making a number of corrections which have significantly improved the presentation. I also express thanks to my English and American publishers.

L. A. ARTSIMOVICH

*20th September 1962*

# EDITORS' NOTE

We believe that this book is of value on a number of grounds to those studying controlled thermonuclear reactions and plasma physics: it constitutes a major review of the subject by one of the most distinguished pioneers in the field; it succeeds in presenting difficult ideas in lucid and simple fashion without losing the essential physical content; the extensive research programme in the Soviet Union is authoritatively discussed, including the underlying scientific motivations; and finally it contains independent assessment of much of the research programmes carried out in western countries.

The text used for the translation is basically that of the first Russian edition. Corrections and some extensive additions sent to us by Academician Artsimovich have been added and also, in a few cases, emendations and clarifications suggested by us and discussed with him. The text is now close to, but not identical with, that of the second Russian edition which we received while the present text was in page proof.

The subject does not, in all aspects, possess a widely accepted standard terminology. In editing this translation we have had to make some arbitrary decisions in order to provide as far as possible a self-consistent notation related to that used in already published English-language books. While much of this is self-explanatory, the following points may assist the reader. In discussing devices possessing or treated as possessing cylindrical symmetry, such as the linear ($z$-) pinch or the $\theta$-pinch, the cylindrical polar coordinates $r$, $\theta$, $z$ are denoted where necessary radial, azimuthal and axial respectively. Devices with toroidal or topologically toroidal geometry, such as the stabilised toroidal pinch, the Tokomak systems and the Stellarator, may possess two axes to which the cylindrical polar coordinates can be related. If an initially straight tube of circular cross-section is bent into a closed toroid, then the axis about which it is bent (marked $z$ in Figs. 28 and 29) we have called the major axis, and quantities referring to this axis are prefixed major. For example, $R$ of Fig. 29 is the major radius. The circular cross-section—shown in Fig. 30—of the initially straight tube we refer to as the minor cross-section, and quantities pertaining to it are prefixed minor. The locus of the centre of the minor cross-sections forms the centre line of the tube bore. Vector quantities parallel to this centre line we refer to as longitudinal; thus the current $J$ of Fig. 29 is a longitudinal current. In some discussions of topologically toroidal devices, the cylindrical polar coordinate system is used with the $z$-axis coincident with the centre line of the tube bore (assumed straight). The term 'magnetic axis' is reserved for the line defined at the beginning of Chapter VIII. We have reserved the term 'longitudinal' for the above-mentioned use alone, with the exception that the well-established term 'longitudinal wave' is retained for waves in which the particle motion is parallel to the wave vector.

In the discussion of wave motion in plasmas, we have retained the translated Russian terminology. The English terminology is at present very confused, and the reader can place reliance only on the mathematical description of the mode when comparing the discussion in different texts. The reader is particularly warned that the Russian usage of the terms 'ordinary' and 'extraordinary' is at variance with that of some English-language authors. We have eliminated some, but not all cases of synonymous terms. Thus the term Larmor frequency is not used and the frequency $eH/mc$ is referred to throughout as the cyclotron frequency; on the other hand the heating produced by the collisional resistance to the passage of current is referred to variously as Joule and ohmic heating. We have added a detailed table of contents, a subject index, a number of additional references and a list of the principal symbols.

We wish to thank Academician Artsimovich and a number of our colleagues for discussions which have clarified our understanding of the text; and we are particularly grateful to J. Fortna and J. D. Jukes for reading the entire proofs of the translation. We are very grateful to P. Kelly and A. Peiperl, and to Messrs. Oliver & Boyd and Messrs. Gordon and Breach for their cooperation in producing this translation.

A. C. KOLB
R. S. PEASE

# CONTENTS

FOREWORD TO THE RUSSIAN EDITION v

FOREWORD TO THE ENGLISH EDITION .. vii

EDITORS' NOTE ix

I INTRODUCTION .. .. .. 1

1.1. Thermonuclear reactions and energy balance with radiation 1

1.2. Magnetic confinement of plasma—reactor efficiency—minimum confinement time—optimal temperature—transformation of fusion energy to electrical energy—fuels—tritium breeding 9

1.3. Classification of confinement and heating schemes 18

II THE MOTION OF PARTICLES IN PLASMAS 22

2.1. Single particle motion: adiabatic invariance—motion parallel to the magnetic field 22

2.2. Motion in non-uniform fields: drift—motion perpendicular to the magnetic field—adiabatic trapping—experiments 26

2.3. Drift in combined electric and magnetic fields—quasi-periodic motion in time-varying non-uniform fields 33

2.4. Collisions between charged particles: cross-sections—mean-free-paths—collision times 38

2.5. Collisional relaxation—ions and electrons—slowing down rates—scattering 42

2.6. Collisions with neutral atoms — ionisation — impurity radiation 49

2.7. Charge-exchange processes 56

III TRANSPORT PHENOMENA IN PLASMAS .. .. .. 61

3.1. Electrical transport coefficients: conductivity—dielectric constant—polarisation 61

3.2. Runaway electrons and thermal conductivity 64

3.3. Transport phenomena in magnetic fields: electrical conductivity—dielectric constant—anisotropy of conductivity 67

3.4. Diffusion across a magnetic field: collisions between like particles and between unlike particles—heat conduction—Bohm diffusion and relation to experiment 71

IV MAGNETOHYDRODYNAMIC THEORY OF PLASMA 77

- 4.1. Magnetohydrodynamic equations: two-fluid equations—equations of motion—Ohm's law—validity of MHD approximation 77
- 4.2. Magnetostatics: pressure balance—pinch effect—Joule heating 82
- 4.3. Toroidal configurations: toroidal drift—toroidal pinch—effect of conducting walls—stabilised toroidal pinch 87
- 4.4. Collisional diffusion of plasma boundary 94
- 4.5. The collisionless plasma boundary 96
- 4.6. Motion of plasma with the lines of force 100
- 4.7. Oscillations and waves: electron plasma oscillations—sound waves—Alfvén waves—magnetosonic waves 102

V FAST HIGH-POWER DISCHARGES .. 109

- 5.1. Pinch effect: historical comments—experimental apparatus—diagnostic techniques 109
- 5.2. Experimental studies of plasma motion in the dynamic pinch 113
- 5.3. The dynamic pinch—measurements of plasma density and temperature—instabilities—impurities—the theory of Leontovich and Osovets (snow-plow model)—MHD calculations—microscopic processes 117
- 5.4. Neutron and X-ray emission from linear pinches—acceleration process—thermonuclear prospects of the dynamic pinch 132
- 5.5. The Triax hard core pinch 144
- 5.6. Theta-pinches: experimental 146
- 5.7. Theta-pinches: theoretical interpretation—inertial heating—effect of particle loss—trapped magnetic field—origin of nuclear reactions 154
- 5.8. Plasma loop in a transverse field 162
- 5.9. Plasma accelerators (injectors)—rail sources—coaxial guns 165

VI HEATING AND CONFINEMENT OF A PLASMA BY SUSTAINED ELECTRICAL DISCHARGES .. 172

- 6.1. General theory: 'slow' and 'fast' discharges—kink and sausage instabilities—the stabilised pinch—Kruskal-Shafranov stability condition—normal modes—the Suydam criterion—theoretical uncertainties 172
- 6.2. Experimental apparatus: insulated versus conducting discharge chambers—transformer design consideration—Zeta—pre-ionisation 182
- 6.3. Experimental techniques: discharge resistance and electron

temperature—electron density from microwave transmission —spectroscopy—infra-red measurements—energy loss measurements 189

6.4. Stabilised toroidal pinch, experimental results: typical parameters—plasma pressure—electron and ion temperatures—mass motion—emission of neutrals—X-ray emission —neutron radiation—energy balance 197

6.5. Stabilised toroidal pinch, general conclusions: instability—particle energies—acceleration processes—energy exchange —anomalous resistance—magnetohydrodynamic instabilities—runaway electrons—thermonuclear prospects 205

6.6. Toroidal discharges in strong longitudinal fields: the use of limiters—equilibrium position—Tokomak installations and experimental results: properties of the discharges—instability—influence of stray fields on equilibrium—electron density and 'pump-out'—hard X-ray emission and runaway electrons—new Tokomak installations and experimental results 208

6.7. Conclusions from studies of Tokomak systems: stability—ion temperature—force-free field configurations—pressure balance considerations—anisotropic conductivity and turbulent diffusion—future experiments—Joule heating expectations 223

6.8. Other varieties of sustained pinches: compressional heating —stabilisation by internal conductors—the Levitron 231

VII MAGNETIC TRAPS: GENERAL PRINCIPLES 236

7.1. Definition of magnetic trap—general approach to the problem—initial work in the Soviet Union 236

7.2. Single particle motion, qualitative ideas:—drift motions—the current-carrying ring—practical magnetic systems: Levitron, Astron, Stellarator, bumpy-torus 238

7.3. Single particle motion: general theory in axially symmetric magnetic fields—adiabatic motion—trapping of particles with large Larmor radii 242

7.4. Stability of plasmas in magnetic traps: magnetohydrodynamic and kinetic-type instabilities—flute and interchange instabilities—stability criteria—stability theory based on the motion of individual particles—mirror traps with anisotropic plasma pressure 249

7.5. Magnetohydrodynamic instabilities: growth rates—influence of a diffuse boundary—finite Larmor radius effects —influence of conducting walls and end-plates in mirror traps—Kadomtsev theory of turbulent diffusion 258

7.6. Other MHD-type instabilities: centrifugal instability—connection with anomalous diffusion and Rayleigh-Taylor instability—theory of instability, of the positive column—waves generated by temperature gradients 262

7.7. Kinetic instabilities: beam instability—velocity space instabilities—Landau damping—growth rates—excitation of plasma oscillations—excitation of ion-sound waves—wave excitation and confinement time—anomalous diffusion coefficient—instabilities due to anisotropic velocity distribution—some unsolved theoretical problems 269

7.8. Betatron radiation: its origin—relativistic effects—absorption in the plasma—implications for thermonuclear reactors 281

VIII SPECIFIC TYPES OF MAGNETIC TRAP 286

THE STELLARATOR: 8.1—8.6

8.1. Single particle motion—rotational transform and magnetic surfaces—figure-eight configuration—helical windings—shear stabilisation—construction tolerances—particle trajectories—mirror effects 286

8.2. Magnetohydrodynamics: equilibrium plasma configuration—influence of plasma diamagnetism—maximum plasma pressure—stability against flute perturbations—stability during ohmic heating 292

8.3. Construction and plasma heating: the race-track Stellarator—the divertor and impurities—ohmic heating—magnetic pumping at the collision frequency—magneto-sonic resonance—transit-time heating 297

8.4. Ion cyclotron resonance heating: single particle theory—in rarefied and high-density plasma—cyclotron waves and the magnetic beach 301

8.5. Experimental results: ohmic heating phase—Kruskal-Shafranov limit—spectroscopic observations—anomalous diffusion 304

8.6. Anomalous diffusion mechanisms: runaway electrons and plasma oscillations—ion oscillations—Kadomtsev mechanism—universal instabilities—trend of future research 308

MAGNETIC MIRROR TRAPS: 8.7—8.14

8.7. Axially symmetric adiabatic traps: particle distributions—influence of electrostatic fields—the high-$\beta$ limit—mirror losses by collisions—confinement time—ratio of diffusion losses and scattering losses—production of net fusion power 311

8.8. Injection of high-energy particles: molecular ion dissociation—trapping in a rising field—injection across a rising magnetic field—non-adiabatic trapping in spatially varying fields—fast neutral injection—ionisation on background gas or other beams—vacuum requirements—Lorentz ionisation of neutral atoms 318

8.9. Heating methods: ion magnetron—plasma injection—magnetic compression 32
8.10 Experiments with compressional mirror traps: hot electron plasmas—X-rays—electron temperature—plasma volume—confinement time—interchange instabilities—'line-tying'—an interpretation of Pyrotron experiments—ion temperature—multi-stage compression experiments 325
8.11. Ion magnetron experiments: charge-exchange losses and containment time—losses due to instability—loss of energetic ions—influence of geometry on losses 329
8.12. Rotating plasma experiments: plasma currents—enhanced mirror ratio—plasma capacitance and electrical characteristics—future possibilities 336
8.13. Experiments with Ogra: molecular ion dissociation on residual gas—'burn-out'—vacuum conditions—critical current—Ogra design features—status of Ogra experiments—non-stationary effects—space charge—ion cyclotron radiation 340
8.14. The DCX experiments: molecular ion dissociation with an arc—ion beam characteristics—charge exchange losses in the arc—special nature of plasma 347
8.15. Astron: relativistic electron current ('E-layer') 349

HIGH-FREQUENCY CONFINEMENT: 8.16—8.18

8.16. Theory: the skin effect—motion of single particles in HF fields—HF fields combined with static magnetic fields (high-frequency plugs)—compensation of toroidal drift 351
8.17. Confinement of plasmas: equilibrium conditions—boundary between plasma and confining fields—particle losses 356
8.18. Experimental: travelling waves in a toroidal chamber—an experiment with two waves travelling in opposite directions—high-frequency magnetic 'plugs' for axial confinement—confinement in resonant cavities—HF stabilisation 358

CUSP-SHAPED FIELDS: 8.19—8.20

8.19. Cusp-shaped fields—field distribution near field-zero—non-adiabatic particle motion—loss rates—influence of boundary layer structure—diffusion broadening of boundary layer—thermonuclear prospects—confinement at low $\beta$ 361
8.20. Experimental investigation of cusp-shaped fields: plasma injection and penetration into a strong field—finite conductivity effects—trapping mechanisms—heating by compression—experimental apparatus—life-time of the plasma—the search for non-adiabatic losses 367

8.21. Hybrid magnetic field traps: defects of, simple geometries—general requirements—examples of hybrid geometries—Ioffe's apparatus—Ioffe's experimental results 375

IX CONCLUSION .. 380

BIBLIOGRAPHY .. .. 383

LIST OF SYMBOLS .. 397

INDEX .. .. .. .. 399

CHAPTER I

# INTRODUCTION

§ **1.1** Thermonuclear reactions arise from collisions between the fast atomic nuclei in matter heated to a very high temperature. If the colliding nuclei have sufficiently large relative speed, they can overcome the potential barrier of mutual electrostatic repulsion, approach very closely to one another and react. When the temperature $T$ is not too high, so that the quantity $kT$, representing the energy of the random thermal motion of the particles, has a value small compared to the barrier potential, only an insignificant proportion of the thermal collisions will result in nuclear reactions. As $T$ is raised, the thermonuclear reaction rate increases rapidly.

Thermonuclear reactions are, apparently, the main source of stellar energy and must therefore play an important part in astrophysical processes. Inside stars, the temperature and the density are very high. Therefore in stellar matter an intensive process of nuclear synthesis must go on, during which the basic component of matter—hydrogen—is converted into helium by a succession of nuclear fusion reactions, and a vast amount of energy is released.

It is natural that the idea of producing similar reactions here on earth, in order to make use of the power from them, should have been current for many years. The problem of how to do this has now come to the forefront of nuclear energy research. Its solution will provide access to the well-nigh inexhaustible energy resources of the light elements—energy which can be released by thermonuclear fusion processes at very high temperatures, but cannot be obtained in surplus by any other known method.

From the point of view of both scientific research and practical applications, the greatest interest attaches to producing nuclear fusion in deuterium or in a mixture of deuterium and tritium. Here only the minimum temperature, relatively speaking, is required in order to obtain intense thermonuclear reactions.

The reactions in deuterium can take place in two ways, as follows:

$$\begin{tikzcd}[row sep=small] & {}^3\mathrm{He}+n, \\ d+d \arrow[ur] \arrow[dr] & \\ & t+p. \end{tikzcd}$$

The two branches of the reaction have almost equal probability. The energy released is 3·3 MeV for the reaction giving a neutron and 4·0 MeV for that giving a proton.

Figure 1 shows the total cross-section for the *d-d* reaction as a function of the deuteron energy $W_d$ (in the co-ordinate system where one deuteron is at rest). When $W_d \leqq 1{\cdot}5\times10^5$ eV the variation of this cross-section can be expressed with sufficient accuracy by the formula

$$\sigma = (2{\cdot}4\times10^{-19}/W_d)\exp(-1{\cdot}4\times10^3/W_d^{\frac{1}{2}});\ \text{cm}^2,\ W_d \text{ in eV.} \qquad \ldots\ldots\ldots(1.1)$$

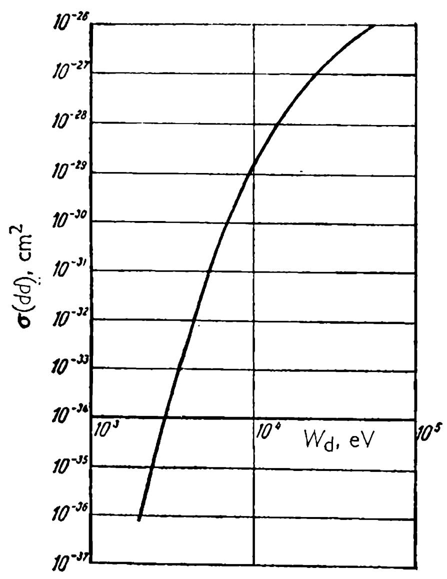

FIG. 1. Dependence of the total *d-d* reaction cross-section on deuteron energy

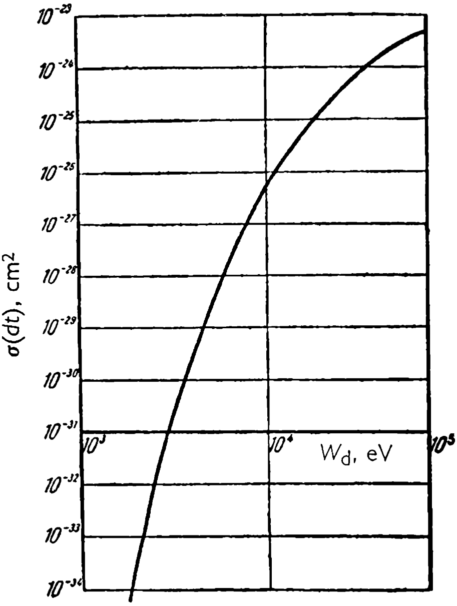

FIG. 2. Dependence of the *d-t* reaction cross-section on deuteron energy

In a mixture of deuterium and tritium, the reaction

$$d+t \rightarrow {}^4\text{He}+n$$

takes place, liberating 17·6 MeV of energy; 80% of this energy, i.e. about 14·1 MeV, is acquired by the neutron. The cross-section as a function of deuteron energy (the tritium nucleus is assumed to be at rest) is shown in Fig. 2. The cross-section for this reaction is given approximately by the formula

$$\sigma = (6\times10^{-17}/W_d)\left[1+\frac{(W_d-10^5)^2}{3\times10^{10}}\right]^{-1}\exp\left(\frac{-1{\cdot}5\times10^3}{W_d^{\frac{1}{2}}}\right);\ \text{cm}^2,\ W_d \text{ in eV.} \qquad \ldots\ldots\ldots(1.2)$$

This is in good agreement with experimental data for energies below about 1 MeV. When $W_d \leqq 10^5$ eV the *d-t* reaction cross-section is about a hundred times greater than the total *d-d* reaction cross-section. This is because the *d-t* reaction involves a resonance process.

Given the cross-section as a function of particle energy, it is possible to calculate the thermonuclear reaction rate in matter. The number of nuclear reactions taking place in 1 cm$^3$ during 1 sec is given by the expression

$$g = n_1 n_2 \overline{v\sigma}. \qquad \text{.........}(1.3)$$

Here $n_1$ and $n_2$ are the numbers of nuclei per cm$^3$ (number density) of the two reacting species, and $\overline{v\sigma}$ is the product of the relative velocity of the nuclei and the reaction cross-section averaged over the velocity distribution of the nuclei. In calculating the reaction rate in pure deuterium the product $n_1 n_2$ is replaced by $n^2/2$, where $n$ is the number density of deuterium nuclei.

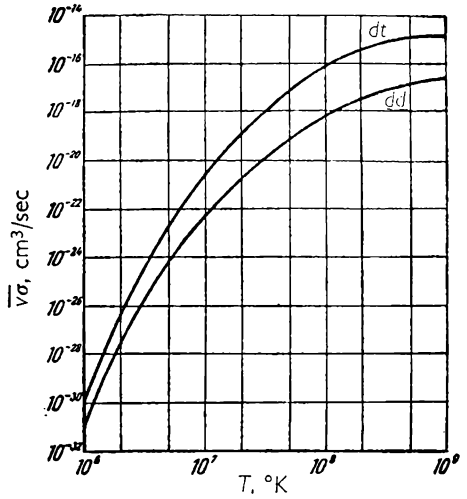

FIG. 3

Mean $v\sigma$ values (cm$^3$ sec$^{-1}$) for *d-d* and *d-t* reactions when the distribution of particle energy in the plasma is maxwellian

Where the value of $T$ is fixed† (i.e. where there is a given value for the mean kinetic energy of the random motion of the particles) the quantity $\overline{v\sigma}$ is still not determined uniquely because it is very sensitive to the particle velocity distribution. Where temperatures are not too high ($T \leqq 10^8$), the marked dependence of the cross-section on the relative velocity $v$ results in the major part of the thermonuclear reactions being due to collisions between particles whose energy is several times greater than the mean value of the thermal energy $3/2kT$. Thus the reaction rate depends markedly on the detailed shape of that part of the energy spectrum made up by the small proportion of particles with an energy considerably in excess of the mean value. It may be assumed that where 'randomising' processes take place rapidly compared to all other processes, a Maxwellian velocity distribution will be established. Figure 3 shows values of $\overline{v\sigma}$ for the *d-d* and *d-t* reactions in the temperature range $10^6$ to $10^9$ °K, i.e. from $10^2$ to $10^5$ eV, for Maxwellian velocity distributions. When the temperatures do not exceed $10^8$ °K ($10^4$ eV), use can also be made of the following formulae to determine the reaction rate:

---

† Henceforth $T$ will be used to signify temperature measured in °K. Temperature in electron-volts will be designated by $\theta$. As is familiar, $T = 11{,}610\,\theta$.

$$g_{dd} = 7.5\times 10^{-10}(n^2/T^{\frac{2}{3}}) \exp(-4{\cdot}25\times 10^3/T^{\frac{1}{3}}) \text{ reactions cm}^{-3}\text{ sec}^{-1}; \quad \text{.........}(1.4a)$$

$$g_{dt} = 1{\cdot}6\times 10^{-7}(n_1 n_2/T^{\frac{2}{3}}) \exp(-4{\cdot}52\times 10^3/T^{\frac{1}{3}}) \text{ reactions cm}^{-3}\text{ sec}^{-1}. \quad \text{.........}(1.4b)$$

However, the assumption of a Maxwellian velocity distribution is not by any means justified in all cases of interest to us. When a heating pulse of short duration takes place in a low density plasma, it may well be that there is insufficient time to establish a Maxwellian velocity distribution. This may mean that, although the random motion of the particles can be defined by a specific temperature (meaning by this a quantity proportional to the mean particle energy), the proportion of particles which populate the very high energy part of the energy spectrum is nevertheless negligible. In such a situation the reaction rate is reduced significantly. Figure 4 shows how the *d-d* reaction rate compares for two different velocity distributions, the temperatures being the same: $g_1$ corresponds to a Maxwellian distribution, $g_2$ to the case where all the particles have the same energy. Admittedly the second of these distributions, here selected for purposes of comparison, is not a realistic one; nevertheless the comparative values of $g_1$ and $g_2$ illustrate how greatly the shape of the energy spectrum influences the reaction rate. We see that for a temperature of about $10^6$ °K a significant departure from a Maxwellian distribution can diminish the nuclear reaction rate by several orders of magnitude. As $T$ increases, the ratio $g_1/g_2$ decreases until at $T = 10^8$ °K it approaches unity. This change in $g_1/g_2$ is qualitatively quite understandable: when the energy is high, $\sigma$ is not nearly so strongly dependent on $W_d$.

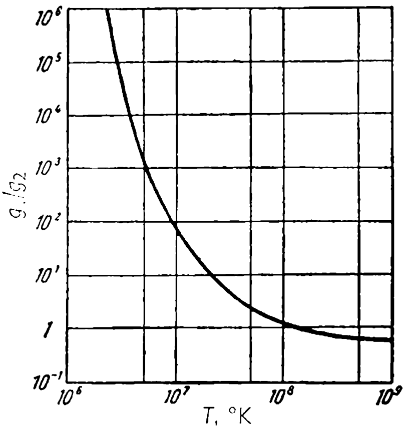

FIG. 4

Ratio of the *d-d* reaction rates for two different particle velocity distributions

From the above data on thermonuclear reaction rates, it follows that the experimentalist can hope to detect the first signs of nuclear reactions in heated matter only when the temperature reaches something like a million degrees. If thermonuclear processes are to be of any practical value for energy production, a considerably higher temperature—hundreds of millions of degrees—is required.

At temperatures of a million degrees or more, matter exists as a plasma with a high degree of ionisation† (the degree of ionisation approaches 100% in stationary conditions). Only a fairly small amount of energy has to be concentrated in a plasma in order that its temperature should be high enough to ensure a high thermonuclear reaction rate. For instance, in hydrogen plasma with number density $n = 10^{15}$ cm$^{-3}$, the energy required for $T = 10^8$ °K amounts to only 4 joules/cm$^3$. If there were a method of heating plasma by which all thermal losses could be eliminated in practice, then a small power source could be used to produce a large thermonuclear yield. However, the main difficulty lies precisely in reducing the thermal losses, which rise extremely rapidly as the temperature is raised. In the absence of magnetic fields, the coefficient of thermal conductivity of fully ionised plasma is proportional to $T^{\frac{5}{2}}$, and therefore the thermal conduction losses increase as $T^{\frac{7}{2}}$.

An idea of the sort of values involved in the heating process, under conditions of unrestricted thermal conduction, can be obtained from an actual example. A sphere with a heat source at the centre is an ideal heating configuration. A simple calculation gives the following relationship between the total thermal flux and the temperature of a small central heat-source in a large conducting sphere:

$$Q = (8\pi/7)\alpha_T r_1 T^{\frac{7}{2}}. \qquad \text{.........}(1.5)$$

Here $Q$ is the heat evolved per second within a region of radius $r_1$, $T$ is the temperature at $r_1$ and $\alpha_T$ is the numerical multiplier in the formula for the coefficient of thermal conductivity

$$\sigma_T = \alpha_T T^{\frac{5}{2}}. \qquad \text{.........}(1.6)$$

In the c.g.s. system the value of $\alpha_T$ is about $10^{-6}$.‡ If we take $T = 10^6$ and $r_1 = 1$ cm we find that $Q$ is about $4 \times 10^5$ kW. The example is instructive in so far as it illustrates the scale of the difficulties that have yet to be overcome before we can generate intense thermonuclear reactions with steady-state heating.

To solve the problem, a method is needed which makes it possible either to reduce the thermal conductivity by many orders of magnitude or to separate the plasma from walls and suspend it in a vacuum.

Let us suppose that a method has been found which eliminates thermal conduction from the plasma. The energy losses will now be caused solely by radiation. As will be explained later, what is wanted in practice is a very high temperature plasma with a number density not exceeding about $10^{15}$ cm$^{-3}$. Plasma as rarefied as this is very transparent to short-wavelength electromagnetic radiation, in particular to those wavelengths corresponding to photon energies of about $kT_e$ at these very high temperatures. Consequently the energy radiated by the plasma is many orders of magnitude less than for a black body at the same temperature. Nevertheless, the radiation loss from a hot plasma can still be very considerable.

---

† A plasma is a gas in which the proportion of atoms ionised is sufficiently large for the motions of the resulting electrons and positive ions to be dominated by their collective electromagnetic interactions.

‡ Strictly speaking, $\alpha_T$ is not a constant: it depends both on the number density and on the temperature. However, over the range of values of $n$ and $T$ of interest to us, this dependence of $\alpha_T$ is only of a weak logarithmic character.

In order to determine the magnitude of this loss the first thing that must be done is to establish what processes can be a source of electromagnetic radiation. The greater part of the electromagnetic radiation from wholly ionised high-temperature plasma is bremsstrahlung; that is, radiation due to the motion of the free electrons in the Coulomb fields of the nuclei. This radiation has the same physical origin as the X-rays in the continuous spectrum from an ordinary Röntgen tube, where the anode of the tube is bombarded by a stream of fast electrons. The quantum-mechanical theory of bremsstrahling of non-relativistic electrons was derived by Sommerfeld. Its predictions are in agreement with the experimental data obtained from continuous spectra of X-rays. According to the theory, when a fast electron moves through matter it radiates energy at a rate equal to

$$-dW_e/dt = 1{\cdot}5\times 10^{-25} n Z^2 W_e^{\frac{1}{2}} \text{ ergs sec}^{-1}. \qquad \ldots\ldots\ldots(1.7)$$

In this expression $n$ is the number density of atomic nuclei, $Z$ is their atomic number and $W_e$ is the kinetic energy of the electron in electron-volts. The intensity of bremsstrahlung from the plasma is obtained by integrating equation (*1.7*) over the electron energy distribution. With a Maxwellian distribution, the total energy radiated by unit volume of plasma per second is calculated to be

$$Q_{\text{rad}} = 1{\cdot}6\times 10^{-27} n_e n_i Z^2 T_e^{\frac{1}{2}} \text{ ergs sec}^{-1}, \qquad \ldots\ldots\ldots(1.8)$$

where $n_e$ and $n_i$ are the number densities ($\text{cm}^{-3}$) of electrons and ions respectively, and $T_e$ is the electron temperature. For the frequency range $\nu$ to $\nu+d\nu$ the power radiated is equal to

$$f(\nu)\,d\nu = 6{\cdot}8\times 10^{-38} n_e n_i Z^2 T_e^{-\frac{1}{2}} \phi\left(\frac{h\nu}{kT_e}\right) \exp\left(-\frac{h\nu}{kT_e}\right) d\nu. \qquad \ldots\ldots\ldots(1.9)$$

The variation of the numerical factor $\phi$ with $(h\nu/kT_e)$ is shown in Fig. 5.

Equation (*1.8*) for the bremsstrahlung intensity is accurate enough when $T_e$ is not too high, so that the electrons can be considered as non-relativistic. However, when relativistic electron temperatures are reached (i.e. when $T_e$ exceeds about $10^9$ °K), the intensity of the radiation caused by interactions between electrons and the Coulomb field of the nuclei rises more rapidly with $T_e$ than indicated by formula (*1.8*). Furthermore, at relativistic speeds collisions of electrons with other electrons also give rise to intense bremsstrahlung; thus the total radiation loss is still further enhanced.

Figure 6 shows the ratio of the actual bremsstrahlung intensity to the value determined from equation (*1.8*), for a broad range of electron temperatures. We see that this ratio starts to diverge appreciably from unity at $T_e \simeq 5 \times 10^8$ °K. When temperatures and plasma densities are high, energy losses due to bremsstrahlung become very large. Thus, for example, at $T_e \simeq 10^9$ °K and $n \simeq 10^{15}$ cm$^{-3}$ the power radiated by 1 m$^3$ of hydrogen plasma is equal to $7 \times 10^3$ kW.

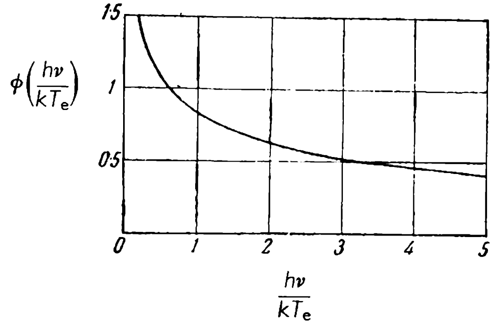

FIG. 5. The function $\phi(k\nu/kT_e)$ of equation (*1.9*)

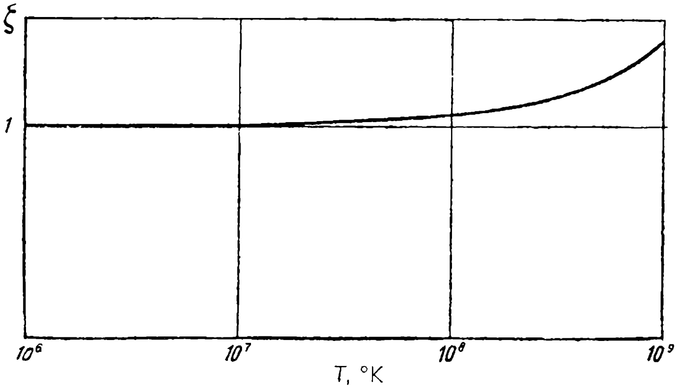

FIG. 6. The ratio $\zeta$ of the total energy radiated as bremsstrahlung to that given by equation (*1.8*)

It should be noted that even comparatively small concentrations of heavy impurity matter in high temperature hydrogen plasma can considerably increase the bremsstrahlung losses. For example, if hydrogen plasma is contaminated with 0·1% of copper nuclei, then this contamination will nearly double the bremsstrahlung intensity.

When the electron temperatures are comparatively low ($T_e < 10^8$), the enhancement of the radiation from a hydrogen plasma by contamination is even greater, because the processes of radiative recombination and line radiation become very intense when conditions are insufficient to strip all the atoms of their bound electrons. We shall return to this topic in the next chapter.

Bremsstrahlung of fast electrons causes an unavoidable loss of energy from plasma heated to high temperature. No known method of thermally insulating hot plasma can have any noticeable effect on this loss. A thermonuclear generator can, therefore, produce surplus energy only when the total energy produced in fusion reactions exceeds these radiation losses. The nuclear energy produced and the radiation losses depend alike on the plasma number density (both are proportional to $n^2$), and consequently their ratio for a given nuclear fuel is solely a function of the plasma temperature.

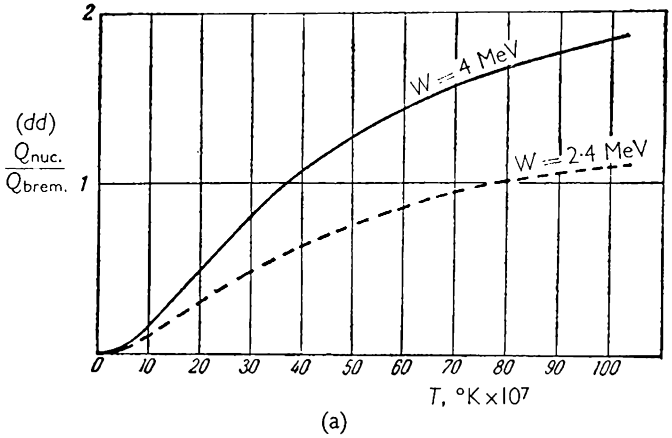

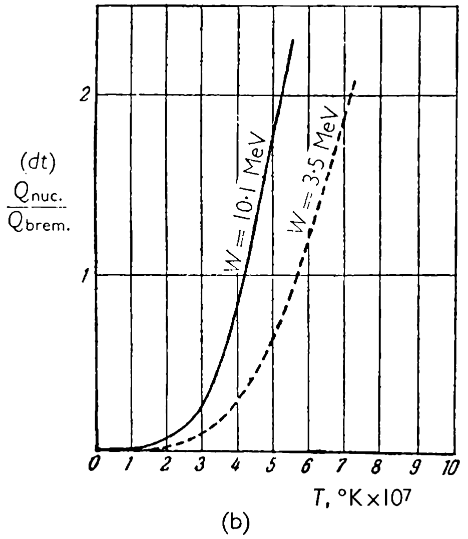

FIG. 7. Ratio of the energy released by thermonuclear reactions to that lost by bremsstrahlung:

(a) for the *d-d* reaction
(b) for the *d-t* reaction

The curves reproduced in Figs. 7a and 7b show this ratio as a function of plasma temperature $T$: (a) for pure deuterium, and (b) for a 50 % mixture of deuterium and tritium. The dotted curves do not take into account all the energy released by the fusion reactions, but only that part of it which appears as kinetic energy of the charged reaction products, i.e. that part of the energy which can be directly deposited as heat in the plasma and which, in principle, can be converted with high efficiency into electrical energy. That part of the energy carried away by the neutrons (to which has been added a neutron binding energy† of 8 MeV which is assumed to be released when the neutron is finally captured) is deposited in some moderating medium outside the volume occupied by the plasma, and can be utilised in the form of electrical energy with a normal thermal efficiency of only about 0·3. Allowance for this second portion of energy (adopting 0·3 for the efficiency) raises the energy output by 65% (from 2·4 to 4 MeV) in pure deuterium and by 180% (from 3·5 to 10·1 MeV) in a mixture of deuterium and tritium. The corresponding curves are shown in Figs. 7a and 7b by unbroken lines. It should be noted that the graphs of Fig. 7 were obtained by taking the ion temperature $T_i$ as equal to the electron temperature $T_e$. It may be that in practice this equality cannot be maintained. In particular, if the entire heating flux were to go directly into the positive ions, and losses were due solely to bremsstrahlung, then $T_e$ would be less than $T_i$: indeed the ratio $T_e/T_i$ would be far from unity.

We can see from Figs. 7a and 7b that a system generating thermonuclear reactions can serve as a nuclear power station only if the plasma temperature exceeds some critical temperature $T_c$ which amounts to about $3{\cdot}5 \times 10^8$ °K for deuterium, and to about $4 \times 10^7$ °K for a 50% mixture of deuterium and tritium.‡ These critical temperatures are calculated assuming that optimum use is made of the thermonuclear energy released. If one counts only that part of the energy carried by the charged reaction products, then the calculated values of $T_c$ are correspondingly higher.

Bremsstrahlung of fast electrons accounts entirely for the radiation from high-temperature hydrogen plasma in the high-frequency region ($h\nu \simeq kT_e$). In the low-frequency region other physical processes also can contribute to the radiation losses. In particular, at very high temperatures (beginning at about $10^8$ °K) losses due to so-called betatron radiation (also called 'magnetic bremsstrahlung', 'cyclotron radiation' and 'synchrotron radiation') can become large. We shall consider this type of loss later when analysing the properties of proposed thermonuclear generators.

§ **1.2** The fundamental and very difficult problem requiring solution, if intense controlled thermonuclear reactions are to be realised, is how to insulate the very high-temperature plasma from the surrounding walls of the containing vessel. The fast particles which comprise the plasma must be contained for a sufficiently long time to allow a high probability of their reacting with one another before striking the walls of the chamber.

---

† The neutron binding energy added is the energy released when neutrons are captured by atomic nuclei. For most stable nuclei this energy varies between 7 and 11 MeV, and has an average value of about 8 MeV over the whole periodic table.

‡ If one assumes partial utilisation of the energy lost as bremsstrahlung, the values of $T_c$ go down. They drop further if, when calculating the energy yield for *d-d* reactions, one allows for the additional sources of nuclear energy provided by the formation of tritium (see below).

In principle it is possible to solve this problem because at a high temperature matter can exist only in the form of an essentially fully-ionised plasma containing only charged particles. Therefore it is possible to use a strong magnetic field for thermal insulation. In a magnetic field charged particles can move freely only in helical trajectories along the direction of the vector $\boldsymbol{H}$. If the lines of force are parallel to the walls of the chamber containing the plasma then the escape of particles from the plasma should become inhibited in strong fields, and the flow of heat to the walls sharply diminished. Ideally, one would like the plasma to be separated from the walls by a region containing no particles at all. Although particle diffusion prevents the plasma boundary from being ideally sharp (and therefore complete detachment of the plasma from the surrounding walls is, strictly speaking, unattainable), it is apparently possible in principle to come near enough to such an ideal. Where $H$ and $T$ are large, the collisional diffusion of particles in a plane perpendicular to $\boldsymbol{H}$ is slight; therefore the blurring of an initially sharp boundary should take place slowly.

We shall look from a macroscopic standpoint at the balance of forces on the free boundary of a hot plasma (for the sake of simplicity the boundary is assumed static). A fully-ionised hydrogen plasma at a temperature $T$ has a gas-kinetic pressure:

$$p = 2nkT, \qquad \text{.........}(1.10)$$

where $n$ is the number density of positive ions. At the boundary which divides the plasma from the vacuum, the pressure $p$ must be balanced by the pressure exerted by the magnetic field. Let the magnetic field strength be $H_0$ outside the plasma and $H_i$ inside the plasma.† For equilibrium it is necessary that the difference between the magnetic pressures should equal the plasma pressure, i.e.

$$(H_0^2 - H_i^2)/8\pi = 2nkT. \qquad \text{.........}(1.11)$$

Although this relationship has been obtained here for a quite special and idealised case, it expresses the essential aim of all methods for solving the problem of controlled thermonuclear fusion: this aim is to contain the hot plasma by a strong magnetic field. The minimum external field strength needed to contain the pressure of the plasma corresponds to the condition $H_i = 0$; then

$$H_0 = 4\sqrt{\pi nkT}. \qquad \text{.........}(1.12)$$

For a given temperature the thermonuclear reaction rate is proportional to $n^2$, and consequently the maximum reaction rate increases with the magnetic field as $H_o^4$. It follows that in an ideal thermonuclear generator a practical limit for the reaction rate per unit volume of plasma is set by the mechanical stresses in the system maintaining the strong magnetic fields. To illustrate this point we note that when $T = 4 \times 10^8$ °K and $n = 10^{15}$ cm$^{-3}$, the required field strength is $5 \times 10^4$ Oe. A magnetic field of this strength is already near the present practical limit for large installations working for prolonged periods.

---

† When a plasma is at high temperature its electrical conductivity is very great, and therefore the different values of the magnetic field on either side of the boundary equalise very slowly. Because of this, the supposition of a jump in the field strength at the boundary is a legitimate idealisation of the true picture.

Any system proposed for the practical solution of the problem of obtaining thermonuclear energy must satisfy one essential condition: the energy released by nuclear fusion must more than compensate for the energy expended from other sources in generating and maintaining a high temperature in the plasma. To fix ideas, we shall introduce the concept of the efficiency of a thermonuclear generator in terms of these energies, and we shall try, though only in a rough approximation, to express this efficiency in terms of the main parameters describing the envisaged operation of a thermonuclear reactor.

We shall designate the efficiency $R$ of a thermonuclear generator as the ratio of the nuclear energy released per unit time to the energy losses. If the insulation of the plasma against thermal conduction losses could be made complete, so that not a single particle would escape from the plasma to the walls, then bremsstrahlung would be the only source of energy loss; and to determine the efficiency of a thermonuclear generator one could use the curves reproduced in Figs. 7a and 7b. The efficiency would then be simply a function of temperature and would not depend on other parameters in the system. However, one can hardly expect that energy losses in a thermonuclear generator will be caused solely by plasma radiation. It seems more probable that even with very good thermal insulation there will be a flow of particles to the walls which will transport energy greatly exceeding the radiation loss.

We shall not consider here the physical mechanisms which can lead to such fluxes of particles bombarding the walls of a thermonuclear generator; and in assessing the associated energy loss we shall grossly simplify the true picture of what is likely to happen. Looked at phenomenologically, the quality of the thermal insulation can be characterised by the mean lifetime of particles in the plasma. The energy carried away by the particle fluxes can be related to this quantity.

If the mean life of an individual particle in the plasma is $\tau_p$ (taking it to be the same for electrons and ions), and if the number density of particles of the same sign within the plasma is $n$, then the number of particles which disappear from unit volume per unit time and reach the walls is $2n/\tau_p$. They carry away energy

$$\Delta Q_p = 3nkT/\tau_p. \qquad \text{.........}(1.13)$$

We shall take this expression as defining the thermal losses due to imperfect confinement of particles.

The total heat loss is the sum of $\Delta Q_p$ and the radiated energy $\Delta Q_{rad} = n^2 f_{rad}(T)$. However, part of the energy leaving the plasma in the form of heat and electromagnetic radiation can be converted into electrical energy, and therefore it should not be written off as a complete loss. To determine what proportion of the losses must be written off completely, the sum of $\Delta Q_p$ and $\Delta Q_{rad}$ must be multiplied by a coefficient $1-\eta_0$, where $\eta_0$ is the thermal efficiency with which the energy deposited outside the plasma is transformed into electric energy. We shall allow some optimism in assessing $\eta_0$ and take it to be $\frac{1}{3}$. The following expression can now be written for the efficiency of a thermonuclear generator:

$$R = \alpha n^2 \overline{v\sigma} W_n \times 1{\cdot}6 \times 10^{-6} \Big/ \left[\frac{2nkT}{\tau_p} + \frac{2}{3} n^2 f_{rad}(T)\right]; \quad \ldots\ldots\ldots (1.14)$$

$W_n$ is in MeV, the other quantities being in c.g.s. units. The numerical multiplier $\alpha$ is $\frac{1}{2}$ for a generator working on pure deuterium, and is $\frac{1}{4}$ when a 50% mixture of deuterium and tritium is used. For the *d-t* reaction the effective nuclear energy released $W_n$ is taken to be 10·1 MeV, as discussed above.

For a generator working on pure deuterium the choice of a suitable value for $W_n$ is somewhat complicated by the fact that in *d-d* reactions not only is nuclear energy released but tritium nuclei are formed as well, and these in turn can be utilised as thermonuclear fuel; as such they are considerably more efficient than deuterons. A part of this tritium will be consumed in the same thermonuclear cycle in which it is formed. The unconsumed tritium can be separated off, mixed with an equal quantity of deuterium, and used in another thermonuclear cycle. Now let us assume that it is possible to build a system in which a 50% mixture of deuterium and tritium is used and which produces thermonuclear energy in excess of the energy losses. This additional nuclear energy can be written into the energy sum for a *d-d* thermonuclear generator in which tritium nuclei are formed as a result of *d-d* reactions. Earlier we took $W_n$ to be 4 MeV for the *d-d* reaction. To allow for the additional energy obtained by consuming the tritium reaction product, a correction has to be applied to the value of $W_n$ quoted. The maximum value of this correction is obtained by assuming that in the reactor using the deuterium-tritium mixture, the energy losses are negligible compared to the nuclear energy released. Bearing in mind that tritium is formed only in one branch of *d-d* reaction, we thus take the maximum value of the correction to $W_n$ as equal to one-half the useful energy released in the *d-t* reaction, i.e. equal to 5 MeV. When this correction is applied, the value of $W_n$ which has to be put into the expression for the efficiency of a thermonuclear generator working on deuterium becomes 9·0 MeV. Henceforth this maximum value for $W_n$ is adopted in the text.

It follows from formula (*1.14*) that a thermonuclear generator will serve as a source of energy on condition that

$$n\{\alpha\overline{v\sigma}W_{\mathrm{n}}\times 1{\cdot}6\times 10^{-6}-\tfrac{2}{3}f_{\mathrm{rad}}(T)\} > \frac{2kT}{\tau_{\mathrm{p}}};$$

where $W_{\mathrm{n}}$ is in MeV, and other quantities are in c.g.s. units.

The maximum permissible number density is determined by the magnetic field strength supporting the plasma pressure. Substituting equation (*1.12*) for $n$, we obtain

$$H^2\tau_{\mathrm{p}} > 32\pi(kT)^2/[\alpha\overline{v\sigma}W_{\mathrm{n}}\times 1{\cdot}6\times 10^{-6}-\tfrac{2}{3}f_{\mathrm{rad}}(T)]. \quad \text{.........}(\mathit{1.15})$$

Obviously, this inequality will be meaningful only if the right-hand side is positive. When this is so, the value of the right-hand side first of all falls, as the temperature rises, from $\infty$ to a minimum, and then rises slowly. The temperature for which the right-hand side is a minimum can be termed optimal since it corresponds (at least in principle) to the most favourable operating conditions. For pure deuterium the optimal temperature is $3\times 10^8$ °K; at this temperature condition (*1.15*) becomes

$$H^2\tau_{\mathrm{p}} > 5\times 10^9\ (\mathrm{Oe}^2\ \mathrm{sec}). \qquad \text{.........}(\mathit{1.16a})$$

If allowance is not made for the additional energy available from the tritium reaction product, the right-hand side of the inequality must be increased to $2\times 10^{10}$. In this case the optimal temperature goes up to $5\times 10^8$ °K.

For a 50% mixture of deuterium and tritium the optimal temperature is $1{\cdot}8\times 10^8$ °K. At this temperature the condition for a positive energy yield is:

$$H^2\tau_{\mathrm{p}} > 6\times 10^7\ (\mathrm{Oe}^2\ \mathrm{sec}). \qquad \text{.........}(\mathit{1.16b})$$

The shorter the mean lifetime of a particle in the plasma, the higher is the required magnetic field strength. To give an example, when $\tau_{\mathrm{p}} = 10^{-5}$ sec, the magnetic field in a reactor working on pure deuterium must, by (*1.16a*), exceed $2{\cdot}2\times 10^7$ Oe. The magnetic pressure will then be of the order of $2\times 10^7$ atmospheres, and the power produced in 1 cm$^3$ reaches $3\times 10^8$ kW. A system with characteristics like this, which are those of an explosion of enormous strength, offers absolutely no promise as a source of controlled thermonuclear power.

To keep the basic parameters of a thermonuclear reactor within the bounds of what is conceivable in practice, it is necessary to devise a method of containing plasma particles for times measured in seconds or even tens of seconds. Thus, if we take $\tau_{\mathrm{p}} = 10$ sec, the strength of the field in a deuterium-fuelled reactor would have to be of the order of $2\times 10^4$ Oe, which is well within the bounds of possibility. It should be noted, however, that in this case the power generated per unit plasma volume is small (about 0·3 W/cm$^3$), and if such a complex installation is to have any practical value its dimensions will have to be extremely large (a volume of hundreds or even thousands of cubic metres). We also note that at the optimal temperatures the total power released per unit volume by thermonuclear reactions amounts to:

(a) for a reactor using pure deuterium,

$$Q = 1{\cdot}2\times 10^{-18} H^4, \qquad \mathrm{W/cm^3}; \qquad \text{.........}(1.17a)$$

(b) for a reactor using a 50% mixture of deuterium and tritium,

$$Q = 7\times 10^{-17} H^4, \qquad \mathrm{W/cm^3}. \qquad \text{.........}(1.17b)$$

$H$ is the strength of the field containing the plasma, according to equation (*1.12*), in oersted.

As already said, the method used in this chapter to make an initial estimate of the efficiency of a thermonuclear reactor is very simplified. The simplification distorts the true picture in one particularly important respect: all types of energy loss associated with particle losses have been lumped together regardless of the physical mechanism involved, and the mean particle life-time $\tau_p$ is taken as characteristic of their total effect. In the formula for the efficiency, this quantity appears as a parameter independent of $n$, $T$ or $H$. (Only on this condition is it possible to introduce the concept of optimal temperature in the way that was done above.) Thus this quantity, which is obviously appropriate to a simplified approach, is a provisional one; and this must be borne in mind. If exactly defined, $\tau_p$ is that interval of time during which particles transfer to the walls thermal energy equal to the total kinetic energy of the particles in the plasma.

In practice, of course, $\tau_p$ will be a function of such basic parameters as the temperature, the number density and the field strength. But the nature of this dependence can be discussed only in conjunction with an examination of the principles of operation and construction of actual systems devised to obtain high-temperature plasma; and this will be done in later chapters. At that stage the necessary refinement to the estimated losses by electromagnetic radiation from the plasma will also be introduced. This refinement will include making allowance for the energy leaving the plasma in the form of betatron radiation.

Apart from the simplification involved in introducing the phenomenological constant $\tau_p$, we introduced a further idealisation by assuming that the plasma pressure is fully equal to the pressure of the external magnetic field. The available results of both theoretical analysis and experimental data suggest that when $p = H^2/8\pi$, the plasma confinement is not stable. It is very likely (though not actually proved) that the stable confinement of plasma in a magnetic field can be realised only on the condition that $8\pi p/H^2 \ll 1$. If this is so, then the minimum values of $H^2\tau_p$ necessary to reach conditions giving a surplus energy must be correspondingly increased (by the ratio of the magnetic to the plasma pressure). It is easy to satisfy ourselves on this point if we recall the steps in the calculation which led us to equations (*1.16a*) and (*1.16b*). This increase in $H^2\tau_p$ leads to a further multiplication of the difficulties.

To conclude our general analysis of the efficiency of a thermonuclear reactor, we shall explain how the efficiency is affected by the time for which a high plasma temperature is maintained. This explanation is necessary in order to estimate the efficiency of a thermonuclear reactor operating in a series of periodically recurring cycles.

We shall designate the duration of the high-temperature state by $\tau_1$. It should be noted that, in principle, there need be no connection between $\tau_1$ and the mean life-time of particles in the plasma $\tau_p$, although in practice there may be some correlation between these quantities. To avoid complicating our explanation of the dependence of $R$ on $\tau_1$, we shall suppose that the thermal insulation is ideal ($\tau_p = \infty$). In this case, thermal losses of energy take place only when the plasma temperature falls at the end of a working cycle. To cool the plasma a part of the energy stored in it must, by one mechanism or another, be transferred to the walls. It is this amount of energy which constitutes the thermal losses. It is assumed here that the greater part of the thermal energy stored in the plasma will be directly transformed into electrical energy.

By considerations analogous to those used to derive formula (*1.14*), it is easy to establish that in the case being considered the expression for the efficiency is†

$$R = \frac{\tau_1 \alpha n \overline{\sigma v} W_n \times 1{\cdot}6 \times 10^{-6}}{3kT(1-\eta)+\frac{2}{3}n\tau_1 f_{\mathrm{rad}}(T)}, \qquad \text{.........}(1.18)$$

where $\eta$ is the efficiency of conversion of plasma thermal energy into electric energy. Dividing the numerator and denominator in equation (*1.18*) by $\tau_1$ we obtain an expression for $R$ which differs from (*1.14*) in one respect only, viz: the term expressing thermal losses is $\frac{2}{3}\,\tau_1/(1-\eta)$ instead of $\tau_p$.

Corresponding changes occur in conditions (*1.16a*) and (*1.16b*). If thermal losses occur only because of the incomplete transformation of the plasma energy into electric energy then it is required that $H^2\tau_1$ should exceed $5 \times 10^9(1-\eta)$ Oe$^2$ sec for a power-producing reactor operating on pure deuterium, and $6 \times 10^7(1-\eta)$ Oe$^2$ sec for one operating on a mixture of deuterium and tritium (for the case when $p = H^2/8\pi$).

We shall now examine the question of transforming thermonuclear energy into electrical energy. We have already touched on the fact that the energy released in fusion reactions consists of two portions which make different contributions to the operation of a thermonuclear reactor. That portion of the energy which is carried off by neutrons exerts no direct influence on the processes taking place in the plasma, and can be utilised with an efficiency of about $\frac{1}{3}$. The second portion of the energy arising from nuclear fusion (that associated with the charged reaction products) is deposited directly in the plasma. This portion of the energy compensates directly for losses, and raises the temperature of the nuclear fuel. This portion of the nuclear energy can, in principle, be turned into electrical energy with an efficiency $\eta$ close to unity.

---

† It is assumed that during the time $\tau_1$ the plasma temperature $T$ is constant.

So efficient a conversion is possible because, when we use magnetic thermo-insulation, the high-temperature nuclear fuel is surrounded on all sides by a powerful magnetic field which serves as an elastic envelope compressing the plasma. If the plasma, heated to a high temperature, expands against the magnetic pressure, then its thermal energy will be transformed into electromagnetic energy. This process is entirely analogous to the expansion of gas against a moving piston.

We shall not analyse the actual methods for further transforming the energy passed on to the magnetic field by an expanding plasma, because what concerns us here is only the value of the coefficient $\eta$. If the highest temperature of the plasma, at the onset of expansion, is $T_1$, and if $T_2$ is the lowest temperature to which the plasma cools at the end of each cycle, then the maximum value of $\eta$ is given by the familiar formula:

$$\eta = 1 - T_2/T_1.$$

It follows from this that in theory it is possible to make $\eta$ very close to unity, because the upper temperature in the thermal cycle of the reactor is very high, and the ratio $T_2/T_1$ can thus be made quite small. However, a big reversible temperature drop during expansion can be achieved only by a large increase of the plasma volume.

In the most favourable case, when the expansion proceeds adiabatically, the temperature changes in inverse proportion to $\Omega^{\frac{2}{3}}$, where $\Omega$ is the volume occupied by the plasma. Therefore, in order to convert 90% of the total thermal energy of the plasma into electrical energy, it is necessary to increase the plasma volume approximately 30 times. This means that during the time when the plasma is at its highest temperature and is a source of thermonuclear energy, it occupies only a very small part of the vacuum chamber of the thermonuclear reactor, the rest of the vacuum chamber being filled by a strong magnetic field. This difficulty can be avoided to a certain extent by expanding the plasma along the lines of force from a region which has small volume but a powerful field into a region having large volume and a weaker field. Even so, it may well be found impracticable to raise $\eta$ much above $\frac{1}{2}$.

The above considerations provide the basis for a sufficiently clear answer to the question, what advantages are gained by transforming the thermal energy of the plasma directly into electrical energy.

By our original estimate the electrical energy from *d-d* reactions should amount to about 9 MeV per *d-d* reaction. For *d-t* reactions the corresponding figure is approximately 10 MeV. These figures have been

PLATE I

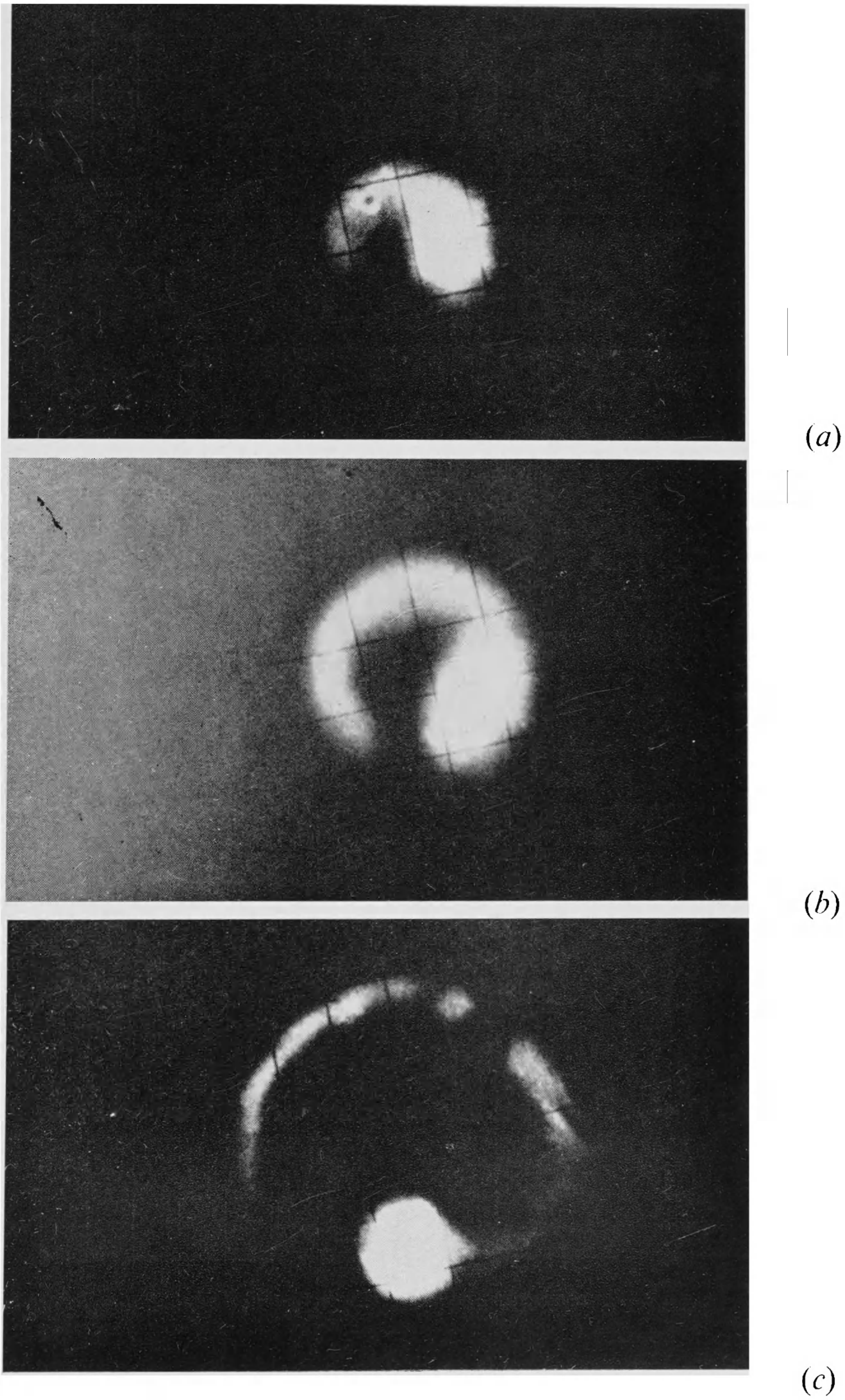

The formation of plasma protuberances in Zharinov's experiments. The magnetic field is perpendicular to the plane of the figure.

obtained on the assumption that the energy of the charged reaction products is utilised fully and the energy of the neutrons only 30%.

If we now reject these assumptions and assume instead that the total energy released by the nuclear reactions is transferred to a heat-exchange medium and is then used in an ordinary heat engine with an efficiency of 0·3, then the electrical energy is reduced by 2·6 MeV, that is by 28% of its previous value for the *d-d* reaction and, for the *d-t* reaction by 2·5 MeV, that is by 24%. In practice, the effect on the overall energy efficiency must be even less, because direct conversion of plasma energy cannot be complete. It thus turns out that the amount of useful energy produced by a thermonuclear reactor need not be strongly dependent on whether or not the thermal energy of the plasma is directly transformed into electric energy.

However, in certain conditions the direct transformation of heat into electrical energy could be very significant for the operation of a thermonuclear generator because it could change such a generator from an energy-absorbing system into an energy-producing one. This would occur in a case where $H^2\tau_1$ was approaching the critical value at which thermal losses were balanced by the generation of thermonuclear energy. This critical value is proportional to $1-\eta$, where $\eta$ is the conversion efficiency of the plasma thermal energy. A change in the value of $\eta$ from 0·3–0·33 to 0·75–0·8, consequent upon a change in the method of utilising the total thermal energy in the plasma, reduces the critical value $H^2\tau_1$ by at least a factor of two; and this could carry the generator over into working conditions in which surplus energy is produced.

Summing up, one can say that the direct transformation of the heat generated in the plasma into electrical energy is important, not because it makes possible any large increase in the energy released by the thermonuclear reactions, but because it can lead to a considerable reduction in the unconvertible thermal losses. In addition, direct conversion of the plasma thermal energy alleviates the thermal stress on the system by reducing the heat load on the walls of the chamber containing the plasma.

At the present time, the study of controlled thermonuclear reactions is based on the assumption that the fuel must be either deuterium or a mixture of deuterium and tritium. Which of these two types of nuclear fuel is the more promising?

The chief and obvious advantage of the *d-t* fuel is the high value of the reaction cross-section. As has been said above, the reaction rate in a 50% *d-t* mixture is 50–100 times greater than the reaction rate in pure deuterium over the entire temperature range likely to be of practical value.

As against this, it might perhaps be objected that tritium is an extremely expensive nuclear fuel, and that the gain from using tritium in a thermonuclear reactor could not compensate for the energy expended by producing it in ordinary nuclear reactors. This objection is, however, groundless. Every *d-t* reaction produces a 14·1 MeV neutron which leaves the plasma. If the reaction chamber is surrounded by a sufficiently thick layer of a substance in which (*n*, 2*n*) reactions take place, it will be possible to increase the initial neutron flux considerably.

To multiply neutrons by (*n*, 2*n*) reactions either beryllium or some heavy element such as lead or bismuth can be used. Given a neutron energy of 14·1 MeV, the cross-section of the (*n*, 2*n*) reaction in these substances exceeds that of all other competing nuclear processes put together. In the case of beryllium $\sigma(n, 2n)$ is $2\times 10^{-24}$ cm$^2$; in the case of lead and bismuth it is $2{\cdot}4\times 10^{-24}$ cm$^2$. If the reaction chamber is surrounded by a blanket of any of these substances, the number of neutrons can be increased at least 1·5–2·0 times. This increased neutron flux can be used to enhance the breeding of tritium by moderating and then absorbing the neutrons in the light isotope of lithium. In lithium the slow-neutron reaction is

$$^6\mathrm{Li}+n \rightarrow t+{}^4\mathrm{He},$$

the cross-section of which is very great. Analysis of experimental results for (*n*, 2*n*) reactions and for the tritium-forming reaction shows that, even with the most conservative assumptions (making allowance for possible reductions in the neutron flux due to other nuclear processes), the coefficient for tritium breeding in a single operating cycle of a thermonuclear reactor can easily be raised to a value exceeding unity. Moreover, this coefficient is the multiplier in the geometrical progression determining the growth of the total quantity of tritium arising from successive repetitions of the reactor's working cycle.

Thus with a *d*-*t* mixture it is possible to ensure that the tritium stock will constantly increase as the reactor operates. Therefore until there is a danger of exhausting all accessible stocks of $^6$Li by utilizing them to regenerate tritium, thermonuclear reactors will operate mainly on a *d*-*t* mixture, even though the associated technological process will be more complicated than for operation with pure deuterium.

Even if, for some reason, it becomes necessary to work with pure deuterium fuel, most of the nuclear energy will nevertheless be yielded by consuming the tritium formed in the *d*-*d* reactions.

§ **1.3** At the present time, research on controlled thermonuclear reactions is at a stage when various approaches to the problem are being tried out. Not one of these has been investigated so thoroughly that a convincing claim of ultimate success can be made for it. Seemingly, all that can be regarded as universally accepted is the conviction that the solution of the problem must lie in finding the right method of magnetic thermo-insulation. To simplify analysis that will follow later, it is useful to give a general classification of the methods of using magnetic fields to isolate and heat the plasma.

These methods can be divided into two main groups:

(1) methods based on equilibrium conditions, i.e. states in which the plasma pressure is balanced by the magnetic pressure;

(2) pulsed methods, in which acceleration of the plasma by electrodynamic forces is used both for confining and for heating the plasma. In this case, the processes in the plasma are not in equilibrium and take place over very short intervals of time.

The difference between these two groups of methods takes a precise form if we express it in the language of magnetohydrodynamics. As we know, magnetohydrodynamics is concerned with the behaviour of conducting fluids in electromagnetic fields. Looked at macroscopically, a plasma can be considered as a conducting fluid. The conditions under which this approximation is justified will be examined in Chapter IV; here we shall simply assume that these conditions have been fulfilled.

In this approximation the basic equation characterising the motion of plasma under the action of electrodynamic forces can be written in the following form:

$$\rho \frac{d\boldsymbol{v}}{dt} = \boldsymbol{F}_{\mathrm{M}} - \operatorname{grad} p \qquad \text{.........}(1.19)$$

where $\boldsymbol{v}$ and $\rho$ designate respectively the velocity and the mass density of an elementary volume of plasma which is being displaced under the action of an electrodynamic force $\boldsymbol{F}_{\mathrm{M}}$ and of a pressure gradient. All the terms of equation (*1.19*) are related to a unit of plasma volume, and therefore $\boldsymbol{F}_{\mathrm{M}}$ is the electrodynamic force acting per unit volume on the plasma. From a macroscopic point of view the force $\boldsymbol{F}_{\mathrm{M}}$ arises from interaction between the magnetic field and the electric currents flowing in the plasma. If there were no currents, the plasma would not be affected by the magnetic field. If the field strength is $\boldsymbol{H}$ and the current density is $\boldsymbol{j}$, then the force with which the field acts on a unit of volume of plasma is

$$\boldsymbol{F}_{\mathrm{M}} = \frac{1}{c} \boldsymbol{j} \times \boldsymbol{H}.$$

It should be noted that this force is zero not only when $\boldsymbol{j} = 0$ but also if the current in the plasma is parallel to the magnetic field.

Thus the basic equation of motion for a plasma in a magnetic field becomes:

$$\rho \frac{d\boldsymbol{v}}{dt} = \frac{1}{c} \boldsymbol{j} \times \boldsymbol{H} - \operatorname{grad} p, \qquad \text{.........}(1.20)$$

where $c$ is the velocity of light. A glance at this equation is all that is needed to distinguish the two extreme cases mentioned above.

If the gas-kinetic pressure is small, the second term on the right-hand side of equation (*1.20*) can be neglected and the electrodynamic forces will be balanced by the 'inertial forces':

$$\rho \frac{d\boldsymbol{v}}{dt} = \frac{1}{c} \boldsymbol{j} \times \boldsymbol{H}. \qquad \text{.........}(1.21)$$

Under these conditions the plasma as a whole will acquire a directed velocity whose magnitude can be considerably greater than the random thermal speed of the ions. The kinetic energy of directed motion can in principle be used for the subsequent heating-up of the plasma. This occurs in shock wave processes, or when a moving plasma blob strikes a target, or the like. In such circumstances, the process is characterised by a comparatively short time-scale, justifying the use of the expression 'non-stationary case'. The duration of the acceleration process must be about $a/v$ where $a$ is the distance over which the plasma is displaced and $v$ is the directed velocity. If we take $a = 10^2$ cm (a relatively large apparatus) and take $v$ as equal to $10^8$ cm/sec, which corresponds to a deuteron kinetic energy of about $10^4$ eV, then the acceleration time-scale will be of the order of $10^{-6}$ sec. It is clear that such conditions will be of interest in practice only if they can be used as the first phase of the plasma heating process. This phase has to end with the transformation of the accumulated kinetic energy into heat, that is, by a change to a quasi-stationary state in which the rapid mass motions of the accelerating phase must be dissipated in a very short space of time. Anticipating what will be said in a more detailed analysis of pulsed methods of heating, we note that the main difficulty of this method lies precisely in bringing about a controlled transition from the accelerating phase to the quasi-stationary phase.

The opposite limiting case occurs when the acceleration of the plasma is small so that the 'inertial term' on the left-hand side of the equation can be neglected by comparison with the pressure gradient. In this case the gas-kinetic pressure and the magnetic pressure always balance one another, viz:

$$\operatorname{grad} p = \frac{1}{c} j \times \boldsymbol{H}. \qquad \text{.........}(1.22)$$

Equation (*1.11*) is a particular ideal case of this relationship, corresponding to infinite plasma conductivity (current flowing only on the plasma surface). It will be necessary to take account of the forces of inertia in equilibrium plasma configurations of this type only at a subsequent stage of analysis, when we investigate stability in relation to various perturbations of the equilibrium configuration.

Among the various routes that may be attempted towards obtaining hot plasma in equilibrium conditions, the following main ones are indicated pretty clearly at the present time:

(1) development of methods of heating plasma in systems with a toroidal plasma current and an externally generated magnetic field to stabilise it;

(2) investigation of systems in which high-temperature plasma is accumulated in magnetic traps by injecting either fast particles or plasma blobs into the trap from outside.

There are wide possibilities, some of them already tried out, for combining both these approaches in various ways. To give a rough idea of the distinguishing marks of thermonuclear systems based on the general principles described we can use a homely comparison. A system of the first type is a kettle inside which plasma is made and heated, whereas a trap with injection from outside is a thermos flask to be filled with fast particles.

From the discussion in this section, we can provide the following preliminary classification of systems for obtaining high-temperature plasmas:

1. systems in which the plasma is accelerated by a magnetic field (pulsed processes);
2. quasi-stationary systems with a ring-shaped plasma carrying a large current;
3. magnetic traps with injection of either particles or plasma;
4. systems based on a combination of different principles.

This extremely imperfect classification is given here with one aim alone: to make it easier in subsequent pages to understand the properties of practical systems used to investigate the possibility of producing thermonuclear reactions.

## CHAPTER II

# THE MOTION OF PARTICLES IN PLASMAS

§ **2.1** The basic knowledge of plasma physics necessary to understand the phenomena expected in a thermonuclear reactor is expounded in this and the following chapters. From a practical point of view, the behaviour of a fully ionised plasma in a strong magnetic field is of the most interest. We shall begin by analysing the motion of the charged particles in a plasma.

For a plasma in a magnetic field, the nature of the particle motion depends first and foremost on the ratio of the collision mean-free-path $\lambda$ to the radius of gyration of the trajectory, $\rho_{\mathrm{H}}$. If $\lambda/\rho_{\mathrm{H}} \ll 1$ (weak magnetic field, dense plasma), then the action of the field is too weak to deflect the particle significantly between successive collisions, and the particle trajectories can be simply represented by successive short straight lines. This means that in this limit the magnetic field does not have any significant influence on any of the main plasma processes.

In the opposite limit, when $\lambda/\rho_{\mathrm{H}} \gg 1$ (strong field, rarefied plasma), a particle on the average makes many turns along a helical trajectory between successive collisions; the field has a strong effect on the particle motions, and in particular it greatly limits displacements of the particles in the direction perpendicular to $\boldsymbol{H}$. Consequently, the character of a number of basic processes taking place in the plasma undergoes considerable alteration.

For given values of $n$ and $H$, the higher the plasma temperature, the greater is the ratio $\lambda/\rho_{\mathrm{H}}$; as will be shown below, this ratio increases as $T^{\frac{3}{2}}$. For values of $n$, $T$ and $H$ which are of practical significance for envisaged thermonuclear reactors, the condition $\lambda/\rho_{\mathrm{H}} \gg 1$ is generally satisfied, both by the electrons and by the ions. For example, if $n = 10^{14}$ cm$^{-3}$, $T = 10^8$ °K, and $H = 10^4$ Oe, which are values probably not very different from those needed in future thermonuclear reactors, the ratio $\lambda/\rho_{\mathrm{H}}$ is about $5 \times 10^5$ for the ions, and about $3 \times 10^7$ for the electrons.

The circumstances in which a magnetic field strongly influences the motion of particles in a plasma can also be expressed in a somewhat different form if we introduce $\omega_{\mathrm{H}}$ the angular frequency of rotation of particles in a magnetic field and $\tau$ the mean time between successive collisions. It is obvious that

$$\lambda/\rho_{\mathrm{H}} = \frac{\lambda/v}{\rho_{\mathrm{H}}/v} \simeq \omega_{\mathrm{H}}\tau,$$

consequently the inequality $\lambda/\rho_{\mathrm{H}} \gg 1$ is equivalent to $\omega_{\mathrm{H}}\tau \gg 1$.

We now consider the main laws governing the motion of single charged particles in magnetic fields. In most cases of practical importance for our problem, the radius of gyration of the trajectory of a particle in the magnetic field is small in comparison with distances over which the vector ***H*** changes significantly. This means that to a first approximation the field may be regarded as constant throughout one revolution. This considerably simplifies the analysis of the particle motion because it becomes possible to use an approximate theory to investigate trajectories. The basic conclusions of this theory can be deduced from some very simple considerations whose clarity redeems their lack of strict accuracy.

We take first the case where ***H*** is constant in time and where there is no electric field. A charged particle in a uniform magnetic field moves along a helical trajectory whose axis is one of the magnetic lines of force. The radius of the helix (the Larmor radius) is equal to

$$\rho_{\mathrm{H}} = \frac{pc}{qH}\sin\alpha. \qquad \text{.........}(2.1)$$

Here $p$ is the momentum of the particle, $q$ is its charge and $\alpha$ is the angle between the velocity vector and the magnetic field. The angular frequency of revolution (the cyclotron frequency) of the particle is independent of $p$, and is given by

$$\omega_{\mathrm{H}} = \frac{qH}{mc} \qquad \text{.........}(2.2)$$

where $m$ is the mass of the particle.

Let us now suppose that the field strength changes slowly along a line of force, so that the field changes significantly only over a distance many times greater than the Larmor radius. Therefore, short lengths of the trajectory will continue to appear as a helix of constant radius and pitch. However, when we consider long sections of the trajectory in a varying field, there is an important change in the values of the parameters characterising the particle motion. It is not only the radius of the helical path that changes, but also the angle $\alpha$; i.e. there is a change in the ratio of the components of the velocity parallel and perpendicular to ***H***. This happens because, when the field strength varies along the direction of ***H***, the lines of force are no longer parallel; instead they form a converging or diverging bundle. A force then appears which acts on the particle in the direction of the magnetic lines of force. If the particle moves in the direction of increasing $H$ this force retards the parallel motion; in the opposite case, the parallel motion is accelerated. Essentially, this is the same force which makes it possible to focus particles in accelerators and prevents them from escaping along the lines of force.

The origin of this parallel component of the magnetic force is indicated in Fig. 8. It arises from a magnetic field component $H_{\perp}$ which is perpendicular to the axial line of motion. This component of ***H*** is directed along the radius of the Larmor orbit. It acts on the transverse (azimuthal) component of the particle velocity and produces a $\boldsymbol{v}\times\boldsymbol{H}$ force directed towards the region of smaller $H$.

To derive the variations of the geometrical parameters of the helical trajectory in a non-uniform field, we note that particle motion can be considered not only in the laboratory system of coordinates but also, with equal validity, in a coordinate system where the instantaneous value of the parallel velocity component is equal to zero. In this coordinate system, the

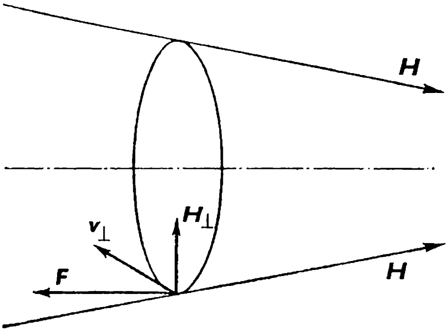

FIG. 8. Origin of the force slowing down the parallel motion of a particle in a non-uniform magnetic field

rotational motion normal to the field is preserved, but the field moves along the axial line with velocity $u$, and passes through the circular trajectory of the particles. In this moving coordinate system the magnetic field, because it is non-uniform, changes with time. Therefore it creates a solenoidal electric field in the plane of the orbit, which either accelerates or decelerates the rotation of the particle. To be specific, let us suppose that a positively charged particle is moving along a line of force towards a region of higher field strength. Then, in the above moving coordinate system, the solenoidal electric field $\boldsymbol{E}$ is in the same direction as that of the particle rotation. In one revolution of the particle, the field $\boldsymbol{E}$ will do work

$$\Delta W_\perp = 2\pi\rho_H qE.$$

But

$$2\pi\rho_H E = \pi\rho_H^2 \frac{1}{c}\frac{dH}{dt};$$

therefore

$$\Delta W_\perp = \frac{\pi\rho_H^2 q}{c}\frac{dH}{dt}. \qquad \text{.........(2.3)}$$

Because the field strength changes only insignificantly during one revolution, $dH/dt$ can be replaced by $\Delta H/t_H$ where $\Delta H$ is the increase of field strength during the period of revolution $t_H$. Consequently

$$\Delta W_\perp = \frac{\pi\rho_H^2 q}{ct_H}\Delta H. \qquad \text{.........(2.4)}$$

The energy of the transverse motion is related to the Larmor radius by

$$W_\perp = q^2\rho_{\mathrm{H}}^2H^2/2mc^2. \qquad \text{.........}(2.5)$$

Substituting the expression

$$t_{\mathrm{H}} = 2\pi mc/qH \qquad \text{.........}(2.6)$$

in equations (*2.4*) and (*2.5*), we obtain:

$$\Delta W_\perp/\Delta H = W_\perp/H. \qquad \text{.........}(2.7)$$

Consequently, in a slowly varying magnetic field, the ratio of the kinetic energy $W_\perp$ of the rotational motion to the strength of the magnetic field $H$, is a constant.

This means that the quantity $W_\perp/H$ is an adiabatic invariant. Because $W_\perp/H$ is constant, the angular momentum of the particles must also be constant, because it differs from $W_\perp/H$ only by a constant coefficient. By (*2.5*), $\rho_{\mathrm{H}}^2H$ is also a constant of the motion. Consequently the Larmor radius varies as $H^{-\frac{1}{2}}$.

These results may be differently interpreted if we consider the particle moving in a Larmor orbit as an elementary diamagnetic unit. It can be seen that the magnetic moment generated by the rotating charged particle is numerically equal to $W_\perp/H$. The force arising from the interaction of a magnetic moment $\mu$ with a field gradient along the lines of force, is:

$$F = -\mu\frac{\partial H}{\partial l} \qquad \text{.........}(2.8)$$

where the derivative is taken along the direction of ***H***. The equation of motion for the parallel component of velocity $v_\parallel$ of an elementary diamagnet is thus:

$$m\frac{dv_\parallel}{dt} = -\mu\frac{\partial H}{\partial l} = -\frac{W_\perp}{H}\frac{\partial H}{\partial l}.$$

Multiplying both sides of this equation by $v_\parallel$ we obtain:

$$\frac{dW_\parallel}{dt} = -\frac{W_\perp}{H}\frac{\partial H}{\partial l}v_\parallel = -\frac{W_\perp}{H}\frac{dH}{dt}$$

($W_\parallel$ is the kinetic energy of parallel motion).

The total energy is conserved, and so

$$\frac{dW_\parallel}{dt} = -\frac{dW_\perp}{dt}.$$

Consequently

$$\frac{dW_\perp}{dt} = \frac{W_\perp}{H}\frac{dH}{dt},$$

that is

$$\frac{W_\perp}{H} = \text{const.}$$

Thus the adiabatic invariance of $W_\perp/H$ is also demonstrated by considering the interaction as being between a small diamagnetic current loop and the non-uniform field.

Let us now consider the motion parallel to the magnetic field. Because the total kinetic energy of a particle is constant in a static magnetic field, any change in $W_\perp$ must lead to a corresponding change in the kinetic energy $W_\parallel$ associated with the parallel motion. Let us suppose that a particle is initially at a point where the magnetic field strength is $H_0$, and is moving at an angle $\alpha_0$ to the magnetic field. Initially, the ratio of the transverse energy to the field strength is

$$(W_0 \sin^2 \alpha_0)/H_0,$$

where $W_0$ is the total kinetic energy of the particle.

Because this ratio is a constant of the motion, the angle $\alpha$ between the direction of motion and $\boldsymbol{H}$ is given at any other point on the particle trajectory by

$$\sin \alpha = \sqrt{H/H_0} \sin \alpha_0. \qquad \text{.........}(2.9)$$

When the particle moves in the direction of increasing $H$, $\alpha$ increases; and when the particle reaches a point where $H$ equals $H_0/\sin^2 \alpha_0$, this angle becomes $\pi/2$. Consequently, the parallel component of velocity becomes zero at this point, and the particle starts to move in the opposite direction. One can say that a field which increases as one moves along the lines of force acts as a magnetic mirror which reflects the particles that fall on it.

The first distinguishing feature of a mirror of this type is that the point at which the reflection takes place does not depend on the total energy of the particle; a second is that the particles reflected are only those whose velocities are initially inclined to the magnetic field at an angle greater than a certain minimum size. If a stream of particles is directed from a region where the magnetic field strength is $H_0$ into a region where the maximum value of the field is $H_m$, then the only particles which pass through this mirror are those whose initial angle of inclination $\alpha_0$ lies within the loss cone defined by the condition

$$\sin \alpha_0 \leqq \sqrt{H_0/H_m}. \qquad \text{.........}(2.10)$$

The particles with larger initial angle of inclination will be reflected back; and the larger the initial angle is, the sooner will reflection take place.

§ **2.2** So far we have restricted the discussion to cases where the field strength changes in the direction of the lines of force. However, the field strength can also change in a direction perpendicular to $\boldsymbol{H}$. An example is the field generated by a straight current-carrying conductor. Here the lines of force run parallel to one another, and the field strength varies inversely as the distance from the conductor.

To elucidate the motion of particles in such fields, we will consider the simple case of motion in a plane. Let a particle move in the $xy$ plane under the action of a field which is directed along the $z$ axis. Let us suppose that the field strength increases in the direction of $x$. The particle trajectory in the $xy$ plane cannot be circular because the radius of curvature on the right (that is, where $H$ is greater) is less than the radius of curvature on the left (Fig. 9). It is clear that the trajectory cannot be a closed line: with every revolution that it makes, the particle moves along the $y$ axis (that is, normal to the gradient of $H$). Thus the trajectory is a series of successive unclosed loops lying within a narrow strip parallel to the $y$ axis. The particles move in the positive or negative direction of $y$, depending on the sign of their charge. If this directed motion—which is usually called 'drift motion'—is small compared with the total velocity, the particle motion can be regarded as being compounded from two simple motions: circular motion around a guiding centre; and a steady displacement of the guiding centre. The second of these is the drift velocity in a non-uniform magnetic field.

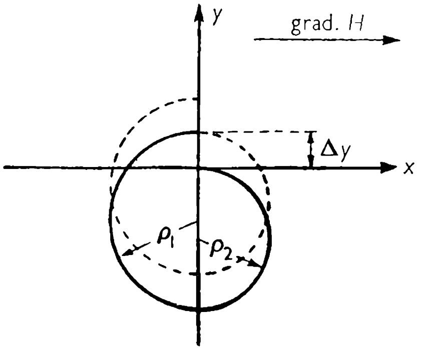

FIG. 9

Drift of a particle in a non-uniform magnetic field

To determine the magnitude of this drift velocity, we consider the trajectory shown in Fig. 9. If the displacement after one revolution is small compared with the mean radius of the trajectory, then this displacement can be taken as equal to $2(\rho_1-\rho_2)$, where $\rho_1$ and $\rho_2$ are respectively the mean radii of curvature for the left- and right-hand halves of the loop (each half can be considered as approximately semi-circular). If the field varies only slightly over the loop, the difference between $\rho_1$ and $\rho_2$ is

$$\frac{d\rho_H}{dH}(H_1-H_2),$$

where $H_1$ and $H_2$ are average values of the field strength for the left-hand and right-hand halves of the loop. As an approximate estimate, the difference between $H_1$ and $H_2$ can be taken as $-\rho_H(dH/dx)$.

The following expression for the displacement $\Delta y$ (see Fig. 9) is then obtained:

$$\Delta y = -2\rho_H\frac{d\rho_H}{dH}\frac{dH}{dx};$$

so that the drift velocity is given by

$$v_\mathrm{d} = \frac{\Delta y}{t_\mathrm{H}} = -\frac{2\rho_\mathrm{H}}{t_\mathrm{H}}\frac{d\rho_\mathrm{H}}{dH}\frac{dH}{dx}. \qquad \text{.........}(2.11)$$

Since $\rho_\mathrm{H}$ is inversely proportional to $H$

$$(d\rho_\mathrm{H}/dH) = -\rho_\mathrm{H}/H.$$

Using this relationship together with equations (*2.5*) and (*2.6*), equation (*2.11*) becomes:

$$v_\mathrm{d} = \frac{mcv_\perp^2}{\pi qH^2}\frac{dH}{dx}. \qquad \text{.........}(2.12)$$

Here $v_\perp$ is the component of the particle velocity in the plane perpendicular to $\boldsymbol{H}$.† The direction of $\boldsymbol{v}_\mathrm{d}$ is that of $\boldsymbol{H}\times\operatorname{grad} H$.

Of course it cannot be expected that such a very rough calculation will give the correct numerical value of the coefficient in the formula for $v_\mathrm{d}$. A precise value can be obtained by means of a somewhat long calculation which we shall not give here. The correct coefficient turns out to be $\frac{1}{2}$ instead of $1/\pi$ given in equation (*2.12*).

The expression for the drift velocity in vector form is

$$\boldsymbol{v}_\mathrm{d} = \frac{mcv_\perp^2}{2qH^2}\boldsymbol{h}_1\times\operatorname{grad} H \qquad \text{.........}(2.13)$$

where $\boldsymbol{h}_1$ is the unit vector in the direction of $\boldsymbol{H}$.

The ratio of the drift velocity $v_\mathrm{d}$ to the speed of the particle $v_\perp$ is

$$\frac{v_\mathrm{d}}{v_\perp} \approx \frac{1}{2}\frac{\rho_\mathrm{H}}{H}\frac{dH}{dx};$$

and it is of the same order of magnitude as the relative change in field strength over a distance of one Larmor radius. All the above calculations depend on this quantity being small.

It is a basic property of drift perpendicular to the lines of force in a non-uniform field that the field strength is constant along the drift path of the particle. The fact that $H$ remains unchanged means that the ratio $W_\perp/H$ also remains constant throughout the drift.

In examining drift phenomenon, we have so far confined ourselves to the case when both the velocity and grad $H$ are perpendicular to $\boldsymbol{H}$. In the general case, it can be shown that the drift velocity depends not only on the transverse velocity component $v_\perp$ but also on the parallel component $v_\parallel$. In the case of a particle whose trajectory never intersects any flow of current,‡ the drift velocity is given, in the general case, by the formula

---

† In the case we are considering of motion in a plane, it coincides with the total velocity.

‡ This means that in the region where particle motion can occur curl $\boldsymbol{H} = 0$.

$$\boldsymbol{v}_{\mathrm{d}} = \frac{mc(v_{\perp}^2+2v_{\parallel}^2)}{2qH^2}\boldsymbol{h}_1\times \operatorname{grad} H, \qquad \text{.........}(2.14)$$

which is valid for any ratio of $v_{\perp}$ to $v_{\parallel}$.

$\boldsymbol{v}_{\mathrm{d}}$ can also be related to the curvature of the lines of force. If $R$ is the radius of curvature, equation (*2.14*) becomes:

$$v_{\mathrm{d}} = (2v_{\parallel}^2+v_{\perp}^2)/2\omega_{\mathrm{H}}R. \qquad \text{.........}(2.15)$$

$\boldsymbol{v}_{\mathrm{d}}$ is perpendicular to both $\boldsymbol{H}$ and $\boldsymbol{R}$; that is, it is directed along the binormal to the line of force.

This study of particular cases of particle motion in magnetic fields lends support to the assumption that even in the general case of motion in a field of arbitrary form, the quantity $W_{\perp}/H$ is invariant; that is, it will remain constant for a given particle over the whole length of its trajectory. This assumption follows from the fact that $W_{\perp}/H$ is conserved both when a particle moves along the lines of force in a field gradient directed parallel to $\boldsymbol{H}$ and also when drift movement is caused by a field gradient directed normal to $\boldsymbol{H}$.

A detailed theoretical analysis does indeed show that $W_{\perp}/H$ is an adiabatic invariant of motion in the general case; that is, it is constant provided only that the relative changes in the field are small over distances of the order of the Larmor radius.

The analysis of the individual cases considered above enables us to form a clear picture of the motion of a particle in a non-uniform field of any form. When we examine a particular section of a particle trajectory, we can always break down its motion into the following three constituents:

1. circular Larmor motion around the line of force;
2. movement of the centre of the Larmor circle (guiding centre) along the lines of force;
3. drift of the guiding centre in a direction perpendicular both to $\boldsymbol{H}$ and the gradient of $H$.

The locus of the guiding centre forms the axis of the helical trajectory of the particle. The form of this axis is the main geometric characteristic of particle motion in a strong magnetic field. The axis can be regarded as a mean of the particle trajectory. In the general case, movement of the particle along the axis is made up of motion parallel to $\boldsymbol{H}$ and of drift in a direction perpendicular to $\boldsymbol{H}$.

As the field strength increases, the drift velocity decreases and the axis of the trajectory diverges less and less from the line of force on which the particle was initially located. In the limit where the field strength is infinite, the trajectory of a particle will be represented by a helical line with infinitely small radius and infinitely small pitch length, disposed along one of the lines of force.

However, if we are considering the motion of a particle which is confined within a limited region of space then, even with very large field strength, the drift motion cannot be neglected. Over a sufficiently long time interval a particle can, as a result of drift, move very far from the line of force on which it was originally located.

In a non-uniform field there are always regions of space with high field strengths which are inaccessible to those particles which have a large angle of inclination $\alpha$ in regions of relatively small $H$. As such a particle approaches a high field region, the motion parallel to the line of force is retarded, and the particle is either reflected back or drifts around the inaccessible region.

Figure 10 shows schematically the locus of the guiding centre of a particle moving in an axially symmetric field whose strength increases on both sides of a central region where $H$ is minimum. In such a field, a particle moving at a sufficiently large angle of inclination to the lines of force is trapped within a limited region of space between the 'magnetic plugs' (or 'magnetic mirrors'). In the region of the magnetic mirrors, where the field is non-uniform, a particle undergoes drift in the azimuthal direction. Therefore the form of the guiding centre locus is to some extent reminiscent of a squirrel cage. Such a system is a typical example of a magnetic trap for charged particles, based on the principle of adiabatic invariance. In 1953 it was proposed by Budker as the basis of a thermonuclear reactor.

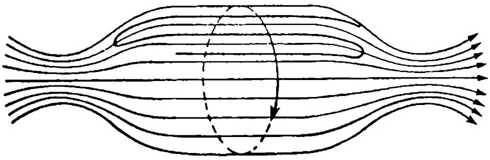

FIG. 10. Locus of the guiding centre of a particle moving in a magnetic mirror trap

In nature, the outer magnetic field of the earth serves as a grandiose trap for charged particles of cosmic origin. The lines of force bunch together near the earth's magnetic poles, and these regions act as magnetic mirrors. Measurements made by artificial earth satellites and by space rockets have shown that charged particles, formed in the space around the earth by various nuclear processes, are efficiently captured by this geomagnetic trap.

The approximate theory, outlined above, of the motion of charged particles in a non-uniform magnetic field very greatly simplifies the analysis of trajectories in fields of complex form. However, if we are to use the results of this theory with complete confidence—particularly for the motion of particles in magnetic traps—it will be necessary further to refine the principle of adiabatic invariance. This refinement will have to include a discussion of the conditions in which this principle can be applied to problems involving the motion of particles in a restricted region. When the region within which a particle can move is determined by the condition that the value of $W_\perp/H$ must be conserved, the motion has an oscillatory character. In some conditions, a gradual amplification of these oscillations can take place, and this can lead to a breakdown of adiabatic invariance and to particles leaving the magnetic system. Since we are concerned with systems where particles have to remain for a period in which an extremely large number of oscillations will take place, the conditions for applicability of the principle of adiabatic invariance are very important and must be a subject of special study.

The question of how long adiabatic invariance can be preserved in a magnetic mirror trap was the subject of an outstanding series of experiments by Rodionov. The idea underlying this work, which was suggested by Budker, is that in a magnetic trap filled with tritium, measurements of the confinement time can be made on the $\beta$-particles formed by radioactive decay. If a $\beta$-particle is emitted in the region between the magnetic mirrors, it can escape from the magnetic trap either because its velocity vector is scattered into the loss cone by collisions with gas atoms, or because $W_\perp/H$ changes significantly as a result of a slow accumulation of small changes (that is to say, by the breakdown of adiabatic invariance). Let us suppose that the latter cause does not arise; that is to say, we assume that the $\beta$-particle when moving in a vacuum will never be able to leave the trap. In this case the confinement time $\tau$ of a particle in a real system will be determined by the probability of collisions with gas atoms, and $\tau$ must therefore be inversely proportional to the gas pressure in the trap. In these circumstances the equilibrium number density of $\beta$-particles in a trap filled solely with tritium is independent of the tritium pressure, as shown by the following simple argument. When equilibrium is established, the number density $n_\beta$ of $\beta$-particles must equal the number of tritium $\beta$-disintegrations per unit time per unit volume, multiplied by the mean confinement time $\tau$. But the first of these quantities is proportional to the pressure of the tritium $p_t$, and the second is inversely proportional to this pressure; therefore, although $p_t$ may change, the equilibrium value of $n_\beta$ must remain constant, even down to the very small values of $p_t$ where one may expect to detect limitations of the confinement due to other processes.

Direct measurement of $n_\beta$ is difficult, and experimentally it is very much easier to determine the number of ions formed by the $\beta$-particles in the trap during a unit of time. This number is proportional to the product $n_\beta p_t$. Given that $n_\beta$ is independent of the pressure, the number of ion pairs formed per second must be proportional to $p_t$. Figure 11 shows the experimental apparatus of Rodionov. A degassed glass vessel $C$ in which a high vacuum has been produced is filled with tritium; the pressure is measured by the ionisation manometer $M$. A magnetic field is created by the iron-cored electromagnet $K_1$ and two additional coils $K_2$. The ratio of the field strength in the magnetic mirrors to the field strength in the centre of the chamber can be varied over a wide range. The ionisation produced by the $\beta$-particles in the gas is measured with aluminium electrodes placed on the inside surface of the chamber. A low voltage is applied between them, which ensures that all the slow ions and electrons are collected. When the number of ion pairs produced at a given tritium pressure is known, it is possible to determine $n_\beta$ and hence to calculate the mean life-time of the $\beta$-particles. Measurements carried out over a wide range of tritium pressures showed that the particles may undergo up to $10^7$ reflections from the magnetic mirrors. From this follows a conclusion of great practical importance: breakdown of adiabatic invariance leading to a serious loss of particles does not occur in a properly constructed magnetic mirror trap.

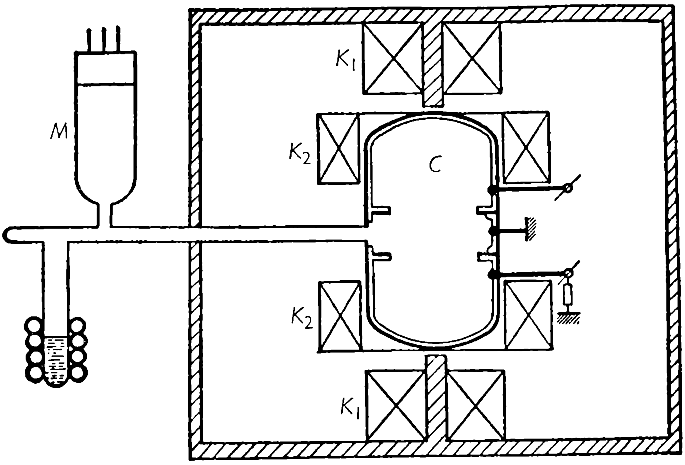

FIG. 11. Diagram of Rodionov's apparatus

The conclusions drawn from Rodionov's experiments are confirmed by the experiments carried out by Gibson, Jordan and Lauer at the Radiation Laboratory of the University of California. In this work a magnetic mirror trap was used to confine positrons formed by the decay of radioactive neon. Owing to the large energy of the positrons and to the high vacuum achieved the confinement time in these experiments amounted to several seconds. The confinement time was estimated by measuring the current of positrons leaving the chamber through a small thin foil window situated on the magnetic axis behind one of the mirrors. The observations agreed completely with theoretical calculations of the particle loss caused by collisions with gas atoms. It is interesting to note that in these experiments it was possible for the first time to confine particles in a magnetic trap for periods of about 10 seconds. During such a period, a positron is reflected by the mirrors about $10^9$ times, and it makes more than $10^{10}$ Larmor revolutions. Unfortunately in these experiments no attempt was made to study the loss rate of those positrons whose trajectories are located some distance off axis. The point at issue is that particles whose Larmor circles enclose the axis are predicted to have a long confinement time not only because of conservation of the adiabatic invariant, but also by the precise theory of charged particle motion in axially symmetric fields (see Chapter VII, § 7.3). The main interest lies in the experimental determination of the confinement time of particles whose Larmor orbits do not enclose the axis, because precise theory gives no indication of the confinement time of such particles.†

§ **2.3** The above results can be generalised to include the case of charged particle motion in the presence of an electric and a magnetic field. The component of the electric field parallel to ***H*** accelerates or retards the particle motion in that direction. The component of *E* which is perpendicular to ***H*** produces a drift of the particles in the direction of the vector ***E*** × ***H***. The drift velocity is given by

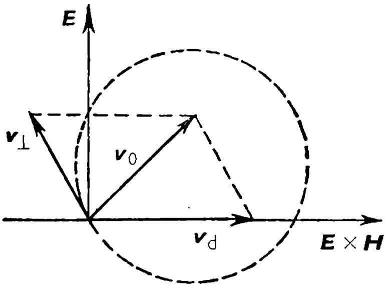

FIG. 12

The velocity components of particle motion in crossed fields

$$\boldsymbol{v}_d = c\boldsymbol{E}\times\boldsymbol{H}/H^2. \qquad \ldots\ldots\ldots(2.16)$$

The particle motion in the plane perpendicular to ***H*** can be regarded as being compounded of Larmor rotation with speed $v_\perp$ and a rectilinear drift motion of magnitude $v_d$. The particle trajectory is trochoidal. The relationship between $v_d$ and $v_\perp$ depends on the initial conditions. Let us assume that a particle is formed (for instance by ionisation of an atom) with an initial velocity $\boldsymbol{v}_0$. In crossed fields the initial velocity of rotation, that is $\boldsymbol{v}_\perp$, is $\boldsymbol{v}_0 - \boldsymbol{v}_d$ both in magnitude and direction (Fig. 12). In a weak electric field $v_\perp \simeq v_0$, and the particle trajectory appears similar to the drift path in a non-uniform magnetic field. In strong electric fields, when the initial speed is comparatively small, the magnitude of $v_\perp$ is equal to $v_d$. In this case, the particle moves in a cycloid of amplitude $2mc^2E/qH^2$. In the most general case when the magnetic field is not uniform and an electric field is present, the drift velocity in the direction perpendicular to ***H*** is the sum of the velocities given by equations (*2.14*) and (*2.16*).

The particle motion parallel to the magnetic field is given by

---

† Such experiments have now been performed by the Livermore group; see Gibson, Jordan and Lauer, *Phys. of Fluids*, **6**, 116, January 1963.

$$m\frac{dv_{\parallel}}{dt} = -\frac{W_{\perp}}{H}\frac{\partial H}{\partial l}+qE_{\parallel}, \qquad \text{.........}(2.17)$$

where $E_{\parallel}$ is the component of $\boldsymbol{E}$ parallel to $\boldsymbol{H}$.

A strong parallel electric field can have an important influence on the properties of magnetic mirrors. If $E_{\parallel}$ is sufficiently large and if it is so directed that it accelerates charged particles of one sign towards the high-field region, then the magnetic mirrors may fail to reflect these particles. On the other hand reflection of particles of opposite charge sign from the magnetic mirror is enhanced under these conditions.

Integrating equation (*2.17*) along the line of force we obtain:

$$W_{\parallel}-W_0\cos^2\alpha_0 = -W_0(\sin^2\alpha_0)\frac{H-H_0}{H_0}-q\phi. \qquad \text{.........}(2.18)$$

The electrostatic potential $\phi$ at the initial point is taken as zero. The relation between $\sin\alpha_0$ and the magnetic field strength $H$ at the point of reflection is:

$$\sin^2\alpha_0 = (1-q\phi/W_0)H_0/H. \qquad \text{.........}(2.19)$$

This represents a generalisation of the simple law, given in § **2.1**, for the reflection of particles from magnetic mirrors. Thus in a given magnetic field the loss cone, which defines the limits of the directions of motion of trapped particles, is altered significantly by the electric field when $q\phi \approx W_0$.

In particular, an electric field can arise as a consequence of a change in the magnetic field strength with time. Such cases are of special interest in studying the motion of charged particles. Let us suppose that a magnetic field in some region of space around an axis $z$ can be considered uniform, and let us examine how an increase in $H$ affects the motion of a particle which initially moved along a helical trajectory around one of the lines of force parallel to the $z$ axis. The transverse velocity component increases as $\sqrt{H}$, and the parallel component $v_z$ remains unchanged. Therefore the angle made by the trajectory with the axis increases, i.e. the helical trajectory is compressed. In addition, the Larmor radius of the helical trajectory varies inversely as $\sqrt{H}$.

Under the action of the induced electric field there must also be a radial drift of particles towards the axis of cylindrical symmetry. This drift speed is

$$-\frac{dr}{dt} = c\frac{E}{H} = c\frac{1}{H}\frac{1}{2\pi rc}\frac{d\Phi}{dt}, \qquad \text{.........}(2.20)$$

where $\Phi = \pi r^2 H$, is the magnetic flux through a circle of radius $r$. Consequently

$$\frac{dr}{dt} = -\frac{r}{2H}\frac{dH}{dt}, \qquad \text{.........}(2.21)$$

i.e.

$$r \propto 1/\sqrt{H}. \qquad .........(2.22)$$

Thus, the distance to the axis of symmetry decreases with $H$ in the same way as does the Larmor radius.

Let us now suppose that there is a large number of particles evenly distributed throughout the uniform magnetic field. As the field strength grows, the trajectories of the particles are drawn towards the axis, and therefore the number density $n$ must increase. The total number of particles must be conserved, and so:

$$nr^2 = \text{const.}$$

Therefore the number density must be proportional to $H$. The sum of the values of $W_\perp$ for particles in a unit of volume is proportional to $H^2$; that is to say, the ratio of the kinetic energy density involved in the Larmor revolution of particles to the magnetic energy density must remain constant.

When a non-uniform field varies with time, the parameters describing the trajectories change in a more complicated way. If a particle is oscillating between two magnetic mirrors, then when $H$ increases, the trajectory comes closer to the axis of cylindrical symmetry and, at the same time, the amplitude of the oscillations along the $z$ axis decreases.

By way of example we can take the motion of particles in an axially symmetric magnetic mirror field whose strength both varies along the axis according to a parabolic law and also increases with time:

$$H(z, t) = H_0\phi(t) + \frac{k^2z^2}{2}f(t). \qquad .........(2.23)$$

We will suppose that the field strength increases so slowly (as described by the functions $\phi(t)$ and $f(t)$) that the change of $H$ is small during the period of one oscillation by a particle between the magnetic mirrors. The equation describing the parallel oscillations of a particle under the action of a force $F = -(W_\perp/H)(\partial H/\partial z)$ has the form

$$m\ddot{z} = -k^2f(t)zW_\perp/H. \qquad .........(2.24)$$

Because $W_\perp/H$ is constant, the frequency $\omega$ increases as $\sqrt{f}$. As we know from the theory of oscillations, when $\omega$ changes slowly, the energy of oscillatory motion is proportional to $\omega$. But this energy is also proportional to the product of $\omega^2$ and the square of the amplitude of oscillation. Therefore the amplitude of the oscillations is inversely proportional to $\sqrt[4]{f}$.

Thus, as the field increases, the region in which the particle moves is compressed, and the energy of parallel motion increases. Furthermore, these changes of the parallel motion are independent of the field variation represented by the first term in the expression for $H$, i.e. the term describing the field strength at its minimum.

The mechanism which increases the energy of parallel motion is readily explained. The induced electric field in the magnetic mirror regions accelerates the particles so that they acquire additional rotational energy, which is subsequently transformed into energy of parallel motion when the particle is reflected from the mirror. Alternatively, one can say that the particles are being reflected from moving mirrors which approach one another along the $z$ axis, because increasing the mirror fields is equivalent to shifting the boundaries of the high-field regions. Figure 13 shows a very simple example of a configuration with moving mirrors. In this idealised case it is supposed that the high-field regions (the mirrors) move as a whole with a constant speed $u$ which is small compared with the parallel component of the particle velocity $v$. A charged particle situated between the approaching magnetic mirrors behaves just like a molecule in the space between two moving pistons. At each reflection from the mirror, the parallel velocity of a particle increases by $2u$. When $u \ll v$ the acceleration is given by:

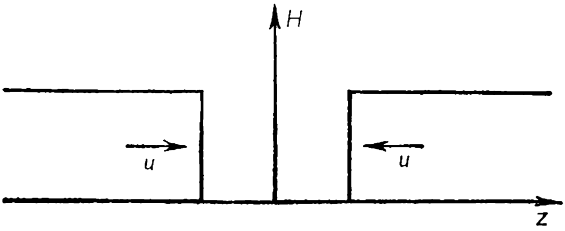

FIG. 13. Magnetic mirrors moving towards one another

$$\frac{dv}{dt} t_p = 4u. \qquad \text{.........(2.25)}$$

Here $t_p$ is the period of oscillation and is equal to $2l/v$, where $l$ is the distance between the mirrors. This distance decreases with time: $l = l_0 - 2ut$. Consequently

$$\frac{dv}{v} = \frac{2u\,dt}{l_0 - 2ut}, \qquad v = v_0 \frac{l_0}{l_0 - 2ut}. \qquad \text{.........(2.26)}$$

The kinetic energy of parallel motion $W_{\parallel}$ and the frequency of oscillation $\omega$ are given by:

$$W_{\parallel} = W_{\parallel}(0) l_0^2 / l^2;$$
$$\omega = \omega(0) l_0^2 / l^2.$$

Thus $W_{\parallel}$ and $\omega$ are proportional to one another, just as in the example analysed above.

It should be noted that the parallel energy of a particle trapped between two approaching magnetic mirrors cannot increase beyond a certain limit. When $W_{\parallel}$ reaches the value $\mu(H_{\max} - H_0)$, where $\mu$ is the magnetic moment associated with the Larmor orbit (the adiabatic invariant of motion), the particle can pass through the strong field region and is lost.

These particular examples illustrate the general pattern which occurs with such quasi-periodic motions. By the laws of analytical dynamics not only is $W_{\perp}/H$ an adiabatic invariant for this class of motions, but so also is the integral

$$\oint p_{\parallel}\, dl. \qquad \text{.........}(2.27)$$

In this integral $p_{\parallel}$ is the component of the momentum parallel to $H$. The integration is carried out along the trajectory of the particle for one cycle of oscillation. This invariant of parallel motion can also be written in the form

$$\int_0^{t_p} v_{\parallel}^2\, dt,$$

from which it follows that if the period $t_p$ of the oscillation is shortened by a change in the magnetic field, then the energy of parallel motion increases roughly in inverse proportion to $t_p$, i.e. in proportion to $\omega$. As strict theory shows, the invariant of parallel motion is conserved not only when $H$ changes with time, but also when the trajectory is gradually altered by drift motion due to non-uniformity of the field.

The increase in the kinetic energy of particles trapped in a space between moving magnetic mirrors represents a very simple particular example of the mechanism proposed by Fermi to explain the acceleration of cosmic ray particles. According to the Fermi theory, cosmic ray particles gain energy as a result of collisions with magnetic fields moving at random in cosmic space. Even though a particle can either gain or lose energy as a result of a single collision with any such 'magnetic cloud' (depending on the direction in which the 'magnetic cloud' is moving), the net statistical effect of many collisions is an increase in the energy of the particles at the expense of the energy of the moving magnetic fields.

This mechanism of particle acceleration may also be very important for certain plasma heating processes; this is particularly so when instabilities develop in a plasma and lead to fluctuations of the magnetic field which move at great speed.

In concluding this brief review of the main laws governing the motion of charged particles in a strong magnetic field, we make one observation which will be useful when we analyse such phenomena as the passage of a current or the diffusion of particles in plasma. This observation is that equation (*2.16*) which determines the drift velocity of particles in an electric field can, after minor modification, also be used for calculating the drift velocity caused by any non-electric force. Let us suppose that a force $\boldsymbol{F}$ acts on a particle with charge $q$. The electric field $\boldsymbol{E}$ equivalent to this force is given by:

$$\boldsymbol{F} = q\boldsymbol{E}.$$

In this field a particle drifts with velocity

$$\boldsymbol{u} = (c/qH^2)\boldsymbol{F}\times\boldsymbol{H}. \qquad \text{.........}(2.28)$$

If the force $\boldsymbol{F}$ is the same for particles of either sign (electrons and ions), the resulting drift velocities are equal in magnitude but opposite in sign. If $F_e = -F_i$, particles of both signs drift with the same speed in the same direction.

The results given in this section will be used later when we discuss the properties of various systems which might serve as the basis for future thermonuclear reactors. The motion of charged particles in high-frequency electromagnetic fields will be briefly examined in Chapter VIII.

§ **2.4** If the number density of electrons and ions in a plasma is not too small, the collisions between the charged particles of the plasma acquire great importance. Analysis of these collisions is necessary in order to understand such phenomena as diffusion, heat conduction and the passage of current in a plasma. This section gives a brief account of the collision processes due to the electrostatic interaction between charged particles. An elementary encounter of this type is represented by the case, familiar from atomic physics, where one particle is scattered in the Coulomb field of another. In the simplest case, when we consider the motion of a fast light particle amongst practically immobile heavy particles (an electron interacting with the ions of a plasma), the collision probability is given by Rutherford's formula:

$$n\sigma(\theta)\,d\theta = \pi n\left(\frac{Z_1Z_2e^2}{mv^2}\right)^2 \frac{\cos(\theta/2)}{\sin^3(\theta/2)}\,d\theta. \qquad \text{.........}(2.29)$$

Here $n\sigma(\theta)\,d\theta$ is the probability per unit path length that a moving particle will undergo a collision in which its velocity is deflected through an angle which lies between $\theta$ and $\theta+d\theta$; $n$ is the number density of scattering centres; $Z_1e$ and $Z_2e$ are the charges of the colliding particles; $m$ is the mass and $v$ is the speed of the moving particle. When $\theta$ is sufficiently small compared to unity, the expression turns out to be valid whatever the ratio of the masses of the colliding particles (in particular, the expression is valid for collisions of ions with ions or of electrons with electrons).

There is, however, a certain lower limit to $\theta$ below which formula (*2.29*) can no longer be used to calculate the probability of a scattering collision. Scattering through a very small angle occurs when the distance between the colliding particles is large. When this distance is sufficiently great, the Coulomb interaction between the colliding particles is weakened because the field of the scattering centre is screened by intervening particles of opposite sign. The field of the scattering centre cannot penetrate the plasma for an indefinitely large distance because, when acted on by this field, the particles of the plasma start moving and, as a result, the field is cancelled out.

It can be shown that the region within which one can distinguish the field of a single particle against a background of the fluctuating electric fields of the plasma as a whole, has linear dimensions $d$ given by

$$d \approx \sqrt{\frac{kT}{8\pi n e^2}}, \qquad \text{.........}(2.30)$$

where $T$ is the plasma temperature. The quantity

$$2^{1/2}d = (kT/4\pi n e^2)^{1/2} \equiv r_D \qquad \text{.........}(2.30a)$$

is called the Debye shielding distance.†

In order to derive equation (*2.30*) let us consider the simplest example of shielding. Suppose that an electric field is generated by an infinite plane electrode placed in a plasma. The resulting potential $V$ in the plasma is a function of the distance $x$ between a given point and the surface of the electrode. The variation of $V$ with $x$ is determined by Poisson's equation:

$$\frac{d^2V}{dx^2} = -4\pi e(n_i - n_e). \qquad \text{.........}(2.31)$$

For the case of thermodynamic equilibrium, the spatial distribution of particles in the potential $V$ is given by Boltzmann's expression, that is:

$$n_i = n_0 \exp(-eV/kT); \qquad n_e = n_0 \exp(eV/kT). \qquad \text{.........}(2.32)$$

Here $n_0$ is the number density of electrons in the quasi-neutral unperturbed plasma at $x \to \infty$, where the potential is taken as zero. We will limit ourselves to the case when $eV \ll kT$. Expanding $n_i$ and $n_e$ in powers of $eV/kT$ and substituting in equation (*2.31*), we find as a first approximation

$$\frac{d^2V}{dx^2} = \frac{8\pi n_0 e^2}{kT} V.$$

With the convention $V \to 0$ as $x \to \infty$,

$$V = V_0 \exp(-x/d), \qquad \text{.........}(2.33)$$

where $d$ is given by equation (*2.30*).

The physical interpretation of this result is that the electric field tends to polarise the plasma, while thermal motion tends to weaken the polarisation. Consequently, screening of the field occurs at some non-zero distance which increases with temperature and decreases as the number density of charged particles increases.

One can talk of elementary binary collisions only when the distance between the colliding particles is considerably less than $d$. The angle of scattering corresponding to an impact parameter of $d$ is:

---

† The numerical factor in equation (*2.30*) is smaller by a factor of $\sqrt{2}$ than that often used (cf. Spitzer *loc. cit.*, Eqn. 2.3).

$$\theta_{\min} \approx \frac{2Z_1Z_2e^2}{mv^2d}. \qquad \text{.........}(2.34)$$

The quantity $\theta_{\min}$ is the lower limit of the scattering angle for which Rutherford's formula is applicable; when $\theta \ll \theta_{\min}$ the probability of scattering will be many times less than indicated by the Rutherford formula. In all cases of practical interest $\theta_{\min}$ is very small. To give an example, the value of $\theta_{\min}$ is about $10^{-7}$ radians for a hydrogen plasma at a temperature of $10^3$ eV and with a number density of $10^{14}$ cm$^{-3}$.

As Rutherford's formula shows, the main peculiarity of Coulomb collisions is the very great probability of small-angle collisions. Compared with these 'weak' collisions, encounters involving large changes in the direction of motion are of negligible probability. This peculiarity means that the nature of the movement of charged particles in a plasma is very different from that of atoms in a neutral gas. When we use the elementary concepts of the kinetic theory of gases we imagine the molecular trajectories to consist of straight sections with sharp bends at the points where collisions occur. In contrast to this, the trajectory of an electron or an ion in a plasma should be represented by a smooth and slightly wavy line, with an almost continuous change in direction. Therefore such concepts as the mean-free-path and the mean time between collisions lose their clarity when applied to collisions in a plasma, and retain only a conventional meaning. Nevertheless, when analysing basic plasma processes, we shall make frequent use of these concepts, so as not to complicate the exposition by introducing the cumbersome apparatus of strict theoretical methods. The cost of this simplification is an inevitable inaccuracy of the numerical coefficients found in all the main formulae.

In order to define the mean-free-path of particles in a plasma, we note that it must represent the average distance traversed by the particles in randomising their direction of motion. The ultimate quantitative formulation of this definition is:

$$dv = -(v/\lambda)\,dx. \qquad \text{.........}(2.35)$$

Here $dv$ is the mean change in velocity parallel to $dx$ over a distance $dx$ for a parallel monoenergetic beam of particles and $\lambda$ is the mean-free-path for particles with speed $v$.

Using equation (*2.29*), we can express $\lambda$ as an integral over the angular distribution of the velocities of the scattered particles. If a particle undergoes a collision which changes its direction of motion by an angle $\theta$, the component of $v$ in the initial direction is reduced by $v(1-\cos\theta)$. As it passes through a layer of plasma of thickness $dx$, a particle undergoes $n\sigma(\theta)\,d\theta\,dx$ collisions with scattering angle between $\theta$ and $\theta+d\theta$. Multiplying this quantity by $v(1-\cos\theta)$ and integrating over all scattering angles, we obtain the mean value of $dv$:

$$dv = -vn\,dx \int_0^\pi \sigma(\theta)(1-\cos\theta)\,d\theta.$$

Therefore,

$$\frac{1}{\lambda} = n \int_0^\pi \sigma(\theta)(1-\cos\theta)\,d\theta. \qquad \text{.........}(2.36)$$

Using Rutherford's formula for $\sigma(\theta)\,d\theta$ and integrating from $\theta_{\mathrm{min}}$ to $\pi$, we find

$$\lambda = \frac{1}{4\pi n}\left(\frac{mv^2}{Z_1Z_2e^2}\right)^2 \frac{1}{\ln(2/\theta_{\mathrm{min}})}. \qquad \text{.........}(2.37)$$

The quantity $2/\theta_{\mathrm{min}}$ in the logarithmic term is very large; therefore even a relatively inaccurate estimate of $\theta_{\mathrm{min}}$ will not introduce much error in determining the mean-free-path. If the colliding particles have a Maxwellian energy distribution, we obtain for the average value of $\lambda$:

$$\lambda = 4\times10^5T^2/Z_1^2Z_2^2nL_c = 6\times10^{13}\theta^2/Z_1^2Z_2^2nL_c, \qquad \text{.........}(2.38)$$

where $L_c = \ln(2/\theta_{\mathrm{min}})$.

The quantity $L_c$ is called the Coulomb logarithm. It can be found from equations (*2.30*) and (*2.34*). Over a very broad range of densities and temperatures, the value of $L_c$ varies between 10 and 20; henceforth, unless stated otherwise, it is taken to be 15.

Equation (*2.37*) has been derived for the case when the scattering centres can be regarded as immobile. Therefore, when $Z_1 = 1$, it gives the mean-free-path of an electron between two 'collisions' with plasma ions. As noted above, such an interpretation of $\lambda$ is conventional: in actual fact, an electron moving a distance $\lambda$ undergoes a great number of small-angle deflections, the statistical effect of which is to randomise the direction of motion.

From equation (*2.38*) we can evaluate several other quantities which describe the encounters between electrons and ions. The effective cross-section for electron-ion collisions can be found from the relationship $\lambda = 1/n\sigma$. The effective mean collision time is found from $\tau = \lambda/v$; and the effective ion-electron collision frequency $\nu$ is $1/\tau$. These quantities are given by the following numerical formulae†:

$$\sigma_{\mathrm{ei}} = 4\times10^{-5}Z_{\mathrm{i}}^2/T_{\mathrm{e}}^2 = 3\times10^{-13}Z_{\mathrm{i}}^2/\theta_{\mathrm{e}}^2; \qquad \text{.........}(2.39)$$

$$\tau_{\mathrm{ei}} = 4\times10^{-2}T_{\mathrm{e}}^{\frac{3}{2}}/n_{\mathrm{i}}Z_{\mathrm{i}}^2 = 5\times10^4\theta_{\mathrm{e}}^{\frac{3}{2}}/n_{\mathrm{i}}Z_{\mathrm{i}}^2; \qquad \text{.........}(2.40)$$

$$v_{\mathrm{ei}} = 25n_{\mathrm{i}}Z_{\mathrm{i}}^2/T_{\mathrm{e}}^{\frac{3}{2}} = 2\times10^{-5}n_{\mathrm{i}}Z_{\mathrm{i}}^2/\theta_{\mathrm{e}}^{\frac{3}{2}}. \qquad \text{.........}(2.41)$$

---

† The subscript ei designates quantities characterising collisions of electrons with ions.

For a more complete description of the statistical effect of Coulomb collisions between particles in a plasma, it is necessary to introduce parameters defining the interaction between particles of the same type (electrons with electrons and ions with ions). However, because we shall not have to work with these parameters in what follows, we will confine ourselves merely to some general remarks about them.† The mean-free-path for Coulomb collisions is determined, roughly speaking, by the energy of the particles. Therefore the mean-free-path $\lambda_{ee}$ which can be introduced to describe electron-electron collisions is of about the same magnitude as $\lambda_{ei}$ (the expressions for $\lambda_{ei}$ and $\lambda_{ee}$ differ only by a numerical coefficient of order unity which arises because, in an electron-electron encounter, the colliding particles are moving at comparable speeds). Therefore it is also the case that $\tau_{ee} \simeq \tau_{ei}$ and $\nu_{ee} \simeq \nu_{ei}$. The mean-free-path $\lambda_{ii}$ which characterises ion-ion collisions is determined by an expression completely analogous to $\lambda_{ei}$, with the difference that in equation (*2.38*) the ion temperature $T_i$ must replace $T_e$. The corresponding mean time, $\tau_{ii}$ is greater than $\tau_{ee}$ (and $\tau_{ei}$) by the ratio $v_e/v_i$; assuming equal electron and ion temperatures, we have†

$$\tau_{ii}/\tau_{ee} = (m_i/m_e)^{\frac{1}{2}}.$$

§ **2.5** The establishment of thermal equilibrium in the plasma is of great importance in the problem of controlled thermonuclear reactions. Two aspects of the matter should be distinguished: (a) the relaxation of differences between the ion temperature and the electron temperature; (b) the rate at which a Maxwellian velocity distribution is established for each constituent of the plasma. We begin by considering the first of these aspects.

If a fast particle with momentum $p_1 = m_1 v_1$ passes a stationary scattering centre of mass $m_2$ and is deflected by a small angle $\theta$, then the momentum imparted to $m_2$ is $\Delta p = 2p_1 \sin(\theta/2)$. The scattering centre thus acquires kinetic energy:

$$\Delta W = (\Delta p)^2/2m_2 = (2p_1^2/m_2)\sin^2(\theta/2).$$

The energy lost by the fast particle per unit time can be determined by multiplying $\Delta W$ by the scattering probability $v_1 n\sigma(\theta)\,d\theta$, and integrating with respect to $\theta$ from $\theta_{\min}$ to $\pi$. For Coulomb interaction (equation *2.29*),

$$-\frac{dW}{dt} = \frac{4\pi n e^4 Z_1^2 Z_2^2 L_c}{m_2 v_1}. \qquad \text{.........}(2.42)$$

This expression can be used to determine the rate at which energy is transferred from fast to slow particles, in the limiting case when both the kinetic energy and the speed of the scattering centres are much smaller than those of the particle which is being slowed down. For example, equation (*2.42*) gives the correct value for the transfer of energy from electrons to ions in a plasma if $T_e \gg T_i$; by averaging equation (*2.42*) with respect to $v_1$ over a Maxwellian velocity distribution, we obtain for this case:

---

† These remarks and results are valid only for the case of singly-charged ions.

$$-\frac{dW_e}{dt} = n_i Z_i^2 e^4 L_c \sqrt{32\pi m_e}/m_i\sqrt{kT_e}. \qquad \ldots\ldots\ldots(2.43)$$

The rate of energy loss for electrons in a hydrogen plasma is (when $L_c = 15$)

$$-\frac{dW_e}{dt} = 1{\cdot}2\times10^{-17} n_i/T_e^{\frac{1}{2}} = 1{\cdot}1\times10^{-19} n_i/\theta_e^{\frac{1}{2}}. \qquad \ldots\ldots\ldots(2.44)$$

In a deuterium plasma, the electrons lose energy at half this rate, other conditions being equal.

Equation (*2.42*) can also be used to determine the deceleration of a very fast ion by collision with cold electrons. The mean energy loss rate for very energetic ions at temperature $T_i$, colliding with cold electrons of a plasma is given by an expression analogous to (*2.43*):

$$-\frac{dW_i}{dt} = n_e Z_i^2 e^4 L_c \sqrt{32\pi m_i}/m_e\sqrt{kT_i}. \qquad \ldots\ldots\ldots(2.45)$$

This expression is applicable provided $v_i \gg v_e$, i.e.

$$T_i \gg (m_i/m_e)T_e.$$

The formulae describing the exchange of energy between electrons and ions in a plasma become more complicated when the motion of the scattering centres is not negligible. It is inadmissible to neglect such motion in the first place when $T_e$ and $T_i$ are comparable, and in the second place when the ions have a greater kinetic energy but a smaller velocity than the electrons ($T_i \gg T_e$, but $v_i < v_e$). In the general case the energy transferred per unit time from particles of one plasma constituent to particles of the other can be expressed:

$$Q = \frac{\overline{W_e} - \overline{W_i}}{\tau_{eq}} = \frac{3}{2}k\frac{T_e - T_i}{\tau_{eq}}. \qquad \ldots\ldots\ldots(2.46)$$

Here $Q$ is the energy transferred per unit time per particle. Conventionally we consider $Q$ a positive quantity when $T_e > T_i$. The parameter $\tau_{eq}$ is a time characteristic of the energy exchange rate in a plasma; it can be called the electron-ion energy relaxation time. When the speed of the particles of one constituent of the plasma is much larger than that of the other constituent, $\tau_{eq}$ can be determined by comparing equation (*2.46*) with the limiting formulae (*2.43*) and (*2.45*); when $Z_i = 1$ the following limiting expressions are obtained for $\tau_{eq}$:

1) when $v_e \gg v_i$,

$$\tau_{eq} = 3m_i(kT_e)^{\frac{3}{2}}/2ne^4L_c\sqrt{32\pi m_e} = 17AT_e^{\frac{3}{2}}/n; \qquad \ldots\ldots\ldots(2.47)$$

2) when $v_i \gg v_e$,

$$\tau_{eq} = 3m_e(kT_i)^{\frac{3}{2}}/2ne^4L_c\sqrt{32\pi m_i} = 2{\cdot}2\times 10^{-4}T_i^{\frac{3}{2}}/n\sqrt{A}; \qquad \text{........}(2.48)$$

where $A$ is the atomic weight of the ions and $n = n_e = n_i$.

Because of the large value of $m_i/m_e$, the electron speed greatly exceeds the ion speed not only when the electron temperature is higher than the ion temperature, but also in the opposite case provided $T_e \gg (m_e/m_i)T_i$. Therefore when $T_e/T_i$ is greater than $10^{-3}$, we must insert $\tau_{eq}$ from equation (*2.47*) into (*2.46*), to obtain the energy exchange rate for a hydrogen plasma. The formula then becomes:

$$Q = 1{\cdot}2\times 10^{-17}n(T_e - T_i)/AT_e^{\frac{3}{2}}. \qquad \text{........}(2.49)$$

We encounter one of the particular cases to which this formula applies when we study heat exchange between ions and electrons during shock heating processes in a magnetically accelerated plasma. For fast enough shock waves†, $T_i$ can considerably exceed $T_e$, but the ion thermal speed remains considerably less than that of the electrons. The rate of energy transfer from ions to electrons in this case is many times less than the value obtained by using equation (*2.48*), which gives the ion energy loss to virtually stationary electrons.

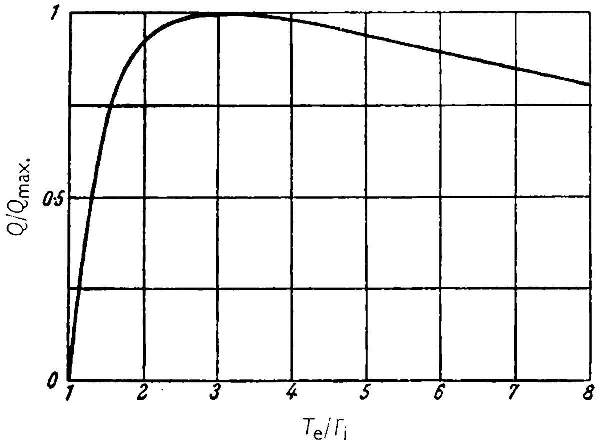

FIG. 14. Dependence of $Q$ on $T_e$, for the case when $T_e > T_i$, and $T_i$ is fixed

If $T_e/T_i$ is considerably less than $m_e/m_i$ (this corresponds to the slowing down of high energy ions in a cold plasma), then we have to use equation (*2.48*) to determine $\tau_{eq}$. In this case $T_e$ can be neglected in comparison with $T_i$, so that equation (*2.46*) for $Q$ reduces to equation (*2.42*). In the intermediate region, i.e. when $v_i \approx v_e$, it is necessary to use strict theory to evaluate $\tau_{eq}$. For singly-charged ions, the required expression is:

---

† For low Alfvén Mach numbers, the electron temperature can exceed the ion temperature due to ohmic heating.

$$\tau_{eq} = \frac{3m_e m_i}{8(2\pi)^{\frac{1}{2}} n e^4 L_c}\left(\frac{kT_e}{m_e}+\frac{kT_i}{m_i}\right)^{\frac{3}{2}}. \qquad \text{.........(2.50)}$$

The expressions already obtained for $\tau_{eq}$, which relate to limiting cases, are, of course, in full agreement with the general expression (*2.50*).

Let us now examine some of the consequences of the theory of heat exchange between electrons and ions in a plasma. Figure 14 shows $Q$ as a function of $T_e$ for a fixed value of $T_i$, when $T_e > T_i$. The maximum rate at which the electrons heat the ions occurs when $T_e = 3T_i$. Given this condition, $Q_{max} = 5\times 10^{-18} n A^{-1} T_i^{-\frac{1}{2}}$. Figure 15 shows how the quantity $-Q$ varies with $T_i$, when $T_i > T_e$ and $T_e$ is constant. When $T_i$ lies between $T_e$ and about $\frac{1}{2}(m_i/m_e)T_e$, the ion energy loss rate grows linearly with $T_i$. At the start of this region, $Q$ is determined by expression (*2.49*). When $T_i = \frac{1}{2}(m_i/m_e)T_e$, the quantity $-Q$ reaches a maximum value $-Q_{max} = 9\times 10^{-15} n A^{-1} T_e^{-\frac{1}{2}}$. Further increase in $T_i$ has the result that the rate of energy transfer is reduced, first very slightly, but eventually to vary as $T_i^{-\frac{1}{2}}$ (as follows from (*2.48*) which is valid when $v_i \gg v_e$).

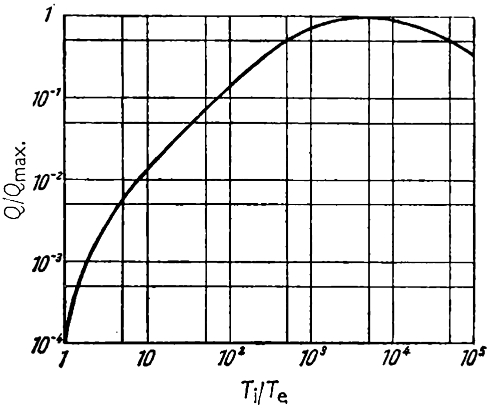

FIG. 15. Dependence of $-Q$ on $T_i$, for the case when $T_i > T_e$, and $T_e$ is fixed

Let us now use these formulae to estimate the rate at which thermal equilibrium is established between electrons and ions in a plasma. Suppose that the thermal relaxation takes place in adiabatic conditions, so that the total kinetic energy is conserved. In this case,

$$T_e + T_i = \text{const},$$

$$-dT_e/dt = B(T_e - T_i)/T_e^{\frac{3}{2}}, \qquad \text{.........(2.51)}$$

where $B = n/17A$ (we assume that $v_i \ll v_e$, so that $\tau_{eq}$ is obtained from equation (*2.47*)). Expressions can be found from equation (*2.51*) which describe the change of $T_e$ and $T_i$ with time for given initial conditions.

Figure 16a shows the ratio $T_i/T_e$ as a function of time, $t/\tau_0$, with the initial condition $T_e = T_0$ and $T_i = 0$. The unit of time $\tau_0$ is the value of the parameter $\tau_{eq}$ calculated from equation (*2.47*) with $T_e = T_0$. In the problem given, $\tau_0$ is a characteristic parameter defining the time needed to establish thermal equilibrium. With $t = 0{\cdot}5\tau_0$ the ratio $T_i/T_e$ is about 0·7; when $t = \tau_0$, $T_i$ and $T_e$ differ by only 3 %.

Figure 16b illustrates the relaxation when the initial conditions are

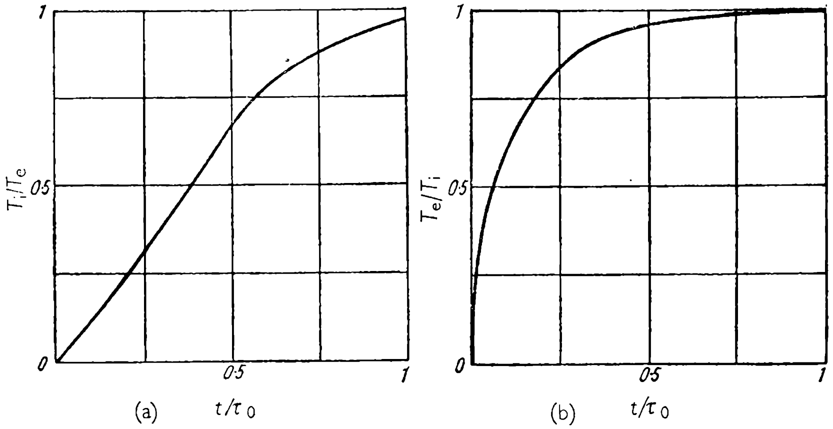

FIG. 16. Relaxation of ion-electron temperature difference:

(a) ions being heated by electrons; (b) electrons being heated by ions

$T_e = 0$ and $T_i = T_0$. We see that, for given $T_0$, the rate of relaxation of the temperature difference is considerably faster when the ion constituent has the higher temperature: with $t = 0{\cdot}3\tau_0$, the ratio $T_e/T_i$ is approximately 0·9. In order to get an impression of the approximate value of the time taken to establish equilibrium in a plasma, we note that with $n = 10^{14}$ cm$^{-3}$ and $T_0 = 10^8$ °K the parameter $\tau_0 = 0{\cdot}17A$ sec (i.e. for deuterium about one third of a second).

Both these very simple cases of the establishment of equilibrium involves the assumption that the total thermal energy of the plasma is conserved. In the general case, when the total thermal energy varies with time, the relation between $T_e$ and $T_i$ becomes more complex. If there is a rapid accumulation of energy in the plasma, or if processes take place which involve large energy losses, the gap between the electron temperature and the ion temperature can be as big as one pleases and can increase with time.

The heating of the plasma by fast charged particles formed by fusion reactions between light nuclei could be an important process in a thermonuclear reactor. The fast charged particle (a proton, a triton or the nucleus of one of the isotopes of helium) as it moves in a plasma will be slowed down by collisions both with electrons and ions. The energy losses due to collisions with electrons can be estimated from either equation (*2.42*) or (*2.49*), depending on the ratio of the particle energy—which we can conventionally express by some effective temperature—to the energy of the electrons. The energy loss due to ion collisions is described by a formula similar to (*2.42*), $m_2$ representing in this case the mass of the plasma ion, and $v_1$ the speed of the fast particle. By using these theoretical relationships, we can easily establish that if the plasma temperature is about $10^4$ eV, and the energy of the fast particle is some MeV, most of the energy of the particle is expended in heating the electrons. Only after the particle energy has fallen to about $10^5$ eV does the slowing down caused by ion collisions compare with that caused by collisions with electrons.

When the rate of energy transfer by Coulomb collisions from a fast particle to plasma electrons falls as the electron temperature increases, the range of a fast particle in the plasma increases with $T_e$. This increase of range begins at values of $T_e$ such that the thermal speed of the plasma electrons is comparable with the speed of the fast particle. The increase in the range will, naturally, produce an enhanced yield of nuclear reactions caused by the fast particles in the plasma.

Let us consider a particular case. Suppose that a beam of fast deuterons, of initial energy $W_0$, come to rest in a tritium plasma. If the plasma temperature is low, so that the speed of the deuterons considerably exceeds that of the plasma electrons, the yield of nuclear reactions is very small. With $W_0 = 100$ keV the proportion of deuterons which undergo a nuclear reaction over the full range is $2 \times 10^{-6}$. The energy efficiency is 0·04%, if we define it as the ratio of the nuclear energy released to the initial deuteron energy. In the example we are considering, the reaction yield and the energy efficiency both increase rapidly when the electron temperature reaches $10^3$ eV. The variation of these quantities with $\theta_e$ is shown in Table 1 (where slowing down by ion collisions is also taken into account). With $\theta_e = 6 \times 10^3$ eV the energy efficiency becomes unity. This result shows that it is in principle possible to generate nuclear fusion energy not only when it is released by thermal collisions of plasma ions, but also when a stream of fast particles passes through a plasma of sufficiently high electron temperature. The realisation of the latter process by injecting a beam of deuterons from an accelerator into a plasma does not appear to be at all practicable for obtaining a net energy gain. In some

*Table I*

| $\theta_e$ (eV) | 0 | $1 \times 10^3$ | $3 \times 10^3$ | $5 \times 10^3$ | $1 \times 10^4$ |
|---|---|---|---|---|---|
| Reaction yield | $2 \times 10^{-6}$ | $8 \times 10^{-4}$ | $3 \times 10^{-3}$ | $5 \times 10^{-3}$ | $8 \times 10^{-3}$ |
| Energy efficiency | $4 \times 10^{-4}$ | 0·14 | 0·5 | 0·9 | 1·4 |

conditions, however, fast particles can arise directly in the plasma itself because of accelerating mechanisms associated with various forms of plasma instability. If the electron temperature of the plasma is high enough, such internal injection of fast ions can (at least in principle) lead to a high nuclear reaction rate. Such a chain of events, while possible and of importance in the analysis of experiments, has almost certainly no long-term practical significance.

When fast heavy particles are slowed down in plasma, the scattering processes also alters their direction of motion. So long as the particle energy is sufficiently large compared to the energy of the plasma electrons, the particle loses the greater part of its energy through collisions with plasma electrons before its direction of motion is significantly altered. This can be seen by analysing the relation between the parameters that characterise the scattering and the slowing down of fast particles in a plasma. The scattering process is characterised by the mean square angle of scatter $\theta_s$. An expression defining $\theta_s$ for a sufficiently small path length $\Delta x$, within which the energy of the particle is constant, can be found from Rutherford's formula. By definition

$$\theta_s^2 = n\Delta x \int \theta^2 \sigma(\theta)\, d\theta.$$

By using (*2.29*) and by taking into account that, when integrating, only the region of small angles ($\sin\theta \simeq \theta$, $\cos\theta \simeq 1$) is important, we find

$$\theta_s^2 = 8\pi n \left(\frac{Z_1 Z_2 e^2}{mv^2}\right)^2 \Delta x L_c. \qquad \ldots\ldots\ldots(2.52)$$

To derive the scattering of a fast particle of mass $m_1$, charge $Z_1 e$ and energy $W$ slowing down in a plasma of ion number density $n_i$ and ionic charge $Z_i e$, we have to allow for scattering both on ions and on electrons. $Z_2^2$ is therefore replaced by $Z_i^2 + Z_i$ and $n$ by $n_i$; the modified expression (*2.52*) is then integrated over $x$ (owing to the statistical character of the process, the mean square angle of scatter is an additive quantity). Thus, the mean square angle of scatter over the path from $x = 0$ to $x = x_f$ is:

$$\theta_s^2 = 2\pi n_i Z_1^2 (Z_i^2 + Z_i) e^4 L_c \int_0^{x_f} \frac{dx}{W^2}. \qquad \ldots\ldots\ldots(2.53)$$

Equation (*2.53*) can be evaluated by integrating over the particle energy instead of over its path, thereby relating the scattering to the loss in energy. If the particle speed exceeds the thermal speed of the plasma electrons (slowing down in a cold plasma), the quantity $dW/dx$ can be derived from (*2.42*) and substituted in (*2.53*). On integrating we obtain

$$\theta_s = \sqrt{(Z_i + 1)\frac{m_e}{m_1} \ln \frac{W_0}{W_f}}. \qquad \ldots\ldots\ldots(2.54)$$

Here $W_0$ is the initial energy of the particle and $W_f$ is its final energy over the section of path being considered. It follows that the direction of motion of a fast heavy particle changes significantly only after it has lost almost all its initial kinetic energy. Thus, for example, a proton emitted in a *d-d* reaction and slowed down in a cold deuterium plasma, is deviated through an angle of about 1° only when it has lost 90% of its energy.

The relation between scattering and slowing down is qualitatively different for fast electrons. In this case, as equation *(2.54)* shows, the magnitude and direction of the particle velocity change, roughly speaking, at the same rate: the value of $\theta_s$ is about unity for an *e*-fold reduction in the electron energy.

This difference between the behaviour of ions and of electrons is explained by the fact that, if they have the same initial energy, they undergo the same scattering in the plasma, but different energy loss: the electrons lose energy much more slowly (because of their higher speed). These results should be borne in mind particularly when analysing the processes that take place in magnetic traps in which plasma is obtained by injecting fast ions. The main process determining the behaviour of the fast ions during the initial phase of accumulating particles in a trap, is the slowing down of the ions on the cold electrons.

At the beginning of this section we mentioned the rate at which a Maxwellian velocity distribution is established in a plasma. Calculations show that a time several times larger than the mean collision time for identical particles is in practice sufficient to establish a Maxwellian velocity distribution, whatever the initial energy distribution of the particles. For collisions between electrons this latter time is less than the quantity $\tau_{eq}$ (introduced above) by a factor of about $m_e/m_i$. For ions, this factor is about $(m_e/m_i)^{\frac{1}{2}}$. It follows that the times needed to establish Maxwellian distributions are in all cases far shorter than the energy relaxation time between particles of different type.

§ **2.6** A fully ionised and completely pure hydrogen plasma, in which there are no neutral atoms or impurity ions, is a theoretical abstraction. In actual installations for heating plasma to high temperatures, the surface of the plasma is always bombarded by neutral atoms and molecules. These neutral atoms and molecules arise mainly through the evaporation of gases adsorbed on the surface of the chamber containing the plasma, or absorbed in the material of the chamber walls. Neutral particles may also be emitted owing to bombardment of the walls by fast charged particles and by ultraviolet or soft X-radiation (photo-dissociation of adsorbed molecules).

If we are to assess the possible effect of neutral particles getting into a high-temperature plasma, we shall have to acquaint ourselves with the main interactions of fast electrons and protons with atoms, molecules and impurity ions. In this and the following section, a brief summary is given of the relevant data, particular attention being paid to cases where electrons and protons interact with atoms and molecules of hydrogen. In the graphs given below, all the cross-sections for interactions between fast particles and molecules of hydrogen or other substances are given with reference to a single molecule (and not with reference to a single atom, as is sometimes done).

For the problem with which we are concerned, the greatest importance attaches to the ionisation of atoms and molecules, to radiation associated with impurity ions, and to charge-exchange processes. Let us look first at the main characteristics of ionisation processes.

Figure 17 shows measured ionisation cross-sections of atomic and molecular hydrogen by electrons, as a function of electron velocity $v_e$ for a range of values which corresponds to an electron energy ranging from the threshold to 400 eV. The ionisation curve for atomic hydrogen contains the recent measurements of Fite and Brackmann. The cross-sections for ionisation of molecular hydrogen are taken from the early work of Tate and Smith. When the electron energy is large compared with the ionisation potential, the ionisation cross-sections $\sigma_e(H_2)$ and $\sigma_e(H)$ vary as $v_e^{-2}$, and the ratio $\sigma_e(H_2)/\sigma_e(H)$ approaches two. It should be noted that in the ionisation of molecular hydrogen by electron impact, the predominant process is the formation of molecular ions (when the electron energy is much greater than the ionisation potential, approximately $10^3$ $H_2^+$ ions are formed for every $H^+$ ion formed). Measured cross-sections for the ionisation of certain other elements by electron impact are given in Fig. 18.

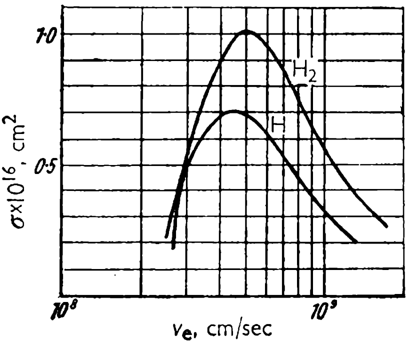

FIG. 17. Cross-sections for the ionisation of atomic and molecular hydrogen by electron impact

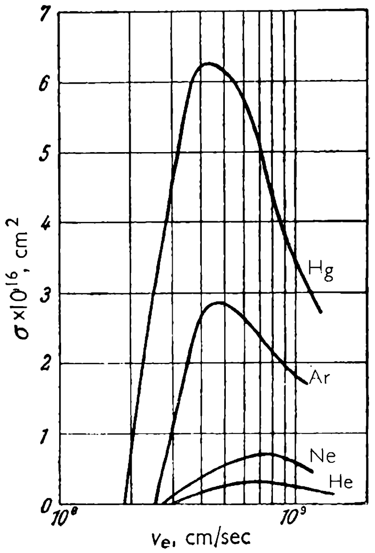

FIG. 18. Cross-sections for the ionisations of various elements by electron impact

In a plasma where the ion temperature is sufficiently high, neutral atoms can also become ionised when they collide with ions. Figure 19 shows the total ionisation cross-section of molecular hydrogen by protons as a function of proton velocity. The curve shown was constructed from the measurements obtained by Ilin, Afrosimov and Fedorenko (proton velocities of $10^8$ to $6\times 10^8$ cm/sec), and from the results of Gillbody (proton velocities of $3\times 10^7$ to $7\times 10^7$ cm/sec). The term 'total ionisation cross-section' means that account is taken of all forms of ionising collision. The ionisation cross-section rises rapidly with proton velocity at low proton energies; it reaches a maximum value when $v_p = 3\times 10^8$ cm/sec and then decreases monotonically (it varies as $v_p^{-2}$ at high velocities). On the same graph are shown measurements by Fite of the ionisation cross-section of atomic hydrogen for a narrow range of proton speeds (from $1{\cdot}2\times 10^8$ to $3\times 10^8$ cm/sec). For rough estimation, it can be taken that the ionisation cross-section of atomic hydrogen is half that of the hydrogen molecule $H_2$ when the proton energy exceeds 30 keV.

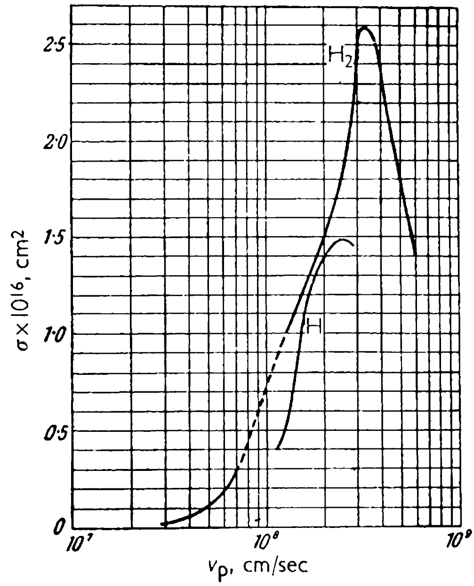

FIG. 19

Cross-sections for the ionisation of molecular and atomic hydrogen by protons

Given the ionisation cross-section for an atom or molecule under the action of electron and ion impact, we can determine both the mean life-time of such a neutral particle in a plasma, and the depth to which it can penetrate into a plasma from outside. The mean life-time of a neutral particle, which we shall also term henceforth 'ionisation time', is given by the following relationship:

$$\tau_{\text{ion}} = 1/n(\overline{v_e\sigma_e}+\overline{v_i\sigma_i}), \qquad \text{.........}(2.55)$$

where $n$ is the plasma number density, $v_e$ and $v_i$ are the electron and ion velocities, $\sigma_e$ and $\sigma_i$ are the cross-sections for ionisation by electron and ion impact and $\overline{v_e\sigma_e}$ and $\overline{v_i\sigma_i}$ are averaged over the velocity distribution.

When the electron and ion temperature is about a million degrees in a hydrogen plasma, the ionisation of atomic or molecular hydrogen occurs essentially only when there is a collision with an electron. However, when the temperature is about a hundred million degrees (10 keV) the main ionisation process is collisions between neutral particles and protons. To illustrate this point we give a numerical example. Let $T_e = T_i = 2\times 10^8$ °K and $n = 10^{14}\,\text{cm}^{-3}$; then for atomic hydrogen, $\overline{v_e\sigma_e} \simeq 3\times 10^{-9}\,\text{cm}^3\,\text{sec}^{-1}$, $\overline{v_i\sigma_i} \simeq 0{\cdot}8\times 10^{-8}\,\text{cm}^3\,\text{sec}^{-1}$ and $\tau_{\text{ion}} \simeq 1\times 10^{-6}$ sec. The variation of the ionisation time with plasma temperature is shown in Fig. 20 (for atomic hydrogen in a hydrogen plasma with $n = 10^{14}$). The depth of penetration of a neutral atom into a plasma is roughly equal to $v_0\tau_{\text{ion}}$, where $v_0$ is the speed of the atom. If, in the particular example just considered, we put

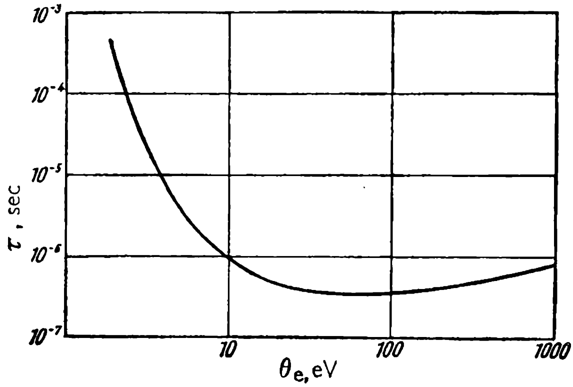

FIG. 20. Time of ionisation for a hydrogen atom in a hydrogen plasma ($n = 10^{14}\,\text{cm}^{-3}$)

$v_0 = 2\times 10^5$ cm/sec (which corresponds to room temperature for atomic hydrogen), we obtain a value of about 1 mm for the depth of penetration. Atoms of heavier elements are ionised more rapidly and penetrate a shorter distance than hydrogen atoms.

Ions of elements with $Z \gg 1$, which are formed when impurities get into a hydrogen plasma, enhance the radiated power and thus represent an additional source of energy loss. Knorr, Kogan, Dolgov and others have explored theoretically the contribution of impurity radiation to the energy balance of a plasma. We give here some results of these studies.

Three types of radiation are associated with impurity ions: (a) bremsstrahlung, (b) recombination radiation and (c) line radiation of excited ions. Energy loss through bremsstrahlung due to impurity ions is especially important when the plasma temperature is high, because the intensity of this radiation increases as $T^{\frac{1}{2}}Z^2_{\text{eff}}$. If the mean electron energy exceeds the K-shell binding energies, equation (*1.8*) can be used to estimate the bremsstrahlung intensity, $Z_{\text{eff}}$ being taken as the atomic number of the impurity element. Screening of the nuclear charge by bound electrons has little effect on the bremsstrahlung intensity for sufficiently fast electrons.

Recombination radiation displays a quite different pattern of behaviour. The total power radiated by radiative recombination between ions and free electrons varies as $T_e^{-\frac{1}{2}}$. The power radiated increases very rapidly with the charge of the ion. To estimate the energy removed from the plasma by continuum recombination radiation, the following formula can be used:

$$Q_{\text{rec}} = 5\times 10^{-22} n_e T_e^{-\frac{1}{2}} Z_{\text{eff}}^4. \qquad \text{.........}(2.56)$$

Here $Q_{\text{rec}}$ is the recombination energy radiated per second by an impurity ion, and $Z_{\text{eff}}$ is the effective charge of the ion in the plasma. The value of $Z_{\text{eff}}$ is itself a function of the temperature. When it gets into a plasma, an impurity atom loses one electron after another until such time as the capture of free plasma electrons in recombination processes† balances the loss of the remaining bound electrons by ionisation processes. The bigger $T_e$, the larger is the effective charge. Obviously, the limiting value of $Z_{\text{eff}}$, given a sufficiently high electron temperature, is the atomic number of the element.

The third of the radiation processes mentioned above is associated with radiative transitions between the quantum mechanical states of the electrons bound to impurity ions. The resulting radiation has a line spectrum; it is produced either by electron impacts which excite the ion from its ground state to a higher level (this mechanism is the chief one) or it can follow recombination of a free electron into an energy level other than the ground state. The intensity of the line spectrum is a complex function of $Z$, $T_e$ and the energy level structure of the given ion. This form of radiation predominates when the plasma temperature is comparatively low.

To estimate the effect of impurity ions on the overall energy balance of a hydrogen plasma we must calculate the total energy lost through all forms of radiation. The total power radiated by a small concentration of impurity is proportional to the number density of the impurity ions $n^*$, and the electron number density $n_e$ in the hydrogen plasma. The total power radiated can be expressed in the form:

$$Q_{\text{rad}} = n_e n^* f(Z, T_e). \qquad \text{.........}(2.57)$$

The quantity $Q_{\text{rad}}$ denotes the power radiated by impurity ions per unit volume of plasma. In Figs. 21 and 22, the quantity $f(Z, T_e)$ is shown for the cases $Z = 6$ (carbon) and $Z = 8$ (oxygen) as a function of temperature, assuming a steady-state exists in which the rate of ionization by electron impact is balanced by the radiative recombination rate. There is a marked fluctuation of the intensity of line and recombination radiation at an electron temperature in the region of 10–200 eV; this is caused by the great difference between the ionisation potentials of the outer (valence) and inner (K-) electron shells of the C and O atoms. The first maximum is due mostly to radiation from the lithium-like ions CIV and OVI, which is associated with the $2s$–$2p$ transitions between energy levels with the same principal quantum number. For these transitions $\Delta E \approx 10$ eV, and as a consequence of this the main factor which determines the rate of excitation, $\exp(-\Delta E/kT_e)$, is close to unity.

---

† In the conditions of interest to us (rarefied plasma) the main recombination mechanism is two-body recombination, i.e. radiative recombination.

As shown by Kogan and Vasilev, when $Z \simeq 10$ and $T_e \simeq 10^6$, a rough estimate of $f(Z, T_e)$ can be obtained from:

$$f(Z, T_e) = 1{\cdot}6\times 10^{-27}Z^2\sqrt{T_e}+6\times 10^{-22}\frac{Z^4}{\sqrt{T_e}}+8\times 10^{-17}\frac{Z^6}{T_e^{\frac{3}{2}}}, \qquad \ldots\ldots\ldots(2.58)$$

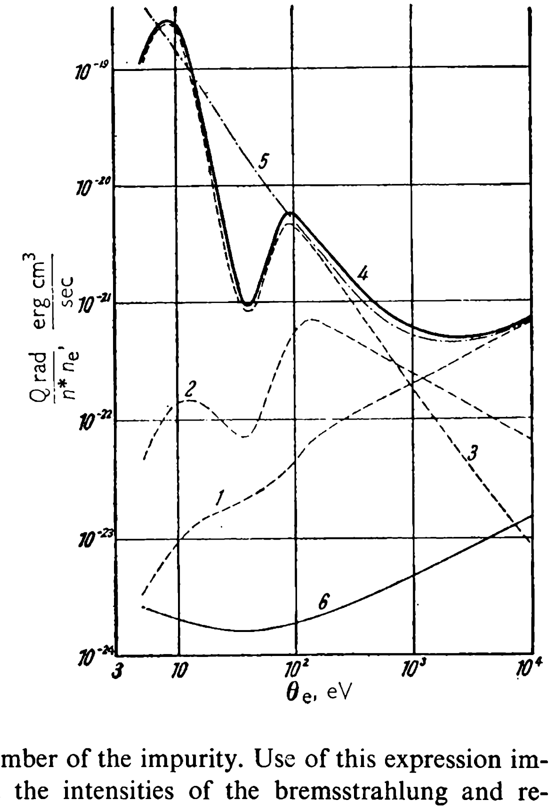

FIG. 21

Curves showing radiation intensities for carbon. The broken curves 1, 2 and 3 show respectively the intensity of bremsstrahlung, of recombination radiation and of line radiation. The unbroken curve 4 represents the intensity of the total radiation, i.e. the function $f(Z, T_e)$. The broken curve 5 is obtained from the extrapolation of equation (*2.58*). Curve 6 shows the intensity of hydrogen radiation

where $Z$ is the atomic number of the impurity. Use of this expression implies, in particular, that the intensities of the bremsstrahlung and recombination continuum are taken as being the same as for fully ionised impurities. As can be seen from Figs. 21 and 22, when $T_e < 10^6$, equation (*2.58*) gives a rough estimate of the power radiated.

The same figures also show, for purposes of comparison, the corresponding curve for a pure hydrogen plasma. For this curve, the value of $f(1, T_e)$ given by the ordinate corresponds to the power radiated by unit volume of hydrogen plasma with $n_e = 1$. At electron temperatures above about $3\times 10^5$ °K, the main radiative process in pure hydrogen plasma is bremsstrahlung, the intensity of which increases as $T_e$ increases.

The ratio of the power radiated by impurities to that radiated by the pure hydrogen plasma is

$$\alpha \frac{f(Z, T_e)}{f(1, T_e)},$$

where $\alpha = n^*/n_e$ is the relative number density of impurity atoms. The curves in Figs. 21 and 22 show that even at relatively low $Z$, the power radiated by an impurity ion exceeds by several orders of magnitude that due to a single proton. Therefore even a slight contamination by impurity atoms can increase by many times the radiation from a hydrogen plasma. For example, if 1 % oxygen is present in a comparatively cold hydrogen plasma with a temperature of about 10 eV, the power radiated from the plasma is enhanced approximately a thousand times. It follows that in those methods of obtaining high-temperature plasma where the starting state is cold plasma, losses through impurity radiation can dominate the energy balance during the initial heating phase.

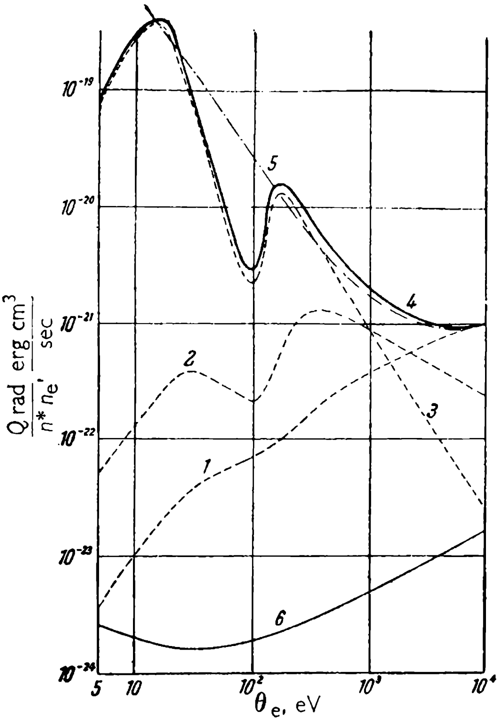

FIG. 22

Graph showing radiation intensities for oxygen. The significance of the curves is as in Fig. 21

It must be pointed out that all the above remarks about the significance of impurity radiation in the energy balance of a hydrogen plasma are based on quite rough theoretical calculations. At present there are few reliable experimental data bearing on this.

When drawing up the overall energy balance for the heating of hydrogen plasma which contains impurity ions, account must be taken not only of radiation but also of the energy absorbed by forming ions with an equilibrium charge $Z_{\text{eff}}$. The ion acquires this charge as the result of a series of ionisation processes at the expense of the thermal energy of the plasma electrons. The energy in the hydrogen plasma is also expended by passing on the mean thermal energy $\frac{3}{2}kT$ to each ion and to the electrons stripped off it. On the average, the energy expended on each impurity atom in the plasma is equal to

$$\tfrac{3}{2}kT(Z_{\text{eff}}+1)+e\sum V_i, \qquad \text{.........}(2.59)$$

where $\sum V_i$ is the sum of the ionisation potentials of the stripped electrons. By taking this energy into account, we allow for the heat capacity of the impurity atoms. The first term in (*2.59*) is related to the heat capacity of free particles; the second term takes account of the ionisation energy. The heat capacity of impurities can be very important in the energy balance of a highly contaminated hydrogen plasma.

We must emphasise that the above remarks on the radiative power and thermal capacity of impurity ions, and also the numerical estimates are fully applicable only if the confinement times are long enough for the charge of the impurity ions to reach the steady state value $Z_{\text{eff}}$. Roughly speaking, the time needed to establish this charge is equal to the ionisation time of an ion with a charge $(Z_{\text{eff}}-1)$. In plasma with a temperature $T \simeq 10^6$ °K and number density $n_e \simeq 10^{14}$ cm$^{-3}$ this time is about $10^{-4}$ sec; it usually increases when the electron temperature increases (as a consequence of the dependence of $Z_{\text{eff}}$ on $T_e$).

§ **2.7** Charge-exchange of ions on neutral atoms and molecules can be very important in high-temperature plasma under certain conditions. The charge-exchange process in its essential and simplest form can be represented by:

$$A^{+}+B^{(0)} \rightarrow A^{(0)}+B^{+}.$$

This expresses the fact that, during a collision, the charge of an ion $A^+$ can be transferred to a neutral particle $B^{(0)}$ and the initial ion itself becomes a neutral atom or molecule.

The charge-exchange cross-section is a function of the relative speed of the colliding particles, and depends also on the nature of the particles. At low relative speeds the charge exchange cross-section can be large only when the charge-exchange is not accompanied by a change in the internal energy of the combined system. This occurs when charge-exchange takes place between an atomic ion and an atom of the same element (or between a molecular ion and a molecule of the same substance). Such processes are called resonant charge-exchange. Examples are:

$$H^{+}+H \rightarrow H+H^{+};$$

and

$$H_2^{+}+H_2 \rightarrow H_2+H_2^{+}.$$

Figure 23 shows the charge-exchange cross-section of $H^+$ in atomic hydrogen as measured by Fite, Stebbing, Hummer and Brackmann. Experimental results, in agreement with theory, indicate that for resonant charge-exchange the cross-section $\sigma$ increases steadily as $v_i$ decreases. For slow protons moving in atomic hydrogen the charge-exchange cross-section reaches $3\times 10^{-15}$ cm$^2$.

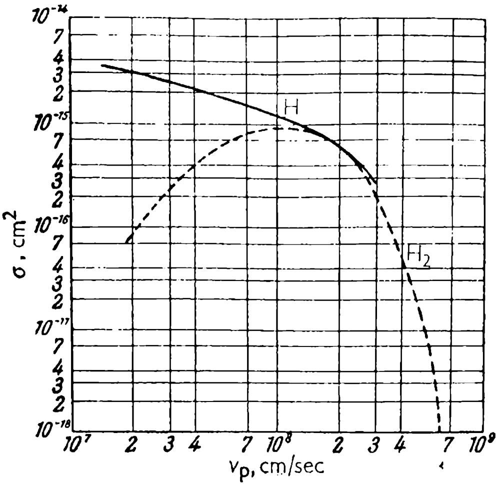

FIG. 23

Charge-exchange cross-sections for protons in atomic and molecular hydrogen

If the internal energy of a system of colliding particles is altered by charge-exchange, the variation of $\sigma$ with $v_i$ is quite different. To provide a comparison with the curve for resonant charge-exchange, Fig. 23 also shows the charge-exchange cross-section for the process

$$H^+ + H_2 \rightarrow H + H_2^+.$$

The form of the curve is typical of non-resonant charge-exchange. As the relative velocity increases, $\sigma$ grows rapidly at first, and reaches its maximum when $v \simeq 10^8$ cm/sec; thereafter it falls rapidly. The cross-sections for resonant and non-resonant charge-exchange differ substantially only in the region of low relative velocities. Where the proton energies are high (above 100 keV) the charge-exchange cross-section of molecular hydrogen is twice that of atomic hydrogen. The effective charge-exchange cross-

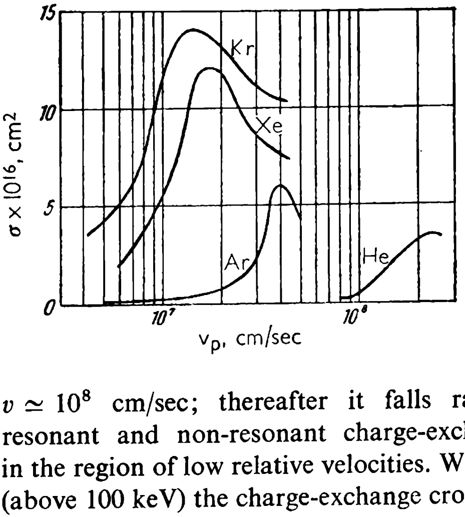

FIG. 24

Charge-exchange cross-sections for protons on atoms of various elements sections of protons on atoms of certain heavy elements are shown in Fig. 24. These are not resonance processes; nevertheless, for optimum values of $v_p$, the corresponding cross-sections are quite high.

We will now examine the importance of charge-exchange as a plasma-cooling mechanism. If a 'cold' neutral atom enters a hydrogen plasma, it can, by an elementary act of charge-exchange, pass on one of its electrons to a fast proton of the plasma which thus becomes a fast neutral hydrogen atom and may escape from the plasma, taking with it kinetic energy $\frac{3}{2}kT_i$ ($T_i$ is the temperature of the protons in the plasma).

The importance of such energy losses in the energy balance of a hydrogen plasma depends on the state of the plasma and the conditions at its boundary. We shall first assume that the effect of impurities can be wholly neglected, so that only hydrogen is present in the region surrounding the plasma. Normally the hydrogen is in a molecular state, and therefore the surface of the hydrogen plasma is bombarded by $H_2$ molecules. On penetrating into the plasma, the molecules quickly dissociate, and the resulting hydrogen atoms undergo resonant charge-exchange collisions. These are the processes which predominate at plasma temperatures up to some tens of keV (at a higher ion temperature, charge-exchange does not have time to occur because the probability of ionisation of hydrogen atoms by collision with protons is much greater than the probability of charge-exchange). The energy carried away from the plasma by the fast neutral hydrogen atoms formed by charge-exchange is proportional to the flux of hydrogen molecules at the boundary of the plasma. If the number density of the plasma is high enough and if its geometrical dimensions are not too small, the plasma surface is black to neutral molecules; that is, each molecule falling on the surface is captured by the plasma. In this case, the flux of energy leaving the plasma is equal to

$$\frac{3}{4}n_0 v_0 kT_i S,$$

where $n_0$ is the molecular number density in the surrounding gas, $v_0$ is the average molecular velocity and $S$ is the surface area of the plasma.

The ratio of this quantity to the energy lost in the form of electromagnetic radiation is, for hydrogen plasma,

$$6\times 10^{10} n_0 v_0 T_i^{\frac{1}{2}} S/n^2\Omega,$$

where $n$ is the plasma number density and $\Omega$ is the plasma volume. To achieve this simple expression, $T_e$ is taken as equal to $T_i$, and only bremsstrahlung is taken into account.

For the sake of illustration we take a particular example, using the sort of numerical parameters which might be of practical interest. Suppose that a plasma with a number density $n = 3\times 10^{14}$ cm$^{-3}$ and a temperature $T = 10^8$ °K occupies a long cylindrical region of 25 cm diameter. The space surrounding the plasma contains hydrogen at a temperature of $10^3$ °K and a number density of $3\times 10^9$ cm$^{-3}$ (which, at normal temperature, corresponds to a pressure of $10^{-7}$ Torr). In these conditions, $10^{17}$ molecules per second fall on each centimetre length of the cylindrical plasma column, and the power loss due to charge-exchange is 170 W/cm. Thus in the example we are considering the loss of energy by charge-exchange is roughly the same as the loss by bremsstrahlung in a pure hydrogen plasma.

In cold hydrogen plasma at a temperature of a few electron-volts, charge-exchange processes are not significant in the same way; this is because in the range of temperatures mentioned the hydrogen can be incompletely ionised, and atomic hydrogen is present in the plasma with a relatively high number density. In the low energy region charge-exchange of protons on atoms of hydrogen has a very large cross-section, and is the main process of interaction between these particles. It is responsible for a very rapid heat-exchange between ions and neutral atoms in a hydrogen plasma. Therefore in cold plasma with a temperature of a few electron-volts, the protons and the atoms have essentially the same temperature; and one of the main plasma cooling mechanisms is then ordinary thermal conduction in the neutral gas which, in these conditions, removes heat from the plasma very quickly and impedes an increase in the ion temperature (because of this there can be a big difference between the values of $T_e$ and $T_i$). It should be noted however that at low temperatures there is also a rapid exchange of energy between the protons and atoms in a plasma due to ordinary elastic collisions, and therefore even if charge-exchange were entirely absent the losses caused by the heat conductivity of the neutral constituent of the plasma would be essentially the same.

Charge-exchange on heavy impurity atoms can be very important in the energy balance of a plasma when two conditions are simultaneously fulfilled: (a) the probability of charge-exchange for an impurity atom exceeds the probability of its ionisation by electron or ion impact; (b) the properties and the linear dimensions of the plasma are such that an atom passing through the plasma has little chance of being ionised by electron impact. The first condition is self-evident; the second is easily understood if we consider what happens when it is not satisfied. In this case the plasma is still an absolutely black body to the neutral atoms that fall on its surface, even when charge-exchange processes are absent. Charge-exchange does not increase the number of captured atoms and the associated energy loss ($\frac{3}{2}kT_i$ for each charge-exchange) is less than the energy expended in forming ions with the steady-state charge.

However, if the plasma temperature is insufficient to strip all the bound electrons from the impurity atoms, account must be taken of the additional energy loss caused by charge-exchange of protons on impurity ions which have retained some of their bound electrons. It is very difficult to estimate the importance of this effect since there are no data whatsoever on the charge-exchange of moderately energetic protons on multiple ionised atoms. It can be assumed that if the mean thermal energy of the electrons and protons is about the same as or greater than the ionisation potential of the impurity ion when it has lost all but one of its electrons, then the proportion of incompletely ionised atoms will be very small for well-confined plasmas, and their participation in charge-exchange processes can be neglected.

Charge-exchange of fast ions on neutral atoms or molecules can be very important in those devices where the high-temperature plasma is created by the injection of fast ions into a magnetic trap. The current delivered by such injectors is limited, and therefore, in order to create a plasma with a high number density inside a trap, a long time is needed: given an injection current of 0·1 amp, 150 seconds are needed to fill 1 cubic metre with plasma with a number density of $10^{14}$ $\mathrm{cm}^{-3}$ (assuming that all the particles are trapped). Consequently, during the initial stage of accumulation, when the plasma still has a low number density and the residual gas in the trap is not fully ionised, charge-exchange may lead to the loss of a high proportion of the injected ions.

However, one can also imagine a situation where charge-exchange might play a positive part in the capture of injected particles in a trap. This will be so if a stream of fast neutral atoms is injected into a cold plasma of high number density, created by other means in the volume of the trap. The fast atoms become ionised by charge-exchange collisions with the slow ions, and the temperature of the ion constituent of the plasma increases due to the replacement of slow ions by fast ones. In later chapters we shall return to the part played by charge-exchange processes in magnetic traps of various types.

To conclude this preliminary review of the behaviour of neutral particles in high-temperature plasma it remains to make one comment. In the graphs given in this section, various interactions of the particles in a hydrogen plasma are described. However, practical importance attaches only to processes which take place in deuterium or in a mixture of deuterium and tritium. It is therefore necessary to recall that the cross-sections for all types of interaction are a function of the relative speed of the particles. Therefore the graphs describing the ionisation and charge-exchange processes for ordinary hydrogen remain valid for deuterium and tritium as well, provided the particle speed is used for the abscissae scales.

CHAPTER III

# TRANSPORT PHENOMENA IN PLASMAS

§ **3.1** Directed fluxes of energy and of particles appear in plasmas under the action of electric fields, of density gradients and of temperature gradients. Processes of this type have the general name of transport phenomena. We shall first consider such phenomena for the case when no magnetic field is present.

If an electric field $E$ is generated in a plasma, the charged particles are set in motion and produce an electric current. In the general case, the strength of the electric field can be an arbitrary function of time $t$. Let us calculate the current density arising from a uniform electric field $E(t)$ whose magnitude changes with time, taking into account the motion of the electrons only and regarding the ions as immobile.

The equation of motion of an electron in the field is

$$\ddot{x} = -(e/m_e)E(t). \qquad \text{.........}(3.1)$$

Here $x$ is the electron coordinate in the direction of $E$. If we integrate this expression from the time $t_0$ of the last collision between the electron and an ion, to the time $t$, we obtain

$$\dot{x} = -(e/m_e)\int_{t_0}^{t} E(t')\,dt'. \qquad \text{.........}(3.2)$$

It is here assumed that $\dot{x}$ is reduced to zero at each collision.

To determine the current density at time $t$ we must find the mean value of the velocity $\dot{x}$. Let us consider the time interval $t_0$ to $t_0+dt_0$ which precedes the time $t$. Out of the total number of electrons a proportion equal to $(dt_0/\tau_{ei})$ collide with ions during this interval. Of this proportion, a fraction equal to $\exp[-(t-t_0)/\tau_{ei}]$ undergo no further collisions until after time $t$. Therefore the quantity

$$(dt_0/\tau_{ei})\exp\left[-(t-t_0)/\tau_{ei}\right] \qquad \text{.........}(3.3)$$

is the proportion of electrons at time $t$ whose last collisions with ions occurred in the time interval $t_0$ to $t_0+dt_0$.

To find the mean value of the velocity $\dot{x}$, we have to multiply (*3.2*) by (*3.3*) and integrate with respect to $t_0$ between $-\infty$ and $t$:

$$\bar{\dot{x}} = (-e/m_e\tau_{ei})\int_{-\infty}^{t}\left[\exp\left[-(t-t_0)/\tau_{ei}\right]\int_{t_0}^{t} E(t')\,dt'\right]dt_0.$$

Integrating this expression by parts:

$$\bar{x} = (-e/m_e) \int_{-\infty}^{t} E(t_0) \exp\left[-(t-t_0)/\tau_{ei}\right] dt_0.$$

The current density is given by:

$$= -ne\bar{x} = (ne^2/m_e) \int_{-\infty}^{t} E(t_0) \exp\left[-(t-t_0)/\tau_{ei}\right] dt_0, \qquad \text{.........}(3.4)$$

where $n$ is the electron number density. Equation (*3.4*) can be rearranged so as to express $E$ as an explicit function of the current density $j$ and its rate of change, $dj/dt$; differentiating (*3.4*) yields

$$\frac{dj}{dt} = -(ne^2/m_e\tau_{ei}) \int_{-\infty}^{t} E(t_0) \exp\left[-(t-t_0)/\tau_{ei}\right] dt_0 + (ne^2/m_e)E(t).$$

$$\text{.........}(3.5)$$

Multiplying by $\tau_{ei}$ gives:

$$j + \tau_{ei}\frac{dj}{dt} = \frac{ne^2\tau_{ei}}{m_e}E(t). \qquad \text{.........}(3.6)$$

From these expressions we can find the complex conductivity of a plasma for the case when $E(t)$ is a periodic function of time. Let $E(t) = E_0 \exp i\omega t$. It then follows from (*3.6*) that

$$j = \frac{ne^2\tau_{ei}}{m_e}\frac{E(t)}{1+i\omega\tau_{ei}}. \qquad \text{.........}(3.7)$$

For a constant current

$$i = \frac{ne^2\tau_{ei}}{m_e}E_0, \qquad \text{.........}(3.8)$$

and therefore the quantity

$$\sigma = \frac{ne^2\tau_{ei}}{m_e} \qquad \text{.........}(3.9$$

represents the conductivity of the plasma.

With this particular plasma model, an expression for the conductivity can also be obtained more simply, using from the outset the condition for steady-state flow of electrons. The force exerted on the electrons by the constant electric field is balanced by the friction force due to collisions with the ions. This friction force is defined as the mean value of the momentum lost by electrons per unit time as a result of collisions with ions. An electron undergoes $(1/\tau_{ei})$ collisions per unit time; in each collision a mean momentum equal to $mu$ is transferred to the ions, where $u$ is the electron drift velocity relative to the ions. The friction force per electron is thus equal to $(m_e u/\tau_{ei})$, and under steady-state conditions, it is exactly balanced by the electric force $-Ee$; hence,

$$-eE = m_e u/\tau_{ei}.$$

By setting $j$ equal to $-neu$, equation (*3.8*) is obtained. For a fully-ionised plasma $\sigma$ is independent of the electron number density $n$ because $\tau_{ei}$ is inversely proportional to $n$; substituting equation (*2.40*) for $\tau_{ei}$, we find

$$\left.\begin{aligned}\sigma &= 0{\cdot}9\times 10^7 T_e^{\frac{3}{2}} = 1{\cdot}1\times 10^{13}\theta_e^{\frac{3}{2}} \quad \text{(e.s.u.)}\\ &= 1{\cdot}2\times 10^2 \theta_e^{\frac{3}{2}}\ \text{mho cm}^{-1}\end{aligned}\right\}\dots\dots\dots(3.10)$$

We note that when $\theta_e = 1{\cdot}4\times 10^3$ eV ($1{\cdot}6\times 10^7$ °K), the electrical conductivity of hydrogen plasma is roughly equal to the conductivity of copper at room temperature. When $\theta_e = 1{\cdot}4\times 10^5$ eV the conductivity exceeds that of copper or silver by about 1000 times.

For time-varying fields, equation (*3.7*) can be rewritten in the form

$$E = j(\eta + i\omega L), \qquad \dots\dots\dots(3.11)$$

where $\eta = 1/\sigma$ and $L = m_e/ne^2$.

It follows from this expression that in a time-varying field, the plasma behaves as though it possessed not only resistivity but also a form of 'non-magnetic' inductivity. This apparent inductivity is due to the inertia of the electrons; when $\omega$ is large, it can significantly reduce the value of the current compared with that in a constant electric field.

Continuing the calculations to establish the relation between $j$ and $E$, we can also find the dielectric constant $\varepsilon$ of the plasma. By definition,

$$\varepsilon = 1 + 4\pi P/E,$$

where $P$ is the electric polarisation per unit volume. We shall consider the electric field to be a sinusoidal function of time with frequency $\omega$, and neglect the oscillations of the ions in view of their small mobility. We can then express the polarisation as:

$$-P = ne\bar{x} = ne\int \bar{\dot{x}}\, dt.$$

Only the time-varying part of the integral has to be counted because the time-average value of $P$ is zero. From (*3.5*) and (*3.7*) it follows that

$$P = -\frac{ne^2 E}{m_e\omega^2(1 - i/\omega\tau_{ei})}, \qquad \dots\dots\dots(3.12)$$

and hence

$$\varepsilon = 1 - \frac{4\pi ne^2}{m_e\omega^2(1 - i/\omega\tau_{ei})}.\dagger \qquad \dots\dots\dots(3.13)$$

---

† The derivation of $\varepsilon$ used here assumes that, unlike the case of a gas of neutral atoms, the electric polarisation $P$ makes no contribution to the force on the electron, defined by (*3.1*). This assumption has been justified by calculation and observation (see V. L. Ginzburg, *loc. cit.*, Ch. 2, p. 27). In an infinite uniform plasma, the uniform displacement of the electrons in a single direction does not produce any additional electric fields to alter the average field experienced by the electrons.

For a high-temperature plasma in a high-frequency field, $\omega\tau_{ei} \gg 1$. In this case

$$\varepsilon = 1-\omega_0^2/\omega^2 \qquad \text{........}(3.14)$$

where $\omega_0 = \sqrt{\dfrac{4\pi ne^2}{m_e}}$ is the frequency of the so-called Langmuir electron plasma oscillations (§*4.7*). When $\omega < \omega_0$ the dielectric constant becomes negative. From this it follows specifically that if an electromagnetic wave with frequency less than $\omega_0$ falls on the surface of such a plasma, it is completely reflected, and is not transmitted through the plasma.

§ **3.2** The characteristic feature of the current flow which we have been considering is the linear relation between the electric field strength and the resulting drift velocity of the electrons. Because of this relation between $u$ and $E$, the electric current satisfies Ohm's law. Nevertheless, an electric field in a plasma can also lead to accelerating processes which increase the energy of a proportion of the electrons without limit. Such electrons are often called 'runaway electrons'. It should be noted that these two different forms of motion are by no means mutually exclusive: when there is an electric field in a plasma, part of the electrons can become involved in a runaway process and, simultaneously, other electrons produce a quasi-stationary ohmic current. The fact that a quasi-stationary current and a non-stationary acceleration process can exist in the plasma together is accounted for by the main characteristic of Coulomb collisions, namely that the cross-section for electron-ion interaction falls very rapidly as the electron speed increases. The equilibrium state, described for a constant electric field by the relation

$$-m_e u = eE\tau, \qquad \text{.........}(3.15)$$

requires that, on average, an electron is accelerated between successive collisions to a velocity that is small compared to its random thermal speed $v$. For Coulomb collisions, the collision time $\tau$ is proportional to $v^3$ and hence, for a given electric field, the ratio of the drift speed $u$ to the random thermal speed $v$ is proportional to $v^2$. Therefore if the energy spectrum of the electrons spreads into a region of high enough energies, some electrons will always be found which, in traversing their mean-free-path, acquire a drift velocity greater than their thermal speed. For such electrons there is no equilibrium between the accelerating action of the electric field and the frictional drag due to Coulomb collisions, and therefore these electrons are in a runaway state of continuous acceleration. This is easier to see if we appreciate that when electrons are slowed down by Coulomb forces, the collision processes do not, on the whole, correspond to the conventional concept of a collision as being a process in which the particle momentum is quasi-instantaneously changed by a large amount. Instead the process consists of numerous small-angle collisions whose effects add statistically to produce a quasi-continuous slowing down. When an electric field is applied the resulting acceleration can not only counteract this slowing down, but can exceed it; so that a state can be created in which no equilibrium is possible between the forces accelerating the electron and those that slow it down.

The dividing line between the runaway state and the equilibrium ohmic drift state is given by the condition

$$eE\lambda(v) \simeq m_e v^2, \qquad \text{.........}(3.16)$$

where $\lambda(v)$ is the mean-free-path for an electron with a given velocity $v$. It is easy to show from equation (*2.37*) that this condition is equivalent to the relation†

$$EW_e/n \simeq 2\times 10^{-12}Z^2; \qquad E \text{ in volts/cm, } W_e \text{ in eV.} \qquad \text{.........}(3.16a)$$

Condition (*3.16a*) determines the lower limit of electron energy $W_e$ above which electrons are in the runaway state. This limit is lowered as the ratio $E/n$ increases. When both $E/n$ and the electron temperature are large enough, the acceleration can involve the greater part of the energy spectrum of the electrons. In this circumstance there is virtually no ohmic plasma current. Calculations by Dreicer show that this occurs if the electric field strength exceeds a critical value $E_c$ given by

$$E_c = 10^{-8}nZ^2/T_e \text{ Volts/cm.} \qquad \text{.........}(3.17)$$

This result is in good agreement with the rough estimate which can be obtained by putting $W_e$ equal to the mean electron thermal energy in equation (*3.16a*). In the opposite case, when $E \leqq E_c$, condition (*3.16a*) is satisfied only for electrons with speeds greatly exceeding the mean thermal speed, and these represent only a small proportion of the total number of plasma electrons. We cannot, however, ignore the effects which might be caused by the continuous acceleration of even a relatively small proportion of the plasma electrons. The flux of fast electrons resulting from such acceleration can generate oscillations in the plasma and produce various types of instability.

In electrodeless plasma devices where the electric field is solenoidal, all the electrons must eventually become runaway electrons if the electric field is maintained for long enough and there is no escape of particles to the walls. This must happen because that part of the energy spectrum depleted by the runaway process is continuously replenished with electrons scattered into it by collisions from the main part of the Maxwellian spectrum. The greater $E/E_c$ is, the faster is the increase in the flux of runaway electrons. It is possible, however, that mechanisms also exist which hinder the growth of the runaway electron flux. Such a mechanism might be a strong interaction between the directed beam of fast electrons and plasma oscillations, the consequence being an anomalous slowing down of the beam.

---

† All that is taken into account here is the slowing down caused by collisions with ions. If $W_e$ greatly exceeds $\theta_e$, i.e. if we consider the conduct of an electron belonging to the 'tail' of the Maxwell distribution, it becomes necessary also to take account of slowing down caused by collisions with electrons in the main part of the energy spectrum. However, the condition (3.16a) still remains approximately valid. Electron-electron collisions are allowed for in the work of Dreicer.

This phenomenon of runaway electrons in the plasma of a toroidal discharge forms the basis of a possible high-current electron accelerator. The idea was first suggested by Steenbeck, who also carried out the first experimental research to verify this principle of acceleration. The theory of runaway electrons in plasma, first discussed by C. T. R. Wilson, has been developed by a number of authors (Spitzer, Harm, Giovanelli). The fullest treatment available is that of Dreicer, who investigated the time-variation of the electron velocity distribution in an infinite plasma in the presence of a constant uniform electric field. Dreicer calculated the time necessary, in a constant field $E$, for the main bulk of the plasma electrons to go over to the runaway state. The time is given by the expression

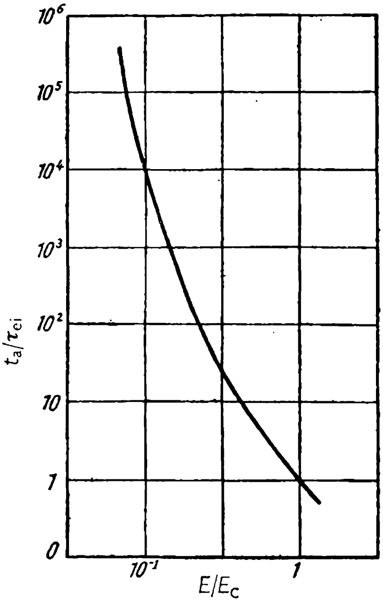

FIG. 25

Time taken for the main bulk of electrons to diffuse into the runaway region as a function of $E/E_c$

$$t_a = \tau_{ei} f(E/E_c). \qquad \text{.........}(3.18)$$

The function $f(E/E_c)$ is shown in Fig. 25.

It is probably somewhat easier to grasp the significance of equation (*3.18*) if we note that the ratio $E/E_c$ is equal to the ratio of the Ohmic drift speed $u$ in the electric field $E$, to the electron thermal speed. Indeed, by using equations (*3.15*) and (*3.17*), which define $u$ and $E_c$, and also equation (*2.40*) which defines $\tau_{ei}$, it is possible to obtain the following relation

$$u/v_e = E/E_c. \qquad \text{.........}(3.19)$$

Here $v_e$ is the root-mean-square thermal speed of the electrons $\sqrt{3kT_e/m_e}$.

To illustrate these theoretical results, we consider a numerical example.

Let $u/v_e = 0{\cdot}1$. From the graph in Fig. 25 it follows that the corresponding value of $f(E/E_c)$ is $9 \times 10^3$. Thus the time necessary for the main bulk of the electrons to runaway is some ten thousand times greater than the mean Coulomb collision time.

Let us further suppose $n = 10^{14}$ cm$^{-3}$, $T_e = 10^6$ °K and $Z = 1$; we then find $\tau_{ei} = 4 \times 10^{-7}$ sec and so $t_a \approx 10^{-3}$ sec. It follows from equations (*3.18*) and (*2.40*) that, for a given value of $E/E_c$, $t_a$ is proportional to $T_e^{\frac{3}{2}}$. Therefore, if the temperature of the plasma is low, the argument of the function $f(E/E_c)$ must be sufficiently small to prevent a rapid transition of all the electrons to the runaway state. It is sufficient in practice that at any temperature the field strength is some 25–30 times less than the critical value $E_c$ (due to the extremely rapid growth of $f(E/E_c)$ as $E/E_c$ decreases).

In devices for heating plasma with toroidal discharge currents, runaway acceleration of electrons in the solenoidal electric fields is a parasitic effect which can be responsible for various types of instability in the plasma, and for additional energy losses. Experimental results on these effects are given in Chapters VI and VIII.

To conclude this discussion of transport properties in an unmagnetised plasma, some remarks on thermal conduction are necessary. As already stated in Chapter I, the thermal conductivity of fully-ionised high-temperature plasma is very large. The rapid increase of thermal conductivity with temperature is due to the increase of the mean-free-path of the particles. With $T_e$ equal to $T_i$, the electron thermal speed is many times greater than that of the ions; and therefore the transfer of heat is predominantly due to the electron constituent of the plasma. When the electron mean-free-path is small compared with the distance over which a significant change of temperature occurs, the thermal flux $Q$ can be determined from the usual formula

$$Q = -\sigma_T \operatorname{grad} T, \qquad \text{.........}(3.20)$$

where the coefficient of thermal conductivity $\sigma_T$ is given by equation (*1.6*). When $T_e = 10^6$ °K, hydrogen plasma has a thermal conductivity 30 times greater than that of copper at room temperature.

Equation (*3.20*) cannot be used if the mean-free-path exceeds the dimensions of the plasma-filled region.

§ **3.3** Magnetic fields have practically no influence on transport processes which take place along the lines of force, but they have a strong influence on transport processes which are directed perpendicular to the lines of force. We can see this by considering such properties of a plasma as electrical and thermal conductivity, and diffusion.

In a steady state, with $\boldsymbol{E}$ perpendicular to $\boldsymbol{H}$, the current flowing in a fully-ionised infinite homogeneous plasma is zero. This can be shown by simple arguments based on the laws governing the drift motion of charged particles in a magnetic field. Let us suppose that the established drift motion of the electrons is described by the vector $\boldsymbol{u}_e$, and the ion drift motion by the vector $\boldsymbol{u}_i$. The mean slowing-down force acting on the electrons is determined by the rate at which momentum is transferred from the electrons to the ions by collisions. The force is proportional to the relative drift velocity and is given by

$$-m_e(\boldsymbol{u}_e-\boldsymbol{u}_i)/\tau_{ei}.$$

The mean total force acting on an electron due to the electric field and to the ions is thus:

$$\boldsymbol{F}_e = -e\boldsymbol{E}-m_e(\boldsymbol{u}_e-\boldsymbol{u}_i)/\tau_{ei}. \qquad \text{.........}(3.21)$$

A force $\boldsymbol{F}_i = -\boldsymbol{F}_e$ acts on the ions (assumed here to be singly charged). In the steady state, $\boldsymbol{u}_e$ and $\boldsymbol{u}_i$ must equal the drift velocities of the electrons and the ions in the magnetic field under the influence of the non-magnetic forces $\boldsymbol{F}_e$ and $\boldsymbol{F}_i$. According to (*2.28*), these drift velocities are given by the expressions:

$$-\boldsymbol{u}_e = \frac{c}{eH^2}\boldsymbol{F}_e\times\boldsymbol{H}, \qquad \text{.........}(3.22)$$

$$\boldsymbol{u}_i = \frac{c}{eH^2}\boldsymbol{F}_i\times\boldsymbol{H}, \qquad \text{.........}(3.23)$$

Consequently $\boldsymbol{u}_e = \boldsymbol{u}_i$. Therefore the electrons and ions drift in the direction perpendicular to $\boldsymbol{E}$ and $\boldsymbol{H}$ with the same speed:

$$u = cE/H. \qquad \text{.........}(3.24)$$

Thus there is no drift motion of the electrons relative to the ions, and so the current in the plasma is zero. At the same time the plasma as a whole moves perpendicularly to $\boldsymbol{E}$ and $\boldsymbol{H}$ at a speed $u$. The absence of steady-state current in crossed $\boldsymbol{E}$ and $\boldsymbol{H}$ fields can also be regarded as a consequence of the fact that the electric field as seen from the plasma moving at the drift velocity $\boldsymbol{u}$ is zero ($\boldsymbol{E}' = \boldsymbol{E}+\boldsymbol{u}\times\boldsymbol{H}/c = 0$).

In real conditions, however, we always have to deal with a plasma which occupies some finite region of space. The behaviour of plasma in crossed fields then depends largely on conditions at its boundaries. In particular, the transverse current is zero only when the boundary conditions do not impede the free drift of the plasma. This can be expected, however, only when the drift movement is parallel to the plasma boundary. An important case where this condition is fulfilled is the one in which the plasma occupies a region shaped like a hollow cylinder, the magnetic field is parallel to the axis of the cylinder and the electric field is entirely radial.

The absence of a steady-state current in crossed fields means that the plasma behaves like a dielectric in a direction perpendicular to $\boldsymbol{H}$. The main quantity characterising this state is the dielectric constant of the plasma in crossed fields. To evaluate this quantity (which is henceforth designated $\varepsilon_m$) we use the most obvious method and make several simplifying assumptions, which do not affect the final result. Suppose that a plasma is in a parallel plane capacitor and is subjected to orthogonal **E** and **H** fields (Fig. 26). Suppose that the length of the capacitor along the $x$ axis is infinite and further, that the thermal energy of the particles is very small. In this case, the plasma particles will move in cycloids when the electric field is switched on instantaneously. As has been said in the previous chapter, the drift speed and the speed of Larmor rotation are the same during the cycloidal motion, and are equal to $cE/H$. If we eliminate the drift motion by changing to a coordinate system which moves with the plasma, we can see that a particle of mass $m$ and charge $q$ which was originally at point $A$ on the $x$ axis moves in a circular trajectory due to the action of the electric field, and that the centre of the circular path is displaced normal to the $x$ axis by a distance

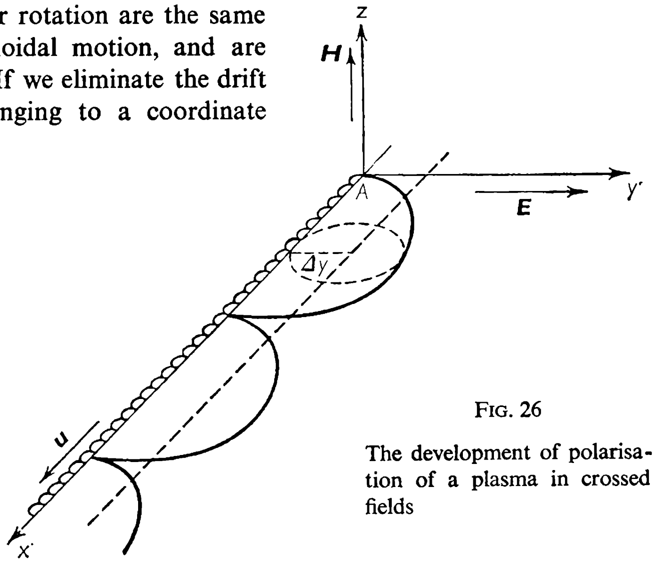

Fig. 26

The development of polarisation of a plasma in crossed fields

$$\Delta y = (mc/qH)(cE/H) = mc^2E/qH^2.$$

The ions are displaced in the direction of $E$, and the electrons in the opposite direction. The time-average polarisation per unit volume is

$$P \equiv ne(\Delta y_i - \Delta y_e) = n(m_i + m_e)c^2E/H^2.$$

From this it follows that

$$\varepsilon_m \equiv 1 + 4\pi P/E = 1 + 4\pi\rho c^2/H^2, \qquad \ldots\ldots\ldots(3.25)$$

where $\rho$ is the plasma mass density.

Even in comparatively rarefied plasma and with fairly high values of $H$, $\varepsilon_m$ can be very large. For instance with $n = 10^{10}$ cm$^{-3}$ and $H = 1000$ Oe, the transverse dielectric constant of deuterium plasma is about $10^2$. Thus the component of an applied electric field perpendicular to **H** is diminished many times on penetrating from a vacuum into a freely drifting plasma.

Equation (*3.25*) can also be derived from the general magnetohydrodynamic equations of a plasma, which are given in the next chapter. It there becomes apparent that the above expression for $\varepsilon_m$ can also be used to describe the behaviour of plasma in alternating electromagnetic fields provided that the frequency is low compared to the cyclotron frequency of the ions.† The design of the plasma capacitor (see Chapter VIII § **8.12**) is based on the high polarisability of plasma in crossed fields.

If the plasma drift velocity has a component perpendicular to a plasma boundary, conditions can be created (and regularly are created in steady-state conditions) which hinder the drift motion. Drift in a finite plasma normally leads to a redistribution of the number density of the particles; as a result, diffusion fluxes arise which counteract the drift motion. If the diffusion flux exactly balances the crossed-field drift, a stationary state is achieved in which the net flow of ions and electrons in the direction of $\boldsymbol{E}\times\boldsymbol{H}$ is zero. Plasma conductivity perpendicular to $\boldsymbol{H}$ is then re-established, and the current is related to the electric field strength by approximately the same relationship as applies when no transverse magnetic field is present. The correctness of this affirmation can be checked by analysing the expressions for the electron and ion drift motions.

Let $\boldsymbol{E}$ and $\boldsymbol{H}$ be parallel to the $x$ and $y$ axes respectively. Then the drift velocities in the direction $\boldsymbol{E}\times\boldsymbol{H}$ are the $z$ components of $\boldsymbol{u}_e$ and $\boldsymbol{u}_i$. It follows from (*3.22*) and (*3.23*) that the necessary condition for there being no drift along the $z$ axis is that the $x$-component of the total forces $\boldsymbol{F}_e$ and $\boldsymbol{F}_i$ should be zero. The factors which stop the drift parallel to the $z$ axis do not give rise to any new forces in the $x$-direction. We can thus write:

$$F_{ex} = -F_{ix} = -eE - m_e(u_{ex} - u_{ix})/\tau_{ei}.$$

Setting this equal to zero we obtain for the current $j$,

$$j = ne(u_{ix} - u_{ex}) = ne^2\tau_{ei}E/m_e$$

which is what had to be proved.

We shall leave to the next chapter a more detailed analysis of the connection between the current and the electric field in a plasma when there is a transverse magnetic field. However, we may note that quasi-stationary situations in which $\boldsymbol{E}$ is perpendicular to $\boldsymbol{H}$ and the transverse conductivity is re-established are typical of those methods of obtaining high-temperature plasma by means of high-current discharges.

It should also be noted that the crude analysis given above cannot bring out certain significant details of the conduction mechanism. One of the interesting prizes won by a more profound analysis of transport processes in fully ionised plasma is the prediction of a residual anisotropy of the electrical conductivity for the case when the transverse conductivity is re-established. This anisotropy is such that the conductivity parallel to $\boldsymbol{H}$ is twice that perpendicular to $\boldsymbol{H}$. This effect does not, unfortunately, admit of a simple interpretation. We can merely note that it is brought about by the specific character of Coulomb interaction between the particles. Because of this anisotropy of conductivity, the direction of current flow does not normally coincide with the direction of the applied electric field when a magnetic field is present. When the directions of $\boldsymbol{E}$ and $\boldsymbol{H}$ are arbitrary, the current density is given by:

---

† The above deduction of equation (*3.25*) is essentially not a magnetohydrodynamic one because the field $E$ is switched on instantaneously (i.e. in a time short compared to the ion cyclotron period). As a consequence, the field itself imparts a cycloidal motion to the particles, which doubles the energy stored in the plasma compared with that expected from the standard expression $\varepsilon_m E^2/8\pi$. In the magnetohydrodynamic approximation, the field must be switched on in a time long by comparison with the ion cyclotron period; any circular motion of the particles is then only their initial thermal motion, and the energy discrepancy is removed.

$$\boldsymbol{j} = \sigma_{\parallel}\boldsymbol{E}_{\parallel} + \sigma_{\perp}\boldsymbol{E}_{\perp}, \qquad \text{.........}(3.26)$$

where $\boldsymbol{E}_{\parallel}$ and $\boldsymbol{E}_{\perp}$ are the components of $\boldsymbol{E}$ parallel and perpendicular to $\boldsymbol{H}$, and $\sigma_{\parallel}$ and $\sigma_{\perp}$ are the corresponding values of the conductivity. Because $\sigma_{\parallel} = 2\sigma_{\perp}$, the vector $\boldsymbol{j}$ is inclined to the magnetic lines of force at a lesser angle than is the vector $\boldsymbol{E}$.

As we shall see later, the anisotropic conductivity and its related effects can be important in high current pulsed discharges. Experimental data show that in such discharges $\sigma_{\perp}$ is many times less than $\sigma_{\parallel}$. This result is very different from the theoretical predictions given above. The reason for the discrepancy is that the plasma in these experimental installations is not always sufficiently stable.

§ **3.4** A strong magnetic field also markedly affects the character of plasma diffusion across the field. In the absence of a magnetic field, an increase in the rate of collisions between the particles is a factor which reduces the rate of diffusion. When considering the transverse diffusion of plasma in a strong uniform magnetic field, however, we encounter the opposite situation: if the electrons and ions did not collide with one another at all, they could move freely only along the magnetic lines of force, and there would be no diffusion perpendicular to $\boldsymbol{H}$; the diffusion of particles across the field becomes possible only because of collisions (that is, assuming there are no instabilities). A rough estimate of the diffusion coefficient can be obtained by very simple arguments. Suppose that during time $\tau$ a particle effectively undergoes one collision which on average displaces it normal to the lines of force by a distance roughly equal to the Larmor radius $\rho_H$. By the laws of statistics, when the particle has undergone a large number of uncorrelated collisions, one adds the squares of the individual displacements to obtain the square of the total displacement. Thus, during time $t$ a particle will be displaced normal to the magnetic field by distance $x$:

$$x \approx \rho_H\sqrt{t/\tau}.$$

This displacement is simply Brownian motion of the particles in the direction normal to $H$. In terms of a diffusion coefficient $D_\perp$, the mean displacement over time $t$ is about $\sqrt{D_\perp t}$. Thus

$$D_\perp \approx \rho_H^2/\tau \simeq \lambda v/(\omega_H \tau)^2. \qquad \text{.........(3.27)}$$

In a fully ionised plasma, $\tau$ is proportional to $T^{\frac{3}{2}}$; therefore

$$D_\perp \propto n/H^2 T^{\frac{1}{2}}.$$

When $H$ and $T$ are large, $D_\perp$ is very small. This means that for high-temperature plasma in a state of equilibrium in a strong magnetic field, diffusion across the lines of force can, in theory, be reduced to a value at which it is no longer a major factor limiting the life-time of fast particles in a plasma.

As with other transport processes, diffusion along the lines of force is the same as when $H = 0$. Therefore a plasma in a strong magnetic field behaves with respect to diffusion processes as a very anisotropic medium.

This qualitative estimate of the diffusion rate across a magnetic field leaves unexplained certain essential features of the diffusion process. One important peculiarity is that diffusion is caused only by collisions between particles of different types, i.e. collisions between ions and electrons. Collisions between identical particles cannot lead to macroscopic changes in the spatial distribution of particles.

This statement can be proved as follows. Let us define the position of a particle by means of the radius vector $\boldsymbol{r}$ joining the particle to the centre of its Larmor orbit. This vector is proportional to the particle momentum $\boldsymbol{p}$, and is at right angles to it; viz., $\boldsymbol{r} = (\boldsymbol{p} \times \boldsymbol{H})/qH^2$. The sense of the right angle is different for particles of different charge sign. When two particles collide the total momentum is conserved; therefore, if the colliding particles have charge $q$ of the same magnitude and sign, the vector $\boldsymbol{r}_1 + \boldsymbol{r}_2$ is also conserved. A study of Fig. 27 shows that in this case the mid-point of the line joining the centres of the Larmor orbits remains fixed in space during a collision. In Fig. 27, $S$ is the point where a collision occurs; $M$ is the mid-point of the line joining the centres of the Larmor orbits $O_1$ and $O_2$. In accordance with what has been said above, when the particles collide, the line $O_1O_2$ changes its magnitude and direction, but always goes through the point $M$. The straight dashed line, drawn through M, divides the plane perpendicular to $\boldsymbol{H}$ into two regions (I and II). The collision does not alter the distribution of particles between these regions because, if $O_1$ changes from region I to region II, then $O_2$ changes from region II to region I. This occurs whatever the direction of the boundary line may be. This behaviour of the particles means that no diffusion results from collisions between like particles.

One can see that these kinematic effects no longer occur when the collisions are between particles of different type; therefore such collisions lead to a change in the macroscopic distribution of the particles, i.e. to diffusion.

This peculiarity of the diffusion mechanism is automatically included in the formal derivation of the diffusion coefficient from the theory of particle drift in a magnetic field. In this derivation, the motion of particles of a given kind can be regarded as due to forces arising from the gradients of partial pressure. The electrons in a unit volume are acted on by the force grad $p_e$ per unit volume, where $p_e$ is the partial pressure of the electron constituent of the plasma; thus the mean force acting per electron is $-(1/n)$ grad $p_e$. Similarly, the mean force acting per ion is $-(1/n)$ grad $p_i$ ($p_i$ is the partial pressure of the ion constituent). Interaction of the particles through collisions manifests itself in the same way as with motion due to an electric field. Therefore the diffusion velocities of the electrons and ions are given by the formulae

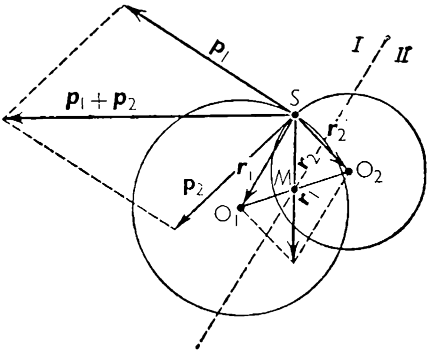

Fig. 27. Vector diagram of the collision of two identical particles in a magnetic field

$$\boldsymbol{u}_e = \frac{c}{eH^2}\left\{\left(\frac{\text{grad}\, p_e}{n}+\frac{m_e(\boldsymbol{u}_e-\boldsymbol{u}_i)}{\tau_{ei}}\right)\times\boldsymbol{H}\right\}, \qquad \text{.........(3.28)}$$

$$\boldsymbol{u}_i = \frac{c}{eH^2}\left\{\left(-\frac{\text{grad}\, p_i}{n}+\frac{m_e(\boldsymbol{u}_e-\boldsymbol{u}_i)}{\tau_{ei}}\right)\times\boldsymbol{H}\right\}. \qquad \text{.........(3.29)}$$

Suppose that the pressure gradient is in the $x$ direction and the field $\boldsymbol{H}$ is in the $z$ direction; then

$$u_{ex} = u_{ix} = \frac{m_e c}{eH\tau_{ei}}(u_{ey}-u_{iy}),$$

$$u_{iy}-u_{ey} = \frac{c}{eHn}\frac{\partial p}{\partial x},$$

where $p$ is the total pressure.

We will assume for the sake of simplicity that the temperature of the electrons and ions does not depend on $x$. The diffusion velocity of the two plasma constituents in the direction of grad $p$, perpendicular to $\boldsymbol{H}$, is then given by the expression

$$u_x = -\frac{m_e c^2}{e^2 H^2 \tau_{ei}} \frac{k}{n}(T_e + T_i)\frac{\partial n}{\partial x}. \qquad \text{.........}(3.30)$$

By definition

$$n u_x = -D_\perp \frac{\partial n}{\partial x}. \qquad \text{.........}(3.31)$$

Consequently

$$D_\perp = \frac{mc^2}{e^2 H^2 \tau_{ei}} k(T_e + T_i). \qquad \text{.........}(3.32)$$

Because $u_{ix} = u_{ex}$ it follows that the diffusion is ambipolar. By simple transformations the formula for $D_\perp$ can be written:

$$D_\perp = D_0 \frac{T_e + T_i}{T_e} \frac{1}{(\omega_{He}\tau_{ei})^2}, \qquad \text{.........}(3.33)$$

where $D_0 = \lambda v_e/3$ is the ordinary form for the diffusion coefficient encountered in the kinetic theory of gases, and $\omega_{He}$ is the electron cyclotron frequency. Strictly speaking, formula (*3.33*) is valid only when $\omega_{He}\tau_{ei} \gg 1$.

In the presence of a magnetic field $\boldsymbol{H}$, a transverse pressure gradient not only causes diffusion; it also produces an electric current perpendicular to grad $p$ and to $\boldsymbol{H}$. Using the above coordinate system, the magnitude of this current density is:

$$j = ne(u_{iy} - u_{ey}) = \frac{c}{H}\frac{\partial p}{\partial x}. \qquad \text{.........}(3.34)$$

This current is so directed that it reduces the magnetic field strength in the regions where $p$ is large. Because of the existence of this current, which flows along the lines of constant pressure, the plasma is diamagnetic; the pressure of the plasma pushes the magnetic force lines outwards; and indeed equation (*3.34*) is a simple form of equation (*1.22*).

The current determined by equation (*3.34*) is remarkable in a further respect: it plays the chief part in the re-establishment of the transverse electrical conductivity of plasma in crossed electric and magnetic fields. As discussed in § **3.3**, conductivity is re-established when the drift motion in crossed fields is counteracted by a diffusion flux. But this compensation can occur only because a pressure gradient is created in the plasma. This pressure gradient gives rise to a diffusion flux proportional to $\partial p/\partial x$, and also generates the current density $j$ which, as can easily be verified, flows in the direction of $\boldsymbol{E}$. Thus in the crossed-field conditions being considered, it is this current $j$, caused by the pressure gradient, which acts as the re-established conduction current.

By restricting the particle motion in the direction perpendicular to $\boldsymbol{H}$, the magnetic field reduces the transverse conduction of heat. In strong fields, the thermal conductivity perpendicular to $\boldsymbol{H}$ is many times less than in the absence of a field; parallel to the lines of force the thermal conductivity is unchanged. Therefore, the thermal conductivity of the plasma is markedly anisotropic in the presence of a strong magnetic field.

The conduction of heat across a strong magnetic field is due mainly to the ions, not to the electrons. Calculations for the case $\omega_{\mathrm{Hi}}\tau_{\mathrm{ii}} \gg 1$ provide the following expression for the thermal conductivity $\sigma_{\mathrm{T}}$ of hydrogen plasma in the direction perpendicular to $\boldsymbol{H}$:

$$\sigma_{\mathrm{T}} = 2\times 10^{-16} n^2/H^2\sqrt{T_{\mathrm{i}}}, \qquad \mathrm{erg\ sec^{-1}\ deg^{-1}\ cm^{-1}}. \tag{3.35}$$

A comparison of (*3.35*) with (*1.6*) shows that in a strong magnetic field the transverse thermal conductivity is approximately $50(\omega_{\mathrm{Hi}}\tau_{\mathrm{ii}})^2$ times less than the field-free value. With $T_{\mathrm{e}} = T_{\mathrm{i}} = 10^8$ °K, $n = 10^{14}$ cm$^{-3}$ and $H = 10^4$ Oe, $\sigma_{\mathrm{T}}$ is reduced by 14 orders of magnitude.

Although the above 'classical' theory of transport processes in a magnetic plasma was worked out some decades ago, it has still not been properly vindicated by experiment. Indeed, there is much to indicate that the formulae defining the coefficients of diffusion and thermal conduction in a transverse field do not correspond to what is observed experimentally; to be more precise, observations indicate that the theory can be regarded as valid only in certain very limited conditions which are of no real interest to us (weakly ionised, cold plasma with low electron number-density situated in a comparatively weak magnetic field).

From an analysis of experimental results obtained when investigating low-voltage low-pressure arc-discharges in strong fields, Bohm, in 1948, reached the conclusion that plasma diffuses across the lines of force far more quickly than suggested by the classical calculation of the diffusion rate, which takes account only of binary collisions between particles.

To explain this discrepancy between theory and experiment, Bohm advanced the supposition that, besides the classical mechanism of diffusion, there is a completely different mechanism associated with collective motion in the plasma. It is customary to connect this postulated but still undiscovered mechanism with a somewhat vague hypothesis as to the 'turbulence' which is alleged to be an incurable feature of a magnetised plasma. So far there have been no definite results from all the attempts to find a universal mechanism of collective motion which can explain the enhanced diffusion rate. Up to now these attempts have borne only one fruit—an expression for the coefficient of turbulent diffusion which Bohm postulated without giving any theoretical basis. Its form is as follows

$$D_{\perp} = ckT/16eH.$$

We cannot at this time attach great importance to this essentially empirical formula because it is based mainly on the results of early experiments, whose interpretation can still not be regarded as unambiguous.†

---

† However, it must be allowed that recent measurements of particle leakage in Stellarators (§§ **8.5**, **8.6**) during ohmic heating are in satisfactory agreement with Bohm's formula if the numerical coefficient in the formula is increased by approximately three times (see W. Stodiek *et al.*, *Nuclear Fusion* Suppl. **1**, 193, 1963).

Over the last few years, there have been a number of experimental studies of plasma diffusion in magnetic fields, using ordinary low-power discharges in rarefied gases. Measurements have been made of diffusion across a field in the positive column of a decaying discharge, and of diffusion in a hot-cathode arc discharge (in this case the plasma is traversed by a beam of fast electrons from the cathode). According to Lehnert's results, when the number density of charged particles is low and the field strength is below a certain critical value, the diffusion rate in a positive column conforms to the prediction of classical theory. When $H$ is increased above the critical value, the diffusion coefficient increases greatly and becomes many times larger than the value given by equation *(3.32)*. At the same time the shape of the positive column changes and it acquires a helical structure. Kadomtsev and Nedospasov accounted for this effect by invoking an instability of the plasma column associated with the radial gradient of the number density. Thus, in this case, there is a specific mechanism of anomalous diffusion which has no direct relation to the assumed universal turbulence.

Using an ingenious electro-optical technique (the 'plasmascope'), Zharinov has observed the behaviour of a plasma column formed by an intense hot-cathode discharge in hydrogen. He discovered that, when there is a strong axial magnetic field, the plasma column does not have cylindrical symmetry and is not stable. The instability consists of the formation of curious plasma protuberances, which rotate at high speed, on the lateral surface of the plasma column which initially is well defined from the surrounding space. Plate I shows successive stages in the formation of these protuberances. Up to the present, no convincing explanation of these results has been given; but they can also be regarded as a manifestation of one of the possible forms of anomalous diffusion. However, we cannot find here any correspondence with the Bohm formula.

Later, when we come to analyse the processes that take place in various devices built to obtain and confine high-temperature plasma, we shall frequently return to the question of what laws govern the diffusion of plasma across a magnetic field. We shall then see that the character of the diffusion processes cannot be separated from the empirical properties of the devices under investigation, because the diffusion rate depends on the specific forms of instability which afflict the plasma in the particular conditions of each experiment.

## CHAPTER IV

# THE MAGNETOHYDRODYNAMIC THEORY OF PLASMA

§ **4.1** The theoretical calculations in the preceding chapter are concerned with transport processes in a plasma in the presence of a strong magnetic field. The results could also have been obtained by using a more general method which is very useful for analysing various problems in plasma statics and dynamics.

By using this general method, which is based on the Boltzmann equation, it is possible to obtain the basic equations of plasma dynamics in a form which is referred to as the 'magnetohydrodynamic approximation'. This term is justified because, according to these equations, a plasma should behave like an electrically conducting fluid; or more exactly, like a mixture of two conducting fluids. By analysing the various processes which give rise to motion in a plasma, it can be shown that in many instances one can make use of this analogy and apply the methods of magnetohydrodynamics which provide a general description of the phenomena occurring in a conducting fluid acted upon by external fields.

The two fluids making up the plasma are the electron constituent and the ion constituent. We shall assume in what follows that they are uniformly mixed with equal number densities of singly-charged ions and electrons, so that the plasma is everywhere quasi-neutral. The two fluids interact because space charge electric fields, which maintain the quasi-neutrality, arise from otherwise negligible differences between the two number densities; and also because of the frictional forces arising from the motion of the fluids relative to each other.

The basic equations of magnetohydrodynamics which characterise the behaviour of the two constituents are as follows:

$$\rho_e \frac{d\boldsymbol{v}_e}{dt} = -ne\left(\boldsymbol{E}+\frac{1}{c}\boldsymbol{v}_e\times\boldsymbol{H}\right)-\operatorname{grad} p_e-\boldsymbol{F}_{ei}, \qquad \text{.........}(4.1)$$

$$\rho_i \frac{d\boldsymbol{v}_i}{dt} = ne\left(\boldsymbol{E}+\frac{1}{c}\boldsymbol{v}_i\times\boldsymbol{H}\right)-\operatorname{grad} p_i+\boldsymbol{F}_{ei}. \qquad \text{.........}(4.2)$$

In these equations, $\rho_e$, $\rho_i$ is the mass density, $\boldsymbol{v}_e$, $\boldsymbol{v}_i$ the velocity and $p_e$, $p_i$ the pressure of the electron and the ion constituent respectively. $\boldsymbol{F}_{ei}$ represents the frictional force exerted by the ions on the electrons, and $n$ is the number density of each constituent.

Equations *(4.1)* and *(4.2)* are expressions of Newton's second law, in which all the quantities refer to a unit volume of the plasma. The quantities on the right-hand side of each equation represent the forces acting upon all the particles of a given type in a unit volume. These forces arise from the presence of an electromagnetic field, a pressure gradient and collisions with particles of the other plasma constituent.

It is assumed that the pressure is isotropic so that the force due to a pressure drop can be characterised by the gradient of a scalar. In reality, this is not always so. In particular, isotropic pressures do not occur in a broad class of experimental devices, the so-called 'magnetic mirror traps'. For this reason, one may use equations (*4.1*) and (*4.2*) to analyse such systems only after an appropriate modification of the terms representing the pressure forces. The conditions in which the anisotropy of the pressure must be considered will be discussed in Chapter VIII; in the remaining chapters, we shall use equations (*4.1*) and (*4.2*) in the form given above.

The expression for the frictional force $\boldsymbol{F}_{\mathrm{ei}}$ may be related to the current density in the plasma. It is evident that

$$\boldsymbol{F}_{\mathrm{ei}} = \frac{\rho_{\mathrm{e}}(\boldsymbol{v}_{\mathrm{e}}-\boldsymbol{v}_{\mathrm{i}})}{\tau_{\mathrm{ei}}}, \qquad \rho_{\mathrm{e}} = m_{\mathrm{e}}n, \qquad \text{.........}(4.3)$$

$$\boldsymbol{j} = ne(\boldsymbol{v}_{\mathrm{i}}-\boldsymbol{v}_{\mathrm{e}}). \qquad \text{.........}(4.4)$$

Hence

$$\boldsymbol{F}_{\mathrm{ei}} = -\frac{m_{\mathrm{e}}}{e\tau_{\mathrm{ei}}}\boldsymbol{j} = -\frac{ne}{\sigma}\boldsymbol{j}. \qquad \text{.........}(4.5)$$

When the behaviour of a quasi-neutral plasma is studied, it is not always necessary to treat the electron and the ion constituents separately. Thanks to the quasi-neutrality, the plasma usually behaves to a first approximation as a homogeneous conducting fluid whose state at every point is characterised by the mass density $\rho$, the velocity $\boldsymbol{v}$ and the current density $\boldsymbol{j}$, where $\boldsymbol{v}$ and $\rho$ are defined by the relations

$$\rho = n(m_{\mathrm{e}}+m_{\mathrm{i}}), \qquad nm_{\mathrm{i}} = \rho_{\mathrm{i}}, \qquad \text{.........}(4.6)$$

$$\boldsymbol{v} = \frac{1}{\rho}(\rho_{\mathrm{e}}\boldsymbol{v}_{\mathrm{e}}+\rho_{\mathrm{i}}\boldsymbol{v}_{\mathrm{i}}). \qquad \text{.........}(4.7)$$

In practically all cases where the plasma moves as a whole, $\boldsymbol{v} = \boldsymbol{v}_{\mathrm{i}}$ to a high degree of approximation.

In this approach, the basic equation of motion should express the velocity $\boldsymbol{v}$ as a function of the forces. Combining equations (*4.1*) and (*4.2*) and taking into account (*4.6*) and (*4.7*), we find:

$$\rho\frac{d\boldsymbol{v}}{dt} = \frac{1}{c}\boldsymbol{j}\times\boldsymbol{H}-\mathrm{grad}\, p. \qquad \text{.........}(4.8)$$

This is the fundamental equation of magnetohydrodynamics. The quantity $p$ represents the total plasma pressure ($p = p_{\mathrm{e}}+p_{\mathrm{i}}$).

In order to obtain a complete system of equations describing variations in the properties of the plasma and changes in the field caused by the motion of the plasma, the continuity equation

$$\frac{\partial \rho}{\partial t}+\operatorname{div}(\rho \boldsymbol{v}) = 0 \qquad \text{.........}(4.9)$$

must be added to equation (*4.8*), as well as the Maxwell equations:

$$\operatorname{curl} \boldsymbol{H} = \frac{4\pi}{c}\boldsymbol{j}, \qquad \text{.........}(4.10)$$

$$\operatorname{div} \boldsymbol{H} = 0, \qquad \text{.........}(4.11)$$

$$\operatorname{curl} \boldsymbol{E} = -\frac{1}{c}\frac{\partial \boldsymbol{H}}{\partial t}, \qquad \text{.........}(4.12)$$

$$\operatorname{div} \boldsymbol{E} = 4\pi e(n_i - n_e). \qquad \text{.........}(4.13)$$

In almost all cases of interest to us, the neglect of the displacement current is justified.†

The above system of equations is not complete, since it does not permit a unique determination of the parameters characterising the state of the plasma. $\boldsymbol{E}$ and $\boldsymbol{H}$ may be found from Maxwell's equations if the current density is given as a function of space and time. Therefore, only two equations remain for the determination of the four quantities $\boldsymbol{j}$, $\boldsymbol{v}$, $p$ and $\rho$.

One of the missing equations is a relation between the current density and the strength of the electric and magnetic fields. In magnetohydrodynamics, it is usually assumed that Ohm's law is valid in a coordinate system moving with the fluid. On this assumption,

$$\boldsymbol{j} = \sigma \boldsymbol{E}', \qquad \text{.........}(4.14)$$

where $\boldsymbol{E}'$ is the electric field strength in the moving coordinate system and $\sigma$ is the electrical conductivity. Using the equality

$$\boldsymbol{E}' = \boldsymbol{E}+\frac{1}{c}\boldsymbol{v}\times\boldsymbol{H} \qquad \text{.........}(4.15)$$

one can obtain the following expression for the current density:

$$\boldsymbol{j} = \sigma\left(\boldsymbol{E}+\frac{1}{c}\boldsymbol{v}\times\boldsymbol{H}\right). \qquad \text{.........}(4.16)$$

The derivation of this formula is based on the assumption that the magnetic field does not affect the conductivity of the fluid directly: the effect of the magnetic field is assumed to be confined to a change of the electric field strength in the moving fluid. This assumption is generally valid for the description of phenomena occurring in a conventional conducting fluid, such as a liquid metal. However, it is not at all evident *a priori* that the relation (*4.14*) should also be valid for an ionised gas. As discussed in § **3.3**, the magnetic field has a direct effect upon the conductivity of an ionised gas, and the relation between $j$ and $E'$ can therefore be very complex, especially for non-stationary processes. In order to determine the nature of this relation in the general case, we return to the equations characterising the behaviour of both plasma components. Multiplying equation (*4.1*) by $e/m_e$ and (*4.2*) by $e/m_i$ and subtracting one from the other, we obtain:

---

† This approximation is valid at low frequencies when $H^2/4\pi\rho \ll c^2$.

$$\frac{dj}{dt}-\frac{j}{n}\frac{dn}{dt} = \frac{ne^2}{m_e}\left(E+\frac{1}{c}v\times H\right)-\frac{e}{m_e c}j\times H+\frac{e}{m_e}\operatorname{grad} p_e-\frac{j}{\tau_{ei}}. \qquad \text{.........}(4.17)$$

Terms of the order of $m_e/m_i$ are neglected on the right-hand side of this expression. Using equation (*3.9*) and assuming that the number density changes much more slowly than does the current density $j$, one can write equation (*4.17*) in the form

$$j+\tau_{ei}\frac{dj}{dt} = \sigma\left(E+\frac{1}{c}v\times H+\frac{\operatorname{grad} p_e}{ne}-\frac{1}{nec}j\times H\right). \qquad \text{.........}(4.18)$$

This relation is Ohm's law generalised to the case of a plasma in a magnetic field. In the special case where the current flows parallel to the magnetic field and where there is no pressure gradient, equation (*4.18*) agrees with equation (*3.6*) derived in the preceding chapter, with the exception that $E$ is replaced by $E'$.

When the current density changes appreciably in a time much greater than the electron-ion collision time $\tau_{ei}$, then the second term on the left-hand side of equation (*4.18*) can be neglected. In this case, however, the equation for $j$ differs from the simple Ohm's law because of the presence of additional terms on the right-hand side; the first of these terms is proportional to the gradient of the electron pressure, and the second contains the vector product $j\times H$. These terms have a simple physical interpretation. The quantity grad $p$ appears in the expression for $j$ because the current density may be produced not only by an electric field, but also by differences between the electron pressures at different points in space. The term containing $j\times H$ expresses the influence of the magnetic field on the motion of the electrons in the plasma.†

Owing to the presence of these additional terms there is, generally speaking, no definite relation between the current density and the electric field: for given values of $E' = E+(v\times H)/c$ and $\sigma$, the current density may have wide variations. This indefiniteness is substantially reduced when the plasma is in a quasi-stationary state, i.e. when the relative change in the current during the time $\tau_{ei}$ is small and when

$$\left|\rho\frac{dv}{dt}\right| \ll |\operatorname{grad} p|.$$

---

† The effect represented by this term is closely analogous to the Hall effect in ordinary conductors.

In the quasi-stationary state, the fundamental equations (*4.8*) and (*4.18*) take the form

$$\frac{1}{c}\boldsymbol{j}\times\boldsymbol{H} = \text{grad } p, \qquad \text{.........}(4.19)$$

$$= \sigma\left(\boldsymbol{E}+\frac{1}{c}\boldsymbol{v}\times\boldsymbol{H}-\frac{1}{ne}\text{ grad } p_i\right). \qquad \text{.........}(4.20)$$

Making the natural assumption that grad $p_e$ and grad $p_i$ are parallel to each other, we find from (*4.19*) that grad $p_i$ is perpendicular to $\boldsymbol{j}$. Turning to (*4.20*) we see that $\boldsymbol{E}'$ can be resolved into two mutually perpendicular components, $\boldsymbol{E}'_{\parallel}$ and $\boldsymbol{E}'_{\perp}$ : $\boldsymbol{E}'_{\parallel}$ is parallel to $\boldsymbol{j}$, and $\boldsymbol{E}'_{\perp}$ is parallel to grad $p_i$. From equation (*4.20*) we have

$$\boldsymbol{j} = \sigma\boldsymbol{E}'_{\parallel}.$$

Consequently, Ohm's law is valid for the component $\boldsymbol{E}'_{\parallel}$. The component $\boldsymbol{E}'_{\perp}$ does not produce a current; it balances the ionic pressure gradient

$$\boldsymbol{E}'_{\perp} = (\text{grad } p_i)/ne. \qquad \text{.........}(4.21)$$

The physical meaning of these results can be deduced from a few simple considerations. Since the current is created by the electrons, the $\boldsymbol{j}\times\boldsymbol{H}$ force acting on the plasma is exerted on the electron gas. In particular, this force creates gradients in the electron pressure $p_e$. By reason of the requirement of quasi-neutrality, $p_i$ follows changes in $p_e$. However, the gradient of $p_i$ can be sustained only if another force prevents an equalisation of the ion pressures. This force must be oriented in the same direction as grad $p_i$, i.e. perpendicular to $\boldsymbol{j}$ and $\boldsymbol{H}$. Such a force is precisely provided by $\boldsymbol{E}'_{\perp}$, the electric field component perpendicular to $\boldsymbol{j}$. It ensures the conservation of the quasi-neutrality of the plasma by preventing the separation of the ions from the electrons. Ohm's law obviously does not apply to this component of the electric field. When the plasma is stationary (static case), Ohm's law in its usual form applies to the electric field component parallel to the current:

$$\boldsymbol{j} = \sigma\boldsymbol{E}_{\parallel}.$$

At this point, we terminate our discussion of the relationship between the current and the field strength by noting that the anisotropy of the electrical conductivity (equation (*3.26*)) was ignored in the above considerations so as not to complicate the arguments.

At least one more relation, independent of those given above, is necessary for a complete solution of problems in plasma dynamics; for example, a relation between the plasma density and the pressure would serve the purpose. A universal law of this kind does not exist, however, and in order to go much further in the general formulation of the problem it is necessary to make use of the equation of state of the plasma. Specifically, assuming that $T_e = T_i = T$ and that the plasma is an ideal gas, this equation can be written as follows:

$$p = 2nkT. \qquad \text{.........}(4.22)$$

Thus, yet another parameter appears—the plasma temperature; and it is necessary to introduce another equation, one which describes the thermal balance of the plasma. However we shall not here consider a general analysis of the thermal balance, because in studying specific cases one can often use simple integral relations which follow from the particular circumstances of each case.

The magnetohydrodynamic approximation, which represents the plasma as a conducting fluid or a mixture of two fluids, is applicable only when certain conditions are satisfied. These are:

(1) the dimensions of the region occupied by the plasma should be much larger than a characteristic length—the Debye shielding distance. Otherwise, the particle density is too low to ensure the maintenance of quasi-neutrality by electrostatic interactions.

(2) the Larmor radii of the electrons and ions in the magnetic field should be much smaller than the dimensions of the plasma and the distances over which there are appreciable changes in the magnitude of the field strength. Strictly speaking, this condition is not absolutely necessary, and deviations therefrom do not invalidate the magneto-hydrodynamic equations. On the other hand, if this condition is not fulfilled, the concept of a plasma boundary is obscured, and the graphic analogy between the properties of a plasma and those of an ordinary fluid is impaired.

§ **4.2** Let us now turn our attention to the consequences of the fundamental equations characterising the state of a plasma in an electromagnetic field. Here we will deal only with quasi-stationary states without touching upon the question of their stability. In the static case, the pressure gradient is perpendicular to $\boldsymbol{H}$. Hence, the plasma pressure must be constant along the lines of magnetic force. For the case where the lines of force are straight and parallel to each other, it is possible to obtain from equation (*4.19*) a formula relating the pressure to the field strength. Let the $z$ axis be parallel to the lines of force. Then $\boldsymbol{H}$ will have only the component $H_z$, whose value is a function of $x$ and $y$ and is independent of $z$ (due to the condition $\operatorname{div} \boldsymbol{H} = 0$).

From equations (*4.10*) and (*4.19*) it follows that in a quasi-stationary state

$$\operatorname{grad} p = \frac{1}{4\pi}[\operatorname{curl} \boldsymbol{H}] \times \boldsymbol{H}. \qquad \text{.........}(4.23)$$

In the present case, the components of the pressure gradient are given by

$$\frac{\partial p}{\partial x} = -\frac{1}{4\pi} H_z \frac{\partial H_z}{\partial x} = -\frac{1}{8\pi}\frac{\partial}{\partial x} H_z^2,$$

$$\frac{\partial p}{\partial y} = -\frac{1}{4\pi} H_z \frac{\partial H_z}{\partial y} = -\frac{1}{8\pi}\frac{\partial}{\partial y} H_z^2.$$

Therefore,

$$\frac{\partial}{\partial x}\left(p+\frac{1}{8\pi}H^2\right) = \frac{\partial}{\partial y}\left(p+\frac{1}{8\pi}H^2\right) = 0.$$

Consequently,

$$p+\frac{1}{8\pi}H^2 = \text{const.} \qquad \text{.........}(4.24)$$

This result is interesting from a number of viewpoints. First, it follows that a plasma is diamagnetic, since the field strength within the plasma is less than that outside. Second, the equation (*4.24*) is the mathematical expression of the idea of confining a plasma by means of a magnetic field. The magnetic pressure outside the plasma is greater than the magnetic pressure inside by the value of the kinetic pressure of the plasma.

Relatively speaking, the plasma pressure attains its greatest value $p_{\max}$ when the field inside the plasma becomes zero; that is:

$$p_{\max} = \frac{H_0^2}{8\pi}, \qquad \text{.........}(4.25)$$

where $H_0$ is the field strength just outside the plasma boundary.

The pressure balance equations (*4.24*) and (*4.25*) are also valid if the external magnetic field has a curvature, provided that the magnetic field within the plasma is zero; then the kinetic pressure $p$ is constant within the plasma, and drops abruptly to zero at its boundary. However, in the general case of curved fields, the sum of the kinetic pressure and magnetic pressure $H^2/8\pi$ is not a constant. Even then, as can easily be shown, the pressure-balance relation (*4.24*) remains valid if it is taken as a boundary condition: if there is a pressure jump at the plasma surface, the relation

$$p+H_i^2/8\pi = H_0^2/8\pi \qquad \text{.........}(4.26)$$

should apply, where $H_i$ and $H_0$ are the field strengths on the two sides of the boundary.

With equations (*4.10*), (*4.11*) and (*4.19*) it is possible to examine the conditions for the existence of a wide range of quasi-stationary, or—as they are often called—equilibrium plasma configurations. The simplest example of such a configuration is an infinite cylindrical column of plasma surrounded by a vacuum and confined by electrodynamic forces created by a current flowing in the axial direction through the plasma—the so-called 'pinch'.

In this case, $H$ and $p$ depend only on the radial coordinate $r$. The current density is related to the field strength by the expression

$$j = \frac{c}{4\pi r}\frac{d}{dr}Hr.$$

Hence, (*4.23*) reduces to

$$-\frac{dp}{dr} = \frac{H}{4\pi r}\frac{d}{dr}Hr. \qquad \text{.........}(4.27)$$

Multiplying both sides of this relation by $r^2$ and integrating between $r = 0$ and $r = a$, where $a$ is the radius of the plasma column:

$$-\int_0^a \frac{dp}{dr} r^2\, dr = \frac{1}{4\pi}\int_0^a Hr\frac{d}{dr} Hr\, dr. \qquad \text{.........}(4.28)$$

The right-hand side of this equation can be expressed in terms of the total pinch current $J$:

$$\frac{a^2}{8\pi}H^2(a) = \frac{J^2}{2\pi c^2}.$$

The left-hand side of (*4.28*) can be transformed as follows:

$$-\int_0^a \frac{dp}{dr} r^2\, dr = 2\int_0^a pr\, dr = S\bar{p}/\pi.$$

Here $\bar{p}$ is the mean plasma pressure and $S = \pi a^2$ is the cross-sectional area of the plasma column. Consequently, irrespective of the radial distributions of the current density and the pressure inside the plasma, the following general relation applies:

$$\bar{p} = J^2/2c^2S. \qquad \text{.........}(4.29)$$

According to (*4.22*),

$$\bar{p} = \frac{4k}{a^2}\int_0^a nTr\, dr. \qquad \text{.........}(4.30)$$

In general, $T$ designates $(T_e+T_i)/2$.

A detailed analysis of the diffusion and heat transfer processes in the plasma column leads to the conclusion that, in spite of the presence of the current-generated magnetic field which sharply reduces the heat conductivity of the plasma, a uniform temperature across the pinch is established very quickly under quasi-stationary conditions. In contrast, particle diffusion takes place very slowly. Thus, the radial pressure gradient is essentially determined by spatial variations in the density, whereas the temperature $T$ is virtually constant over the whole cross section. For this reason, $T$ can be brought outside the integral (*4.30*), which then becomes

$$\bar{p} = \frac{2kT}{\pi a^2}\int_0^a 2\pi nr\, dr = \frac{2kT}{S}N,$$

where $N$ is the total number of electrons per unit length of the plasma column. Substituting this expression for $\bar{p}$ in (*4.29*), we obtain

$$T = \frac{J^2}{4c^2kN}. \qquad \text{.........}(4.31)$$

It should be emphasized that this formula has been obtained on the basis of very general assumptions.

An examination of the energy transfer between ions and electrons (§ **2.5**) in a plasma shows that for $N \gtrsim 10^{16}$ cm$^{-1}$, $T_e$ and $T_i$ are usually rather close to each other, and $T$ then simply represents the plasma temperature.

Equation (*4.31*) does not, of course, constitute a definitive description of the properties of the plasma column. A complete description would involve all the parameters characterising the properties of the plasma expressed as functions of radius $r$ and time $t$. The variation of the effective plasma radius with time is a matter of particular interest. To determine this, it is necessary to use the complete set of magnetohydrodynamic equations together with the energy balance equation. A detailed exposition of the complete time-dependent theory of the pinch effect is outside the scope of this work; we confine ourselves to only a few brief observations.

In a perfectly confined plasma, the sources of energy are the Joule heating and the work done by the electrodynamic forces, while the losses are due to radiation. Let us consider the simplest case where the radius of the plasma column remains constant, and neglect the loss by radiation. Under these conditions, the energy stored in the plasma will increase, owing to the Joule heating. For the radius $a$ to remain constant, the current must increase with time, because at constant current with a constant radius, the kinetic pressure rises with time and cannot be balanced by a constant magnetic pressure.

The energy equation for a unit length of the plasma column has the following form:

$$3Nk\frac{dT}{dt} = \int_0^a \frac{j^2}{\sigma} 2\pi r\, dr. \qquad \text{.........}(4.32)$$

The conductivity $\sigma$ of the plasma is a function of temperature only, and can therefore be placed in front of the integral sign. The remaining integral

$$2\pi \int_0^a j^2 r\, dr \qquad \text{.........}(4.33)$$

depends upon the current distribution in the plasma.

In the absence of the skin effect, $j$ is independent of radius and the integral (*4.33*) becomes

$$j^2 \pi a^2 = \frac{J^2}{\pi a^2}. \qquad \text{.........}(4.34)$$

However, with a rising current, the skin effect should lead to a redistribution of the current over the cross section, and the true value of the integral (*4.33*) should therefore differ from (*4.34*) by some numerical factor greater than unity. Designating this factor by $f$ and using equation (*3.10*) to determine $\sigma$, we can write the energy balance equation as follows:

$$3Nkb_0T^{3/2}\frac{dT}{dt} = \frac{J^2}{\pi a^2}f, \qquad \text{.........}(4.35)$$

where $b_0$ is the numerical coefficient in (*3.10*). Taking (*4.31*) into account, we obtain

$$\frac{3}{2}T^{1/2}\frac{dT}{dt} = \frac{2fc^2}{\pi a^2 b_0}.$$

Integrating this equation yields

$$T^{3/2} = \frac{2fc^2}{\pi a^2 b_0}t.$$

Here $t$ is time measured from the start of heating.

Thus, the temperature in a column of constant radius will vary as $t^{2/3}$, and it follows that the current should increase as $t^{1/3}$:

$$J = At^{1/3}\ \text{(e.s.u.)}, \quad \text{where} \quad A = 3{\cdot}6\times 10^7\ N^{1/2}/a^{2/3}. \qquad \text{.........}(4.36)$$

The smaller the radius of the pinch, the faster must the current increase if the equilibrium between the kinetic and magnetic pressure is to be preserved. The distribution of the current in the plasma may be obtained from the solution of Maxwell's equations. The factor $f$ in the present case is close to unity.

If the radius of the pinch changes with time, the energy balance should also take into account the work done by the electrodynamic forces. As is shown by a calculation which considers this additional source of energy, equation (*4.36*) (which relates $J$ to $a$ and $t$) remains approximately valid when $a$ changes as the current increases. Here, however, the factor $f$ may differ substantially from unity.

At high current densities, the energy loss due to bremsstrahlung radiation becomes of major importance. Let us compare this loss with the Joule heating. According to equation (*1.8*), the energy radiated per unit time per unit length in a plasma pinch is

$$\Delta Q_{\text{rad}} = 1{\cdot}6\times 10^{-27}\pi a^2\overline{n^2}\sqrt{T}.$$

Here $\overline{n^2}$ is the mean square number density within the radius $a$. To a rough approximation, it may be assumed that $n$ varies as $- r^2$ (this is valid in the absence of the skin effect), so that $\overline{n^2} = 4N^2/3\pi^2a^4$; therefore,

$$\Delta Q_{\text{rad}} = 2{\cdot}1\times 10^{-27}N^2\sqrt{T}/\pi a^2. \qquad \text{.........}(4.37)$$

With this particular assumption, the rate of Joule heating is

$$\Delta Q_{\text{Joule}} = J^2/\pi a^2\sigma = 2{\cdot}2\times10^{-7}J^2/\pi a^2T^{3/2}. \qquad \ldots\ldots\ldots(4.38)$$

The ratio of these two quantities is a function of the current alone:

$$\Delta Q_{\text{rad}}/\Delta Q_{\text{Joule}} = 0{\cdot}4\times10^{-31}J^2 \qquad (J \text{ in e.s.u.});$$

it becomes unity at a current of about $2\times10^6$ Amp. This value of the limiting current, at which any further rise of temperature due to Joule heating should cease, was derived by Braginskii in the U.S.S.R. and by Pease in Great Britain. At currents of the order of $10^5$ A, the bremsstrahlung radiation from a hydrogen plasma should play virtually no part whatever in the energy balance.

The magnetohydrodynamic theory of quasi-stationary high-current pinch processes has not yet been verified experimentally, because it has so far been impossible to obtain a quasi-stationary column of completely ionised plasma heated to a high enough temperature and confined only by the self-magnetic field of the current. The results of experiments involving the heating of plasmas in high-current gas discharges will be discussed in the following chapters.

§ **4.3** With practical applications in view it is obvious that closed systems without electrodes are among the most interesting of the various conceivable plasma configurations. The simplest system of such a type is the plasma torus in a surrounding magnetic field. Such a configuration is the first idea that occurs to an inventor trying to give practical expression to the concept of magnetic confinement.

Suppose that the magnetic field has only the component $H_\theta$ (Fig. 28), so that the lines of force constitute circles the centres of which lie on the major axis $z$. In general the field strength and the plasma pressure will be some function of $z$ and the distance $r$ from the major axis. From the fundamental equilibrium equation (*4.23*), it follows that:

$$\frac{\partial p}{\partial r} = -\frac{H_\theta}{4\pi r}\frac{\partial}{\partial r}rH_\theta, \qquad \ldots\ldots\ldots(4.39)$$

$$\frac{\partial p}{\partial z} = -\frac{H_\theta}{4\pi}\frac{\partial H_\theta}{\partial z}. \qquad \ldots\ldots\ldots(4.40)$$

The second of these equations can be reduced to the form

$$\frac{\partial}{\partial z}\left(p+\frac{1}{8\pi}H_\theta^2\right) = 0.$$

Hence,

$$p+H_\theta^2/8\pi = f(r).$$

Differentiating with respect to $r$ and using (*4.39*), we obtain

$$\frac{\partial p}{\partial r}+\frac{1}{4\pi}H_\theta\frac{\partial H_\theta}{\partial r} = -\frac{H_\theta^2}{4\pi r} = \frac{\partial f}{\partial r}. \qquad \ldots\ldots\ldots(4.41)$$

Consequently, $H_\theta$ depends only upon $r$; therefore, $\partial p/\partial z = 0$; i.e. both $p$ and $H_\theta$ are independent of $z$. This result shows that equilibrium can be established in fields of this type only when the plasma is in the form of a hollow cylinder of infinite extent parallel to the $z$-axis; when the plasma forms a toroidal shape of limited extent and the confining field has only the component $H_\theta$ (Fig. 28), equilibrium cannot be established.

This result can be elucidated by a simple example. Let the plasma be inside a toroidal chamber whose surface is surrounded by a winding which generates the field $H_\theta$ (Fig. 28). Suppose that the plasma is distributed longitudinally to form a ring of circular cross-section, and that the magnetic field has been completely forced out of the region occupied by the plasma. In this case the equilibrium condition will require that $p = H_\theta^2/8\pi$ at the boundary. However, the field strengths at points $M_1$ and $M_2$ must be different because curl $H = 0$ outside the plasma, and so the field strength diminishes as $r^{-1}$; consequently the equilibrium condition cannot be satisfied at all points on the plasma surface.

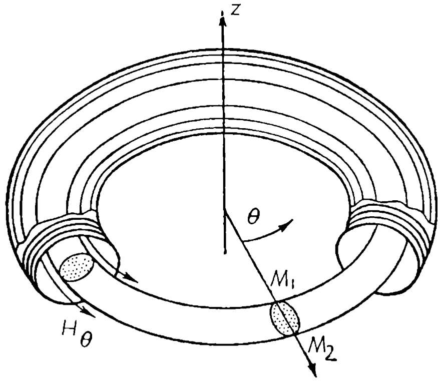

FIG. 28

Plasma ring in the field of a toroidal solenoid

FIG. 29

Plasma ring carrying a longitudinal current

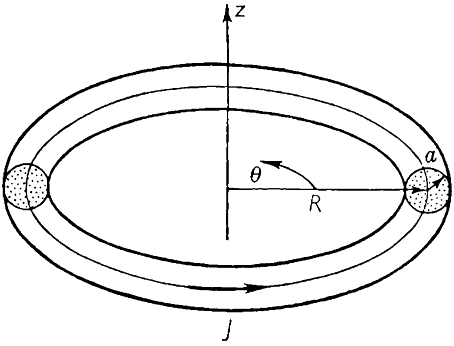

In searching for equilibrium magnetic confinement configurations, axially symmetric systems having ring currents flowing in the plasma must be considered. The simplest system of this type is the toroidal plasma pinch with a longitudinal current (Fig. 29). If the ratio $a/R$ is small enough, the toroidal plasma pinch exhibits properties similar to those of a linear pinch, discussed in § **4.2**. In particular, the pressure balance should be governed by equation (*4.29*), which follows from the equilibrium between the internal pressure of the plasma and the magnetic pressure generated by the current. However, there will be one very substantial difference between the two systems: equation *(4.29)* fully describes the equilibrium conditions in a linear pinch; but for the toroidal configuration, the equilibrium condition is much more complex. A longitudinal current flow around a toroidal conductor generates a force which tends to expand the major radius $R$. This force arises because every segment of the current-carrying ring is acted upon by the magnetic field of the current flowing in the opposite direction on the opposite side of the ring. This tendency of the major radius to expand is a particular example of the general rule according to which the electrodynamic forces in a system of current-carrying conductors are always directed in such a way as to increase the inductance of the system. When a circuit is composed of thin conductors, i.e. conductors whose transverse dimensions are small compared to their length, the expression for the generalised electrodynamic force acting to alter the geometrical configuration of the circuit has the following form:

$$F_q = \frac{J^2}{2c^2}\frac{\partial L}{\partial q}. \qquad \text{.........}(4.42)$$

Here $q$ is a generalised coordinate describing the size and shape, which changes under the influence of the generalised force $F_q$, and $L$ is the self-inductance of the circuit in centimetres. If $a/R \ll 1$, the toroidal plasma may be regarded as a thin conductor, and the net force acting to increase $R$ is

$$F_R = \frac{J^2}{2c^2}\frac{\partial L}{\partial R}.$$

To simplify the calculations, we shall assume that the plasma may be treated as a superconductor, so that the current flows on the plasma surface, the internal magnetic field is zero, and the pressure $p$ is the same at all points in the plasma. With these assumptions:

$$L = 4\pi R\left(\ln\frac{8R}{a}-2\right), \qquad \text{.........}(4.43)$$

$$F_R = \frac{2\pi J^2}{c^2}\left(\ln\frac{8R}{a}-1\right). \qquad \text{.........}(4.44)$$

The electrodynamic force $F_R$ is not the only force which tends to expand a toroidal pinch: a force $F_p$ is also exerted by the plasma pressure. To find this force, it is necessary to calculate the work done by the internal pressure when the major radius of the plasma ring changes by an infinitesimal amount, and to divide this work by the increment of radius $\delta R$. The work done by the pressure is

$$p\delta V = p2\pi\delta R\pi a^2,$$

and therefore the stretching force $F_p$ is given by the expression

$$F_p = 2\pi^2 a^2 p. \qquad \text{.........}(4.45)$$

The total expansion force $F_R + F_p$ can be counteracted if the plasma ring is placed in a magnetic field $H_z$ whose lines of force are parallel to the major axis of the torus. If this field is uniform, the compressive force acting on the current-carrying plasma is

$$\frac{JH_z}{c} 2\pi R.$$

We can now write down the equilibrium conditions for a current-carrying plasma ring in the external field $H_z$:

$$2\pi a^2 p = \frac{J^2}{c^2}, \qquad \text{.........}(4.46)$$

$$2\pi^2 a^2 p + \frac{2\pi J^2}{c^2}\left(\ln\frac{8R}{a} - 1\right) = \frac{JH_z}{c} 2\pi R. \qquad \text{.........}(4.47)$$

The first of these equations defines the equilibrium condition with respect to the minor radius of the plasma ring and differs in no way from the analogous equation (*4.29*) for a linear plasma column. The second equation is specific to the toroidal case and characterises the equilibrium of the forces with respect to the major radius $R$. This condition can be reduced to a simpler form if $p$ is eliminated by using equation (*4.46*), to give the following equation for $H_z$:

$$H_z R = \frac{J}{c}\left(\ln\frac{8R}{a} - \frac{1}{2}\right). \qquad \text{.........}(4.48)$$

The field $H_z$ may be created by means of a solenoid or a system of coils surrounding the vacuum chamber within which the current-carrying plasma ring is located. In either case, to preserve the equilibrium while the current $J$ varies, it is necessary that $J$ and $H_z$ vary with time in the same way.

Compensation of the expansion forces occurs automatically if the plasma ring is inside a toroidal chamber with highly conducting walls. The compensating fields in such systems are generated by the Foucault currents which arise when the ring expands. If the plasma ring expands, the magnetic lines of force cut across the chamber walls (Fig. 30). An electromotive force is thus created which generates a current in the metallic wall. This current flows in a direction opposite to that of the plasma current, and its magnetic field fulfils the function of the field $H_z$. If, simplifying the actual conditions, we suppose that the chamber wall has an infinite conductivity, and that $a \ll r_0$ and $r_0 \ll R$ ($r_0$ is the minor radius of the toroidal metallic shell), the equilibrium conditions assume a simple form. Infinite conductivity implies that the magnetic lines of force cannot penetrate the wall of the chamber, and therefore adjacent to the wall they run parallel to it. The magnetic field produced by the plasma current satisfies this boundary condition only if the plasma is central in the minor cross-section of the chamber. However, when the plasma ring is in this position, the compressing force which should compensate for the expansion forces is zero. Such a force arises only when the plasma is displaced somewhat toward the outer wall of the chamber. Therefore, in order that the above boundary condition be satisfied, currents must flow in the chamber wall and create a magnetic field superimposed on the field produced by the plasma current. In attempting to find the distribution of these currents over the surface of the chamber, we are faced with a problem that is mathematically fully equivalent to the classical electrostatic problem of

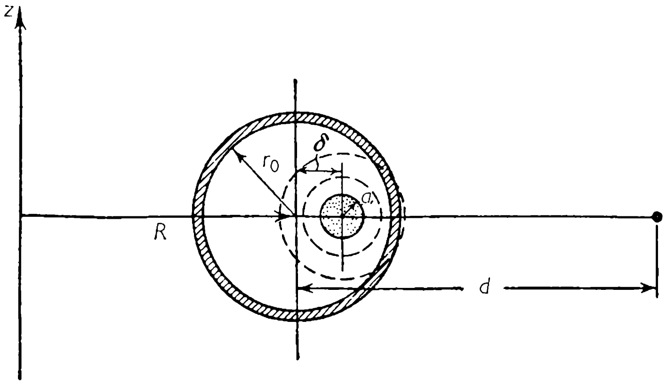

FIG. 30. Minor cross-section of a current-carrying plasma ring inside a conducting shell

finding the electric field generated by a charged filament inside a metal cylinder. By using this fact and borrowing the image method from electrostatics, we find that the boundary condition at the surface of a conductor with infinite conductivity will be fulfilled if, in addition to the magnetic field of the plasma ring, there is also a field generated by a longitudinal image current, flowing in a direction opposite to the plasma current. The image current should be equal in magnitude to the plasma current, and its distance $d$ from the centre of the minor cross-section is given by the condition $\delta d = r_0^2$. If the major radius $R$ of the torus is very large compared with $r_0$, $d \ll R$ even at small displacements of the plasma current from the centre. The magnetic field of the image current acting on the plasma is then

$$H_z = 2J/c(d-\delta).$$

For small displacements, $\delta \ll d$, and therefore,

$$H_z = 2J\delta/cr_0^2. \qquad \text{.........}(4.49)$$

To find the displacement at which equilibrium is attained, it is necessary to substitute the above expression in equation (4.48). It must also be kept in mind that the inductance of the toroidal plasma pinch contained in a conducting shell differs from the value given by equation (*4.43*), and is equal to

$$4\pi R \ln (r_0/a).$$

Taking this into account, we obtain

$$\delta = (r_0^2/2R) \ln (r_0/a). \qquad \text{........}(4.50)$$

In actual fact, because of the finite conductivity of the metallic wall there will be no true steady state, and the plasma ring should gradually expand as the magnetic field penetrates the walls. The time $t$ for the plasma ring to expand to the walls is given by:

$$t \approx 4\pi R \Delta r \sigma / c^2 \ln (r_0/a),$$

where $\sigma$ is the wall conductivity, and $\Delta r$ is the wall thickness. In devices used for the experimental investigation of the toroidal pinch system, one or more insulating sections must be inserted in the metallic shell of the chamber, so that the e.m.f. required to excite the pinch current in the plasma is not shorted-out. As can be easily understood, such insulating sections reduce the stabilising action of the metallic shell. Calculations show that in the presence of $n$ insulating sections, the displacement $\delta$ increases to approximately $(1 + nr_0/2\pi R)$ times the value given by equation (*4.50*).

In recent years, a large number of theoretical and experimental papers have been devoted to the study of toroidal current-carrying plasmas, situated in longitudinal magnetic fields and carrying longitudinal currents flowing around the plasma ring. The interest shown in such systems is due to the fact that, according to theoretical predictions, a plasma ring in the combined field should be free of certain forms of instability which are unavoidable if the field created by the pinch current is acting alone. In this chapter we shall not discuss the problems of instability, but examine only the equilibrium conditions of a current-carrying plasma ring in an external longitudinal field.

It is immediately evident that in this case also a compensating field $H_z$ is needed, since the longitudinal field $H_\theta$ cannot avert the expansion of the current-carrying ring.

In order to describe the equilibrium of a toroidal pinch situated in a longitudinal magnetic field, the additional forces associated with the presence of the longitudinal field must be taken into account. These forces arise when the strength of the longitudinal field inside and outside the plasma are not the same. Let us suppose, as was done above, that the plasma has infinite conductivity and a very weak toroidal character, and that at its surface the strength of the longitudinal field changes abruptly from $H_i$ inside the pinch to $H_0$ outside it. As a result, a difference in the magnetic pressures arises at the boundary of the plasma. If this pressure difference is taken into account, the equilibrium condition for the minor radius can be written in the form

$$2\pi a^2 p = J^2/c^2 + a^2(H_o^2 - H_i^2)/4. \qquad \text{.........}(4.51)$$

This condition also remains valid in the more general case of a plasma with finite conductivity, if the quantity $H_i^2$ is taken to be the mean square field strength inside the plasma. It may also be written in a form similar to equation (*4.31*):

$$4c^2 NkT = \beta J^2, \qquad \text{.........}(4.52)$$

where

$$\beta = 1 + a^2c^2(H_o^2 - H_i^2)/4J^2. \qquad \text{.........}(4.53)$$

In order to derive an equation for the balance of forces tending to alter the major radius of the plasma ring, we consider a small segment which subtends an angle $\Delta\theta$ at the major axis, as shown in Fig. 31. In addition to the forces exerted by the gas pressure and the interaction of the current with the self-magnetic field, the segment is also acted upon by forces which arise from the fact that, with $H_o \neq H_i$, the Maxwellian stresses due to the longitudinal field are not balanced. The circular lines of force of the longitudinal field within the plasma try to contract. The resulting forces on the faces of the plasma segment are represented in Fig. 31 by vectors $F_1$ and $F_2$, which are equal in magnitude and inclined at an angle $\pi - \Delta\theta$. Obviously,

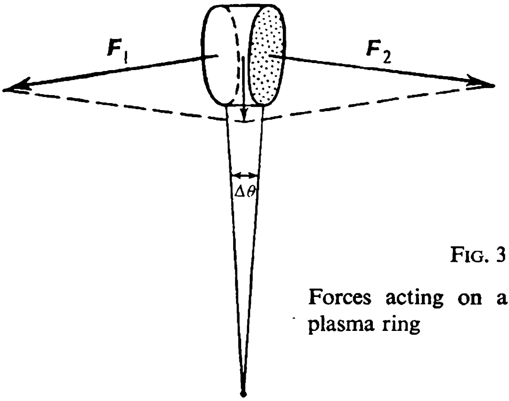

FIG. 31

Forces acting on a segment of a plasma ring

$$F_1 = F_2 = \frac{H_i^2}{8\pi}\pi a^2 = H_i^2 a^2/8.$$

The resultant of the forces $F_1$ and $F_2$ is directed toward the major axis of the torus, and its magnitude is:

$$F_1\Delta\theta = H_i^2 a^2 \Delta\theta/8.$$

If the field strength inside and outside the pinch were the same then the resultant force due to the longitudinal stresses would be balanced by the lateral pressure exerted by the longitudinal lines of force acting from without on the lateral surfaces of the plasma segment. Thus, for $H_i = H_o$, the resultant of the lateral pressure forces, directed outward from the centre of the torus, would be equal in magnitude to $H_{\mathrm{i}}^2 a^2 \Delta\theta/8$.

If, however, $H_{\mathrm{o}} \neq H_{\mathrm{i}}$, the resultant of the lateral pressure forces will obviously be equal to $H_{\mathrm{o}}^2 a^2 \Delta\theta/8$. Thus for $H_{\mathrm{i}} = H_{\mathrm{o}}$, the segment of angular width $\Delta\theta$ is acted upon by an additional radial expansion force equal to

$$a^2 \Delta\theta (H_{\mathrm{o}}^2 - H_{\mathrm{i}}^2)/8. \qquad \text{.........}(4.54)$$

Multiplying (*4.54*) by $2\pi/\Delta\theta$ yields the expansion force for the entire plasma ring, and adding the resulting expression to the left-hand side of equation (*4.47*), we find the total expansion force which must be balanced by the action of the field $H_z$. The desired equilibrium condition is then

$$2\pi^2 a^2 p + \frac{2\pi J^2}{c^2}\left(\ln \frac{8R}{a} - 1\right) + \frac{H_{\mathrm{o}}^2 - H_{\mathrm{i}}^2}{4}\pi a^2 = \frac{JH_z}{c} 2\pi R.$$

Substituting $p$ from (*4.51*), we obtain an equation for $H_z$

$$H_z \frac{JR}{c} = \frac{J^2}{c^2}\left(\ln \frac{8R}{a} - \frac{1}{2}\right) + \frac{H_{\mathrm{o}}^2 - H_{\mathrm{i}}^2}{4} a^2. \qquad \text{.........}(4.55)$$

As indicated above, in a chamber with conducting walls the field $H_z$ arises automatically from the small displacement $\delta$ of the plasma from the centre line of the tube bore. The value of $\delta$, which determines the equilibrium position of the pinch, may be found in this case from the formula

$$\delta = \frac{r_0^2}{2R}\left\{\ln r_0/a + (1 + a^2/r_0^2)\left(\frac{8\pi p}{H_{\mathrm{J}}^2} - \frac{1}{2}\right)\right\}. \qquad \text{.........}(4.55a)$$

In this expression, $H_{\mathrm{J}}$ is the self-magnetic field strength at the surface of the pinch. In particular, it follows from this formula that when the ratio of $p$ to $J$ changes as the plasma is heated, the position of the equilibrium also changes.

Equations (*4.51*), (*4.55*) and (*4.55a*) constitute the theoretical basis for the study of the processes taking place in quasi-stationary discharges in toroidal chambers. These processes will be considered in Chapter VI.

§ **4.4** The dynamic properties of a plasma depend to a large extent on its electrical conductivity. If the conductivity of a plasma is high enough, the currents which arise from the motion of the plasma relative to the magnetic field are distributed over the surface of the plasma because of the skin effect, provided that the time-scale is not too long. Therefore, the forces acting on the plasma are exerted on its boundary, and the balancing pressures should change abruptly in the vicinity of the boundary. These considerations naturally lead to the conclusion that the concept of an equilibrium plasma configuration with a sharply defined boundary has meaning only if the conductivity of the plasma is high enough.

Even so, such a configuration will never be in a strict electrodynamic and thermodynamic steady-state, because the magnetic field within the plasma can be smaller than the external field only for an interval of time determined by the lifetime of the skin currents.

Let us consider in some detail the structure of the plasma-field boundary, supposing it to be in a state of equilibrium and with no externally generated electromotive forces present.

The thickness of the skin layer increases in proportion to $\sqrt{t/\sigma}$, where $t$ is time and $\sigma$ is the plasma conductivity. Hence, if at some initial moment there is a discontinuous change in the field strength associated with surface currents at the plasma boundary, then subsequently there is field penetration which cancels-out the diamagnetic field in successively deeper layers of the plasma. A geometrical blurring of the plasma boundary will take place due to diffusion simultaneously with the penetration of the electromagnetic field into the plasma.

The penetration of a magnetic field into the diamagnetic plasma and the diffusive blurring of the plasma boundary formally represent two independent processes. In reality, however, they are closely related, since they reflect two aspects of the same phenomenon, inasmuch as the electrical resistance of the plasma which increases the thickness of the skin layer, and the diffusion which causes the spreading of the plasma, are both produced by the same interparticle collisions. A magnetic field discontinuity at the plasma boundary levels off only because collisions lead to an expansion of the magnetically confined plasma and to a corresponding fall in the pressure gradients.

This may also be understood from a somewhat different point of view if it is observed that the difference between the magnetic fields inside and outside the plasma is caused by the diamagnetism associated with the Larmor rotation of the charged particles. At constant temperature, the diamagnetic currents can be weakened only by reducing the gradients of the number density, i.e. by the process of diffusion. We thus arrive at the conclusion that the penetration of the external magnetic field into the plasma takes place at the rate determined by the diffusion coefficient $D_\perp$ of the plasma. If at zero time the plasma boundary is sharply defined, then during a time interval $t$ it becomes blurred as the result of diffusion to a depth

$$\delta \approx \sqrt{D_\perp t},$$

and the magnetic field penetrates to the same depth. Consequently $\delta$ represents the thickness of the skin layer. In general, it does not coincide with the value obtained from the classical theory of the skin effect in a solid conductor with a stationary boundary. By using equation (*3.32*) for the diffusion coefficient the following relation is readily obtained:

$$\delta \approx \sqrt{D_\perp t} \simeq \sqrt{\frac{c^2 t}{4\pi\sigma}}\sqrt{\frac{8\pi p}{H^2}}, \qquad \text{.........(4.56)}$$

where $p = nk(T_e+T_i)$ is the kinetic pressure of the plasma. The first factor on the right-hand side of *(4.56)* represents the thickness of the skin layer corresponding to the classical electromagnetic case. If the plasma pressure attains its maximum value, i.e. $p = H^2/8\pi$, the usual electrodynamic formula yields the correct value for the penetration depth. However, if the plasma pressure is very small as compared with the magnetic pressure, the penetration rate diminishes in proportion to the square-root of the ratio of these pressures. Viewed in the light of the ordinary skin-effect theory, this result may appear strange at first sight. In order to understand its physical meaning, one should note that in this case the equalisation of the field occurs not at the fixed boundary of an ordinary conductor, but at the mobile boundary of a plasma which is expanding towards the stronger field. In its diffusive motion, the plasma pushes aside, as it were, the lines of force of the external field penetrating it, and the equalisation rate of the fields is therefore reduced.

§ **4.5** Within the framework of ordinary magnetohydrodynamics, the thickness of the boundary layer between the plasma and the magnetic field may be considered to be equal to zero if the time-scale is much less than the time for the diffusive blurring of the plasma boundary. In reality, this layer must always have a finite thickness. To estimate it, one has to consider the microstructure of the boundary. So far, no general solution to the problem of the boundary microstructure has been found. It is apparent that before this goal is reached a number of obstacles must be cleared away, some of which are purely mathematical in character, while others arise from an almost inevitable impreciseness in formulating the boundary conditions for the general case. We will consider here only the case where the diamagnetic currents exclude the field completely from the region of space occupied by the plasma, and we will assume that there are no collisions between the particles. In this special case the charged particles inside the plasma travel in straight lines over considerable distances. When approaching the boundary, an ion or electron will 'bounce off' the magmetic field and return to the plasma. The region within which there is a deflection of the trajectories constitutes the boundary layer. If the electric field within the boundary layer were equal to zero, then for comparable values of $T_e$ and $T_i$ the ions and electrons would penetrate into the magnetic field to different depths, due to the large difference between the Larmor radii $\rho_{Hi}$ and $\rho_{He}$. However, this difference between the penetration depths of the ions and of the electrons signifies that the quasi-neutrality is disrupted inside the boundary layer, so that an electric field must appear. This electric field will be negligible only if the plasma density is so small that the Debye shielding distance considerably exceeds the mean value of $\rho_{Hi}$. As may be easily verified, this is equivalent to the condition

$$H^2/4\pi\rho c^2 \gg 1.$$

In practice, we usually deal with the opposite limiting case, and we should therefore assume that the electric field produced by the charge separation is so strong that it sharply brakes the ion motion and equalises the electron and ion penetration depths. The general character of the ion and electron motions within the boundary layer may be represented as follows: the electrons rebound off the magnetic field over a distance of the order of $\rho_{He}$, while the ions cannot penetrate much farther, since they are effectively attached to the electrons by electrostatic forces. The calculation detailing this qualitative picture may be performed with comparative ease for only a few special cases involving assumptions which simplify the problem considerably. We shall discuss here the simplest of such cases in the manner of Chapman and Ferraro.

Suppose that all the plasma particles entering the boundary layer have the same initial velocity $\boldsymbol{v}_0$, perpendicular to the boundary. Let $\boldsymbol{v}_0$ be in the $x$ direction, and let $\boldsymbol{H}$ be in the $z$ direction. Inside the plasma, at a large enough distance from the boundary (i.e. when $x \to -\infty$), the magnetic field strength approaches zero. In the vacuum outside the boundary layer, the magnetic field is constant, and equal to $H_0$. In the boundary layer itself, $H$ is a function of $x$. The direction of the electric field must be antiparallel to $\boldsymbol{v}_0$ (this field brakes the ions), and the corresponding potential $\phi$ depends on $x$. We may assume that within the boundary region the ions are acted upon only by the electric field; the effect of the magnetic field upon the ion trajectories may be neglected because the thickness of the layer should be of the order of $\rho_{He}$, whereas the magnetic field has a substantial influence upon the motion of the ions only over distances of the order of $\rho_{Hi}$. Hence, the ion velocity $\boldsymbol{v}$ at any point in the boundary layer has only an $x$ component, whose magnitude can be easily found from the conservation of energy to be

$$v = \sqrt{v_0^2 - \frac{2e\phi}{m_i}}. \qquad \text{.........}(4.57)$$

The ion density in the layer may be determined from the conservation of particle flux,

$$n_0 v_0 = nv. \qquad \text{.........}(4.58)$$

Here $n_0$ is the number density in the main body of the plasma. In the special case under consideration, the conservation of particle flux, as expressed above, applies because the motion of all the ions is characterised by the same initial conditions. From (*4.57*) and (*4.58*) it follows that

$$n = n_0 v_0 / [v_0^2 - 2e\phi/m_i]^{\frac{1}{2}}. \qquad \text{.........}(4.59)$$

The $x$-component of the electron velocity can be determined from an equation completely analogous to (*4.57*). The ion flux is equal to the electron flux at any point within the layer, and since, in accordance with the quasi-neutrality condition, the density of ions and electrons must be almost exactly the same, the $x$-component of the electron velocity should be equal to the ion velocity at the same point. Therefore, in this special case, all the particles penetrate into the magnetic field, travel exactly the same distance, and are reflected back into the plasma at the same plane. We choose a coordinate system such that this plane coincides with the *yz* plane. Hence, at $x = 0$, the velocity component normal to the boundary is zero for all the particles.

We now write the equations of motion for the electrons:

$$m_e \frac{dv}{dt} = e\frac{\partial \phi}{\partial x} - \frac{e}{c}v_y H, \qquad \text{.........}(4.60)$$

$$m_e \frac{dv_y}{dt} = \frac{e}{c}vH. \qquad \text{.........}(4.61)$$

It has been assumed here that the electron velocity component $v_x$ is equal to the ion velocity $v$. The term on the left-hand side of equation (*4.60*) may be neglected, because $m_i\, dv/dt$ is equal to $-e\, \partial\phi/\partial x$, and the magnitude of $m_e\, dv/dt$ should thus be very small compared with the force exerted on the electron by the electric field. Consequently, equation (*4.60*) can be written in the simpler form

$$\partial\phi/\partial x = v_y H/c. \qquad \text{.........}(4.62)$$

Under stationary conditions, all the quantities entering into the equations of motion may be regarded as functions of $x$ only. In particular,

$$\frac{dv_{ye}}{dt} = \frac{\partial v_{ye}}{\partial x}v.$$

Substituting this expression in equation (*4.61*), we obtain

$$m_e \frac{\partial v_{ye}}{\partial x} = \frac{e}{c}H. \qquad \text{.........}(4.63)$$

The relation between the magnetic field strength and the current density yields another equation characterising the properties of the boundary layer:

$$\frac{\partial H}{\partial x} = -\frac{4\pi}{c}j_y = \frac{2\pi n e v_{ye}}{c}. \qquad \text{.........}(4.64)$$

The problem now amounts to solving a system of three differential equations (*4.62*), (*4.63*) and (*4.64*) for the unknowns $\phi$, $H$ and $v_y$. It follows from (*4.62*) and (*4.63*) that

$$\frac{\partial\phi}{\partial x} = \frac{m_e}{e}v_{ye}\frac{\partial v_{ye}}{\partial x}; \qquad \phi = \frac{1}{2}\frac{m_e}{e}v_{ye}^2 + \text{const.}$$

When $x \to -\infty$, $v_{ye}$ approaches zero. Assuming that the electrostatic potential is equal to zero inside the plasma, we obtain

$$v_{ye}^2 = 2e\phi/m_e. \qquad \text{.........}(4.65)$$

Substituting in (*4.59*) yields:

$$n = n_0 v_0/[v_0^2-(m_e/m_i)v_{ye}^2]^{\frac{1}{2}}. \qquad \text{.........}(4.66)$$

Using (*4.63*) and (*4.66*), we can eliminate $n$ and $H$ from (*4.64*) to obtain an equation for $v_{ye}$

$$\frac{m_e c^2}{4\pi n_0 e^2}\frac{d^2 v_{ye}}{dx^2} = v_0 v_{ye}/[v_0^2-(m_e/m_i)v_{ye}^2]^{\frac{1}{2}}. \qquad \text{.........}(4.67)$$

The boundary conditions for $x \to -\infty$ are:

$$v_{ye} \to 0; \qquad dv_{ye}/dx \to 0. \qquad \text{.........}(4.68)$$

Integration of equation (*4.67*) with the boundary conditions (*4.68*) yields the following relation between $x$ and $v_{ye}$:

$$x = \left(\frac{m_e c^2}{4\pi n_0 e^2}\right)^{\frac{1}{2}} f(v_{ye}), \qquad \text{.........}(4.69)$$

where

$$\begin{aligned} f(v_{ye}) = {} & \sqrt{2}\{[1+\sqrt{(1-m_e v_{ye}^2/m_i v_0^2)}]^{\frac{1}{2}}-1\} \\ & +\ln\{(1+\sqrt{2})[1-\sqrt{(1-m_e v_{ye}^2/m_i v_0^2)}]^{\frac{1}{2}}/[\sqrt{2}+[1+\sqrt{(1-m_e v_{ye}^2/m_i v_0^2)}]^{\frac{1}{2}}]\}. \end{aligned} \qquad \text{.........}(4.70)$$

This expression is very cumbersome; therefore, we will not write down the corresponding equations for $\phi$ and $n$. A much clearer picture of the variation of $v_{ye}$, $n$ and $\phi$ in the boundary layer can be given by a graphical representation of these quantities as functions of $x$ (Fig. 32).

All quantities vary rapidly over a length of $[m_e c^2/4\pi n e^2]^{\frac{1}{2}}$, which is of the order of the critical wavelength corresponding to the Langmuir electron plasma frequency (see equation (*3.14*)). As would be expected, this distance is also approximately equal to the electron Larmor radius $m_e v_{ye} c/eH$ in the boundary layer.† The fact that the density approaches infinity at the point $x = 0$ should come as no surprise. This is due to the simplifying assumption of constant initial velocity, so that all the reflections take place at $x = 0$. In real conditions, owing to the thermal distribution of velocities, this singularity would not occur.

Also of importance in the above calculation is the assumption that all the particles arrive at the plasma boundary from infinity and, after reflection, leave the boundary layer. However, it is also possible to imagine a case where some particles remain within the range of influence of a strong magnetic field. The presence of such so-called trapped particles can blur the boundary region, inasmuch as they can be arbitrarily distributed over the region occupied by the magnetic field. In essence, this means that in addition to those plasma configurations which have a sharply defined boundary, plasma configurations with an arbitrarily smooth decrease of density and pressure across the boundary layer can also occur. As already pointed out in § **4.4**, if it were possible to create a sharp boundary between the plasma and the magnetic field at some initial time, this boundary would gradually be blurred as the result of interparticle collisions. These collisions will gradually alter the motion of a larger and larger number of ions and electrons, so that they become part of the above-mentioned class of trapped particles.

---

† The electron Larmor radius at the boundary is substantially greater than $m_e v_0 c/eH$; this is because the electric field which retards the ions also accelerates the electrons to the substantially larger velocity $v_{ey}$.

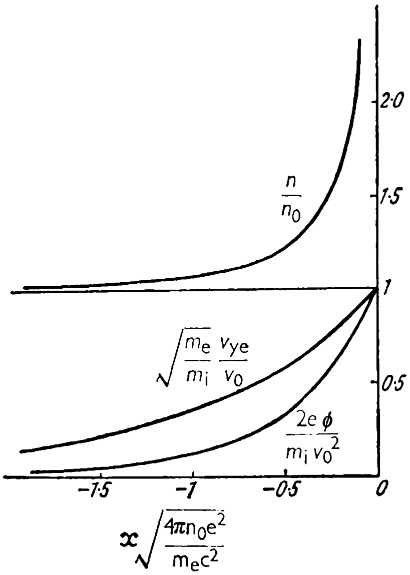

FIG. 32

Variation of the density, potential and tangential velocity component in the vicinity of the plasma boundary

§ **4.6** The picture of the electrodynamic processes associated with a moving plasma is relatively simple only when there is a very high electrical conductivity, which requires a high electron temperature. In a magnetic field, a plasma with high enough conductivity assumes sharply defined anisotropic properties: plasma flows freely along the field but cannot diffuse in a direction perpendicular to it. One of the characteristic features of the flow processes of a high-conductivity plasma in a magnetic field is the so-called 'freezing-in' of the magnetic lines of force. This expression signifies that the lines of force move with the conducting fluid as though they were stuck to it. The concept of the 'frozen-in' lines makes it possible to provide a vivid picture of the variation of the field for different cases of plasma motion. It should be kept in mind, however, that such pictures can be misleading because the line-of-force concept itself is only a convenient auxiliary convention used to represent the geometry of a static field. This concept must be applied with caution to the case of a time-dependent field moving with the fluid and, even so, only to the simplest cases of such motion.

In order to elucidate the mechanisms governing the variations of a field in a moving conducting medium, and to establish the conditions for the 'freezing-in' of the lines of force, let us suppose that the magnetic field vector is everywhere oriented along the $z$-axis. It follows from $\operatorname{div} \boldsymbol{H} = 0$

that the magnitude of the field strength is then independent of $z$ and can change only in a direction perpendicular to the lines of force. Let us also suppose that a highly conducting fluid is distributed in space so that its density $\rho$ as well as $H$ is independent of $z$, but may be any function of the $x$ and $y$ coordinates. Suppose that a fluid element undergoes a deformation, and that its density changes accordingly. The fluid situated at time $t_1$ within a cylindrical region of cross-section $ds_1$ in the $xy$ plane will, because of the deformation, occupy a cylinder of cross-section $ds_2$ at time $t_2$. It is evident that

$$\rho_1\, ds_1 = \rho_2\, ds_2, \qquad \text{.........}(4.71)$$

where $\rho_1$ and $\rho_2$ are the densities of the fluid element at times $t_1$ and $t_2$ respectively.

If the conductivity is very high and if deformation does not take place too slowly, the magnetic flux through the cross-section of the deformed cylinder must remain unchanged. Indeed, if the flux suffers even a minute change, then according to the law of induction an electromotive force arises around the contour bounding the surface. This causes the appearance of a large current whose magnetic field annuls the initial flux change.

Thus, in addition to (*4.71*), the following equation also applies:

$$H_1\, ds_1 = H_2\, ds_2, \qquad \text{.........}(4.72)$$

where $H_1$ and $H_2$ are magnetic field strengths at times $t_1$ and $t_2$. From (*4.71*) and (*4.72*) it follows that

$$H_1/\rho_1 = H_2/\rho_2 = \text{const.} \qquad \text{.........}(4.73)$$

This result represents a quantitative formulation of the concept of the 'freezing-in' of the lines of force. The constancy of the ratio $H/\rho$ is not a general law. It is strictly valid only for rapid deformations of the plasma perpendicular to the lines of force. When a plasma spreads along the lines of force, the ratio $H/\rho$ may vary over a rather wide range.

Owing to the fact that a plasma has finite conductivity and is not an ideal conductor, the field which is 'frozen' into the plasma tends to assume its original configuration as the plasma moves. The rate at which the 'frozen' lines of force 'thaw', leaving regions of space where they have been too strongly compressed and return to occupy regions from which they had been expelled due to the motion of the plasma, is determined by the characteristic time for the skin-effect. During a time $t$, an electromagnetic field penetrates into a conductor to a depth of the order of $(c^2t/4\pi\sigma)^{\frac{1}{2}}$. Hence it follows that if $x$ is a characteristic geometric dimension of the plasma in a direction perpendicular to $H$, the field relaxes in a time of the order of $4\pi\sigma x^2/c^2$. As an example of the magnitudes involved, we note that when $T = 10^8$ °K and $x = 10$ cm, the relaxation time of the fields is about 12 sec.

In particular, the phenomenon of the 'freezing-in' of the lines of force may be observed in systems which are of considerable interest to our main problem. For instance, it occurs in a cylindrical plasma column of high conductivity located in an initially uniform externally generated magnetic field ($H_z$ in Fig. 33) when a rapidly rising current flows along the lines of force of the external field. The current generates a self-magnetic field, the circular lines of which surround and compress the conducting plasma. The initial field $H_z$ is trapped and compressed with the plasma. If the rate of current rise and the plasma conductivity are high, the current flows only in a thin surface layer, and the compression can be considered as due to forces applied at the surface of the plasma cylinder. In a quasi-stationary process (without the formation of shock waves) the plasma density may be considered constant over the cross-section, and therefore $H_z$ should also be the same at all points within the plasma column and should change with time as $1/a^2$, where $a$ is the radius of the conducting plasma.

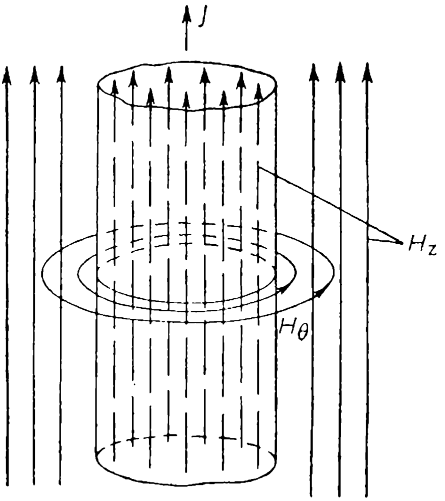

FIG. 33

Trapping of the magnetic lines of force by a compressed plasma

The pinch effect with a trapped axial field has been experimentally observed in work done at the Kurchatov Atomic Energy Institute between 1953 and 1954 on the stabilisation of high-power pulsed discharges. These experiments will be referred to in the following chapter. However, they pertain to cases which are rather far removed from quasi-stationary conditions.

§ **4.7** Various types of oscillations and waves may be initiated by perturbations from an equilibrium state. In this sense a plasma may be regarded as an elastic medium. The origin of the quasi-elastic restoring forces depends on the type of perturbation. Charge separations are restored by forces that are electrostatic in nature, and displacements of the plasma as a whole can be restored by the 'elasticity' of the magnetic lines of force which are displaced with the conducting plasma. In addition, a plasma, just as any other gas, exhibits elasticity towards pressure changes. Owing to the existence of these quasi-elastic forces, the initial perturbation, independent of its cause, may lead to the appearance of various oscillatory motions and wave processes. First we shall briefly describe processes leading to the appearance of oscillations and waves in a plasma in the absence of a magnetic field. Then we shall consider the effect of the magnetic field on the wave properties of a plasma.

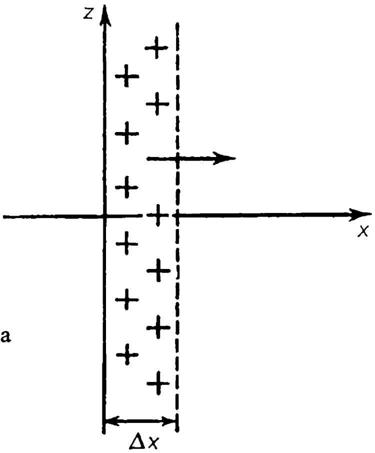

FIG. 34

Displacement of electrons in a plasma

The simplest type of plasma oscillations are longitudinal electron oscillations, usually termed Langmuir oscillations after their discoverer. In discussing the mechanism responsible for the appearance of such oscillations, we shall assume that in an infinite homogeneous plasma a perturbation occurs in which all the electrons initially located on the right-hand side of a certain plane are displaced a distance $\Delta x$ perpendicular to the plane (Fig. 34), while the ions remain stationary. Thus an excess positive charge is produced in a layer of thickness $\Delta x$ adjoining this plane. The charge per unit area is given by $ne\Delta x$, where $n$ is the number density in the unperturbed plasma. The electric field acting upon the displaced electrons is then $4\pi ne\Delta x$ (left of the positive charge the electric field is zero). The equation of motion of the electrons subjected to this electric field is:

$$m_e\, d^2(\Delta x)/dt^2 = -4\pi ne^2\Delta x,$$

which is the equation of simple harmonic motion.

The fundamental frequency of the oscillations—the so-called Langmuir frequency—is

$$\omega_0 = (4\pi ne^2/m_e)^{\frac{1}{2}}. \qquad .........(4.74)$$

The motion of the ions can be neglected due to their large mass. If these oscillations propagate through the plasma, they have the character of longitudinal electrostatic waves. There is no relation between the frequency $\omega_0$, which has a fixed value, and the wavelength $\lambda$ or the wave vector $k = 2\pi/\lambda$. Therefore, the phase velocity of the waves is inversely proportional to the wave vector.

$$v_p = \omega/k = \omega_0/k. \qquad .........(4.75)$$

However, the frequency is independent of the wave vector only when the electron thermal motion may be neglected. This assumption is valid as long as the phase velocity of the wave is many times larger than the mean thermal electron speed $v_e$, that is when the wavelength is large enough. But when $v_p \simeq v_e$, the thermal motion has substantial effect on the properties of the Langmuir waves. Indeed in this case $k \approx \omega_0/v_e$ and the wavelength is comparable to the Debye shielding distance $r_D$, so that fluctuations of the electric microfields of the plasma exert a considerable influence upon the propagation of longitudinal electrostatic waves.

The strict theory of wave propagation in a plasma, taking into account the thermal motion of the electrons, shows that the frequency of the longitudinal waves depends on the wave vector, viz: $\omega^2 = \omega_0^2(1+3k^2r_D^2)$, where $r_D$ is given by equation (*2.30a*). However, this relation is valid only when $\lambda > r_D$. No longitudinal oscillations with a wavelength smaller than the Debye shielding distance can be propagated in a collision-free plasma.

Another important property of these longitudinal plasma oscillations, which is due to the electron thermal motion, is that the energy of the longitudinal oscillations may be absorbed by the plasma even in the absence of collisions (the so-called 'Landau damping'). The physical interpretation of this phenomenon is that plasma particles (electrons or ions) whose velocities are slightly less than the phase velocity of the wave move with the wave for a long time, gain energy from it, and hence cause attenuation. It is obvious that if $v_p \gg v_e$ in an equilibrium plasma with a Maxwellian velocity distribution, there are very few particles able to remove energy from the wave by moving along with it. The fraction of such particles is proportional to $\exp -(mv_p^2/2kT)$, i.e. it is exponentially small. Therefore, when $v_p \gg v_e$, the damping decrement associated with this effect will also be exponentially small. If the particle velocity distribution is not Maxwellian, then different conditions arise, and indeed the energy exchange between the wave and the particles may have a different sign, i.e. the wave amplitude will increase instead of decreasing. We shall discuss this case in Chapter VII in connection with certain types of plasma instabilities associated with electron and ion beams.

Ion-electron collisions have a substantial influence on wave propagation when the electron temperature is low. Collisions dissipate the energy of the ordered motion of electrons, decreasing the wave energy. This damping mechanism occurs both when longitudinal waves associated with electron oscillations of the Langmuir type and when transverse electromagnetic waves are propagated in a plasma.

In addition to the Langmuir electron oscillations, longitudinal ion oscillations may also be excited. These oscillations, in which the entire plasma mass participates, are essentially sound waves. As we know, the concept of sound waves in an ordinary gas has meaning only if the wavelength is substantially larger than the mean-free-path of the atoms or molecules. It turns out that in a plasma, owing to the presence of long-range Coulomb forces (which form the so-called self-consistent field), sound waves may also exist in the opposite limiting case, i.e. when the wavelength is much shorter than the mean-free-path. The frequencies and velocities of these ion waves are both much lower than the frequencies and velocities of the electron waves, and so the plasma preserves its quasi-neutrality, i.e. the electrons follow the motion of the ions. The velocity of propagation of sound waves may be estimated from the usual formula, $v_s^2 = dp/d\rho$, where $p$ is the pressure and $\rho$ is the mass density. For a quasi-neutral plasma $p = k(T_i+ZT_e)\rho/m_i$, and hence $v_s^2 = k(T_i+ZT_e)/m_i$. If $T_e \simeq T_i$, the velocity of sound is of the order of the mean ion thermal speed, and so the number of ions with velocities sufficiently close to the velocity of sound will be so large that Landau damping should be very pronounced. Theory shows that under these conditions sound waves are severely damped in a distance comparable to the wavelength, even in the absence of collisions. Then the concept of wavelength itself obviously loses meaning. If, however, $ZT_e \gg T_i$, the wave velocity substantially exceeds the thermal velocity of the ions, and the number of ions participating in the Landau damping will be very small. Such sound waves can, in principle, have any frequency smaller than the so-called ion Langmuir frequency $\omega_{0i} = [4\pi ne^2/m_i]^{\frac{1}{2}}$. When $\omega$ approaches $\omega_{0i}$, the wavelength approaches the Debye shielding distance, and therefore the plasma is no longer quasi-neutral with respect to the oscillations. Strict theory shows that sound waves do not exist for $\omega > \omega_{0i}$.

A strong magnetic field can be expected to have a substantial effect on the wave properties of a plasma, since it strongly affects the motion of the electrons and ions. In particular, in the presence of a magnetic field, new types of oscillations may arise in a plasma. The most important of these are the magnetohydrodynamic oscillations called Alfvén waves. To describe the physical meaning of Alfvén waves, we note that their occurrence is closely associated with the change in the dielectric properties of a plasma in a magnetic field. As was shown in Chapter III, the dielectric constant $\varepsilon$ of a field-free plasma is always less than unity. When $\omega$ is equal to the Langmuir frequency $\omega_0$, $\varepsilon$ becomes zero, and still smaller frequencies correspond to negative values of $\varepsilon$. However, in the presence of a constant magnetic field, a plasma has a positive dielectric constant which always exceeds unity for transverse electric fields that vary slowly during an ion Larmor period, i.e. for frequencies that are much smaller than the ion cyclotron frequency $\omega_{Hi}$.

Let us now discuss electromagnetic waves with frequencies $\omega < \omega_{Hi}$ which propagate along the lines of force. It is natural to assume that the behaviour of the plasma with respect to such a wave will be characterised by the dielectric constant $\varepsilon_m$. Therefore (from equation (*3.25*)) the phase velocity $v_p$ of the wave is given by the expression

$$v_p^2 = c^2/\varepsilon_m = H_0^2/4\pi\rho(1+H_0^2/4\pi\rho c^2). \qquad \text{.........}(4.76)$$

In a sufficiently dense plasma, $H^2 \ll 4\pi\rho c^2$ and the propagation velocity is equal to $H_0/\sqrt{4\pi\rho}$, which is called the Alfvén velocity. In an extremely rarefied plasma, $v_p$ approaches the velocity of light. Thus, Alfvén waves are simply low-frequency transverse electromagnetic waves in the magnetised plasma. Because $\varepsilon_m \gg 1$, the amplitude of the alternating electric field in an Alfvén wave is very small compared with the amplitude of the alternating magnetic field.

The nature of the wave process changes as $\omega$ approaches $\omega_{Hi}$. Without going into the details of the mathematical theory, we shall confine ourselves to the qualitative aspects of the phenomena which determine the fundamental properties of transverse electromagnetic waves in a plasma when $\omega \simeq \omega_{Hi}$. The simplest linearly polarised plane wave travelling along the direction of a uniform magnetic field may be represented as a superposition of two circularly polarised waves whose electric vectors rotate in opposite directions. If $\omega \ll \omega_{Hi}$, the properties of the two waves are identical. However, as the cyclotron frequency of the ions is approached, the situation changes. Indeed, the wave whose electric vector rotates around the constant field in a direction coinciding with the Larmor rotation of the ions is subject to anomalous dispersion in the region where $\omega \simeq \omega_{Hi}$. This phenomenon should always be observed close to resonance since the phase velocity of this wave (in optics it is called the ordinary wave) varies rapidly in the vicinity of $\omega_{Hi}$. On the other hand, the so-called extraordinary wave† (which corresponds to the opposite direction of rotation of the electric vector) has, for frequencies close to $\omega_{Hi}$, an increasing phase velocity as $\omega$ increases. Therefore, for frequencies close to $\omega_{Hi}$, the plasma is optically active.

Figure 35 shows a graph of the refractive index $\sqrt{\varepsilon}$ as a function of frequency for the two waves with opposite circular polarisations; the index $\alpha$ refers to the ordinary wave, and the index $\beta$ to the extraordinary wave. At low frequencies, the two curves merge, and this corresponds to the transition to an Alfvén wave. At very high frequencies, in the region where $\omega$ is comparable to the electron cyclotron frequency $\omega_{He}$, an anomalous dispersion is observed for the extraordinary wave whose electric vector rotates about the magnetic field in the same direction as the plasma electrons. The anomalous dispersion is always accompanied by an anomalous absorption, i.e. there is a sharp increase in the wave damping. In a plasma this absorption is due to the fact that if the frequency of the ordinary wave approaches $\omega_{Hi}$, the ions are constantly in resonance with the electric field of the wave. The acceleration under the influence of this field continuously transfers energy from the wave to the particles. This phenomenon is utilised in the so-called cyclotron heating of plasmas. The same thing occurs in the case of the extraordinary wave when $\omega \simeq \omega_{He}$.

---

† The terms 'ordinary wave' and 'extraordinary wave' are used for other modes by other authors (see, for example, Spitzer, *loc. cit.*, ch. III).

A magnetic field may also affect the longitudinal oscillations of a plasma. The influence on Langmuir electron oscillations is very weak under ordinary conditions where, as a rule, the frequency of such oscillations is much greater than the electron cyclotron frequency $\omega_{He}$. For this reason, the magnetic field is unable appreciably to influence the rapid oscillatory motion of the electrons. In contrast, the character of the ion oscillations in a plasma may be altered substantially in the presence of a strong magnetic field. The field will not have any effect upon sound waves propagating along the lines of force. But if the sound travels across the field, every compression or rarefaction of the plasma produces a compression and a rarefaction of the lines of force, since the field is frozen to the plasma, so to speak, and they move together. The magnetic field imparts an additional elasticity to the plasma, causing an increase in the sound velocity. For frequencies considerably smaller than the ion cyclotron frequency, the propagation velocity of these magnetosonic waves can be found from the relation $v_s^2 = dp/d\rho$ where $p$, however, must be taken as the sum of the plasma pressure and the magnetic pressure $p_m = H^2/8\pi$. In differentiating, one must keep in mind that because of the freezing of the magnetic field to the plasma, $H$ is proportional to $\rho$. Hence

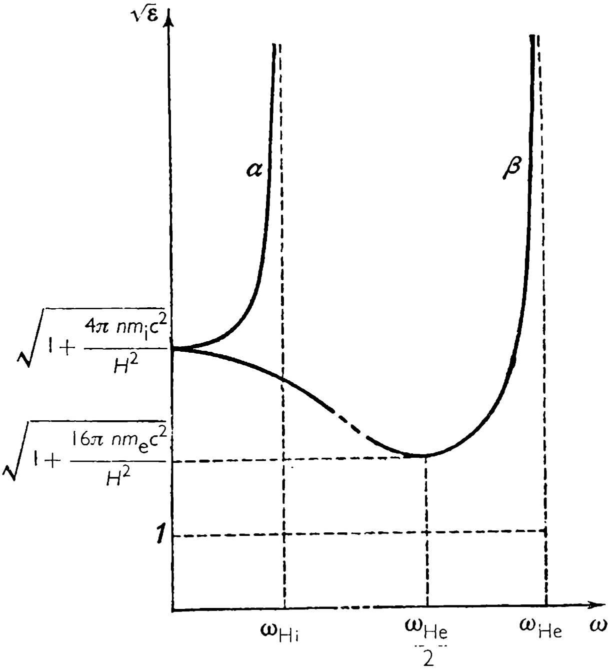

FIG. 35. Index of refraction as a function of frequency (schematic diagram)

$$\frac{\partial H}{\partial \rho} = \frac{H}{\rho} \quad \text{and} \quad \frac{\partial p_{\mathrm{m}}}{\partial \rho} = \frac{H^2}{4\pi\rho}. \qquad \text{.........(4.77)}$$

In determining the plasma pressure, we observe that at low frequencies ($\omega \ll \omega_{\mathrm{Hi}}$) and neglecting collisions, the ratio $W_{\perp}/H$ is a constant for each particle. Hence, the 'temperature' $T$ which determines the mean value of the kinetic energy perpendicular to the lines of force is proportional to $H$. Let $p_0 = nk(T_{\mathrm{e}}+T_{\mathrm{i}})$ designate the corresponding plasma pressure. This quantity is proportional to $\rho H$, and because $H$ varies in proportion to $\rho$, the pressure should be proportional to $\rho^2$. Consequently

$$\partial p_0/\partial p = 2p_0/\rho = 2k(T_{\mathrm{e}}+T_{\mathrm{i}})/m_{\mathrm{i}}. \qquad \text{.........(4.78)}$$

Using (*4.77*) and (*4.78*), we can write the following expression for the sound velocity

$$v_{\mathrm{s}}^2 = 2k(T_{\mathrm{e}}+T_{\mathrm{i}})/m_{\mathrm{i}}+H^2/4\pi\rho. \qquad \text{.........(4.79)}$$

In practice, we very often deal with cases where the kinetic pressure of the plasma constitutes only a small fraction of the magnetic pressure; in which case the first term in equation (*4.79*) may be neglected, and consequently, the velocity of the sound waves travelling normal to the magnetic field turns out to be the same as for Alfvén waves.

## CHAPTER V

# FAST HIGH-POWER DISCHARGES

§ **5.1** This chapter deals with experimental and theoretical studies of the processes for plasma heating in devices where the acceleration by electrodynamic forces is important. For many years the greatest efforts in this direction have been concentrated on the study of powerful electric discharges in which both the magnetic confinement and the heating depend on the current flowing in the plasma itself. Confinement of the plasma arises from the electrodynamic forces which will drive the plasma away from the walls of the discharge chamber, to form an isolated pinched plasma column. The work done on the plasma by these forces together with the Joule heat constitutes the source of plasma heating.

Before the experimental investigation of high-power pulsed discharges, it was believed that the processes involved in passing current through a plasma would turn out to be of a quasi-stationary character, and that the kinetic pressure of the ions and electrons would be counterbalanced by electrodynamic forces. On this initial hypothesis, the prospects of producing thermonuclear reactions in a current-carrying plasma column looked quite rosy. One could envisage a cyclic heating process arising from a gradual increase in the current from zero to some peak value $J_{\max}$ in each cycle. It was supposed that as the current increased, the plasma temperature would rise correspondingly. A simple numerical example suggests that for values of $J_{\max}$ which are entirely feasible technologically very high plasma temperatures may be obtained. With $J_{\max} = 10^6$ A and $N = 10^{17}$ cm$^{-1}$, the plasma temperature given by equation (*4.31*) is $1{\cdot}8 \times 10^8$ °K (16 keV). At this temperature a plasma would be a powerful source of thermonuclear reactions. During each cycle, involving currents of several million amperes, the thermonuclear reaction rate might be expected to be particularly high during the period of peak discharge current.

Calculations of the expected thermonuclear yield led to a conclusion which was unexpected at first glance: it turned out that for given values of $N$ and $J_{\max}$ the total number of nuclear reactions during one heating cycle should be independent of the duration of the cycle, i.e. independent of the time taken for the current to rise from zero to $J_{\max}$. This conclusion is not difficult to explain. According to equation (*4.36*), for a given $J_{\max}$, the rise time $t$ of the current and the plasma radius $a$ are related by

$$t/a^2 = \text{const.}$$

If the total number of particles per unit length of the pinched plasma is also given, the number density is inversely proportional to $a^2$. The reaction rate per unit length of the plasma column is proportional to the product of the density squared and the cross-sectional area, i.e. it varies inversely with $a^2$. Therefore, the thermonuclear yield integrated over the time during which the current rises should be proportional to $t/a^2$, and depends only upon $J_{\max}$. This predicted independence of the thermonuclear yield and the duration of the discharge cycle was one of the arguments supporting the optimistic appraisal of the possibilities of producing thermonuclear reactions by the use of large pulsed currents; for it might be expected that intense thermonuclear reactions could be produced in powerful discharges with a rise time of $10^{-6}$ to $10^{-5}$ sec. The achievement of such electrical discharges is not beyond the limits of technological feasibility. However, the difficulties multiply rapidly as soon as we consider heating times measured in hundredths or tenths of a second, in conjunction with million ampere currents.

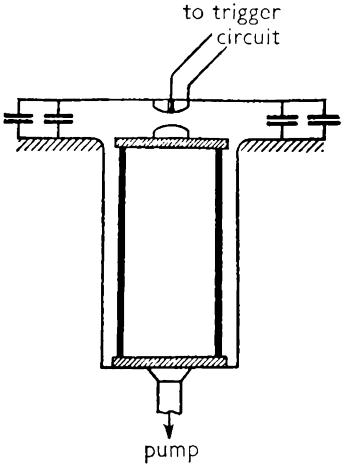

FIG. 36

Diagram of a typical linear pinch apparatus

Our present concept of the nature of plasma processes taking place within fast high-power discharges comes almost exclusively from experimental data.

The phenomena occurring in pulsed discharges in rarefied gases have been the object of a great number of experimental investigations. For discharge times of a few microseconds it is preferable to conduct the experiments with straight discharge tubes (the linear pinch), rather than with electrodeless toroidal chambers: the energy lost by the plasma to the electrodes may be disregarded during the first stages of the compression; and, for a given pulse power source and characteristic tube dimensions, one can obtain higher currents than in a toroidal chamber because the tube is connected directly to the external circuit, whereas in a toroidal pinch the gas current is generated by induction. For this reason all the principal measurements made in the U.S.S.R. have been performed with linear pinch tubes, while toroidal chambers have been used only in control experiments to make sure that the physical processes are independent of the presence of electrodes.

Figure 36 shows a typical experimental arrangement. A battery of high-voltage capacitors connected in parallel is the energy source. The capacitors are connected to the tube through a switch with an independent trigger system. The sketch shows the simplest possible design of a three-electrode spark gap. In practice, a number of more advanced designs of the switching system have also been developed. The gas current is returned to the capacitor bank through a coaxial metal cylinder surrounding the discharge tube. The circuit elements feeding the current from the capacitors to the discharge tube are designed so as to minimise the parasitic external inductance which limits both the maximum current and its rate of rise. In experiments carried out to date, the maximum discharge current varies from a few tens of kiloamperes to two million amperes, and the initial rate of current rise from $10^{10}$ to $10^{12}$ A/sec. Capacitors charged to between 3 and 120 kV have been used with a total stored energy up to $10^6$ J. In experiments where the object was to study processes connected with a high rate of current rise, the parasitic inductance of the circuit amounted to 0·01–0·02 $\mu$H. The main experiments have been performed with discharge tubes made of insulating materials such as glass, quartz or porcelain, the tubes being capped with metal electrodes between which the discharge takes place.

The dimensions of the discharge tubes used cover a very wide range: length, from a few centimetres to two metres; diameter, from a few centimetres to 60 cm. Most attention has naturally been concentrated on the low-pressure régime since it is here that one expects to achieve the highest temperatures.

Of prime interest in controlled fusion research is the study of the processes involved in the passage of large currents through hydrogen and deuterium, and abundant experimental data have been amassed in pinch studies using these gases over a pressure range from $5 \times 10^{-3}$ Torr up to several hundred Torr. Powerful pulsed discharges have also been investigated in helium, argon, and xenon, and also in gas mixtures (D–He, D–Ar, D–Xe).

The experimental study of the plasma in such discharges consists of the measurement of a large number of parameters characterising the plasma properties. Diagnostic methods are required to record changes in the state of the plasma during times measured in microseconds. For this reason, oscillographic recording is mandatory and the main difficulty which must be combated and overcome in developing this technique is the strong electrical interference that inevitably arises from high-power pulsed discharges.

Experimental studies of pulsed gas discharges involve the oscillographic recording of the following quantities:

1. *Discharge current.* This is measured by means of Rogovskii coils. When the oscillograph records the open-circuit output voltage of the coil directly, then $dJ/dt$, and not $J$, is observed. Therefore, in order to obtain an oscillogram of $J$ directly, the output from the Rogovskii coil must be integrated. An $LR$ integrator can be formed by connecting a small inductionless resistance $R$ across the Rogovskii coil which itself forms the

inductance $L$. The voltage across the resistance is then proportional to the current $J$.

2. *Voltage across the discharge tube.* This can be measured by means of a low-impedance potential divider connected in parallel with the tube.

3. *Magnetic field in the plasma.* Magnetic probes—small search coils placed inside the discharge chamber—first developed for plasma studies in the U.S.S.R. by Andrianov, yield very valuable information on the magnetic field configuration. However, the magnetic probes cannot withstand more than one discharge at the highest currents.

4. *Electric field strength.* The axial component of $E$ may be determined from the law of induction by the use of a probe with a number of search coils disposed radially. Double electric probes may also be employed in the measurement of the electric field. It should be noted, however, that both these methods provide a very rough average picture of the electric field distribution in the plasma. Probe techniques have not yet permitted the observation of the strong local electric fields responsible for the appearance of fast particles in the plasma (see below), although these fields undoubtedly exist.

5. *Intensity of the spectral lines and continuum emitted by the plasma.* Spectral intensities are usually measured with monochromators or spectrographs equipped with photoelectric detectors. To determine the intensities of both spectral lines and the recombination-bremsstrahlung continuum, time-resolved photographic recording of the spectrum by means of a rotating mirror has also been used successfully. This technique is discussed in detail in § **5.2**. This instrumentation can also be employed for measuring the widths of spectral lines as a function of time.

6. *X-ray and neutron emission from a plasma.* The time-resolved measurements are performed with scintillation counters. A Wilson cloud chamber with a magnetic field has also been used to determine the energy of the X-rays. The energy spectrum of the neutrons is obtained by examining the tracks of recoil protons in nuclear emulsions. It is also possible to measure the energies of the fast electrons and ions which escape through an opening in the electrodes or tube wall by measuring the deflection of the beam in a magnetic field or by using the Thomson parabola method.

7. *Plasma pressure.* Pressure pulses have been measured with the aid of piezoelectric crystals inserted inside the discharge chamber. However, the quantitative interpretation of the signal is a difficult problem. So far, it has been possible to determine only the order of magnitude of the plasma pressure and the time at which it is large.

In addition to oscillographic techniques, high-speed framing cameras (up to two million frames per second) and streak cameras are also widely used in studies of pulsed discharges. For streak photography of the radial motion, an image of a slit perpendicular to the axis of the discharge tube is swept along a film by means of a rotating mirror. To obtain instantaneous photographs of the discharge, use is also made of Kerr cells and of special explosively operated shutters.

All the above methods for determining the state of the plasma also find applications in the study of quasi-stationary discharges, discussed in the next chapter.

It is evident that the greatest interest is in the experimental determination of the principal quantities characterising the state of a plasma: number density $n_e$, ion temperature $T_i$, and electron temperature $T_e$. Unfortunately, however, the whole arsenal of methods enumerated above produces only rough estimates of the ion and electron temperatures and the plasma density; and even these estimates are obtained by indirect methods and combinations of data obtained by various means, not from direct measurements. We shall discuss further the methods for determining the plasma temperature and density in the following paragraphs which deal with the results of investigations of high power pulsed discharges.

§ **5.2** A typical gas discharge, with a capacitor bank as the source of energy, is oscillatory with a large resistive damping. During the first half-period, a substantial part of the energy initially stored in the capacitors is dissipated in the discharge tube. As is shown by the spectral distribution of plasma radiation, the composition of the gas changes markedly during the discharge owing to the injection of impurities by the strong interaction between the plasma and the walls. In all the cases of practical interest, the plasma becomes contaminated by the end of the first half-period. For this reason, observation of the subsequent stages of the discharge is not of essential importance in plasma physics.

The principal object of study is the first quarter-cycle of the discharge, during which the plasma current builds up to a maximum. The duration of this phase in 'fast' discharges ranges from about 1 $\mu$sec to 10 $\mu$sec. An examination of the current and voltage oscillograms shows that the development of the discharge goes through a series of stages. In the first stage, immediately after the breakdown of the spark-gap switch, both the current and the voltage vary smoothly. Then an inflection is observed in the current wave-form. At the same instant, the voltage drops suddenly. Following this characteristic moment, the voltage and the current rise quickly. After a certain time interval, a second inflection point appears on the current oscillogram accompanied by a second abrupt voltage drop. In some cases, three consecutive inflections are observed on the current oscillogram with a corresponding drop in the voltage.

Typical current and voltage dual-beam oscillograms of a high-power fast discharge in deuterium are shown in Plate II for various initial conditions. These photographs clearly show two inflections in the current trace and the corresponding discontinuities on the voltage trace. These characteristic features of high-current pulsed discharges are most striking when the discharge takes place in a gas with a low atomic weight (hydrogen, deuterium), and for moderate initial gas pressures.

In analysing the relation between the current and the voltage during the initial stage of a fast discharge, one may, to a first approximation, neglect the resistive impedance of the discharge as compared with its inductive impedance. This is justified not least by the fact that all the predictions made with this omission agree with the experiments. The discharge inductance is time-dependent so that the relation between the current and the voltage has the form

$$V = \frac{d}{dt}(LJ). \qquad \text{.........}(5.1)$$

Here, $V$ is the voltage across the tube, $J$ is the total plasma current, and $L$ is the inductance of the discharge. From (*5.1*) it follows that

$$L = \frac{1}{J}\int V dt. \qquad \text{.........}(5.2)$$

By using this relation, it is possible to estimate $L$ from the current and voltage oscillograms. Assuming that the current-carrying plasma column is cylindrical and knowing $L$, one can find the effective radius $a$ of the plasma column from the formula

$$L = 2l \ln (b/a), \qquad \text{.........}(5.3)$$

where $l$ is the length of the pinch tube and $b$ is the radius of the coaxial return conductor. Analysis of the oscillograms along these lines reveals that the plasma inductance increases up to the first inflection on the current waveform. This means that the radius of the plasma column decreases, i.e. the plasma is compressed along the axis of the discharge tube by the 'pinch effect'. At the instant when the point of inflection appears on the current oscillogram, the plasma column contracts into a narrow filament and its radius reaches a minimum value. After this moment the plasma column begins to expand, but then undergoes a second stage of compression. Thus, analysis of the oscillograms shows that the plasma undergoes rapid radial oscillations during the first quarter-period of the discharge. Radial plasma oscillations can be observed more directly from high-speed photographs of the radiation emitted by the discharge. Examination of the frames shown in Plate III (*a*) ,which depict the development of a discharge in deuterium, shows the compression of the plasma into a narrow pinch followed by an expansion. These frames cover an interval of time near the instant when the current inflection occurs, and they can be time-correlated with the current and voltage oscillograms. By these means, complete agreement has been obtained between values of the plasma radius measured by the two different methods; in particular, the frame on which the pinch diameter is minimum corresponds to the time of the current inflection.

Plate III (*b*) shows a streak camera photograph of a $1{\cdot}6 \times 10^6$ A discharge in deuterium at an initial pressure of 1 Torr. This picture shows very clearly the instant of the maximum plasma compression. The subsequent expansion of the column and its secondary compression can also be seen.

A systematic analysis of the voluminous experimental data obtained from the current and voltage oscillograms shows that the processes taking place in a contracting plasma are governed by very specific mechanisms. The implosion time during the first compression increases with the mass of gas per unit length inside the tube, and decreases with increasing $dJ/dt$ (the rate of current rise $dJ/dt$ at the beginning of the discharge is proportional to the applied voltage). The following relation has been established experimentally:

$$t_c \propto \sqrt[4]{M}/(dJ/dt)_0^{\frac{1}{2}}, \qquad \ldots\ldots\ldots(5.4)$$

where $t_c$ is the implosion time, $M$ is the mass per unit length and $(dJ/dt)_0$ is the rate of current rise at the beginning of the discharge. Figure 37 shows the experimental variation of $t_c$ with $M$, obtained for discharges in $H_2$, $D_2$, He, Ar and Xe. The dependence of $t_c$ on $\sqrt[4]{M}$ is obeyed rather closely over a wide range of $M$ (from $10^{-6}$ to $10^{-3}$ g/cm).

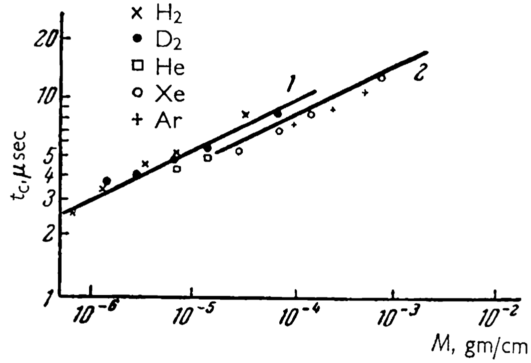

FIG. 37. Dependence of the implosion time $t_c$ on the mass per unit length $M$

Data for $H_2$ and $D_2$ (curve 1) correspond to a somewhat lower value of the initial rate of current rise. Curve 2 is plotted from data obtained with He, Ar and Xe discharges

Valuable data on the dynamics of the electromagnetic processes involved in pulsed discharges can be obtained by the magnetic probe method, widely employed in the investigations of Andrianov, Bazilevskaya and Prokhorov. By measuring the strength of the magnetic field at various radial positions in the discharge tube, one can determine the field distribution as a function of time and also find the distribution of current density over a cross-section of the discharge. Measurements of the field strength in the plasma show that the current distribution is cylindrically symmetrical up to the end of the first implosion if one ignores the region close to the axis where it is difficult to obtain reliable data. Because of the cylindrical symmetry, the current density $j(r)$ is related to the field strength $H(r)$ as follows:

$$j(r) = (c/4\pi r)\, d[rH(r)]/dr. \qquad \text{.........(5.5)}$$

For lack of a better one, this relation may also be used to obtain $j(r)$ at times after the first contraction, but with the reservation that it gives a current density averaged over the azimuth and also neglects axial non-uniformity.

The experimental data lead to the following picture of the current distribution in the pinch. After breakdown the skin-effect causes the current to flow in a thin cylindrical layer adjoining the wall of the discharge tube. This current sheath is driven towards the axis, slowly at first, but then faster and faster. The time at which the current sheath reaches the axis coincides closely with the break on the voltage oscillogram. At that moment the current density near the discharge axis is ten to fifty times greater than the current density averaged over the cross-section of the tube. However, the current distribution has no sharply defined boundary; and the central region, with a radius of a few centimetres, accounts for less than half the total current. During the subsequent expansions and contractions the current density in the inner region remains very high, although it exhibits appreciable oscillations.

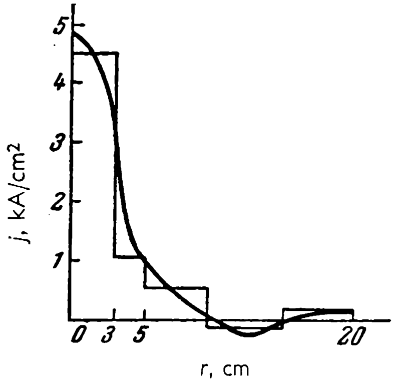

FIG. 38

Histogram of the current density distribution in a pinch discharge at the end of the second bounce of the plasma column

Figure 38 represents a typical example of the radial current distribution during the second contraction in deuterium with an initial compression of 0·05 Torr and an initial field strength of 450 V/cm. A characteristic feature of this distribution is the change in direction of the current (because of the skin-effect) in the outer region. Knowing the field distribution as a function of time, one can determine the velocity $v$ at which the inner boundary of the current sheath moves towards the axis during the first implosion. The maximum value of $v$ occurs at a time very close to the time of maximum compression of the discharge. Measurements show that the maximum radial velocities obtained with hydrogen and deuterium lie between the limits of $1\text{–}3 \times 10^6$ to $2\text{–}3 \times 10^7$ cm/sec, depending on the initial conditions. The velocity increases with $(dJ/dt)_0$ and decreases with increasing initial pressure.

The velocity found by this method directly characterises the motion of the electromagnetic field, and not necessarily the plasma motion. However, in a fast discharge the velocity of the plasma cannot differ appreciably from the velocity with which the field moves because the difference between these two velocities is due only to the finite conductivity of the plasma. The conductivity may be found from the width of the current sheath, and this width can be measured from the magnetic probe data. The analysis shows that, for the fast discharges under consideration, the velocity of the current sheath and that of the imploding plasma should have about the same value. A direct experimental proof of this conclusion is the fact that the velocity of the inner boundary of the current sheath coincides with the propagation velocity of the pressure wave recorded by the piezoelectric pressure detectors. Near the axis, the plasma pressure is negligibly small until the time of maximum contraction. When the current reaches the axis, however, the pressure rises to a very high value for times of the order of a few tenths of a microsecond.

Measurements by Filippov on discharges in an initial gas pressure of 0·2 Torr and an initial rate of current rise of $4 \times 10^{11}$ A/sec show that the pressure at peak compression reaches 200 atm, i.e. it increases by a factor of about one million. Plate IV (*a*) shows an oscillogram of the pressure pulse when the imploding plasma first reaches the axis.

If $v$ is interpreted as the plasma velocity, it turns out that the ions may acquire a rather high kinetic energy during the early stages of a powerful pulsed discharge. For instance, an implosion velocity of $2{\cdot}5 \times 10^7$ cm/sec has been attained, and this corresponds to a deuteron kinetic energy of 600 eV. The presence of high-velocity directed motion of the plasma ions is one of the outstanding features of fast pulsed discharges.

§ **5.3** The experimental facts discussed above lead to the following conception of the mechanisms underyling the behaviour of pulsed discharges. During the initial phases of the discharge when the current is rising rapidly, the electrodynamic forces, which vary as $J^2/a$, cannot be balanced by the internal pressure of the ionized gas (despite the original hypothesis of the quasi-stationary character of the compression). Initially pressure balance is impossible because the current flows only near the tube walls, while inside the thin cylindrical current sheath the gas is unaffected by the discharge and remains at a low pressure. For this reason the cylindrical plasma shell adjoining the tube walls is accelerated toward the axis under the influence of the electrodynamic forces. At this stage a considerable part of the work done by the electrodynamic forces is converted into directed kinetic energy of the particles in this converging shell. The ions and electrons move at the same velocity, so that the ions acquire a large kinetic energy, while the energy of the electrons is almost unchanged due to their small mass. The compression process may be regarded just as the formation of a cylindrical shock wave converging at the axis. Initially, neutral gas is located ahead of the shock wave. As the plasma layer moves inward, the neutral gas is swept up by the charged particles (mainly as a result of charge-exchange processes) and is ionised. Thus the mass which is set into motion increases, and the number of ions and electrons in the imploding plasma shell rises rapidly.

In the final stage of the contraction the magnetically accelerated plasma reaches the axis and a large part of the directed ion energy is converted into thermal energy so that the pressure and temperature rise sharply. Spectroscopic data show conclusively that the temperature and density increase rapidly at the end of the first implosion. Spectral lines of highly ionised impurity ions are observed at this time. Such ions can appear only in a plasma having a high density of fast electrons and therefore the appearance of the corresponding spectral lines means that the electron temperature rises suddenly at this particular moment.

An effective demonstration of the phenomena occurring at the time of the first compression maximum is provided by time-resolved spectrograms of the discharge. By this means Luk'yanov and Sinitsyn also demonstrated that the continuum intensity increases suddenly at the moment of maximum compression. The photograph in Plate IV (*b*) shows a time-resolved spectrogram for an initial pressure of 0·1 Torr and an initial field strength of 450 V/cm. An oscillogram showing the variation in the continuum intensity in the red region of the spectrum, recorded with a monochromator and a photomultiplier, is shown in Plate IV (*c*).

The continuous spectrum which appears at the moment of maximum compression results from both bremsstrahlung (free-free electron transitions) and radiative recombination (the capture of an electron by an ion accompanied by the emission of a photon). Whichever of these two mechanisms predominates, the abrupt character of the flare-up in the continuum can be explained only by assuming that at the moment when the shock wave reaches the axis, the number density of free electrons rises rapidly. The state of the plasma at the time of maximum compression is of especial interest for experimental research because, at this stage, the plasma is virtually completely ionised and at its maximum temperature (for a very short period of time). It is therefore necessary to discuss briefly the measurements of plasma temperature and density at maximum compression.

Rough estimates of $T$ during the compression maximum can be made in three ways: first by assuming that the kinetic energy of the directed motion is converted into heat; second, by measuring the pressure change and using the spectroscopically determined electron density; and third, by measuring the widths of spectral lines (assuming that the broadening is produced by the thermal motion of the radiating ions).

In estimating the temperature by assuming that the directed kinetic energy of heavy particles (ions and atoms) is converted into heat, we employ the relation

$$W_i = 3kT,$$

where $W_i$ is the directed kinetic energy of the ions just before the moment of maximum compression. It is also assumed that because of the high density, the ions and electrons relax to a common temperature even though the electron temperature was low during the implosion (this assumption is also invoked to determine the plasma temperature from the pressure data by using the equation of state). This method of analysis yields an underestimate of $T$ because, in reality, heating also occurs during the compression of the plasma column. During the compression, the accelerated mass per unit length does not remain constant, but increases gradually. For this reason, the work done by the electrodynamic forces in compressing the plasma cannot be converted completely into directed kinetic energy; a substantial part is probably converted into thermal energy before the imploding plasma shell converges at the axis.†

The determination of temperature from the pressure and number density is based on the ideal gas law, $p = 2nkT$. The pressure can be measured to within about 30% and $n$ may be determined with about the same, and perhaps a somewhat greater, accuracy. Therefore, this method may yield a value for the temperature in a pulsed discharge within a factor of 1·5 to 2 times the true value, and it is difficult to decide beforehand the sign of the error. Actually no systematic attempt to estimate the plasma temperature over a wide range of conditions has been made using measurements of the plasma pressure; only a few fragmentary data on the magnitude of $T$ have been obtained by this method.

The techniques discussed above give a value for the temperature that is intermediate between the ion and the electron temperatures. Therefore, the method based on the Doppler broadening of spectral lines is of particular importance because it enables one, in principle, to obtain a direct estimate of $T_i$. The main problem connected with this method is the elimination of the influence of ordered motion. To a first approximation, this may be accomplished if the plasma radiation is observed axially through an aperture in one of the electrodes. It may be assumed that the plasma column is cylindrical and does not have a mean component of velocity parallel to the axis of the discharge tube, so that in this case the broadening of the lines cannot be caused by the ordered motion.

For non-hydrogen-like lines of multiply-ionised impurity ions, the line broadening is determined almost exclusively by the Doppler effect. Therefore, if the influence of the ordered motion is eliminated by the observational conditions, the line width becomes a measure of the ion temperature. It must be kept in mind, however, that the nature of particle motion in the plasma may be considerably complicated by various forms of dynamic instability which are sometimes difficult not only to predict but also to observe directly. Therefore, in order to be able to rely completely on temperature determinations from Doppler line-broadening, one has to make sure that the lines emitted by radiating species with different masses yield the same temperature. If this broadening is even partly caused by a collective ordered motion in which ions and atoms of different mass participate with identical velocity, then the 'temperature' determined from the line width is larger, the larger the mass of the radiating species. Unfortunately, from the scanty experimental data at present available on fast high-power discharges, the existence of a common ion temperature has never been demonstrated. That is why the magnitude of $T_i$ determined from spectral line widths should be approached with caution.

---

† See below, p. 130.

In principle, the most precise direct method for determining $T_i$ is the measurement of the intensity of thermonuclear neutron radiation. Except at the highest temperatures, neutron yield varies exponentially with the temperature so that it is possible by measuring the neutron flux to find $T_i$ with sufficient accuracy, even if the plasma density is known only to within an order of magnitude. However, in order to be able to use this method, one has to make sure that the observed neutron emission is indeed caused by a thermal effect, and is not the result of complex acceleration processes characteristic of pulsed discharges. So far, it has not been possible to create conditions under which the neutron radiation is caused primarily by thermonuclear reactions and that is why temperature measurements from neutron emission have not yet been made.

The flare-up of the bremsstrahlung continuum may also be used for the determination of the electron temperature. It is then necessary to measure the relative intensity of the continuous spectrum at higher frequencies, where the dependence of the spectral density upon $\nu$ is determined mainly by the exponential factor $\exp -h\nu/kT_e$. Such measurements, which encompass the soft X-ray region, may be carried out by means of a vacuum spectrograph with a diffraction grating, thin foils which act as filters, together with scintillators and photomultipliers, or a crystal spectrometer.

We are not going to cite disconnected data on plasma temperatures obtained by different methods and under different conditions, since they produce too wide a dispersion of points to enable one to demonstrate quantitative regularities. Let us only mention that under typical experimental conditions, the plasma temperature at the moment of maximum compression amounts to $1 \times 10^6$ to $2\text{–}3 \times 10^6$ °K (according to conservative estimates).

Of great interest for the complete characterisation of the development of a pulsed discharge is the determination of the plasma temperature at different stages. The data we have just discussed pertain to one moment of time only—the time of maximum contraction of the plasma column. However, the problem of determining the temperature as a function of time turns out to be quite complex, and no serious steps towards its solution have yet been undertaken.

Let us now consider techniques for the determination of the particle densities in a plasma.

A direct method for determining $n_e$ is to probe the plasma with a beam of microwave radiation. The fundamental principles as well as the results of such measurements are described in the next chapter, which deals with plasma heating by quasi-stationary currents. For powerful pulsed discharges in gases where the initial pressure is not very small, the study of microwave transmission through the plasma cannot produce interesting results. Owing to the very high plasma densities (particularly at the time of maximum compression), the plasma column is opaque to the shortest wavelengths now available. This being the case, the main hopes in the search for a method of measuring $n_e$ in fast discharges lie in the spectroscopic investigation of the plasma. The most reliable method for the spectroscopic determination of $n_e$ is based on the measurement of the absolute intensity of the continuous spectrum. As was pointed out earlier, the intensity of the continuous radiation is very small, except during the first compression maximum. During this very brief interval of time an abrupt flare-up in the continuous emission is observed covering a very wide wavelength range.

If the electron temperature of a hydrogen plasma exceeds $\sim 30$ eV, the continuous emission spectrum is almost exclusively due to the bremsstrahlung of electrons in the Coulomb field of the ions. The spectral intensity of this emission is given by equation (*1.9*) for a completely ionised plasma. By measuring the absolute magnitude of the radiant energy in a given spectral range and using equation (*1.9*) one can find $n_e$ during the maximum compression. If the measurements of the intensity are made in the visible region of the spectrum, then $h\nu \ll kT_e$. In this case, the correction factor in (*1.9*) increases logarithmically with $T_e$, and the product of this factor and $T^{-\frac{1}{2}}$ is a slowly varying function of the temperature. As a result, an almost arbitrary choice of $T_e$ has little effect upon the determination of $n_e$ from absolute intensity measurements of the visible continuum.†

Although relatively few measurements of the plasma density have been carried out to date, the continuum measurements can provide hopeful material for the verification of the theory of fast discharges. At an initial deuterium pressure of $5 \times 10^{-2}$ Torr and an initial rate of current rise of the order $10^{11}$ A/sec, the number density at maximum compression is of the order of $10^{17}$ cm$^{-3}$, which corresponds to an increase of the density by factors of ten.

Among other effects used for measuring $n_e$ spectroscopically we should mention the so-called Holtsmark effect, in which fluctuating electric microfields in the plasma blur the energy levels (owing to the Stark effect in fields of slow ions) or cause transitions (fields of fast electrons) in the radiating atoms or ions. The Stark splitting of levels varies linearly with the electric field in hydrogen and hydrogen-like ions (e.g., He$^+$, Li$^{++}$) where the levels are degenerate; it varies quadratically where the levels are non-degenerate, as is usual in all other atomic and ionic species.

---

† Another possibility for measuring $n_e$ and $T_e$ is based on the recent development of techniques for determining the intensity of the continuum in the far infra-red (Harding and Roberts, *loc. cit.*, and §6.3).

For the field strengths which are typical in a plasma, the linear Stark effect in hydrogen-like atoms and ions gives the greatest broadening. The half-width of lines broadened by this effect is roughly proportional to the so-called Holtsmark mean field strength, and varies as $n^{\frac{2}{3}}$ (this result is essentially correct even when electrons are taken into account). To give a numerical example, for plasma densities of the order of $10^{15}$ cm$^{-3}$, the Stark broadening of hydrogen lines will be substantially greater than the Doppler broadening up to temperatures of the order of $10^5$ °K. For sufficiently large $n_e$ and moderately high temperature both effects contribute to the line broadening, so that in principle both $n_e$ and $T_e$ could be determined by a detailed analysis of spectral line profiles.

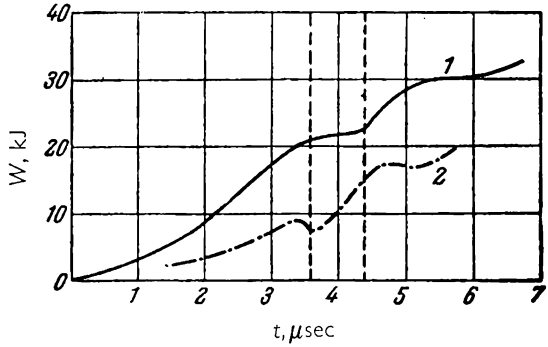

FIG. 39. Time variation of the energy balance. Curve 1 represents $\int JV\,dt$; curve 2, the energy stored in the magnetic field, $(1/8\pi)\int H^2\,d\Omega$

The nature of the process taking place after the first maximum in the compression are not yet known. It is evident, however, that the maximum compression should be followed by an expanding shock wave moving outward towards the walls. The expanding wave should be decelerated by the electrodynamic forces, leading to a second compression phase, followed by a second expansion of the pinch. During the expansion, some of the kinetic energy of the plasma is transferred to the magnetic field. This conversion of energy is not difficult to observe from an examination of Fig. 39, which shows the variation of $\int JV\,dt$ and $(1/8\pi)\int H^2\,d\Omega$ for a typical pulsed discharge. The first of these integrals represents the total energy provided by the electrical energy source, and the second represents the energy contained in the magnetic field. We see that in the expansion phase following the first compression (in the figure this phase corresponds to the time interval between 3·6 and 4·4 μsec), the energy stored in the discharge tube is practically constant, but the energy stored in the magnetic field increases due to the cooling and deceleration of the expanding pinch.

During the expansion and second compression several different kinds of instability begin to appear which are characteristic of a plasma pinch with large current densities. As a result, the shape of the pinch may change considerably, as is observed primarily with magnetic probes. The probe oscillograms show that by the time of the second compression the circular symmetry of the field usually disappears; and that, in addition, radial and axial components of $H$ appear. During this phase of the discharge, the intensity of spectral lines from impurities rises very rapidly (Plate V).

The chief factor responsible for the penetration of impurities into the plasma is the interaction of the discharge with the tube walls. An appreciable part of the current flows in the vicinity of the walls during the entire course of the discharge, so that a significant portion of the energy dissipated during the passage of the current is expended in heating and vaporising the wall surfaces. As the discharge power is increased by increasing the initial value of the voltage across the tube, the role played by the impurities in the discharge becomes more important. In discharges with an initial field strength exceeding $10^3$ V/cm, the impurities substantially alter the plasma density even during the first compression. The contamination of the gas in the discharge chamber by impurities resulting from the evaporation and atomisation of the wall material increases the number of particles in the plasma and causes a drop in the temperature.† This places a real limitation on the attempts to achieve very high temperatures by raising the power of the discharge. No radical methods exist for combating the injection of impurities during the development of a powerful pulsed discharge. One can only hope to reduce the interaction between the discharge and the walls to some extent by magnetic shielding. Such shielding would involve the generation of very high local magnetic fields by external currents, which might protect the walls from a strong interaction with the discharge.

The rough qualitative picture of the acceleration of a cylindrical plasma shell by electrodynamic forces, discussed above, has been refined and the analysis has gone through two stages of development. At first, to describe the dynamics of a plasma column, a very simple model was used to compute the macroscopic motion of an ionised gas acted upon by given electrodynamic forces. We shall briefly state the original assumptions and the results of this calculation, which first took into account the inertial forces which are very important.

Owing to the skin-effect, the current flows along a relatively thin shell during the initial stages of the discharge. Consequently, the electrodynamic forces, which cannot be balanced by the internal pressure of the unperturbed neutral gas, accelerate the plasma shell. To a very rough first approximation, one may neglect the plasma pressure at the start of the compression and write the equation of motion in the form

---

† Even if the impurity is very low (less than 1 %) radiation losses from a high-density plasma can hold the electron temperature down.

$$-\frac{d}{dt}\left(m\frac{da}{dt}\right) = \frac{aH^2(a)}{4}, \qquad \text{.........}(5.6)$$

where $a$ is the radius of the pinch, $m$ is the mass of the moving plasma per unit length of the pinch, and $H(a)$ is the magnetic field strength generated by the gas current at the plasma surface (for a sufficiently high plasma conductivity, the magnetic field inside the pinch may be assumed to be zero). It is also assumed that the moving plasma is contained within the boundaries of a very thin cylindrical layer. During the compression of the pinch, the accelerated mass increases steadily if one assumes that the converging cylindrical plasma shell sweeps up and captures the undisturbed gas located in front of the advancing wave. Using this simplified model (the snowplow model), we can write the following expression for $m$:

$$m = \pi(a_0^2 - a^2)\rho_0, \qquad \text{.........}(5.7)$$

where $\rho_0$ is the initial mass density of the gas and $a_0$ is the radius of the discharge tube. Expressing the magnetic field strength in terms of the total current, we obtain

$$aH^2(a)/4 = J^2(t)/c^2a. \qquad \text{.........}(5.8)$$

From equations (*5.6*), (*5.7*) and (*5.8*) it follows that

$$\frac{d}{dt}\left\{(a_0^2 - a^2)\frac{da}{dt}\right\} = -J^2(t)/\pi c^2\rho_0 a. \qquad \text{.........}(5.9)$$

This equation, together with the initial conditions $a(0) = a_0$ and $(da/dt)_0 = 0$, characterises that phase of the compression when the kinetic pressure is small compared to the electrodynamic forces. This condition is approximately satisfied at early times when the width of the annular current sheath is small compared with its radius.

In order to find $a$ from equation (*5.9*), it is necessary to know the time-dependence of $J$. Strictly speaking, then, it is necessary to solve equation (*5.9*) together with the circuit equation, since the total circuit inductance depends on $a$. However, to avoid complicating the problem, we shall assume that during the times of interest the current rises linearly with time:

$$J(t) = (dJ/dt)_0 t. \qquad \text{.........}(5.10)$$

Let us now introduce the dimensionless variables $x$ and $\tau$:

$$x = a/a_0, \qquad \tau = t/t_1.$$

The quantity $t_1$ characterises the time-scale of the compression. To simplify equation (*5.9*) we shall put

$$t_1 = [a_0 c/(dJ/dt)_0]^{\frac{1}{2}} M^{\frac{1}{4}}, \qquad \text{.........}(5.11)$$

where $M = \pi a_0^2 \rho_0$ is the mass of gas per unit length initially in the tube. If the current rises linearly with time, the equation of motion in dimensionless variables is of the form

$$\frac{d}{d\tau}\left\{(1-x^2)\frac{dx}{d\tau}\right\} = -\frac{\tau^2}{x}, \qquad \text{.........}(5.12)$$

and the corresponding initial conditions are

$$x(0) = 1 \quad \text{and} \quad (dx/d\tau)_0 = 0. \qquad \text{.........}(5.12a)$$

Solving equation (*5.12*) by numerical integration, we obtain the graphical results shown in Fig. 40 as a solid line. The radius of the pinch reaches zero at $\tau = 1{\cdot}5$, i.e. at the time

$$t_c = 1{\cdot}5 t_1, \qquad \text{.........}(5.13)$$

which should correspond to the time of appearance of the first inflection on the current oscillogram.

In the calculation described above, our picture of the physical process has been drastically simplified. It can no longer be used beyond the time of the first compression, because it follows from equation (*5.12*) that if $a = 0$, the acceleration becomes infinite. This result is directly related to the fact that in this calculation the plasma pressure is taken to be zero during the entire compression. In reality, however, the plasma pressure cannot be completely neglected even within the framework of the simple model under discussion, since the capture of the gas by the converging plasma shell is an inelastic process which is accompanied by heating.

Multiplying the left-hand side of equation (*5.6*) by $da$ and performing the integration, we find that the work done by the electrodynamic forces in compressing the pinch from the initial radius to some radius $a$ will be

$$\int \frac{da}{dt}\frac{d}{dt}\left(m\frac{da}{dt}\right)dt = \frac{m}{2}\left(\frac{da}{dt}\right)^2 + \frac{1}{2}\int\left(\frac{da}{dt}\right)^2 dm. \qquad \text{.........}(5.14)$$

The first term on the right-hand side represents the kinetic energy of ordered motion, the second term is the thermal energy evolved in the capture of plasma during the compression process. It is obvious that, at least during the final stages of the compression, the pressure term will have an appreciable influence on the development of the discharge and it should therefore be taken into consideration in the equation of motion. Thus, a term $2\pi a p$ should be added to the right-hand side of equation (*5.6*) (assuming that the pressure remains constant over the cross-section of the pinch). Introducing the dimensionless variables, we obtain

$$\frac{d}{d\tau}\left\{(1-x^2)\frac{dx}{d\tau}\right\} = -\frac{\tau^2}{x} + \frac{p}{p_1}x, \qquad \text{.........}(5.15)$$

where $p_1$ is a quantity having the dimensions of pressure,

$$p_1 = a_0^2\rho_0/2t_1^2. \qquad \text{.........}(5.16)$$

In order to make a qualitative appraisal of the importance of the pressure term, it is necessary to introduce an additional relation between $p$ and $a$. The simplest (although completely unfounded) assumption† is that the pressure varies according to the laws which govern the adiabatic compression of a monatomic gas:

$$p\Omega^{5/3} = \text{constant}. \qquad \text{.........}(5.17)$$

For a contracting cylinder the volume $\Omega \propto a^2$, and therefore

$$p = p_0 x^{-10/3}, \qquad \text{.........}(5.18)$$

where $p_0$ is the initial pressure of the contracting plasma. After substitution of this expression for $p$, equation (*5.15*) becomes

$$\frac{d}{d\tau}\left\{(1-x^2)\frac{dx}{d\tau}\right\} = -\frac{\tau^2}{x} + \alpha x^{-7/3}, \qquad \text{.........}(5.19)$$

where the dimensionless coefficient $\alpha$ is equal to $p_0/p_1$. If the initial pressure is not zero, the compression does not begin until the current builds up to a point which makes the right side of equation (*5.19*) positive. For this reason, in terms of dimensionless variables, the initial conditions are:

$$x = 1, \qquad dx/d\tau = 0 \quad \text{at} \quad \tau = \sqrt{\alpha}.$$

The solution of equation (*5.19*) under these initial conditions for different values of $\alpha$ is represented by the dashed lines in Fig. 40. These curves do not differ appreciably from the curve representing a purely inertial process before the time of maximum compression, even at relatively large values of $\alpha$. Therefore, the expression (*5.13*) for the time of maximum compression is subject to only a minor correction for conditions corresponding to $\alpha$ different from zero. With reasonable assumptions concerning the magnitude of the parameter $\alpha$, this correction amounts to increasing the numerical factor in the formula for $t_1$ by a small percentage.

The above method for taking into account the influence of pressure is based on arbitrary hypotheses and is therefore completely artificial. It has the merit, however, of making it possible to extend the numerical analysis to radial oscillations of the plasma column following the first implosion.

When $p_0$ is not zero, the plasma column contracts to some minimum radius followed by an expansion and second compression under the influence of the electrodynamic forces. The pressure reaches a maximum when the pinch radius is a minimum. According to equation (*5.15*), at that moment the pressure exceeds the value $J^2/2\pi a^2$ expected in quasi-stationary conditions. This excess in pressure is caused by the fact that the left-hand side of equation (*5.19*) is positive at the time of maximum compression. The physical meaning of this result is as follows: at maximum compression, the accelerated plasma is rapidly brought to rest; and this can be considered as an interaction of the plasma with inertial forces which add to the electrodynamic forces and reinforce the compression. Obviously then, the temperature in a dynamic pinch at maximum compression should also be higher than it would be in a quasi-stationary pinch discharge at the same total current.

---

† One neglects the departure from adiabatic laws due to such effects as shock waves, ohmic heating, ionisation and radiation.

The rough estimates which can be made on the basis of this phenomenological theory of the pinch show that the additional effect of the inertial forces lead to temperatures at maximum compression which may exceed the value given by equation (*4.31*) by factors of 1·5–2 at small values of $p_0$. However, this high temperature should last only for a very short time, followed by a cooling of the expanding plasma.

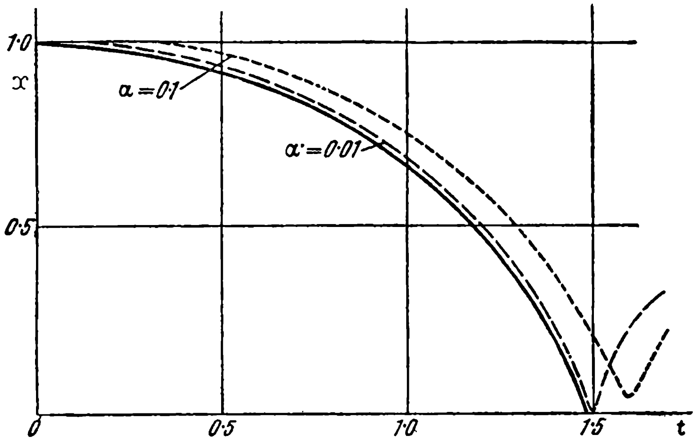

FIG. 40. Theoretical radius-time curves for various values of α as discussed in the text

The above theory of the phenomena occurring in a powerful pinch discharge was submitted in 1953 by Leontovich and Osovets,† and has played an important part in the development of our concepts of the nature of 'fast' discharges. Its primary function was to ascertain the relative importance of the principal factors affecting the electrodynamic compression of a plasma.

The fundamental assumptions upon which Leontovich and Osovets based their calculations now appear obvious, because they incorporate the simple observation that at the beginning of the discharge, the skin-effect disturbs the equilibrium of the forces which act upon the plasma. It should be noted, however, that at the outset of the theoretical investigations (when the idea of quasi-stationary plasma processes was prevalent), the role of the skin-effect in the dynamics of fast discharges was completely ignored. The credit due to the authors of the above dynamic theory lies in the fact that in attempting to find an explanation for the discrepancies between the experimental data on the properties of powerful discharges and the conclusions of the quasi-stationary theory, they were the first to deduce that inertial forces play an important part in the first implosion and that this is closely connected with the influence of the skin-effect.

---

† The theory is presented here in a somewhat altered form. It should be noted that the same conclusions were reached independently a little later by Rosenbluth and Garwin in the U.S.A.

As was pointed out above, the inertial-compression theory can be refined somewhat by taking into account the circuit equation representing the effect of variations in the plasma radius $a$ on the total discharge current $J(t)$. This improvement enables one to describe the compression over a wider range of initial conditions than was possible in the case where it is simply assumed that $J(t)$ rises linearly with time.

The expression for the compression-time $t_c$ is the main theoretical quantitative prediction that can be compared with experimental findings. The calculated values of $t_c$ and the experimental results are in satisfactory agreement, as is shown in Fig. 37, where the theoretical values of $t_c$ are represented by solid lines.

In the second stage of development of the theoretical concepts, an attempt was made to predict by a more accurate calculation the compression and radial oscillations of the plasma—one which would take into account the formation of a shock wave in the plasma as well as the time variation of the mass of the moving gas. Such a calculation was carried out on the basis of magnetohydrodynamic equations, coupled to an equation for the external electrical circuit. The plasma was considered as a monatomic gas with a constant electrical conductivity. It was assumed that during the compression process and subsequent radial oscillation, all the neutral gas moved with the ions (due to charge-exchange processes), so that the velocities of the atoms and ions were identical. Radiation losses, heat transfer to the walls, ionisation and atomic excitation were not considered.

Even with these idealisations, the problem still involves a complex system of partial differential equations which can be solved only by numerical integration with the aid of large electronic computers. The numerical solutions (with a given set of initial conditions) provide information on the temperature, density and flow-velocity as a function of radius, as well as on the distribution of the current density and the strength of the magnetic and electric fields. This theoretical information considerably exceeds that obtained from measurements of the various discharge parameters.†

---

† These computer methods have been extensively developed and many of the above-mentioned assumptions eliminated. See K. Hain, G. Hain, K. V. Roberts, S. J. Roberts and Köppendörfer. Fully ionised pinch collapse. *Zeitschrift fur Naturforschung*, vol. 15a, no. 12, pp. 1039–1050, December, 1960.

PLATE II

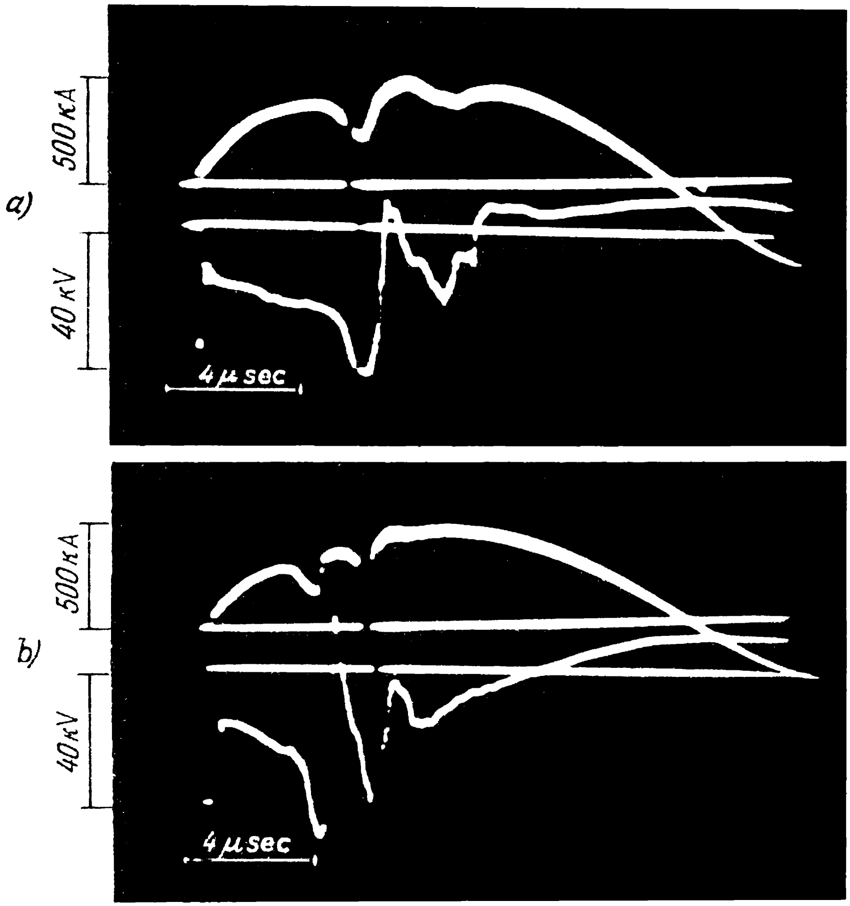

Current (upper) and voltage (lower) oscillograms for discharges in deuterium ($J_{max} \approx$ 450 kA):

($a$) $p_0 = 0{\cdot}2$ Torr
($b$) $p_0 = 0{\cdot}05$ Torr

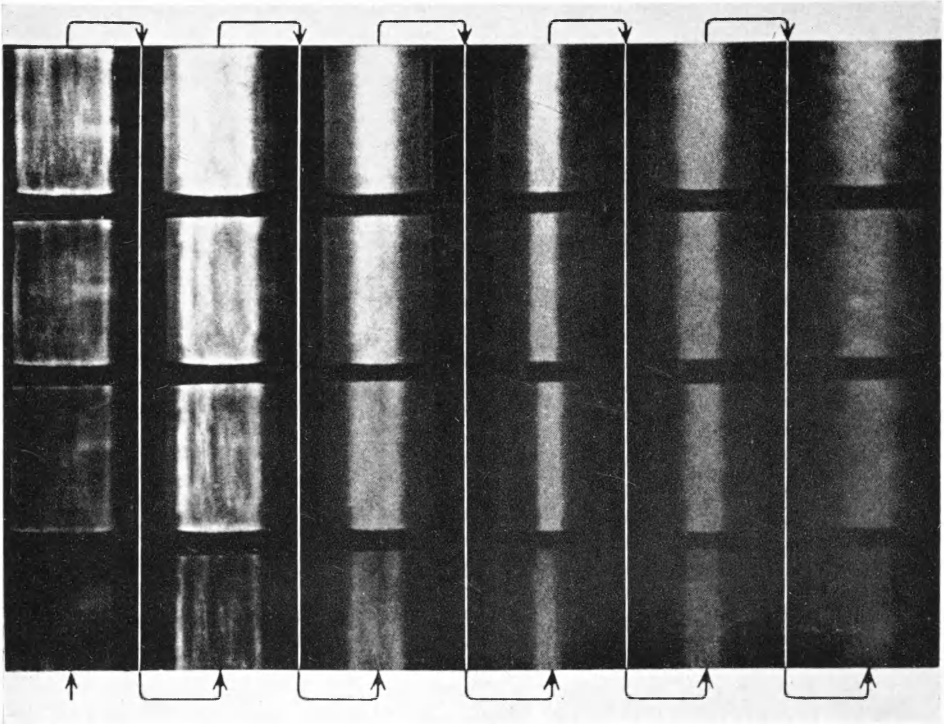

(*a*) Framing camera photographs of a deuterium discharge with an initial pressure of about 1 Torr. Maximum current, 380 kA. The frame sequence is indicated by arrows with 0·5 $\mu$sec between exposures.

PLATE III

(*b*) Streak photograph of a deuterium discharge. Maximum current $1 \cdot 6 \times 10^6$ A.

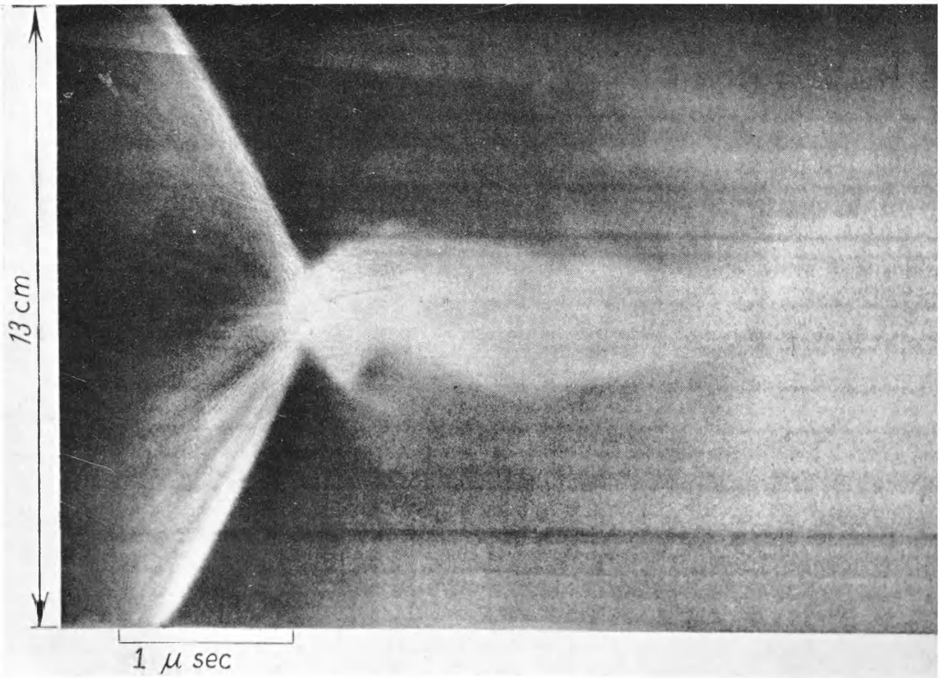

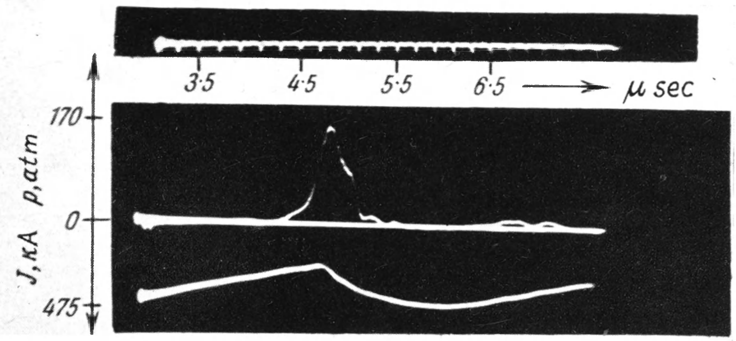

(*a*) Signal from a piezoelectric pressure probe together with a current oscillogram.

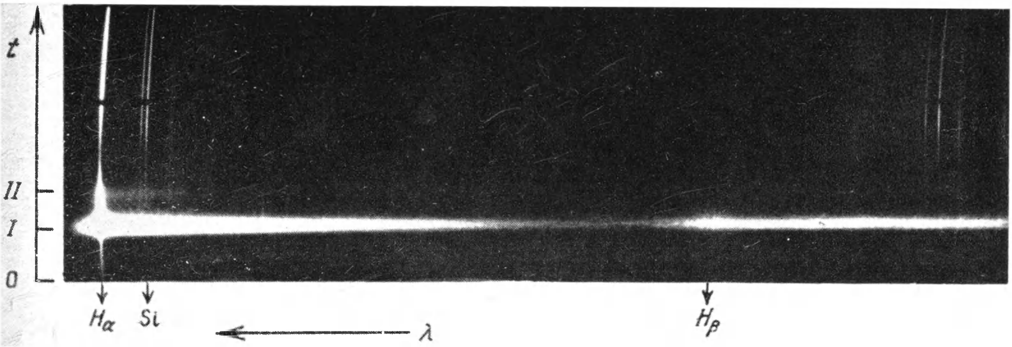

(*b*) Behaviour of the plasma spectrum as a function of time. The marks *I* and *II* on the *t* axis correspond to the times of first and second compression of the plasma column.

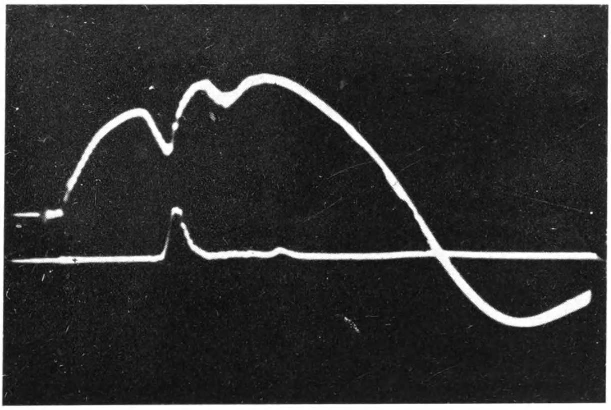

(*c*) Oscillogram of the continuum intensity in the red region of the spectrum, together with a current oscillogram (upper curve).

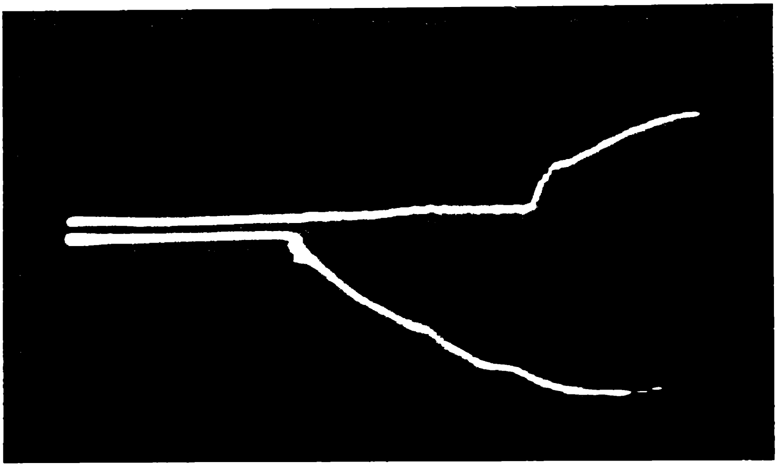

Oscillograms of the intensity of a typical impurity line, SiII 4128Å (top) and the current (bottom).

However, in many respects the reliability of the theoretical results may be verified by comparison with experimental findings; for example, with the considerable amount of existing experimental data concerning current distribution and the radial plasma velocity. In this comparison of the theoretical and experimental results for a number of special cases, the agreement was satisfactory, at least during the initial stages of a pulsed discharge before the second compression. Therefore, it is justifiable also to use the results of the theoretical computations for the estimation of quantities which have not been measured with sufficient accuracy. Two of the most important quantities which characterise the state of a plasma are the temperature and density distribution at the time of maximum compression. Numerical results obtained from the solution of the magnetohydrodynamic equations show that the plasma temperature at maximum compression is given by

$$\bar{T} = 4{\cdot}6\times 10^{13}J^2/N. \qquad \text{.........}(5.20)$$

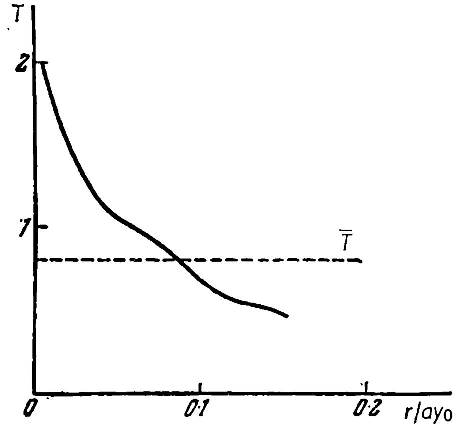

Fig. 41

Variation of $T$ with the pinch radius according to the numerical solution of the magnetohydrodynamic equations

With the assumption that $T_e = T_i$, this expression gives an average value $\bar{T}$ of the plasma temperature which is 2·5 times larger than the temperature calculated for a quasi-stationary discharge with the same $J$ and $N$. This result also follows qualitatively from the simplified compression model where the inertial forces are roughly taken into account. The radial distribution of temperature for a discharge with typical initial conditions is shown schematically in Fig. 41. The dotted line corresponds to the mean value $\bar{T}$. Because of the convergence of the shock wave the temperature rises abruptly near the axis and may exceed the mean value by several times. In considering the dependence of $T$ on $r$, it is obvious that the use of equation (*5.20*) cannot lead to an over-estimate of the maximum ion temperature in a real plasma column.

Figure 42 shows the theoretical time-dependence of terms which contribute to the energy balance of the discharge. One characteristic feature of the energy distribution at early times must be noted: during almost the entire course of the compression phase, the plasma energy is divided about equally between the thermal and the ordered motion; at the stage of maximum compression, the energy in the ordered motion is converted into heat, and the thermal energy of the plasma is approximately doubled. Hence it also follows that the experimental evaluation of the plasma temperature, based on the assumption that the thermal energy is equal to the maximum energy of ordered motion, should yield values of $\bar{T}$ which are about half as large as the true values.

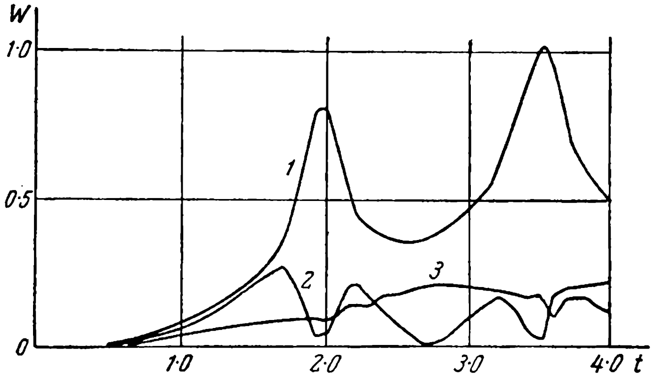

Fig. 42. Terms contributing to the energy balance of a typical pinch discharge

(1) $\int_0^a \frac{3}{2}p2r\,dr$; (2) $\int_0^a \frac{\rho v^2}{2}2r\,dr$; (3) $\int_0^a \frac{H^2}{8\pi}2r\,dr$

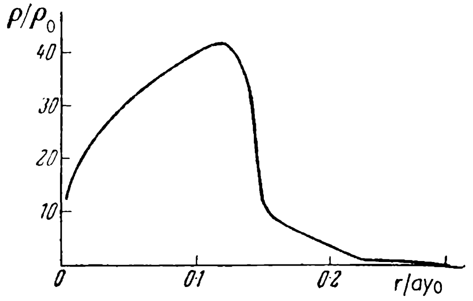

Fig. 43

Radial density distribution at the time of maximum compression in a dynamic pinch, obtained from numerical calculations

The density distribution at the peak compression is shown in Fig. 43. The maximum value of the density is 30 to 40 times the original gas density. This result is confirmed by spectroscopic measurements of the number density. We should emphasise and explain one interesting property of the distribution of $\rho(r)$: it drops abruptly near the plasma axis. The plasma pressure, which is proportional to $\rho T$, should be approximately constant in a small region close to the axis. Therefore, the rapid rise in $T$ near the axis must be compensated by a corresponding decrease in $\rho$.

Of course, it should not be expected that a magnetohydrodynamic theory erected on a whole series of simplifying assumptions will be entirely confirmed by experiments. The theory does not take into consideration the interaction of the discharge with the wall, and therefore cannot explain the large persistent currents in the vicinity of the wall. In these calculations there is no place for instabilities, and that is why the theory provides too idealised a picture of the oscillations of the plasma column which follow the first compression. In particular, the theoretical calculations predict that the plasma temperature at the second compression maximum will be considerably higher than at the first compression. However, there are no experimental data of any kind to substantiate this result. There is also no experimental verification of the theoretical result that the plasma density reaches a very high value during the second compression. As has been shown by spectroscopic measurements of the continuum intensity, the mean plasma density during the second compression is at least four to five times lower than during the first.

In order to complete the discussion of questions involved in the theory of the dynamic pinch, it is necessary to make one observation concerning the nature of the microscopic processes occurring in a plasma. In the above presentation it was pointed out repeatedly that in an 'inertial' compression of a plasma the work done by the electrodynamic forces is converted into kinetic energy of the ions, and that during the expansion of the pinch this ion kinetic energy is transformed into magnetic field energy. Thus the electron component of the plasma is of secondary importance in the over-all energy balance. However, this does not mean that the electrons play a wholly passive role in the dynamics of the pulsating plasma. In fact the electrons, and not the ions, play the primary role in all the processes involved in the compression and expansion of the pinch, because the electrodynamic forces which produce the radial pressure act directly upon the electrons. This is easy to verify if it is recalled that the electrodynamic forces act upon the particles which carry the current, and in a plasma these are the electrons. The plasma current is generated by a flow of electrons moving at some mean velocity $u = j/n_e e$, where $j$ is the current density. The average force $euH/c$ which acts upon an electron moving in the magnetic field is directed along the radius toward the pinch axis. As soon as the electrons begin to move inward under the action of this force, a radial electric field is produced, and it is this which accelerates the ions. The radial electric field should almost completely offset the Lorentz force acting upon the electrons. Thus

$$eE = euH/c.$$

On the other hand,

$$eE = m_i dv_i/dt$$

(because of the small axial velocity of the ions, the force exerted on them by their motion through the magnetic field may be neglected). The strength of the radial electric field under typical conditions in a pulsed discharge lies between a few tens and a few thousand volts per centimetre.

§ **5.4** One of the most characteristic features of powerful pulsed discharges in light gases is that under certain conditions the discharge becomes a source of high-energy radiation. Neutron radiation from pulsed discharges in deuterium was first observed in the U.S.S.R. in 1952. Soon afterwards it was established that hard X-rays are emitted simultaneously with the neutrons. High-energy X-rays (up to 350 keV) also arise in discharges in ordinary hydrogen. To start with, let us confine ourselves to the properties of the neutron radiation.

In the usual discharge tubes with porcelain, quartz or glass walls, neutron emission is observed if the initial pressure lies within the range of a few thousandths to 0·3–0·5 Torr. The neutron yield fluctuates very widely from one discharge to another and attains an appreciable value only after the discharge tube has been conditioned by discharges in hydrogen, deuterium or helium. For a maximum current of 200 to 500 kA and an initial deuterium pressure of about 0·1 Torr, the number of neutrons emitted per discharge usually varies between $10^6$ and $10^8$. The neutron yield is very strongly influenced by a small concentration of foreign gases, i.e. if a few parts per thousand of oxygen, argon or xenon is added to deuterium at a pressure of the order of 0·1 Torr, the neutron emission is quenched.

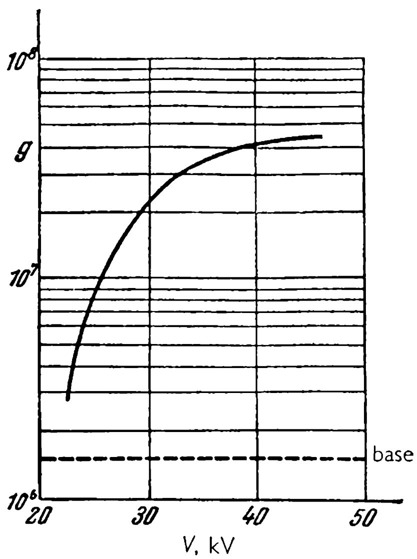

FIG. 44

Variation of the neutron yield with the initial voltage $V$ across the discharge tube

The irreproducibility of the neutron radiation hinders the establishment of quantitative relationships between the neutron yield and the parameters of the discharge. Indeed, these relationships are rather more qualitative than quantitative in nature. Figure 44 shows the dependence of the neutron yield $g$ on the initial voltage across the tube, obtained in a series of experiments with long porcelain discharge tubes with an initial deuterium pressure of 0·02 Torr. The data given in this figure were obtained by averaging the results of a large number of individual experiments and provide a good illustration of the functional dependence of $g$ on $V$. At lower voltages a very fast rise in the neutron yield is observed, followed by saturation at higher voltages. Curves of $g$ versus $V$ obtained for other pressures are similar. The initial pressure which corresponds to the maximum neutron yield for typical discharge tubes is in the range 0·05 to 0·1 Torr.

Measurements of the spatial distribution of the neutron radiation have shown that the emission sources are distributed over the whole length of the discharge and occupy a region close to the axis. Hence, the observed radiation is not a trivial effect, and cannot be explained by assuming that the deuterons accelerated at the plasma boundary bombard the deuterium absorbed on the electrodes or the walls of the tube. Oscillographic studies of the neutron radiation show that in all cases it is characterised by steep-rising short bursts whose duration usually does not exceed 0·3–0·5 $\mu$sec. The neutron bursts appear only at certain definite times of the discharge; those at which the compression of the pinch is a maximum.

The analysis of a very large number of oscillograms shows that if the initial value of $E_0$ the electric field strength in the tube does not exceed 200–300 V/cm, the neutron emission starts at the time of the second compression maximum. The neutrons do not appear during the first compression, but sometimes two neutron bursts are observed—during the second and third maximum compression. The second neutron burst can be observed when the third compression manifests itself clearly on the current and voltage oscillograms. This occurs in discharges with a low initial gas pressure.

As an illustration of these facts, Plate VI shows two oscillograms of the neutron radiation, recorded simultaneously with the current on a dual-beam oscillograph. The first picture (*a*) shows one neutron burst at the time of the second compression, the second (*b*) shows two consecutive neutron bursts.

If the discharge power is increased by raising $E_0$ to 1500–2500 V/cm, the neutron burst also begins to appear during the first compression maximum (see the oscillograms in Plate VII), and usually lasts about 1 $\mu$sec.

Analysis of the neutron energy spectrum is of considerable importance in determining the mechanism causing neutron radiation, since this spectrum characterises the energy of those deuterons which are responsible for the generation of the nuclear reactions in the plasma. The study of the angular dependence of the neutron energy spectrum enables one to go further. If such a dependence is observed, it provides evidence that there is a preferred direction of motion of the fast deuterons which participate in the reactions. An analysis of the kinematics of the $d+d \rightarrow {}^3\mathrm{He}+n$ reaction shows that in a coordinate system where one of the deuterons is at rest before the collision, the kinetic energy of the neutron is given by the expression

$$W_n = W_0 + (W_0 W_k/2)^{\frac{1}{2}} \cos \phi. \qquad \text{.........}(5.21)$$

Here $W_0 = 2{\cdot}46$ MeV is the neutron energy corresponding to the interaction of two deuterons having zero velocities, $W_k$ is the initial kinetic energy of the moving deuteron and the angle $\phi$ designates the direction of the ejected neutron with respect to the direction of motion of the fast deuteron. Equation *(5.21)* is applicable when $W_k \ll W_0$.

If nuclear reactions arise as the result of a process in which a group of fast deuterons moves in a definite direction through a relatively cool plasma then, according to equation *(5.21)*, this should be reflected in the angular dependence of the neutron spectrum. The largest shift in the neutron spectra should be observed by comparing the results obtained from energy measurements of neutrons travelling in the same direction as the fast deuterons, and those travelling in the opposite direction. The difference between the neutron energies observed in these two directions is $\sqrt{2W_0 W_k}$. In this expression, the neutron kinetic energy $W_0$ is also under the square root sign; therefore, even at relatively small energies $W_k$ of directed deuteron motion, a shift in the spectrum should be detectable experimentally (at $W_k = 1$ keV it amounts to about 70 keV).

The technique for examining the neutron energy spectrum is based on the measurement of the range of recoil protons in nuclear emulsions, which are exposed at some distance from the tube during pulsed discharges. In these measurements, the recoil proton tracks chosen for analysis are those inclined at a small angle to the direction of the neutrons.†

All measurements of the energy spectrum of neutrons produced in pulsed discharges (in dynamic linear pinches) show that acceleration processes are mainly responsible for the neutron radiation. As a result of the presence of accelerating electric fields, deuterons with energies of several tens of kilovolts appear at certain times in the plasma. Measurements of the neutron energy distribution as a function of angle also show that the accelerated deuterons move predominantly along the axis of the discharge tube—from the anode to the cathode. As an illustration, Fig. 45 shows two histograms of the energy distribution of neutrons emitted in opposite directions along the axis of a discharge tube. Despite the large width of the energy distributions, it is possible to determine without much difficulty that the neutrons moving toward the cathode have a higher average energy. Direct proof of the existence of fast deuterons in the plasma was obtained by a mass-spectroscopic analysis of the particles emitted from the discharge. Values of $e/m$ and of the energy of the ions which escape from the tube through an orifice in the wall or an electrode, were measured by the Thomson parabola method. It was established that 200 keV deuterons are present in ordinary discharges.

---

† This method was apparently first employed by Colgate in the U.S.A. for the determination of the energy spectrum of neutrons produced in pulsed discharges.

In describing the main properties of the neutron radiation from pulsed discharges, we must mention its variation with the strength of an externally generated axial magnetic field. Measurements have shown if an an axial magnetic field is applied to the discharge tube, the neutron yield drops sharply and the reduction is already appreciable at initial fields of only 50–100 Oe. The neutron radiation disappears completely when the initial magnetic fields exceed a few hundred oersteds.

A pulsed discharge with a rapidly increasing current is also a source of hard X-rays. The X-rays, like the neutrons, are always emitted in short bursts lasting up to a few tenths of a microsecond. Various experimental techniques have been used for studying the properties and production mechanisms of the hard X-rays. The time-dependence of the X-ray pulse is recorded with a scintillation counter. The quantum energies may be measured by the absorption method (using filters of light and heavy elements), and from the energy spectra of Compton electrons and photoelectrons observed in a Wilson cloud chamber or in nuclear emulsions.

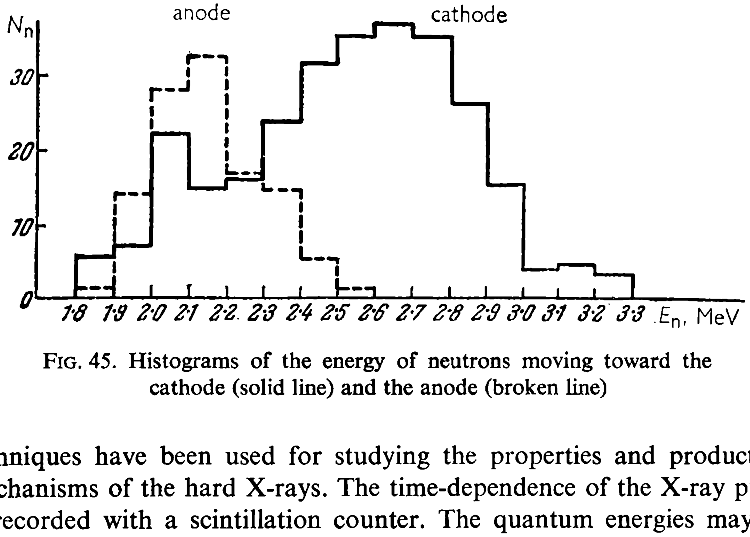

FIG. 45. Histograms of the energy of neutrons moving toward the cathode (solid line) and the anode (broken line)

Hard X-rays are emitted with discharges in hydrogen and deuterium, and the oscillograms show that in deuterium the X-rays appear simultaneously with neutrons. The most convincing proof of this fact is provided by experiments where the neutron and X-ray bursts, detected by the same scintillation counter, become separated by the difference between the time of flight of the neutrons and that of the X-ray quanta. The greater the distance from the discharge tube to the counter, the greater is the delay between the appearance of the X-ray burst and the neutron burst. These measurements show that the bursts occur at the same time, to within hundredths of a microsecond.

Bursts of hard X-rays usually appear at the second and third maximum compression. When the initial electric field is raised to 1000–2500 V/cm, a narrow X-ray burst (lasting about 0·3 μsec), is also observed at the time of the first compression. The X-ray intensity is even more irregular than the neutron radiation. For this reason, the study of the mechanisms governing the dependence of this radiation on the main parameters of the discharge yields only qualitative results. The intensity of the X-ray bursts varies by 1 or 2 orders of magnitude from one discharge to another. It can be roughly stated that at an optimum gas pressure (about 0·1 Torr), the total number of hard quanta (photons with energies exceeding 100 keV) amounts to approximately $10^{10}$–$10^{11}$ per discharge. The variation of the X-ray intensity with pressure is qualitatively similar to that of the neutron radiation.

Measurement of the ranges of recoil electrons in a Wilson cloud chamber allows one to deduce the maximum energy of the X-ray quanta. Figure 46 shows a typical energy distribution for electrons produced in a Wilson chamber during a pulsed discharge in hydrogen at $p_0$ = 0·05 Torr and $E_0$ = 400 V/cm.

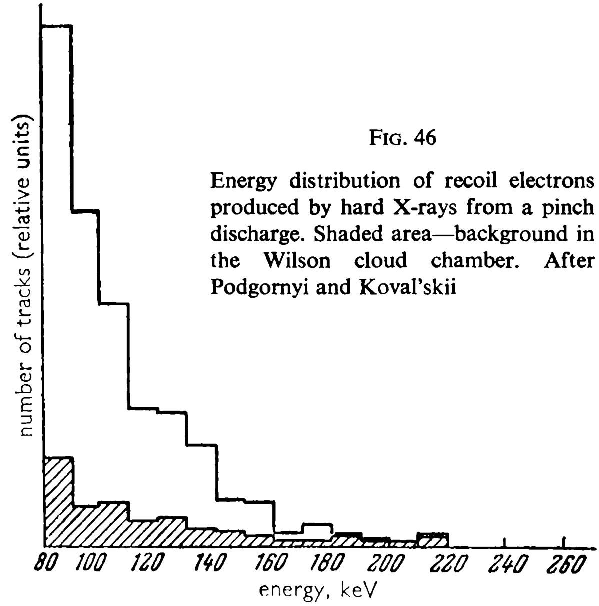

Fig. 46

Energy distribution of recoil electrons produced by hard X-rays from a pinch discharge. Shaded area—background in the Wilson cloud chamber. After Podgornyi and Koval'skii

In determining the maximum energy of X-ray quanta it is most convenient to compare the electron spectrum produced by these quanta with that produced by an X-ray source whose spectrum is already well known (Fig. 47), e.g. an ordinary X-ray tube. Such a comparison shows that quanta with energies up to 300 keV are definitely present in the spectrum of X-rays emitted during pulsed discharges in hydrogen and deuterium. It is interesting to note that during the emission of these quanta, the external voltage applied to the discharge may be no greater than 10 to 15 kV.

The X-ray emission from a pulsed discharge is governed by the usual bremsstrahlung mechanism, involving fast electrons which appear at certain definite phases of the discharge. These fast electrons may be observed directly if they are allowed to escape from the discharge tube through an aperture in the anode. Measurement of the energy spectrum of the escaping electrons shows that the maximum energy is about 300 keV. The fast electrons appearing in the discharge move in a definite direction: they travel towards the anode (more exactly, toward the electrode which acts as the anode in the first half-cycle of the discharge).

No definitive and widely accepted theory exists as yet of the mechanism for the generation of hard X-rays and neutrons. Nevertheless, some features of this mechanism are delineated fairly clearly. As mentioned above, a geometrical investigation of the neutron radiation shows that the flux of fast deuterons is confined to a narrow region in the discharge tube. The same can be said of the flux of fast electrons. By allowing the electrons to leave the discharge tube through an aperture in the anode, it is possible to determine the radius of the accelerating region of the discharge. The width of this zone is found to be a few millimetres in all. Thus it follows directly from the experimental evidence that the particle acceleration occurs in strong electric fields which are produced near the axis of the plasma column during the time of maximum contraction. Hence, to discover the origin of the fast particles, it is necessary to find the origin of these strong electric fields.

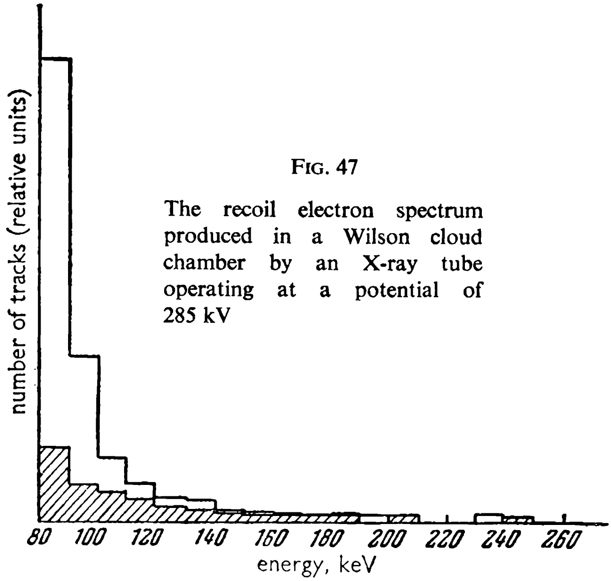

FIG. 47

The recoil electron spectrum produced in a Wilson cloud chamber by an X-ray tube operating at a potential of 285 kV

The electric field in the plasma is primarily due to inductive e.m.f.'s which arise from radial oscillations of the plasma column. We first assume that the plasma column retains cylindrical symmetry so that the electric field strength is given by

$$E_z = j/\sigma - (dr/dt)\, H_\theta(r)/c, \qquad \ldots\ldots\ldots(5.22)$$

which follows from equation (*4.16*). In the compression phase, $dr/dt < 0$. Neglecting resistive voltages, we can write:

$$E_z \approx v_r H_\theta / c \qquad \ldots\ldots\ldots(5.23)$$

where $v_r$ is the velocity of radial compression. When $H = 10^4$ Oe and $v \simeq 10^7$ cm/sec, the electric field strength should be of the order of 1000 V/cm and, if the discharge tube is 100 cm long, the total potential across the plasma column will be about 100 kV. It would seem that these calculations indicate the origin of fast particles: the acceleration of the electrons and ions may be due to the voltage which arises from the radial compression of the plasma column. Actually, however, the problem is considerably more complicated.

Let us note, first of all, that owing to the invariance of $W_\perp/H$ the particle acceleration in a direction perpendicular to the magnetic field cannot start in a region where $H$ is large, since the energy increases only in proportion to $H$. Therefore, only those electrons and ions which were originally close to the axis can be involved in the acceleration process. Moreover, it follows from equation (*5.23*) that $E$ has a maximum value in a region which may be arbitrarily called the boundary of the plasma column. As the axis is approached, $v$ and $H$ decrease approximately in proportion to $r$ (if the additional attenuation of $H$, due to the skin-effect, is disregarded). Consequently, the strength of the axial electric field varies as $r^2$. The mean radius of the plasma column at the time of maximum compression amounts to a few centimetres under typical experimental conditions. With such a large plasma diameter, a particle which begins its acceleration in a region close to the axis cannot acquire a large amount of energy because it moves in a region with a weak electric field.

This is especially so in the case of electrons where, even for the highest observed energies, the radius of gyration is very small compared with the radius of the plasma column. Thus the difficulty is that for large values of the plasma radius at the time of maximum compression, the electric field near the axis will be too small to accelerate the particles sufficiently. Furthermore, measurements under usual conditions (initial field strength in the discharge tube of about 400 V/cm, gas pressure of about 0·05 Torr) show that for $r$ about 3–5 cm, the mean value of $E$ attains several hundred volts per centimetre at the first compression and drops to 100–200 V/cm at times corresponding to the second and third compression, i.e. just when electrons and ions having energies up to 200–300 keV appear. It is certain, therefore, that the appearance of fast particles in a pinch is caused by a more complex mechanism. It appears that the voltage produced by a simple radial compression of the plasma is probably not sufficient for the acceleration of ions and (especially) electrons to the high energies observed experimentally.

It follows from the above that one must look for processes in the plasma which might lead to the appearance of large over-voltages near the axis of the pinch—over-voltages which have the property of not being detected with the usual methods of observation. Such over-voltages may arise as a result of various types of instability peculiar to a high-current pinch.

It may be assumed that one specific type of instability plays a substantial part in the particle acceleration mechanism. It is the appearance of random fluctuations in the radius of the plasma column (Fig. 48). When they have once appeared, they do not disappear, but on the contrary grow very rapidly. As a result, very narrow constrictions are formed at various points along the plasma column (sausage instability). The driving mechanism for the formation of this instability may be easily explained: at the place where the pinch is constricted, the magnetic pressure $H_\theta^2/8\pi$ is greater than in the neighbouring regions, because $H_\theta^2$ is inversely proportional to $r$. The increase in the electrodynamic pressure is not balanced by a corresponding increase of the plasma pressure in the constriction, because the plasma can flow freely into neighbouring portions of the pinch. The formation of a narrow constriction in the final stages of the plasma confinement is associated with very high radial velocities (due to the rapid increase in the magnetic pressure). Therefore, in the constricted region, $H_\theta$ may reach values differing by an order of magnitude from the magnetic field strength at the mean radius of the plasma column. The consequent electric over-voltages in the portions of the pinch where narrow constrictions arise would then be responsible for the appearance of fast electrons and ions in the plasma.

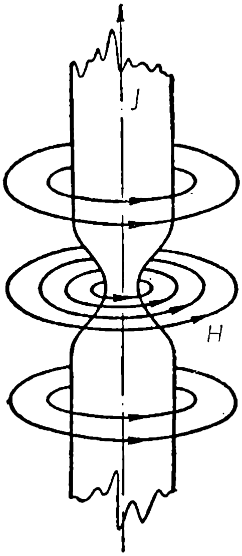

FIG. 48

Local constriction of the plasma pinch and probable cause of large accelerating voltages

If this view is accepted, it is possible to answer the question why neutrons and hard X-rays appear only in the second and third phase of the compression at moderate potentials. The answer is that a certain time interval is necessary for the development of pinch instability. Estimates of this interval, based on theoretical considerations, are too rough to permit one to attribute the development of instability to the second and not the first compression. However, an oscillographic examination of magnetic probe data does permit the measurement of the time interval during which instabilities begin to develop rapidly in a pinch. These data lead to the conclusion that the pinch is virtually stable and retains its cylindrical shape up to the beginning of the second compression; thereafter, the deviation of the field from cylindrical symmetry is shown very clearly on the probe oscillograms.

These considerations concerning the nature of acceleration processes explain the influence of an axial magnetic field on the intensity of neutron radiation. In its motion toward the axis, the cylindrical plasma sheath compresses the trapped axial magnetic field, and produces a rapid increase in field strength on the axis. Herein lies the peculiar 'dynamic paramagnetism' of the plasma pinch, produced by the 'freezing-in' of the lines of force. If the magnetic flux is conserved, the strength of the axial field in the plasma rises in proportion to $1/a^2$ and the resulting magnetic back-pressure varies as $1/a^4$. Therefore, even a low initial axial field very effectively counteracts the formation of the narrow constrictions which, according to the above view, play a decisive part in the creation of strong accelerating electric fields.

At very high initial values of the electric field, the voltage produced by simple cylindrical compression may be sufficient to accelerate deuterons in pinch tubes. Therefore, the neutron radiation may in this case appear during the first compression. In this connection, we recall that, in accordance with theory (see Fig. 43), at the moment of maximum contraction the density in the neighbourhood of the axis is very small, so that collisions do not prevent particles from acquiring energy in the electric field.

A particular manifestation of the Fermi mechanism, which was discussed in Chapter II, can be seen in the particle acceleration processes. To clarify the meaning of this remark, let us consider the behaviour of a particle located near the axis of the pinch at the end of the first compression. In this region, the magnetic field is small and the particle can travel across it without any appreciable deflection. However, the particle cannot move a considerable distance from the axis, because in so doing it would encounter the converging inner wall of the magnetic channel formed by the pinch current. Thus the particle should rebound successively from the wall of the magnetic channel, and with each rebound its kinetic energy will increase.

The above considerations of the acceleration of particles in a pinch cannot claim to constitute an exhaustive explanation of all the related phenomena. There is no reliable quantitative theory of the acceleration mechanism at present, and probably none will appear until experimental studies of certain minute details of these processes are completed.

The production of fast electrons may be due to an entirely different mechanism, also associated with one of the special types of instability characteristic of a high current pinch. Instability of this type leads to a helical twisting of the pinch, which produces an axial magnetic field having a strength of the same order as that of the azimuthal field.† The formation of the axial magnetic field induces an electromotive force which accelerates the plasma electrons along the magnetic field. The azimuthal component of the electron momentum $p_\theta$ will be proportional to the axial magnetic field strength, i.e.

$$p_\theta = eH_z r/2c,$$

where $r$ is the distance to the axis. According to rough estimates, such a 'betatron' acceleration mechanism may result in the acceleration of electrons up to energies of the order of several hundred keV during characteristic instability growth times of tenths of a microsecond. However, the corkscrew instability appears to be unrelated to the acceleration of deuterons, because the energy acquired by a particle during the inductive acceleration is inversely proportional to its mass.

Although the conditions under which the neutron radiation from pulsed discharges has been observed until now are favourable to acceleration processes, one should not consider it impossible for a certain part of this radiation to have a predictable thermonuclear origin. This observation applies particularly to pulsed discharges in tubes with metal walls. In such discharges, studied in detail by Filippov and Filippova, a strong compression of the plasma takes place within the confines of a small segment of the tube axis, and a very high temperature and density are attained in the compression zone. Plate VIII shows a picture of this zone taken through a beryllium foil window with a pin-hole camera, using the soft X-radiation emitted by the plasma. Measurements of the soft X-ray intensity at the time of maximum compression show that the electron temperature reaches about $10^7$ °K at a number density of $\sim 10^{18}/\mathrm{cm}^3$. Obviously, the ion temperature under these conditions should not be lower than the electron temperature, since the electrons take energy away from the shock-heated ions.

It appears that the thermonuclear reaction rate may be raised considerably if higher voltage discharges with higher rates of current rise are used. The kinetic energy of the deuterons converging towards the axis of the pinch should increase in proportion to $(dJ/dt)_0$, resulting in higher ion temperature at the time of maximum compression. However, it must be kept in mind that as $(dJ/dt)_0$ increases, the power dissipated at the walls of the discharge tube also increases; and this increases the emission of gas from the walls and the consequent level of contamination of the deuterium by heavy impurities. For this reason, in designing experiments involving more extreme electrotechnical parameters, it is necessary simultaneously to work out efficient methods of reducing the gas emission from the walls.

---

† The corkscrew instability is a special case of the instabilities which bend the plasma column. In its development, the plasma shows a tendency toward the formation of 'force-free' magnetic configurations (see next chapter).

Let us suppose that these technological difficulties have been overcome. What then are the prospects of generating thermonuclear power by methods based on the utilisation of powerful pulsed discharges?

To answer this question let us recall that a measure of the energy efficiency of a thermonuclear generator is the quantity $H^2\tau$, where $H$ is the strength of the magnetic field confining the plasma and $\tau$ is the confinement time during the compressed state. For a generator with positive energy yield, operating with a 50% deuterium and tritium mixture, the value of $H^2\tau$ should be no lower than $10^8$ Oe$^2$ sec (an optimistic estimate). In the case under consideration,

$$H \simeq 0{\cdot}2J/a_{\text{min}}, \qquad \tau \simeq a_{\text{min}}/v_{\text{T}},$$

where $J$ is the current in amperes at the time of maximum compression, $a_{\text{min}}$ is the minimum radius of the pinch, and $v_{\text{T}}$ designates the ion thermal velocity at the optimum temperature, which is about $10^8$ cm/sec for a deuterium-tritium mixture. A positive energy yield can be obtained if the condition $J > 10^9\sqrt{a_{\text{min}}}$ is satisfied. From the general theory of shock waves it follows that the maximum density at the time of maximum compression cannot surpass the initial density by more than 10–100 times. Therefore, the minimum radius of the pinch can be no less than one-tenth of the radius $a_0$ of the discharge tube.

In proceeding to yet higher-power discharges, it is scarcely feasible to reduce $a_0$ at the same time. Even with a maximum effort at optimism we can hardly envisage a tube radius of less than 10 cm. This value corresponds to $a_{\text{min}}$ of the order of 1 cm, and a total current in the compressed pinch of the order of $10^9$ A. If we consider a discharge several centimetres long, the energy concentrated in the discharge tube at this high current will be of the order of $10^{10}$ $J$. This tremendous energy, which is originally stored in the power supply, is converted into thermal and magnetic energy in a short time interval and, during the expansion of the pinch, is next transformed into shock wave energy, which would destroy the apparatus. By a rough estimate, such a process should be equivalent to the explosion of several tons of TNT.

This result is a good illustration of the technological hopelessness of power generation from thermonuclear reactions in short-term pulsed discharges, in which the duration of compressed state is determined by the transit time of a fast particle across the pinch (in essence, this means that the magnetic field only serves the function of compressing, not of confining the plasma).

This disconcerting résumé should not be taken as an epitaph on the study of fast pulsed discharges; at any rate, it should not be taken to mean that the results of these studies are of no real value. To convince ourselves that the opposite is true, let us note that to date we do not have a more effective method of producing a dense plasma with hot ions than by fast 'inertial' compression which was discovered in the course of studies of fast pulsed discharges. As we shall see later, all attempts to obtain hot ions in a Joule heated plasma have thus far failed to yield positive results. Moreover, the use of the 'inertial' compression as the initial phase of plasma heating has yielded promising results in systems of the '$\theta$-pinch' type, which will be discussed later in this chapter. It is also beyond question that the combination of results obtained in experiments with pulsed discharges has an independent scientific value in plasma physics, especially because of the observation of such interesting phenomena as the generation of fast particles. In particular, these phenomena may serve as a model for the understanding of some astrophysical processes, such as solar flares accompanied by the production of high-energy particles.

Finally, it should be noted that studies of powerful pulsed discharges have provided the first evidence for the stabilizing properties of various plasma-field configurations. Of course, the results thus obtained are purely preliminary, and should not be unconditionally extrapolated to quasi-stationary states of long duration. However, their heuristic value in the search for effective methods of stabilizing plasma instabilities cannot be doubted, since they anticipated much of what was later established in studies of the so-called slow discharges. We refer in particlar to the results of numerous experiments devoted to studies of the influence of external fields on the stability of plasmas in fast discharges.

A substantial part of this work was reported at the Geneva conference in 1958. Most of these investigations were carried out by means of rather simple techniques, and despite their apparent diversity, accentuated by a multitude of arbitrary names, were devoted chiefly to the study of a few simple cases involving the action of an axial field upon an electric discharge in a straight discharge tube. If we sum up the results obtained, they amount chiefly to the observation that in the presence of an externally generated axial field, some of the most frequently encountered pinch instabilities disappear, while others are markedly reduced. However, in all cases a very rapid escape of energy from the pinch, a low conductivity, and a moderate plasma temperature are observed.

At the present time these data are mainly of historical interest, since they have been superseded by results obtained from studies of the so-called quasi-stationary ('slow') discharges in toroidal chambers involving more sophisticated experimental techniques and more refined experimental conditions. Results of these experiments are given in the next chapter; so we will not stop here to consider earlier research on the stabilisation of the linear pinch by an axial magnetic field.

§ **5.5** Special attention should be paid to one of the varieties of the pinch geometry which has not yet been achieved under quasi-stationary conditions. The system in question is shown in Fig. 49. The plasma forms a hollow cylindrical shell carrying a longitudinal current $J_p$. A metallic rod down the axis carries a current $J_1$ flowing in the opposite direction; and this generates a magnetic field which inhibits the normal pinch compression of the plasma shell and permits the confinement of the plasma in a state of equilibrium at some distance from the axis.

The equilibrium conditions have a particularly simple form if it is assumed that the plasma is perfectly conducting and completely excludes the magnetic field and that, in addition, the thickness of the plasma shell is very small as compared with its radius. For an equilibrium to exist, it is necessary that the equality

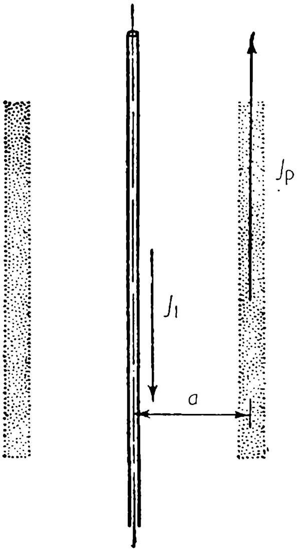

FIG. 49

Hollow plasma column in a tubular pinch with a metal rod down the axis

$$p = H_1^2/8\pi \qquad \text{.........}(5.24)$$

be obeyed at the inner boundary of the layer, $H_1$ being the field strength created by the current in the rod; and that the equality

$$p = (H_2 - H_1)^2/8\pi \qquad \text{.........}(5.25)$$

be satisfied at the outer boundary, $H_2$ being the field strength generated by the current flowing through the plasma. Since we have assumed the plasma shell is very thin, all the magnetic field quantities entering into equations (*5.24*) and (*5.25*) refer to the same value of the coordinate $r$, namely, to the radius $a$ of the shell; thus

$$H_1 = 2J_1/ca \quad \text{and} \quad H_2 = 2J_p/ca.$$

From (*5.24*) and (*5.25*) it follows that $H_2 - H_1 = H_1$, i.e. $H_2 = 2H_1$; hence to achieve equilibrium the current in the plasma must be twice that in the rod.

It is also relatively easy to find a relation between the mean plasma

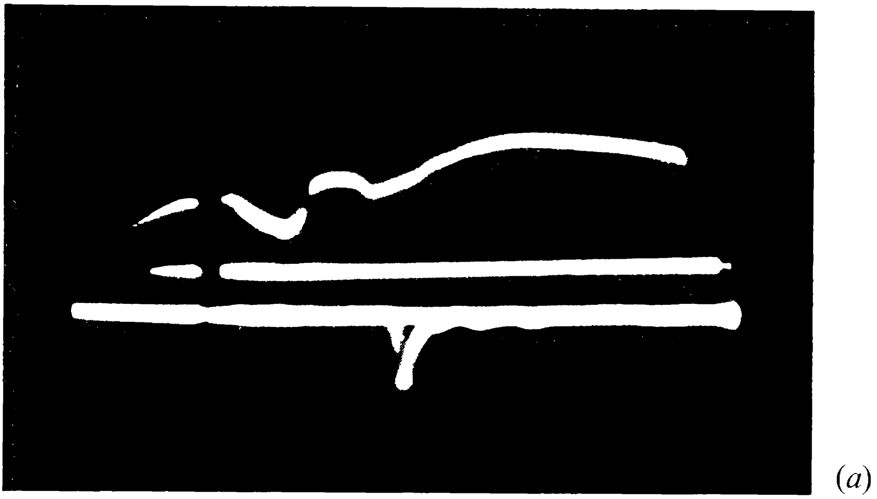

(*a*)

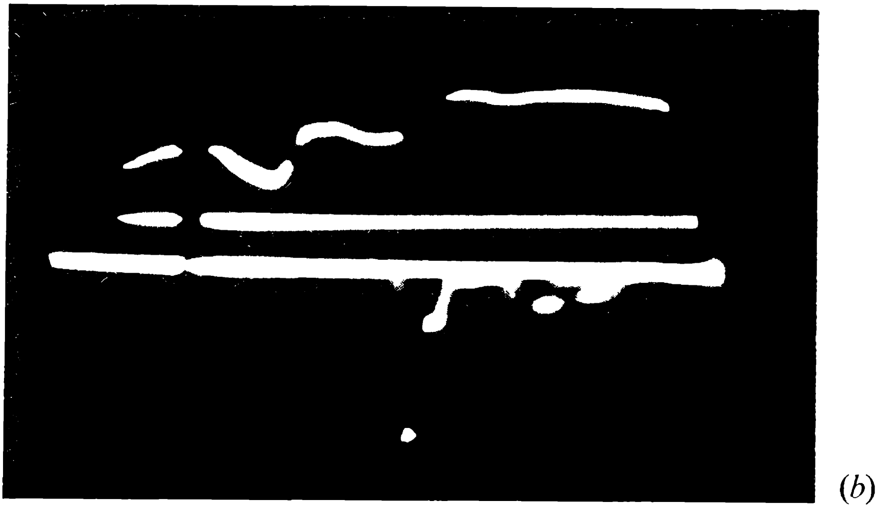

(*b*)

Oscillograms of neutron radiation and pinch current.

PLATE VII

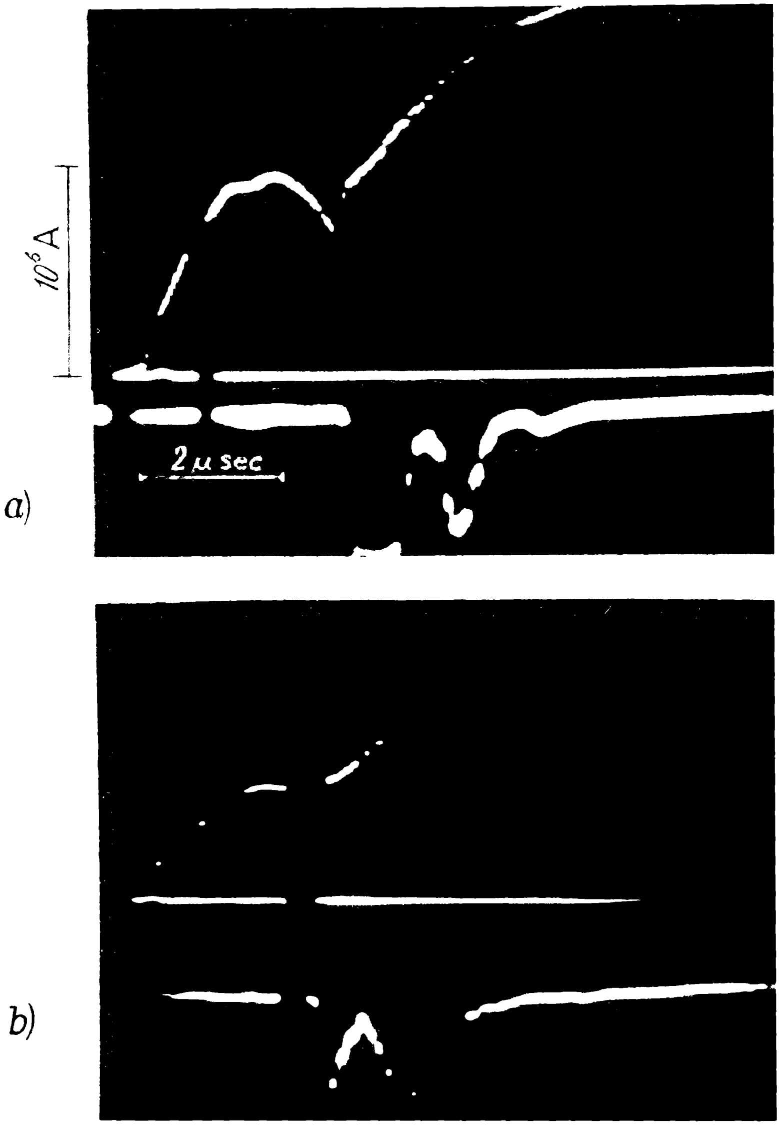

Neutron emission with high initial voltages across the tube.

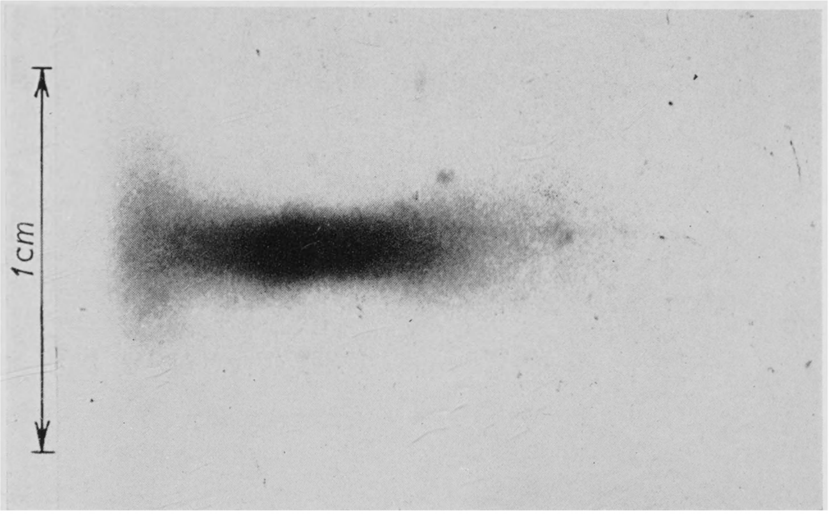

X-ray photograph of the compression zone in a metal wall pinch tube.

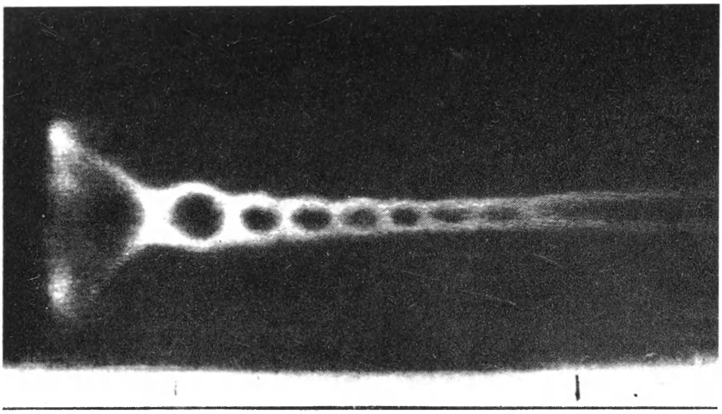

(*a*) Streak camera photographs of the radial compression in a $\theta$-pinch which show 'bouncing' due to the trapping of a field inside the plasma. After Bodin *et al.*

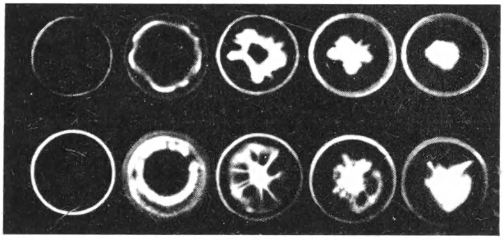

(*b*)

Framing camera photographs of the radiation from a compressed plasma in a $\theta$-pinch. Top row—air, bottom row—helium, 2 $\mu$sec between frames. After Kvartskhava.

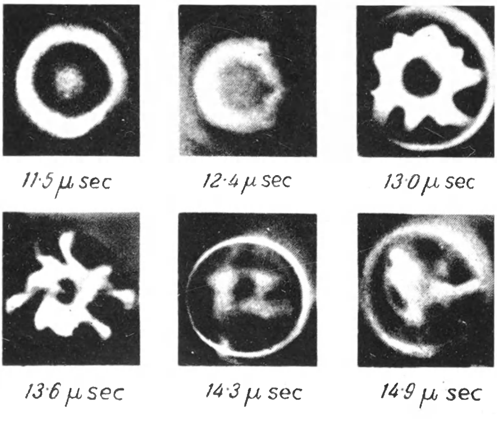

(*c*)

Framing camera photographs of a plasma forming during a $\theta$-pinch discharge in deuterium. Initial gas pressure, 0·1 Torr. After Josephson.

temperature and the total current—a relation similar to (*4.31*) for an ordinary linear pinch. Assuming for the sake of simplicity that the temperature and density are constant over the cross-section of the plasma shell, and taking into account the relation between $J_1$ and $J_p$, we can reduce equation (*5.24*) to

$$J_p^2 = 16c^2\pi a^2 nkT. \qquad .........(5.26)$$

The number density $n$ is related to the total number $N$ of ions or electrons per unit length of the pinch and to the cross-sectional area $S$ by $n = N/S$. Hence,

$$J_p^2 = 16c^2(\pi a^2/S)NkT. \qquad .........(5.27)$$

Comparing these relations with equation (*4.31*) and considering that for a thin plasma shell the value of $\pi a^2$ is considerably greater than the cross-sectional area $S$ occupied by the plasma, we see that for a given plasma current and line density $N$ the mean plasma temperature in the thin cylindrical layer will be much lower than in an ordinary pinch.

Let us reiterate that the above equilibrium results have been obtained assuming the plasma has infinite conductivity (since only perfectly conducting plasma can completely expel a field from the region it occupies). If we exclude the possibility of the field being expelled completely, equations (*5.24*) and (*5.25*) can no longer characterise the equilibrium conditions, and in particular the relationship $J_1 = \frac{1}{2}J_p$ no longer holds; nor does it hold in the more general case when an axial magnetic field is present in addition to the azimuthal field. For the plasma configuration under consideration, it is possible to develop a theory analogous to the theory of the ordinary pinch effect, and to describe how the main parameters characterising the plasma vary for the quasi-stationary case and also for a fast discharge, in which inertial forces play an important part.

We will not here dwell on the results of the theoretical analysis of the properties of a cylindrical plasma layer, since the greatest interest attaches rather to the quasi-stationary case which is dealt with in the next chapter. Anticipating later discussion, we merely note that, in combination with an axial magnetic field, such a tubular plasma column can be stable with respect to certain deformations which are unstable in an ordinary linear pinch.

A tubular plasma layer has for a long time been regarded in the U.S.S.R. and the U.S.A. as one of the plasma configurations which offers hope for obtaining high temperature. However, in our country, only rough experiments have been carried out with a system of this type. In the U.S.A. a cylindrical plasma layer formed by a fast discharge was first studied in fair detail in the Triax device. This device, built at Berkeley by Anderson, Baker and their co-workers, is shown schematically in Fig. 50. The discharge takes place in a hollow cylindrical quartz tube. The plasma current returns along the inner metallic cylinder 4 and the outer shell 3. Tubes about 1 m long were used in the experiments. The outer diameter of the discharge tube was a little over 10 cm, and the diameter of the inner conductor in different experiments was 5, 2·5 and 1·25 cm. Measurements of the principal quantities characterising a discharge (voltage, current, time-derivative of the current, spectral line intensities) were made with a range of initial deuterium pressures from 0·05 to 1 Torr for discharge currents up to $1{\cdot}3\times10^6$ A. The time to maximum current was 2 to 3 $\mu$sec.

As the experiments have shown, the behaviour of the cylindrical plasma layer depends strongly on the ratio of the maximum magnetic pressure $H^2/8\pi$ to the initial value of the gas pressure. If this ratio does not exceed $5\times10^4$, corresponding to initial pressures above 0·2 Torr, the plasma shell does not show any visible signs of instability.

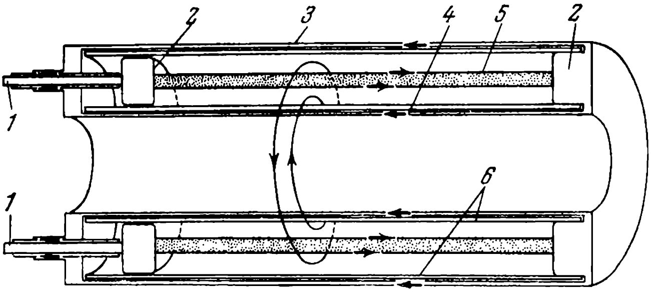

FIG. 50. Diagram of the discharge tube of the Triax device

| | |
|---|---|
| *1.* current input | *4.* inner conductor |
| *2.* electrode | *5.* plasma |
| *3.* outer conductor | *6.* insulators |

According to equation (*5.27*), the plasma temperature will not be very high under the indicated experimental conditions. Thus, for instance, at $p_0 = 0{\cdot}5$ Torr and $J_{\max} = 6\times10^5$ A, the maximum temperature of the compressed plasma layer should not exceed 15–20 eV, theoretically. If the temperature is derived from the conductivity, it indeed turns out to be close to 15 eV at the time of maximum compression. As the ratio of the electrodynamic forces to $p$ increases, the properties of the discharge gradually begin to change. This is primarily indicated by the appearance of definite signs of instability in the form of sharp breaks and jumps on the voltage and current oscillograms, corresponding to bursts of neutron radiation. Subsequently, the experimental study of the properties of tubular plasma columns has continued in the U.S.A., Britain and France on a whole series of installations. The most interesting of these installations is the Levitron, a toroidal device built by Colgate (see § **6.8**).

§ **5.6** Plasma processes in which acceleration by electrodynamic forces plays an important part cover a broad category of phenomena. Hitherto we have considered only those special cases of the pinch effect in which the magnetic field compressing the plasma is generated by an axial current. We now discuss these phenomena as observed in other configurations.

To preserve the natural sequence of exposition, we describe the processes in those experiments where the plasma compression takes place in a rapidly rising external axial field. At the present time, the term '$\theta$-pinch' is usually used to designate such experiments. In terms of the predominant physical processes, they stand together with the 'linear pinch effect', discussed in earlier sections of this chapter. For comparison, Fig. 51 shows a diagram of (a) the linear pinch, and (b) the compression of a cylindrical plasma column by the electrodynamic forces of an external axial field. In the first case, the compressional force arises from the interaction between the azimuthal field $H_\theta$ and the axial current $J_z$. In the second case, the axial field $H_z$ interacts with the azimuthal current $J_\theta$. The analogy between the two configurations would be complete if the currents flowed only in a thin surface layer of the plasma, and the internal fields in both cases were equal to zero. Under this condition, which in theory may be satisfied in discharges of short enough duration (due to the fact that the current sheath is then very thin), a magnetic pressure equal respectively to $H_\theta^2/8\pi$ and $H_z^2/8\pi$ is applied to the plasma surface. If the magnetic field rises at the same rate in both cases for the same initial radius and initial mass, the processes resulting from the compression will proceed in identical fashion, irrespective of whether the pinch is compressed by the azimuthal or the axial field.

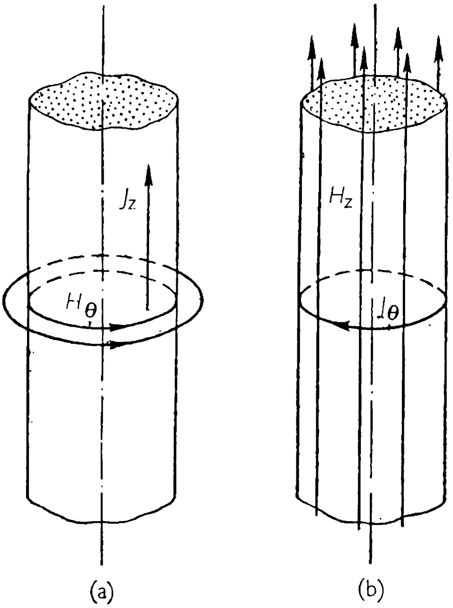

FIG. 51

Plasma column compressed by (a) an azimuthal field (linear pinch), and (b) an axial field ($\theta$-pinch)

However, the premises necessary for such a complete analogy are realised only in the case of a very rapid compression of the plasma. In the other extreme, where the skin-effect is ill defined, either because of a low conductivity or a slow rate of compression, the distribution of the magnetic pressure in configuration (a) differs from that in (b). These distributions for the case of small skin-effect are shown in Fig. 52. For the ordinary pinch, the pressure generated by the field $H_\theta$ is in this case still applied, roughly speaking, at the surface layer of the plasma and is small inside the pinch. In contrast, the pressure in the $\theta$-pinch, due to the axial field $H_z$ now varies only slightly over the cross-section of the pinch. Therefore, even if the magnitude of the field at the pinch boundary is the same, the compression forces will be completely different in the two cases. In the usual linear pinch, the field well inside the plasma column is always relatively small; and the electrodynamic force is always greater than when the pinch is compressed by an axial field which, in cases of insufficient conductivity, easily diffuses into the plasma and generates a counterpressure that offsets the greater part of the compressing force.

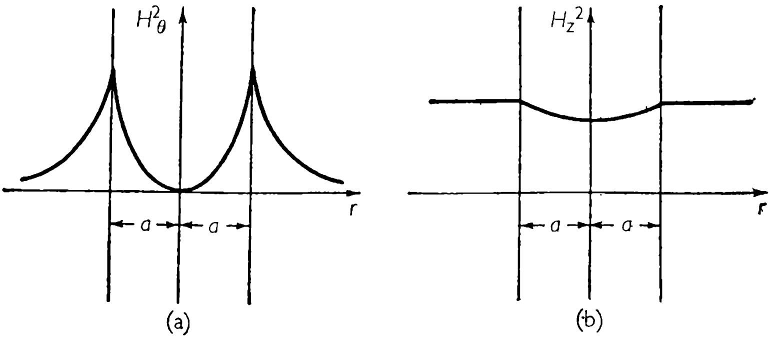

FIG. 52. Distribution of magnetic pressures in (a) an ordinary linear pinch, and (b) $\theta$-pinch due to finite conductivity

At present it is already possible to cite a whole series of papers devoted to the elucidation of the laws governing the rapid compression of a plasma by an external field. In the U.S.A. studies along these lines have been conducted by Tuck's group at Los Alamos and by Kolb and co-workers at the Naval Research Laboratory in Washington. Similar work in England has been done by Niblett and co-workers at the Aldermaston Research Centre. In the U.S.S.R., $\theta$-pinches are being studied by Kvartskhava and co-workers at the Physics Institute of the Georgian Academy of Sciences.

The design of the devices and their power supplies are basically the same in all the above-mentioned experiments. A capacitor bank charged to several tens of kilovolts with an internal inductance as low as 3–5 m$\mu$H is discharged into a single-turn coil producing a strong and rapidly rising magnetic field which compresses the deuterium plasma. The energy stored in the capacitors is measured in tens or hundreds of kilojoules. Figure 53 shows a diagram of one of the first coil designs used in the Scylla device at Los Alamos; it consists of a massive loop surrounding a ceramic tube which contains the deuterium. The shape of the magnetic field produced in such devices is usually selected so that the lines of force are concentrated at the ends and form magnetic mirrors. This is done in order to reinforce the compression effect, and also to reduce the escape of the plasma in the axial direction from the region where it is subjected to the action of the compressing field. However, as we shall see later, the second of these functions performed by the magnetic mirrors is not absolutely necessary because, under certain experimental conditions, during the compression of the plasma, magnetic fields are formed which have configurations such that they themselves prevent the particles from escaping.

Among the parameters characterising the operation of the $\theta$-pinch devices are the rate of rise of the magnetic field and its maximum value. Elmore, Little and Quinn, members of the Los Alamos group, in their report to the Geneva Conference of 1958 cited data to the effect that

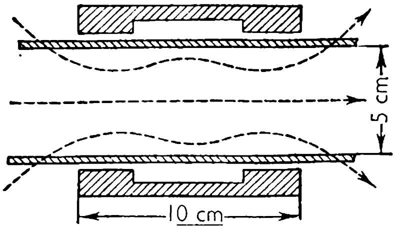

FIG. 53. Single-turn coil of the Scylla device. Dotted lines indicate the lines of force

their device could attain magnetic fields of 100,000 Oe in a time of about 1·3 μsec. In the initial experiments made by Kolb *et al.* fields of up to 200,000 Oe were obtained in short coils, and the build-up time was 5–10 μsec. However, in all these investigations the compressed plasma column was very short so that the escape of plasma along the axis (end losses) had a substantial effect. As a result, it is now common practice to use the devices with long coils and long compression chambers. The biggest device is the Pharos system, recently† put into operation at the U.S. Naval Research Laboratory by Kolb. With this new experimental equipment, the maximum energy which can be stored in the capacitor bank amounts to about 2 megajoules. A magnetic field of about 100,000 Oe, building up in 15 μsec, can be produced in a coil ~2 m long with an inner diameter of about 10 cm. These figures indicate, incidentally, that these fast-compression devices yield the highest power per unit volume used in present-day research on controlled thermonuclear reactions.

As was shown above, fields inside the plasma play an important part in rapid-compression experiments. One should not expect optimum compression and heating with operating conditions in which the rising magnetic field and induced electric field act upon a neutral gas which, during the field build-up, first ionises and is then compressed. Under such conditions, at the beginning of the discharge the field diffuses freely into the volume occupied by the gas or the poorly conducting plasma. Moreover, a dense plasma is formed only after a considerable delay—as late as the second or even third half-period of the alternating magnetic field.

---

† In 1961.

Some improvement of the initial conditions may be achieved if a preliminary high-frequency discharge is employed. However, the usual type of r.f. discharge is too weak to form a plasma with a high enough conductivity. The methods used on Pharos have gone further in this direction by introducing, prior to the onset of the main compressing discharge, an intermediate stage, during which the plasma is subjected to a relatively weak alternating magnetic field which provides a certain amount of initial ohmic heating. A capacitor bank charged to moderately high voltages (up to 30 kV) and relatively small capacity is used for this purpose. This auxiliary bank is discharged into the main coil shortly before the main magnetic field pulse. The magnetic field generated by the auxiliary circuit oscillates with a frequency which is several times larger than that of the main circuit. At the time when the auxiliary discharge is initiated, the gas has already been weakly pre-ionised, e.g. by a high-frequency capacitively-coupled discharge. It thus heats up rapidly to a temperature of between 1 and 5 eV, depending on the initial density. The conductivity is sufficiently high so that a partial trapping of the field invariably occurs at the same time. It turns out, however, that if the initially trapped field has a direction opposite to the main compression field, then it has, so to speak, a favourable effect on the processes involved in the ensuing compression by raising the ion and electron temperatures. To obtain optimum initial conditions for compression in the Pharos device, the following more complicated programme of the different magnetic fields is used. First, there is the usual weak preliminary ionisation of the gas. Then the coil is connected to a capacitor bank which creates a quasi-static magnetic field of up to 10,000 Oe, which is frozen into the plasma during the main compression. The direction of this slowly changing field may be selected parallel as well as antiparallel to the main compressing field. Shortly after the quasi-static field begins to rise, the auxiliary preheat capacitor bank is discharged into the coil. The discharge from this bank decays in about 5–10 $\mu$sec. During this time interval a plasma is formed with a degree of ionisation from 50% to about 100%, depending on the initial gas pressure; the plasma is heated ohmically to several eV, and is drawn away from the walls of the cylindrical vacuum chamber by the slowly rising field. The main capacitor bank is discharged into the coil after preheating and in the presence of the quasi-static magnetic field. In the initial experiments, this device was used to study only the case where the quasi-static field was directed antiparallel to the main compressing field.

All the important studies of the rapid compression of a plasma by an external magnetic field have been carried out with deuterium, at initial pressures in the range 0·03–0·5 Torr. Observations on the magnetically compressed plasma are obtained by the following methods: (1) streak camera photography of the plasma radiation, from which the implosion velocity and volume compression can be measured; (2) measurement of the absolute intensity of the optical continuum, from which the electron density can be determined (see p. 121); (3) measurement of the slope and absolute intensity of the soft X-ray energy spectrum, from which the electron temperature and density can be deduced; (4) recording the neutron emission rate from the plasma and measurement of the neutron spatial distribution and energy spectrum (mass-spectrometric analysis of the fast particles, protons and tritium nuclei generated in (*d*-*d*) reactions). Experimental techniques based on magnetic and piezoelectric probes, which have been widely used in investigations of the linear pinch, cannot be as useful in high-energy rapid compression experiments because in this case a small probe element inserted into the plasma is destroyed in a few discharges. Nevertheless, magnetic probes have provided some very useful evidence on the configuration of the magnetic field in the compressed plasma for the case when the trapped field is antiparallel to the external compression field.

The experimental results obtained so far are still somewhat crude in character and are insufficient to enable us to sketch a reliable overall picture of the phenomena involved. Here we shall attempt to summarise those results of research on magnetic compression by axial fields which may be considered more or less established at the present time, together with all the qualifications that must be made due to the preliminary nature of these exploratory researches.

Streak camera photographs of the visible plasma radiation show that when the main compression pulse follows the preheating, a shock wave is formed that converges toward the axis at a velocity of about $0{\cdot}7$–$1{\cdot}5 \times 10^7$ cm/sec which depends on the voltage, initial pressure and coil radius. Then the plasma undergoes a rapid expansion and subsequent oscillations which are followed by a relatively slow compression. These various phases of the radial motion of the plasma column generally last for a period of time shorter than a quarter-period. By the time the compression field reaches a maximum, the luminous plasma has the shape of a thin column (alternatively, the luminosity can disappear altogether in the case of short coils and relatively long quarter-period). Sometimes, the photographs may show the formation of irregular plasma oscillations in the slow compression phase. There are indications that these oscillations are due to an instability, and that the plasma rotates, sometimes breaking up into two separate filaments.

If there is no preheating and only the high-frequency ionisation of the gas is used, the compression takes place in the second half-period of the discharge, but the overall character of the compression is similar. Streak camera photographs of the plasma radiation obtained under different experimental conditions indicate many individual characteristics which make it difficult to determine the general mechanisms. Nevertheless, it should be noted that such pictures indicate that a field is trapped by the plasma. This is indicated by the low intensity of radiation inside a bright plasma envelope (see Plate IX (*a*), reproduced from the paper by Bodin, Green, Niblett and Peacock, which shows a typical streak photograph of plasma radiation through a slit in the coil perpendicular to the axis).

The clearest picture of the shape of a plasma compressed by a fast-rising magnetic field is provided by high-speed photographs taken end-on along the magnetic axis, i.e. an image of the plasma is obtained in a plane perpendicular to $H$, by photographing the radiation through a window at one of the ends of the cylindrical discharge chamber. Framing camera photographs of the formation and development of the $\theta$-pinch were first obtained by Kvartskhava. Two of the series of pictures he obtained are shown in Plate IX (*b*) for discharges in air and helium at an initial pressure of about 0·1 Torr. Subsequently, similar photographs of discharges in hydrogen and deuterium were obtained at many other laboratories (see Plate IX (*c*) reproduced from a paper by Josephson).

From the photographs on Plate IX we see that the process of plasma formation begins with the appearance of a thin, luminous circle near the tube walls. This circle then begins to contract, and in a few microseconds a dense plasma forms along the axis of the chamber. However, this plasma is by no means a joy to behold when one examines its boundaries. Its cross-section is more reminiscent of an ink blot than of a regular circle. The little tongues which can be seen at first on the thin plasma ring are rapidly transformed into something resembling the tentacles of an octopus, and alter the shape of the plasma column completely. Obviously, this is a manifestation of an instability characteristic of $\theta$-pinch formation.† We shall discuss the causes of this instability later.

In many of the framing camera pictures obtained by photographing the compressed plasma through a window at the end of the discharge tube, one can observe a hollow region inside the plasma that lasts for a certain time after the first maximum compression. As indicated above, a similar effect, apparently produced by the trapping of the initial antiparallel magnetic field by the plasma, is also observed in side-on streak camera photographs through a slit in the coil perpendicular to the axis.

Measurements of the absolute intensity of the optical continuum indicate that a plasma of very high density is obtained in the compression process (for example up to $4 \times 10^{17}$ cm$^{-3}$ in the latest experiments with Pharos). The electron temperature in the compressed plasma column (determined from the energy of the emitted X-rays) may range from 200–300 eV to the keV range, depending on the initial conditions. The pressure in the compressed plasma, which can be evaluated from measurements of $n_e$ and $T_e$, is found to be roughly comparable to the magnetic pressure $H^2/8\pi$. In different experiments carried out up to 1963 on various devices, the time from the beginning of the compression to the instant when the plasma loses its definite geometrical contours and begins to interact violently with the walls amounted to several microseconds (up to about 10 microseconds in the initial experiments with Pharos).

---

† Recent studies indicate that the development of this instability depends strongly on the initial conditions of the discharge. When the initial ionisation (before the beginning of the main compression) is good, the plasma tongues are formed later and may be less distinct.

In the experiments performed on the rapid compression of a plasma by an external axial field, attention has usually been concentrated on the study of the neutron radiation accompanying processes of this kind. If certain experimental parameters are high enough, i.e. at a high rate of rise of the field and a large value of $H_{\max}$, the emission of neutrons is observed in every experiment over a wide range of initial deuterium pressures (0·05–0·5 Torr in experiments by the Los Alamos group). Apparently, both in experiments with Scylla and in those conducted by Kolb with a 200 kJ capacitor bank with coils up to 70 cm long and a bore of 6 cm, the optimum pressure for neutron emission is 0·1 Torr. At this pressure the total number of neutrons in one burst attains a maximum value of the order of $10^7$–$10^8$ if $H_{\max}$ is 70,000–80,000 Oe. The intensity of the neutron emission increases rapidly with the maximum field strength.

The time at which neutrons appear depends on the experimental conditions. If the plasma is not preheated by a short oscillatory discharge from a source of relatively low power, the neutron radiation as a rule appears on the second half-cycle of the primary current. In this case, the emission is often repeated on the third half-cycle of the primary current. The duration of the neutron emission usually lies between 0·1 and 2 $\mu$sec. If the plasma is preheated before the main compression, and the main magnetic field pulse is superimposed on the initial trapped field so that they are antiparallel then, the neutron pulse appears on the first half-cycle of the compressing field up to the time when the field strength goes through a maximum. The neutron burst lasts several microseconds, and up to 10 $\mu$sec with long coils (Pharos).†

The energy spectrum of the neutrons was studied in some of the experiments mentioned above by measuring the ranges of recoil protons in nuclear emulsions. In addition, the energies of protons and tritons produced by (*d-d*) reactions have been measured at Los Alamos using a magnetic spectrograph especially built for this purpose. The measurements of the energy spectra of neutrons and other reaction products made thus far apparently do not contradict the hypothesis that the neutrons are produced in the plasma owing to its high temperature. However, they can also be accounted for by the hypothesis of an acceleration mechanism.

---

† Recent experiments (L. M. Goldman *et al.*, *Phys. Rev. Letters*, 9, 361, 1962) show that neutrons can also be produced during the first half-cycle at low initial pressures (0·01 Torr) with no initial magnetic field, when the rise-time of the main field is sufficiently short.

§ **5.7** We now give some general considerations which may be used for the interpretation of the experimental results obtained from studies of the 'fast $\theta$-pinch'. We first base our considerations on some very rough models of the relevant mechanisms, and in particular we assume that the magnetic field inside the compressed plasma is equal to zero from the very beginning, i.e. the trapped field is not taken into consideration. The first rapid compression phase should be approximately described by an equation analogous to (*5.9*):

$$\pi\rho_0 \frac{d}{dt}\left\{(r_0^2-r^2)\frac{dr}{dt}\right\} = -2\pi r\frac{H^2}{8\pi}. \qquad \text{.........}(5.28)$$

Here $r_0$ is the initial radius of the contracting plasma cylinder and $\rho_0$ is the initial gas density. Assuming that the magnetic field rises linearly with time, and introducing dimensionless variables, we may write the equation of motion in the more compact form

$$\frac{d}{d\tau}\left\{(1-u^2)\frac{du}{d\tau}\right\} = -u\tau^2. \qquad \text{.........}(5.29)$$

Here $u = r/r_0$ and $\tau = t/t_0$, where $t_0$ is a characteristic time dependent upon $r_0$, $\rho_0$ and the rate of rise of the field, viz:

$$t_0 = (4\pi r_0^2\rho_0)^{\frac{1}{4}}/(dH/dt)^{\frac{1}{2}}. \qquad \text{.........}(5.30)$$

For parameters which characterise the existing experimental devices, $t_0$ turns out to be a few tenths of a microsecond. The function $u(\tau)$, which satisfies equation (*5.29*) with the initial conditions $u(0) = 1$ and $(du/d\tau)_0 = 0$ may be expressed by the series

$$u(\tau) = 1-\tau^2/\sqrt{12}+\tau^4/360+ \ldots \qquad \text{.........}(5.31)$$

For all practical purposes it is sufficient to take the first two terms of the expansion, because the extremely idealised assumptions under consideration do not justify a greater accuracy in the determination of the function $u(\tau)$.

The contracting cylindrical plasma shell reaches the axis at $\tau \approx \sqrt[4]{12}$; at that time the kinetic energy $W$ associated with the ordered motion of the ions reaches a maximum value of:

$$W = \frac{10^{11}m_i r_0}{\rho_0^{\frac{1}{2}}}\left(\frac{dH}{dt}\right)\text{eV}. \qquad \text{.........}(5.32)$$

In the experiments at Los Alamos $W$ attained a value in the range 100–200 eV. If the compression had a purely mechanical character after the time of maximum compression, its further development should be described by

$$d^2u/d\tau^2 = -u^2\tau. \qquad \text{.........}(5.33)$$

This equation does not contain a coefficient $1-u^2$, to allow for the gradual increase in the mass of the gas set into motion. Following the first compression maximum, the mass should remain constant, since all the gas has already been set into motion with the same ordered velocity. Equation (*5.33*) describes the radial oscillations of the cylindrical plasma shell which follow the first compression phase. The time-dependence of the plasma radius $u(\tau)$ is shown in Fig. 54, calculated from the series (*5.31*), during the first implosion and thereafter by the numerical integration of equation (*5.33*). Actually, of course, one must not expect this simplified model to yield even a qualitative description of the dynamics which follow the first compression, since by the time of the first contraction a considerable part of the directed kinetic energy is converted into heat and the purely mechanical treatment of the compression process is no longer valid.

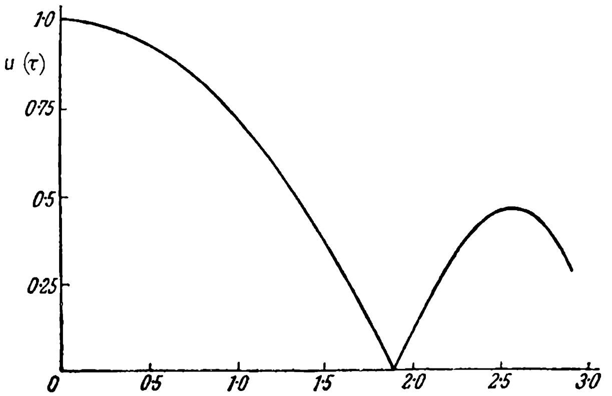

FIG. 54. The radius $u(\tau)$ of the plasma as a function of time $\tau$ during inertial compression in a $\theta$-pinch as calculated from the mechanical 'snowplow' model

The photographs of the plasma radiation which are discussed above show that after several bounces (which are 'softer' than expected from the mechanical model) a much longer compression phase follows, lasting up to the time of maximum field. These general characteristics are observed, at any rate in cases where the plasma is preheated by a relatively low-energy auxiliary discharge prior to the main pulse of the magnetic field. Photographs of the radiation displayed in Kolb's report at the Geneva Conference (they are typical and show the general phenomenon observed in $\theta$-pinch experiments) indicate that the slow compression phase begins approximately one microsecond after the main compressing field is switched on. By that time, $H$ attains about 20–25% of its maximum value and the plasma radius is approximately one-half of the radius of the tube. Assuming that an equilibrium is established at that moment between the magnetic and the gas pressure, one can estimate the plasma temperature. At $p = 0{\cdot}1$

Torr and $H_{\max} = 65{,}000$ Oe, the plasma temperature should be about 100 eV at the start of the slow compression.

If it is assumed that the slow compression of the plasma proceeds adiabatically, the temperature will increase in proportion to $H^{4/5}$(since for a monatomic gas $T \propto p^{2/5}$ and $p \propto H^2$). It should be expected, therefore, that during the first quarter-period of the discharge, the temperature will rise to about three times its initial value and reach 300–600 eV. At the same time, the plasma radius should be reduced by a factor of 2·5, that is to about 1/5 the tube radius.

However, the streak photographs show that the plasma actually contracts much more. At the time of maximum field, the radius of the luminous region is less than 10% of the tube radius. The over-compression is apparently due to the leakage of the hot plasma through the magnetic mirrors, which reduces the density and pressure of the plasma. However, the temperature of the remaining plasma at peak field may turn out to be higher than should have been expected from an adiabatic process in the absence of losses, since the magnetic field performs additional work in compressing the plasma to a smaller radius, and this work is expended in heating a smaller and smaller number of particles.

In order to understand how the leakage of particles from the plasma may influence the process of slow compression, we shall attempt to find a relation between the volume, the temperature and the pressure of the plasma as the total number of particles changes. Let us assume that at any given time the average kinetic energy of the particles escaping from the plasma is equal to the average kinetic energy of the particles remaining behind. Under these conditions, the escape of particles alone will not lead either to a cooling or heating of the plasma. The law of conservation of energy for a plasma contracting under the influence of an external field may be written

$$-p\,d\Omega = d(N\overline{W}) - \overline{W}\,dN, \qquad \text{.........}(5.34)$$

where $N$ is the total number of particles, and $\overline{W}$ is their average energy, equal to $\frac{3}{2}kT$. From equation (*5.34*) it follows that

$$-p\,d\Omega = N\,d\overline{W} = \tfrac{3}{2}Nk\,dT. \qquad \text{.........}(5.35)$$

Substituting $p = NkT/\Omega$ into (*5.25*) we obtain

$$d\Omega/\Omega = (\tfrac{3}{2})\,dT/T; \qquad T\Omega^{2/3} = \text{const.} \qquad \text{.........}(5.36)$$

Thus, the relation between the temperature and volume in this case is the same as when the total number of particles is conserved. Equation (*5.36*) and the expression for the pressure $p$ enable us to establish the relation between $T$ and $p$:

$$T \propto (p/N)^{2/5}. \qquad \text{.........}(5.37)$$

For a given rise of the magnetic pressure, the plasma temperature changes in inverse proportion to $N^{2/5}$. A tenfold decrease in $N$ should raise the temperature 2·5 times. It should be pointed out, however, that the derivation of equation (*5.37*) is based on a number of explicit and implicit assumptions which simplify our picture of the processes involved. In reality, the relation between $T$ and $p$ may be considerably more complex, particularly because under actual experimental conditions the work done by the external forces not only heats the plasma, but also increases the energy of the field trapped inside the contracting plasma shell. Furthermore, the character of the relation between $T$ and $p$ may be affected by the redistribution of energy between the ions and electrons, leading to equal ion and electron temperatures, and by the change in the axial dimensions of the region occupied by the plasma (due to the presence of magnetic mirrors or closed field lines in the case of a reversed trapped field, which generate an additional axial pressure as $H$ rises). For these reasons equation (*5.37*) has a purely illustrative character and can only characterise the qualitative aspects of the effect of particle losses upon the plasma temperature.

The question of the mechanisms responsible for the escape of particles is a rather difficult one—not because such mechanisms are difficult to find but because the relative importance of the various factors which can cause the leakage largely depends upon the density and temperature of the plasma, and also upon the dimensions of the system and the configuration of the magnetic field. Let us assume first of all that the plasma fills a cylindrical region in a field whose lines of force are everywhere parallel to the axis (which approximates to the case when there are no mirrors in the magnetic system). Then the plasma will leak out of the two ends of the discharge tube at a velocity approximately equal to the axial velocity of the ions. When the number density is of the order of $10^{16}$ to $10^{17}$ cm$^{-3}$ and the temperature is several hundred electron volts, the velocity distribution should be completely randomised during the time the field rises from zero to its maximum value, i.e. in a few microseconds. Therefore, the escape velocity of the plasma out of the ends should be of the order of $10^7$ cm/sec.

In systems with magnetic mirrors, the charged particles are contained between the regions where the field is relatively high, and can escape from the plasma only through collisions which change the angle between the particle velocity and the line of force. At low densities, the flow of particles through the mirrors will be proportional to the number of Coulomb collisions per unit time, i.e.

$$-dN/dt \simeq N^2\overline{\sigma v}/\Omega \simeq \text{const}\, N^2/\Omega T^{3/2}. \qquad \text{.........}(5.38)$$

This method of estimating $dN/dt$ is applicable when the length of the region occupied by the plasma is substantially smaller than the ion mean-free-path (an ion can escape from the trap after undergoing only one collision). In the opposite case, the leakage of particles should occur as a free expansion of a gas into a vacuum, and the flow of particles through the mirrors is given by the expression

$$-dN_i/dt \simeq n_i v_i S/2, \qquad \text{........(5.39)}$$

where $S$ is the cross-sectional area of the plasma column in the mirror region and $n_i$ is the particle density in this region. However, these methods for determining $dN/dt$ are of very limited value when applied to actual conditions, because we have disregarded the change in the geometrical structure of the lines of force which is associated with the trapping of the field by the plasma.

On the basis of experimental data obtained by means of high-speed streak photography and a few magnetic probe measurements, the field configuration in the contracting plasma has the form shown schematically in Fig. 55. This configuration for the magnetic lines of force is the inevitable result of the field trapping during the preheating phase preceding the main compression pulse (preheating with an auxiliary discharge or in the preceding half-cycle of the main field). The strength of the trapped field may be relatively small at the beginning of the compression, but it should rise quickly as the plasma radius decreases since the flux remains approximately constant because of the moderately high conductivity and relatively short implosion time. For the indicated field configuration, it is difficult to predict the shape of the plasma or the spatial distribution of the density and temperature. A reasonably natural hypothesis is that a large part of the compressed plasma will be situated inside the region bounded by the closed lines of force. Leakage of particles from this region along the lines of force is inhibited. Therefore, if the plasma remains stable during compression, the total number of particles is conserved. In this case, only those particles which were initially located outside the boundaries of the ring-shaped field lines are able to escape from the system.

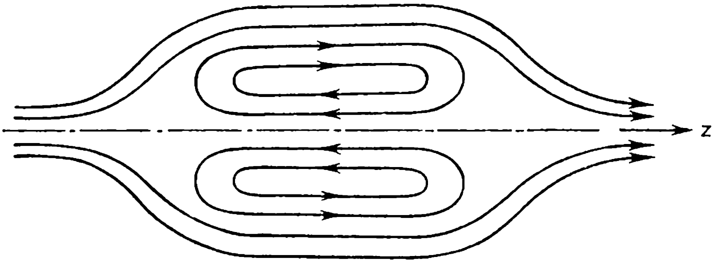

FIG. 55. Configuration of the magnetic field in a $\theta$-pinch with a trapped reverse field

The part played by the trapped field in the dynamics of a contracting plasma has for some time been the subject of a lively debate which has not yet led to any final conclusions, largely owing to the scarcity of and the inadequate agreement between the experimental results. Only the following facts can be considered to be more or less solidly established. A dynamic compression of the plasma with large inertial forces occurs only when the gas is sufficiently ionised before the start of the main compression. If there is no reverse trapped field in the initial phase, the temperature of the compressed plasma is found to be relatively low. In experiments carried out so far, electron temperatures of about 1 keV were obtained only when a reversed field was trapped inside the plasma. In this case the rise in the plasma temperature appears to be related directly or indirectly to a relaxation (or rapid disappearance in some cases) of the reverse field during the compression. These processes also have a direct bearing on the various unsteady deformations which can be observed in some intermediate phases of the compression.

In trying to interpret the above experimental observations, we should first of all describe the causes of the relaxation of the internal field and the influence of this effect on the plasma heating. The simplest model for the relaxation of the internal field is based on the assumption that ordinary Joule losses in the plasma are responsible. When the shape of the field is that depicted in Fig. 55, the azimuthal current maintaining the magnetic configuration must flow inside the region bounded by closed lines of force. Because of the finite conductivity of the plasma this current must decay, thus causing the disappearance of the trapped magnetic field. The energy stored in the field goes into heating the plasma, and this may cause the rise in $T_e$ during the relaxation of the internal field. If this mechanism is idealised to some extent, it is possible to obtain some simple estimates of the field relaxation time and the relative change in $T_e$. Suppose the plasma has the shape of a hollow cylinder with inner and outer radius initially equal to $a_0$ and $b_0$, respectively. Suppose further that the plasma pressure is equal to the external magnetic pressure which, for the sake of simplicity, we will consider constant. The trapped field is located inside the plasma cylinder and has a strength numerically equal to the field strength on the outer surface of the plasma. Thus a quasi-stationary process is considered. Making an energy balance and taking note of the fact that the total magnetic flux inside the coil is preserved, we obtain the following estimate of the relative change in $T_e$

$$\frac{T_e(1)-T_e(0)}{T_e(0)} \simeq 1{\cdot}6\times\frac{a_0^2}{b_0^2-a_0^2}.$$

Here $T_e(0)$ and $T_e(1)$ designate the initial and final electron temperature respectively. The temperature change may be abrupt if the initial plasma pressure is substantially smaller than the magnetic field pressure, since in this case the initial energy content of the plasma is relatively small.† It follows that a two or threefold increase in the electron temperature during the disappearance of the internal field may be explained when reasonable assumptions are made concerning the ratio $a_0/b_0$. Furthermore, it should be noted that if $a_0$ and $b_0$ are comparable, the relaxation of the internal field can no longer be separated from the simultaneous diffusion of the external field into the plasma. The relaxation time $\tau_r$ will be approximately $\bar{\sigma}a_0^2/c^2$ in order of magnitude, where $\bar{\sigma}$ is the mean conductivity during the process. For $\bar{\sigma} = 1 \times 10^{17}$ (which corresponds to a mean electron temperature of about 500 eV) and $a_0 = 0{\cdot}3$ cm, the relaxation time should be $\sim 10^{-5}$ sec. This estimated time is several times longer than the observed build-up time of the electron temperature in experiments with long coils. However, one should not conclude from this result that the theoretical model is completely contradicted by experiment; because there is a very strong dependence of $\tau_r$ on the geometrical parameters and the value of $\bar{\sigma}$ (and also because the above estimates are extremely rough). An entirely different explanation of the field relaxation is also possible, based on the assumption that the hollow plasma ruptures lengthwise as a result of an instability.

---

† However, the value of $8\pi p/H^2$ cannot be too small, otherwise a hollow plasma column with a reverse field will not be in a quasi-stationary state.

The instability of a rapidly contracting plasma, so clearly demonstrated in the excellent photographs obtained by Kvartskhava and co-workers, is a relatively ordinary phenomenon. The only particular difficulty in explaining it is that there are too many different mechanisms which could cause this instability. Of these we shall indicate only one that is rather similar to one already mentioned in connection with the radial acceleration of a plasma in the linear pinch (see § **5.2**). The plasma contained by the closed lines of force constitutes a tubular conductor with a large azimuthal current, which separates the external field from the reverse trapped field. This plasma conductor should be unstable with respect to deformations of the sausage-type. In this case, these necks will appear as length-wise creases on the surface of the plasma and, as a result, the cross section of the plasma assumes a shape reminiscent of a cogwheel—in exact agreement with the photographs. In the final stage of the development of such deformations the ring may burst, accompanied by an instantaneous disappearance of the internal field. At the same time, there should arise a very large electric over-voltage, and bursts of hard X-rays and neutrons should be expected. All these effects are in fact observed experimentally. However, neutrons are generally observed at higher pressures in the absence of hard X-rays. Hard X-rays have been observed if the initial pressure is small.

In general, the picture of the processes taking place in systems of the $\theta$-pinch type remains very obscure and there is as yet no basis for a positive answer to the basic question of instability. There is no doubt, however, that the compression of the plasma in a strong external field represents a more effective method of obtaining high temperatures than the linear pinch. One would think, therefore, that the study of this method will be continued intensively and that it will be developed further. Of considerable interest may be experiments conducted under conditions when the magnetic field is maintained at a high level for a long time after reaching a maximum.

A few words should be said about the nature of the short bursts of neutron radiation observed during the compression of a plasma, as this question is the constant topic of discussion in the papers of some physicists who are chiefly interested in the mechanisms of neutron production and devote much less attention to getting data which characterise the basic physical processes in a contracting plasma. At this point it seems hardly appropriate to try to engage in a detailed discussion of whether or not anyone has yet been successful in obtaining neutrons of thermonuclear origin in a $\theta$-pinch. One can only note the obstacles encountered in attempts to answer this question, which is of limited and merely incidental interest here. In some of the experiments whose results have been published to date, hard X-rays with energies up to several hundred keV have been observed in addition to the neutrons. It is evident, therefore, that in a contracting plasma, fast particles can also appear as a result of accelerating processes. The degree of pre-ionisation seems to be connected with these phenomena, particularly with the production of the hard X-rays.

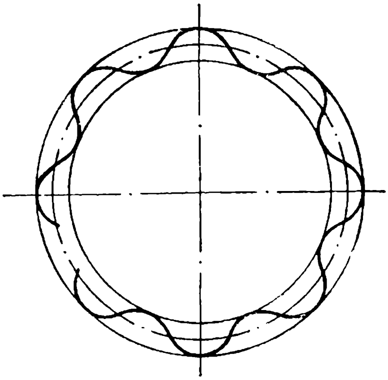

FIG. 56

Possible particle trajectories in the region where the field strength changes sign in a $\theta$-pinch with a reverse trapped field

It is not at all difficult to point out one of the possible acceleration mechanisms. Between the external confining field and the internal reversed field there must be an annular zone in the plasma in which the magnetic field strength is zero. Particles located in the vicinity of this zone can be accelerated in the electric field and may acquire a very substantial energy (see Fig. 56, which shows one of the possible trajectories of such a particle). To this we should add that a plasma compressed by an external field has a well-known mechanism for neutron production in reserve—the acceleration of deuterons as a result of the development of sausage-type instabilities. However, one should not exclude the possibility that a minute amount of hot plasma can remain in the chamber at the time of maximum compression and this might attain a high enough temperature to become a source of thermonuclear radiation.†

§ 5.8 Among the studies devoted to rapid plasma processes, a somewhat special place is occupied by the work of Osovets and co-workers, who have investigated the behaviour of a plasma loop in an alternating, transverse magnetic field. The alternating magnetic field fulfils two functions: first, it creates an annular plasma loop (by means of an electrodeless discharge) and second, it maintains the latter in a state of equilibrium for a certain interval of time.

We first consider the theoretical description of such a system, without touching upon the earliest stage of the discharge. Let an axially symmetric magnetic field (Fig. 57) be induced in a gas at low pressure by means of a system of conductors. The generation of this field will be accompanied by the appearance of an induced electric field whose lines of force will be in a plane perpendicular to the axis of the magnetic system. Let us assume further that, under the influence of the induced field, a discharge takes place in the gas and a ring of plasma is formed. We postulate that this plasma first appears when the magnetic field strength is very small, and we assume at first that the plasma has infinite conductivity. Under these conditions, the total magnetic flux through a major cross-section of the ring should remain equal to zero. Let $J$ be the current in the plasma ring and $L$ be the characteristic inductance of the ring. $\overline{H}$ is the average strength of the external field inside the ring which has a major radius $R$. The condition that the total flux is zero can be expressed

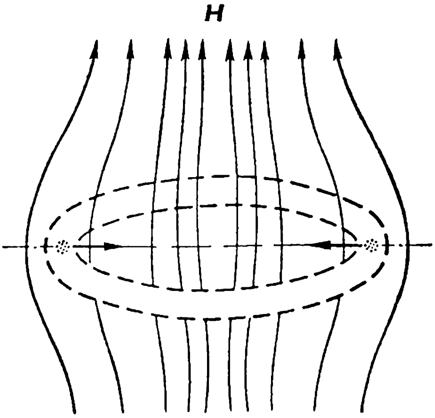

FIG. 57

Plasma ring in a rising axial field. After Osovets *et al.*

$$LJ = -\pi R^2 c\overline{H} = -2\pi c \int_0^R Hr\,dr. \qquad \text{.........(5.40)}$$

---

† Using this issue of the neutron radiation as an appropriate pretext, the author deems it necessary to make one general observation. In his view, the artificial excitement created every time anyone announces the detection of 'real' thermonuclear neutrons introduces an unnecessary element of publicity into the work on one of the most arduous scientific and technical problems in existence today.

The inductance of the ring is given by the familiar formula

$$L = 4\pi R[\ln(8R/a)-2] \equiv 2\pi R\mu, \qquad \text{.........}(5.41)$$

where $a$ is the minor radius.

The plasma ring will be in equilibrium if the sum of the electrodynamic forces acting on it is zero (if the processes are rapid enough we may disregard the plasma pressure). Hence, at equilibrium,

$$2\pi RJH+(J^2/2c)\,\partial L/\partial R = 0, \qquad \text{.........}(5.42)$$

where $H$ is the strength of the external field at the perimeter of the ring. Taking equations (*5.40*) and (*5.41*) into consideration, it is easy to find the following relation between the strength of the external field at the perimeter of the ring and the field strength inside this perimeter:

$$H = \bar{H}(1+2/\mu)/4. \qquad \text{.........}(5.43)$$

In this elegant form, the equation for a plasma ring is very similar to the familiar condition for the existence of an equilibrium orbit in a betatron:

$$H = \bar{H}/2. \qquad \text{.........}(5.44)$$

The value of $2/\mu$ usually lies between 0·2 and 0·3. A comparison of equations (*5.43*) and (*5.44*) shows that the existence of a plasma ring in equilibrium with an external field which creates the ring requires a steeper decrease of the field with radius than is the case in a betatron.

The above theoretical considerations are an extreme idealisation of the actual conditions under which the plasma is formed. The main element of this idealisation is the assumption that the resistance of the plasma can be neglected. If this assumption is eliminated, the equations describing the behaviour of the ring become considerably more complicated. However, from a qualitative point of view at least, one can anticipate the result of taking finite conductivity into account. A resistive plasma ring which initially satisfies condition (*5.43*) is not in complete equilibrium: the radius decreases with time, slowly at first, then with increasing speed. For this reason, after its formation the plasma ring will contract toward the magnetic axis during a certain time interval.

When the conductivity of the plasma has a finite value, the electromotive force inside the plasma is finite and equal to the product of the current and the resistance of the ring. Therefore, the magnetic flux enclosed within the ring of plasma will no longer be identically equal to zero (this flux is equal to the time integral of the electromotive force). Consequently, if the plasma is driven toward the axis rapidly enough, it should compress the trapped magnetic field. Part of the work done by the electrodynamic forces is spent in compressing the field, so that only a part of this work is used to impart kinetic energy to the contracting plasma. The counterpressure of the field surrounded by the contracting ring also limits the degree of compression and final radius of the plasma.

Figure 58 shows a device for the study of a ring-shaped plasma in an increasing transverse field. The discharge takes place in a short cylindrical vacuum chamber made of glass or some other ceramic. Two views of the coil system are shown in Fig. 59. A solenoid coil A surrounds the discharge chamber with disc coils B and C placed at the ends. As indicated in Fig. 58, all the coils are connected in parallel and the field configuration is determined by the dimensions $D_1$, $D_2$, $D_3$, $H$ and $h$ (Fig. 59). The search coils shown in Fig. 58 are used to measure the current distribution and motion of the plasma. Coil I records the total value of the annular gas current. Coils II and III enable one to determine the plasma boundaries, or at least the position of the main portion of the current at any given time.

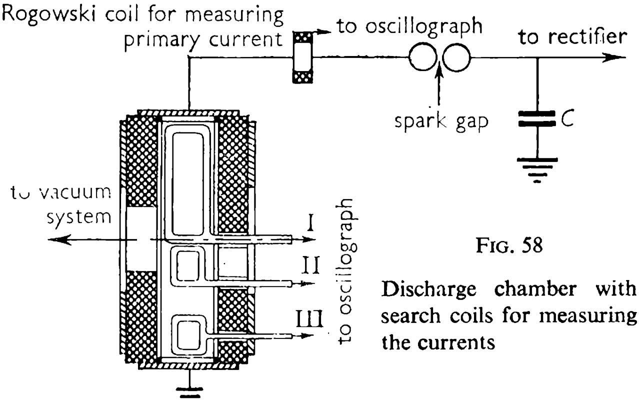

FIG. 58

Discharge chamber with search coils for measuring the currents

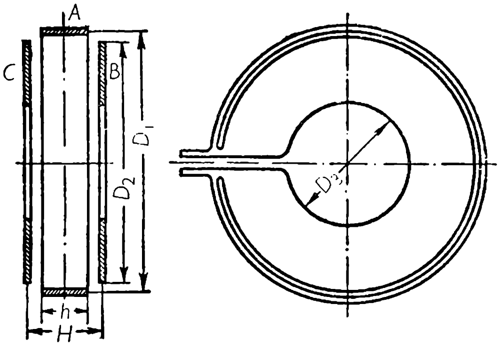

FIG. 59. Coil arrangement used to generate the magnetic field in Osovets' experiment

The initial pressure of the gas (hydrogen or deuterium) is usually about 0·1 Torr. Analysis of the search coil oscillograms and high-speed photographs demonstrates that the formation and compression of the ring of plasma takes place in good agreement with the predictions of theory. In typical experimental conditions the speed of compression lies between $10^6$–$10^7$ cm/sec. Hence the maximum energy of the deuterons in the plasma ranges up to some tens of electron volts.

The total number of particles in the plasma loop during the course of the discharge has not yet been determined experimentally. It is natural to assume that the plasma contains about the same number of particles at the end of the compression as were originally contained within the plasma ring in its equilibrium position, because during its formation and compression the plasma supposedly ionises and carries with it the gas contained in this region. This volume is equal to $\pi a^2 \times 2\pi R$, where $a$ is the minor radius of the plasma ring. When $a = 1{\cdot}5$ cm, $R = 20$ cm and $p = 0{\cdot}1$ Torr, the total number of particles in the compressed plasma ring should be approximately $10^{19}$ according to this estimate.

If it were possible to change the course of events in such a way that the magnetic field inside the plasma ring was cancelled during the compression, one could expect to obtain higher velocities and to obtain plasmas with higher densities and temperatures. In that case, the greater part of the electrodynamic energy $LJ^2/2$ should be ultimately converted into thermal energy. Preliminary experiments have shown that with a suitable bias field the plasma ring has a smaller major diameter than when there is no such field. Though the experimental investigations of the conditions prevailing when the internal field is compensated are still at an early stage, it may be expected that as the compensation methods for large-current devices are improved, it may be possible to obtain plasmas heated to very high temperatures.

§ **5.9** The acceleration of a plasma by electrodynamic forces is displayed in its purest form in devices called ‘plasma injectors’ (also ‘plasma accelerators’ and ‘plasma guns’). The purpose of such injectors is to create dense plasmoids with a high velocity which are then injected into some sort of magnetic trap. Actually, of course, in every plasma injection experiment, the injector should be regarded as a part of the system in which the chief element is the magnetic trap itself.

In this chapter, however, we shall be mainly interested in the primary function of the plasma injector—the creation of accelerated plasmoids. That is why we shall not at this point discuss how best to inject such plasmoids into magnetic traps. In principle, the simplest system for accelerating a plasma appears to be a device of the ‘rail’ type, such as that studied at the Institute of Atomic Energy in 1953. It is shown in Fig. 60. Two rigid parallel conductors (‘rails’) are connected to a capacitor bank through a spark gap. A thin metal wire is stretched between these conductors. When the spark gap is fired, current flows in the wire and the large energy which is suddenly deposited causes it first to vaporise and then to ionise. Thus the wire is transformed into a section of a plasma pinch. Owing to the interaction between the current flowing in this section and the magnetic field produced by the rail conductors, an electrodynamic force is generated which accelerates the plasma along the rails. This force is given by the expression

$$F = (J^2/2c^2)\,\partial L/\partial x, \qquad \text{.........}(5.45)$$

where $L$, the inductance of the circuit, is a function of the distance $x$ travelled by the plasma.

If we simplify the problem considerably by assuming that the plasma moves in a vacuum and retains the shape of a column with infinite conductivity, it is easy to calculate the velocity of the plasma along the rails. We shall not carry out the calculation for a specific system, but only indicate the results. These boil down to the fact that in devices of this type, plasma velocities of the order of $10^7$–$10^8$ cm/sec can be expected. Such velocities should be attained when metal wires a few tens of microns in diameter are vaporised and the length of the rails is some tens of centimetres. In principle, such an acceleration method is applicable not only to a plasma which is formed by the vaporisation of a wire, but may also be used to accelerate a hydrogen or deuterium plasma formed, for instance, by injecting a jet of gas across the rails at the same time as a voltage is applied.

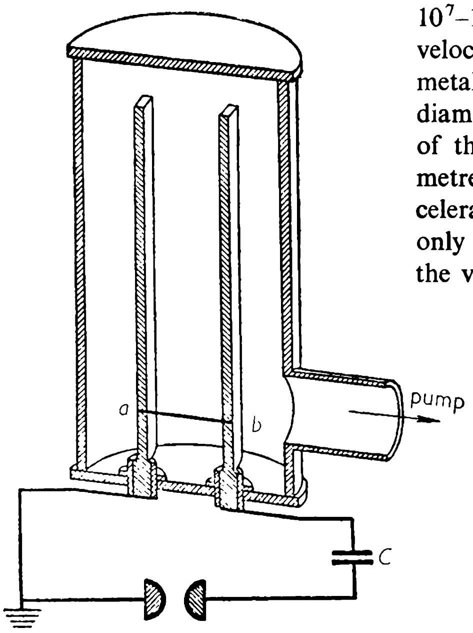

FIG. 60

Device for accelerating a plasma produced by exploding wires

The early experiments were conducted with a simple rail source and thin copper wires. The velocity of the plasma was measured with magnetic probes and by high-speed photography. These measurements showed that a plasma formed from the explosion of a copper wire $2 \times 10^{-3}$ cm in diameter can be accelerated to 1–$2 \times 10^7$ cm/sec over 30 cm. However, the experimental data contradict in many ways the results of calculations based on the elementary equations of motion. In particular, the velocities obtained are considerably smaller than those predicted by theory. High-speed photographs show that the plasma is not a bright, sharply defined entity that moves along the rails, but is a broad luminous cloud with diffuse boundaries.

The experimental attempts to accelerate plasmas with a rail gun, as described above, were purely exploratory. Later experimental studies in the U.S.S.R. and the U.S.A. made use of devices in which the plasma was formed and accelerated in the space between two coaxial cylinders. The discharge occurs in a gas which is introduced into the evacuated system by means of a fast-opening gas valve. In order to operate such a plasma gun at the highest possible efficiency—imparting a high velocity to the largest possible mass—it is necessary to reduce the parasitic inductance of the circuit to a minimum, since it limits the initial rate of current build-up. It is also necessary to have adequate synchronisation between the introduction of the gas and the application of the voltage at the coaxial electrodes. If the discharge starts prematurely, only a small portion of the gas leaks into the gun and is accelerated. If the voltage is applied too late, the gas spreads not only along the entire coaxial system but ahead of the gun as well, so that later on it will retard the motion of the plasma thrown out of the accelerator.

It is clear from the above that in order to obtain good results, the design of the fast-opening valve which admits gas into the gun is of considerable importance. The first essential requirement of its design is to minimise the time necessary for admitting the gas. Figure 61 shows the construction of a plasma accelerator with a fast opening valve, as suggested by Marshall (Los Alamos, U.S.A.). A hollow rod (1) held in place by a strong spring (2) forces a cap (3) against a teflon sleeve (4). The gas under the cap is introduced into the gun by means of an electrodynamic shock at the opposite end of the rod. This shock takes place when the circuit supplying current to the coil (5) is suddenly closed. The magnetic field in the coil creates a pressure pulse which acts on an aluminium bushing (6) fastened to the rod. This pulse is transmitted to the cap at the other end of the rod at the speed of sound, opening a gap between the edges of the cap and the teflon sleeve. The gas enters the gun through the open gap in about 100 $\mu$sec. During this time the gas can travel 5–10 cm from the point of admission. By selecting the time interval between the opening of the valve and the application of the high voltage, it is possible to vary the initial conditions over a wide range. However, to simplify the calculations, we shall assume that the gas is uniformly distributed over the whole length of the accelerator at the moment when the voltage is applied. A rough picture of the plasma motion in a coaxial accelerator may be obtained from a simplified theoretical analysis, in which the basic ideas have been borrowed from the theory of the rapid compression of a plasma in a pinch as discussed in § **5.3**. The equation of motion is of the form

$$\frac{d}{dt}\left(m\frac{dx}{dt}\right) = (J^2/2c^2)\frac{\partial L}{\partial x}. \qquad \text{.........}(5.46)$$

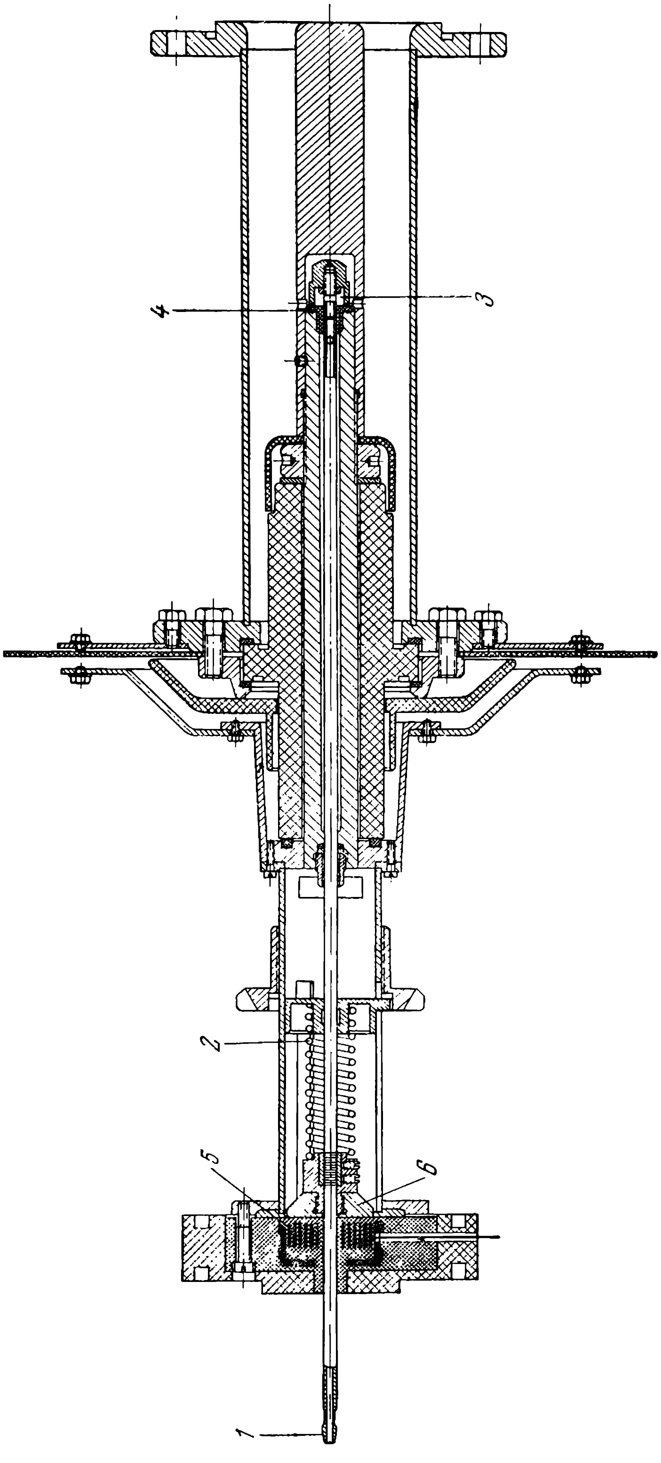

FIG. 61. Design of a coaxial plasma accelerator. After Marshall

If the motion takes place along a linear system of conductors, the inductance is given by the expression

$$L = L_0 + \xi x, \qquad \text{.........}(5.47)$$

where $L_0$ is the parasitic inductance of the external circuit and $\xi$ is the inductance per unit length. For a coaxial system, $\xi = 2 \ln (r_2/r_1)$, where $r_1$ and $r_2$ are the radius of the inner and outer electrode respectively. If the length of the coaxial system is large compared with the skin depth, the gas current may be regarded as flowing only within the boundaries of a relatively thin layer which sweeps up and ionises the gas along the coaxial system. Thus the mass of accelerated plasma increases in proportion to the distance $x$ travelled by the current layer. Therefore,

$$m = S\rho_0 x, \qquad \text{.........}(5.48)$$

where $\rho_0$ is the initial mass density and $S = \pi(r_2^2 - r_1^2)$ is the cross-sectional area of the annulus. Hence equation (*5.46*) becomes

$$(S\rho_0/2)\, d^2x^2/dt^2 = (\xi/2c^2)J^2. \qquad \text{.........}(5.49)$$

The current and voltage are determined by the circuit equations

$$J = -C\, dV/dt, \qquad \text{.........}(5.50)$$

$$V = \frac{1}{c^2}\frac{d}{dt}(L_0 + \xi x)J. \qquad \text{.........}(5.51)$$

The elementary model we have selected can give only a qualitative picture of the acceleration process because of the simplifying assumptions involved; consequently there is hardly any point in considering the detailed behaviour of the general solutions to equations (*5.49*)–(*5.51*). It is sufficient to confine ourselves to the simplest case. Let us assume that the capacitor potential is practically constant; during the acceleration of the plasma this approximation is valid if the capacitance C is large enough. Furthermore, we shall assume that $L_0 \gg \xi x$. In this particular case

$$J = V_0 t c^2/L_0, \qquad \text{.........}(5.52)$$

where $V_0$ is the initial voltage.

Substituting (*5.52*) into (*5.49*), we find

$$x = \gamma t^2/2; \qquad dx/dt = \gamma t. \qquad \text{.........}(5.53)$$

The constant $\gamma$ denotes the acceleration of the plasma, and depends on the parameters of the system in the following manner:

$$\gamma = [(cV_0)^2\xi/3\rho_0 S L_0^2]^{\frac{1}{2}}. \qquad \text{.........}(5.54)$$

The plasma velocity depends on the distance covered:

$$dx/dt = [4\xi(V_0 cx)^2/3S\rho_0 L_0^2]^{\frac{1}{4}}. \qquad \text{.........}(5.55)$$

This is the expression most interesting experimentally. For an accelerator with given parameters, the plasma velocity is proportional to $(V_0^2/\rho_0)^{\frac{1}{4}}$. We should note in this connection that for all processes where the electrodynamic acceleration of plasma plays an important part, the variation of the velocity with the initial voltage and mass density has a somewhat universal character. We encounter the same dependence between $v$, $V_0$, and $\rho_0$ when we consider both a dynamic linear pinch and also the implosion of a plasma in a fast $\theta$-pinch. This similarity is associated with the fact that in all of these processes the electrodynamic forces initially increase in proportion to $t^2$.

To illustrate the above relations let us take a concrete example: 0·1 cm$^3$ of deuterium at atmospheric pressure is admitted through a valve into a 30 cm long accelerator, and spreads uniformly along the entire coaxial line. The initial capacitor potential is 30 kV, the parasitic inductance is equal to 0·1 $\mu$H and $\xi = 0{\cdot}5$. With these parameters, the plasma velocity at the end of the line should reach $3 \times 10^7$ cm/sec, which corresponds to a deuteron energy of 900 eV. The total number of deuterons in the accelerated plasma should be $6 \times 10^{18}$ (if the ionisation of the neutral gas is complete). A further increase in $v$ may be achieved by reducing the parasitic inductance and increasing the capacitor potential. The velocity cannot be increased appreciably by decreasing the density, because the dependence of $v$ on $\rho_0$ is very weak, and also because the trapping of the gas by the moving plasma is impaired if $\rho_0$ is too small.

The elementary theory described here is useful only for exploratory estimates and is unable to answer many important questions. In particular, this theory provides no information on how the radial coordinate $r$ influences the accelerator (the magnetic pressure in the plasma layer decreases from the inner to the outer cylinder inversely as $r^2$). A more thorough physical analysis is also needed to evaluate the role which may be played by the interaction between the moving plasma and the walls. The question of the stability of the acceleration process also remains essentially open until a genuine magnetohydrodynamic theory is developed. On the basis of the general considerations presented in Chapter VII, the plasma-magnetic field interface in the accelerator is expected to be unstable.

Experimental studies carried out so far have shown that coaxial plasma guns can be used to accelerate $10^{17}$–$10^{18}$ deuterons to a velocity of 3–$5 \times 10^7$ cm/sec. Apparently, as the accelerator design and electrical systems are improved, it will be possible to attain plasma velocities of the order of $10^8$ cm/sec. The neutral component can be almost completely removed when the accelerated plasma is driven over a sufficiently long distance in a vacuum.

The axial thickness of the plasma annulus in the accelerator is theoretically determined by the skin depth and it should not exceed a few centimetres in ordinary experimental conditions. However, owing to the distribution of particle velocities, the accelerated plasma extends over a considerable distance after leaving the accelerator, with a corresponding decrease in density. At distances of the order of one metre from the plasma gun, the maximum number density does not usually exceed $10^{15}$ cm$^{-3}$. In models involving infinite conductivity and 'frozen' lines of force, one may expect that an azimuthal magnetic field is trapped for a certain period of time inside the plasma after it leaves the injector. However, because the conductivity of the accelerated plasma is not especially high, this field relaxes quickly. The field trapping can be greatly reduced by selecting the initial conditions so that the current drops to zero at the instant when the plasma leaves the end of the gun.

Besides rail and coaxial type accelerators, pinch-type devices may be used to accelerate a plasma. The idea underlying this method is as follows: with suitable initial conditions a pinch discharge can be formed such that the contracting plasma has an approximately conical shape and produces a cumulative jet directed along the axis of the discharge tube. Study of the various kinds of pinches shows that the conditions favouring the formation of such jets are created by pulsed discharges in tubes with metallic walls, and also in conical ceramic tubes. Measurement of the current distribution and motion of the luminous front in chambers with metallic walls shows that the compression begins in a region close to the anode, and then spreads toward the cathode at a speed of up to $3 \times 10^7$ cm/sec for an initial deuterium pressure of 0·1 Torr. The motion of the current sheath toward the cathode is shown schematically by the dotted lines in Fig. 62, and appears to be related to the motion of the plasma. Therefore if a small aperture is made in the electrode, an accelerated plasma jet should pass through it. This has been verified experimentally and the plasma velocity (measured by the Doppler effect) in high-power discharges can reach $2 \times 10^7$ cm/sec. However, the mass of plasma ejected at this high velocity in the first devices of this type did not exceed a few tenths of one per cent of the total mass in the discharge chamber. Further improvements in this method may so greatly increase its efficiency that it will be possible to obtain plasmas with a much larger total mass and number density. Moreover, to prevent the expansion of the plasma caused by the high transverse particle velocities, the plasma jet must be guided by a strong axial magnetic field.

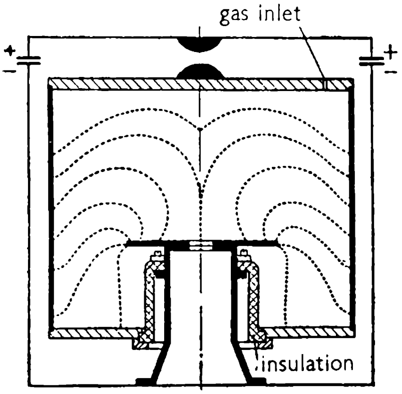

FIG. 62

Successive positions of the current sheath of a discharge in a tube with a metallic wall

## CHAPTER VI

# HEATING AND CONFINEMENT OF A PLASMA BY SUSTAINED ELECTRICAL DISCHARGES

§ **6.1** The lack of prospective practical applications of fast high-power pinch discharges (§ **5.4**) does not detract in any way from the idea of confining a plasma in the self-magnetic field of a high-current discharge, the high-temperature plasma being produced by the associated Joule and compressional heating.

Fast discharges cannot result in quasi-stationary equilibrium states in which the magnetic forces are at all times balanced by the internal pressure of a high-temperature plasma. However, it does not follow that such a state is unattainable in powerful discharges of long duration. If the current rises slowly enough, one can expect to obtain conditions which differ radically from those obtained with high rates of current rise. A quantitative criterion for distinguishing between 'slow' and 'fast' discharges is provided by the ratio of the current rise-time to the period of the inertial radial oscillations. When electric discharges with a peak current of $10^5$–$10^6$ A and a half period of the order of several milliseconds (or more) take place in rarefied gases, hundreds of inertial oscillations can occur within the first half-period. We shall refer to such discharges as slow, as opposed to the fast ones in which only a few radial oscillations can occur up to the time of peak current.

It may be expected that the magnetic forces are balanced by the kinetic pressure of the plasma in slow discharges. The temperature gradually increases due to the Joule heating and, under certain conditions, also due to the compression of the plasma. In order to produce a high-temperature plasma in such an equilibrium condition, the following requirements must be met:

1. the energy loss to the electrodes must be prevented, i.e. the plasma pinch must be closed;
2. the plasma must be confined and isolated from the walls;
3. the equilibrium state must be stable.

The first of these requirements means that we are dealing with electrodeless discharges. We shall assume henceforth that the discharge takes place in a toroidal chamber, and that the current is excited by induction.

Under certain initial conditions the second requirement is automatically fulfilled as a result of the compression of the plasma which initially fills the entire chamber. Compression occurs both in the absence of an externally generated longitudinal field and in discharges with a relatively weak one (see § **6.4** for a detailed discussion of toroidal pinches with a longitudinal stabilising field). However, if the discharge takes place in a longitudinal field whose strength greatly exceeds the field strength produced by the discharge current, it is not easy to form a completely isolated plasma because the strong longitudinal field prevents all but a very small pinch compression. We shall return to this case in § **6.6**.

As shown by the results of extensive experimentation, the main and most difficult task in the quasi-stationary heating of a plasma is the achievement of plasma configurations possessing a stable equilibrium. The basic equilibrium conditions for quasi-stationary pinches were discussed in § **4.3**. Although, in deriving the equations determining the equilibrium of a toroidal pinch, we made idealising assumptions (in particular, it was assumed that the plasma has a sharply defined boundary and that the pinch radius is small compared with the major radius of the torus), the results obtained can nevertheless be used as the basis of a first approximation to the theory of quasi-stationary discharges.

It is immediately evident that the problem of stability is the most dangerous and highly difficult obstacle to the realisation of quasi-stationary plasmas. A plasma is a system with an almost infinite number of degrees of freedom. Thus, strictly speaking, the stability problem is theoretically insoluble; and an answer to the question as to the existence or otherwise of stable states can be provided only by direct experiment. This fact cannot, however, serve as an excuse for dismissing the theoretical investigation of the various special problems which comprise the general problem of the stability of plasma configurations. Specifically, when a given class of quasi-stationary plasma states are considered, it is usually possible to predict which perturbations are the most dangerous to the preservation of a high degree of thermal insulation. It is these particularly dangerous perturbations that should be the object of theoretical research: it must be determined if the occurrence of one of these perturbations leads either to a deviation from the equilibrium state which grows with time, or to small oscillations of only limited amplitude in the neighbourhood of the equilibrium state.

Let us now turn directly to the problem of the stability of a pinch carrying an electric current which generates a strong magnetic field. In analysing the stability problem, we shall restrict ourselves to the framework of the magnetohydrodynamic approximation, i.e. we shall identify the plasma with a conducting fluid. The various manifestations of instability which may be caused by the microstructure of the plasma and the specific character of the interaction between the particles are not considered in such an analysis (they will be discussed in the following chapter).

Some graphic representations of a qualitative nature are helpful in a preliminary exploration of the stability of an equilibrium pinch. Figures 48 and 63 show the form of two of the simplest perturbations which can occur in a linear pinch. The first is a local constriction of the pinch, the second is a kink deformation. In the absence of a stabilising magnetic field, an isolated pinch compressed by its self-magnetic field should be unstable against both types of perturbations. The first of these two types of instability has already been mentioned (§ **4.4**): it is due to the fact that the rise of magnetic pressure in the region of the constriction is not offset by a corresponding increase in the plasma pressure $p$; the plasma can flow freely along the pinch from one section to another, and consequently the value of $p$ should be about the same everywhere. For this reason, each deformation arising at random grows, and will disrupt the pinch wherever a narrow constriction forms.

In the kink deformation, as shown in Fig. 63, the field strength produced by the current is less on the outside of the bend than that on the inside; so that the amplitude of this perturbation also increases with time, until the sharply bent pinch touches the wall of the discharge tube. The instability of the pinch with respect to the sausage and kink instabilities may be regarded as a graphic illustration of certain properties of the magnetic lines of force, a picture associated with the concept of Maxwell stresses. The lines of force associated with the magnetic field are analogous to stretched elastic bands which, in the first case, try to contract radially, and in the second, repel one another in the longitudinal direction. The contraction of these bands leads to the formation of constrictions; their mutual repulsion is reminiscent of a compressed spring—which we know is unstable against buckling.

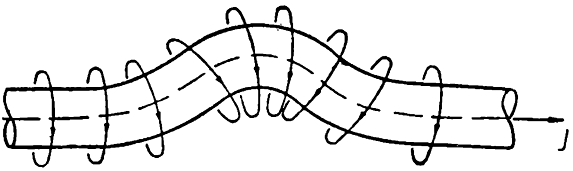

FIG. 63. Kink deformation in a plasma pinch

To stabilise the pinch, a longitudinal magnetic field and an external conducting shell may be used. Let us first consider the stabilising mechanism of the longitudinal magnetic field. For simplicity, we shall assume that the pinch has infinite conductivity so that the electrodynamic forces are applied to its surface. Let us also assume at first that the longitudinal magnetic field $H_z$ is uniform inside the plasma and is equal to zero outside. The longitudinal field inside the pinch generates a magnetic pressure opposed to the pressure produced by the pinch field and consequently hinders the formation of sausage-type instabilities. Let the radius of the pinch change locally from $a$ to $a-\delta a$. The magnetic pressure due to the pinch current then increases by

$$(H_J^2/8\pi)(2\delta a/a).$$

Because the longitudinal field is frozen into the pinch, $H_z a^2$ is constant during the deformation so that the magnetic pressure produced by the longitudinal field varies inversely with $a^4$ (i.e. faster than that of the pinch field). Thus, when the radius of the pinch decreases by $\delta a$, the internal magnetic pressure increases by

$$(H_z^2/8\pi)(4\delta a/a).$$

This additional pressure prevents the radius of the pinch from decreasing if the condition

$$H_z^2 > H_J^2/2$$

is satisfied; and the pinch is then stabilised with respect to sausage-type deformations.

The longitudinal magnetic field frozen into the pinch also helps to stabilise the kinking. In kinking, the pinch becomes elongated; and consequently the longitudinal lines of force, which behave like stretched rubber bands, try to contract and straighten the bent portion of the pinch. However a longitudinal field is less effective for stabilising kinks than for stabilising sausage-type instabilities. Calculations show that the force arising from the stretching of the longitudinal lines of force cannot balance the force produced by the pinch field when the wavelength $\lambda$ which characterises the kink distribution along the pinch is large compared with the plasma radius. When the strength of the trapped longitudinal field is a maximum, i.e. when $H_z = H_J$ (in this case the plasma pressure is zero), only those kinks for which $\lambda < 14a$ can be stabilised.

An internal longitudinal field is insufficient by itself to stabilise the pinch against long-wavelength kinks. However, this does not mean that difficulties connected with the presence of such perturbations are insurmountable. A conducting metallic shell may be quite effective in reducing the instability of a pinch against long-wavelength kinks. The mechanism of the stabilising action of a metallic shell has already been mentioned in Chapter IV. When the pinch is displaced, the magnetic flux between the plasma and the metallic shell cannot change because the lines of force cannot penetrate the metal. Thus the pinch field must undergo a deformation—it will be squeezed and consequently enhanced in the space between the side of the displacement and the wall, and weakened on the opposite side. As a result, a force arises which tends to restore the displaced part of the pinch to its original position. In essence, we are dealing here with an effect that is completely analogous to the one which restricts the expansion of the major radius of the plasma ring in the metal torus. To explain this property of the metallic shell, we presented a somewhat different picture in Chapter IV, making use of the concept of the 'image current'. This explanation of the action of the shell is completely equivalent in physical terms to the picture of the deformation of the lines of force, and can also be used to analyse the stabilising properties of the shell. It can therefore be stated that, when the pinch is kinked, image currents arise in the conducting shell whose field suppresses the growth of the deformation.

It is necessary to emphasise, however, that the metallic shell is only effective against kinks which are characterised by large enough wavelengths; the order of magnitude of the wavelength $\lambda$ must be comparable with, or greater than, the radius of the metallic shell. The distortion of the pinch field by the kinking occupies a region with a radius of the order of $\lambda$. Therefore, when $\lambda$ is small compared with the tube radius, the lines of force are not distorted appreciably near the conducting shell, and cannot lead to the appearance of image currents which are large enough to stabilise the kink. It is also easy to see that the metallic shell is incapable of ensuring pinch stability with respect to radial deformations such as the sausage-type instabilities. In deformations with azimuthal symmetry, the self-magnetic field outside the plasma does not change, and so image currents which would suppress this distortion of the pinch cannot arise in the conducting shell. Consequently, to stabilise the pinch two stabilising factors must act at the same time: a trapped longitudinal magnetic field, and a metallic shell. The first of these stabilises the short-wavelength kinks and the sausage instabilities; the second stabilises the long-wavelength kinks.

Another supplementary condition is necessary to stabilise perturbations of arbitrary wavelength: the range of wavelengths over which these stabilising factors are effective must overlap. This is possible only when the radius $a$ of the pinch is not too small compared with the radius $b$ of the metallic shell. If the ratio $a/b$ is very small, there will be a range of wavelengths over which kink stabilisation is impossible. This is a wavelength range in which the ratio $\lambda/a$ is too large for the influence of the longitudinal field to be exerted and, at the same time, is too small for the image currents arising in the metallic shell to be effective. Calculations show that for the idealised case considered here (infinite plasma conductivity and complete freezing-in of the longitudinal field), all wavelengths will be stabilised provided that $a/b$ exceeds a certain value which increases with the ratio $H_J/H_z$. The minimum permissible value of $a/b$ is $\frac{1}{5}$, and is obtained when $H_J = H_z$, i.e. when the magnetic pressure generated by the pinch field is used to confine the trapped longitudinal field only, and the plasma pressure is zero. When $(H_z/H_J)^2 = 0{\cdot}5$, the minimum permissible value of $a/b$ is $0{\cdot}4$.

The stability is decreased if a longitudinal field $H_0$ exists outside the plasma which is comparable in magnitude with the trapped field $H_i$. Figure 64 shows a theoretical stability diagram for different values of the ratio $H_0/H_i \equiv \varepsilon$. The region of stable equilibrium for a given value of $\varepsilon$ begins at a certain definite value of $a/b$ and is bounded at the top by a straight line which corresponds to the maximum equilibrium value of $H_i/H_J$, in accordance with the condition for equilibrium,

$$H_J^2 = H_i^2 - H_0^2 = H_i^2(1-\varepsilon^2).$$

At the top boundary of the stability region, the plasma pressure is zero. The stability region for the special case where $\varepsilon = 0{\cdot}3$ is shaded in the figure. As follows from the general stability diagram, the region of permissible values of $a/b$ is reduced as the ratio $H_0/H_i$ increases. A stable state in a strong longitudinal field (in the infinite cylindrical approximation) can be obtained only when the plasma almost touches the surface of the metallic shell. In practical terms, this means that the pinch cannot be stabilised under such conditions.

This deterioration of the stability when there is an external longitudinal field is associated with the change in the magnetic field geometry. When $H_0 \neq 0$, the lines of force outside the pinch are helical. As can easily be proved, the pitch length of such a helical line located on the outer surface of the plasma is $2\pi a(H_0/H_J)$, and increases with the strength of the longitudinal field. Among the various perturbations which can occur on the surface of the pinch, those which take place along a helical line having the same pitch as that of the field line (Fig. 65) present a special hazard. Deformations of this type result in the minimum distortion of the field outside the pinch. The plasma may be said to squeeze itself between the lines of force, moving them apart slightly. At a large distance from the surface of the pinch the field is almost undisturbed. For this reason, such deformations can be stabilised by the metallic shell only when the pinch almost touches its surface.

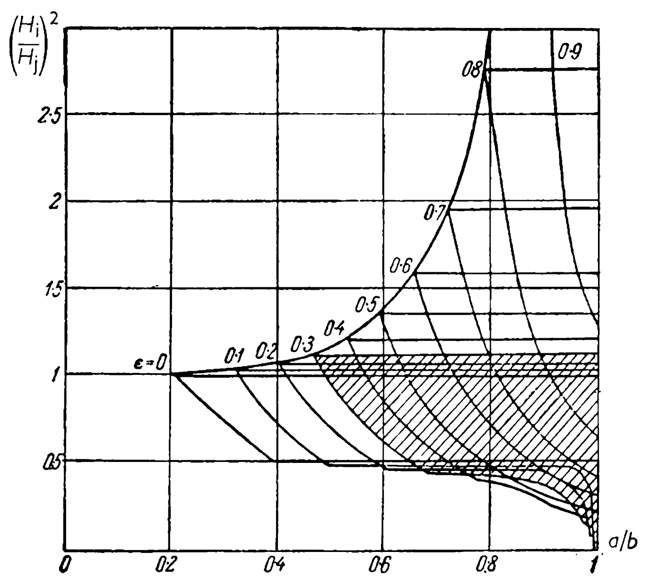

FIG. 64. Stability diagram for an infinitely conducting cylindrical plasma column (stabilised pinch); $\varepsilon = H_0/H_i$. After Shafranov

If, in selecting methods for stabilising a pinch, we use the stability diagram shown in Fig. 64, we are led to the conclusion that the best system is one in which the external longitudinal magnetic field $H_0$ is zero, and the strength of the trapped field $H_i$ is comparable with $H_J$. Such a situation may arise if the contracting plasma carries with it a large part of the longitudinal magnetic flux initially present in the discharge tube. The strength of the longitudinal field inside such a 'paramagnetic' pinch is approximately equal to $H_{i0}(b/a)^2$, where $H_{i0}$ is the initial field strength.

To achieve such an operating régime, the strength of the initial longitudinal field must be relatively small. An inherent advantage is due to the fact that the proper initial conditions occur naturally in the development of a pulsed discharge; initially the plasma is distributed over the entire cross-section of the chamber and then, as $H_J$ begins to exceed $H_{i0}$, it contracts and carries inward the trapped longitudinal lines of force. A necessary condition for maintaining such a discharge is a high plasma conductivity. The duration of the 'paramagnetic' state is determined by the laws governing the skin-effect; in order of magnitude, it is equal to the time taken for the trapped field to diffuse out of the pinch.

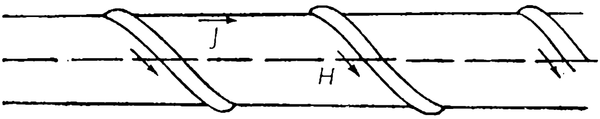

FIG. 65. Screw deformation of the pinch

However, this method of stabilising a pinch is not the only possible one, even within the framework of the above theoretical ideas. In order to convince ourselves of this, we observe that all the above theoretical results refer to a pinch of infinite length. In an infinitely long pinch, perturbations of any wavelength may arise. However, in practical circumstances, the length of the pinch is a finite quantity; and the wavelength characterising the distribution of the deformation along a toroidal pinch cannot exceed the length of the major circumference. Taking this into account, we come to the conclusion that an infinitely conducting pinch can be stable not only when $H_{i0} < H_J$ and $H_0$ is very small, but also when the strength of the longitudinal field both inside and outside the plasma is practically identical and is much greater than $H_J$.

In this latter case, the stability condition requires that the wavelength of the particularly dangerous helical deformation referred to above should exceed the length of the pinch, viz.:

$$2\pi a(H_0/H_J) > 2\pi R. \qquad \text{.........}(6.1)$$

Consequently, in order to stabilise a toroidal pinch with a strong longitudinal field it is necessary that the ratio $H_0/H_J$ be greater than $R/a$. The condition (*6.1*) was obtained independently by Kruskal and by Shafranov.

However, even when this condition is fulfilled, certain perturbations are not necessarily stabilised. These are the so-called high-mode deformations which we shall discuss a little later.

In the case under consideration, the longitudinal magnetic field is distributed over the entire cross-section of the discharge tube, and does not vary significantly at the plasma boundary. One of the advantages of such a method for stabilising a discharge is that the confinement time is not limited to the duration of the skin-effect, but is determined only by the duration of $H_0$ and $J$. However, a high price is paid for this advantage, because it is necessary to work with very high magnetic fields.

In this discussion of pinch stability we have not considered the mathematical aspects of the theory and have given only the results. However, a few remarks about the classification of elementary plasma deformations used in the theory will make it easier for a reader studying these problems for the first time to understand specialised papers which very often contain terms used for classifying plasma deformations but do not provide explanations. Familiarity with this terminology is also necessary for the formulation of a criterion of pinch stability with respect to surface perturbations which are more complex than sausage and kink deformations.

If the pinch has a sharply defined boundary and the current flows only along the surface, the picture of the deformation is wholly determined by changes in the shape of the pinch surface. Let us suppose we are dealing with a straight cylindrical pinch of radius $a_0$ and of infinite length. When the deformation occurs, the surface of the pinch ceases to be cylindrical. The perturbation changes the distance from the surface to the axis by an amount $\delta r$, which is in general an arbitrary function of the axial coordinate $z$, the azimuth $\theta$ and time $t$. The displacement $\delta r$ may be represented as a superposition of Fourier components of the form

$$\delta r = \xi_0 \exp i(kz+m\theta-\omega t),$$

where $\xi_0$ is the amplitude of the component. The quantities $k$, $m$ and $\omega$, which enter into the exponential factor, have a simple physical meaning. The quantity $k$ is the wave-number characterising the axial periodicity of the perturbation; it is related to the wavelength of the deformation by $k = 2\pi/\lambda$. The coefficient $m$ is called the 'mode' of the perturbation; it determines the azimuthal periodicity of $\delta r$. When the azimuth changes by $2\pi$, $\delta r$ returns to its original value, so that $m$ can have only integral values ($m = 0, \pm 1, \pm 2, \ldots$). When $m = 0$, the displacement is independent of the azimuth. This corresponds to the sausage-type instabilities already familiar to us. The value $|m| = 1$ corresponds to the dangerous kinks for which the axis of the pinch assumes the shape of a screw or a sine wave. When $|m| > 1$, the pinch axis is not displaced and the deformations have helical structures, with $m$-fold symmetry, i.e. the pinch assumes a shape resembling a braid twisted from several strands. Figure 66 indicates the shape of the deformations corresponding to $m = 2$, 3 and 4. If the value of $\omega$ (which determines the time-dependence of $\delta r$) is real, the amplitude of the perturbation is limited, i.e. the pinch is stable against a given type of perturbation. When $\omega$ is imaginary or has a positive imaginary part, we are dealing with a perturbation which grows in time, i.e. an example of pinch instability.

The aim of the theory is to establish criteria determining the range of characteristic parameters for which the pinch should be stable for every given pair of values of $k$ and $m$. The most important of such criteria have already been indicated, i.e. they characterise the circumstances in which the pinch can be stable against the most dangerous deformations—those with modes $m = 0$ and $m = 1$. Although perturbations corresponding to the higher modes are less dangerous, it is difficult to evaluate in advance of experiment the part they play in increasing energy losses from a pinch. It is possible that under certain conditions the instability of such perturbations will be an important obstacle to confining a high-temperature pinch plasma. For this reason, it is useful to know the stability criterion for perturbations with $|m| > 1$. We shall discuss here the most important practical case, when $H_z \gg H_J$. In this case, it may be shown by reasoning very similar to that which leads to condition (*6.1*) that the inequality

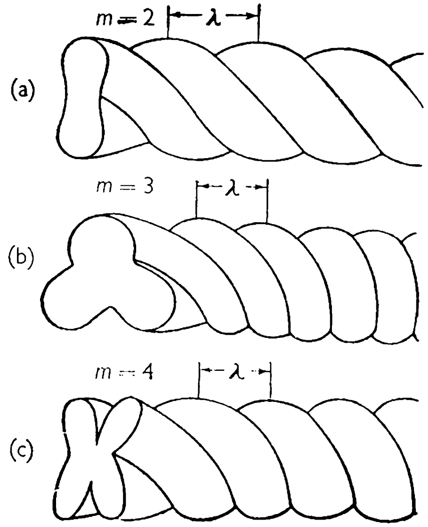

FIG. 66

Deformations with higher modes ($|m| > 1$)

$$|H_z/H_J| > |mR/a|$$

must be satisfied for the stabilisation of a toroidal pinch against deformations of the $m$th mode.

Obviously, this condition cannot be satisfied for all values of $m$: however large the ratio $H_z/H_J$ may be, there will always exist some deformations with a large enough $m$ for which the stability criterion will not be obeyed. It can only be hoped that because the pinch as a whole does not change its position in the chamber and has no tendency to pinch itself off, these instabilities will not lead to a catastrophic escape of particles and energy from the plasma.

The above theoretical analysis of pinch stability indicates the basic possibility of heating a current-carrying plasma, and that the stability of the most dangerous perturbations can be predicted. These results provide a supporting argument for an optimistic appraisal of the study of slow toroidal discharges. However, we should not forget that the conclusions drawn from the simplified magnetohydrodynamic theory of stability are based on a drastic over-simplification of the physical picture of a discharge, from which many important details are excluded. Strictly speaking, the theory presented is valid only for the case where the pinch has infinite conductivity, so that the thickness of the current-carrying skin is infinitesimally small. For this reason, the theory cannot be used for deformations of the plasma which are characterised by a wavelength smaller than the skin-depth. A more thorough analysis shows that in practice such deformations can be unstable. Obviously, one cannot expect to stabilise these by methods used to suppress long-wavelength instabilities.

A large number of investigations have been reported whose purpose was to develop and improve the theory of pinch stability. These further studies have taken into consideration the structure of a pinch with a diffuse boundary. In addition, these studies included not only macroscopic deformations of the plasma but also local deviations from the state of equilibrium, i.e. deformations developing over some limited region inside the plasma. These studies have not yet produced results agreeing well enough with experiment to be regarded as the next great step in the development of stability theory. Nevertheless, some of the concrete results of the more rigorous theory may take on a great importance if they are confirmed experimentally.

One of the most interesting conclusions of the theoretical analyses of the local properties of a pinch is the stability criterion discovered by Suydam. According to this criterion, the stability of a cylindrical pinch requires that the following inequality be satisfied at every point inside the pinch:

$$\frac{8\pi}{H_z^2}\frac{dp}{dr}+\frac{r}{4}\left(\frac{1}{\mu}\frac{d\mu}{dr}\right)^2 > 0, \qquad \ldots\ldots\ldots(6.2)$$

where $r$ is the distance from the pinch axis and $\mu = H_\theta/rH_z$ ($H_\theta$ is the strength of the azimuthal field at a given point). As follows from the derivation, the inequality (*6.2*) provides only a necessary condition for the stability of the pinch. From the point of view of the experimentalist, an unquestionable advantage of Suydam's criterion is the fact that it can be used to determine the stability of any state with a known radial distribution of $p$ and $\mu$.

It follows from equation (*6.2*) that the quantity $d\mu/dr$ (the shear) should everywhere be large enough for the positive value of the second term to outweigh the negative first term which contains the plasma pressure gradient. As shown by studies of specific examples, such compensation in the case of a diffuse plasma boundary can be achieved most easily in practice in a discharge with a strong longitudinal field $H_z \gg H_\theta$. Suydam's criterion can also be satisfied in situations where the external field changes its direction sharply at the plasma boundary. However, in this case the pinch turns out to be unstable against perturbations having a wavelength greater than the skin-depth.

Although the conclusions which follow from Suydam's criterion appear seriously to deflate the optimism concerning the prospects of a wide variety of studies devoted to 'quasi-stationary' discharges, they do not themselves justify stopping experimental work along these lines. The point is that the pinch theory is still at a stage where it cannot form the basis of a final judgment as to the stability or instability of specific configurations of plasma in a magnetic field. The author has arrived at this conclusion after many consultations with theoreticians. When these consultations were concerned with the question of the desirability of working in some definite régime or other, the diagnosis of the stability has always turned out to be very evasive. At the present time, the experimentalist ought not to think that his hands are completely tied by the theoretical predictions. On the contrary, the principal objective of experiments today is the creation of reliable points of reference for the further development of theoretical concepts. To reach this goal, we require long and tedious work in the investigation of the plasma properties associated with slow discharges and of various methods of stabilising plasma pinches by means of externally generated fields.

§ **6.2** Experimental investigations of the processes which take place in the plasma of a sustained discharge can be carried out, in principle, both in long straight tubes and in toroidal chambers. In practice, however, linear pinch tubes can be used only for exploratory experiments with limited objectives. The release of a very large amount of energy on a small area of the electrodes leads to considerable vaporisation of the electrode material. In contrast to the effects in fast discharges discussed in the preceding chapter, the contamination of the gas associated with the heating of the electrodes has a substantial effect on the entire course of events in slow discharges. For this reason, the most valuable experimental data on the quasi-stationary states of a plasma during sustained discharges are obtained with toroidal discharge chambers.

In the first stage of the experiments, most of the basic studies in the U.S.S.R. as well as in England and the U.S.A. were conducted with chambers made of insulating materials (glass, porcelain, quartz). Due to the large amount of gas evolved from the walls, significant results with such chambers can be obtained only at relatively high initial gas densities and for discharges of moderate power. In most of the present-day large-scale experimental devices, quasi-stationary discharges are produced in chambers with metal walls. Such a chamber may consist either of a series of circular sections insulated from one another (Fig. 67), or it may be made in the form of a continuous torus of thin material of moderate electrical conductivity and good vacuum qualities (Fig. 68), e.g. thin, non-magnetic, stainless steel. The all-metal chamber can then be heated under a good vacuum to a high temperature for a preliminary bake-out, thanks to which its vacuum properties are substantially improved and the discharge occurs in relatively pure conditions. The wall-thickness of the continuous metallic chamber has to be selected on the basis of a compromise between two requirements: it must have first the necessary rigidity of construction, and second a high enough resistance to current flowing through the metal around the torus (this current shunts the discharge and creates an additional load on the energy source which supplies electrical power to the discharge). In large experimental devices with a minor diameter of tens of centimetres, the thickness of the stainless steel has to be a few tenths of a millimetre. In this case, however, the chamber cannot withstand a pressure of one atmosphere, and therefore it is placed inside a vacuum-tight casing which, if it is a thick metal conductor, also serves as the stabilising shell. In order to prevent the formation of parasitic discharges in the gas between the inner chamber (called a 'liner') and the outer casing, the space between them is highly evacuated by means of auxiliary pumps. Thus the entire discharge volume constitutes a double vacuum system. As a result, the gas leakage into the inner chamber is reduced to a minimum.

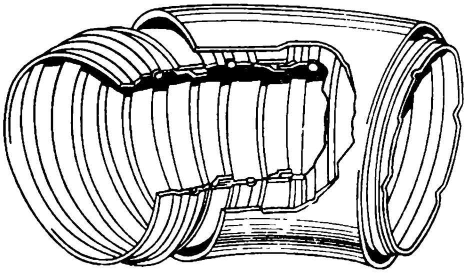

FIG. 67

A toroidal discharge chamber consisting of insulated rings

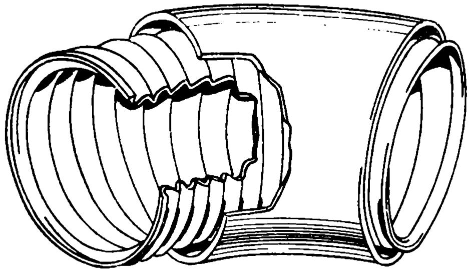

FIG. 68

Chamber made in the form of a continuous metallic torus

In the other version, where the liner consists of a series of annular metallic sections separated by layers of electric insulation, the stabilisation

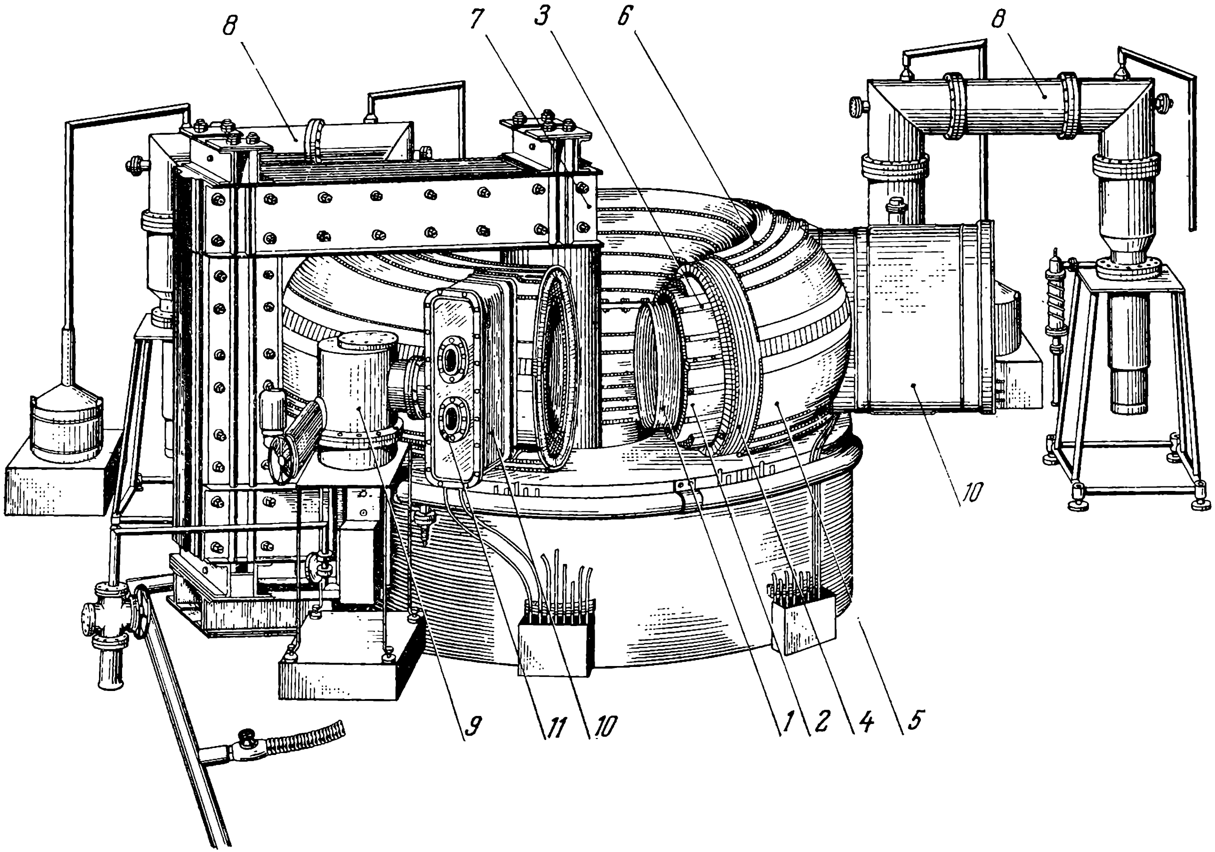

*1:* liner

*2:* vacuum casing

*3:* tube for water-cooling the casing

*4:* longitudinal field coil

*5:* metallic casing

*6:* primary winding of the transformer

*7:* iron yoke

*8, 9:* pumps for evacuating the discharge tube and the gap between the liner and the outer casing of the chamber

*10:* pumping port

*11:* apertures for insertion of diagnostic instruments

FIG. 69. Large toroidal pinch apparatus with a continuous metallic liner

of the pinch also requires a continuous, conducting envelope which can at the same time serve as a vacuum chamber which must be evacuated separately. When the metallic sections have a large enough wall-thickness, the longitudinal magnetic flux within them is constant during the discharge. This version is used, therefore, in investigations of the 'paramagnetic' pinch régime.

Figure 69 is a diagram of a device with a continuous liner (including the basic elements of the vacuum system). For simplicity the electrical supply system and discharge circuit are not shown.

The toroidal gas column acts as the secondary winding of a transformer, so that the gas current is generated by induction. In all the experimental devices which have been built so far, the current in the primary winding is supplied from a large capacitor bank. In the simplest design, the primary winding is the single turn formed by the metallic shell surrounding the discharge chamber (Fig. 70).† However, such a system is suitable only for producing discharges with a short duration. If one wishes to study the properties of discharges having a duration of the order of one millisecond or more, the ratio of secondary to primary turns must be lowered by increasing the number of turns in the primary winding; the reduction of the turns-ratio from 1:1 to values such as 1:5 or 1:10 also provides a better utilisation of existing capacitor banks (by reducing the impedance of the primary circuit relative to the secondary).

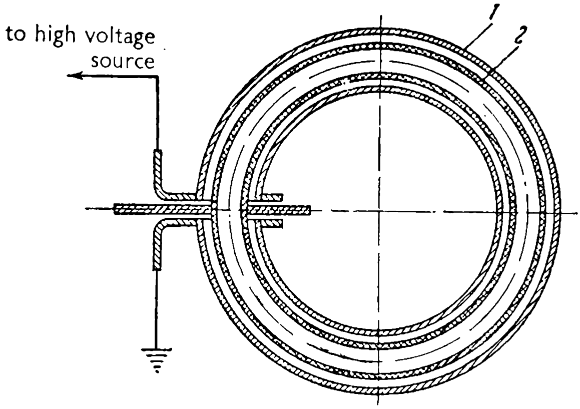

FIG. 70. The simplest original design of the transformer. 1, Metallic shell acting as the primary winding of the transformer; 2, discharge chamber

The design of the assembly depends primarily on whether or not an iron core is used to generate the changing magnetic flux. In devices without an iron core, the coils of the primary winding are placed next to the surface of the discharge chamber in order to improve the coupling. The coupling coefficient between the primary winding and the gas column in such a system can be increased to 0·6–0·65 (i.e. the gas current is up to 0·65 of the total primary ampere-turns). One of the disadvantages of systems without an iron transformer is the presence of excessive stray magnetic fields from the primary windings. These stray fields partially penetrate into the discharge chamber, distorting the magnetic field produced by gas currents and the stabilising windings. Consequently, the magnetic thermal insulation of the plasma may deteriorate considerably and, in addition, the experimental conditions are ill-defined.

---

† Experimental investigations of high-current toroidal pinch discharges were first described by Cousins and Ware in 1951.

An effective means of preventing stray fields is the use of metal screens which are placed on the surface of the discharge chamber. One of these screens serves as the outer metallic casing whose main function is to stabilise the discharge by means of image currents. However, this casing perforce contains insulating gaps and is insufficient for a complete elemination of the stray fields, particularly at the feed points. Additional screens are therefore necessary.

With an iron-cored transformer, the coupling coefficient between the primary winding and the secondary gas column can be brought very close to unity, and the stray fields from the primary winding itself can be negligible when the operating conditions are 'properly' selected. 'Proper' conditions in this case include the requirement that the ferromagnetism of the core must not be saturated, i.e. the value of the induction field during the discharge cycle must remain substantially below the saturation value $B_{\text{max}}$ available in the given type of iron.

In view of these advantages, the use of iron cores is preferable for large experimental devices. It should be kept in mind, however, that an iron core is advantageous only when its cross-section is compatible with the required discharge conditions; that is to say, in order to achieve particular discharge conditions it is necessary that, over a time interval $t$ (for example from the start of the discharge to the time when the current drops to zero), the mean electric field $\bar{E}$ in the plasma is maintained at some required value. According to the law of induction

$$2\pi R\bar{E}t = \pi R_{\text{m}}^2(B_1 - B_0)/c. \qquad \ldots\ldots\ldots(6.3)$$

Here $R$ is the major radius of the plasma ring, $\pi R_{\text{m}}^2$ is the cross-section of the core (Fig. 71) and the quantities $B_1$ and $B_0$ designate the induction in the core at the initial and final time. If the induction in the iron core is zero initially, it follows from equation (*6.3*) that the condition

$$R_{\text{m}}^2/R > 2c\bar{E}t/B_{\text{max}} \qquad \ldots\ldots\ldots(6.4)$$

must be satisfied. For example, if we take $B_{\text{max}} = 1{\cdot}5\times10^4$ gauss, $t = 2\times10^{-3}$ sec and $\bar{E} = 3\times10^{-3}$ (i.e. $\approx 1$ V/cm), we obtain from (*6.4*), $R_{\text{m}}^2 > 24R$. On the other hand, it follows from Fig. 71 that $R_{\text{m}} < R - b$, where $b$ is the minor radius of the chamber. If $b$ is taken to be 30 cm, the minimum value of $R$ for which both of these inequalities can be satisfied is 72 cm.

The condition determining the minimum geometrical dimensions of the chamber is less stringent if the magnetic polarity of the core is reversed during the discharge. Let us assume that initially the magnetic induction in the iron is $-B_{\text{max}}$. This induction is produced by direct current flowing from a D.C. generator or a rectifier through a supplementary winding on the transformer. If it is assumed that during the time $t$, the discharge of the main capacitor bank through the primary winding changes the induction from $-B_{\text{max}}$ to $+B_{\text{max}}$, then in the condition (*6.4*) which determines the ratio $R_{\text{m}}^2/R$, the right-hand side is reduced by a factor of two. This leads to a corresponding reduction of the values of $R_{\text{m}}$ and $R$ for a given required $\bar{E}t$.

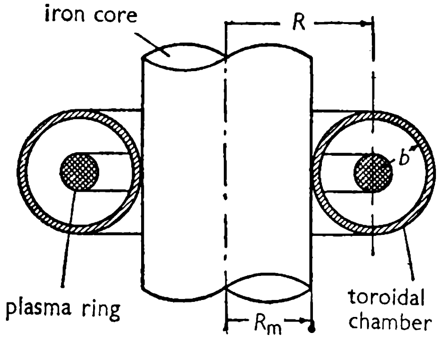

FIG. 71. Outline of toroidal chamber and iron core

As an example of an efficiently designed system with an iron core, we can take the arrangement of the Zeta assembly. Figure 72 shows the structure of the transformer used in this device. The transformer consists of two separate ring-shaped cores which interlink the toroidal discharge chamber. The cores are made up of ring sections 10 cm wide, with an outer diameter of about 3 m and an inner diameter of 1·5 m. Each section consists of a thin ribbon of transformer steel which is coiled like a tightly compressed clock spring. The primary coils are uniformly distributed over the surface of each core. By interconnecting individual sections of these windings it is possible to change the turns-ratio from 1:3 to 1:27. In order to obtain the maximum possible change in the magnetic induction, the cores are biased by direct current from a rectifier. The biasing circuit is protected from the high voltage arising during the main capacitor discharge by a choke in the biasing circuit.

In the supply system of Zeta, an additional circuit is provided to extend the time over which magnetic energy is stored in the secondary circuit, thereby prolonging the current pulse in the discharge chamber. This electrical circuit (a 'clamp' circuit) consists of low-resistance ignitrons connected as a shunt across the main capacitor bank. The ignitrons are ignited at the instant when the capacitor potential goes through zero and they thus prevent the capacitors from charging up in the reverse direction and stopping the gas currents. Obviously the secondary (discharge) circuit is effectively shorted at the same time. The subsequent decay of the current in the plasma is determined by the inductance and resistance of the gas column and the short-circuited primary. As a result, the gas current drops much more slowly than in the case when the primary is not shorted and the capacitor potential reverses.

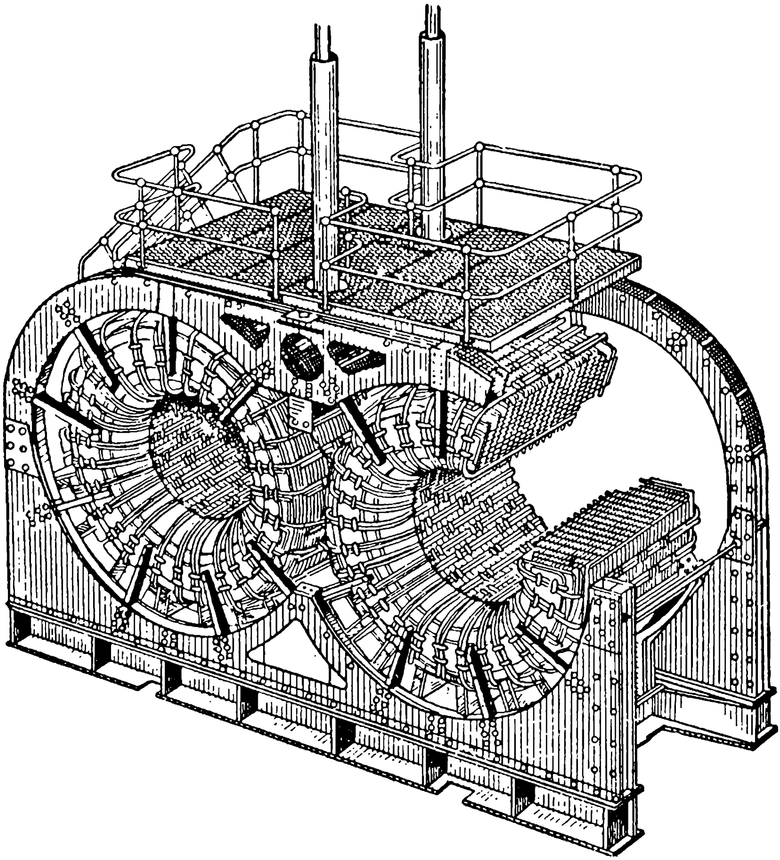

FIG. 72. Structure of the transformer of the Zeta toroidal pinch assembly

To initiate the discharge, the neutral gas in the chamber is often pre-ionised by a high-frequency discharge in the chamber. There are many methods of coupling the high-frequency power to the chamber, and we shall not discuss them here. When the power is relatively small, the RF discharge produces a high enough initial ionisation so that, when the voltage from the main capacitor bank is applied, the necessary initial conditions exist for the formation of a pinch with a large and fast-rising current. The use of high-frequency pre-ionisation lowers the minimum pressure for which a pinch will form, which is of the order of $10^{-4}$ Torr in large-bore installations filled with hydrogen.

We can imagine other methods of producing a considerable initial degree of ionisation to facilitate the breakdown. For instance, if an electron beam is directed round the torus near the surface of the chamber, then, in the presence of a longitudinal field, the electrons will move along the chamber and at the same time will be displaced towards the opposite wall (due to the drift in the non-uniform field). Such a helical electron beam facilitates the gas breakdown by its existence alone, since the beam itself constitutes an initial concentration of charged particles in the chamber. In addition, it should be noted that as a result of the ionisation of the gas along this beam, the total number of charged particles in the chamber may be increased by an order of magnitude.

§ **6.3** The experimental techniques for studying quasi-stationary discharges are far from perfect, both in the variety of methods employed and in the accuracy of the results which can be obtained by different measurements. However, this unsatisfactory state of affairs is partly explained if we take into account the specific properties of the object studied—the plasma—for which it is very difficult to obtain reliable and exact knowledge of all its parameters even in the best of circumstances. Getting a step ahead of ourselves, we should note that these high-current discharges produce plasmas which show very little justification for the term 'quasi-stationary'. At any rate, a spiral of cigarette smoke in air is as much deserving of such a name. In a pinch, all the basic physical parameters—density, pressure, temperature, current density, electrical conductivity—vary over very wide ranges from point to point and, for a given element of volume, from one instant of time to another. In view of the marked inhomogenity of the plasma and the very rapid variation in its local properties, most of the experimental methods used at present provide only very rough average values of the measurable characteristics of the plasma.

There is one other specific factor which considerably complicates the experimental studies of plasma properties in these discharges. It lies in the fact that in trying to produce as pure a discharge as possible, we select a design of the whole assembly such that the plasma column is surrounded on all sides by a multilayer metallic casing. It is very difficult to reach the plasma with any diagnostic instrumentation through the hermetic casing, parts of which are also heated to a high temperature. None the less, the existing and newly developed diagnostic methods used to investigate 'quasi-stationary' discharges provide, at least in principle, much more complete information on the plasma state than is the case for powerful discharges of very short duration.

The experimental techniques employed at the present time make it possible to study the shape of the plasma pinch, to perform measurements of the electric and magnetic characteristics of the discharge (voltage, current and the spatial distribution of the magnetic field), to determine the mean value of the charged particle density, to study the character of the plasma radiation over a wide range of wavelengths and to measure the energy loss by radiation. The methods of determining the current, voltage and the distribution of the magnetic field in pinches were described in the preceding chapter. They need no reviewing and no substantial change when used to investigate slow discharges.

In sustained discharges, the resistive voltage drop in the plasma, $\Omega J$ (where $\Omega$ is the discharge resistance), is comparable with the inductive drop $c d(LJ)/dt$. Therefore, it is possible to estimate such an important quantity as the plasma resistance from measurements of $V$, $J$ and $L$ as functions of time. However, there is no special need for an accurate determination of the inductance $L$ since it can be calculated from the simple formula

$$L = 4\pi R \ln (b/a)$$

which depends only weakly on one geometrical parameter associated with the pinch—its radius $a$—the determination of which may, however, give rise to some doubts.

Knowing the resistance $\Omega$, one can find the plasma conductivity $\bar{\sigma}$ averaged over the cross-section of the pinch. It is evident that

$$\bar{\sigma} = 2R/\Omega a^2.$$

With all the qualifications regarding the accuracy with which $\bar{\sigma}$ can be determined and the uncertainty which is inevitably introduced into the interpretation of this quantity due to the averaging, the measurement of the plasma conductivity has some significance. The electrical conductivity of a plasma may be correlated with the electron temperature, and therefore the data obtained in measurements of $\bar{\sigma}$ are an indication of the success or otherwise of the attempts to heat a current-carrying plasma.

The average value of $T_e$ is determined from $\bar{\sigma}$ by the use of equation (*3.10*). It must also be kept in mind that this equation is valid only for a completely ionised hydrogen plasma which contains no impurities. If these conditions are not met, low values of $T_e$ are obtained from the conductivity data. If, for example, the plasma is contaminated by 10% of quadruply-charged ions, equation (*3.10*) yields a value of $T_e$ which is 30% too low. If the relative concentration of impurities with charge $Ze$ are known, it is not difficult to make the necessary corrections in the determination of $T_e$. In this case, the calculation requires the use of the following more accurate formula:

$$\bar{\sigma} = 0{\cdot}9 \times 10^7 T_e^{\frac{3}{2}} \sum \alpha_i Z_i / \sum \alpha_i Z_i^2, \qquad \text{.........}(6.5)$$

where $\alpha_i$ is the relative concentration of ions with charge $Z_i e$.

In discussing the determination of electron temperature from the electrical conductivity, we should not overlook one fact which may, under certain conditions, considerably hamper the interpretation of the results obtained in this way: the formula relating $\bar{\sigma}$ and $T_e$ is, strictly speaking, valid only for a quasi-stationary plasma. All the existing experimental information shows that in real high-current pinches, a certain degree of non-stationary behaviour is always observed. It is manifested by small, separate elements of plasma which are in a state of disordered (or, at any rate, not fully ordered) macroscopic motion at rather high velocities. Fluctuating electric fields arise in the plasma as a result of these motions. The scattering of electrons by these fields may play a part similar to that of collisions between electrons and ions, and lead to a reduction in the electron mobility in the direction of the main applied field. Thus, owing to transient motions in the plasma, its electrical conductivity may decrease and no longer be related to the electron temperature by formulae which take into account only the elementary Coulomb collisions. We shall return to this question later.

A direct method of determining the electron density in the plasma is suggested by the formula for the dielectric constant derived in Chapter III. According to equation (*3.14*), the dielectric constant is zero when the following relation between $\lambda$ and $n$ is satisfied:

$$\lambda = 3{\cdot}3\times 10^6/\sqrt{n} \quad \text{(cm)}. \qquad \ldots\ldots\ldots(6.6)$$

This relation determines the limiting wavelength $\lambda$ of radiation which can pass through a plasma with an electron number density of $n$. Electromagnetic radiation with longer wavelength will be reflected at the plasma boundary and cannot traverse the plasma.

Because of the availability of a large number of high-frequency signal generators emitting radiation in the millimetre and centimetre wavelength range, one could determine the plasma density in the various stages of the pinch development. At the present time, we must be content with considerably more modest results, because no single laboratory actually has a large selection of generators producing a variety of wavelengths in the desired range. By using one generator it is possible to determine whether $n$ is larger or smaller than a certain value, but an accurate determination the electron number density is impossible.

Figure 73 shows an experimental arrangement where a directed beam of electromagnetic radiation with a low-frequency modulation is passed through the plasma in a pinch discharge and falls on a receiver whose output is connected to an oscilloscope. At the time when the electron number density exceeds the value of $n$ (given by equation (*6.6*)) for the given generator wavelength, the low-frequency signal on the oscilloscope disappears. It follows from the experimental arrangement shown in the diagram that if the electron density is not uniform over the cross-section, the disappearance of the signal is determined by the maximum value of $n$ along the path of the electromagnetic waves. The upper limit of the density which can be measured in this way is determined by available millimetre wave generators. At the present time, this limit is about $2 \times 10^{14}\ \mathrm{cm}^{-3}$ ($\lambda = 2$ mm).

If the diameter of the plasma column is large enough, then by moving the source and receiver so that the electromagnetic radiation passes through the plasma at various distances from the pinch axis, one can also find, in principle, the radial density distribution. However, such experiments have not yet been performed with microwaves.

The measurement of $n$, based on the determination of the cut-off wavelength, is only the first step in the use of radio-frequency plasma diagnostics. A much better method of measuring the density employs a radio-interferometer to determine the phase shift between microwave beams which propagate along two different paths, one of which traverses the plasma. A diagram of a radio-interferometer for measuring plasma densities is shown in Fig. 74. The radiation generated by a klystron is split in two and propagated along two parallel paths. The plasma index of refraction is a function of the frequency (see equation (*3.14*)), and the phase shift is proportional to the length of the path travelled in the plasma and to the difference between the plasma index of refraction and unity (the refractivity). After passing through the plasma, the two waves are combined and interfere. The amplitude of the resulting signal depends on the phase shift between the two beams, and hence on the plasma density.

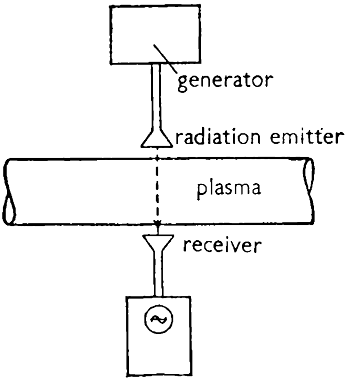

FIG. 73

Diagram of an experiment for estimating the electron density by the passage of microwaves through a plasma

Although the basic method is very simple, its practical application entails the use of rather complex electronic apparatus. We shall not consider here different versions of the technique nor the methods of observing the interference effects since they are constantly being improved and rapidly supersede one another.†

Amongst recently proposed methods of probing a plasma with microwaves, we should mention radiolocation of the motion of the plasma boundary. This technique was developed at the Leningrad Institute of Physics and Technology and was used to study the motion of the plasma in the Alpha toroidal pinch. A radio signal with a wavelength $\lambda$ penetrates into the plasma and is reflected from the regions where the electron density exceeds $n = 1{\cdot}12 \times 10^{13}/\lambda^2$. By analysing the amplitude and the form of the reflected signals, we can estimate the position of the reflecting boundary and describe its motion during the discharge.

---

† A particularly convenient extension of this kind of measurement has recently been described by Ashby and Jephcott, Measurement of plasma density using a gas laser as an infra-red interferometer, *Applied Physics Letters*, **3**, 13, 1963.

Spectroscopic methods have found widespread applications in studies of quasi-stationary discharges. The apparatus used includes ordinary spectrographs for the visible region (7000–4000 Å), spectrographs with quartz optics for the near ultraviolet (from 4000 Å to 2000 Å) and vacuum spectrographs with diffraction gratings for studying the spectrum emitted by a plasma in the far ultraviolet and soft X-ray regions (from 2000 Å to 20 Å). By the use of high-speed shutters, it is possible to obtain spectrograms with a short exposure-time at selected phases of the discharge. For this purpose, spectral intensities are also measured photoelectrically and recorded on an oscilloscope. Prism spectrographs will detect the plasma radiation which passes through a glass or quartz window in the wall of the discharge tube. Far ultraviolet and soft X-ray measurements can be made only if one eliminates windows between the spectrograph and the plasma, because they absorb this radiation.

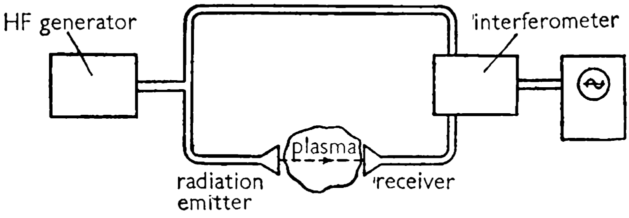

FIG. 74. Diagram of a radio-interferometer for measuring electron number density

Using the spectrographic data, one can first of all determine the composition of the plasma and measure the relative concentration of the various impurities which are invariably present. In principle, the technique for determining the concentration of impurities is very simple. It is based on the measurement of impurity line intensities as a function of known added quantities of the impurity. Unfortunately, however, such direct determinations of the impurity content have not been carried out systematically to date; instead, only the relative abundance of various impurities has been estimated from the measurement of the relative intensity of the lines belonging to different elements. This procedure always introduces great uncertainty into the results.

Spectroscopic measurements provide valuable information on the velocity of the plasma ions and may also serve to determine the electron temperature. The spectroscopic method of estimating the electron temperature is based on a determination of the relative intensities of the lines emitted by atoms and ions in different excited states. Use is made of the fact that the intensity of a spectral line is proportional to the population of the quantum level from which the optical transition originates, so that the expression for the relative intensity of two lines contains the factor $\exp(-\Delta E/kT_e)$, where $\Delta E$ is the energy difference between the two initial excited levels.† Actually, the interpretation of the results obtained from measurements of relative intensities is complicated by the fact that the optical transition rate is determined not only by the above exponential factor; it also depends on the wave functions of the initial and final states, which determine the transition probabilities. Unfortunately, the transition probabilities are not known in the majority of cases. If runaway electrons exist in the plasma, the determination of $T_e$ from spectroscopic data is complicated still more, since the exponential dependence of the intensity of the spectral lines on $\Delta E/kT_e$ is valid only if the electron velocity distribution is Maxwellian. For these reasons, all the spectroscopic measurements of $T_e$ in pinches have so far, strictly speaking, provided only an order-of-magnitude estimate.‡

As pointed out in the preceding chapter, the widths of spectral lines can be a very important index of the motion of ions and atoms in a plasma. The interpretation of line width measurements should be approached with a good deal of caution. This applies particularly to attempts at deriving the ion temperature from the measured widths. Many such attempts have ended in failure because there are non-equilibrium regions in the plasma which are associated with local high-velocity mass-motion of the plasma. Owing to the rapid changes in the direction and velocity of such mass motion, the spectral lines are broadened. The assertion that the line broadening is caused by the thermal motion and not by mass motion is possible only in the case where thorough control experiments show that, first, the temperatures determined from the broadening of the lines emitted by ions with different masses are identical; second, that the line shapes do not depend on the direction of observation; and third, the line shapes must be Gaussian as predicted by the theory of the thermal Doppler effect.

Spectroscopic analysis may also be used to determine what portion of the radiation emitted by the plasma lies in the visible part of the spectrum, in the near and far ultraviolet, and in the soft X-ray region. These losses can be determined from absolute measurements of line intensities and the continuum. The simplest method, although a very rough one, of measuring the radiation loss is based on the use of phosphors which convert a major part of the far ultraviolet radiation into visible light. Let us suppose that a thin layer of a luminescent substance is placed (in a vacuum) in the path of the radiation emerging through an aperture in the chamber wall. The phosphor absorbs all the ultraviolet rays striking it and converts part of the absorbed energy into visible radiation whose intensity can be measured with an ordinary photocell or from the exposure of a photographic film placed behind the luminescent screen. For absolute measurements of the radiation loss by this method, it is necessary to know the spectral energy distribution of the radiation and the conversion efficiency of the luminescent material.

---

† The exponential factor $\exp(-\Delta E/kT_e)$ arises from Boltzmann statistics in a plasma where the excited level population densities are in thermodynamic equilibrium. Such equilibrium does not usually occur in sustained discharges, because the electron excitation rates are much slower than radiative decay rates. However, in this latter case, the same exponential factor usually occurs; it arises from the integration of the electron-collision excitation cross-section over the Maxwellian distribution of free electrons.

‡ Use of this method in the ultra-violet region considerably improves the precision. See L. Heroux, A spectroscopic method of measuring electron temperature in plasmas, *Nature*, **198**, 1291, 1963.

Some interesting possibilities for the study of the properties of a dense plasma in quasi-stationary discharges are opened up in connection with the application of a new spectroscopic method, developed in England by Harding and co-workers. It involves the measurement of plasma radiation in the far infra-red range adjoining the radio-frequency range. The plasma radiation at wavelengths of the order of 0·1–1 mm consists of the long-wavelength portion of the continuous spectrum produced by the bremsstrahlung of electrons in the Coulomb field of the ions. The expression for the spectral density of this radiation is given by equation (*1.9*). When $h\nu \ll kT_e$, the factor $\Phi(h\nu/kT_e)$ is equal to $\frac{\sqrt{3}}{\pi}\ln\left(2{\cdot}2\frac{kT}{h\nu}\right)$. If the plasma has a high enough density, it is necessary to consider the self-absorption of the radiation by the plasma. In the long-wavelength region of the spectrum, the linear absorption coefficient $\mu$ can be determined from the formula

$$\mu \simeq 10^{-2} n_e n_i Z^2 \ln(2{\cdot}2kT_e/h\nu)/T_e^{3/2}\nu^2.$$

At very large wavelengths, where the product of $\mu$ and the thickness of the radiating layer becomes greater than unity, the radiation intensity of the plasma should approach that of a black body at the temperature $T_e$ as determined by the Rayleigh-Jeans law. In principle, the measurement of the spectral radiation density in such a wavelength range may provide a direct method for determining the electron temperature. If $T_e$ is known, it is also possible to find $n_e$ from measurements of the radiation intensity in the wavelength region where the absorption may be neglected. Let us take a specific example. In a deuterium plasma at a temperature of 10 eV and a number density of $10^{15}$ cm$^{-3}$, the absorption coefficient for $\lambda = 1$ mm is about 0·03 cm$^{-1}$. Hence at this wavelength, a plasma which has a diameter of several tens of centimetres radiates almost as a black body. On the other hand, with these densities and temperatures, the absorption can be practically neglected at a wavelength of 0·1 mm; and this means that the radiation intensity per unit volume is given by equation (*1.9*) with the above indicated value of $\Phi(h\nu/kT_e)$. Harding and co-workers employed photoconducting SbIn placed in a strong magnetic field and cooled by liquid helium as a sensitive infra-red detector with a short time-constant. They were the first to use this technique successfully for the determination of the basic constants of a plasma in quasi-stationary discharges at $n_e \simeq 10^{15}$ cm$^{-3}$. For much smaller electron densities, the separate determination of $n_e$ and $T_e$ is difficult, due to the small value of $\mu$ over the entire spectral range under consideration. When $n_e \leqslant 10^{14}$ cm$^{-3}$ this method is also difficult to use in the measurement of densities because of the low radiation intensity.

The measurement of the energy flux at the wall of the chamber as a function of time is of great interest. In order to perform such measurements, it is necessary to have a detector with a broad spectral response as well as a short time-constant. Andrianov has proposed that the thermal radiation from a thin foil heated by the plasma radiation be used as such a detector. The radiation from the foil may be measured with a photomultiplier. With a short pulse of radiation, the temperature change in the thin foil is proportional to the amount of energy absorbed by its surface, since the losses due to thermal conductivity may be neglected. The change in the intensity of the thermal radiation from the foil is proportional to the temperature increment $\Delta T$ and depends very strongly on the absolute temperature of the foil. For this reason, the sensitivity of such a device can be increased by two or three orders of magnitude if the foil is heated by an auxiliary electric current. With an initial foil temperature in the 300–600° K range, the sensitivity varies approximately as $T_0^7$. A radiation detector of this type was constructed and studied by Prokhorov, who used a platinum foil 6$\mu$ thick, heated to 800° C. To achieve a time-resolution of the order of 0·5 $\mu$sec, the smallest energy which can be measured is $3 \times 10^{-3}$ J/cm$^2$. This sensitivity is fully adequate for studying the energy balance of sustained high-current discharges, since in this case the energy flux reaching the wall is measured in hundreds and thousands of watts per square centimetre.

A substantial part of the energy exchanged between the plasma and the walls may be due to the flux of fast neutral atoms which are formed in the outer layers of the pinch as a result of charge exchange between slow atoms dislodged from the walls and fast ions in the plasma. The energy spectrum of these neutral atoms is directly related to the energy distribution of the ions. Therefore, it is necessary to develop methods for measuring the flux, energy spectrum and masses of neutral atoms leaving the plasma. One such method has been worked out at the Leningrad Institute of Physics and Technology by Afrosimov, Gladkovskii, Gordeev, Kalinkevich and Fedorenko, and used successfully with the Alpha device. A diagram of their apparatus is shown in Fig. 75. Charged particles are separated from the flux of atoms leaving the plasma by passing the particle beam through deflector plates $C_1$. The neutral beam enters the ionising chamber $K$, which is filled with nitrogen at a pressure of $10^{-5}$—$10^{-4}$ Torr. Some of the fast atoms which pass through the chamber are ionised by collisions with nitrogen molecules. The plates $C_2$ deflect the ions to the target $M$. They knock out secondary electrons which are accelerated to 10–20 keV and detected by a plastic scintillation-counter with a photomultiplier. Neutral atoms with energies of from 300 eV to several tens of kiloelectron volts can be detected with such an instrument.

§ **6.4** Turning now to a presentation of the experimental data concerning the behaviour of the plasma in slow discharges, we shall first of all consider the results of experiments with systems in which a longitudinal stabilising field is trapped in the contracting plasma. Studies of this type were first carried out by the British physicists who built Zeta and a similar but somewhat smaller device, Sceptre. Later, a number of interesting results were also obtained in U.S.S.R. with the Alpha device, modelled after Zeta.

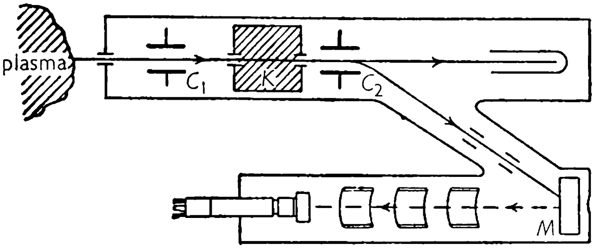

FIG. 75. Instrument for measuring the flux of neutral atoms to the walls of Alpha

In Zeta, the minor diameter of the discharge tube is 100 cm, and the average circumference is about 1200 cm. The main measurements on Zeta reported in 1958 were conducted with automatic controls so that discharge pulses could be repeated every 12 sec. The maximum potential at the primary of the transformer varied approximately between 8 and 18 kV. For a turns-ratio of 1:9, the corresponding value of the e.m.f. around the discharge chamber was 1–2 kV. The peak gas current $J_m$, for given values of the initial pressure $p_0$ and initial strength of the stabilising field $H_0$, was proportional to the electric field induced in the chamber. The dependence of $J_m$ on $p_0$ was very weak. As $p_0$ rises, the current increases a little at first, then remains practically constant.

In the experiments with Zeta described at the Geneva Conference of 1958, $J_m$ varied between 70 and 200 kA. The investigations were devoted mainly to discharges in deuterium at an initial gas pressure of $10^{-4}$ to $10^{-3}$ Torr. The stabilising field $H_0$ ranged from 100 to 350 Oe in different experiments. The largest number of measurements were made with rather rigidly fixed parameters: $H_0 = 160$ Oe; $J_m$, 140 to 200 kA; deuterium pressure, about $1{\cdot}2 \times 10^{-4}$ Torr. To attenuate the electrical overvoltages, 5% nitrogen was usually added to the deuterium (an empirically found medicine).

Typical oscillograms of the gas current and voltage around the chamber are shown in Plate X for discharges in deuterium. It should be remembered that they were obtained with an electrical system whose characteristic feature is the automatic shorting (clamping) of the transformer primary when the capacitor potential goes through zero. Because of this feature the gas current does not alternate. After the primary voltage falls to zero, the current fall is reduced by the electromotive force due to self-induction. If the inductance and resistance of the plasma remained constant, the current would decrease exponentially after clamping. Actually, these quantities vary with time and the current decreases in a more complicated fashion.

The first feature which strikes the eye from an inspection of the oscillograms is their complete disagreement with the concept that the discharge has a 'quasi-stationary' character. Although the time-behaviour of the current might still be called relatively smooth (by stretching a point), the voltage oscillogram is typical of sharply transient processes. The amplitude of the high-frequency overvoltages is comparable with the mean voltage around the discharge chamber. The frequency characterising these overvoltages lies in the region $10^4$–$10^6$ cps.

The instability of the plasma is observed indirectly from high-speed streak photographs of the discharge. Plate XI shows such photographs of the pinch, taken through a narrow slit perpendicular to the tube axis. The upper picture was made in visible light, the lower in the near ultraviolet. The bright horizontal lines show the position of the walls of the discharge chamber. We see that the bright transverse flashes ('barring'), succeeding one another at intervals of several tens of microseconds, fill the chamber out to its walls.

As the authors of the Zeta papers have pointed out, in many cases a time correlation is observed between the optical flashes and the high-frequency transients in the voltage oscillograms. By increasing the time-constant of the measuring gear, one can filter out the high-frequency oscillations and obtain smooth voltage oscillograms to estimate the mean resistance of the plasma pinch.

Assuming that the discharge inductance is not changing at peak current, so that $d(LJ)/dt = 0$, it is possible to obtain an estimate of the resistance at peak current from the formula $V = J_m\Omega$. In the standard experimental conditions ($p_0 = 1 \times 10^{-4}$ Torr, $H_0 = 160$ Oe), the discharge resistance determined in this fashion varies between $3 \times 10^{-3}$ and $3{\cdot}8 \times 10^{-3}$ ohm.

To find the plasma conductivity from $\Omega$, one must know the cross-sectional area of the plasma through which the current flows. This area, as well as the radial distribution of the current, may be determined by means of magnetic probes. Under standard conditions, the radius of the discharge is approximately 15–20 cm (if the value of the radius is taken to be the distance from the pinch axis to the point at which the self-magnetic field reaches a maximum). Within this region, the current is evenly distributed and no signs of the skin-effect are to be seen. The mean conductivity determined from $\Omega$ is $3\text{–}4 \times 10^{14}$ c.g.s. e.s.u.

Magnetic search coil measurements provide interesting and in some respects unexpected results. The main features of these measurements are as follows:

(1) In the initial stage the current flows over the entire cross-section of the chamber. The compression of the current-carrying channel begins 100–200 $\mu$sec after the breakdown, and ends when the current is a maximum.

(2) The current density $j_z$ has a maximum value near the axis of the pinch. The value of $j_z$ in this region exceeds the mean current density in the pinch by a factor of 1·5 to 2·5. Consequently, the longitudinal conductivity of the plasma near the axis is also considerably higher than the mean conductivity quoted earlier.

(3) The strength of the longitudinal field trapped in the pinch in the course of the compression rises continually. At the moment when the discharge current reaches a maximum, the value of $H_z$ at the pinch axis can be 12 to 15 times as great as the initial field $H_0$.

(4) $H_z$ decreases rapidly with distance from the axis, and it can become negative in the outer regions (i.e. the longitudinal field $H_z$ is reversed outside the pinch).

These experimental facts may be interpreted more or less satisfactorily from a qualitative point of view. The absence of any appreciable skin-effect is caused by the low conductivity. Indeed, the thickness of a current-carrying skin corresponding to the measured value of $\bar{\sigma}$ (indicated above) and to a current rise-time (from zero to a maximum) of $\approx 1$ msec is $\approx 20$ cm, i.e. it is comparable with the radius of the pinch. No freezing-in of the magnetic lines of force can be expected in such a poorly conducting plasma column. For this reason, the pinch, which contracts under the action of the electrodynamic forces, does not carry along the longitudinal lines of force. To the natural question—what in this case causes the increase in $H_z$ inside the pinch?—we can give the following answer: this experimental fact is explained by the presence of an anisotropic conductivity, which is related to pinch instabilities. In a helical magnetic field with components $H_\theta$ and $H_z$, the current flows along helical lines as a result of a strongly anisotropic conductivity. Thus the azimuthal component $j_\theta$ rises with the $z$-component of the current, $j_z$. This component produces a supplementary longitudinal field which adds to the initial field $H_0$.

However, there is one curious phenomenon—the appearance of a reversed longitudinal field near the inner wall of the toroidal chamber—which can be explained neither by the anisotropy of the conductivity nor by the trapping of the initial field. This reversed longitudinal field arises in cases where the initial longitudinal field is comparatively small and it can be expected that the pinch is at the limit of its stability against helical kinking. This phenomenon appears to be associated most of all with the appearance of helical perturbations of the pinch, during which the azimuthal field may be converted into a longitudinal one, i.e. the longitudinal current may 'generate', so to speak, an additional longitudinal field.

The magnetic probe measurements can be used, in principle, for the determination, or at least a rough evaluation, of the most interesting physical parameter characterising the properties of a plasma—the value of the pressure $p$. Disregarding the toroidal nature of the pinch, we can write the following relation for $p$:

$$-\frac{\partial p}{\partial r} = \frac{1}{c}(j_z H_\theta - j_\theta H_z) \qquad \dots\dots\dots(6.7)$$

which is a special case of the more general expression (*4.19*). Expressing the components of the current density in terms of $H_z$ and $H_\theta$, we obtain

$$-\frac{\partial p}{\partial r} = \frac{1}{4\pi}\left(\frac{H_\theta}{r}\frac{\partial}{\partial r}rH_\theta + H_z\frac{\partial}{\partial r}H_z\right). \qquad \dots\dots\dots(6.8)$$

The right-hand side of this equality contains only the quantities $H_z$ and $H_\theta$, which are measured directly in the experiments, and their derivatives with respect to the radial coordinate. When equation (*6.8*) and the integral relations resulting from it are used to process the experimental data obtained in studies with Zeta, it turns out that the kinetic pressure in the pinch is very small and plays an insignificant part in the establishment of an equilibrium between the forces which act on the plasma. This is partly expressed by the fact that the proportionality factor $\beta$ which relates the current with $T$ in equation (*4.52*) is small compared to unity. In the report of the British physicists on the operation of Zeta, it was pointed out that $\beta$ could not exceed $\frac{1}{3}$. It is probable, however, that even this modest estimate of an upper limit for $\beta$ is unnecessarily optimistic.

Thus, in the experiments considered, the self-magnetic compression force produced by the gas current is off-set by the pressure of the longitudinal field in the pinch, and only a very small part of this force balances the plasma pressure. In view of the small value of $p$, it follows from equation (*3.7*) that $j_z/j_\theta = H_z/H_\theta$. This means that the direction of the current follows the direction of the magnetic lines of force. Such a magnetic configuration may be termed force-free, since $\boldsymbol{j} \times \boldsymbol{H}$ is very small. A force-free field configuration corresponds to a very pronounced difference between the values of plasma conductivity in the directions parallel and normal to $\boldsymbol{H}$ ($\sigma_{\parallel} \gg \sigma_{\perp}$). Let us note that in such a magnetic configuration, the values of $H_z$ and $H_\theta$ under stationary conditions are uniquely determined by the value of the pinch current $J$ and the strength of the longitudinal field at the plasma boundary. When these values are given and the conditions are stationary, the entire topography of the fields can be found.

Since the plasma pressure in a paramagnetic pinch is small, its tem-

PLATE X

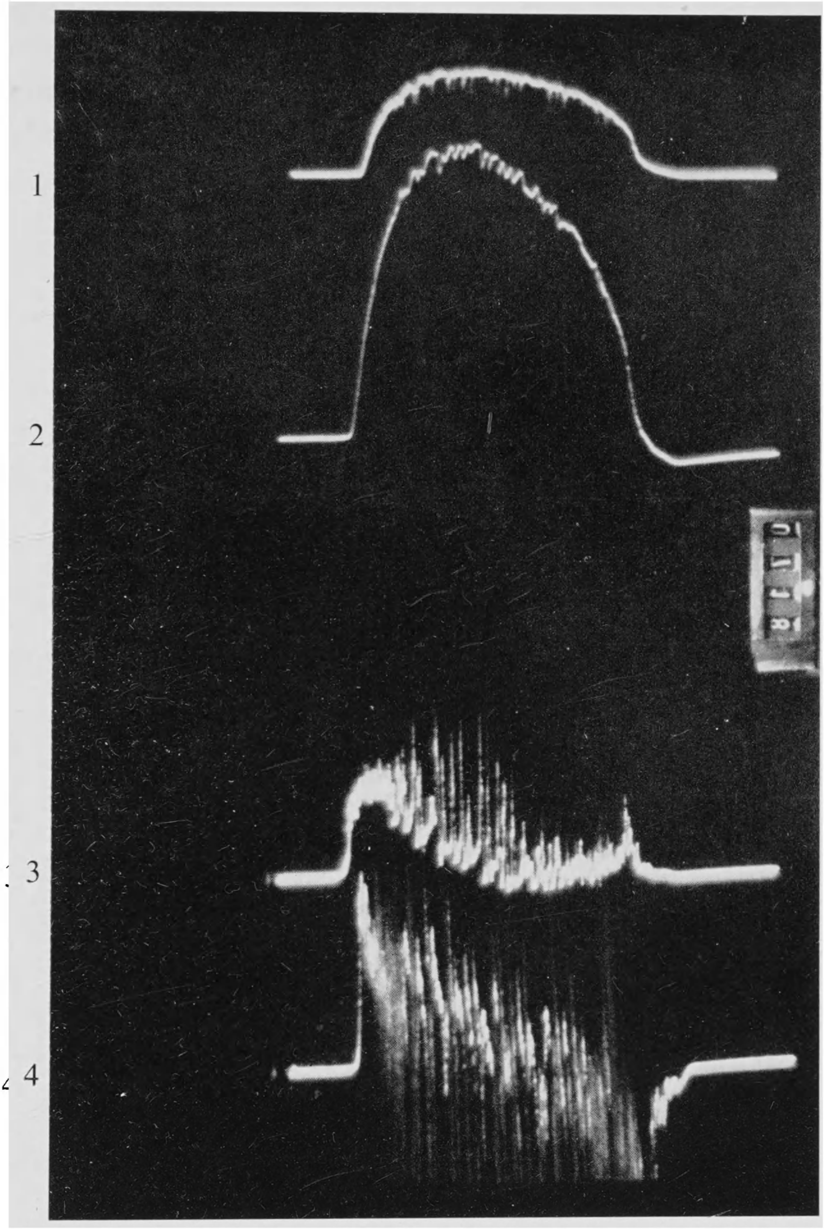

Oscillograms of a discharge in Zeta.

1, primary winding current; 2, secondary (discharge) current; 3, discharge voltage; 4, $dJ/dt$ of the discharge current. Sweep time, 5 msec.

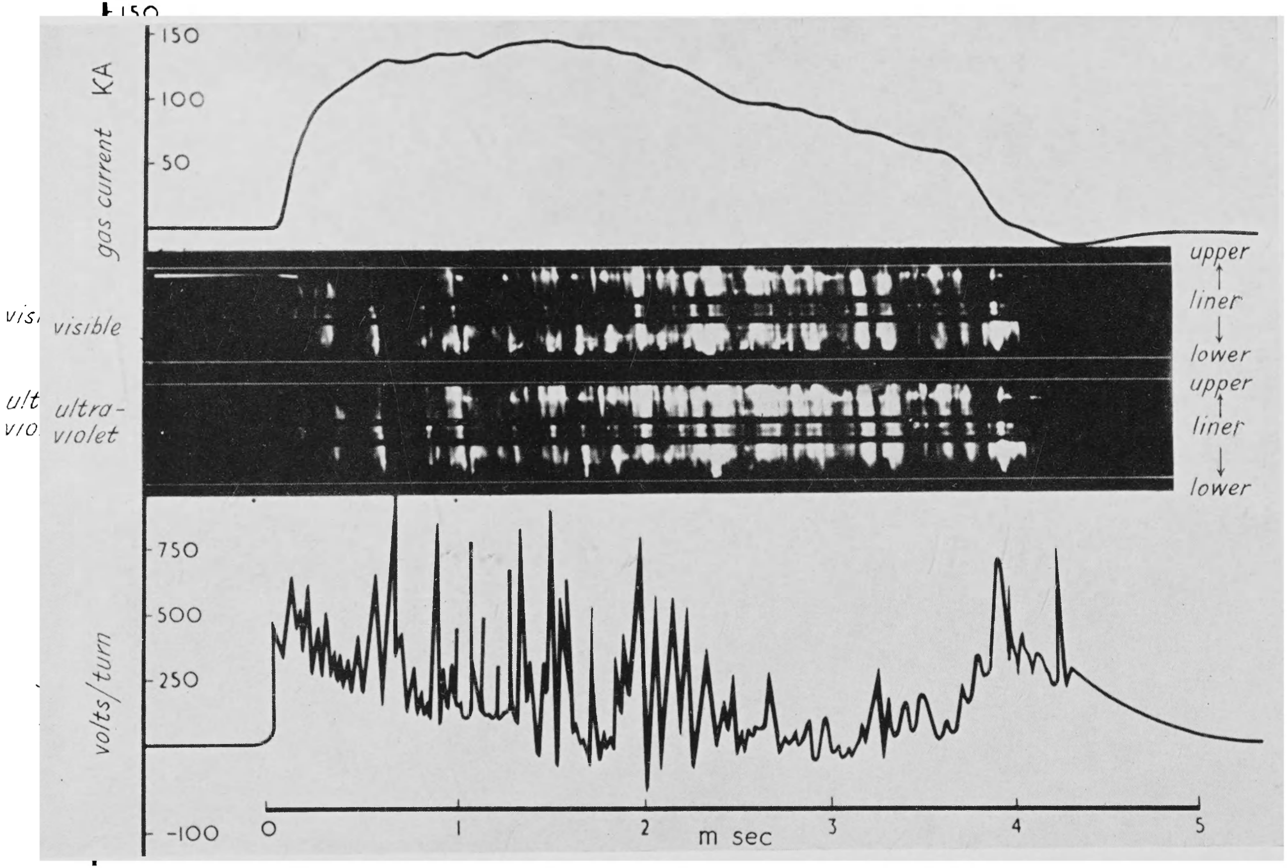

Time-resolved photograph of a large toroidal pinch, correlated in time with current (top) and voltage (bottom) oscillograms.

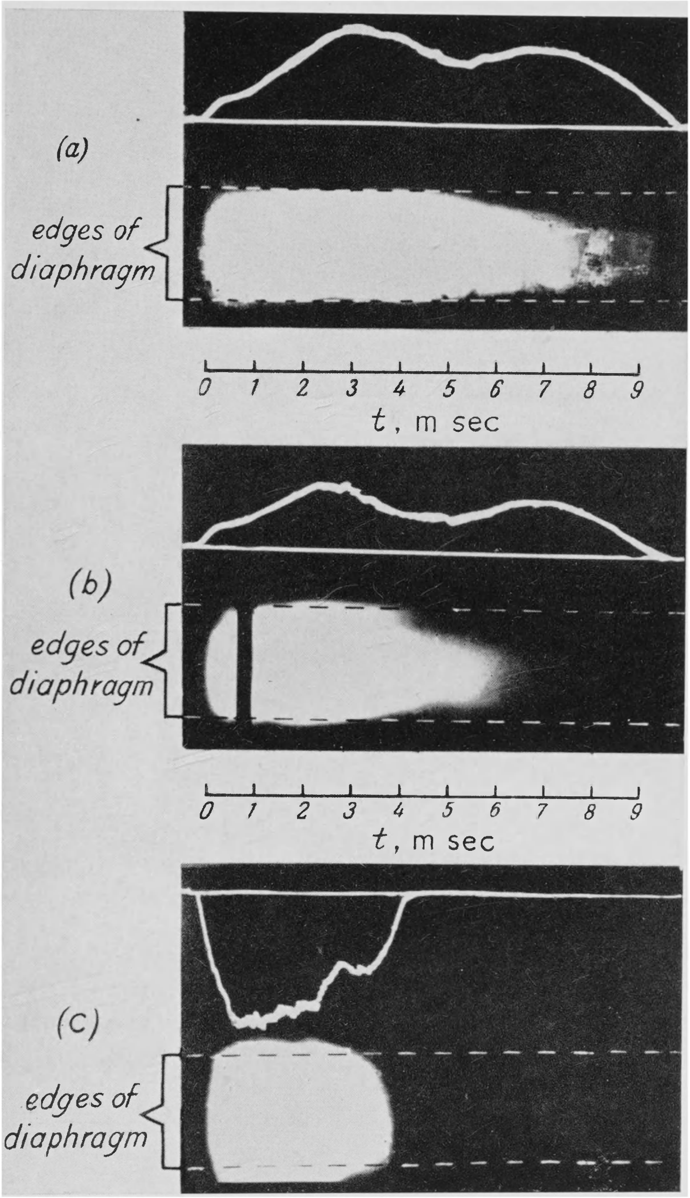

Time-resolved vacuum ultraviolet photographs of a toroidal discharge with a high longitudinal field strength.

(*a*) $E_0 = 0{\cdot}09$ V/cm, $p_0 = 5 \times 10^{-4}$ Torr $D_2$, $H_0 = 10$ kOe, $q = 4{\cdot}1$;
(*b*) $E_0 = 0{\cdot}09$ V/cm, $p_0 = 5 \times 10^{-4}$ Torr $D_2$, $H_0 = 6$ kOe, $q = 3{\cdot}5$;
(*c*) $E_0 = 0{\cdot}24$ V/cm, $p_0 = 5 \times 10^{-4}$ Torr $D_2$, $H_0 = 6$ kOe, $q = 1{\cdot}6$.

perature should not be high either. The electron temperature can be estimated first from the electrical conductivity data, and second from the results of spectroscopic measurements. Using equation (*6.5*) and considering that under stationary experimental conditions the 5% added nitrogen forms triply- or quadruply-charged ions, we find (disregarding other impurities) that $T_e$ averages 10–15 eV in the experiments described. Spectroscopic data indicate somewhat higher values of $T_e$.

The answer to the question of what ion temperature is actually attained in a paramagnetic pinch still remains unclear. In the determination of $T_i$, the only data available are the widths of spectral lines emitted by impurity ions. If it is assumed that the line widths depend only on the thermal motion of the ions, unexpectedly high values of the ion temperatures are obtained from the experimental data. It turns out, however, that these values for the temperature depend substantially on which spectral lines are used for analysis. From the first spectroscopic determinations of the ion temperature, carried out with Zeta, it was evident that the value of the temperature calculated from the width of one of the spectral lines of triply-charged nitrogen (N IV) is about half as large as that determined from the lines of quadruply-charged oxygen (O V).

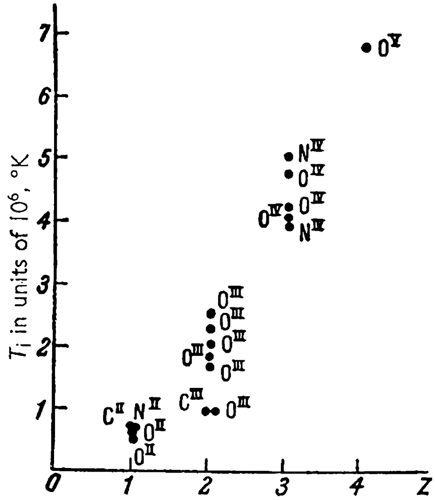

FIG. 76

Results of measurements of the 'temperature' of impurity ions in Alpha. The abscissa represents the charge of the ion

A detailed spectroscopic analysis of ion temperatures has been carried out by Zaidel' and co-workers in Leningrad with the Alpha device. They found that the dependence of ion temperature, determined from spectral line broadening, on the ionic charge has a very regular character. Figure 76 shows some results of the ion temperature measurements using lines of multiply-ionised carbon, nitrogen and oxygen. They were obtained from the line contours plotted from exposures lasting over the entire course of the discharge. Each point on the graph corresponds to a measurement of $T_i$ from specific lines of various ionic species. Data obtained from the deuterium line spectrum are not given in these graphs because neutral deuterium atoms are concentrated mainly in the outermost regions of the discharge, and a measurement of their temperature cannot provide a correct picture of the temperature of the deuterium ions in the plasma. Despite a rather appreciable scattering of the points pertaining to the different measurements, the general character of the regularity is expressed quite clearly. The larger $Z$, the higher is $T_i$.

However, new measurements of the spectral line widths of tracer ions performed on Zeta in 1961 lead to a rather different conclusion. It was found that if a comparison is made between the widths of different lines emitted by the plasma within the same short time interval, the values of the temperature $T_i$, determined at this time, do not depend on $Z$ and are a linear function of the ionic mass, i.e. $T_i = A + Bm_i$, where $A$ and $B$ may be considered constant for a fixed time interval. For moderately heavy ions (from deuterium to oxygen) the constant $A$ substantially exceeds $Bm_i$; which indicates a rapid equalisation of temperature between different ions. If this result, established at present on the basis of the measurement of a relatively small number of spectral lines, is widely confirmed, the experimental data given in Fig. 76 will have to be interpreted anew. Such an interpretation might be based on the assumption that $T_e$ is to some extent correlated with $T_i$ due to the fact that the heating of the electrons is partially caused by the transfer of energy from the ions, which acquire it from fluctuating electric fields associated with the instability. If this assumption is made, the rate of formation and excitation of highly charged ions is greatest (owing to the corresponding rise in $T_e$) at those times when the ion temperature is highest. In other words, this means that in Fig. 76 the cause is plotted along the ordinate, and the effect along the abscissa.

Spectroscopic methods make it possible to measure not only the widths but also the shifts of the line, and thus to determine the direction of any ordered ion motion. These measurements have shown that the mean ion velocity (averaged along the line of sight of the spectrograph) is many times smaller than the velocities of disordered motion from which the values of $T_i$ are calculated.

Leaving further discussion of results of the spectroscopic measurement of $T_i$ to later paragraphs, we shall not take up here the question of how legitimate is the use of the term 'temperature' in this situation. We shall only observe that, regardless of any subsequent interpretations, there is one important result of a general character: the kinetic energy of the impurity ions in a paramagnetic pinch substantially exceeds the average energy of the electrons.

The fact that the ions in a plasma may have comparatively very high energies also follows from measurements of the energy spectrum of neutral atoms bombarding the wall. Such measurements were first made on Alpha by the method described earlier (p. 196). They showed that deuterium atoms are the chief constituent of the flux of neutral particles. Figure 77 shows a typical energy distribution of atoms escaping from the plasma. This curve clearly does not correspond to a Maxwellian velocity distribution. It also follows from Fig. 77 that a rather substantial part of the neutral flux is carried by atoms having an energy of thousands of electron volts. This result indicates that the plasma contains a large number of deuterium ions having energies in this range.

Measurements of the electron density in the pinch have shown that in discharges with a total current of 100 kA and above, the gas appears to be completely ionised. However, the radial density distribution across the pinch remains unexplained.

The development of a discharge in deuterium and other light gases is accompanied by a rather intense X-ray emission with a very broad spectrum (the measured photon energy is in the range of 1 keV to 1–2 MeV). This radiation arises in all probability from the bombardment of the inner surface of the discharge chamber by electrons accelerated by the applied electric field. If this hypothesis is accepted, one may try to estimate the fraction of the discharge current associated with the fast electrons, using measurements of the intensity of the X-rays. Under standard experimental conditions, this fraction is very small: in Zeta its order of magnitude does not on average exceed $10^{-4}$.

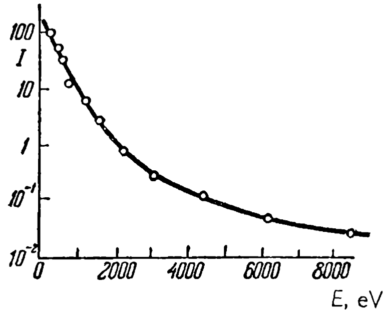

FIG. 77

Energy spectrum of neutral atoms bombarding the wall of a discharge chamber. The ordinate is the energy distribution function in relative units

A paramagnetic pinch with a high total current is also, as a rule, a source of neutron radiation. The first observation of this effect gave rise to the short-lived hope that genuine thermonuclear reactions were produced in the plasma, but the enthusiasm thus created subsided rather quickly. Measurement of the neutron energy spectrum showed that the neutrons in devices of the Zeta type are produced by acceleration processes, just as in the case of fast pulsed discharges. The average energy of the deuterons responsible for the observed neutron radiation amounted to several tens of kiloelectron volts.

The results of investigations of the energy balance of these discharges are of great significance in the understanding of the processes taking place. Let us consider the distribution of the energy transferred from the capacitor bank to the discharge up to the time of peak current. The energy released in the discharge tube is equal to $\int JV\,dt$. Part of it is expended in the generation of the self-magnetic field and in the enhancement of the longitudinal field in the pinch. The total magnetic energy, minus the energy originally stored in the initial longitudinal field, is equal to

$$\frac{1}{8\pi}\int\limits_{\Omega}(H_\theta^2+H_z^2)\,d\Omega-\frac{\overline{H_0^2}}{8\pi}\Omega. \qquad \text{.........}(6.9)$$

Here $\Omega$ is the total volume of the vacuum chamber and $d\Omega$ is a volume element. The bar over $H_0^2$ denotes that an average value is taken, i.e. account is taken of the non-uniformity of the initial field, caused by the toroidal shape of the chamber. The difference between the integral of $JV$ and the value of (*6.9*) is partly accumulated in the plasma as particle kinetic energy and ionisation energy, and is partly expended in energy losses, i.e. is lost to the chamber walls. The explanation of the relationship between these two components of the energy balance is of great interest. A qualitative characteristic of this relationship is obtained without any difficulty. It lies in the fact that in systems of this type, the energy lost from the plasma exceeds by many times the useful fraction contained in the kinetic energy of the particles. This general, and unfortunately certain, conclusion may be illustrated by a numerical example. At $p_0 = 1{\cdot}2\times10^{-4}$ Torr, $H_0 = 160$ Oe and $J_m = 200$ kA, the total energy released in the chamber of Zeta during the rise-time of the current to peak value amounts to about $2\times10^5$ J. Less than half of this energy appears in the magnetic field, and the remainder is absorbed by the plasma. In estimating the total kinetic energy of the electrons and ions in the plasma we can write

$$W = \tfrac{3}{2}Nk(T_e+T_i)l = 0{\cdot}75\times10^{-2}\beta lJ_A^2. \qquad \text{.........}(6.10)$$

As was indicated above, coefficient $\beta$ is probably less than $\frac{1}{3}$ in any case. Therefore, assuming that $\beta = \frac{1}{3}$, we obtain a very high value for $W$. However, even at this value of $\beta$, the kinetic energy stored in the plasma amounts only to $10^4$ J in all, i.e. less than 10% of the absorbed energy. Thus, it turns out that over 90% of the energy deposited in the pinch is expended in a huge energy loss from the plasma.

No complete interpretation of this loss has been made to date. However, measurements performed both on Alpha and on Zeta show that in many conditions the fraction of the energy transported to the walls by the particles surpasses the energy that escapes from the plasma as radiation (in which the main part is played by impurity ions). If this conclusion concerning the important role of energy transport by particle fluxes is valid†, then this means that the magnetic thermal insulation is virtually absent in the system under consideration. Indeed, for a substantial part of the energy to be transported by the ions and electrons of the plasma, each of these particles must make, on the average, several tens of trips to the chamber walls across the magnetic lines of force during the course of the discharge. That such trips to the wall actually occur in Zeta is shown by spectroscopic measurements.[†]

---

† This is so, see A. Gibson and D. W. Mason, Energy loss processes in Zeta, *Proc. Phys. Soc.*, **79**, 326, 1962.

§ **6.5** The information given above on the behaviour of a plasma in sustained pinches, obtained as the result of numerous experimental studies, permit certain general conclusions to be drawn. First of all, the instability of the paramagnetic pinch should be noted. The external signs of this instability are high-frequency oscillations on the voltage oscillograms and bright flashes of light from luminescent gas which extends out to the walls of the chamber. A direct proof of the instability can be inferred from the energy spectrum of the ions. As was indicated above, the ions are more energetic than the electrons in a paramagnetic pinch. The average energy of the multiply-charged impurity ions is of the order of 100 eV (and increases with the charge on the ion). Furthermore, the plasma contains a relatively large number of ions with energies between 1 keV and several tens of keV; which indicates a sharp deviation from a Maxwellian energy distribution. These facts cannot be explained on the basis of an assumption that the processes involved are quasi-stationary and the plasma is Joule heated, because cool electrons cannot transfer energy to hot ions. Consequently, fast ions must acquire their energy in acceleration processes arising as a result of the development of unstable deformations. If the plasma is not completely stable, the equilibrium of forces in the pinch is preserved only on the average, but it is continuously disturbed in local sections of the pinch. For this reason the plasma is always in a state of macroscopic, extremely disordered motion. 'Turbulence' is a very appropriate term for describing such motion. The only drawback connected with the use of this term is that it is excessively employed to cover all effects which are so far unexplained.

When the turbulence is strongly developed, the motions taking place in a 'quasi-stationary' paramagnetic pinch represent a statistical superposition of processes similar to the inertial pulsations characteristic of the fast discharges discussed in the preceding chapter. These pulsations in different parts of the pinch may be practically independent of one another. From this point of view, the appearance of some very fast ions is not unexpected, since they can be accelerated by means of the Fermi mechanism, as might well occur in an unstable plasma with large-scale turbulence.

The dependence of the ion kinetic energies on $m_i$ and $Z$ is determined by the nature of the spectrum of the electric fields associated with plasma turbulence. An analysis of the high-frequency oscillations which appear on the discharge oscillograms leads to the conclusion that an important part in the dynamics of a pinch is played by electric fields which oscillate with frequencies smaller than the ion cyclotron frequencies. In such electric fields, perpendicular to $H$, the ions should move at velocities close to the drift velocity $cE/H$, and hence, the energies of the ions should be proportional to their masses and be independent of the magnitude of the charge. Owing to the equal velocities of all the particles in an element of the plasma within which the fields retain a given value and direction, no exchange of energy takes place between these particles. When the ions are accelerated by electric fields which oscillate with frequencies comparable to or greater than the ion Larmor frequencies $\omega_{\mathrm{Hi}}$, a quite different situation arises. In the limiting case when $\omega \gg \omega_{\mathrm{Hi}}$, the elementary acceleration process occurs as if the magnetic field were absent. The maximum kinetic energy acquired by the ions in such a process under the influence of a field $E = E_0 \sin \omega t$ is equal to $Z^2 e^2 E_0^2 / 2m_{\mathrm{i}}\omega^2$, which is less than that acquired under the influence of a slowly changing field of the same amplitude in the ratio $(\omega_{\mathrm{Hi}}/\omega)^2$. However, owing to the relatively good thermal contact between the ions, the kinetic energies acquired by them in high-frequency fields should change rapidly to random thermal energy and be uniformly distributed among ions of different charges and masses. This additive component of the ionic energy should grow continuously at the expense of the energy contained in the high-frequency electric oscillations and will be limited only by the thermal loss (also included here is the transfer of energy from the ions to the plasma electrons). Some contribution to this energy component may also be made by collisions between individual elements of the plasma which move at different velocities and by their intermixing along the magnetic lines of force, and finally, by an effect such as the straying of ions having large values of $m_{\mathrm{i}}/Z$ from a region with one value of $E_0$ into a neighbouring region where $E_0$ has another value. It follows that in the case where relatively moderate frequencies predominate in the spectrum of electric plasma oscillations ($\omega < \omega_{\mathrm{Hi}}$), the average kinetic energy of the ions can be represented with sufficient accuracy by a linear mass function—in accordance with recent observations made in spectroscopic studies with Zeta. The part of the energy which is independent of $m_{\mathrm{i}}$ represents the true thermal energy of the plasma. The more distinct the expression of the turbulence, the higher is the value of the other term proportional to $m_{\mathrm{i}}$ in the expression for the average energy. Owing to the exchange of energy between the ions and electrons in the plasma, the additive component of the energy of the ions may prove to be an important supplementary source of energy for the heating of electrons. Thus, in the energy balance of a turbulent plasma, the stepwise process of energy conversion has a rather unique character. Energy from the electrical circuit supplying the discharge is transferred directly to the electrons of the plasma. A small part of this energy is accumulated as heat in the electron gas, whose temperature is relatively low, and a substantial part is used to excite oscillations and waves in the plasma by mechanisms whose nature has not yet been eludicated. Ions get their thermal energy from these waves and oscillations; the ion constituent is heated to a considerably higher temperature than the electron constituent, and returns part of its energy to the electron gas. In addition, because there exists a mechanism for the transfer of energy from the electric currents to the plasma fluctuations, there should also be an associated transfer of momentum, i.e. additional electron scattering. For this reason, the electrical resistance of the plasma should be higher than predicted by equation *(3.10)*, in which only Coulomb collisions have been taken into consideration (but a theoretical estimate of this correction cannot be made as yet). This assumption is supported by measurements performed on Zeta in 1961, when it was observed that in discharge regimes with a marked degree of turbulence the relation between $\sigma$ and $T_e$ breaks down and that the plasma exhibits a supplementary, 'anomalous', resistance. A similar anomalous resistivity appears also to play a part in the rapid disappearance of the skin currents at the start of the discharge.

---

[†] W. M. Burton and R. Wilson, Spectroscopic measurements of plasma containment in Zeta, *Proc. Phys. Soc.*, **78**, 1416. 1961.

These general remarks should have been a preface to a theoretical analysis of the complex motions of the plasma in a paramagnetic pinch. Such an analysis should provide a velocity spectrum of the directed motions, should show how the heating of the ionic component takes place as a result of the dissipation of the directed motion, and should establish a relation between the directed and the thermal velocities of the particles. However, almost nothing has been done along these lines so far.

The turbulence of the plasma in Zeta-type devices may be due to a number of causes. Most important is the magnetohydrodynamic instability of the paramagnetic pinch with a diffuse boundary. Theory predicts that a pinch can be stable only when the longitudinal field is not displaced with the field generated by the main pinch current, i.e. when the regions of space in which $H_\theta$ and $H_z$ are non-zero do not overlap appreciably. As was pointed out above, a skin-effect has been observed to disappear very rapidly in a paramagnetic pinch. Therefore, the $H_\theta$ and $H_z$ fields are not separated in practice. Suydam's criteria can be fulfilled for such a field distribution only when the plasma pressure amounts to less than a few per cent of the magnetic pressure. As soon as the plasma pressure exceeds this value, the configuration is predicted to be unstable, and small-scale motions arise which 'dump' the excess energy at the walls.

The bright bands observed on time-resolved photographs of a slow pinch may represent a manifestation of this instability. In particular, one of the forms of the instability corresponds to a deformation which consists in the expulsion of the plasma from the pinch along the spiral lines of force located on the surface of the pinch. Since near the boundary of the pinch $H_\theta \gg H_z$, this deformation, when observed through a narrow slit in the chamber, may have the external appearance of flares moving in a direction normal to the pinch axis.

A certain part in the development of instabilities may also be played, in principle, by the acceleration of electrons by the electric field inside the pinch. As discussed in Chapter III, the transition of the electrons into a state of continuous acceleration (runaway electrons) depends on the ratio of $u$, the mean velocity in the direction of the electric field, to the thermal velocity $v_e$. The number of runaway electrons begins to increase rapidly at $u/v_e > 0{\cdot}07$. In Zeta-type devices, the electron temperature is apparently very low, and therefore, at large currents the acceleration of a large number of electrons could be expected. Thus, for instance, if it is assumed that $T_e \simeq 10$ eV, then for $N \simeq 5 \times 10^{16}$ cm$^{-1}$ and a total current of 200 kA, the ratio $u/v_e$ is about 0·1. If the graph shown in Fig. 19 is used to estimate the time necessary for the plasma electrons to go into the runaway mode, this time is found to be of the order of 300 $\mu$sec.

Comparison of such estimates with experiment is difficult in those cases where there is no direct measurement of the line density $N$; for if the energy loss is taken to indicate a rapid loss of particles to the wall, followed by re-injection, the line density $N$ during most of the discharge need bear no close relation to the initial gas content of the discharge chamber. However, such estimates have recently been made, using ultraviolet and microwave techniques on Zeta; and these observations indicate that when the line density falls below $6 \times 10^{16}$ cm$^{-1}$, there is a rapid increase in the flux of runaway electrons accompanied by an extremely violent instability which largely disrupts the discharge current. The observed critical line density is in good agreement with that calculated above. In addition, however, runaway processes may arise during the bulk of the discharge due to inhomogeneities of the plasma density—especially in the outer regions; and these may contribute to the turbulence.

If we consider the results of investigations carried out with Zeta, Sceptre, Alpha and other apparatus from the standpoint of the prospects they offer for solving the problem of controlled thermonuclear fusion, these prospects appear very dim. Indeed, all the experiments indicate that despite the original expectations, the paramagnetic pinch is unstable and rapidly transfers its energy to the walls of the chamber. Even although the resistance of the plasma has proved considerably higher than could have been expected, the Joule heating is insufficient to raise the electron temperature above ten to twenty electron volts because the energy escapes from the pinch extremely rapidly. From the standpoint of scientific research, however, experiments with paramagnetic plasma pinches in weak magnetic fields have not yet exhausted all the interesting physical data they should yield. This pertains primarily to transport processes in an unstable plasma and to the mechanism responsible for the fields which accelerate the ions.

§ **6.6** Toroidal systems with a very large ratio of the longitudinal magnetic field to the self-magnetic field generated by the plasma current have been studied in far less detail than systems with a paramagnetic plasma column. The main experimental results have been obtained by Yavlinsky and co-workers at the Kurchatov Institute. The strong longitudinal fields needed are generated by discharging capacitor banks through powerful coils. The longitudinal flux in this case is not constant with time; but it changes slowly during the half-period of the gas discharge in the chamber. For instance, in the device shown in Fig. 69, the longitudinal field strength changes with a period of 0·16 sec, while the gas current in the discharge chamber has a half-period of about 5–10 msec. In order that the longitudinal field may penetrate freely into the discharge chamber, the torus walls must have a high resistance to the currents flowing round the minor axis of the chamber. This condition is met when the inner discharge chamber is made of thin stainless steel and the outer copper jacket has a longitudinal insulation slit around the entire circumference (see Fig. 69).

In systems of the type under consideration the ratio of the self-magnetic field to the longitudinal magnetic field must be small in order to suppress the instabilities (see equation (*6.1*)): therefore the plasma column should not exhibit much compression during the discharge. Indeed, if the pinch were strongly compressed after its formation, this would lead to an increase of the strength of the axial field in the plasma. But, since $H_J^2 \ll H_z^2$, even a relatively small increase of $H_z$ inside the plasma could not be balanced by the pressure generated by the self-magnetic field. This fact gives rise to a wholly understandable difficulty in isolating the plasma column from the walls.

If, at the outset, the discharge developed over the whole cross-section of the chamber, the pinch could be isolated from the walls merely by raising the strength of the longitudinal field. Such a method of isolating the plasma from the walls necessitates a very rapid increase of the magnetic field in a large volume, a requirement that is very difficult to accomplish technically. A far simpler method of achieving the same goal consists in providing the chamber with diaphragms having apertures ('limiters') considerably smaller than the cross-section of the discharge chamber. Experiments show that when this design is employed the pinch has a cross-section that is limited by the size of the limiter. Furthermore, to prevent the pinch from partly touching the edges of the diaphragm, the centres of the limiter should be displaced somewhat toward the outer wall of the chamber (see Fig. 78). This requirement follows from the fact that the equilibrium position of the pinch should be displaced with respect to the centre of the minor cross-section by a distance $\delta$ which is given, to a first approximation, by equation (*4.55a*). A more accurate determination of the location of the limiter is provided by direct experiments: if the limiter is not positioned properly, one can see marks left by the discharge on the diaphragm.

To obtain a pure hydrogen or deuterium plasma with a minimum content of foreign ions, it is necessary to observe very strict vacuum hygiene. No organic substances should be used in the construction of the liner or anywhere else in the high-vacuum system. In addition, the liner should be degassed by a prolonged heating at the highest possible temperature. In the studies described here, the discharges in the chamber were carried out under two different vacuum régimes: (1) with a cool liner which had been outgassed by heating to 400–450° C for several hundred hours by an alternating current; (2) with a hot liner whose temperature lay in the 400–450° C range. The experiments indicate that the degree of contamination of the plasma by foreign matter is approximately the same for both régimes. The pressure of the residual gases in the chamber before the discharge under usual experimental conditions is typically $1 \times 10^{-7}$ to $1 \times 10^{-6}$ Torr.

The main subject of the experimental research has been deuterium plasma. Additionally, discharges in hydrogen and argon have been studied. In experiments performed with various installations, the initial parameters have varied over the following limits: initial gas pressure $p_0$, from $2 \times 10^{-4}$ to $2 \times 10^{-3}$ Torr; $H_z$, from $2 \times 10^3$ to $2 \times 10^4$ Oe; initial electric field $E_0$ from 0·05 to 0·6 V/cm; quarter period of the electric field, from 3 msec to 10 msec. The duration of the first phase of the discharge in the experiments now being discussed depends to some extent on other initial parameters. In particular, the duration is reduced when the electric field $E_0$ is very large.

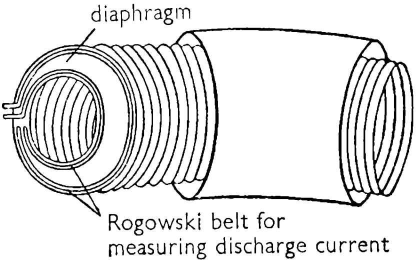

FIG. 78

Structure of the discharge chamber used in experiments where the ratio $H_z/H_\theta$ is large (Tokomak systems)

When studying quasi-stationary discharges in a strong external field, the measuring techniques used are basically the same as those discussed in the last section. Information is obtained from oscillograms of the discharge, photographs of the radiation from the plasma column, spectrograms of the radiation in the visible and ultraviolet region, hard X-ray detectors and from radio-interferometric measurements.

Before describing the experimental results there is one particular characteristic of the available material which is worth noting. This is that all the results so far obtained are clearly coloured in various ways depending on which particular installation was used to carry out the experiments. What we learn about the plasma properties in any particular series of experiments inevitably includes some contribution arising from such factors as defects in the design of the apparatus, shortcomings in the technology used and inability to arrange the proper initial formation of the plasma; and it is difficult for us to separate out this contribution. It therefore behoves us to be cautious and to speak not so much of the properties of a plasma in general but of the behaviour of the plasma in some particular experimental device. Only the gradual accumulation of results on installations of different types will enable us at some future date to identify adequately the 'apparatus effect' and to clarify the true behaviour of the plasma column—the behaviour, that is, which in principle corresponds to 'ideal' conditions, in so far as these are attainable. For the present, the attainment of this goal is made the more difficult by an unremoved defect in our experimental results, namely the ambiguity to which their interpretation is open even at the initial purely phenomenological stage. For example, it is not possible from available data to determine with adequate accuracy a unique absolute value of the number density of charged particles $n_e$, or even the change in $n_e$ during the discharge. Radio-interferometric measurements give us not $n_e$ but the product of $n_e d$, where $d$ is the diameter of the plasma column. The best one can say about $d$ is that it does not exceed some limiting value (the diameter of the limiter), but for the time being we do not have available any precise numerical data bearing either on the true value of $d$ or on its variation with time. Clearly, this particular example represents merely a certain stage in experimental research on plasma columns. Later, when methods have been devised for simultaneous radio-interferometric analysis at various wavelengths, our measurements will become quite unambiguous. However, this example is not the only one that could be given. The ambiguity caused by the lack of precise information as to the diameter of the plasma column also obtrudes when we try to determine the conductivity of plasma from the measured resistance of the plasma column. Furthermore, there is the question as to what proportion of the current and energy stored in a plasma can be accounted for by runaway electrons. The fact that this question is unanswered means that the determination of the plasma temperature from the conductivity is additionally ambiguous because one cannot *a priori* rule out the possibility that a significant part of the current is carried by a small number of very fast electrons.† There is also some indefiniteness about the loss of particles from the plasma, and therefore one can still only submit working hypotheses as to the nature of the diffusion processes in these so-called Tokomak installations.

The greatest volume of experimental information was obtained on two installations of the Tokomak type: T-1 and T-2, which are practically identical in design and dimensions. The discharge chambers of these devices have the following dimensions: major diameter, 125 cm; diameter of liner, 40 cm; diameter of limiter, 20–25 cm. The maximum strength of the longitudinal magnetic field is about 10 kOe. We shall first present the main results of experiments carried out with T-1 and T-2.

Plate XII shows streak photographs of the plasma column obtained with a drum camera. This method employs a simple optical system of the pinhole camera type: narrow slits perpendicular to the optical axis of the camera admit light from a small portion of the discharge into a vacuum chamber, inside which revolves a photographic film sensitised with a phosphor and wound on a drum. The image of the plasma on the revolving film is produced by the integrated radiation flux emitted by the discharge (from the visible to the far ultraviolet and including X-rays).

---

† Though this certainly seems unlikely, as we shall see later.

The three pictures shown in Plate XII correspond to discharges with different values of the ratio $H_z/H_J$. This ratio decreases from the upper to the lower picture, and the transverse dimensions of the plasma column change accordingly. In the top picture the radiating plasma lies within the region bounded by the limiting apertures (whose boundaries are represented by broken lines). In the centre picture the plasma spreads a little beyond the boundaries of this region up to the time of maximum current, and in the bottom picture this expansion of the plasma column is even more pronounced.

In order to compare these observations with the theoretical calculations, let us note that a measure of the stability of a discharge in a strong longitudinal field is the quantity

$$q = \frac{H_z}{H_J}\frac{a}{R},$$

where $H_J$ is the strength of the field due to the discharge at the surface of the plasma at the moment of peak discharge current $J$. If $q$ exceeds a certain whole number $m$, the discharge should be stable against all the helical deformations whose order is smaller than or equal to $m$. Therefore, the larger $q$ is, the greater is the margin of stability of the plasma (for $q < 1$, the discharge is unstable with respect to the most dangerous helical deformation with $m = 1$). These theoretical deductions are well illustrated by the time-resolved photographs of the plasma radiation. The top picture corresponds to $q = 4{\cdot}1$, the middle picture was obtained for $q = 3{\cdot}5$, the bottom picture corresponds to $q = 1{\cdot}5$. We can see that, when the margin of stability is large enough, the streak pictures provide no indications whatsoever of a dilation of the pinch or the appearance of flares and protuberances analogous to those observed in experiments with a paramagnetic pinch in Zeta-type devices.

Rogovskii coils placed on the diaphragms (see Fig. 78) are used to measure the current in the discharge chamber. The inner coil, whose diameter is equal to that of the limiting aperture in the diaphragm, measures the current flowing through the aperture. The outer coil measures the total discharge current. The difference between the two measurements makes it possible to determine the current flowing through plasma in the outer regions beyond the toroidal volume defined by the aperture of the limiter. The dependence of this fraction of the total current on $q$ for typical experimental conditions is given in Fig. 79. The ratio of the current in the outer regions to the gas current inside the limiter decreases rapidly with increasing $q$, and does not exceed 4% when $q \geqq 2$. This result

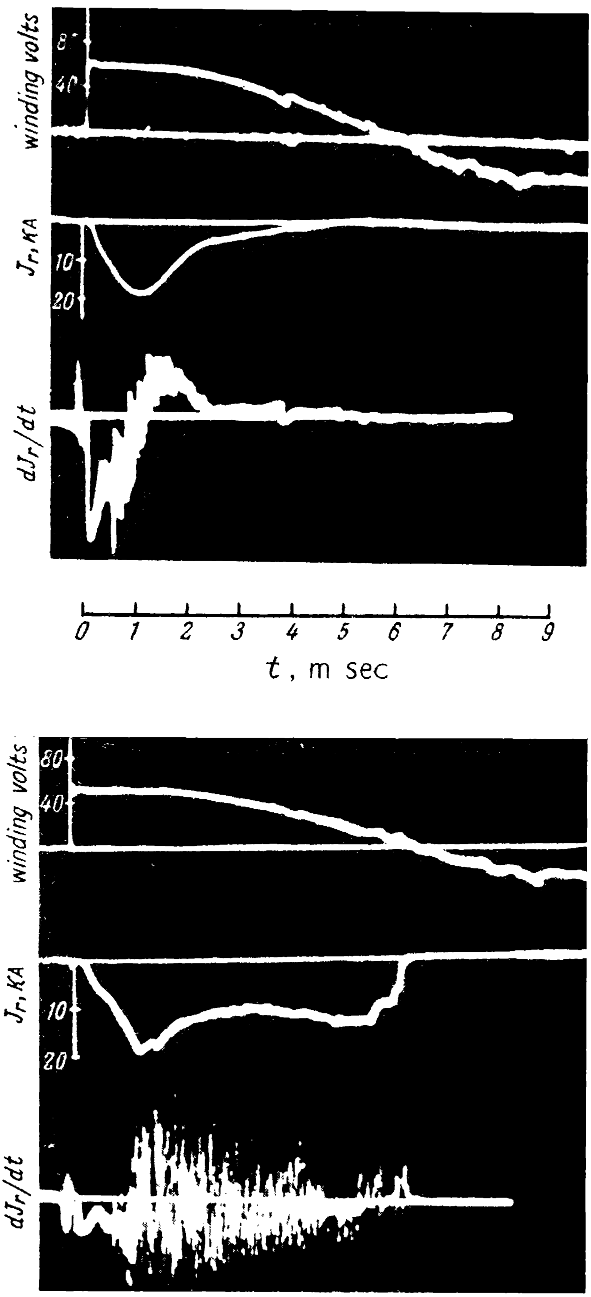

(*a*)

(*b*)

same scale as (*a*) above

Discharge oscillograms for various conditions of the vacuum preconditioning of the walls. Other initial parameters are the same (*a*) 'dirty' chamber; (*b*) 'clean' chamber; $H_0 = 6$ kOe, $p_0 = 5 \times 10^{-4}$ Torr $D_2$.

PLATE XIV

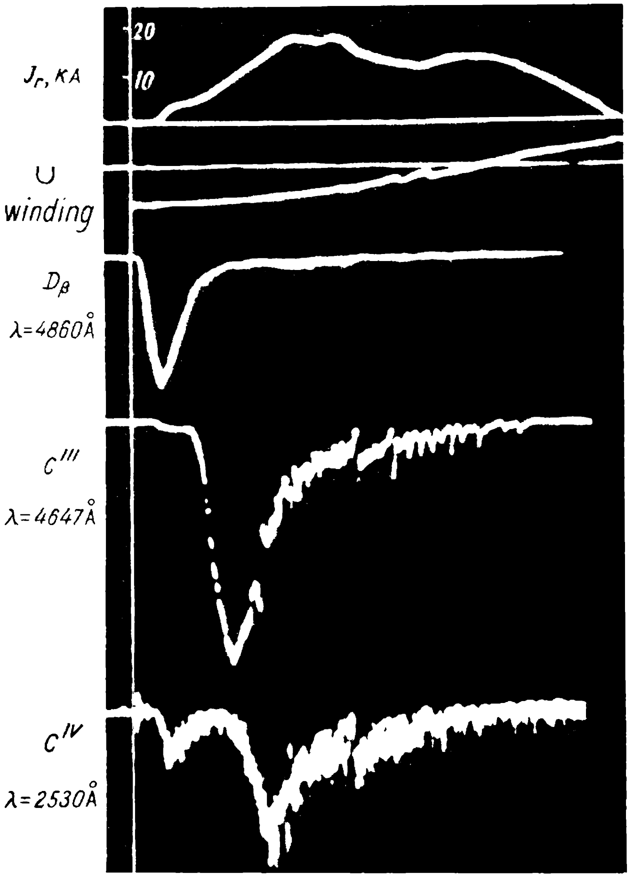

Oscillogram of the intensity of spectral lines.
$E_0 = 0{\cdot}09$ V/cm; $p_0 = 5 \times 10^{-4}$ Torr $D_2$; $H_z = 10$ kOe.

is confirmed by the conclusions drawn from the streak photographs of the plasma column.

The discharge oscillograms are very sensitive to the vacuum conditions. Discharges in tubes with inadequately degassed liners (Plate XIII (*a*)) give oscillograms which differ markedly from those in which the liners have been subjected to a prolonged thermal conditioning (Plate XIII (*b*)). We see that under the good vacuum conditions obtained after a prolonged degassing of the liner, the pulse lasts longer and assumes a double-peaked shape. In an inadequately preconditioned tube the discharge current dies away before the voltage reaches zero; in a clean chamber the current drops to zero much later and, under certain initial conditions, does so only after the start of the second half-period (see Plate XIV). We shall focus our attention on the results of measurements carried out under these relatively clean vacuum conditions.

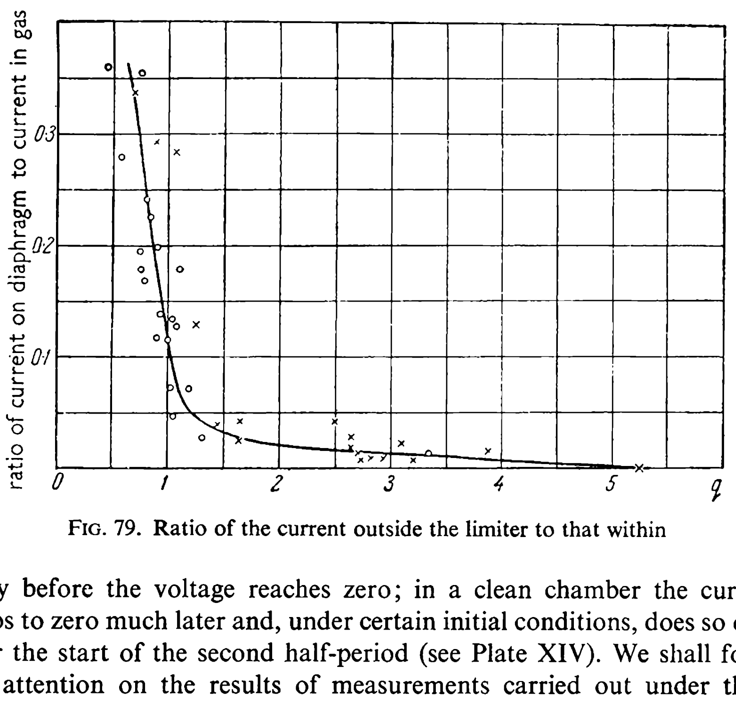

FIG. 79. Ratio of the current outside the limiter to that within

The total current at the first maximum of the double-peaked curve, everything else being equal, increases continuously as $H_z$ rises, and no moderation of this increase at very high values of $H_z$ (up to $H_z = 10^4$ Oe) has been observed. The growth of $J_{\max}$ with $H_z$ indicates that the plasma conductivity increases correspondingly. The variation of the conductivity with $H_z$ is shown in Fig. 80. These data correspond to the time of the first current peak, and are derived on the assumption that the current is uniformly distributed over the area of the limiter. For $H_z = 10^4$ Oe, $\sigma \simeq 7 \times 10^{14}$ c.g.s. e.s.u., which corresponds to an electron temperature of 15–20 eV. The rate of thermal relaxation between the electron and ion constituents of the plasma is high under these conditions, and therefore $T_i$ and $T_e$ should be approximately equal.

A much higher value of the conductivity is obtained at the second maximum of the current. It is difficult to determine the numerical value of $\sigma$ at this point with sufficient accuracy, because the voltage is very small and moreover the cross-sectional area of the pinch is unknown (judging from the time-resolved photographs of the plasma, the diameter of the discharge decreases markedly up to the time of the second current maximum). By a rough and probably low estimate, the plasma conductivity at the second current maximum is at least five times greater than that at the first maximum. It may be assumed, therefore, that the electron temperature corresponding to the second maximum amounts to no less than 50 eV.

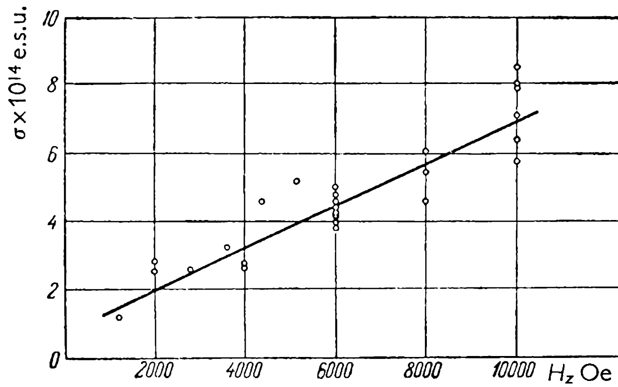

FIG. 80. Electrical conductivity of a plasma in Tokomak at the first maximum of the discharge current as a function of the longitudinal field strength

However, it cannot be excluded that at this phase of the discharge, because of its sharp decrease in radius, runaway electrons may begin to be important: a large part of the current would then be carried by fast electrons while the plasma temperature remained low.

All the oscillograms of the time derivative of the current, which correspond to discharges in an adequately degassed chamber, display extremely-violent oscillations with frequencies of 10 to 100 kc, whose random nature indicates clearly that they are engendered by the development of some kind of transient processes in the plasma. The amplitude of the oscillations varies considerably during each discharge. During the initial stage of the discharge, the current oscillations have a relatively small amplitude; this increases abruptly during a certain time interval whose duration is a function of $E_0/p_0$, and usually amounts to one hundred to several hundred microseconds. The large amplitude of the high-frequency oscillations indicates that even a very strong external magnetic field does not provide an ideal means of ensuring the complete stability of a plasma column.

These oscillations are apparently related to an instability of the magnetohydrodynamic type, since it is possible to conclude from an analysis of the oscillograms that the abrupt increase of the amplitude of the oscillations occurs at the moment when the ratio $J/H_z$ attains some minimum value. If, therefore, the geometrical cross-section of the plasma column is taken as equal to the cross-section of the limiter, the appearance of strong oscillations cannot be explained by the excitation of helical instability with $m = 1$ or even with $m = 2$. It is, however, entirely possible that under these conditions the plasma column does not completely fill the limiting aperture, as a consequence of which instability occurs at lower currents than might have been expected from an *a priori* estimate of the plasma radius.

The energy balance of discharges in a strong magnetic field has not yet been definitely established. To set it up, one must know the energy accumulated in the plasma and the energy associated with changes in the longitudinal field strength during the formation of the plasma column. For quasi-stationary processes these quantities can in principle be found from data on the distribution of the magnetic field. However, in order to obtain a picture of the distribution of both components of the magnetic field in the chamber for the case when $H_z \gg H_J$, it is necessary to perform magnetic probe measurements with very great accuracy, because the local variations in the strength of the field are very small compared with its average value. The order of magnitude of these variations in the longitudinal component of the field may be estimated by assuming that the counterpressure of the compressed field balances the electrodynamic forces associated with the current. In this case, $2H_z\Delta H_z \simeq H_J^2$ and hence,

$$\frac{\Delta H_z}{H_z} \simeq \frac{1}{2}\left(\frac{H_J}{H_z}\right)^2.$$

For stability, it is necessary that the right-hand side be less than $\frac{1}{2}(a/R)^2$. In practice, this means that $\Delta H_z \ll 10^{-2}H_z$.

If account is taken of the technical difficulties arising in the measurement of small changes of field strength, it becomes understandable why, in attempting to determine the thermal energy of the plasma from an accurate balance of the pressures, we cannot expect that magnetic probes will be very helpful. It can be shown that, in principle, to determine the pressure balance (and hence, the energy balance) when $H_z \gg H_J$, it is not necessary to know the entire spatial distribution of the field; it is sufficient to know only one integral characteristic of this distribution. The change of the magnetic flux outside the plasma column is an example of such a characteristic. So far, however, this method has not been used and we shall not describe it here.

Although the magnetic field data necessary for a quantitative determination of the thermal energy of the plasma are not available, the qualitative aspect of the energy balance of the discharge appears clear enough. By estimating the order of magnitude of the thermal energy stored in the plasma and comparing it with the electrical energy dissipated in the gas discharge, we find that under the conditions studied hitherto the electrical energy deposited in the plasma exceeds by many times the energy accumulated in the plasma. As a concrete example, let us consider the discharge for which oscillograms are presented in Plate XIII. The electrical energy fed into the discharge during the rise-time from zero to peak current is in this case $5 \times 10^2$ J (excluding the magnetic energy associated with the current), and the thermal energy stored in the plasma at best does not exceed 60 J. Consequently, about 90% of the expended energy must be accounted for by losses from the plasma.

A significant and perhaps even the largest part of the energy absorbed by the plasma in the initial phase of the discharge is carried off by the radiation from impurity ions. This radiation lies mainly in the far ultraviolet region and, in an adequately degassed chamber, consists of a relatively small number of lines of the ions of C, N and O. Rough measurements of the total radiation losses, using a phosphor to convert the ultraviolet radiation into visible light, were made at an early stage of the experiments. They showed that in discharges in a chamber which had not been subjected to a prolonged thermal preconditioning, ultraviolet radiation is the main source of energy losses from the plasma. In passing to a higher level of vacuum purity, we would need to review these data. It is very probable, however, that impurity radiation also plays an important part in the energy balance of discharges in the degassed chamber.

This supposition is supported by estimates of the radiation intensity from the theoretical curves shown in Figs. 21 and 22. Such estimates indicate that a 5% admixture of carbon or oxygen atoms with hydrogen suffices to radiate all the energy evolved in the plasma during a discharge (under the typical experimental conditions described above).

Spectroscopic studies of discharges in a strong axial field are only of a preliminary nature. However, they have already provided valuable information on the manner in which the plasma properties change in the course of a discharge. Plate XIV shows the oscillograms of the intensity of spectral lines emitted by deuterium and by C III and C IV ions, together with current and voltage oscillograms. We see how the three lines, corresponding to different ionisation states, appear successively in the radiation from the discharge. In the initial phase, when the electron temperature is still moderate, deuterium lines appear which vanish after the ionisation of the bulk of the gas in the chamber is completed. The lines of doubly-ionised carbon, C III, are observed much later. Their intensity begins to decrease before the current reaches a maximum. Hence, one may conclude that when the current goes through the first maximum, most of the carbon ions exist as C IV. The following stage in the ionisation of carbon is apparently reached near the current maximum, since at that moment the intensity of the C IV lines begins to drop. The ionisation energy for the transition from C IV to C V is 64 eV. The minimum excitation energy for the spectral lines of C V is 304 eV. For this reason, such lines in a plasma with an electron temperature of the order of twenty to thirty electron volts will have a low intensity.

The regularities characterising the variation of spectral line intensities with time support the assumption that the radiative de-excitation of the excited impurity ions is one of the elements which determines the energy balance in the plasma. If all other forms of energy loss are excluded from consideration, the heating of the plasma may be represented roughly in the following manner. The electric field imparts kinetic energy to the electrons, which is lost by the excitation and ionisation of impurity atoms and ions. In the earliest phase, when the electron temperature is still very low, the main loss is due to the excitation and ionisation of neutral atoms. As long as not all of the atoms are converted into singly-charged ions, the electron temperature will stay constant (like that of boiling water in a samovar). When first ionisation has been completed, the temperature begins to rise. Now the second stage of the process begins: the singly-charged ions are excited and ionised once more, so that doubly-charged ions begin to appear. During the time when second ionisation takes place, the electron temperature is stabilised once again. It begins to rise again towards the end of the second phase of ionisation, when almost all the impurity atoms are doubly-ionised. If the current-carrying plasma column is maintained, the ionisation of the impurities and the gradual rise of the electron temperature attendant upon it can proceed further.

In actual fact, the heating processes are of a more complex nature: the energy loss is caused not only by radiation, but also by an abnormally fast escape of the particles from the plasma, which we shall discuss below. In addition, a certain part in the cooling of the plasma may be played by the charge-exchange between the hot ions and the cool neutral atoms evaporating from the walls or present as a layer between the plasma column and the wall. It is difficult as yet to say anything definite about the relative roles of these processes in the energy balance of a discharge in a strong axial magnetic field. A simple explanation, which agrees well with all the experimental results is the following. The currents flowing in the primary winding of the transformer (which is on the outer surface of the vacuum chamber itself), and those flowing in the liner, together generate a magnetic field of quite complex structure in a toroidal geometry (particularly under conditions when the iron core is close to saturation). Inside the vacuum chamber this field has a small variable component $H_\perp$, which is parallel to the major axis of the torus and is dependent on time. The slowly changing longitudinal field generated by the coils around the chamber also make their contribution to $H_\perp$, and to all this is added the magnetic field of the compensating return lead of the longitudinal field coil which runs round the chamber (this return lead coil serves to eliminate coupling between the discharge circuit and the longitudinal field coil circuit). Interaction between the plasma current and the field $H_\perp$ leads to the appearance of an additional force which causes expansion or contraction of the major radius of the plasma ring. As a consequence, the equilibrium position (see Chapter IV) changes during the discharge; the displacement of the plasma is also effected by a change in the ratio $p/H^2$. During the initial stage of the discharge the major radius apparently expands, and this results in a strong interaction between the plasma and the edge of the diaphragm as a result of which the current is reduced. Then, as a result of changes in $p$ and $H_\perp$ the plasma ring contracts and no longer touches the diaphragm. This development may be associated with the secondary growth in plasma current and the increase in conductivity. If this supposition is subsequently confirmed (which seems very likely) it may be possible to increase the conductivity (and consequently the plasma temperature as well) by controlling the position of the column by means of specially arranged electrical circuits.

If this explanation is correct, then the two peaks on the current oscillograms can be regarded as a typical example of an 'apparatus effect'. It should be noted, incidentally, that on installations where the external field coils have an improved design and are better shielded from variable magnetic fields, the current oscillograms take on their usual one-humped form. Apparently in these installations the radial movements of the plasma are far less marked.

If one assumes the minor diameter of the plasma column is unchanged and equal to the diameter of the limiter, radio-interferometric methods provide an estimate of $n_e$ as a function of time. A typical curve obtained in this way is shown in Fig. 81. The electron density increases rapidly during the initial phase of the discharge (as should be expected), and, after reaching a certain maximum value, drops exponentially (which is completely unexpected). The rate at which $n_e$ decreases falls as the longitudinal magnetic field is increased. For $H_z = 5600$ Oe and an initial pressure of $5 \times 10^{-4}$ Torr, the electron density drops by half in about 0·5 msec. The maximum density is far less than the value which would be obtained if all the particles initially present in the chamber had been concentrated into the plasma column.

One interesting feature of the variation in the plasma density should be mentioned. After $n_e$ drops to a value of the order 1 to $2 \times 10^{12}$ cm$^{-3}$ it begins to rise again and attains a second maximum at a time close to the second current maximum. Radio-interferometric measurements at different radial positions in the plasma column indicate that the secondary rise of $n_e$ is associated with the fact that there is a region near the core of the discharge with an enhanced electron density, and this is the region which is involved in the second density maximum. At the same time, the plasma density at the periphery continues to decrease monotonically. Near the time of the second current maximum, the value of $n_e$ in the core of the discharge is apparently close to $10^{13}$ cm$^{-3}$ (i.e. about 20% of the value at the first maximum). However, it may be that this variation of $n_e$ is largely due to radial displacements of the plasma column. If this is so, no interest attaches to the quantitative interpretation of the fall and subsequent rise of $n_e$.

Qualitatively, the measurements of $n_e$ can, seemingly, be regarded as evidence of the peculiar instability of the plasma state under study which manifests itself in the anomalous diffusion of particles from the plasma column to the diaphragms in the chamber. An analogous phenomenon (commonly called 'pump out') was first observed in experimental investigations of magnetic traps called Stellarators. Therefore, we shall not give any further consideration here to the mechanism of the anomalous escape of particles, postponing a discussion of this difficult problem to Chapter VIII.

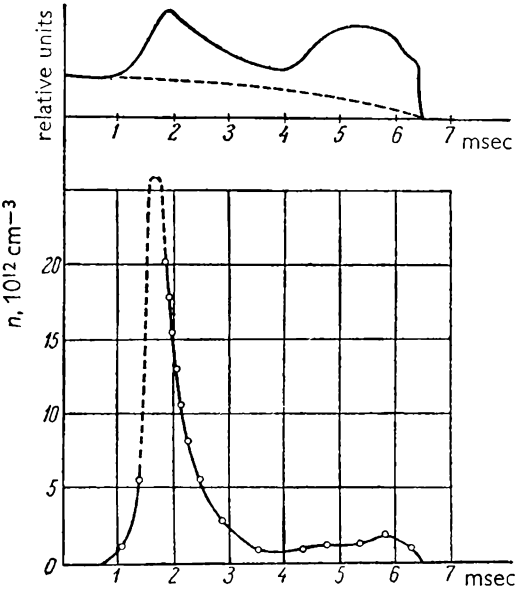

FIG. 81. Variation of the electron density of the plasma in Tokomak during the first half-period of the discharge. The figure also shows an oscillogram of the total secondary current (discharge current + current in liner). $E_0 = 0{\cdot}15$ V/cm; $p_0 = 5 \times 10^{-4}$ Torr $D_2$; $H_z = 5{\cdot}4$ kOe

Among the other experimental facts obtained from studies of toroidal discharges in strong axial fields, we should mention the emission of hard X-rays produced by the accelerated electrons. This radiation, with a maximum energy of some MeV, appears in the initial stage of the discharge and stops before the current reaches a maximum. A correlation between the time when the X-rays disappear and the instant when intense high-frequency oscillations appear on the $dJ/dt$ oscillogram has been observed.

The radiation given off by the fast electrons can serve as an important indicator of the processes taking place in the plasma column. To interpret the meaning of this indicator we must first of all have a clear picture of the motion of fast electrons in the plasma. When an electron is accelerated out of the normal Maxwellian distribution and acquires under the action of an electric field an energy of the order of tens of keV, then it practically ceases to be affected by collisions with other particles. This means that the motion of such an electron takes place only under the action of the solenoidal electric field and of the magnetic fields generated by the coils and by the plasma current. When $H_J/H_z \ll 1$, the character of this motion is quite simple. It can be considered as the combination of two motions—displacement along the line of force and drift in the non-uniform longitudinal field (more detailed analysis shows that the drift under the action of the self-magnetic field can be neglected if the Kruskal-Shafranov condition is fulfilled with a large enough margin). The momentum of the fast electrons makes a small angle with the direction of the longitudinal field, and is determined by the following equality:

$$-\,mv = e\int_{t_0}^{t} E\,dt.$$

Here $E$ is the strength of the solenoidal electric field in the plasma column, with the inductive component subtracted. The integral is taken over the acceleration time. Let us consider the projection of the electron trajectory on to a plane which is perpendicular to the magnetic lines of force and moves around the toroid along with the electron. In the absence of drift, this projection would appear as a circle centred on the minor cross-section of the plasma column. Calculation shows that if drift is taken into account, the centre of the circle is displaced by a distance $\delta$ towards the outside wall of the chamber. The value of $\delta$ depends on the geometry of the field $H_\theta$, i.e. on the distribution of the current density in the plasma over a cross-section of the column. If we assume that the current density is uniform over the entire cross-section, we obtain the following approximate expression:

$$\delta = \frac{mvc}{eH_J}\frac{a}{R},$$

where $H_J$ is the strength of the self-magnetic field at the boundary of the plasma column. With this assumption concerning the current distribution, the runaway electron trajectories projected on to the plane perpendicular to the longitudinal field form a group of concentric circles. The common centre of these circles is shifted from the centre of the minor cross-section by a distance $\delta$, which is determined by the above formula, into which can be inserted the momentum of a fast electron, represented as $e\int E\,dt$. Under typical experimental conditions $\delta$ should be of the order of a few centimetres and should increase continuously with time. The trajectories of runaway electrons are directly related to the value and structure of the self-magnetic field of the discharge current. It follows from this that the behaviour of the electrons during a discharge should reflect any changes which that component of the field undergoes, and which, in turn, are the consequence of changes in the magnitude and distribution of the plasma currents—in particular, in the position and the transverse dimensions of the plasma column. A consequence of this, to give an example, is that an intense, short burst of X-rays can occur as a result of the development of a hydromagnetic instability, which changes the distribution of current in the plasma and, as a result, fast electrons which were originally moving on trajectories in the middle of the column, now emerge at the surface and strike the diaphragm. In the absence of instabilities which break down the field structure, or of fast radial motion of the column, the X-rays can persist during a significant part of the first half-period of the current, the reason being that electrons, as they gain energy, are only gradually displaced towards the outside of the column and approach the diaphragm. At the same time, it must be considered improbable that there is any correlation between the X-rays and the development of those instabilities which may lead to anomalous diffusion but do not break down the structure of the self-magnetic field. Instabilities of this type, which figure very widely in recent theoretical research, will lead to the appearance of electric fields of varying size and direction in different sections of the plasma column. Because of their great speed, the accelerated electrons are not influenced by such fields. A fast electron, during its motion, integrates fluctuating electric fields over a very long distance in a very short time, and therefore it does not undergo any perceptible drift under the action of this field.

As noted earlier, the experimental results described above relate to toroidal discharges in a strong longitudinal field, and were obtained by work on the T-1 and T-2 Tokomak installations. In these experiments $H_z$ did not exceed 10 kOe (and was normally a good deal less), and the geometry of the magnetic fields fell far short of perfection. Recently (in 1962) our understanding of the behaviour of toroidal plasma columns has been enlarged by the first measurements obtained with the TM installations, where the field can be considerably larger and where the design of the chamber and the coils for the generation of the magnetic fields have been greatly improved. In TM the diameter of the toroidal chamber $R$ is 80 cm, and the (minor) diameter of the liner is 20 cm. The yoke of the iron core is Щ-shaped. The primary winding of the discharge circuit is positioned on the side supports of the yoke.

The longitudinal field coil is much more accurately designed than was the case for T-1 and T-2, and the magnitude of stray fields which displace the column has been reduced to a minimum. In experiments carried out so far with TM, the maximum $H_z$ was 22 kOe. Capacitor banks provide the power both for the discharge and for the longitudinal field. The duration of the first half-period of the discharge current is $\approx 3$ msec. The initial deuterium pressure $p_0$ has been varied between $5 \times 10^{-4}$ Torr (the minimum $p_0$ for breakdown) and $3 \times 10^{-3}$ Torr. As a consequence of a change in the leakage inductance of the discharge transformer, due to the turns of the primary winding being placed on the side supports of the yoke, the oscillograms of the discharge current and the voltage also show a change in form (compared with T-1 and T-2).

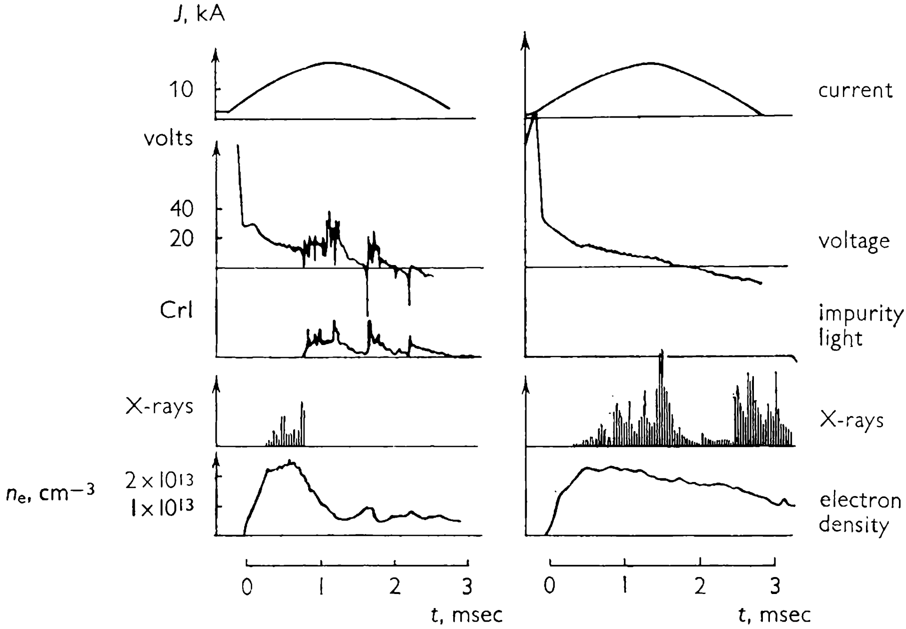

FIG. 82. Oscillograms of a discharge in hydrogen taken on the TM apparatus. The left-hand group of oscillograms were obtained for $H_z = 11$ kOe and the right-hand group for $H_z = 22$ kOe. The initial pressure and the initial discharge voltage were identical for both cases. $p_0 = 1 \cdot 10^{-3}$ Torr, $E_0 = 0{\cdot}1$ V/cm

Figure 82 shows two series of oscillograms characterising the behaviour of the plasma column in the TM installation for two values of the initial parameters (these parameters are $H_z$ and the initial discharge voltage). We can see that particular stages in the development of the discharge are clearly marked on the voltage oscillogram, whereas the current oscillograms are almost simple sinusoids. For a relatively small value of $H_z/E_0$ (the first series of oscillograms) the voltage starts to undergo strong and quite regular oscillations at a certain time after the breakdown. The intensity of the light emitted by the plasma column also varies at the same time as the voltage (Fig. 82 shows oscillograms of the intensity of one of the lines of the impurities present). Hard X-rays with an energy of several MeV appear as separate bursts until the onset of strong oscillations, and are subsequently wholly absent. Apparently under these conditions we are faced with the development of magnetohydrodynamic instability (for instance, helical deformations) just as in the experiments carried out earlier on the T-1 and T-2 installations. The oscillogram of $n_e$ indicates a rapid fall-off in the number density of electrons after the onset of the oscillations. If we estimate plasma life-time from this oscillogram, the result we obtain is about 0·5 msec. The second series of oscillograms, which were obtained while using a very strong longitudinal field ($H_z = 22$ kOe), shows the characteristic behaviour of a 'stable' plasma column. In this case, the marked oscillations on the voltage oscillogram disappear, the X-rays persist during almost the entire current pulse, and the electron number density falls off very slowly once the maximum has been attained. The mean life-time of particles in the plasma under these conditions is approximately the duration of the discharge pulse itself (it exceeds 3 msec as estimated from the oscillogram of $n_e$). In stable operation the conductivity of the plasma reaches $5 \times 10^{15}$ c.g.s., if it is calculated at the time of maximum current on the assumption that the column fills the entire free cross-section of the limiter (whose diameter is 16 cm); this conductivity corresponds to $T_e \approx 60$ eV. It seems, however, that in fact the (minor) diameter of the plasma column at maximum current is likely to be considerably less than 16 cm. It can therefore be assumed that the electron temperature actually achieved in experiments on TM is really not less than 100 eV.

This record value of $T_e$ is many times greater than those obtained from measurements with T-1 and T-2. The increase in electron temperature is brought about by two factors: the larger $H_z$ and the improvement in the shape of the magnetic fields. Associated with this, there is also a much more favourable energy balance for the discharge in the TM device. In stable operation about 30% of the electric energy expended on the discharge up to the moment of current maximum accumulates in the plasma in the form of particle kinetic energy (it is assumed that $T_i \approx T_e$). Thus, under such operating conditions, the electron temperature is sensitive to the plasma density; it decreases as the initial gas pressure rises, contrary to the situation for discharges where $H_z/E_0$ is relatively small (for such discharges the independence of $\sigma$ and $T_e$ on $p_0$ is characteristic).

Taken overall, the new results obtained with TM, despite their incompleteness and approximate nature, greatly strengthen our confidence that future work with Tokomak type systems will be very rewarding.

§ **6.7** Let us now pass on to an analysis of some of the conclusions to be drawn from these experimental investigations of quasi-stationary discharges in strong fields. A comparison of the properties of a plasma column in a strong field with those of the paramagnetic pinch formed in devices of the Zeta type shows that the strong magnetic field provides a marked increase in the stability of the plasma. This is demonstrated, first by time-resolved photographs of the plasma radiation which show visible signs of instability when $H_z/H_J$ is small, and second by the conductivity measurements. Despite the fact that in experiments with strong fields a comparatively small amount of energy was fed into the plasma, the average electrical conductivity of the plasma was higher in this case than that of the plasma in Zeta and Alpha. Although spectroscopic measurements of $T_i$ in Tokomak systems are preliminary, they so far confirm the hypothesis that in such devices the ion temperature does not exceed the electron temperature. The strong framework, provided by the lines of force of the externally generated field immersed in the plasma, prevents the development of plasma deformations involving a rapid distortion of the field lines, even if the plasma conductivity is low. For this reason, the processes leading to the acceleration of ions and associated with the development of sharply expressed instabilities can hardly play an important part in the energy balance of a discharge with a strong longitudinal field. Thus it may be assumed that in studying such discharges we are dealing with a plasma in which $T_e \approx T_i$ and hence, that one of the main signs of a strong instability is lacking. The remaining instability of the type which leads to anomalous diffusion, although a serious obstacle in attempts to achieve very high temperatures, does not in itself cause the plasma to cool as much as does the direct contact between the violently pulsating plasma and the walls of Zeta and Alpha.

Owing to the unfavourable relation between the energy stored in the plasma and the energy lost by various mechanisms, the kinetic pressure of the plasma cannot balance the compression forces arising from the flow of gas currents. Estimates indicate that under ordinary experimental conditions the plasma pressure is several times less than the magnetic pressure generated by the discharge current. Therefore, in high-current discharges with a strong longitudinal field, the plasma should possess paramagnetic properties—just as in devices of the Zeta-type. Moreover, the compression forces produced by the discharge current must be compensated by an enhanced longitudinal field in the plasma, i.e. the following relation should be applicable:

$$J_z/J_\theta \approx H_z/H_\theta,$$

which characterises a force-free magnetic configuration. Consequently, an azimuthal current should exist in the plasma column. For this current to appear, an electromotive force is necessary, and our problem now is to explain its origin.

We shall assume at the outset that the plasma has an isotropic conductivity, i.e. that the conductivity in the directions normal and parallel to $\boldsymbol{H}$ are the same. If this is the case, an azimuthal electric field $E_\theta$, which forms a right-handed spiral system in the direction of the discharge current, should be responsible for the appearance of the azimuthal component of the current. In reality, however, no appreciable compression of the plasma occurs in the initial stage of the discharge; on the contrary, the opposite process—a rapid expansion of the plasma due to the abnormally high diffusion rate—takes place. We do not observe this on the photographs of the plasma column because the outer layers of the expanding plasma pinch are continuously peeled-off by the diaphragms, but we can evaluate the rate of the diffusional motion from the drop in the electron density. Let us now note that if the plasma expands, $E_\theta$ will have a sign opposite to that which is necessary to maintain the azimuthal current in the force-free paramagnetic configuration.

The difficulty arising in an attempt to ascertain the pressure balance becomes particularly clear when one tries to determine the pressure jump associated with the azimuthal currents. The electric field arising from the radial motion of the plasma across the axial lines of force is equal to $vH_z/c$, where $v$ is the velocity of the plasma. This motion across the field will generate a current density

$$j_\theta = \sigma v H_z/c.$$

Owing to the appearance of the azimuthal current, the strength of the longitudinal field inside the plasma changes as follows:

$$dH_z/dr = 4\pi\sigma v H_z/c^2.$$

The difference between the magnetic pressures at the periphery and at the axis of the plasma column will be

$$\frac{H_z^2(a)}{8\pi}-\frac{H_z^2(0)}{8\pi} = \frac{H_z^2\sigma}{2c^2}\int_0^a v\,dr = \frac{H_z^2\sigma\bar{v}a}{2c^2}.$$

Here $\bar{v}$ is the mean radial velocity. It is assumed that the change in the field is small compared with its magnitude. According to the experimental data available, we take $\sigma \simeq 5\times 10^{14}$ c.g.s., $v \simeq 10^4$ cm/sec, $H_z = 10^4$ Oe, $a = 10$ cm. For these particular parameters, the difference between the magnetic pressures is about $3\times 10^6$ dynes/cm².† However, if one evaluates the maximum possible plasma pressure $p$ which could balance the total force of magnetic compression, it turns out that it is not even of the order of magnitude of $10^4$ dynes/cm². We thus arrive at the following contradiction: the extremely strong diamagnetism produced by the azimuthal currents in the expanding plasma should arrest the expansion and generate a gas flow in the opposite direction; this is not observed in actual fact.

An attempt may be made to resolve this contradiction by dismissing the assumption that the conductivity is isotropic and supposing instead that $\sigma_\perp$ is far smaller than $\sigma_\parallel$. This point of view is supported by another independent argument. It is obvious that if, due to the turbulent motion, the particles in the plasma column diffuse rapidly from the axis toward the walls, this means that the turbulence imitates, so to speak, an increase in the number of collision centres in the path of a moving particle. Only if the number of collisions is increased (i.e. the mean-free-paths are shortened) can the particles move perpendicularly to the strong magnetic field. And, since the conductivity is proportional to the mean-free-path, the anomalous diffusion may be described phenomenologically by a corresponding decrease in $\sigma_\perp$.

---

† These results were obtained in experiments with T-1 and T-2.

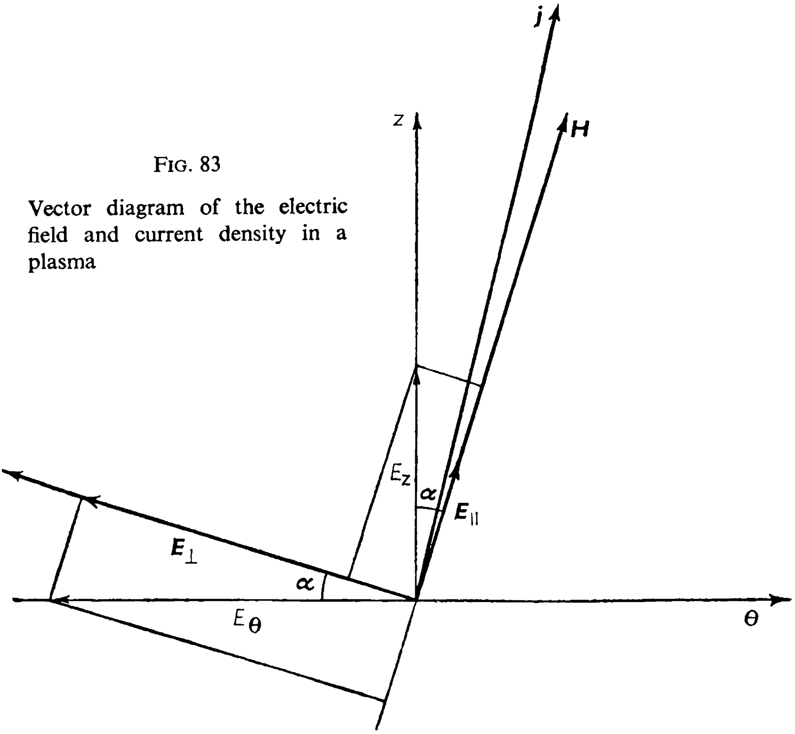

FIG. 83

Vector diagram of the electric field and current density in a plasma

Let us put $\sigma_\perp = \varepsilon\sigma_{\|}$, and we shall assume that ε is much smaller than unity. By analogy with equation (*3.26*), we can write

$$\boldsymbol{j} = \sigma_{\|}(\boldsymbol{E}_{\|} + \varepsilon \boldsymbol{E}_\perp). \qquad \text{.........}(6.11)$$

To find the components of $\boldsymbol{E}$ and $\boldsymbol{j}$ which are parallel and perpendicular to $\boldsymbol{H}$, let us turn to Fig. 83, which is a vector diagram of the fields and currents. The azimuthal component of the magnetic field, generated by the longitudinal discharge current, is small compared to $H_z$. That is why the angle α between the vector $\boldsymbol{H}$ and the (minor) axis z is small. The electric field in the expanding plasma has two components. The longitudinal component $E_z$ is equal to $E_0 + v_r H_\theta / c$, where $E_0$ is the field strength produced in the discharge by the external electrical circuit. The azimuthal component $E_\theta$ is equal in magnitude to $v_r H_z / c$, and is oriented clockwise (i.e. in the direction of decreasing $\theta$). Because $\alpha \ll 1$, we obtain the following expressions for the components of the current in the directions parallel and perpendicular to $\boldsymbol{H}$ for the stationary case:

$$j_{\parallel} = \sigma_{\parallel}(E_z - \alpha E_\theta) \approx \sigma_{\parallel} E_0, \qquad j_{\perp} = \sigma_{\parallel}\varepsilon E_\theta = \sigma_{\parallel}\varepsilon v_r H_z/c. \qquad \ldots\ldots\ldots(6.12)$$

Under typical experimental conditions, the longitudinal component of the electric field is about 0·1 V/cm, and the azimuthal component $\simeq$0·5 V/cm (at the boundary of the plasma column). The order of magnitude of the coefficient $\varepsilon$ may be determined from pressure balance. The resultant force acting on the plasma is $j_{\perp}H_z/c$ and should be counterbalanced by the pressure gradient. Therefore,

$$-dp/dr = \sigma_{\parallel}\varepsilon E_\theta H_z/c.$$

Putting

$$-dp/dr \approx p/a,$$

we find the following expression for a rough estimate of $\varepsilon$:

$$\varepsilon \approx pc/a\sigma_{\parallel}E_\theta H_z.$$

When $p \simeq 3\times 10^3$, $\sigma_{\parallel} \simeq 5\times 10^{14}$, $H = 5\times 10^3$ Oe and $a = 10$ cm, $\varepsilon$ should be of the order of $10^{-3}$. From equation (*6.12*) it follows that

$$j_{\perp}/j_{\parallel} = \varepsilon E_\theta/E_0,$$

which is about $10^{-2}$.

In the above analysis of the pressure balance some doubts may be raised concerning the validity of using equilibrium equations for a pinch with turbulent diffusion. This may be partially justified as follows: under conditions where the diffusion velocity is several orders of magnitude smaller than the thermal velocity of the ions (as is the case under consideration), the inertial terms in the general dynamic equations are negligible so that the plasma may be regarded as being in a state of macroscopic equilibrium. An instability of the anomalous diffusion type, which slowly gnaws at the organism of the plasma pinch, is not able to eliminate completely the magnetic thermal insulation, and so the life-time of the particles in the plasma is hundreds of times longer than the time of the flight across the pinch.

Although from what has been stated it would seem that the above conclusions are valid, the estimate of the magnitude of $\sigma_{\perp}$ nevertheless causes serious doubt. In principle, the following picture can be drawn: owing to an instability the plasma flows outward in narrow streams while the plasma column as a whole contracts slowly. Under these conditions, the magnetic configuration can be force-free even when $\sigma_{\perp} = \sigma_{\parallel}$ since the effective value of $v_r$ is less than zero. The experimental data available at the present time are not sufficient to elucidate the question of the true value of $\sigma_{\perp}$ for a plasma with a high level of turbulence. Solution of this problem may be of considerable importance for the understanding of the processes causing turbulence (i.e. anomalous diffusion).

At the present time, the prospects of further studies on the properties of plasmas heated by a current in toroidal chambers with a strong longitudinal field are quite clear. The principal aim is to establish the limiting temperature to which a plasma can be heated under such conditions by means of the Joule heat evolved by the discharge current. We are at present at a stage where the greater part of the energy expended by the external energy source escapes to the walls as radiation. The energy barrier created by the radiation loss could be overcome in two ways. First, it is necessary to perfect the vacuum technology and to reduce to a minimum the emission of gas by the walls. Second, the strength of the longitudinal field should be increased. In accordance with the Kruskal-Shafranov criterion, $H_z$ determines the maximum value of the total discharge current at which stability with respect to the most dangerous of pinch deformations can be achieved. By increasing $H_z$, we can increase $J_{\max}$ and accordingly raise the electrical power delivered to the discharge. It may be assumed that at high enough values of $H_z$ and $J_{\max}$ it will be possible to go rapidly through all the high ionisation stages of the impurity atoms, and to achieve conditions in which the remaining energy can be used mainly to raise the kinetic energy of the particles. An increase of $H_z$ should be associated with another important advantage: a reduction of the anomalous diffusion rate. A decrease of the diffusion rate should lead to an increase of the lifetime of the particles in the plasma, and this will make it possible to increase the effective heating time.

In the experimental devices used so far, the stabilising field can be raised to $2 \times 10^4$ Oe. At such a field strength the column has an adequate reserve of stability for currents up to 50 kA. Under such conditions the energy fed into the discharge during the first quarter period does not exceed 3000–4000 Joules. A great part of this energy is carried off by line radiation in the extreme ultraviolet. To penetrate the temperature barrier caused by impurity radiation and to raise the plasma temperature to 200–300 electron volts, the energy released in the plasma has to be raised at least 5–10 times. This can be achieved only if the field strength is raised to 40–50 kOe.

Experiments with fields on this scale, which were once a distant hope, have become a task for the immediate future now that the new T-3 installation—the largest of the Tokomak series—has been completed at the Institute of Atomic Energy. This installation, which was assembled in 1961, underwent preliminary tuning up and became an operating experimental device by the summer of 1962. A photograph of T-3 is shown in Plate XV. The major diameter of the toroidal chamber is 200 cm. The minor diameter of the liner is 40 cm; the minor diameter of the outer shell of the chamber is 50 cm. The liner is evacuated through lateral manifolds by two high-vacuum pumps down to a pressure of $\approx 3 \times 10^{-8}$

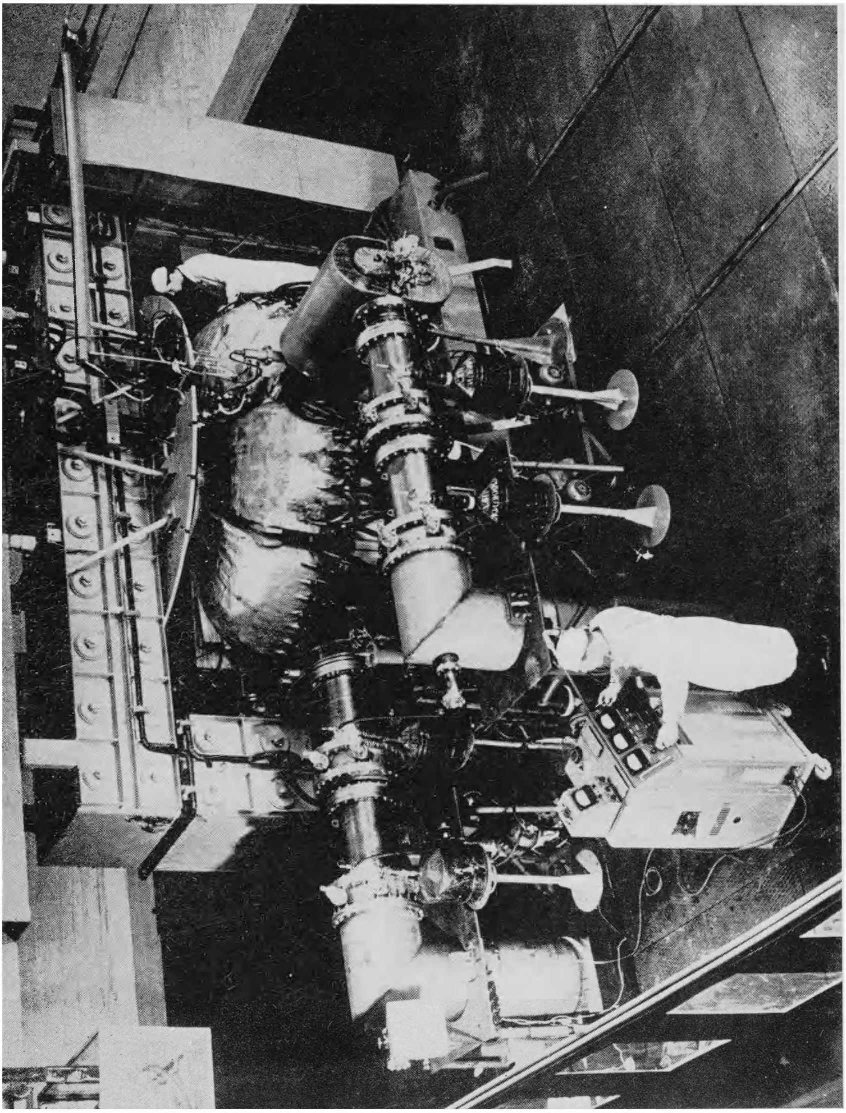

The largest member of the Tokomak family, T-3.

Torr. Two other high-vacuum pumps create a vacuum of about $10^{-6}$ Torr in the gap between the liner and the outer shell. The magnetic field is generated by eight coils, each of which is an independent unit made up of 352 turns coated with epoxy resin. The external diameter of the coils is about 100 cm. A pulse generator with a capacity of 75,000 kVA is used to supply the coil. The design of the coils and the layout of their power-supply is calculated to generate a longitudinal field of up to 40 kOe. The half-period of this field is 0·1 sec. By using a Щ-shaped transformer to enclose the chamber, discharge currents of up to 250 kA can be obtained. The duration of the first half-period of the discharge current can vary between 10 and 20 msec for the simplest switching scheme (without the reverse magnetisation of the core envisaged in the design). In the first half of 1962 nothing more was done on T-3 than a series of commissioning experiments at field strengths of up to 22–23 kOe. With such fields in a well-conditioned chamber, the plasma conductivity can easily be raised to around 2 to $3 \times 10^{15}$ (at a conservative estimate) for a discharge in deuterium at an initial pressure of $5 \times 10^{-4}$ to $10^{-3}$ Torr.

The results that one can hope to obtain by experimenting at high values of $H_z$ lead to a calculation of the Joule heating of the plasma under the assumption that there are no losses. To simplify the calculation, we shall assume that the temperature is uniform over the cross-section of the pinch (a weakly developed turbulence is sufficient to ensure uniformity); and in addition, we shall consider the ion and electron temperatures to be equal. This equality of temperatures can be achieved by choosing a large enough value of $N$. The thermal energy gain of the plasma will be determined by equation (*4.35*), which remains valid if the pinch is immersed in a longitudinal field. Putting $f = 1$ and integrating equation (*4.35*) we find that

$$\frac{6}{5} N k \pi a^2 b_0 T^{5/2} = \int_0^t J^2\, dt, \qquad \ldots\ldots\ldots(6.14)$$

where $\sigma = b_0 T^{3/2}$. Let

$$J = J_{\mathrm{m}} \sin \omega t.$$

Evaluating the integral on the right side of (*6.14*) with an upper limit corresponding to the current maximum, we obtain the following expression for $T$:

$$T = \left( \frac{5 J_{\mathrm{m}}^2 \tau}{12 N k \pi a^2 b_0} \right)^{2/5}, \qquad \ldots\ldots\ldots(6.15)$$

where $\tau$ is the duration of the first quarter-period. For a given field strength $H_z$, the largest value of $J_{\mathrm{m}}$ compatible with the stability requirements is determined by the expression

$$J_{\mathrm{m}} = \frac{a^2 c}{2qR} H_z, \qquad \ldots\ldots\ldots(6.16)$$

where $R$ is the major radius of the torus and $q$ is the assumed value of the magnetohydrodynamic stability margin. Putting $q = 2$ and substituting *(6.16)* into *(6.15)*, we obtain:

$$T = 5\times 10^{4}(a^{2}H_{z}^{2}\tau/N_{1}R^{2})^{2/5}. \qquad \ldots\ldots\ldots(6.17)$$

Here $N_1$ is the line density (electrons or ions) in units of $10^{16}$ cm$^{-1}$ ($N = N_1 \times 10^{16}$ cm$^{-1}$). Let $H_z = 5\times 10^4$ Oe, $\tau = 0{\cdot}01$ sec, $N_1 = 5$ and $a/R = 10^{-1}$. With these parameters, the plasma temperature should be about $4\times 10^6$ °K, i.e. about 400 eV.

Using the formulae derived in Chapter II, which describe the transfer of energy from electrons to ions, we can see easily that $T_e$ and $T_i$ will be rather close to each other for these discharge parameters. In accordance with equation *(6.16)*, the maximum current necessary for such conditions should be approximately equal to 120 kA. Since the average drift velocity of the current-carrying electrons in this case will be two orders of magnitude less than their thermal velocity, the pinch instability associated with runaway of the electrons is unlikely to appear. It goes without saying that these calculations will be valid only if it is found that the velocity of the anomalous diffusion decreases rapidly as $H_z$ rises, and if it does not increase appreciably with the temperature of the plasma. The optimistic expectations may not be fulfilled; in that case, we shall not be able to heat the plasma to a temperature of several million degrees, even in devices with a very high longitudinal magnetic field strength.

The answer to the question, how effective is the heating of a plasma by a toroidal discharge stabilised by a strong longitudinal field, is of great significance for the entire problem of controlled nuclear fusion. The application of this heating method underlies the initial phase of the process of producing a high-temperature plasma in the Stellarator (see Chapter VIII), and therefore the experimental investigations we have dealt with in this chapter fit in with the research of the Stellarator programme.

In view of the fact that the existing theory is unable to predict the behaviour of the anomalous diffusion when $H_z$ and $T$ are raised, the answer to the above question can be provided only by indirect experiments in simple toroidal devices and Stellarators. It is the author's opinion that toroidal discharges have a distinct advantage over Stellarators as a means of studying the efficiency of Joule heating. This advantage is related to the fact that for a given $H_z$ it is much more difficult to attain a high enough $a/R$ ratio in a Stellarator than in an ordinary toroidal chamber which is a considerably simpler structure. Therefore, when the outcome of the fight against contaminations and instabilities is successful, the temperature to which the plasma can be Joule heated will be higher in simple toroidal systems than in those of the Stellarator type. It may be added that, thanks to the relatively large value of $a/R$ for Tokomak-type devices certain types of instability predicted by the present theory do not prove dangerous. This is true specifically for the instability due to the inhomogeneity of the plasma, i.e. where there is a gradient in number density close to the boundary of the plasma column. The Stellarator is one example where this instability may manifest itself as a marked increase in the diffusion coefficient (see § **7.7** and § **8.6**).

The study of quasi-stationary discharges in a strong longitudinal field is also of undeniable value from the standpoint of plasma physics, apart from any future practical applications. In such discharges, a plasma with a very high concentration of charged particles and a not too low temperature appears to us at first as an object of rather distinct geometrical shape free of the catastrophic deformations which alter all the parameters in fast-pulsed discharges within a few microseconds. The relatively high stability of a slow pinch in a high field makes it possible to study thoroughly those mechanisms which are at the basis of the diffusion processes and limit the lifetime of the hot plasma. As far as these questions are concerned, we are still in the initial stage of collecting and classifying the first experimental data.

In order to understand the nature of the phenomena occurring in a plasma, even from a qualitative standpoint alone, there is need for a very abundant flow of fresh and reliable experimental data. First, an explanation must be found for the relative importance of the various mechanisms which lead to energy loss from the plasma; and their dependence on time and the initial parameters of the discharge must be established. Second, it is necessary to determine how the anomalous diffusion rate depends on the discharge current, the initial pressure and $H_z$. Third, there is need for the development and application of optical or other techniques for determining the ion temperature. Moreover, it is necessary to study systematically the X-rays produced during the acceleration of the electrons, to measure the intensity and the energy spectrum of the neutral particles emitted as a result of charge exchange in the peripheral regions of the plasma column and, finally, to try to obtain direct evidence for the structure of the magnetic field by means of probe and integrated flux measurements. Such are some of the most obvious details of the experimental programme in this field to be investigated in the near future.

§ **6.8** To conclude this survey of problems related to the properties of slow discharges, we should at least mention briefly other methods of heating and thermally insulating plasma pinches—methods which are at an initial stage of development or are being tested in preliminary experiments.

The heat evolved by the current flowing along the plasma column is by no means the only possible way of heating the plasma in toroidal chambers. The plasma temperature may also be raised by increasing the longitudinal field strength $H_z$. In Chapter V we considered a few examples of the use of fast-rising fields for producing a high-temperature plasma. Such a method of heating is also applicable to slow toroidal discharges. In principle, this method can be an important adjunct to experiments involving the use of a strong external field for stabilising the plasma column.

Let us suppose that at some time $t_0$ the initially constant longitudinal field begins to increase rapidly. The change in $H_z$ is associated with the appearance of the azimuthal electric field $E_\theta$ which causes the particles to drift toward the axis. As was pointed out in Chapter II, the radial velocity is equal to $-r(dH_z/dt)/2H_z$ If this velocity appreciably exceeds the rate of diffusional expansion of the plasma, the radius of the pinch will vary inversely with $\sqrt{H_z}$. The velocity of anomalous diffusion under typical experimental conditions ($H_z \simeq 10^4$ Oe and $r \simeq 10$ cm) is about $10^4$ cm/sec. Therefore, the compression created by the rising external field will prevail over the expansion due to diffusion only if the relative change in $H_z$ is large during a time considerably shorter than $10^{-3}$ sec. To produce such a rapid increase in $H_z$ in large chambers presents a difficult technological problem; it may be accomplished only if the energy source has sufficient power and is able to deliver to the device energy of the order of several tens of megajoules in several tenths of a millisecond.

The heating of the plasma when $H_z$ increases occurs at the expense of kinetic energy accumulated during the acceleration of ions and electrons by the solenoidal electric field. In the time between two Coulomb collisions, each particle is able to undergo many rotations in the magnetic field; therefore, in accordance with the principle of adiabatic invariance, the kinetic energy $W_\perp$ associated with the transverse motion of a particle will increase in proportion to $H_z$ between collisions. Hence, the kinetic energy gain of a particle per unit time will be

$$\frac{W_\perp}{H_z}\frac{dH_z}{dt}.$$

The role of the collisions is that they redistribute the kinetic energy received from the solenoidal field among all the velocity components, and thus restore the initial isotropy of velocities which is disturbed by the acceleration perpendicular to $H$. If the rise-time of the magnetic field is considerably longer than $\tau_{ei}$ (and this is almost always the case in experimental devices), the collisions will completely eliminate the anisotropy of the velocities; thus $W_\perp$ will, on the average, amount to $\frac{2}{3}$ of the total kinetic energy $W$ of the particle. Consequently, we can write

$$\frac{dW}{dt} = \frac{2}{3}\frac{W}{H}\frac{dH}{dt}. \qquad \text{.........(6.18)}$$

Hence

$$\frac{W}{W_0} = \left(\frac{H}{H_0}\right)^{2/3}. \qquad \text{.........(6.19)}$$

Thus the temperature of a contracting plasma should increase in proportion to $H^{2/3}$. Of course, this law will be valid only if one can disregard the other sources of energy being released in the plasma (such as Joule heat due to the longitudinal current), and also neglect the energy loss. This can be done only when the field rises very rapidly. In the more general case, $dW/dt$, given by equation (*6.18*), should be considered as an additive term in the expression for the energy balance of the plasma, along with the other terms discussed above.

A rapid increase of the longitudinal field in toroidal discharges may be reflected in the character of the discharge, not only because it leads to a supplementary heating mechanism, but also because the rising field, while compressing the plasma, can isolate the plasma from the walls or edges of the limiters. Therefore, the field promotes a decrease in the loss and improves the heat balance of the plasma.

In regard to the problem of the influence of a varying external field on the plasma column, there are as yet no reliable experimental data obtained under conditions of adequate purity. For this reason we are forced to confine ourselves here to the general considerations given above. It should be noted that the latter are valid only for conditions when $\sigma_\perp$ is not too small (i.e. time of compression must be less than the skin diffusion time $\sigma_\perp a^2$). A plasma with a low transverse conductivity can contract appreciably only in a very rapidly increasing field.

In addition to the simplest methods of stabilising a current-carrying plasma column which have been discussed at some length in the preceding paragraphs, there are also other possibilities for solving this basic problem. Various methods have been proposed for improving the thermal insulation of a pinch by introducing supplementary stabilising elements which alter the magnetic configuration in the discharge chamber. We will only mention here one such idea, first expressed by Sakharov in the beginning of 1951, at the earliest stages of the work on magnetic thermal insulation. Sakharov's idea was to remove the fundamental defect of the simplest toroidal magnetic trap—the drift of the particles toward the walls—by placing a toroidal metal conductor along the minor axis of the chamber. A current is induced in the conductor, which in turn creates a strong magnetic field around the conductor (Fig. 84). In this magnetic field configuration, a charged particle of moderate energy located inside the

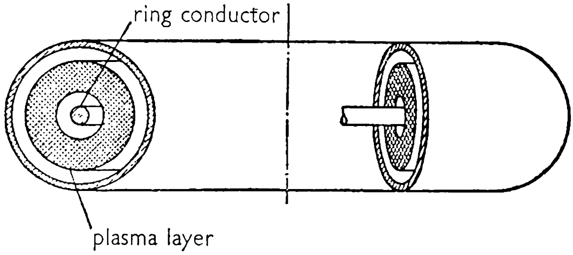

FIG. 84. Levitron—a toroidal pinch with a solid conducting core

torus will be confined and will drift neither to the walls nor to the internal conductor. In a system of this kind, the plasma forms a hollow toroidal layer (shaded in Fig. 84) in the space between the wall of the chamber and the solid conductor (the hard-core) suspended freely in a vacuum.

Recently, this idea became the object of a lively debate in connection with the search for plasma configurations which theoretically should be the most stable (in the magnetohydrodynamic approximation). Colgate, in his discussion of the various methods of stabilising the pinch, came to the conclusion that a toroidal chamber with a longitudinal field $H_z$ and a component $H_\theta$ generated by the current flowing in the hard core should possess a high degree of magnetohydrodynamic stability, since this combination of fields can meet the basic theoretical criteria which must be fulfilled if a stable plasma is to be achieved. For an infinite conductivity plasma, magnetohydrodynamic stability is ensured when the azimuthal and longitudinal fields have a radial distribution as shown in Fig. 85. The dotted lines show the region occupied by the plasma layer. The current in the plasma flows in the opposite direction to that in the metal core. The longitudinal magnetic field serves as an 'outer prop' for the plasma layer. However, the recent calculations of Rebut† have shown that the stability expected for a tubular plasma layer seems less likely when the finite conductivity of the plasma is taken into account. According to these calculations the system can be stable only if the condition

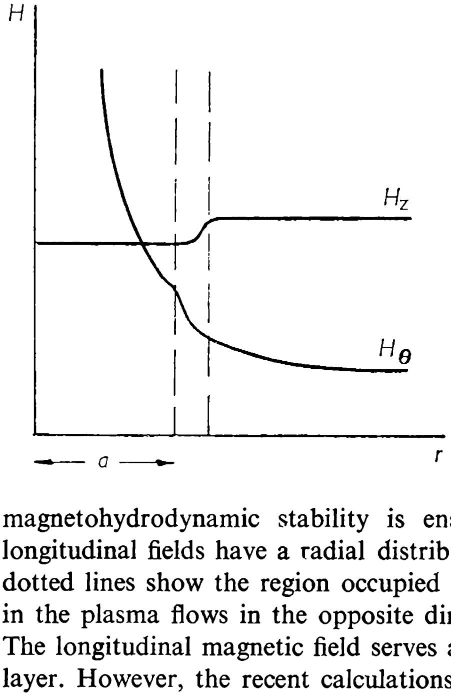

FIG. 85

The components $H_z$ and $H_\theta$ as a function of the radius in the hard-core pinch geometry

$$\frac{4\pi j^2 a^2}{c^2 p} < 1$$

is observed, where $j$ is the longitudinal current density in the plasma, $p$ is the plasma pressure and $a$ is the radius of the plasma layer (it is assumed that its thickness is small compared with $a$). It follows from this condition that a plasma layer can be stable only if the ratio of the plasma pressure to the pressure of the externally generated fields is small.

---

† Paper read at conference on plasma stability at Harwell (1962); see bibliography.

A system with a solid conducting core inside a toroidal chamber has been called a Levitron. An installation of this type, built under Colgate's leadership, has recently been brought into operation at Livermore in the U.S.A. This complex installation fulfils the exacting requirements for vacuum conditions which are now considered obligatory for all experiments with quasi-stationary discharges.

The duration of the heating cycle (the heating mechanisms are not yet established) will be determined by the time during which the conducting core remains near to the minor axis of the chamber. If no current is passed through the conductor, it would simply fall under its own weight. However, if a current flows in the conductor, then the braking mechanism produced by eddy currents begins to act as the conductor begins to fall, and a situation arises that is similar to the case of the expansion of a toroidal current-carrying plasma ring.

A relatively simple calculation shows that under these conditions the time during which the current-carrying core comes to rest after a small displacement downward is approximately the same as the time during which the current exists in the conductor. This time is equal to $L/\Omega$ in order of magnitude, where $L$ is the inductance of the metal ring and $\Omega$ its resistance. In devices of practical interest, this time will be of the order of a fraction of a second.

When the Levitron ends its commissioning phase and becomes an experimental device in regular operation, it will make possible an important step forward in the study of stability problems and methods of producing high-temperature plasmas. Nevertheless, it is difficult to shake off the impression that such an excessively artificial system is unlikely to have ultimate practical application.

## CHAPTER VII

# MAGNETIC TRAPS: GENERAL PRINCIPLES

§ **7.1** The term 'magnetic trap' could refer to any device for producing and confining a hot plasma which operates on the principle of magnetic thermal insulation. It is desirable, however, to restrict the use of the term to systems of a more definite type.

In the preceding chapters we have discussed methods for producing a high-temperature plasma which are based on various forms of the pinch effect. In these devices, the plasma current is generated by external circuits, and this current plays the major role in the confinement of the heated plasma; the particles are, so to speak, attracted to each other by the self-consistent magnetic field which they create. The externally generated magnetic field in such systems is used as a stabiliser for the various plasma perturbations which are unstable in its absence. However, even when external stabilising fields are employed, it is very difficult to avoid all the different types of instability which plague systems based on the pinch effect, especially when the plasma pressure $p$ is of the same order of magnitude as the magnetic pressure, $H^2/8\pi$, associated with the stabilising field. When $8\pi p/H^2 \simeq 1$, the plasma has a strong influence on the distribution of the external magnetic field, and this may lead to the appearance of characteristic instabilities. In addition, the external field may not produce, roughly speaking, enough 'margin of stability' to counteract certain forms of instability peculiar to the pinch effect.

In contrast with systems based on the pinch effect, we use the term 'magnetic trap' for devices in which the external field serves to confine the plasma, and where the fields generated by plasma currents do not, at least in principle, play an essential part. It follows from this definition of magnetic traps that they have a particularly important feature, namely the magnetic field configuration does not depend on the presence of current-carrying plasma; and so $\beta \equiv 8\pi p/H^2$ may be arbitrarily small compared with unity.

Because the external field serves only to confine the plasma, the production of a high-temperature plasma in magnetic traps becomes an independent problem. The solution to this problem may depend to a large extent on the actual shape of the magnetic trap chosen. Various means may be employed to obtain a high-temperature plasma in a magnetic trap: one of them involves filling the trap with fast ions which are injected from a powerful ion source and are trapped in the magnetic field by some irreversible mechanism; in another, preaccelerated plasmoids are injected into the trap; yet again, the trap may be filled with a cool plasma which is then heated by compression with a fast-rising magnetic field or by means of a high-frequency alternating field. There are also methods of obtaining fast ions directly inside the trap by accelerating, with a strong electric field, the ions of a cool plasma within the magnetic system itself.

The first natural step in approaching the problem of magnetic traps is an analysis of the motion of a single charged particle, in order to discover those field configurations which will trap the particle in a restricted region of space. After a satisfactory method of confining single particles has been found, it is then possible to proceed to the study of the behaviour of the large number of particles which make up a plasma in the given field configuration, gradually taking into account such factors as the inter-particle collisions and the electric fields providing quasi-neutrality. Such an approach has the obvious disadvantage that a magnetic field configuration which can trap single particles need not also confine a plasma. However, the approach is very clear; and in addition, the difficulties of developing a theory for the behaviour of the plasma in complicated field geometries can be ignored in the initial stages of the research. Apparently all types of magnetic traps studied so far (on the whole, not very numerous) have been developed by analysing the motion of individual particles in different magnetic field configurations.

The possibility of constructing magnetic traps to confine a high-temperature plasma for an extended period was recognised many years ago. In the initial stages, Soviet, American and English physicists, separated from one another by the high walls of secrecy, tried to arrive at the solution independently. After these barriers had been removed, it became clear that the ideas proposed and developed in these countries were very similar. In the Soviet Union, the investigation of the problem of magnetic traps was given impetus by the work of Sakharov and Tamm who, in 1950, proposed a first model of a thermonuclear reactor based on magnetic confinement. They proposed to ionise and heat a rarefied deuterium gas confined within a toroidal chamber by a strong longitudinal magnetic field generated by coils wound on the outer surface of the chamber. However, such a system has an essential defect as a magnetic trap: in the non-uniform toroidal field, the particles have a drift motion perpendicular to the magnetic lines of force (see § **2.2**). This motion will cause each particle to impinge on the wall of the chamber. This defect was first pointed out by Sakharov and Tamm themselves, who then proposed to eliminate the drift by using either the self-magnetic field of a longitudinal plasma current, or the field of a co-axial current-carrying ring suspended freely inside the chamber. We should also recall that the conclusion that a plasma cannot be confined by the magnetic field of a simple toroidal coil also follows from the magnetohydrodynamic analysis of the equilibrium conditions carried out in § **4.3**.

In further investigations, several different types of magnetic configurations were found in which it might be possible to trap single charged particles in a restricted volume. Thus arose the diversification of the experimental studies of magnetic traps. This chapter is concerned mainly with the properties of traps in which constant magnetic fields are employed to confine the plasma. Systems based on the use of high-frequency electromagnetic fields—alone or in combination with a constant field—are considered in the closing paragraphs of Chapter VIII.

Magnetic traps involving a constant (or a quasi-static) magnetic field may be divided into two chief categories: traps with closed lines-of-force and limited drift; and traps with magnetic 'plugs' (or 'mirrors').

§ **7.2** In devising systems of the first category, the main problem is to find conditions in which the drift motion is restricted so that the particles stay within a limited region of space. The simplest trap with these properties is formed by a current-carrying conductor in the shape of a ring. If the field generated by the current is large enough (so that the Larmor radii are sufficiently small), the particles located near the conductor will be trapped in a restricted region of space. Each particle will move along the magnetic lines of force surrounding the conductor. In addition, they will drift normal to the lines of force and parallel to the surface of the conductor. The general form of the trajectory of a charged particle in such a field is shown in Fig. 86.

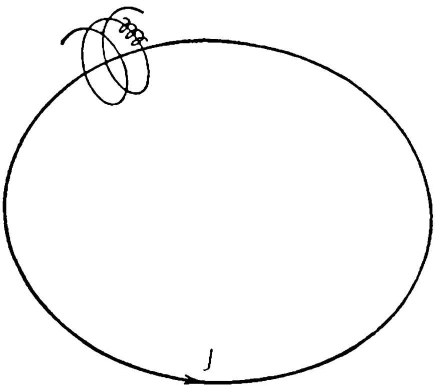

FIG. 86

Trajectory of a charged particle in the field of a current-carrying ring

This simple system is an example of an 'ideal' trap, i.e. a system in which particles can be confined within a restricted region, whatever their directions of motion are, provided that their energies do not exceed a certain value. The current-carrying ring is a particular example of an axially symmetric magnetic system. In studying the behaviour of particles in such systems one can use the general equations of motion, remembering that both the equations and their interpretation are considerably simplified by the axial symmetry of the field. A mathematical analysis of these equations will be given in § 7.3, but here we shall briefly state some qualitative features of the trajectories.

In an axially symmetric field, the motion of a particle with sufficiently low energy may be resolved into two components: the drift in the $\theta$-

direction, as a result of which the trajectory revolves around the symmetry axis $z$ of the magnetic system; and motion in the $r$–$z$ plane, i.e. in a plane containing the symmetry axis $z$.†

The nature of particle motion in an axially symmetric magnetic field is depicted in Fig. 87, which shows a projection of the trajectory onto the $r$–$z$ plane rotating with the particle around the axis of the magnetic system. For an ion or electron of small enough kinetic energy, the region in which the projection of the trajectory is located becomes a narrow band bounded by two of the magnetic lines of force. Such bands, surrounding the current-carrying conductors which generate the magnetic field, define zones of possible motion for single particles whose Larmor radii are small compared with their distance from the $z$ axis. If this condition is not fulfilled, the zones of possible motion may have a different shape. In particular, for particles whose Larmor orbits encircle the axis (Fig. 88), these zones may, under certain conditions, be bounded in the $z$-direction (see § 7.3).

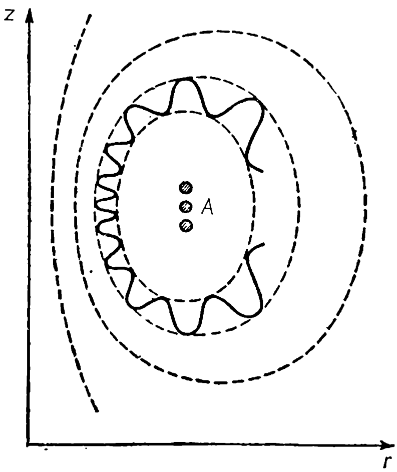

FIG. 87. Projection of the trajectory rotating in the $r$-$z$ plane; $A$—cross-section of conductors which generate the field

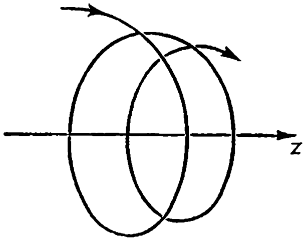

FIG. 88. Trajectory 'captured' on the axis of the magnetic system

In principle, a circular current-carrying conductor is not the only type of ideal trap; any other system of axially symmetrical coils occupying a restricted portion of space can serve as such a trap. It should be observed that such a system can also preserve the properties of an ideal trap when it is placed in an external field produced by other sources. In particular, we can imagine a magnetic field generated by a current-carrying loop together with a linear current-carrying conductor on the axis. The straight conductor generates a magnetic field $H_\theta$ with circular lines of force. The field structure of such a system is equivalent to that generated by a toroidal coil enclosing a circular current, since the configuration of the fields near the current-carrying ring is identical in both cases.

---

† $r$, $\theta$ and $z$ are standard cylindrical polar coordinates, with the $z$ axis being the axis of symmetry, i.e. the major axis, of the current-carrying rings. 'Axially symmetric' fields have components $H_z$ and $H_r$, but $H_\theta = 0$.

In the field generated by the linear conductor (or the toroidal coil) alone, the charged particles drift in the $z$-direction. However, in the presence of the additional field produced by the current-carrying ring, the picture of the motion will be different. The lines of force of the combined field spiral around the ring current, and as a result the particle trajectories assume a form similar to the one they have in the field of the ring current alone. A detailed study of this case shows that the size and shape of the regions of confinement for particles with a small enough Larmor radius change only slightly when the $H_\theta$ component of the field is turned on, i.e. the trap preserves its properties.

At an early stage of the research, this type of system, which involves the superposition of two fields of different character, was recognised as an improvement on the original version of a trap involving only one type of field. In this connection, we should note from the standpoint of pure mechanics the addition of the $H_\theta$ component plays no substantial part in this system, and is in a certain sense useless. However, it must be kept in mind that this statement holds only for the case of the motion of an isolated particle in a given external field. As we have indicated in the preceding chapters, if the ring current is created by the motion of the charged particles themselves, the equilibrium is inherently unstable, and a strong external stabilising field becomes indispensable.

In studying the question of particle confinement in a magnetic field, we have not yet considered the practical limitations on the creation of fields of the required shape. However, only those magnetic systems which can be achieved technologically are of interest in the solution of our basic problem. From this point of view, a magnetic trap with a steady ring current is a mathematical abstraction. In order to sustain a constant current in the ring, an e.m.f. must be applied to the conductor. The circuit can be opened at some point, and the ends diverted to one side. If we analyse in detail the behaviour of the particles in the vicinity of the external leads, it turns out that, whatever the means of supplying the current, there is an unavoidable leakage of particles caused by the drift along the supply leads (or by the direct impingement of the particles on the surface of these leads). The same phenomena also take place in other axially symmetric magnetic systems designed to serve as ideal traps.

In principle, however, there are conceivable variants of axially symmetrical traps in which the supply leads are not necessary. Two such variants are:

1. The current in the conducting ring can be generated by induction, while the conductor itself is levitated in a vacuum by means of magnetic forces due to the interaction with the external circuit or with eddy currents arising in a metallic shell. This idea was proposed by Sakharov as far back as 1950. It is also the basis of the design of the Levitron, discussed in the

preceding chapter. The field of the levitated conducting ring can be combined with fields of a different shape, for instance with the field of a toroidal coil surrounding the conductor.

2. The ring current can also be generated by injecting particles into a magnetic field, almost at right angles to the direction of ***H***. For instance, an intense beam of high-energy relativistic electrons could create, as it were, a special kind of solenoid. The turns of this solenoid will be the successive loops traced out by the trajectories of the injected electrons. This idea underlies the Astron device, proposed by Christofilos in the U.S.A. It will be described further in § **8.5.**

Completely different methods of restricting particle drift in toroidal devices are also possible. The rotation of the lines of force, necessary for counteracting the drift, can be achieved without the aid of a ring current inside the chamber. The simplest example of such a method is the system illustrated in Fig. 89. It consists of a torus bent to the shape of a figure eight. This modification of a toroidal trap was proposed by Spitzer in 1950 and independently by the present author in 1955. Such a system is not an ideal trap, since it confines only those particles whose velocity vector lies within a definite range of allowed directions. A particle will be trapped if its velocity vector forms a sufficiently small angle with the direction of the lines of force. With this condition, the particle passing through a curved part of the chamber (for instance, *AB*) has insufficient time to drift to the wall, and will therefore move on to the second curved part (*CD*), where the drift motion is in the opposite direction. Ideally, the drift displacements in the two curved parts of the chamber exactly counteract each other, and the particle can travel an infinite number of turns around the chamber without reaching the walls. If the ratio of the parallel velocity to the transverse velocity is too small, the particle will be too far displaced normal to the lines of force and, in the very first passage through the curved part of the chamber, the drift will carry it to the wall. The fate of a charged particle in a chamber of the figure-eight type depends on the quantity

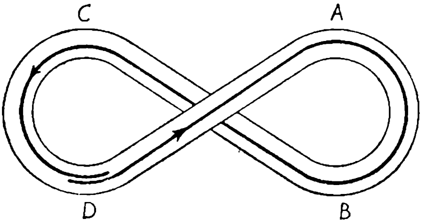

FIG. 89

Magnetic configuration of the figure-eight type; a line of force is indicated by the arrows

$$x = \frac{b \cos \alpha}{\pi \rho_H},$$

where $b$ is the minor radius of the chamber, $\rho_H$ is the Larmor radius of the particle and $\alpha$ is the angle between the direction of the velocity vector and $H$. If $x$ is much smaller than unity, the particle will be lost; if $x$ is much larger than unity, it will be trapped. Although these considerations correctly characterise most of the properties of the trap under consideration, they are too superficial and leave out one of its most important properties thanks to which it assumes a special significance as the prime representative of a broad category of magnetic traps generally called Stellarators. The systems in the Stellarator category are based on the idea of the rotational transform of the magnetic lines of force, originated and developed by Spitzer and co-workers at Princeton (U.S.A.). Sections **8.1–8.6** will be devoted to the exposition of this idea and to the complex of theoretical and experimental research associated with it.

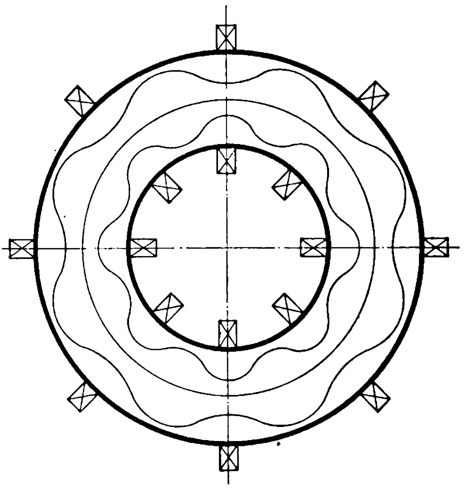

FIG. 90

Corrugated or 'bumpy' torus

The drift should also be restricted when the longitudinal magnetic field in a torus is corrugated (by a non-uniform winding on the surface of the chamber). A chamber with such a 'bumpy' field is shown in Fig. 90. A particle moving in such a field will undergo a helical drift motion as a result of which its trajectory rotates round the minor chamber axis. Thus the particles will not approach the wall as they travel along the chamber (the rotation of the trajectories, caused by the longitudinal non-uniformity of the field, offsets the toroidal drift). Systems of this type were first examined by Budker and Kadomtsev. The most significant results of the theory of particle motion in traps of the corrugated torus type were obtained by Morozov and Solov'ev. They showed that in the guiding centre approximation, for particles having sufficiently small Larmor radii, the bumpy torus represents an 'almost ideal' trap. However, when such a trap is filled with a plasma, its ideal properties seemingly vanish. Theoretical analysis shows that a plasma in a corrugated field should be unstable (see § **7.4**).

§ **7.3** Let us now consider the general theory of the motion of charged particles in axially symmetric magnetic fields and some corollaries of this theory which pertain to magnetic traps.

To characterise a magnetic field in this case it is convenient to use the vector potential $A$ which is defined by the expression curl $A = \boldsymbol{H}$. In the axially symmetric case, both $A$ and $\boldsymbol{H}$ depend on the $r$ and $z$ coordinates alone. Therefore, in cylindrical coordinates the vectorial relationship between $A$ and $\boldsymbol{H}$ is reduced to the following equations:

$$H_r = -\frac{\partial A_\theta}{\partial z}, \qquad \qquad \text{.........}(7.1)$$

$$H_z = \frac{1}{r}\frac{\partial r A_\theta}{\partial r}. \qquad \qquad \text{.........}(7.2)$$

These formulae contain only the $\theta$-component of the vector potential, which we shall refer to simply as $A$. A direct relation exists between the values of $A$ and the shape of the lines of force. The equation of a line of force, $dr/dz = H_r/H_z$, can be reduced by means of (7.1) and (7.2) to the form

$$\frac{1}{r}\frac{\partial rA}{\partial r}\,dr + \frac{1}{r}\frac{\partial rA}{\partial z}\,dz = 0.$$

Consequently, $rA$ is constant along a line of force, i.e. the equation of a line of force is of the form

$$rA = \text{const.} \qquad \qquad \text{.........}(7.3)$$

For a given field defined by some given configuration of the conductors, the value of $A$ can be determined in various ways. We shall indicate only one of them. If the field strength on the axis of the system $H(z)$ is given as a function of the $z$ coordinate, both components of $\boldsymbol{H}$ and the value of the vector potential may be computed by means of the series

$$H_z = H(z) - \frac{r^2}{4}H''(z) + \ldots + (-1)^n \frac{1}{(n!)^2}\left(\frac{r}{2}\right)^{2n} H^{(2n)}(z), \qquad \text{.........}(7.4)$$

$$H_r = -\frac{r}{2}H'(z) + \frac{r^3}{16}H'''(z) - \ldots + (-1)^n \frac{1}{(n-1)!\,n!}\left(\frac{r}{2}\right)^{2n-1} H^{(2n-1)}(z) \qquad \text{.........}(7.5)$$

$$A = \frac{r}{2}H(z) - \frac{r^3}{16}H''(z) + \ldots + (-1)^{n+1} \frac{1}{(n-1)!\,n!}\left(\frac{r}{2}\right)^{2n-1} H^{(2n-2)}(z). \qquad \text{.........}(7.6)$$

It should be remembered that the above expressions are valid only for a vacuum field. They are therefore inapplicable when all the space is taken up by a plasma whose pressure is so high that it alters the field strength substantially.

The equations of motion of a particle of charge $q$ and mass $m$ in an axially symmetrical field are:

$$\ddot{z} = -\frac{q}{mc}r\dot{\theta}H_r, \qquad \text{.........}(7.7)$$

$$\ddot{r}-r\dot{\theta}^2 = \frac{q}{mc}r\dot{\theta}H_z, \qquad \text{.........}(7.8)$$

$$\frac{d}{dt}r^2\dot{\theta} = \frac{q}{mc}r(\dot{z}H_r-\dot{r}H_z). \qquad \text{.........}(7.9)$$

By using (*7.1*) and (*7.2*), it is possible to transform the right-hand side of equation (*7.9*) as follows:

$$r(\dot{z}H_r-\dot{r}H_z) = -\dot{z}\frac{\partial rA}{\partial z}-\dot{r}\frac{\partial rA}{\partial r} = -\frac{d}{dt}rA. \qquad \text{.........}(7.10)$$

Making use of this result and integrating (*7.9*), we obtain

$$-r^2\dot{\theta} = \frac{q}{mc}rA+C_1. \qquad \text{.........}(7.11)$$

The constant $C_1$ is determined from the initial conditions. Substituting the expression for $\dot{\theta}$ into equations (*7.7*) and (*7.8*), we can write these equations, after some relatively simple transformations, in the following form:

$$\ddot{z} = -\frac{\partial}{\partial z}\frac{1}{2r^2}\left(\frac{q}{mc}rA+C_1\right)^2, \qquad \text{.........}(7.12)$$

$$\ddot{r} = -\frac{\partial}{\partial r}\frac{1}{2r^2}\left(\frac{q}{mc}rA+C_1\right)^2. \qquad \text{.........}(7.13)$$

With this notation, the equations for $\ddot{z}$ and $\ddot{r}$ take on a new meaning: they represent the motion of a particle in the $r$–$z$ plane under the influence of forces which are functions of the coordinates. In the field of these forces, the particle has a potential energy for which the following expression can be written:

$$U_p = \frac{m}{2r^2}\left(\frac{q}{mc}rA+C_1\right)^2. \qquad \text{.........}(7.14)$$

The quantity $U_p$ is called the 'meridian potential'.

The above results may facilitate the analysis of the motion of a particle in various concrete cases. Some characteristic features of this motion can sometimes be described even without solving equations (*7.12*) and (*7.13*) by analysing the shape of the potential function $U_p$. In this manner, it is possible to find the boundaries of the possible particle motion and to investigate the geometrical shape of these regions.

Let us first consider the motion of a particle whose Larmor radius is small compared with the distance $r$ from the symmetry axis. In this case, the inequality

$$|r^2\dot{\theta}| \ll \frac{q}{mc}|rA| \qquad \text{.........(7.15)}$$

will apply. Indeed, according to equation (*7.6*), the vector potential is equal to $rH$ in order of magnitude, and $|r^2\dot{\theta}| \simeq rv$ where $v$ is the speed of the particle. Therefore,

$$\left|\frac{r^2\dot{\theta}}{\frac{q}{mc}rA}\right| \simeq \frac{rv}{\frac{q}{mc}r^2H} = \frac{mvc}{qH}\cdot\frac{1}{r} = \frac{\rho_H}{r}. \qquad \text{.........(7.16)}$$

The value of $\rho_H/r$ is, by definition, much smaller than unity, and hence the inequality (*7.15*) is proved.

Let us return to equation (*7.11*). Obviously, it can apply simultaneously with (*7.15*) only when the constant $C_1$ is nearly equal in magnitude and of opposite sign to the term containing the vector potential $A$. For such a compensation to occur over the whole path of the particle, the value of $rA$ must remain virtually constant along the trajectory. According to equation (*7.3*), the constancy of $rA$ means that the particle, in its motion in the space defined by the coordinates $r$ and $z$, follows a selected line of force and travels along it round the current-carrying conductors.

This conclusion may also be interpreted from another point of view. The range of $r$ and $z$ over which the particle can move is determined by the shape of the potential function $U_p$. This function includes the quantity $\left(\frac{q}{mc}rA+C_1\right)^2$ as a factor. One can select a line of force to which the particle will be attached, so to speak. Along this line the above factor is zero, and consequently, $U_p$ is also equal to zero. However, when the displacement in the direction perpendicular to the line of force is small, $U_p$ will increase rapidly (as the square of the displacement). It can be stated, therefore, that the motion of the particle takes place in a deep circular potential well running along one of the lines of force. In moving inside this well, the particle rebounds successively from the inner and outer walls of the potential barrier; thus its trajectory will represent a rapidly oscillating curve (see Fig. 87).

Let us now consider the motion of a particle whose Larmor radius is comparable in magnitude to its distance from the $z$ axis. To simplify the calculations, let us assume that the particle moves in a region so close to the $z$ axis that $A$ can be assumed equal to $\frac{r}{2}H(z)$.† Under this condition,

$$-r^2\dot{\theta} = \omega_H r^2/2 + C_1.$$

---

† It is assumed that in the region of space considered $H(z) > 0$.

The cyclotron frequency $\omega_H$ is a function of $z$. The constant $C_1$ depends on the initial conditions. Designating the values of $r$, $\dot{\theta}$ and $\omega_H$ at the start of the trajectory by $r_0$, $\dot{\theta}_0$ and $\omega_{H0}$, we obtain

$$C_1 = -r_0^2(\dot{\theta}_0+\omega_{H0}/2).$$

Hence,

$$-r^2\dot{\theta} = \frac{\omega_H}{2}r^2-r_0^2\left(\dot{\theta}_0+\frac{\omega_{H0}}{2}\right).$$

The left-hand side of this equality cannot exceed $rv_0$, where $v_0$ is the total velocity of the particle. For this reason, the motion will take place only in that region of space where the condition

$$\frac{\omega_H}{2}r^2-r_0^2\left(\dot{\theta}_0+\frac{\omega_{H0}}{2}\right) \leqq rv_0$$

is satisfied.

To find the boundaries of this region, it is necessary to take the equals sign and solve the resulting equation for $r$. We thus find

$$r = \frac{v_0}{\omega_H}\left[1\pm\left(1+\frac{\omega_H r_0^2}{v_0^2}(2\dot{\theta}_0+\omega_{H0})\right)^{\frac{1}{2}}\right]. \qquad \text{.........}(7.17)$$

An analysis of this expression shows that the shape of the region of possible motion depends primarily on the relation between $\dot{\theta}_0$ and $\omega_{H0}$. If $-\dot{\theta}_0 < \frac{\omega_{H0}}{2}$, the term under the square root sign will be positive for all positive values of $\omega_H$, and hence, both values of $r$ will be real. When $-\dot{\theta}_0 > \frac{\omega_{H0}}{2}$, the root will be real only in the region of space where the condition

$$\left|\frac{\omega_H r_0^2}{v_0^2}(2\dot{\theta}_0+\omega_{H0})\right| < 1 \qquad \text{.........}(7.18)$$

is satisfied.

To explain the meaning of this inequality, we note that under the given initial conditions it imposes a definite restriction on $\omega_H$, i.e. on the value of the magnetic field strength. Let us suppose that a particle located initially at a point where the field strength is $H_0$ moves in the direction of increasing $H$. The left-hand side of the inequality (*7.18*) then increases and, at some value $H = H_1$, reaches unity. The value of $H_1$ determines the boundaries of the region in which the particle can move. In particular, if the field strength increases along the $z$ axis on both sides of some initial point of the trajectory, the particle oscillates along the axis in the region where $H < H_1$. $H_1$ is given by the condition

$$\frac{H_1}{H_0}\frac{\omega_H r_0^2}{v_0^2}(2\dot{\theta}_0+\omega_{H0}) = -1. \qquad \text{.........}(7.19)$$

Introducing the definitions $r_0\dot{\theta}_0/v_0 = \gamma$ and $-2\dot{\theta}_0/\omega_{H0} = \zeta_0$, we can write (*7.19*) as follows:

$$\frac{H_1}{H_0} = \frac{1}{\gamma^2}\frac{\zeta_0^2}{4(\zeta_0-1)}. \qquad \ldots\ldots\ldots(7.20)$$

In the case under consideration, $\zeta_0 > 1$. As can easily be shown, this means that the particle trajectory encircles the axis in each Larmor revolution. Figure 91 shows projections of the trajectories on the plane perpendicular to the $z$ axis for different initial conditions. These projections represent slightly deformed circles (strictly speaking, these trajectories are not closed). In (a) the magnetic axis lies outside the trajectory during the motion of the particle, and the azimuth $\theta_0$ is less than half the angle $\omega_{H0}t$, subtended at the centre of the Larmor circle, i.e. $-\dot{\theta}_0 < \omega_{H0}/2$, or $\zeta_0 < 1$. In (b), as can readily be seen, $-\dot{\theta}_0 > \omega_{H0}/2$, i.e. $\zeta_0 > 1$.

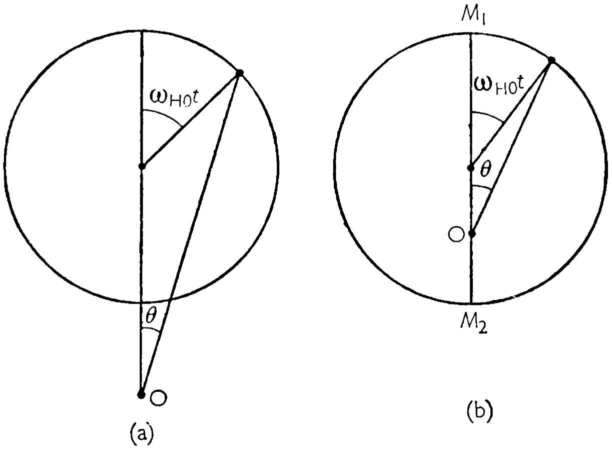

FIG. 91. Projections of trajectories on a plane perpendicular to the magnetic axis O

Thus in a field whose strength increases along the $z$ axis in both directions from the central region, and under specific initial conditions of motion, the particles should be trapped inside a potential well which occupies some portion of space inside the magnetic system. Such a potential well (i.e. the zone of possible motion) in the $r$–$z$ plane is depicted in Fig. 92. At points where condition (*7.20*) is met, the two values of $r$ as given by (*7.17*) coincide. These points mark the boundaries of the zone in the axial direction.

The possibility of trapping particles in systems with magnetic mirrors is also a direct consequence of the adiabatic invariance of $W_{\perp}/H$. However, a weak point of the arguments leading to this conclusion remains, viz. the problem of the duration of adiabatic invariance, which cannot be solved satisfactorily within the framework of the approximate theory. Moreover, so long as the answer to this problem is not known, the time during which the particle remains in the trap cannot be calculated.

The more rigorous theory presented above makes possible a step forward in this direction. It shows that in systems with axial symmetry the particles may indeed be trapped for an indefinitely long period between two regions of strong magnetic field, and this will take place over a rather wide range of initial conditions. This conclusion can be countered with the argument that the above study of the nature of particle motion in the region close to the axis of the magnetic system is not rigorous enough, since it takes into account only the first term of the series expansion of $A$ in powers of $r$. However, as shown by a detailed analysis of specific cases, this restriction does not affect the qualitative aspect of the fundamental result of the above analysis because, when the higher-order terms are considered, the shapes of the zones of allowed motion are not altered substantially. The relation (*7.20*), which determines the boundaries of the zone of allowed motion, is analogous to the relation (*2.10*), which follows from the condition of adiabatic invariance. The agreement between these relations becomes especially clear when the point $M_1$ (or $M_2$) is chosen as the origin of the trajectory in Fig. 92; at this point, the radial component of the particle velocity becomes zero, and therefore, the quantity $r_0\dot{\theta}_0$ represents the velocity component perpendicular to the direction of the magnetic field ($r\dot{\theta} = v_\perp$). When the initial conditions are thus chosen, $\gamma = \sin \alpha_0$, where $\alpha_0$ is the angle between the initial velocity vector and $H$. Consequently, the relation (*7.20*) can be written in the form

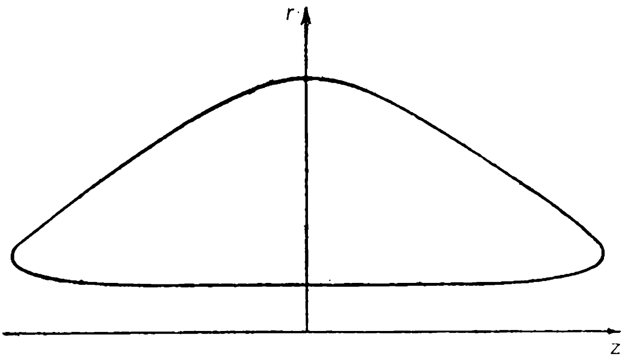

FIG. 92. Region of possible motion in the *r*-*z* plane

$$\frac{H_1}{H_0} = \frac{1}{\sin^2 \alpha_0} \cdot \frac{\zeta_0^2}{4(\zeta_0 - 1)}. \qquad \text{.........}(7.21)$$

When $\zeta_0 = 2$, i.e. when the centre of the initial Larmor circle lies on the $z$ axis, the above expression for $H_1/H_0$ is identical with (*2.10*). In general, when $\zeta_0 \neq 2$, the two formulae give different values of $H_1$. This should not appear strange. Equation *(2.10)*, which follows from the adiabatic invariance of $W_\perp/H$, determines the actual position of the point of reversal of the guiding centre, whereas the relation *(7.21)* determines the limiting depth to which the particle can penetrate in a strong field without violating conservation of energy for motion in the $r$–$z$ plane. It is evident that conservation of energy cannot in general impose more rigorous restrictions on the motion of the particle than those which follow from a detailed analysis of the shape of the trajectory. It is therefore quite natural that *(7.21)* should yield higher values of $H_1$ than *(2.10)*. When $\zeta_0 < 1$, an analysis based on equation *(7.17)* turns out to be less fruitful: it does not yield any results which might be interpreted as indicating that the particle rebounds from a strong field. This does not mean, of course, that in this case the particles move freely across strong field regions. Condition *(2.10)*, which follows from the adiabatic invariance of $W_\perp/H$, holds for both $\zeta_0 > 1$ and $\zeta_0 < 1$.

The theory expounded in this section provides the necessary equipment for an accurate calculation of the trajectories for any value of the ratio of the Larmor radius to the dimensions of the magnetic system. In each special case the problem amounts to a solution of the differential equations *(7.12)* and *(7.13)* with a given function $A$, which can be found when the field distribution along the axis of the magnetic system is known (alternatively, the function may be calculated from known formulae of electrodynamics). An accurate calculation of the trajectories is especially interesting in the analysis of various methods for injecting fast ions into a trap with axially symmetric fields.

§ **7.4** Whatever the method proposed for creating a high-temperature plasma, the main problem to be solved is the stability of the plasma configuration. Some particular aspects of this problem were outlined in the preceding chapter as part of the exposition of the results of studies of powerful quasi-stationary discharges. The analysis of the stability of a plasma confined in a magnetic trap is equally important. It is easily seen that in this case also the various forms of instability constitute the main obstacle to the achievement of the primary goal.

There is as yet no complete and general theory of plasma stability in magnetic fields; one therefore has to use isolated, individual results of theoretical analysis. These results cannot usually be expressed in a form that is categorical enough to permit one either positively to reject some types of magnetic trap or, conversely, to guarantee the stability of plasma in other kinds of magnetic traps. In practical application, the theory of stability provides suggestions rather than rigorous rules.

The problem of instability may be stated in the general form, as follows: let us assume that a plasma having a certain set of characteristic parameters (density, pressure, electron and ion velocity distributions) is in a state of macroscopic equilibrium. Can such an equilibrium be maintained for a sufficiently long time, or will small fluctuations of the parameters lead to disturbances which will grow rapidly and cause the plasma to escape from the volume in which it is trapped? It is important to emphasise at this point that we are not interested in all changes in the plasma state, but only in those which lead to a disturbance of the magnetic confinement, i.e. in the motion of the plasma across the magnetic lines of force.

Every particular stability problem consists of the study of the response of the plasma system to a small change in any given parameter. These disturbances of the equilibrium may at first be divided roughly into two categories. The first comprises disturbances which may be called magnetohydrodynamic. This means that we are dealing with processes in which the plasma behaves very much like a homogeneous conducting fluid (or a mixture of two fluids). The second category comprises more detailed effects which depend on the distribution of the electron and ion velocities. Included here are such phenomena as, for instance, the generation of a fast electron excess at the high-velocity end of the Maxwell distribution; to this group we can also add the different processes connected with electron and ion oscillations, which may be excited by oriented streams of electrons and ions, or may arise with certain kinds of non-Maxwellian velocity distributions. This group of disturbances may be called disturbances of the kinetic type. This classification is rather arbitrary because, in reality, the disturbances of the equilibrium may involve both the magnetohydrodynamic and the kinetic properties of the plasma. Nevertheless we shall differentiate between these two forms of disturbance in order to simplify the presentation of the results obtained from theoretical analysis.

Let us begin with the relatively better studied problem of the stability of a plasma with respect to disturbances of a magnetohydrodynamic nature. Let us first suppose that the plasma—which has an infinite conductivity—excludes the magnetic field completely from some region of space, so that the plasma has a sharply defined boundary at which the field changes abruptly from zero to some finite value. The equilibrium between the plasma and the external field is established when $p = H^2/8\pi$ at the boundary. As shown in Chapter IV, the plasma boundary must follow the lines of force of the external field. To find the conditions under which such an equilibrium will be stable, let us assume that the plasma boundary is deformed so that a limited area is slightly deflected towards the external field. The plasma pressure remains unchanged, but the field strength at the boundary of the deformed segment will either increase if $H$ increases with the distance from the surface of the plasma, or decrease if the gradient of $H$ has the opposite direction. In the first case, the initial deformation causes $H^2/8\pi$ to exceed $p$ at the deformed boundary; therefore, the deflected part of the boundary is acted on by a restoring force. Thus, this is a case of stable equilibrium. In the second case, the force is in the other direction, and so the deflection should increase with time; this is a case of an unstable plasma boundary.

The nature of the change in $H$ near the plasma boundary is related to the geometry of the lines of force. This relation is usually a simple one; so that a glance at the shape of the lines of force near the surface of the plasma is sufficient, in most cases, to tell whether or not stability will prevail. In particular, if the lines of force near the plasma boundary lie in a plane, $H$ will increase towards their centre of curvature, i.e. the gradient of $H$ is oriented along the inner normal to the line of force. Hence, if the plasma has a convex surface (Fig. 93a), its boundary will be unstable, and if the surface of the plasma is concave (Fig. 93b), it will be stable. Under these conditions, the stability or instability is local in character, since it is determined only by the geometry of the external field near a given element of the plasma surface.

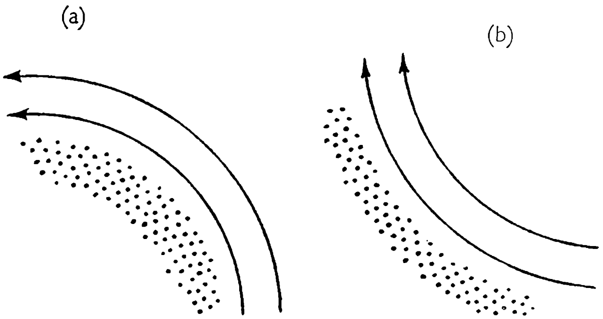

FIG. 93. Unstable and stable forms of the plasma boundary

From the criterion established above it follows that of the various plasma configurations with a sharply defined boundary, only those whose entire surface is bent inwards can be stable. The simplest example of such a configuration is a plasma in a trap with a hyperbolic field (cusp) geometry. Any system in which even a small part of the plasma surface is convex should be unstable.

However, this uncomfortable result is valid only when the plasma in the trap has a sharp boundary and completely excludes the magnetic field from the volume it occupies. This latter condition is most significant. If it is not satisfied, so that the condition $p \ll H^2/8\pi$ is relevant, then the stability criteria may change substantially. The magnetohydrodynamic stability of a plasma whose pressure is considerably smaller than the magnetic pressure has been studied by Rosenbluth and Longmire in the U.S.A. and by Kadomtsev in the U.S.S.R. We shall cite the principal results obtained by these authors. As before, we shall assume that the plasma has infinite conductivity. This condition should almost always be valid when the deformations occur rapidly enough.

If a small amount of plasma is introduced into a magnetic field, it will spread freely along the lines of force, filling a certain flux tube. Since we assume $p^2 \ll H^2/8\pi$, the magnetic field will remain almost unchanged by the plasma. Moreover, thanks to the infinite conductivity, the magnetic field may be considered as frozen to the plasma; therefore, in any deformation, the field should be displaced together with the plasma. This circumstance imposes some severe limitations on the character of the possible deformations.

The flux tube filled with the plasma cannot be bent much because the bending of the lines of force is associated with a substantial increase in the magnetic energy which, for a small value of $\beta$, cannot be offset by the work done by kinetic pressure of the plasma. For this reason, the local deformations encompassing only some small segment of any flux tube are automatically stabilised. However, the plasma pressure may give rise to deformations in which no distortion of the magnetic field takes place. This means that, during the deformation, the elementary plasma-filled flux tube is displaced in such a way that the flux carried out with the plasma is replaced without any net change in $H$.

The plasma located inside the flux tube occupies a volume $\Omega = \int S\,dl$, where $S$ is the area of a cross-section of the tube and the integral is taken along the line of force. Since the magnetic flux in the tube should remain constant, $SH = \text{const.}$ and hence $\Omega = C\int dl/H$ where $C$ is a constant. The plasma-filled tube will attempt to move so as to make the volume $\Omega$ increase, since this corresponds to the natural tendency of a gas to expand. This means that $U = -\int dl/H$ plays the part of potential energy in the process of plasma displacement. The plasma will attempt to move in the direction of decreasing $U$, until it reaches a region already occupied by a plasma with a higher pressure.

The type of deformations examined here are characterised by the displacement of entire flux tubes which change places with one another. They are usually called interchange deformations or convective deformations. When they emerge at the boundary between the plasma and the magnetic field, such deformations impart a special 'fluted' or 'grooved' structure to the plasma surface (Fig. 94). Essentially, the term 'flute' may be used when the plasma has a sharp boundary. The stability condition for flute deformations is that the potential energy of the plasma in an elementary flux tube must increase when the flux tube rises through the plasma surface and forms a ridge on it. This condition for stability can be written as follows

$$\delta \int \frac{dl}{H} < 0. \qquad \text{.........}(7.22)$$

The variation of the integral is taken between two infinitesimally close lines of force along the normal to the plasma surface.

The stability criterion obtained above characterises the properties of the surface layer of the plasma and has meaning only for a plasma with a sharply defined boundary. A more general stability condition may also be derived for the case when the plasma pressure changes continuously in space. According to Rosenbluth and Kadomtsev, it is of the form

$$\operatorname{grad} p \cdot \operatorname{grad} U < -\gamma p U \left( \frac{\operatorname{grad} U}{U} \right)^2, \qquad \ldots\ldots\ldots(7.23)$$

where $\gamma$ is the ratio of specific heats. When this inequality is used, it must be remembered that $U$ is always negative.

A graphic example of the application of conditions (*7.22*) and (*7.23*) is the behaviour of a plasma surrounding a linear current-carrying conductor. In this case, $H = 2J/cr$ and hence $U = -2\pi r/H = -\pi c r^2/J$ per unit length of conductor. The criterion (*7.22*) leads to the conclusion that in such a field, the cylindrical plasma layer can have a stable inner boundary for any value of $r$, but that its outer boundary is always unstable. However, from the more general condition for convective stability, (*7.. 3*), it follows that if the plasma layer does not have a sharply defined boundary but the pressure decreases monotonically with increasing distance from the axis, stability can nevertheless be attained. For this it is only necessary that $p$ varies no faster than $r^{-2\gamma}$.

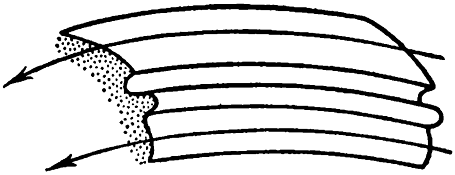

FIG. 94. Flute deformation of a plasma boundary; arrows show the magnetic lines of force

Unfortunately, this approach to the problem of the stability of a rarefied plasma suffers from the disadvantage that it can be applied only to systems with a comparatively simple geometry for the lines of force, with the supplementary condition that the plasma pressure is isotropic. For systems where one line of force can fill a whole surface by swinging round and round (as is the case in the Stellarator, for instance), the concept itself of the interchange deformation loses its simple physical meaning. The inapplicability of the above notions to the analysis of systems with anisotropic plasma pressure (as in magnetic mirror traps) is also rather apparent, since in this case one cannot speak of the free spreading of a plasma along a flux tube. The problem of the stability of a low-pressure plasma can, however, be approached from a completely different point of view by using a method based on an analysis of the motion of individual particles in non-uniform magnetic fields. This method, of course, is not as general as that used to obtain the above stability conditions, but it has the merit of maximum clarity and of permitting the solution of stability problems when the pressure is anisotropic.

We shall restrict ourselves to applying this method to an examination of plasma stability in systems having an axially symmetric magnetic field, and we shall first consider the case where the deformation occurs at the outer boundary of the plasma. Let us assume that in equilibrium the plasma forms some body of revolution bounded by lines of force arranged symmetrically about the axis. Let us suppose further that this equilibrium is disturbed by a surface deformation in which a small ridge (hump) of rectangular cross-section, directed along the lines of force (Fig. 95), is formed on this surface. The formation of such a ridge is a special case of the flute deformation. Let us now describe the motion of the particles inside the ridge. Owing to the non-uniformity of the field, they are subject to drift in the direction perpendicular to $\boldsymbol{H}$ and grad $H$. In the present case, both these vectors lie in the $(r, z)$ plane, so that the drift will take place in the azimuthal direction: the ions and electrons will drift in opposite directions. In the region where the lines of force are convex (i.e. the field decreases with increasing distance from the axis), the ion drift will be counterclockwise if one looks along the lines of force in the direction of $\boldsymbol{H}$. In the region where the field increases with $r$ and the lines of force are concave, the ion drift will be clockwise. As a result of the drift, the ions will move to one side of the rectangular ridge and the electrons to the other side, and thus excess charges of opposite sign accumulate on opposite sides of the ridge. The charge accumulating per unit time on a length $dl$ of a side of the ridge is equal to $en(u_i - u_e)\, dl\, \delta h$, where $n$ is the plasma number density, $u_i$ and $u_e$ are the projections of the drift velocities of the ions and electrons on the direction of the external normal to the side, and $\delta h$ is the height of the ridge. The sign of the charge depends on the curvature of the lines of force at the plasma boundary. If the plasma surface extends some distance along the lines of force, and if the curvature of the lines of force changes sign in the region occupied by the plasma, then

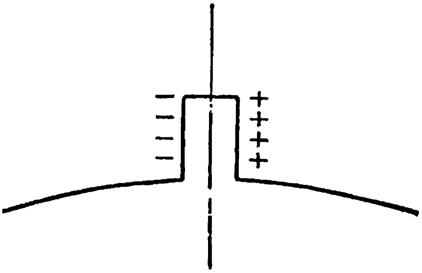

FIG. 95. Rectangular ridge on the plasma boundary (projection on a plane perpendicular to $\boldsymbol{H}$)

positive charges will form on some parts of the side and negative charges on other parts.

Since we have assumed that the plasma has an infinite conductivity, the charges can move freely along the lines of force and any potential difference in this direction will be instantly balanced. As a result, the sign of the electric charge arising on one side of the ridge should be the same along the entire line of force. The total charge collecting on one side of the ridge per unit time is equal to

$$Q = e\int n(u_{\mathrm{i}}-u_{\mathrm{e}})\,\delta h\,dl, \qquad \text{.........}(7.24)$$

where the integration is performed along a line of force.

In accordance with the above, the sign of the integrand depends on the sign of the curvature of a given section of a line of force. The net charges of opposite signs which accumulate on opposite sides of the ridge on the plasma surface produce an azimuthal electric field $\boldsymbol{E}$ which causes the particles to drift in the direction of $\boldsymbol{E}\times\boldsymbol{H}$. If the line of force is convex over the entire surface of the plasma, then $\boldsymbol{E}$, produced by the charge separation, is directed so that the drift caused by it should accentuate the deformation (it drives the particles outwards in the radial direction). If, on the other hand, the lines of force at the plasma boundary are everywhere concave, the drift in the electric field returns the particles to the plasma, and the surface deformation is stable. In general, when the lines of force are convex on some parts of the surface and concave on the others, the stability or instability of the surface will depend on the sign of the resultant charge $Q$ given by the integral (*7.24*).

Let us reduce this integral to such a form that it can be calculated if the distribution of the plasma pressure over the lines of force and the shape of the magnetic field are known. The drift velocities $u_{\mathrm{i}}$ and $u_{\mathrm{e}}$ are quantities averaged over the ion and electron velocity distributions. From (*2.15*) it follows that

$$\left.\begin{aligned} enu_{\mathrm{i}} &= \frac{c}{HR}nm_{\mathrm{i}}(\overline{v_{\parallel}^2}+\tfrac{1}{2}\overline{v_{\perp}^2})_{\mathrm{i}},\\ enu_{\mathrm{e}} &= -\frac{c}{HR}nm_{\mathrm{e}}(\overline{v_{\parallel}^2}+\tfrac{1}{2}\overline{v_{\perp}^2})_{\mathrm{e}},\end{aligned}\right\} \qquad \text{.........}(7.25)$$

where $R$ is the radius of curvature.

If the plasma is in general considered anisotropic, the following expressions can be written for the parallel and transverse components of the pressure of the electron and ion gas:

$$\begin{aligned} p_{\parallel\mathrm{i}} &= 2nm_{\mathrm{i}}\overline{v_{\parallel\mathrm{i}}^2}, & p_{\perp\mathrm{i}} &= nm_{\mathrm{i}}\overline{v_{\perp\mathrm{i}}^2},\\ p_{\parallel\mathrm{e}} &= 2nm_{\mathrm{e}}\overline{v_{\parallel\mathrm{e}}^2}, & p_{\perp\mathrm{e}} &= nm_{\mathrm{e}}\overline{v_{\perp\mathrm{e}}^2}.\end{aligned} \qquad \text{.........}(7.26)$$

The difference between the numerical factors in the expressions for these pressure components is due to the fact that the parallel motion has one degree of freedom, and the transverse motion has two.

Using equations (*7.25*) and (*7.26*), we get

$$ne(u_i - u_e) = \frac{c}{HR}(p_{\parallel} + p_{\perp}). \qquad \text{.........}(7.27)$$

Here, $p_{\parallel}$ and $p_{\perp}$ designate, respectively, the total parallel and transverse pressure components of the anisotropic plasma.

To take into account the dependence of the direction of the drift on the curvature of the lines of force, we shall assume that the radius of curvature $R$ of the line of force is positive in those parts where this line is convex and negative where it is concave. The height of the deformed surface element $\delta h$ changes along the line of force. In order to derive an expression for this change, we observe that the magnetic flux enclosed within the rectangular perturbation must remain constant over the length of a line of force (since the ridge represents a plasma-containing flux tube). Consequently, $H\delta h\, dS = \text{const.}$ In an axially symmetric magnetic field, the width $dS$ of the ridge must be a constant fraction of the circumference of the circular cross-section of the plasma in the $r-\theta$ plane at all values of $z$. Therefore $dS$ is proportional to the distance $r$ from the plasma boundary to the symmetry axis. Thus $\delta h \propto 1/Hr$. Taking this result into account, as well as equation (*7.27*), we can reduce the expression for $Q$ to the following form:

$$Q \propto c \int \frac{p_{\parallel} + p_{\perp}}{H^2 R r}\, dl. \qquad \text{.........}(7.28)$$

With the above convention for the sign of $R$, the positive value of $Q$ corresponds to surface stability with respect to the particular rectangular deformations under consideration. In the special case where the pressure is isotropic, the value of $p = p_{\parallel} + p_{\perp}$ should remain unchanged along the line of force, and hence,

$$Q \propto pc \int \frac{dl}{H^2 R r}. \qquad \text{.........}(7.29)$$

In a plasma with an isotropic pressure distribution, the sign of $Q$ depends only on the shape of the magnetic field. This facilitates the discussion of the stability conditions. As a concrete example we can consider the behaviour of a confined plasma in an axial field of periodic structure (Fig. 96). Let us find the value of the integral (*7.29*) for this case, assuming for simplicity that the plasma is located in a region close to the magnetic axis. From the condition for the conservation of the magnetic flux under these assumptions, it follows that

$$r^2 H = \text{const.}, \qquad r \propto 1/\sqrt{H}, \qquad r' \propto -H'/2\sqrt{H^3}.$$

Here, $r$ corresponds to the boundary of the plasma. Both $r$ and $H$ are functions of $z$ and the prime denotes derivative with respect to $z$. We further obtain

$$\frac{1}{R} = r'' \propto \frac{1}{\sqrt{H^5}}(\tfrac{3}{2}H'^2 - H''H), \qquad \ldots\ldots\ldots(7.30)$$

$$\int \frac{dl}{H^2Rr} \propto \int \frac{dz}{H^4}(\tfrac{3}{2}H'^2 - H''H). \qquad \ldots\ldots\ldots(7.31)$$

Since $H$ is a periodic function of $z$, it suffices to find the value of the integral for one period. Performing the integration by parts, we find that the integral between $a$ and $b$ (Fig. 96) is equal to $-\tfrac{3}{2}\int (H'^2/H^4)\,dz$. This quantity is always negative, and hence a plasma with an isotropic pressure in a periodic axial field is unstable.

The situation becomes more complicated when cases are considered in which the pressure is known to be anisotropic. Of especial interest among the systems in this category are the magnetic mirror traps. In these traps the value of $p_{\parallel} + p_{\perp}$ may change along a line of force over a very wide range, and cases are possible where it is at a maximum in the central region of the trap and drops in the direction of the mirrors, as well as cases where it is represented by a two-humped curve with a minimum in the middle. In a single-humped distribution, the main contribution to the integral (*7.28*) is made by regions with a negative curvature, and hence the plasma should be unstable. If however the pressure is distributed over a two-humped curve, a stable configuration may arise. For this to happen it is necessary that the maxima of the total pressure be sufficiently pronounced and occur in the regions of positive curvature. Such conditions may apparently be realised when the plasma is produced by injecting fast ions into the trap. Practically, this necessitates the fulfilment of very rigid requirements with regard to the angular distribution of the injected particles.

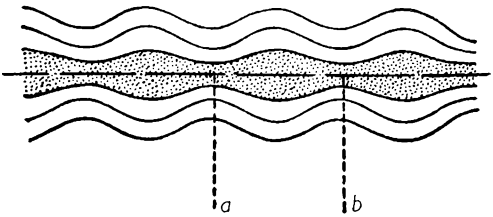

FIG. 96. Plasma confined in a field of periodic structure

The above method may be extended also to the case where the plasma has no sharply defined boundary. Under these conditions, it is possible to select elementary deformations of the interchange-type in which there is a change in the shape of the boundary between two regions located at different distances from the axis. We are not going to give here the expression for the stability condition for this more general case, since it is considerably less elegant than the one established above for a plasma with a sharp boundary. We shall only note that if the plasma pressure decreases rapidly enough in the radial direction (i.e. outward from the symmetry axis), the stability condition does not change in the qualitative sense.

Concluding the discussion of plasma stability conditions in a magnetic field, we observe that these conditions follow essentially from the extensive analogy between a plasma and a highly-conducting diamagnetic fluid. It is precisely because of its diamagnetic nature that a plasma always shows a tendency towards spreading in the direction of decreasing magnetic field when the plasma surface is deformed.

§ **7.5** Of great importance for the entire problem of confinement is the question of the rate at which the deformations grow in unstable plasma states. The time-scale characterising the rate of development of the deformations determines the lifetime of the plasma in a state of unstable equilibrium. When this lifetime is known, it is easier to choose methods of stabilising the disturbances arising in a plasma.

In the simplest version of the stability problem, when it is assumed that the plasma completely excludes the magnetic field from a certain region and that this region has a sharply defined boundary, the question of the growth rate of the deformations is clear enough. For a deformation of the convex part of the plasma surface, the equilibrium between the kinetic and magnetic pressure forces will be the more upset, the deeper the intrusion of the surface ridge into the magnetic field. When the deformed part of the plasma has moved so far that the magnetic pressure it encounters is greatly reduced, then further motion of the deformed part will proceed at a velocity of the order of the expansion velocity of the gas in a vacuum. This means that the growth rate of the deformation should be determined in order of magnitude by the thermal velocity of the ions. We could arrive at the same conclusion by means of the following straight-forward, although very simple-minded, calculation.

Let us suppose that the initial deformation consists in the formation of a small bump of height $\delta x$ on the surface of the plasma. In such a deformation, the magnetic pressure changes by $\frac{1}{4\pi}H\frac{\partial H}{\partial x}\delta x$, while the kinetic pressure will remain almost unchanged. The plasma located inside the deformed part acquires a velocity (due to the difference in pressures) whose value may be estimated from Newton's second law:

$$m_i n\frac{dv}{dt} = -\frac{1}{4\pi}H\frac{\partial H}{\partial x}. \qquad \text{.........}(7.32)$$

Integrating equation (*7.32*) we find that the velocity tends toward a limit equal to $\frac{H_0}{\sqrt{4\pi m_i n}}$ ($H_0$ being the external field strength). This velocity (the Alfvén velocity) is practically the same as the mean thermal velocity of the ions. This result has a very simple meaning. It indicates that if the plasma configuration does not satisfy the stability criteria at all points of the surface, the deformations develop at such a catastrophic rate that the very concepts of equilibrium configuration and magnetic confinement lose all meaning. The plasma collapses in the time taken by a particle to reach the walls of the container at the normal thermal velocity.

It seems natural to expect that the growth rates of unstable deformations might be considerably lower if $p \ll H^2/8\pi$, since the growth of instabilities in a low-pressure plasma arises from particle drifts whose velocities decrease as the magnetic field strength rises. The velocity of the deformed part of the plasma in the direction perpendicular to $\boldsymbol{H}$ is equal to $cE/H$, where $E$ is the electric field arising from the separation of charges due to the drift in a non-uniform magnetic field. Let us evaluate this velocity for a deformation of the rectangular type discussed above. We shall not consider, in the first place, the redistribution of charges along the lines of force.

The electric field strength in the plasma inside the perturbation is equal to $4\pi Q_1/\varepsilon_m$, where $Q_1$ is the charge density which builds up on the side of the ridge as a result of the magnetic drift, and $\varepsilon_m$ is the dielectric constant of the plasma in the crossed fields, given by equation *(3.25)*. Taking $\varepsilon_m \gg 1$ (this is true when the plasma density is high enough), we can write the following expression for $E$:

$$E = \frac{eH^2}{m_i c^2}(d_i - d_e) = \omega_{Hi} H(d_i - d_e)/c, \qquad \text{.........}(7.33)$$

where $d_i$ and $d_e$ are the distances over which the ions and electrons are displaced as a result of the magnetic drift. For the growth rate of deformations, we obtain

$$\dot{y} = \frac{cE}{H} = \omega_{Hi}(d_i - d_e). \qquad \text{.........}(7.34)$$

During the initial growth of the instability, the magnetic drift velocities may be considered constant for the electrons and ions. Therefore, at the outset, the crest height at the surface will rise at the rate

$$\dot{y} = \omega_{Hi} t(u_i - u_e). \qquad \text{.........}(7.35)$$

Thus after a time equal to the ion Larmor period, $\dot{y}$ will approach the total magnetic drift velocity, and will continue to rise.[†] The increase in $\dot{y}$ will not cease until a substantial part of the original reserve of kinetic energy has been converted into electric drift energy of the ions. The limiting value of $\dot{y}$ will depend on the ratio of the original electron and ion temperatures. If $T_i > T_e$, or $T_i \approx T_e$, the limiting velocity with which the plasma ridge penetrates into the magnetic field will be of the order of magnitude of the ion thermal velocity. If, however, $T_e \gg T_i$ the maximum value of $\dot{y}$ will be of the order of $\sqrt{kT_e/m_i}$.

---

[†] In traps with low plasma densities ($\varepsilon_m \simeq 1$), the deformations may develop much more slowly.

We can also evaluate the time it takes $\dot{y}$ to reach the limiting value. For simplicity, let us suppose that $T_i \gg T_e$ and $v_{i\parallel} > v_{i\perp}$. Under these conditions, in the initial stage,

$$\dot{y} \approx \frac{v_i^2 t}{R}.$$

Hence, $\dot{y}$ will be of the order of $v_i$, after a time of about $R/v_i$. It must be said that these estimates of the velocity at which a deformation increases are not rigorous in any sense of the word. They are based on an extremely simplified model, in which the deformation is assumed to be in the form of a plasma protuberance, and furthermore, they implicitly contain the assumption that the initial fluctuation has already led to the formation of a well-pronounced ridge on the surface of the plasma. Therefore, the initial phase during which the deformation arises cannot be discussed in terms of the above model.

If one considers the redistribution of the charges along the lines of force, a redistribution associated with the balancing of the potential, the expressions for $E$ and $\dot{y}$ become much more complicated. It is evident, however, that qualitatively different results can be obtained only when there is an almost complete cancellation of the parts with a positive and a negative sign of $R$ in the integral (*7.28*).

Thus, we see that for a low-$\beta$ plasma with a sharp boundary the violation of the strict stability conditions may lead to as rapid a destruction of the equilibrium configuration as is the case when the plasma completely excludes the magnetic field.

This conclusion, however, is by no means always valid. First of all, it is necessary to point out that under actual experimental conditions, the plasma has no sharply defined outer boundary. This should result in a substantial decrease in the velocities with which the deformations develop in their initial stage. Indeed, if a deformation of the flute-type does not arise on the outer surface of the plasma but somewhere inside it at some arbitrary boundary between two regions having a slightly different density and pressure, the charge forming as a result of the magnetic drift on the lateral faces of such an internal asymmetric irregularity will be many times smaller than the charge forming on the sharp boundary between the plasma and the vacuum. This is easily confirmed by noting that the value of this charge will depend only on a small difference between the pressure inside the flute and that outside it, and this difference will be proportional to the original amplitude of the deformation. For this reason, the initial rate of development of an irregularity may be many times smaller than the value given by equation (*7.35*).

The applicability of the above considerations is also limited by the fact that it makes no sense to talk about the development of deformations whose dimensions are smaller than the Larmor radii of the plasma ions. Thus, for instance, one obviously should not picture the formation of a flute whose width is smaller than $\rho_{\mathrm{Hi}}$ on the outer surface of the plasma, since the deformation cannot produce a sharp local distortion of the Larmor orbits. In particular, it follows from this comment that in the magnetohydrodynamic analysis of experimentally observed instabilities, systems in which the energy of the plasma is measured in tens, or at most hundreds, of electron volts should not be appraised with the same yardstick as traps, such as the Ogra and the Oak Ridge device DCX, filled with high-energy ions.

The effect of a finite value of the Larmor radius on the instability of a plasma has been recently studied by Rosenbluth and co-workers. They examined the case where the radius of curvature $R$ of the lines of force is very large compared with the characteristic dimension over which the plasma density falls to a relatively low value. For all practical purposes this length may be taken as equal to the plasma radius $a$ for an axially symmetric shape. In this case, according to Rosenbluth, owing to the finite value of the ion Larmor radius, not only are perturbations with wavelength $\lambda \approx \rho_{\mathrm{Hi}}$ stabilised, but also perturbations with wavelengths satisfying the condition

$$\lambda < \rho_{\mathrm{Hi}}\sqrt{R/a}.$$

There also exist a number of other factors which can exert a stabilising influence on the development of interchange instabilities by considerably reducing the growth rate of the deformations. In particular, the growth rate of instabilities may be slowed down by the interaction of the plasma with the conducting walls of the chamber. When the plasma boundary comes in contact with the wall, the excess electric charges arising in deformations of the boundary layer have the opportunity to discharge, since the 'superficial' charges can leak on to the wall. The specific mechanism for such a partial stabilisation of instabilities depends to a large degree on the type of magnetic system in which the plasma is located. One such mechanism which prolongs the plasma confinement in mirror-type traps has been discussed by Rosenbluth.

Let us assume that a high-temperature plasma occupies a certain volume between two magnetic mirrors, and that outside this volume there exists a cool plasma extending along the lines of force up to their intersection with the conducting walls of the chamber. This cool plasma represents, as it were, an extension of the hot plasma into the region of the mirrors. It may form, for instance, as a result of a continuous leakage of particles due to Coulomb collisions in the hot region. If the cool plasma has a sufficiently high conductivity then, thanks to its contact with the walls, it will very effectively prevent the formation of electric fields across the magnetic lines of force. Indeed, let us suppose that an electric field perpendicular to ***H*** arises in the hot plasma due to some disturbance. Because the cool plasma is assumed to be a good conductor, all the lines of force are, so to speak, short-circuited through the wall of the chamber, and the electric fields between them will vanish very quickly. We shall return to the effect of this mechanism in § **8.10**, in connection with a discussion of the results of experiments performed with traps using magnetic mirrors.

The direct contact between the plasma and the side walls of the vacuum chamber in a mirror trap has been analysed by Kadomtsev, who studied their influence on the plasma instability. He came to the conclusion that after a rapidly expanding unstable plasma has come in contact with the wall over its entire perimeter, a certain deceleration in the violent development of the deformations on the plasma surface will take place. The phenomena near the walls will be in many respects analogous to convection phenomena in a heated fluid. Let us imagine a flux tube filled with plasma having a slightly higher pressure than the neighbouring flux tubes; this tube is pushed out to the surface of the plasma owing to the diamagnetic effect. When touching the metal wall, the tube gives up its excess pressure and drops back down into the plasma. If inside the volume occupied by the plasma there occurs a sufficiently thorough mixing of the plasma due to the instability caused by the non-uniform field, the rate at which the particles escape from the plasma will be determined by the processes occurring near the walls. The calculation of such convective processes involves some very serious difficulties and, even with greatly simplified assumptions, yields but a rough estimate of the confinement time of the plasma. In Kadomtsev's theory, this time is given by the formula

$$\tau = Ca\left[(1+\gamma^2)\frac{Rm_{\mathrm{i}}}{\rho_{\mathrm{Hi}}kT_{\mathrm{i}}}\right]^{\frac{1}{2}}. \qquad \text{.........}(7.36)$$

Here $a$ is the radius of the chamber, $\gamma$ is the ratio of the ion cyclotron frequency to the ion plasma frequency, $R$ is the radius of curvature of the line of force passing near the wall; the other symbols have their usual meanings (the formula was derived for the case when $T_{\mathrm{i}} \gg T_{\mathrm{e}}$). The most indefinite quantity is the dimensionless coefficient $C$, which depends on the fraction of the density lost by the individual flux tube during contact with the wall. It appears that the value of $C$ should lie between a few units and several tens of units, and in reality may depend strongly on the geometry of the experimental apparatus.

§ **7.6** The convective instability of a plasma is not necessarily associated with a non-uniform magnetic field. It may also occur when the magnetic field is uniform, particularly if there is an electric field causing the plasma to rotate as a whole. In order to elucidate this statement, let us assume that the plasma is located inside a cylinder whose axis is parallel to ***H***. If the strength of the radial electric field $E$ in the plasma is not zero, the electrons and ions undergo a circular drift at a velocity $u_{\mathrm{d}} = cE/H$. A more detailed analysis shows that the rotational drift velocities of the ions and electrons should differ somewhat.† This difference can be qualitatively attributed to the effect of the centrifugal force $F = Mu_d^2/R$, where $R$ is the radius of the drift trajectory. This force is directed along the radius and produces an additional drift velocity $\frac{c}{qH^2}\boldsymbol{F}\times\boldsymbol{H}$ which has opposite sign and different value for ions and electrons respectively. The difference between the total drift velocities of the ions and electrons in the rotating plasma can, in the presence of surface deformations or of azimuthal irregularities inside the plasma, lead to the separation of charges and to the formation of azimuthal electrostatic fields. The mechanism of the electric polarisation of the deformed surface in a rotating plasma is similar to the one which is operative in the presence of a non-uniform field (in both cases, charges accumulate on the deformed portion of the boundary because of the difference between the azimuthal drift velocities of the ions and electrons). The azimuthal electric field in the region of the deformation in turn generates a particle drift along the outward normal to the plasma surface, i.e. it causes the deformation to grow. Using arguments formally analogous to those employed in the analysis of a plasma boundary in a non-uniform magnetic field, we can estimate the time taken for the deformation velocity to equal the original drift velocity of the plasma in the electric field, $u_d(E)$. In order of magnitude, this time interval is $R/u_d(E)$.

This instability mechanism, which is not directly related to the geometry of the magnetic field, is one of the possible causes of 'anomalous' plasma diffusion across a uniform field. The anomalous diffusion rate produced by the rotation of the plasma should be strongly dependent on the conditions at the plasma boundary, and primarily on the strength of the electric field $E$. In particular, we can expect that this effect will be less noticeable in a dense plasma, because the correspondingly large value of the transverse dielectric constant $\varepsilon_m$ decreases $E$. We can also expect the initial shape of the plasma surface to play a part. If the initial plasma boundary is not cylindrically symmetrical, then, if a radial electric field $E$ is produced, the necessary conditions for a rapid growth of deformations are created which should result in a rapid further distortion of the initial asymmetries.

As pointed out in Chapter III, the formation of rotating plasma protuberances having spiral shapes has been observed in certain experiments designed to study the diffusion of a plasma across a uniform magnetic field. It is not impossible that this phenomenon, which phenomenologically constitutes one of the forms of anomalous diffusion, is associated with centrifugal instability.

The centrifugal instability is a special case of a more general mechanism (sometimes called Rayleigh-Taylor instability), which is liable to appear in all cases of plasma acceleration by magnetic fields (for instance when a plasma is compressed very rapidly by a self-magnetic field or by an external magnetic field). When a plasma is accelerated, the ion and electron drift velocities in the direction perpendicular to **H** have different values. This follows from the fundamental equations of plasma dynamics given in Chapter IV. Assuming that the acceleration **a** is the same for both components (this is necessary for quasi-neutrality), and, for simplicity, neglecting the plasma pressure and the frictional forces, we obtain from equations (*4.1*) and (*4.2*) the following expression for the difference between the ion and electron drift velocities:

---

† See § 8.12.

$$u_i - u_e = -\frac{m_i c}{qH^2}\boldsymbol{a}\times\boldsymbol{H}. \qquad \ldots\ldots\ldots (7.37)$$

In the derivation of equation (*7.37*) it is assumed that the plasma is acted upon only by an electromagnetic force.

This expression for the difference between the drift velocities admits of a graphic interpretation. We can say that the difference in $u_i$ and $u_e$ is caused by the inertial force of the ions, $m_i a$ ($m_e$ being small, the electron inertia is negligible). As can easily be seen from an examination of the simplest model of the formation of the flute deformation at the plasma boundary, the difference between the drift velocities of the ions and electrons should result in an instability when the acceleration $a$ is directed toward the plasma. This condition might be expected, for example, in the first phase of a rapid compression of the plasma by a rising axial field in devices such as Scylla, and also in the formation of a pinch in rapid pulsed discharges. Actually, in any dynamic process the stability or instability of a plasma depends on the combined effect of two factors, the field geometry and the acceleration.† In individual cases it is usually easy to establish which of these factors plays the dominant role.

Let us note that the problem of the stability of the boundary layer during an accelerated motion of a plasma can be approached from a somewhat different angle. The difference in the drift velocities of the ions and electrons signifies that a current is flowing in the boundary layer. The presence of this current causes the appearance of the instability in a macroscopic model of the process: the flute deformations, by which this type of instability manifests itself, can be attributed to perturbations of the sausage type when this point of view is taken.

In our analysis of the above stability problem we have considered, for the sake of simplicity, that the plasma behaves like a super-conducting fluid. For this reason, all we have said actually applies only to perturbations developing over periods of time that are substantially shorter than the characteristic time of the skin-effect ($\tau_s \simeq 4\pi\sigma\lambda^2/c^2$, where $\sigma$ is the electrical conductivity and $\lambda$ the characteristic dimension of the perturbation under study, as for example, its wavelength). For periods of time comparable to $\tau_s$ or more, the plasma resistance exerts a considerable influence on the development of the deformation. Under certain conditions, the resistance will act as a stabilizing factor which leads to a damping of the perturbations from equilibrium. This stabilisation mechanism may obviously be related to the conversion of the perturbation energy into heat due to Joule losses. On the other hand, the resistance may lower the stability of the plasma, because the finite conductivity can give rise to types of plasma deformation which are forbidden when infinite conductivity 'freezes' the plasma to the magnetic field. Thus there is reason to fear that new types of instability, not characteristic of fluid with infinite conductivity, will be observed in a plasma having a non-zero resistivity.

---

† See, for example, T. K. Allen and R. J. Bickerton, Experiments on the compression of plasma in cusp geometry, *Nature*, **191**, 794, 1961.

One of the possible forms of such instability, which can occur in an inhomogeneous current-carrying plasma, has been studied by Kadomtsev in connection with research aimed at elucidating the anomalous diffusion of particles observed in experiments with toroidal discharges in strong magnetic fields. We shall present here, in a simplified form, the original ideas and principal results of this interesting study.

Let us consider the case of a plasma located in a uniform externally generated magnetic field with a current, produced by a constant electromotive force, flowing along the magnetic lines of force. We assume that the current is so small that its magnetic field can be neglected. Herein lies the fundamental difference between the basis of the Kadomtsev theory and the theory of pinch stability discussed in Chapter VI. Let the equilibrium magnetic field be directed along the $z$ axis, and let its strength $H_0$ be the same everywhere (this holds for a plasma with a small enough value of $\beta$). Let us suppose further that the density and temperature of the plasma are functions of the $x$ coordinate and do not depend on $y$ and $z$. In this case, the conductivity $\sigma_0$ will also be a function of $x$. The current density in the unperturbed plasma is equal to $\sigma_0 E_0$, where $E_0$ is the electric field strength. A small perturbation of the equilibrium state of the plasma may be expanded into elementary perturbations of the type

$$f(x) \exp [i(k_y y + k_z z + \nu t)]. \qquad \text{.........}(7.38)$$

The quantity $\nu$ may be real as well as imaginary. It is understood that this dependence on the coordinates and the time is common to the fluctuations of all the basic parameters determining the properties of the plasma.

Among the various deviations from equilibrium, the greatest hazard to stability arises from those which do not cause a distortion of the magnetic field. Let us determine the time-dependence of the amplitude of such perturbations. To do this, we must find the corresponding value of $\nu$ or, at least, we must determine the sign of its real part. For these perturbations $\partial H/\partial t = 0$, and hence curl $\boldsymbol{E} = 0$. This means that there are no induced electric fields in the deformed plasma, i.e. $\boldsymbol{E} = -\text{grad}\, U$. This field will have a component $E_0 + \Delta E_z$ along the $z$ axis, and a component $\Delta E_y$ along the $y$ axis (since in the equilibrium plasma, the field is by convention directed along the $z$ axis). The component $\Delta E_y$ will cause the plasma to drift in the $x$ direction. The drift velocity will be

$$\Delta v_x = \frac{c}{H_0}\Delta E_y.$$

Since the increment of the electric potential is determined by the deviation from the equilibrium state, it also must be proportional to $\exp i(k_y y + k_z z)$; consequently the ratio of the components of the perturbed electric field, $\Delta E_y/\Delta E_z$, is equal to $k_y/k_z$. The perturbed increment of the axial current is given by the expression

$$\Delta j_z = \Delta\sigma E_0 + \sigma_0 \Delta E_z.$$

Here,

$$\Delta\sigma = \tfrac{3}{2}\sigma_0\frac{\Delta T}{T}. \qquad \text{.........}(7.39)$$

However, for perturbations which do not distort the magnetic field, $\Delta H = 0$ and hence,

$$\Delta \boldsymbol{j} = \frac{c}{4\pi}\operatorname{curl}\boldsymbol{H} = 0.$$

Therefore,

$$\Delta\sigma E_0 + \sigma_0 \Delta E_z = 0.$$

Substituting the expression for $\Delta\sigma$ into this equation, and taking into consideration the relation between $\Delta E_y$ and $\Delta E_z$, we can express the field component along the $y$ axis in terms of $\Delta T$:

$$\Delta E_y = -\frac{3}{2}\frac{k_y}{k_z}E_0\frac{\Delta T}{T}. \qquad \text{.........}(7.40)$$

Let us now set up the heat balance equation. Neglecting the fluctuations of the Joule losses (since $j_z$ is small) and noting that in a moving plasma the heat is transported together with the mass, we can write the heat balance equation for the perturbed plasma as follows:

$$\frac{\partial}{\partial t}\Delta T + \Delta v_x \frac{\partial T_0}{\partial x} = \chi_{\|}\frac{\partial^2}{\partial z^2}T. \qquad \text{.........}(7.41)$$

The second term on the left describes the heat transport due to the plasma motion.

The right-hand side contains only the thermal conduction term which equalises the temperature along the lines of force; the heat conductivity across the lines of force is assumed to be zero. The coefficient $\chi_{\|}$ is the parallel thermal diffusivity of the plasma (the coefficient of heat conductivity divided by the heat capacity per unit volume). Using equation (*7.40*) we can express the drift velocity $\Delta v_x$ in terms of $\Delta T$. Substituting this expression into the heat balance equation, we find:

$$\frac{\partial}{\partial t}\Delta T - \gamma \Delta T = \chi_{\parallel}\frac{\partial^2}{\partial z^2}\Delta T, \qquad \text{.........}(7.42)$$

where

$$\gamma = \frac{3}{2}\frac{k_y}{k_z}\frac{cE_0}{H}\frac{1}{T_0}\frac{\partial T_0}{\partial x} = \frac{k_y}{k_z}\frac{cE_0}{H}\frac{\partial}{\partial x}\ln \sigma_0. \qquad \text{.........}(7.43)$$

Putting $\Delta T \propto \exp[i(k_y y + k_z z) + \nu t]$, we can derive an expression for $\nu$ from (*7.42*):

$$\nu = \gamma - \chi_{\parallel}k_z^2. \qquad \text{.........}(7.44)$$

If $\gamma > \chi_{\parallel}k_z^2$, the perturbations in the plasma will increase exponentially. Consequently, the plasma will turn out to be unstable when the inequality

$$\frac{k_y}{k_z}\frac{cE_0}{H}\frac{\partial}{\partial x}\ln \sigma_0 > k_z^2\chi_{\parallel} \qquad \text{.........}(7.45)$$

is satisfied. This inequality is satisfied by perturbations with a sufficiently small value of $k_z$.

It should be emphasised that in the mechanism for the development of resistive instabilities of the above type, the main part is played by the inhomogeneity of the plasma, which shows up in the dependence of $\sigma$ on $x$.

By choosing a sufficiently large ratio of $k_y$ to $k_z$, we can always fulfil the inequality (*7.45*); thus it would seem that this mechanism should always produce an instability in a plasma with a current flow along the magnetic lines of force. Actually, however, this is not so. The minimum value of $k_z$ is limited by a whole series of requirements. In particular, for a bounded plasma the minimum value of $k_z$ is determined by the value of $2\pi/l$, where $l$ is the linear dimension of the region occupied by the plasma along the lines of force. On the other hand, the maximum value of $k_y$ is also limited (if only because the wavelength of the perturbation in the $y$ direction cannot be smaller than the ion Larmor radius). In view of these limitations, it may turn out that if the value of the thermal diffusivity $\chi_{\parallel}$ is high enough, i.e. if the temperature is high, the condition (*7.45*) is not satisfied by any of the possible perturbations of the plasma.

At the present time, because of the imperfections in the theory, it is difficult to draw a line between those states of the plasma in which the instability caused by gradients in the conductivity should be observed, and those states in which it is extinguished by the equalising effect of the parallel heat conductivity of the plasma. Nevertheless, one should not dismiss the possibility that in experimental devices such as the Stellarator or in toroidal systems with strong fields, this type of instability could be the chief cause of the abnormally high diffusion of the plasma across the magnetic field.

The explanation of anomalous diffusion on the basis of the previously discussed mechanism governing the excitation of plasma oscillations amounts, from a purely qualitative standpoint, to saying that the statistical addition of the particle drifts, which arise from the fluctuating electric fields, is equivalent to multiple collisions, and should therefore be expressed by a corresponding increase in the diffusion rate across the magnetic field.

Kadomtsev attempted to proceed much further beyond these general considerations, and also developed a quantitative theory of turbulent diffusion for an inhomogeneous plasma with finite conductivity. This theory, based on the instability mechanism described above, leads to the following estimate of the lifetime of particles in a cylindrical plasma immersed in a strong axial magnetic field:

$$\tau_0 = A\frac{a}{v_{\mathrm{i}}}\frac{l}{L_0}\left(\frac{v_{\mathrm{i}}\chi_{\|}}{l}\right)^{\frac{1}{4}}\left(\frac{H}{cE_0}\right)^{\frac{1}{2}}. \qquad \text{.........}(7.46)$$

Here $a$ is the plasma radius, $v_{\mathrm{i}}$ is the velocity of sound, i.e. the ion thermal velocity calculated from the total temperature of the electrons and ions, $L_0$ is the length of the pinch, $l$ the distance between conducting diaphragms bounding the diameter of the pinch, $\chi_{\|}$ is the parallel thermal diffusivity of the electrons, $E_0$ is the applied axial electric field, and $A$ is a numerical factor of the order unity.

It is hardly to be expected that the expression (*7.46*) can give more than the order of magnitude of $\tau_0$, and a rough idea of the dependence of the mean lifetime on the basic parameters determining the plasma state. Let us mention, however, a few corollaries of equation (*7.46*). First, $\tau_0 \propto \sqrt{H}$; second, $\tau_0 \propto E_0^{-\frac{1}{2}}$; third, $\tau_0$ should be virtually independent of the temperature.

This calculation of the turbulent diffusion performed by Kadomtsev is interesting primarily as the first attempt, carried to a definite conclusion, at developing a non-linear theory of plasma instability in which the representation of the initiation of elementary oscillations is related to the macroscopic description of transport phenomena.

One distinguishing feature of the instability mechanism pointed out by Kadomtsev lies in the fact that this mechanism is related neither to the magnetic field geometry nor to the acceleration of the plasma, but only to the plasma inhomogeneity and to the presence of an electric current.

Sagdeev has also predicted that in an inhomogeneous plasma instabilities may sometimes arise in the absence of an electric current parallel to $\boldsymbol{H}$. This 'universal' instability is caused by the generation of compressional waves. Let us assume that such a wave, which consists of alternating regions of compression and rarefaction, propagates in the plasma at a certain angle to a constant magnetic field $\boldsymbol{H}_0$. In this case, the electric field associated with the wave will have a component $E_{\perp}$ perpendicular to $\boldsymbol{H}_0$, so that there will be a drift with a velocity $cE_{\perp}/H_0$. If the temperature of the inhomogeneous plasma is different on different lines of force, heat will be exchanged between regions with different temperatures. Let us now observe that in the wave itself periodic temperature fluctuations should exist, caused by the fact that the plasma heats when compressed and cools upon expansion. Thus if the additional influx of heat produced by the drift is deposited in the plasma on the compression phase, the oscillations should be amplified. The calculations, based on kinetic theory, show that if the ratio of the wave numbers $k_\perp/k_\parallel$ is high enough, oscillations of the plasma will be excited if the temperature gradient perpendicular to the lines of force is much greater than the density gradient. The necessary condition for the oscillation is

$$\frac{d \ln T_0}{d \ln n_0} > 2. \qquad \text{.........}(7.47)$$

The excitation of compressional waves will also occur under conditions when the temperature gradient has a direction opposite to that of the density gradient.

§ 7.7 As mentioned above, in addition to the magnetohydrodynamic instabilities, there may also occur in a plasma kinetic-type instabilities which depend on the velocity distribution of the ions and electrons. In many instances, the appearance of instabilities is associated with the excitation of various types of plasma oscillations. The task of theory with respect to the analysis of kinetic instabilities is to establish, first, under what conditions they can appear, and second, how their development may affect the confinement of the plasma in magnetic traps.

The second of these questions now becomes far from trivial. The kinetic instabilities arise at first in phase space, and for this reason it is difficult to predict, generally speaking, what influence they may have on the plasma configuration. Considering only the qualitative aspects of the phenomena, it is possible to establish that the kinetic instabilities lead to the development of various types of plasma oscillations and waves with which are associated alternating electric fields. If this alternating field has a component perpendicular to $\boldsymbol{H}$, it causes the particles to drift across the lines of force. A statistical addition of such drifts could obviously lead to anomalous particle diffusion. In order to determine, by means of this picture, the main index of the instabilities—the rate of the anomalous escape of particles or the coefficient of anomalous diffusion—it is necessary to know the amplitude of the alternating fields in the plasma and the dimensions of the regions within which the vector $\boldsymbol{E}$ remains approximately constant in magnitude and direction. Such calculations can be carried out more or less adequately only in some simple cases.

Leaving aside this aspect of the problem for the time being, let us investigate the conditions favourable to the development of kinetic instabilities. Of these conditions the most important is the deviation of the velocity distribution function from Maxwell's law. At the present time, most of the detailed theoretical studies have been devoted to instabilities associated with deviations of two types: the so-called 'beam' instability, caused by the presence of additional maxima on the velocity distribution function (Fig. 97), and the instability arising from an anisotropic velocity distribution.

The beam instability is caused by the interaction between a beam of charged particles and the waves which may be propagated in the plasma. This interaction involves the transfer of energy by the particles of the beam to waves whose propagation velocity is close to the velocity of the particles, and thus the beam is decelerated and waves are amplified.

Let us consider the mechanism for the simplest case, when longitudinal oscillations are generated. Let us assume that some perturbation of the electric field exists in the plasma which may be represented as a plane sine wave. Figure 98a shows the instantaneous distribution of the electric potential $V$ in this wave. This potential profile will move at a velocity equal to the phase velocity of the wave, $\omega/k$. The electrons (or ions) whose velocity differs markedly from $\omega/k$ preserve their energy, on the average, as they pass through the region of alternating $V$. In contrast, the particles moving at velocities close to $\omega/k$ will bounce off the potential barriers. In order to describe the conditions in which such rebounding will occur, let us transform to a coordinate system which moves with the wave. In this coordinate system, the picture of the potential distribution shown in Fig. 98b will be stationary. If the component of the electron velocity† in the direction of wave propagation is $v_e$, then in the moving coordinate system it will be equal to $v_e-\omega/k$. It is evident that the electron will rebound from the potential barrier if the following condition is obeyed:

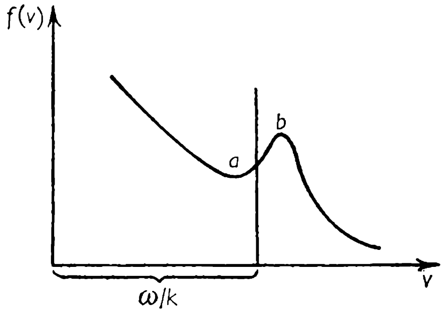

FIG. 97

Additional maximum in the velocity distribution function due to the presence of a particle beam

$$\frac{m_e}{2}\left(v_e-\frac{\omega}{k}\right)^2 < U_m, \qquad \text{.........(7.48)}$$

i.e., if $v_e$ is confined within the limits

$$\frac{\omega}{k}-\sqrt{\frac{2U_m}{m_e}} < v_e < \frac{\omega}{k}+\sqrt{\frac{2U_m}{m_e}}, \qquad \text{.........(7.48a)}$$

where $U_m = -eV_{max}$.

---

† The reasoning which follows is also valid for ions.

The electrons for which condition (*7.48a*) applies can be divided into two groups according to their velocities. The first group includes electrons with velocities exceeding $\omega/k$, the second group has velocities smaller than $\omega/k$. Electrons of the first group overtake the wave, and those of the second group fall behind it. Figure 98b shows the rebounds of electrons of both groups from a potential barrier in a coordinate system moving along with the wave. An electron with $v_e > \omega/k$ will bounce off the potential barrier on the left. In the moving coordinate system, the electron velocity will change sign following the rebound, and become $\frac{\omega}{k} - v_e$. In the laboratory coordinate system, the speed of the reflected electron will be $2\frac{\omega}{k} - v_e$, which is smaller than its initial speed. Hence, when an electron of the first group collides with a moving potential barrier, it loses energy by transferring it to the wave.

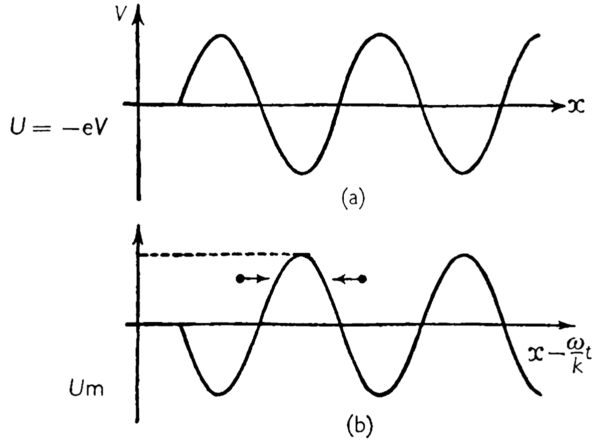

FIG. 98. (a) Potential profile of the wave
(b) Diagram illustrating an electron rebounding from a potential barrier in a coordinate system moving with the wave

In contrast, an electron which lags behind the wave from the outset acquires additional energy by colliding with the moving potential barrier. The complete energy balance in the interaction between the plasma electrons and the wave depends on the relative number of electrons in the two groups. If the electrons of the first group are more numerous, the energy of the wave will increase, which amplifies the oscillations, i.e. the situation corresponds to an instability. Obviously, this will take place if the electron velocity distribution function has a positive derivative in the vicinity of $v_e = \omega/k$.

For a Maxwell velocity distribution, the single maximum of the distribution function $f(v_e)$ occurs at $v_e = 0$; thus no oscillations are developed. In this case, whatever part of the velocity spectrum is considered, the number of electrons of the second group is greater than that of the first group; consequently, any longitudinal wave arising in the plasma will be damped by giving up its energy to the electrons, whatever its frequency $\omega$. This is the wave-damping mechanism established by Landau and referred to in Chapter IV.

However, in the presence of a sufficiently well-defined beam of electrons, the total velocity distribution function may have an additional maximum at a value of $v_e$ different from zero. This case is depicted in Fig. 97. A wave whose phase velocity lies near to the second maximum of the distribution function, between points $a$ and $b$, will be excited by the electron beam because in this region $\partial f/\partial v_e > 0$. Thus, among the waves which are present in the plasma due to fluctuations in the nascent state, the electron beam will pick out a narrow spectral region and will forcibly impart energy to the waves in this part of the spectrum.

We shall try to give a rough estimate of the growth-rate of the wave energy $\nu$; it is directly related to the growth time of instabilities for the process under consideration ($\tau \approx 1/\nu$). By definition, the growth-rate $\nu = \frac{1}{2\varepsilon}\frac{d\varepsilon}{dt}$, where $\varepsilon$ is the energy of the wave. The quantity $d\varepsilon/dt$ is the sum of the energies transferred to the wave by all the electrons per unit time. In one collision, an electron loses the energy

$$\Delta W = \frac{m_e v_e^2}{2} - \frac{m_e}{2}\left(\frac{2\omega}{k} - v_e\right)^2 = 2m_e\frac{\omega}{k}\left(v_e - \frac{\omega}{k}\right). \qquad \text{.........}(7.49)$$

The number of collisions with the potential barriers which one electron undergoes per second is equal to the velocity of the electron relative to the wave velocity divided by the distance between the wave crests. The first of these quantities is equal to $v_e - \frac{\omega}{k}$, the second is the wavelength $\lambda$.

From the above it follows that an electron travelling ahead of the wave gives up an energy $\frac{2m_e\omega}{k\lambda}\left(v_e - \frac{\omega}{k}\right)^2$ per unit time to the wave. The energy acquired by an electron trailing the wave is given by exactly the same kind of expression. Summing up over all the plasma electrons which satisfy the condition (*7.48*), we find that the increase in the energy of the wave is given by the expression

$$\frac{d\varepsilon}{dt} = \frac{2m_e}{\lambda}\frac{\omega}{k}\left[\int\limits_{\frac{\omega}{k}}^{\frac{\omega}{k}+\sqrt{\frac{2U_m}{m_e}}} \left(v_e - \frac{\omega}{k}\right)^2 f(v_e)\, dv_e - \int\limits_{\frac{\omega}{k}-\sqrt{\frac{2U_m}{m_e}}}^{\frac{\omega}{k}} \left(v_e - \frac{\omega}{k}\right)^2 f(v_e)\, dv_e\right]. \qquad \text{.........}(7.50)$$

Supposing that $U_m$ is small, so that $v_e$ differs negligibly from $\omega/k$; we can represent $f(v_e)$ in the form

$$f(v_e) = f\left(\frac{\omega}{k}\right)+\left(v_e-\frac{\omega}{k}\right)\frac{\partial f}{\partial v_e}. \qquad \text{.........( .51)}$$

The derivative is taken at the point $v_e = \omega/k$. Substituting this expression into (*7.50*) yields

$$\frac{d\varepsilon}{dt} = \frac{2}{\pi}\frac{1}{m_e}U_m^2\omega\frac{\partial f}{\partial v_e}. \qquad \text{.........(7.52)}$$

Here $\varepsilon$ designates the wave energy calculated per unit volume. Therefore, the distribution function $f(v_e)$ is normalised to

$$\int f(v_e)\, dv_e = n_e,$$

where $n_e$ is the electron number density. If we now take a distribution function $f_1(v_e)$ normalised to unity $\int f_1(v_e)\, dv_e = 1$, the relation (*7.52*) can be written as

$$\frac{d\varepsilon}{dt} = \frac{2}{\pi}\frac{n_e}{m_e}U_m^2\omega\frac{\partial f_1}{\partial v_e}. \qquad \text{.........( .53)}$$

To determine the energy growth-rate, it is also necessary to calculate the energy stored in the wave. The wave energy per unit volume is

$$\varepsilon = \frac{\overline{E^2}}{8\pi}+\frac{m_e n_e \overline{v_e^2}}{2},$$

where $\overline{E^2}$ is the mean square electric field strength and $\overline{v^2}$ is the mean square velocity of the electrons travelling in the wave. The mean potential and mean kinetic energy should be equal in the longitudinal electron oscillations. Hence $\varepsilon = \overline{E^2}/4\pi$. As can be easily proved, $\overline{E^2}$ is related to $U_m$ as follows: $\overline{E^2} = k^2 U_m^2/e^2$. From equation (*7.53*) we obtain the expression for the energy growth-rate:

$$\nu = \frac{1}{2\varepsilon}\frac{d\varepsilon}{dt} = \frac{4n_e e^2}{m_e}\frac{\omega}{k^2}\frac{\partial f_1}{\partial v_e}. \qquad \text{.........(7.54)}$$

The longitudinal electron plasma oscillations can have different wavelengths and different phase velocities, but the frequency $\omega$ of these oscillations is always equal to the electron plasma frequency $\omega_0$. Therefore, the final formula for the energy increment is

$$\nu \approx \frac{\omega_0^3}{k^2}\left(\frac{\partial f_1}{\partial v_e}\right)_{v_e = v_{ph}}, \qquad \text{.........(7.55)}$$

where $v_{\text{ph}}$ is the phase velocity of the wave whose velocity is close to that of the beam electrons. From equation (*7.55*) it follows that the beam intensity must exceed some minimum value in order that the oscillations may develop. A very weak beam cannot affect the electron velocity distribution function enough to change the sign of its slope.

The above calculation of the growth rate of the beam instability is based on an extremely simplified picture of the process, and thus the applicability of this model is very limited. In particular, this picture does not consider the fate of the electron after its collision with the potential barrier, although this is very essential to the whole mechanism for the development of oscillations. Actually, having given up energy to the wave, the decelerated electron collides with the next wave crest, and acquires energy again. Thus it would seem that there is an almost complete compensation of the energy initially lost to the wave, i.e. the development of electrostatic oscillations should cease at the earliest stage, before the amplitude of the wave, excited by the passage of the beam through the plasma, reaches an appreciable value (if there are no external influences, such as an accelerating electric field which restores the velocity lost by the electron in the collision). In essence, this observation means that the method of calculation employed above is useful only for a linear approximation, i.e. for estimating the rate of increase of the wave amplitude at the very earliest stage of development of the oscillations.

We have so far considered a special example of the interaction between an electron beam and the waves in a plasma, an example which corresponds to the excitation of short-wave electron plasma oscillations. It is possible that such a process is actually achieved under conditions where some fraction of the electron constituent of the plasma, acted upon by an electric field, is continuously accelerated (runaway electrons) and becomes sharply dissociated from the bulk of the electron velocity distribution. Let us imagine that a current flows in the plasma under the influence of an electric field. The passage of current slightly alters the electron velocity distribution, since, on the average, the electrons acquire a small directed velocity $u$ in the direction of the electric field. Because of this, the maximum of this velocity distribution should be displaced from $v = 0$ to $v = u$ (Fig. 99). This means that the electrons in the velocity range from 0 to $u$ can, by means of the above mechanisms, excite plasma waves with phase velocities lying within the same interval. Under typical experimental conditions, the average electron drift velocity amounts to $10^6 - 10^7$ cm/sec. Electron plasma oscillations with phase velocities of this order will have a wavelength of $10^{-4} - 10^{-5}$ cm for a plasma density of the order of $10^{13} - 10^{14}$ cm$^{-3}$. Waves with such a small wavelength will be damped very quickly, and their excitation can therefore be disregarded. For comparison with experiment it appears much more interesting to discuss the case where ion plasma oscillations are excited.

The question of the development of ion plasma oscillations, i.e. the excitation of ion sound waves in a plasma, is a different matter. For these waves the phase velocity does not depend on the wavelength $\lambda$, and is of the order of the ion thermal velocity if $T_i \approx T_e$, or of the order of $\sqrt{\frac{kT_e}{m_i}}$ if $T_i \ll T_e$. Obviously, a necessary condition for the electron excitation of ion waves is the requirement that the directed electron velocities be no less than the phase velocities of the waves. Thus the excitation of ion sound waves should, roughly speaking, begin at a current density which corresponds to the condition $u \approx \bar{v}_i$ or $u \approx \sqrt{\frac{kT_e}{m_i}}$. As was stated in Chapter IV, one more condition must be satisfied before ion sound waves can be excited: the ion temperature should be substantially below the electron temperature.

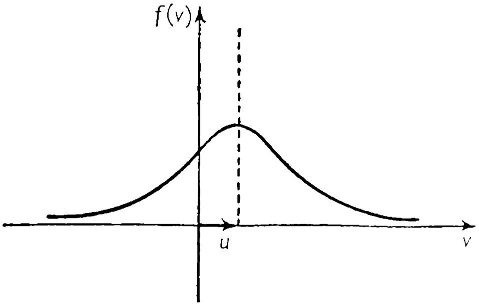

FIG. 99. Velocity distribution function in the presence of a current

In some experiments carried out in recent years, attempts have been made to explain the origin of anomalous diffusion in various magnetic traps as due to the development of this type of oscillation. In this connection, we should take notice of the fact that, on the basis of the above considerations concerning the mechanism of the energy exchange between the beam and the plasma oscillations, a relationship between the excitation of the waves and the confinement of the particles in the plasma depends on additional assumptions. To demonstrate the possibility of such a relationship, it is necessary to abandon a model in which a single plane wave is propagated in an infinite plasma, and to consider instead the independent excitation of oscillations by the interaction between beams and plasma in limited regions of the plasma volume.

In order to define the problem of the influence of the beam instability on the confinement of a plasma, let us consider the case where the electron flow travels parallel to the magnetic lines of force. We encounter such a case, for instance, in the Joule heating of a plasma in toroidal chambers. It may be assumed that this flow consists of a large number of parallel electron streams, each of which is flowing along a certain flux tube. Let us now suppose that each stream causes the appearance of a longitudinal wave that is not correlated in phase and amplitude with the waves forming in the neighbouring parts of the plasma. Under these circumstances, the distribution of the electric potential along two neighbouring lines of force will be different, and hence, fluctuating electric fields perpendicular to **H** will inevitably arise. These fields will produce a plasma drift equivalent to the appearance of anomalous diffusion, which causes a rapid leakage of particles from the plasma across the magnetic lines of force. The anomalous diffusion rate can be correlated with the basic quantities characterising a fluctuating electric field in the plasma: the mean field amplitude $\bar{E}$ and the mean dimensions of the regions within which, roughly speaking, the component of the electric field perpendicular to **H** is constant.

Let us assume for the sake of precision that the irregular electric fields arise from the excitation of long-wavelength ion waves along the lines of force. We shall also assume that the linear scale $l$ characterising the fluctuations of the electric potential in the plane perpendicular to **H** is much less than the scale determining the change of potential along the lines of force (so that $l \ll \lambda$). We shall assume further that, as long as the portion of the plasma moving with a drift velocity $c\bar{E}/H$ is displaced over a distance $l$, the electric field is not able to change appreciably. With these assumptions, an element of plasma will in time $t$ diffuse across the magnetic field a distance $y$ given by:

$$y \approx l\sqrt{\frac{t}{\tau}}, \qquad \text{.........(7.56)}$$

where $\tau$ is the time needed by the element to traverse a distance $l$ at the drift velocity, i.e.

$$\tau \approx \frac{l}{v_{\mathrm{d}}} \approx \frac{lH}{c\bar{E}}. \qquad \text{.........(7.57)}$$

From (*7.56*) and (*7.57*) we obtain

$$y \approx \sqrt{l\frac{c\bar{E}}{H}t}. \qquad \text{.........(7.58)}$$

Thus, we arrive at the following expression for the coefficient of anomalous diffusion:

$$D_{\perp} \approx l\frac{c\bar{E}}{H}, \qquad \text{.........(7.59)}$$

which can also be expressed as follows:

$$D_{\perp} \approx \frac{c^2\overline{E^2}}{H^2}\tau. \qquad \text{.........(7.60)}$$

Here $\tau$ is the average time during which the field may be considered approximately constant in a coordinate system which moves at the drift velocity. It goes without saying that these considerations, which are phenomenological from the theoretical point of view, cannot claim to be anything more than a demonstration of the fundamental possibility of establishing a relationship between anomalous diffusion and the excitation of waves by the directed flow of electrons. However, these discussions may turn out to be useful in the analysis of certain experimental results.

As an example, let us consider the problem of anomalous diffusion in quasi-stationary toroidal discharges. In this case, it is possible to establish a relationship between the diffusion coefficient and the kinetic energy of the ions accelerated by fluctuating electric fields. As was pointed out in § **6.4**, the average ion kinetic energy in a quasi-stationary discharge can be represented as the sum of two terms, one of which corresponds to a thermal energy which is the same for all the ions regardless of their mass and charge, and the other to the kinetic energy of the directed ion motion produced by fluctuating electric fields. To a rough approximation, this second term is equal to $\frac{m_i c^2 \overline{E^2}}{2H^2}$ (if the directed ion motion arises primarily from transverse electric fields with frequencies $\omega < \omega_{Hi}$). This term may be determined experimentally by measuring the widths of spectral lines emitted by ions of different masses. In this manner, measurements of spectral line widths constitute a direct method for estimating the value of $\overline{E^2}/H^2$ which enters into equation (*7.60*). The value of $\tau$ in this formula may be roughly estimated from the spectrum of high-frequency oscillations on discharge oscillograms. Thus, by using measurements of the spectral line widths and the oscillograms of high-frequency oscillations, we are able (at least in principle), to give an *a priori* estimate of the diffusion velocity of a plasma in quasi-stationary discharges. The practical application of such a procedure involves one basic difficulty: the contribution to the spectral line width by that part of the ion energy which is proportional to the mass is comparatively small, and its determination requires some very tedious spectroscopic measurements.

To conclude this analysis of the conditions under which the beam instability develops, let us note that instabilities may arise not only under the influence of electron beams, but also in the presence of an intense flux of accelerated ions.

Let us now examine some oscillation-producing processes associated with the anisotropy of the velocity distribution function in a magnetic field. The above discussion of beam instabilities obviously remains valid for waves which propagate either parallel or at small angles to the magnetic field. However, for waves polarised perpendicularly to $\boldsymbol{H}$, entirely different instabilities can develop by the excitation of oscillations. A necessary condition for their generation is the anisotropy of the velocity distribution. The physical mechanism governing the excitation of oscillations consists of the following: the individual Larmor orbits located along the same line of force are attracted to one another like parallel currents, and therefore have a tendency to 'stick'. This tendency is opposed by the thermal motion of the particles along the lines of force, which disassembles high-density bunches of plasma. However, if the parallel component of the particle velocity happens for some reason to be comparatively small, any fluctuation in the parallel distribution of the plasma density leads to the appearance and excitation of oscillations, the fragmentation of the plasma into plasmoids and the corresponding changes in the distribution of the magmetic field strength. Without dwelling on the explanation of this mechanism in any more detail, we shall give the main conclusions of a theory constructed by Sagdeev, who predicted the existence of this type of instability in an anisotropic plasma.

In an anisotropic plasma, the distribution functions for the velocity components parallel and perpendicular to $\boldsymbol{H}$ are different. The simplest form of the distribution function in this case will be

$$f \propto \exp\left(-\frac{mv_{\perp}^2}{2kT_{\perp}}-\frac{mv_{\parallel}^2}{2kT_{\parallel}}\right). \qquad \text{.........}(7.61)$$

If the 'parallel' temperature $T_{\parallel}$ and the 'transverse' temperature $T_{\perp}$ differ widely enough, waves which have frequencies close to the cyclotron frequencies of the electrons and ions, $\omega_{\mathrm{He}}$ and $\omega_{\mathrm{Hi}}$, and opposite circular polarisations (the ordinary and extraordinary wave) will be excited in the plasma. The instability associated with the development of the extraordinary wave (with an electric field rotating in the same direction as the electrons) should occur when the following condition is met:

$$T_{\perp \mathrm{e}}/T_{\parallel \mathrm{e}} > H/(8\pi nkT_{\perp \mathrm{e}})^{\frac{1}{2}}. \qquad \text{.........}(7.62)$$

In this case, the growth rate of the instability will be of the order of magnitude of

$$\omega_{\mathrm{He}}\frac{8\pi nkT_{\perp \mathrm{e}}}{H^2}.$$

The ordinary wave begins to develop if

$$T_{\perp \mathrm{i}}/T_{\parallel \mathrm{i}} > H/(8\pi nkT_{\perp \mathrm{i}})^{\frac{1}{2}}, \qquad \text{.........}(7.63)$$

with a growth-rate of the order

$$\omega_{\mathrm{Hi}}\frac{8\pi nkT_{\perp \mathrm{i}}}{H^2}.$$

It follows from these conditions that the instabilities under consideration are especially hazardous when the plasma pressure is not very small compared with the magnetic pressure. Moreover, as was pointed out by Sagdeev, in traps with magnetic mirrors unstable regions should always exist because, in the regions where the particles rebound from a strong magnetic field, the parallel energy has to be small compared with the transverse energy, and hence the conditions for the development of the instability will arise. Obviously, if $\beta$ is small the instability can appear only in small regions near the boundaries of the plasma volume. Therefore, for a very low pressure plasma, the comparative role of this type of instability should be a minor one.

The linearised stability theory for an anisotropic plasma cannot provide the answer to the question of how this instability affects the lifetime of particles in magnetic systems. In order to elucidate this question, the calculation must be carried to the second approximation. Such a calculation shows that the development of oscillations in an anisotropic plasma should lead to an equalisation of the transverse and parallel temperatures, i.e. to the re-establishment of an equipartition of energy among the kinetic degrees of freedom. It is clear that such a mechanism will strongly enhance the leakage of particles from the plasma in magnetic mirror traps.

Studies of the problem of plasma stability have until now been of a broadly exploratory and not very deep nature, and have been aimed at including in theoretical analysis the widest possible variety of processes involving the generation and development of various types of perturbations which throw the plasma out of an equilibrium state. In the overwhelming majority of cases, the result of such studies is the establishment of stability criteria and the derivation of expressions for the growth rate of perturbations, valid only in the linear approximation, i.e. for small deviations from the equilibrium position. The applicability of these results to definite predictions is also limited by the fact that they are usually derived on the basis of simplified assumptions which do not correspond to the actual experimental conditions. For instance, in the analysis of instabilities caused by the deviation of the velocity distribution function from Maxwell's law, it is usually assumed that the plasma is unbounded and homogeneous; similarly, the magnetohydrodynamic stability calculations are usually carried out for a plasma with a free boundary and an infinitely high conductivity. Only very recently have papers appeared in which the stated aim was to extend the analysis of the development of small deformations to the determination of the macroscopic rate of collapse of an unstable plasma configuration. An example of this type of profound approach to the problem is Kadomtsev's work on the instability of plasma in magnetic mirror traps and in systems with Joule heating.

Among other problems of a broad nature awaiting treatment by theoretical analysis is the very interesting question of plasma instability in the intermediate case where the kinetic pressure is comparable to the magnetic pressure but is not quite sufficient to expel the field completely. This case has not been systematically investigated as yet.

The main factor hindering the fruitful development of theoretical studies of the stability problem is the almost complete absence of much necessary experimental confirmation. The rare drops of experimental fact are almost unnoticeable in the vast but arid field of theoretical work. Only in the rather narrow category of pinch phenomena has it been possible to establish a connection between theory and experiment. Numerous experiments in this area provide a whole series of characteristic cases which exhibit the development of the main types of magnetohydrodynamic instability associated with the self-field produced by the gas current. According to the predictions of theory, the unstable deformations in pinch discharges develop with considerable violence, at velocities of the order of the ion thermal velocity. It is therefore legitimate to state that as far as the analysis of the most dangerous instabilities involved in the pinch effect is concerned, theory has fulfilled its task to a first approximation.

However, in experiments with magnetic traps, we do not usually encounter such a strong manifestation of instability, even in cases where, according to theory, the plasma configuration does not meet the stability criteria. The instability peculiar to the plasma in magnetic traps usually manifests itself in the form of slowly developing perturbations, i.e. it has the nature of anomalous diffusion. Furthermore, the average confinement times of particles in the plasma may vary over wide ranges, attaining several milliseconds in certain experiments. This anomalous diffusion represents in each case the result of the superposition of perturbations which are characteristic of the plasma instability for a given trap. The fact that the macroscopic velocity associated with the development of the instability in these cases does not show itself to be clearly related to the ion thermal velocity should not appear strange, since the equality of these velocities is, according to theory, more the exception than the rule. Strictly speaking, it should occur only for violent processes involving the development of magnetohydrodynamic instabilities in a plasma having a distinct outer boundary. Unfortunately, apart from this obvious statement, we can say very little about the nature of anomalous diffusion at the present time, since the experimental investigations of this important phenomenon are still in their very early stages.

It can hardly be assumed that anomalous diffusion is an inevitable flaw of a plasma trapped in a magnetic field. It is much more probable that this diffusion is closely related to the characteristic properties of the magnetic trap and depends on the manipulations to which the plasma is subjected. Thus, for instance, despite the extreme scarcity and haphazard nature of experimental data, the impression exists that, when Joule heating takes place, the anomalous diffusion is a calamity difficult to prevent; while in the case of a plasma which is not subjected to the influence of a current, this diffusion either does not appear at all or exists in a considerably attenuated form. Further development of the theory, supported by new experimental data, should provide the answer both to the question of the conditions accompanying the generation of anomalous diffusion and to the question of the possible methods for preventing it. These questions are of decisive importance for our entire problem, since a high thermonuclear yield can be achieved only in a highly stable plasma.

In connection with the problem of verifying theoretical conclusions, let us mention one factor which, although it seems completely trivial, usually escapes one's attention when theory is compared with experiment. What we have in mind is that one must not confuse instability with the absence of an equilibrium, which may be caused by an incomplete compensation of the forces applied to the plasma or by the initial motion of the plasma. In analysing the behaviour of the plasma in a specific magnetic system, one should consider all the forces which act upon it and the initial conditions under which the plasma is formed.

In particular, one example of the breakdown of equilibrium that can be quoted is the influence of stray magnetic fields on the behaviour of a plasma column in a toroidal chamber, which was mentioned in the last chapter. Under the action of these fields the column undergoes a marked radial displacement during a discharge, and under certain conditions this displacement can resemble the development of instabilities. The force of gravity can also break down the stability of a plasma and force it to move across the magnetic lines of force. In a uniform magnetic field this motion will be indistinguishable from a free fall. However, because of the low acceleration, the displacement of the plasma under the influence of gravity can be observed only during a period of time measured in tens of milliseconds.

§ **7.8.** A substantial part in the energy balance of a magnetically confined plasma may be played under certain conditions by the so-called magnetic or betatron radiation associated with the Larmor rotation of the electrons. According to the laws of classical electrodynamics, a charged particle in accelerated motion should radiate electromagnetic energy. For an electron moving in a magnetic field $H$ along a helical path with a centripetal acceleration $v_{\perp}^2/\rho_{He}$, the energy radiated per unit time is given by the expression

$$q_r = \frac{2}{3}r_0^2\left(1+\frac{W_e}{m_0c^2}\right)^2 \frac{v_{\perp}^2}{c}H^2, \qquad \text{.........}(7.64)$$

where $r_0$ is the classical electron radius, $m_0$ is the electron rest mass and $W_e$ is the kinetic energy of the electron (in the cases of interest to us, $W_e < m_0c^2$).

The emission spectrum for an individual electron is a line spectrum. It consists of the fundamental line with a cyclotron frequency $eH/mc$ and its simple harmonics.† If the energy of the electron is small enough compared

---

† Owing to the Doppler effect and considerations of relativity, the frequency, $\omega_n$, of the $n$th harmonic turns out to depend on the velocity of the particle ($v_{\parallel}$ and $v_{\perp}$) and the angle $\theta$ between the direction from which the radiation is observed and the magnetic field. A more accurate formula is

$$\omega_n = \frac{n\omega_{He}\sqrt{1-v^2/c^2}}{1-(v_{\parallel}/c)\cos\theta},$$

where $\omega_{He} = eH/mc$.

with $m_0c^2$, the bulk of the radiated energy should be at the fundamental frequency. As $W_e$ rises, the proportion of the higher harmonics in the total radiation intensity increases rapidly. If it is assumed that all the radiated energy leaves the plasma, the energy lost in magnetic radiation from a plasma with number density $n_e$ and temperature $T_e$ will amount to

$$Q_r = \frac{4e^2}{3c}n_e\Omega\left(\frac{eH}{m_ec}\right)^2\frac{kT_e}{m_ec^2}. \qquad \text{.........(7.65)}$$

Here $\Omega$ is the plasma volume. It is assumed that $kT_e \ll m_ec^2$ and that the velocity distribution is isotropic.

The quantity $Q_r$ may be compared with the evolution of energy occurring as a result of thermonuclear reactions. The energy $Q_{nuc}$ liberated in thermonuclear fusion is proportional to $n^2\Omega f(T)$, where $f(T)$ is a known function of the temperature (we assume that $T_e = T_i$). Therefore,

$$\frac{Q_r}{Q_{nuc}} \simeq \frac{H^2T}{nf(T)} \propto \frac{1}{\beta}F(T),$$

where $\beta$ is the ratio of the plasma pressure to the magnetic pressure, and $F(T) = T^2/f(T)$. A numerical calculation shows that in a deuterium plasma at any temperature and any possible value of $\beta$ (up to unity), the total magnetic radiation is many times greater than the energy evolved as a result of thermonuclear reactions. Thus, for instance, at $T = 5\times10^8$ °K, the ratio $Q_r/Q_{nuc}$ is about 20 even in the optimistic case when $\beta = 1$. However, for a mixture of deuterium and tritium at $\beta \approx 1$, there is a rather wide temperature range in which $Q_{nuc} > Q_r$.

Consequently, if the magnetic radiation could leave the plasma freely, it would constitute one of the chief obstacles to the construction of a thermonuclear reactor with a positive energy balance. In reality, however, the matter is considerably more complicated. In a dense plasma, the major part of the magnetic radiation, which corresponds to the fundamental frequency and the first few harmonics, is absorbed without leaving the plasma, and only the radiation of the relatively weak higher harmonics escapes across the plasma boundary without any substantial attenuation. The difficult problem of the absorption of magnetic radiation in the plasma has been thoroughly analysed and fully elucidated in the work of Trubnikov.

An idea of some of Trubnikov's findings is given by Fig. 100, which shows the spectral distribution of the magnetic radiation intensity leaving a plane plasma layer for the case where $\beta = 1$. The frequency, in units of $\omega_{He} = \dfrac{eH}{m_ec}$ is plotted along the abscissa, and the spectral intensity distribution along the ordinate. The ordinate scale is chosen so that the spectrum of a black body is represented by the parabola $y = 2x^2$ in the low-frequency region (i.e. where this spectrum is described by the Rayleigh-Jeans law).

Absorption in the plasma alters not only the intensity, but also the spectral distribution of the radiation. Low frequencies, i.e. the lower harmonics of the magnetic radiation, are absorbed most readily. For this reason, in the spectrum of radiation emitted from a thick plasma layer, the higher harmonics (which in the primary spectrum account for a relatively small intensity) should predominate. As a result of the absorption, the spectrum should depend on the thickness of the radiating layer. This thickness is conveniently expressed in dimensionless units. The dimensionless thickness $A$ of a layer is given by the relation

$$A = \frac{4\pi n e}{H} a,$$

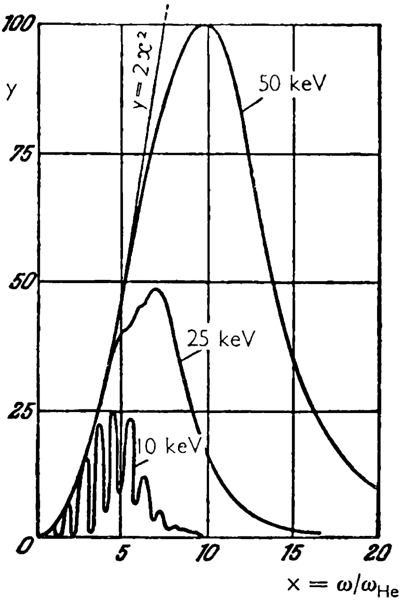

Fig. 100

Magnetic radiation spectrum; the various curves correspond to different values of the electron temperature

where $a$ is the thickness of the layer in centimetres. The graphs shown in Fig. 100 are plotted for the case where $A = 10^4$. The different curves represent the spectrum of magnetic radiation corresponding to different values of the plasma temperature. Attention is drawn to the fact that when $kT_e$ is equal to 10 keV, the individual harmonics show up clearly in the spectral distribution, while at higher temperatures the curves have a shape characteristic of a continuous spectrum. The reason is that, due to the thermal velocity spread, the electrons have different masses, and hence radiate at different frequencies (see footnote on p. 281). Therefore, at high temperatures, the individual lines of the higher harmonics overlap. We should also note that the spectral intensities never exceed the limits of the black-body level, which in this portion of the emission spectrum of a high-temperature plasma is given by the Rayleigh-Jeans formula (as should be expected on the basis of the general laws of radiation theory).

The absorption of the magnetic radiation reduces the flux of electromagnetic energy leaving the plasma surface for thick enough plasma layers, and reduces the radiation losses correspondingly. According to Trubnikov, the total radiation power emerging from a plane plasma layer can be expressed as follows:

$$Q_r = Q_0 f_1(A, T), \qquad \text{........}(7.66)$$

where $Q_0$ is the energy flux in the absence of absorption, and $f_1$ is a factor which allows for the absorption of the magnetic radiation in the layer. $Q_0$ is calculated from equation (7.65), and the graphs shown in Fig. 101 can be used to determine the coefficient $f_1$. It follows from these graphs that when $T_e = 5 \times 10^8$ °K in a layer having a dimensionless thickness of

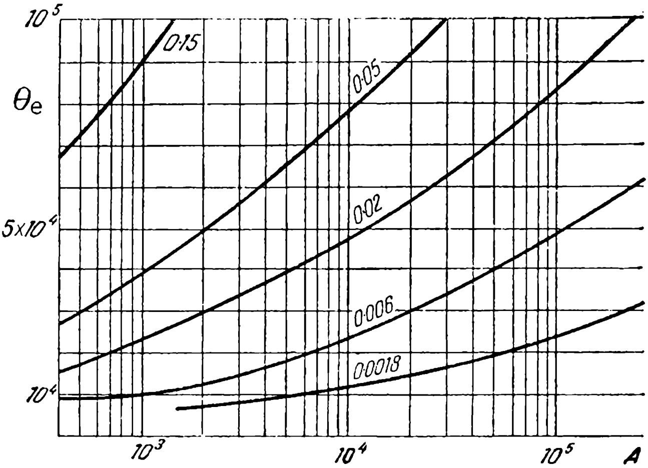

FIG. 101. Graphs for the determination of $f_1$ for different values of $A$ and $\theta_e$

the order of $10^3 - 10^4$, the absorption decreases the radiation loss by two orders of magnitude.

By using these graphs it is possible, for given values of the basic parameters ($T_e$, $H$ and $n_e$), to determine the minimum layer thickness for which the radiation energy emerging from the plasma will be equal to the energy yield produced by thermonuclear reactions. Thus, for instance, when $T = 5 \times 10^8$ °K, $n_e = 10^{14}$ cm$^{-3}$ and $H = 5 \times 10^4$ Oersteds (under these conditions, $\beta \approx 0{\cdot}1$), the minimum thickness for deuterium should be about two metres. In reality, the situation may turn out to be more favourable, because magnetic radiation is mainly in the far infra-red (wavelengths in the range $10^{-1}$–$10^{-2}$ cm) and can be reflected from the metallic walls of the chamber with a coefficient close to unity. Therefore, the major part of the radiation will be reflected back into the plasma. Rough estimates indicate that by using this effect it is possible to reduce the radiation loss by at least one order of magnitude. Under these conditions, this loss will apparently no longer play an important part in the energy balance for thick layers of a high-temperature plasma, at least for a deuterium-tritium mixture (provided $\beta$ is no less than 0·1 and the electron temperature is not above a few tens of kiloelectron volts).

Among the various types of magnetic traps designed for the prolonged confinement of high-temperature plasma and the achievement of controlled thermonuclear reactions, the most sensitive to magnetic radiation are the magnetic mirror systems, because an excessive loss of particles by Coulomb collisions can be prevented only by heating the plasma to much higher temperatures than are necessary in traps with closed lines-of-force.

## CHAPTER VIII

# SPECIFIC TYPES OF MAGNETIC TRAP

### *The Stellarator*

§ **8.1** The plasma in a Stellarator is confined by an externally generated toroidal-type magnetic field with the property that each line of force twists round the centre line of the tube bore and forms, by successive circuits round the torus, a complete toroidal surface (the so-called 'magnetic surface'). It must be emphasised that the magnetic field is created by a winding on the external surface of the chamber. It is this which distinguishes the Stellarator from toroidal systems in which the rotation of the lines of force is obtained by having a ring-shaped current-carrying conductor inside the chamber.

The service rendered by Spitzer and his colleagues lies in their having found a number of methods for producing this 'rotational transform' of the lines of force, both by deforming the chamber itself, and also by introducing additional external windings which twist the otherwise longitudinal lines of force in an ordinary toroidal chamber (or in a chamber of 'race-track' shape). Before presenting the methods used to create such fields in further detail, we shall describe the general geometrical properties of the 'rotational transform', basing the discussion on that given in the Geneva conference paper by Spitzer.

Figure 102 shows a minor cross-section of a toroidal-type chamber enclosing a magnetic field with the relevant properties. Let us consider a line of force which does not pass too close to the chamber wall. Let the point $P_1$ represent this line of force in the given minor cross-section of the tube (i.e. $P_1$ is the point where the line of force intersects the plane of the drawing). If we follow the continuation of this line of force round the major axis of the toroidal chamber, the line of force again cuts the plane shown on the drawing, this time at some point $P_2$. In a chamber with a simple longitudinal field, $P_1$ and $P_2$ coincide. However, when there are windings or geometrical deformations which produce a rotational transform, the point $P_2$ will be displaced with respect to $P_1$, and this displacement will be almost purely azimuthal—that is to say it will not be associated with any very noticeable change in the distance from the centre line of the tube bore. In further circuits round the chamber, the line of force will cut the given cross-section of the tube consecutively at points $P_3$, $P_4$ and so on. When these points are joined up they form some sort of closed curve. To describe this curve accurately, it is necessary to follow the line of force over a large number of circuits around the chamber. After $N$ circuits we obtain on the plane of Fig. 102 $N$ points of intersection between the plane and the line of force, and these points will follow one another along the curve shown by a dotted line and become steadily more closely spaced as $N$ is increased. Given an infinite number of circuits round the chamber, a line of force will trace out a toroidal surface of which the curve in Fig. 102 is a cross-section.

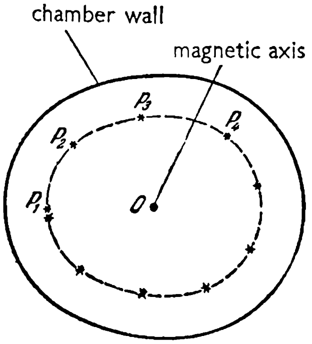

FIG. 102. Diagrammatic representation of a rotational transform

From geometrical considerations of a quite general character, it must be allowed that amongst the various lines of force there will be one which is not displaced and which therefore closes on itself in one circuit round the chamber. This line of force may be termed the 'magnetic axis' of the system. It intersects the given minor cross-section at some central point $O$. In practice it can be considered that the magnetic axis roughly coincides with the geometric centre of the bore of the toroidal chamber.

The simplest system in which a magnetic field undergoes rotational transformation is the figure eight configuration already mentioned (§ **7.2**; Fig. 89). Figure 103 shows a projection of the chamber on to a plane perpendicular to the line joining the centres of the curved sections. $LM$ and $NK$ correspond to curved sections of the chamber. They lie in planes inclined at an angle $\alpha$ to the straight sections $KL$ and $MN$. To demonstrate how the rotational transformation takes place, Fig. 103b shows in one plane the four cross-sections of the chamber at the points $K$, $L$, $M$ and $N$. The projection of the magnetic axis of the system is represented by the full line passing through the centres of the cross-sections. Let one of the lines of force pass through the point $P_1$ in the cross-section $K$. If we carefully investigate the course of this line round the figure eight, we can establish that

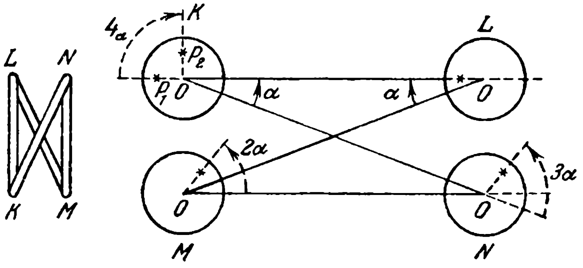

(a) (b)

FIG. 103. (a) Projection of the figure eight onto a plane perpendicular to the line joining the centres of the curved sections;
(b) Simplified projection, illustrating the origin of the rotational transform

in the $L$, $M$ and $N$ cross-sections it passes through the points indicated by small crosses in the figure, as follows. In the straight sections $KL$ and $MN$ the line of force does not undergo rotation. Therefore the radius vector joining the point (representing the line of force) to the centre of the tube in section $K$ is parallel to that in section $L$; and similarly in sections $M$ and $N$. In the curved sections $LM$ and $NK$, the line of force remains parallel to the magnetic axis and curves with it; consequently, it occupies in each cross-section one and the same position relative to the magnetic axis. Taking this into account, we can see that after a complete circuit round the figure eight, a line of force rotates through an angle equal to $4\alpha$ about the centre line of the tube bore. It should be noted that, in this ideal configuration, the rotational transform angle has the same value for all lines of force irrespective of their position relative to the magnetic axis. In practical devices this corollary is only approximately fulfilled.

Rotation of the lines of force can be brought about in other ways as well. The most important of these is probably that based on using additional windings which generate a transverse magnetic field in a toroidal chamber. The strength of this field increases as one moves away from the centre of the minor cross-section, and the direction of the field changes as one moves longitudinally round the tube.

To give an impression of the geometry of this field we shall simplify the problem by replacing the toroidal chamber with an infinite straight cylinder. We shall assume that the transverse field is produced by a winding consisting of $2n$ symmetrically disposed conductors, each of which runs helically around the outer surface; the currents in these conductors are of equal strength but are opposite in direction in adjacent conductors (Fig. 104). When the field created by a helical winding of this type is added to the uniform axial field of a simple solenoid, the lines of force become twisted about the centre line. If one selects some line of force passing not too close to the walls of the cylinder, and follows it along the tube for a distance many times the pitch length of the helical winding, one can easily see that the line of force gradually rotates round the axis of the cylinder. The entire length of the line of force lies on a 'magnetic surface'.

To elucidate the complex geometry of lines of force and magnetic surfaces, we shall use drawings (Figs. 105 and 106) taken from a paper by Morozov and Solov'ev, who have studied the structure of a helical field in detail. Figure 105 shows schematically the cross-section of magnetic surfaces in a plane perpendicular to the axis of the cylinder when $n = 3$. More detail of this cross-sectional structure is shown in Fig. 106. The three-dimensional form of the magnetic surfaces can be visualised if we imagine that, as we move along the cylinder axis, the picture shown in these figures rotates about the axis, one revolution being completed in the pitch length of the helical winding.

From Figs. 105 and 106 we can see that the magnetic surfaces are divided into two classes. One class consists of closed surfaces which enclose the tube axis; the other consists of those surfaces which close externally round the helical conductors. The intermediate magnetic surface, which divides the two different classes, is shown by a thick line on the figures. The sharp apices shown are characteristic of such a surface. The position of this boundary surface ('the separatrix') has great importance in practice because particles are confined in a helical field only if they move within the region bounded by the separatrix (because the lines of force outside this region pass through the wall of the vacuum tube). If we increase the current in the helical winding while leaving the axial magnetic field unchanged, the separatrix is squeezed in towards the axis of the cylinder and there is a corresponding reduction in the volume of the plasma-confining region.

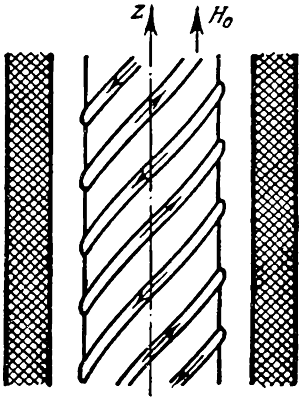

FIG. 104. The system of conductors generating a helical field

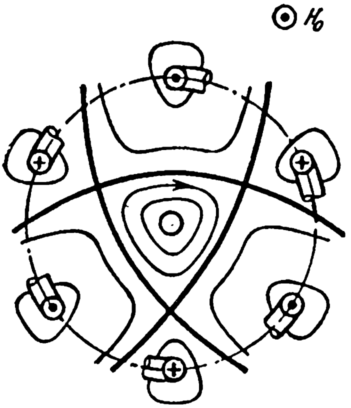

FIG. 105. Rough outline of the magnetic surfaces in a Stellarator with a helical winding

We shall now describe the geometrical properties of the lines of force within the separatrix. A line of force lying on a magnetic surface also revolves as it is followed along the cylinder axis, but it revolves more slowly than the cross-sectional shape of the magnetic surface. Over a sufficient axial distance, a line of force will rotate many times round the magnetic surface created by it. Figure 107 indicates the shape of an individual line of force lying inside the separatrix. It is evident that the line of force has quite a complex helical structure. The line forms a helix with a pitch length $L/n$ ($L$ is the pitch length of the helical winding) and an elliptical projection on the plane perpendicular to the helix axis. This axis is itself a helical line, with a much greater pitch length and a circular projection on the plane perpendicular to the cylinder axis. The field strength changes as one moves along the line of force. It is greatest at points furthest from the cylinder axis $z$; it is smallest at points nearest to the axis. The variation of $H$ along the line of force depends on the ratio

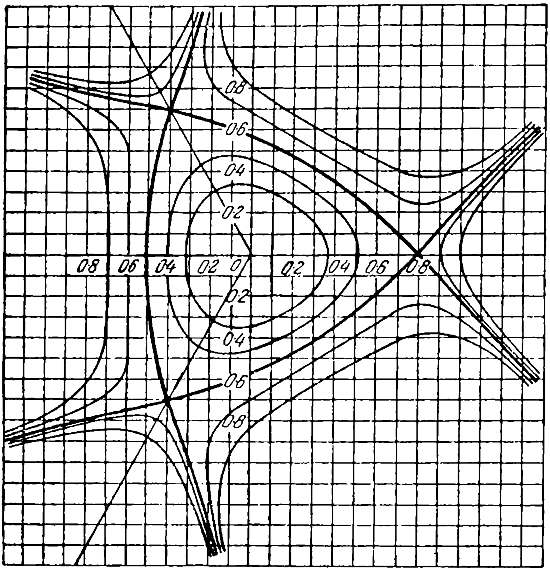

FIG. 106. Structure of the magnetic surfaces when $n = 3$

of the transverse component of the helical field to the axial component lying along the $z$ axis. In existing apparatus this ratio is not large and the change in $H$ along a line amounts to no more than a few per cent—sometimes to a fraction of one per cent—and is zero on the axis.

The sketches given here show the simplest case of a helical field created inside a straight cylinder. In actual installations such fields are created inside a toroidal or race-track chamber. It seems very probable that if the minor radius of the plasma is only a small fraction of the major radius of the torus, then the structure of the magnetic field produced by the helical winding will be qualitatively the same as for a straight cylinder. This is in fact the result given by an exact calculation of helical fields in toroidal systems, made with the help of computing machines.

A helical field of this Stellarator type has an important property which makes a vital contribution to the stability of the plasma column: as one

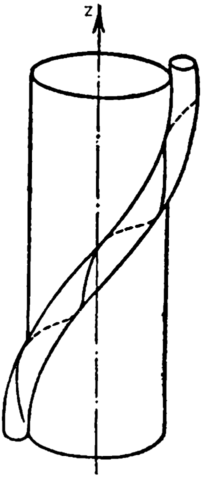

FIG. 107

The shape of a line of force within the separatrix goes from the inner regions of such a field to its periphery, the pitch of the lines of force increases, that is to say the angle which they make with the cylinder axis gets bigger, so that there is shear in the field. The angle through which a line of force rotates over a given axial length is also, in general, a function of $r$. It is independent of $r$ only for a helical winding with $n = 2$, which creates a transverse field proportional to the first power of $r$ near the axis.

It is of great practical importance to know how precisely the windings of a Stellarator need to be made and located in order to ensure the properties of the magnetic field. A detailed study of this question shows that the tolerances admissible for the windings of a Stellarator are extremely stringent. The relative accuracy that must be maintained for such parameters as the pitch of the helical winding, the distance between the conductors, the diameter of the winding and so on, must be of the order of 0·1 %. If this accuracy is not achieved there is an appreciable deformation of the magnetic surfaces and, as a result, a considerable reduction of the volume enclosed by the separatrix.

An approximate theory for the motion of individual particles in a Stellarator with a helical field has been worked out by Morozov and Solov'ev. The theory assumes that, as a particle moves, both the 'transverse adiabatic invariant' $W_{\perp}/H$ and the 'invariant of parallel motion' are conserved. It will be recalled that for particles trapped in some section of a line of force the latter invariant is given by $\int v_{\parallel}\, dl$, the integral being taken between points at which $v_{\parallel}$ becomes zero. In analysing the motion of particles which are freely displaced along lines of force one has to make some change in the expression for the invariant of parallel motion, but we shall not now dwell on this refinement.

For particles whose Larmor radii are sufficiently small, a Stellarator, given the tolerances mentioned, is an ideal trap. The motion of a particle projected on to the minor cross-section (i.e. the plane of the cross-section of the tube) takes place along a trajectory which, to a first approximation, can be considered as closed. The centre of this closed trajectory is displaced relative to the centre line of the tube bore by a distance $\Delta$. For a particle whose velocity is inclined at a relatively small angle to the magnetic field, the displacement $\Delta$ is given by the expression

$$\Delta \approx \frac{L}{2\pi}\left(\frac{2n\rho_{\mathrm{H}}}{R}\frac{H_0^2}{H_{\perp}^2}\right)^{1/(2n-3)}. \qquad \text{.........}(8.1)$$

In this expression $L$ is the pitch length of the helical winding, $R$ is the major radius of the torus, $\rho_{\mathrm{H}}$ is the Larmor radius, $n$ is the order of helical symmetry, i.e. the number of independent helical conductors carrying current in the same direction. $H_0$ is the strength of the longitudinal field, $H_{\perp}$ is the strength of the transverse field created by the helical winding at distance $L/2\pi$ from the centre line of the tube. Equation (*8.1*) relates to the case of $n \geqq 3$. When $n = 1$ and 2 the expression for $\Delta$ is

$$\Delta = \frac{L\rho_{\mathrm{H}}}{\pi R}\left(\frac{H_0}{H_\perp}\right)^2. \qquad \ldots\ldots\ldots(8.1a)$$

Equations (*8.1*) and (*8.1a*) can also be used to determine $\Delta$ in the case when the angle between the particle velocity and $\boldsymbol{H}$ is not too small, if we confine ourselves to analysing the motion of particles which travel freely round the whole chamber without being subject to large reductions of $v_{\parallel}$ in those regions where the field intensity is a maximum. For particles whose motion along the lines of force is limited by mirror effects, the displacement is determined by expressions of different type, which will not be given here.

To get some appreciation of the effect of toroidal geometry on the motion of particles in a Stellarator, we shall consider a numerical example. Let $R = 100$ cm, $H_0/H_\perp = 4$, $L = 60$ cm, $\rho_{\mathrm{H}} = 0{\cdot}5$ cm (Larmor radius of a 10 keV deuteron in a field of 40,000 Oe); then the displacement $\Delta$ of the trajectory from the centre line is calculated to be $\simeq 3{\cdot}5$ cm when $n = 3$ and about $1{\cdot}5$ cm when $n = 1$ and $n = 2$. There is considerable practical interest in the determination of $\Delta$ for a Stellarator with a race-track geometry. However, in work published up to now, this case has not been investigated in sufficient detail, probably because of the difficulties involved in analysing trajectories at points where the semi-circular sections of the tube join straight sections.

One comment must be added to what has been said above about the properties of a Stellarator as a magnetic trap for single particles. Strictly speaking, the drift theory of particle motion cannot answer the question of whether or not a given magnetic trap can be considered as an 'ideal' trap. In particular, if we use the drift approximation to deal with the motion of particles in the helical field of a Stellarator, we are compelled to exclude from consideration the trajectories of those particles with a very small longitudinal velocity. Such particles are trapped by mirror effects within short sections of the lines of force. The drift theory does not allow us to make definite statements about the trajectories of these particles, nor can we establish whether they are confined in the trap for a significant time. Therefore it is more correct and more cautious to describe the Stellarator as an 'almost ideal' trap. The proportion of particles which come into the group with indeterminate properties is extremely small, and consequently the difference between the descriptions 'ideal' and 'almost ideal' is hardly of very special importance.

§ **8.2** The ultimate purpose of the Stellarator is to serve as a magnetic trap for a plasma of useful density. The theory of the Stellarator cannot, therefore, be limited to an analysis of the behaviour of individual particles. The main object of the first stage of theoretical studies is to assist the understanding of the equilibrium and stability of plasma in a Stellarator. In the magnetohydrodynamic approximation, the equilibrium configuration of a plasma with an isotropic pressure is determined by solving the system of equations

$$\operatorname{grad} p = \frac{1}{c}\, \boldsymbol{j} \times \boldsymbol{H}, \qquad \text{.........}(8.2)$$

$$\boldsymbol{j} = \frac{c}{4\pi} \operatorname{curl} \boldsymbol{H}, \qquad \text{.........}(8.3)$$

$$\operatorname{div} \boldsymbol{H} = 0. \qquad \text{.........}(8.4)$$

Because of the complicated structure of the magnetic field, it is hardly to be expected that the solutions of these equations can be presented as simple closed expressions. It is possible, however, to draw some conclusions about the behaviour of plasma in a Stellarator from an analysis of the quite general consequences of equations (*8.2*)–(*8.4*). As remarked in Chapter IV, it follows from equation (*8.2*) that the (isotropic) plasma pressure remains constant along a line of force. Therefore in systems of the Stellarator type, where every line of force generates a complete magnetic surface, the pressure on this surface is a constant. Since $\boldsymbol{j}$ is perpendicular to grad $p$, the current flow must lie wholly on the magnetic surfaces (i.e. the current cannot have a component perpendicular to a magnetic surface).

We shall now point out the difference in behaviour between plasma in a simple toroidal field,† and plasma in the helical field of a Stellarator. In the field of a toroidal solenoid, $\boldsymbol{H}$ has only a longitudinal component and consequently, by equation (*8.3*), the longitudinal component of $\boldsymbol{j}$ equals zero, i.e. the current flows perpendicularly to the lines of force. This is precisely the reason why, in the case we are considering, there are no solutions to the equations corresponding to equilibrium plasma configurations of toroidal form. Indeed, it follows from equation (*8.2*) that

$$\boldsymbol{j} = -\frac{c}{H^2}[\operatorname{grad} p] \times \boldsymbol{H}. \qquad \text{.........}(8.5)$$

As was shown in Chapter IV, if the longitudinal component of current density is zero, this equality is incompatible with the condition div $\boldsymbol{j} = 0$. In other words, a ring-shaped plasma can be in equilibrium only on condition that the current has a longitudinal component. When this longitudinal component of the current is arbitrary, equation (*8.5*) does not define the full value of the vector $\boldsymbol{j}$ but only that component of it which is perpendicular to $\boldsymbol{H}$; it follows that there is then no inconsistency with the requirement that div $\boldsymbol{j} = 0$. This is just the situation that we encounter in changing from a system with a simple toroidal field to a Stellarator. In a plasma confined by the helical field of a Stellarator, the diamagnetic currents flow in such a way that the angle between $\boldsymbol{j}$ and $\boldsymbol{H}$ is not equal to

---

† Without a longitudinal current produced by induction.

90°. The appearance of a component of $\boldsymbol{j}$ parallel to $\boldsymbol{H}$ is caused by the more complicated field structure.† As Spitzer notes, the physical purpose of the parallel currents in the Stellarator is to prevent the separation of charges due to toroidal drift. Charges of opposite sign, which otherwise accumulate due to particle drift in the non-uniform field, are able to flow along the helical lines of force and annul one another.

In a Stellarator the ratio $\beta$ of plasma pressure to magnetic pressure cannot be near to unity because the plasma itself must not cause any significant distortion of the structure of the helical field nor must it bring about any perceptible deformation of the magnetic surfaces. If $\beta$ is sufficiently small, the geometrical structure of the field in the plasma-filled trap preserves its basic vacuum characteristics, and it is then possible to use the method of successive approximations to solve the equilibrium equations.

Let $H_0$ represent the vacuum magnetic field strength. We shall choose an initial pressure distribution for the plasma in the magnetic system. There can be a fair degree of arbitrariness about this distribution, which is limited only by the following two obvious requirements:

(1) at any point $\beta$ must be small compared with unity (its maximum value emerges from the calculation itself);

(2) the plasma pressure does not change along a line of force, and therefore it must be the same at all points on the same magnetic surface.

For magnetic surfaces lying outside the separatrix of the helical field, the pressure should be taken as equal to zero. Clearly it may be assumed that, within the region bounded by the separatrix, the pressure must decrease more or less gradually with increasing distance from the magnetic axis. We shall designate the initial value of the plasma pressure by $p_0$. The first step in the method of successive approximations is to determine the current density $\boldsymbol{j}$ in the plasma from equation (*8.2*)

$$\operatorname{grad} p_0 = \frac{1}{c}\boldsymbol{j}_1 \times \boldsymbol{H}_0 .$$

Knowing $\boldsymbol{j}_1$ one can calculate the small change of magnetic field due to the plasma diamagnetism from the equations

$$\operatorname{curl} \boldsymbol{H}_1 = \frac{4\pi}{c}\boldsymbol{j}_1 \quad \text{and} \quad \operatorname{div} \boldsymbol{H}_1 = 0.$$

After replacing $\boldsymbol{H}_0$ by the refined value of the field strength $\boldsymbol{H}_1$, a correction must be made to $p_0$. The refined value $p_1$ of the pressure is chosen, to satisfy the requirement that there should be no pressure gradients parallel to the magnetic surfaces of the field $\boldsymbol{H}_1$. The new value of the pressure thus gives the following approximation for the diamagnetic current density:

---

† This component should not be confused with the longitudinal current generated in the Stellarator by inductive coupling of the plasma loop to an external power source: such a current serves for the initial heating of the plasma.

$$\operatorname{grad} p_1 = \frac{1}{c} \boldsymbol{j}_2 \times \boldsymbol{H}_1.$$

On finding $\boldsymbol{j}_2$ one can proceed to the next approximation for field strength, and so on.

The method just given for calculating the basic parameters of the equilibrium plasma configuration in a Stellarator is applicable only when $\beta$ is small compared with unity. Detailed theoretical analysis shows that even when $\beta > 0{\cdot}01$ the distortion of the magnetic surfaces caused by diamagnetic currents in the plasma will be so great that the geometry of the resulting field will be very different from the initial geometry, and the trap will lose its ability to confine plasma.

The Princeton theoretical group has paid great attention to the problem of plasma stability in a Stellarator. The main qualitative conclusion that emerges from these studies is that an equilibrium plasma, which is not subjected to the action of an external electro-motive force, will (as far as magnetohydrodynamics is concerned) be stable with respect to the most dangerous perturbations described in § 7.4.

The predicted stability of a plasma column in a Stellarator is determined by the properties of the helical field. The main part here is played by the rapid growth in the transverse component of $\boldsymbol{H}$ as one moves away from the magnetic axis. Because the transverse component of the field increases more rapidly than $r$, the lines of force get more twisted in the outer regions than in the central ones. A sheared field structure like this makes it difficult for flute-like deformations to develop because the lines of force cannot, in the infinite conductivity approximation, disentangle themselves from each other.

However, the prospects of achieving stability appear less rosy when the plasma is being ohmically heated. The weakening of stability under these conditions is associated first of all with the fact that when the longitudinal current in a Stellarator is large, growing perturbations which are of the same type as in a simple toroidal chamber can appear. In both cases, the boundary of the stability region is determined by the Kruskal-Shafranov criterion, the sense of which is (Chapter VI) that the lines of force lying on the surface of a ring-shaped plasma must not complete a minor circuit in the course of a complete major circuit round the chamber. To obtain a mathematical formulation of this criterion in a form applicable to an ohmically heated Stellarator, we shall note that in this case the rotation of the lines of force is due to two causes: first, the helical structure of the magnetic field; and second, the magnetic field generated by the ohmic heating current. The rotational transform angle either increases or decreases depending on the direction of the current. An increase occurs when the direction of the field generated by the heating current coincides with the direction of rotation of the vector **H** of the vacuum field. In the opposite case, the ohmic heating current leads to an untwisting of the helical lines of force.

In the latter case, if the heating current is large enough, the net rotation of the lines of force can be opposite in direction to that produced by the helical winding alone. However, it seems that such a state of affairs is unlikely to be of practical importance because, before it can be reached, the equilibrium of the plasma ring must break down. This breakdown of equilibrium occurs when the heating current is sufficiently large to untwist the lines of force completely; that is, the rotation due to current in the plasma annuls the rotation due to the helical winding.

On the basis of the above remarks, it is relatively simple to derive a stability criterion analogous to the Kruskal-Shafranov criterion for a Stellarator with a longitudinal heating current. If the directions of the rotations caused by the current and by the helical winding are identical, then the condition for stability is

$$\frac{2J}{cr_0} < H_z\frac{r_0}{L}(2\pi-\psi). \qquad \text{.........}(8.6)$$

In the case of opposite rotations, this condition can be written in the following form:

$$\frac{2J}{cr_0} < H_z\frac{r_0\psi}{L}. \qquad \text{.........}(8.7)$$

In these inequalities, $J$ is the total longitudinal current, $H_z$ is the longitudinal component of the external field, $r_0$ is the radius of the column (assuming that the column has a well-defined boundary), $L$ is the length of the major circumference of the Stellarator chamber and $\psi$ is the rotational transform angle. For the sake of simplicity it is supposed that this angle is less than $2\pi$. If $\psi > 2\pi$, then in inequality (*8.6*) the difference $2\pi-\psi$ must be replaced by $2\pi n-\psi$, where $n$ is the smallest positive whole number satisfying the condition $2\pi n > \psi$. Then in (*8.7*), instead of $\psi$, one must write $\psi-2\pi(n-1)$. The geometrical significance of these substitutions is easily explained if we note that if $\psi > 2\pi$, instability will appear for the first time when there is a plasma current of such strength that the total rotational transform angle is a multiple of $2\pi$.

Let us now assume that the Kruskal-Shafranov criterion for stability has been satisfied. One might hope that a quiescent ohmic heating of the Stellarator plasma would now occur. This expectation is indeed correct, but only in certain limited circumstances. The fulfilment of the stability conditions (*8.6*) or (*8.7*) prevents marked distortion of the column form, such as the formation of protuberances on the plasma and ejection of matter to the wall at speeds comparable with the thermal speed of particles. In other words, condition (*8.6*) can be regarded as eliminating 'strong' instabilities. However, there remains a 'weak' instability which, apparently,

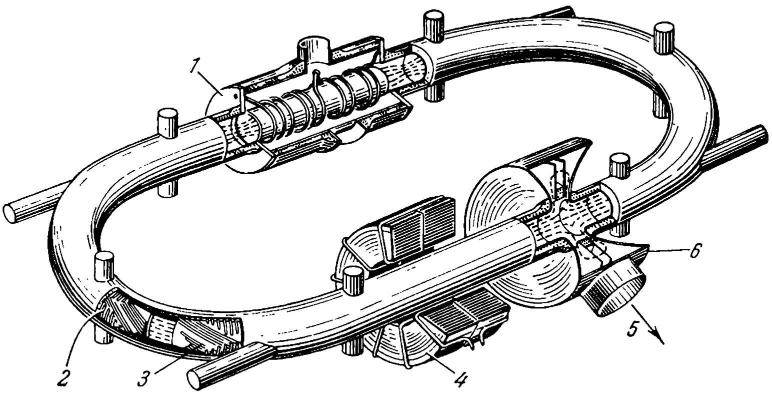

FIG. 108. Race-track type Stellarator with divertor and section for resonance heating

*1:* resonance heating section; *2:* coils generating the longitudinal field; *3:* helical windings; *4:* ohmic heating transformer; *5:* to vacuum pump; *6:* divertor

can give rise to anomalous diffusion, even at current strengths considerably less than those involved in fulfilling the Kruskal-Shafranov criterion.

We make here only passing mention of this instability; apparently it occurs when ohmic heating of plasma takes place both in a simple toroidal field and in the helical field of a Stellarator. The characteristics and possible causes of this instability will be discussed after we have described the main experimental observations of the properties of Stellarators.

§ **8.3** The construction of a race-track Stellarator is shown schematically in Fig. 108. To produce the longitudinal field there is an ordinary winding distributed along the whole length of the chamber. The helical windings are placed on the curved sections. The vacuum chamber is made of thin stainless steel, and can be heated to a high temperature for degassing.

Ionisation of the gas and preliminary plasma heating is at present carried out by a longitudinal current which is excited in the chamber by

FIG. 109

Outline design of a divertor

*1:* chamber walls

*2:* central divertor coil

*3:* main confining field windings

*4:* pumping orifice

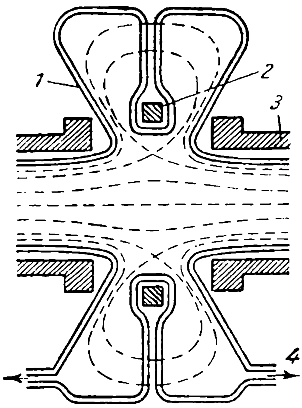

induction. To prevent longitudinal currents appearing in the thin metal walls of the vacuum chamber, a cross-sectional cut is made in it and a ring of heat-resistant dielectric is inserted. In one of the straight sections of the chamber, apparatus can be installed to generate a high-frequency heating field (methods of high-frequency heating of plasma in Stellarators are discussed a little further on). The so-called 'divertor' can be installed in the other straight section.

The purposes of this 'divertor' are to reduce the interaction between the plasma and the walls, and to prevent impurity atoms from penetrating into the middle of the plasma column. In the divertor, the form of the magnetic field is considerably changed, and its strength is reduced, so that the outer lines of force are led outside the main chamber. The construction of a divertor is shown schematically in Fig. 109. To bend the lines of force as shown in the figure, the current in the middle coil 2 is made to flow in an opposite direction to that of the current in the main coil 3. If one follows the lines of force, one can see that the entire flux which, in the uniform field region, lies in a surface region adjacent to the wall, now goes into the divertor. If an impurity atom is dislodged from the wall of the Stellarator tube, it becomes ionised close to the surface of the plasma column; the ion then moves along one of these outer lines of force into the divertor chamber where it once more falls on to a solid surface and becomes embedded in it. A neutral atom emitted from this absorbing surface in the divertor chamber cannot easily enter the Stellarator tube. It will do so only if its initial direction of motion lies inside a comparatively small solid angle subtended by the access aperture of the divertor at the absorbing surface. In other cases, an atom dislodged from the absorbing surface falls on to the inner walls of the divertor chamber. Experiments with a divertor were carried out on the model B-65 Stellarator. The spectroscopically measured impurity content and the plasma temperature were determined with and without the divertor energised. It was found that in practice the impurity content was reduced 2–3 times by energising the divertor.†

Many methods can be used to obtain high-temperature plasma in a Stellarator. The most straightforward of these is to use two heating mechanisms: first, ohmic heating of the plasma by an induced current; and second, further plasma heating by means of a high-frequency alternating field. As regards ohmic heating, the same considerations apply as were discussed in Chapter VI in the analysis of quasi-stationary discharges in toroidal chambers; for this stage to be effective, the stability of the plasma column must be maintained, i.e. inequality (*8.6*) must be preserved. Furthermore, in order to avoid runaway electrons appearing, one has to keep $E$ sufficiently small compared with the critical value $E_c$ defined by equations (*3.17*) and (*3.18*).

The difference between the electron and ion temperatures during ohmic heating has no special importance; in a Stellarator, temperature relaxation between the two constituents of the plasma can take place after the end of the ohmic heating phase, because the confinement of the plasma continues after the longitudinal current has disappeared. For a given magnetic field strength, the maximum ohmic heating current permitted by condition (*8.6*) is usually much lower in a Stellarator than in a toroidal chamber with the same plasma diameter; this is so because the complex winding system required around the Stellarator tube allows only a comparatively small value of $r_0/L$. Consequently, ohmic heating in a Stellarator can provide only a relatively modest power input; it will hardly be possible, by this ohmic heating process, to raise the plasma temperature in a Stellarator very much higher than $10^6$ °K. During the ohmic heating phase, the main danger comes from the weak instability referred to above. As discussed later, this phenomenon represents the main obstacle to carrying out the first heating phase effectively. Quite apart from this difficulty, we shall simply note that, to raise the plasma temperature to thermonuclear levels, other heating methods have to be used.

---

† Results with the Model C Stellarator indicate that with the divertor the impurity level is reduced by an order of magnitude.

For this next heating stage one can use either periodic compression of the plasma by an alternating magnetic field (the so-called 'magnetic pumping') or resonance acceleration of the ions by the action of a high-frequency electromagnetic field oscillating at about the ion cyclotron frequency in the main confining field (cyclotron resonance).

We shall look first at the mechanism of 'magnetic pumping'. In order to heat a plasma effectively by the action of a periodically changing field, there must be a close relationship between the period of the alternating field and a time which is characteristic of one of the plasma processes. By way of example, we can consider a specific type of magnetic pumping in which the applied frequency $\omega$ is close to $\nu$ the frequency of Coulomb collisions between particles. The value of $\omega$ satisfying this condition is very small compared with the ion and electron cyclotron frequencies. It follows that during the intervals between collisions the energy of transverse motion $W_\perp$ must change in proportion to $H$. This variation of $W_\perp$ means that there is a departure from equipartition of kinetic energy between the different directions of motion of the particles. The simple relationship $W_\perp = 2W_\parallel$, which holds good for plasma with an isotropic velocity distribution, is no longer satisfied in an alternating magnetic field. As can easily be understood, the state of a plasma in a periodically changing magnetic field very largely depends on the relationship between $\omega$ and $\nu$. If $\omega \gg \nu$, then $W_\perp$ must undergo oscillations relative to some mean value corresponding to the constant component of $H$, and $W_\parallel$ remains constant. No significant heating of the plasma can be expected in such circumstances. Quite different conditions are created when $\omega \approx \nu$. When this is the case, energy exchange between the different degrees of freedom, directed towards re-establishing isotropy of the velocity distribution, plays an important role. Because of this exchange there must be an irreversible transfer of energy from the field to the plasma, and consequently the plasma temperature increases.

To clarify this heating mechanism we shall consider a simple example. At some moment in time let the field strength increase rapidly from its initial value $H_0$ to $H_1 = H_0(1+\alpha)$. We shall assume that $\alpha$ is small compared with unity. If initially the particles have an isotropic velocity distribution and a mean energy $W_0$, then, after the rapid jump in the field strength, the mean kinetic energy becomes

$$\tfrac{2}{3}W_0(1+\alpha)+\tfrac{1}{3}W_0 = W_0(1+\tfrac{2}{3}\alpha).$$

The entire increase in energy is associated with the increase of transverse velocity, i.e. it is an increase of $W_\perp$. If the field strength is maintained at $H_1$ for an interval of time comparable with $1/\nu$, this anisotropy will be largely evened-out, and $W_\perp$ will fall to approximately $\tfrac{2}{3}W_0(1+\tfrac{2}{3}\alpha)$. If the field strength now returns rapidly to its initial value, then $W_\perp$ falls to

$$\tfrac{2}{3}W_0\frac{1+\frac{2}{3}\alpha}{1+\alpha} = \tfrac{2}{3}W_0(1-\tfrac{1}{3}\alpha+\tfrac{1}{3}\alpha^2+\ldots),$$

but $W_\parallel$ will retain the enhanced value $\tfrac{1}{3}W_0(1+\tfrac{2}{3}\alpha)$. Thus, after the field strength has returned to the value $H_0$, the total mean kinetic energy amounts to

$$W_\perp+W_\parallel = W_0(1+\tfrac{2}{9}\alpha^2).$$

The process can be repeated, the field strength being held at its initial value for a time interval of about $1/\nu$ and $H$ then being raised again to $H_1$. After a second rectangular pulse the total mean kinetic energy of the particles will be $W_0(1+\tfrac{4}{9}\alpha^2)$. It will increase in proportion to the number of pulses, i.e. it is proportional to the heating time. A more realistic calculation shows that if the field strength varies sinusoidally:

$$H = H_0(1+\alpha\sin\omega t), \qquad \ldots\ldots\ldots(8.8)$$

then the mean particle energy will change with time as follows:

$$\frac{dW}{dt} = \frac{\alpha^2}{6}\frac{\omega^2\nu}{\frac{9}{4}\nu^2+\omega^2}W. \qquad \ldots\ldots\ldots(8.9)$$

The most rapid increase in energy takes place when $\omega \approx \nu$. This method of heating is most efficient when the plasma temperature is low, because $\nu \propto T^{-\frac{3}{2}}$; and consequently, for given values of $\alpha$ and $\omega$, $dW/dt$ varies as $T^{-\frac{1}{2}}$.

To carry out this method of magnetic pumping in practice, a special coil (Fig. 108) is installed on one of the straight sections of the Stellarator to generate a high-frequency field of the required frequency and of the greatest possible amplitude.

Amongst variants of magnetic pumping, we may note in particular the use of magneto-acoustic resonance. Here the frequency of the alternating magnetic field is adjusted so that it approximately coincides with one of the normal mode frequencies of the plasma column in the straight section of the Stellarator. The value of these frequencies must be of the order of $H/d\sqrt{4\pi\rho}$, where $d$ is the diameter of the region occupied by the plasma and $\rho$ is the plasma mass density. Plasma heating can also occur when the period of the alternating field is comparable with the time taken by an ion to traverse the alternating field region.

§ **8.4** A particularly interesting ion-heating method is based on the idea of cyclotron resonance. In this method, the alternating field, which is relatively weak, has a frequency $\omega$ equal to the cyclotron frequency of the ions in the confining field $H_0$. Figure 110 represents the projection of a cylindrical plasma column on to a plane perpendicular to the magnetic field. The alternating component of the magnetic field induces an electric field $E_\theta$, also of frequency $\omega$. In conditions of cylindrical symmetry, the vector $\boldsymbol{E}$ must have an azimuthal direction and, consequently, the lines of the electric field are coaxial circles.

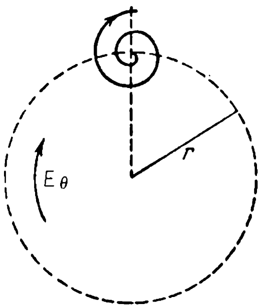

FIG. 110. Resonance acceleration of ions in a plasma

Let us assume in the first place that the plasma is so rarefied that it can be regarded simply as a collection of independent particles. In these conditions resonance acceleration of the ions will occur under the action of the alternating electric field. The ion velocity in the plane perpendicular to $\boldsymbol{H}$ increases in proportion to the duration of the alternating field, and the ion trajectories are of spiral form. If an ion takes a time $t$ to pass through the section of the Stellarator where the alternating field is effective, its energy increases by $\Delta W \approx e^2\bar{E}^2t^2/2m_i$, where $\bar{E}$ is the root-mean-square electric field along the spiral trajectory. Calculation yields $\bar{E} \approx E_0/2$. Consequently $\Delta W \approx \frac{1}{4}e^2E_0^2t^2/2m_i$. Taking into consideration that $E_0 = r\omega H_1/2c$, where $H_1$ is the amplitude of the alternating magnetic field and $r$ is the distance from the centre of the spiral trajectory to the symmetry axis, we find

$$\Delta W \simeq \frac{e^2r^2H_1^2}{32m_ic^2}\left(\frac{\omega l}{v_{\|}}\right)^2. \qquad \text{.........}(8.10)$$

Here $l$ is the length of the region of resonance acceleration and $v_{\|}$ is the parallel velocity of the ion. Equation (*8.10*) has been derived on the assumption that the ion Larmor radius remains much smaller than $r$. Given $H_1 = 25$ Oe, $l = 50$ cm, $r = 5$ cm, $\omega = 10^8$ sec$^{-1}$, $v_{\|} = 10^7$ cm/sec, the energy of a deuteron increases by approximately 10 keV in a passage through the resonance field region. This example shows that resonance between Larmor revolution of ions and magnetic field oscillations can produce rapid heating of the ion constituent of a plasma with a very low number density of charged particles.

In a dense plasma, however, this ion heating technique runs into serious difficulties; the reason is that the applied electric field is distorted by a plasma electric field which itself arises from the resonance heating of ions. The origin and nature of this additional electric field can be easily explained if we consider the trajectory of one of the ions, as represented in Fig. 110. The motion of the ion along its spiral trajectory represents the superposition of two oscillatory motions which are perpendicular to each other and which have a gradually increasing amplitude. These oscillations take place along the radius and along the azimuth. All the ions located in a given section of the plasma column oscillate at one and the same phase, and the amplitudes of their oscillations increase proportionately to $r$. Azimuthal oscillations of ions in a cylindrically symmetrical plasma cannot result in a spatial redistribution of particles and in the appearance of space charges. The situation is different for the radial oscillations: these cause the appearance of alternating space charges, and of radial electric fields associated with them. At the moment when the ions are displaced in the outward direction, a net positive charge appears on the outer surface of the plasma column, and negative charges arise inside the plasma. At the opposite phase of oscillation, the plasma surface is charged negatively while a distributed positive charge is formed within the column. The strength of the alternating radial electric field produced by this space charge must be of the order of $4\pi n\zeta e$ where $\zeta$ is the amplitude of the radial oscillations of the ions arising from their resonance acceleration. For the purposes of rough calculation $\zeta$ can be taken as equal to the Larmor radius of the accelerated ion. The radial electric field will have an important influence on the motion of ions when its strength is comparable with that of the induced azimuthal field $E_\theta$, i.e. when

$$4\pi ne\rho_{\text{Hi}} \approx \frac{r}{2c}\omega H_1. \qquad \text{.........}(8.11)$$

Let us put $n = 10^{10}$ cm$^{-3}$, and take the same numerical values for $r$, $\omega$ and $H_1$ as were used in the above example of resonance acceleration of ions. When these basic parameters are adopted, condition (*8.11*) is fulfilled when $\rho_{Hi}$ reaches $3 \cdot 5 \times 10^{-3}$ cm, i.e. when ions are accelerated to only 0·1 eV. Consequently, even at the very beginning of resonance heating, account has to be taken of the influence of the radial field; which means to say, in effect, that in analysing the ion motion, the problem has to be solved with a self-consistent field. Even without doing any calculations, however, one can foresee the main result of such an analysis. This result will be that, because of the superposition of $E_\theta$ and $E_r$, the motion of the ions will take on a character very different from the motion associated with resonance acceleration of single particles.

On analysing the motion of an ion under the action of a resonance field $E$ it is easy to establish that the radial displacement $\zeta$ is shifted in phase relative to $E$ by an angle $+\pi/2$, if $\boldsymbol{H}$ is directed along the positive $z$-axis. Therefore the radial component of the field directed opposite to $\zeta$ will lag behind $E$ by a phase angle equal to $\pi/2$. Such a field will slow down the ions, and when its amplitude equals $E_\theta$, the acceleration process will stop. When $E_\theta$ and $E_r$ are equal the resulting electric field vector rotates in a counter-clockwise direction, i.e. in the direction opposite to Larmor rotation, and therefore there is no resonance.

As has been noted above, $E_\theta$ and $E_r$ become equal at the earliest stage of acceleration. Thus, in its simplest form, the method of cyclotron resonance heating encounters practical difficulties of a type that render it ineffective. Stix suggested a possible way out of this difficulty which consisted in using an alternating field which changed in phase along a straight section of the chamber. Let us assume that a periodic field is generated by two coils $K_1$ and $K_2$ put at some distance from one another, and that the fields of the two coils differ in phase by 180°. The radial displacement of ions in coil $K_1$ will, at any moment of time, have a sign opposite to that of the radial displacement of the ions inside coil $K_2$. Space charges of opposite sign that arise when ions are accelerated in the regions affected by coils $K_1$ and $K_2$ are then automatically compensated by the free flow of electrons along the magnetic lines of force, either from the $K_1$ region to the $K_2$ region or vice versa.

A number of papers have been devoted to the theoretical analysis of ion acceleration in systems with such a configuration of resonance field. The main outcome of these analyses is that, in a dense plasma, the radial electric field, which damps the ion acceleration, does not fall to zero even when electron currents compensate the space charges. The trouble is that the compensating electron currents themselves generate a changing magnetic field which, in its turn, induces an electric field. The magnetic field caused by the compensating currents running along the lines of force has only an azimuthal component. Therefore, at least one of the two components $E_z$ and $E_r$ of the induced electric field must be non-zero. Due to the high electrical conductivity of the plasma, the parallel component $E_z$ will always be much the smaller of the two. If we visualise how the electron currents and the associated fields are formed, we can see that the radial component of the electric field always lies in such a direction that it hinders the resonance acceleration of the ions.

Nevertheless, despite this conclusion, the idea of using cyclotron resonance to heat plasma has proved to be quite long-lived. Theoretical research has shown that, at frequencies somewhat less than the ion cyclotron frequency $\omega_{Hi}$, a plasma can support oscillations which have been given the name of 'cyclotron waves'. The frequency spectrum of these oscillations consists of a series of closely packed lines, each of which corresponds to a specific form of the radial variation of amplitude, this variation being represented by one of the Bessel functions $J_n(r)$. Cyclotron waves can be regarded as the short-wavelength limit of Alfvén's hydromagnetic waves.† They penetrate freely into the plasma and propagate along the lines of force. When propagated in a uniform field, these waves are relatively feebly damped and therefore cannot heat the ions strongly. One can hope, however, that it will be possible to achieve quite effective heating of plasma with cyclotron waves by resorting to the ingenious idea of creating a 'magnetic beach'. The essence of this idea is that the cyclotron waves are generated in the plasma at a place where the magnetic field strength $H$ is high, and are then propagated into a region where $H$ is lower. During this propagation the waves become shorter and shorter and the damping caused by interaction with ions increases rapidly. Eventually, at some value of $H$ not very different from the initial value, the wavelength becomes so short that all the oscillatory energy goes into heat. This process is analogous to what happens to waves at a sloping shore. As they approach such a shore the waves become shorter and shorter, and more and more precipitous till they finally break, turning their energy into heat.

Experiments carried out to study heating of plasma by the cyclotron resonance method have not so far provided wholly definitive results. However, on the basis of data recently obtained, it appears possible, in devices using a magnetic beach, to raise the ion temperature to some tens of electron-volts (when the plasma number density is about $10^{13}$ cm$^{-3}$).

§ **8.5** In comparison with the profound and important results obtained by theoretical research done in connection with the 'Stellarator programme', the experimental data bearing on the behaviour of plasma in Stellarators are disappointingly sparse. Although experiments have now been in progress for about ten years, their results to date (1961) do not enable us to get a reasonably full or clear impression of the main processes that take place in magnetic traps of this type.‡

Almost all the experimental data available relate to the ohmic heating phase in Stellarators which have been filled with hydrogen or helium at low initial pressure ($10^{-3}$–$10^{-4}$ Torr). The majority of the measurements have been made using figure eight Stellarators. A number of measurements have also been carried out on race-track type Stellarators with helical windings on the curved sections. In all cases, the production and heating of plasma was achieved by using a longitudinal electric field, between about 0·04 and 0·5 V/cm. The strength of the longitudinal magnetic field was from $10^4$ to $3 \times 10^4$ Oe, and the diameter of the plasma column was usually not more than 4 cm (the chamber length being several metres).

---

† Strictly speaking, the left-hand circularly polarised Alfvén wave.

‡ Papers published since 1961, which report further observations—particularly on the Model C Stellarator—are listed in the bibliography.

The bulk of the experimental information was obtained from current and voltage oscillograms, from microwave interferometric measurements

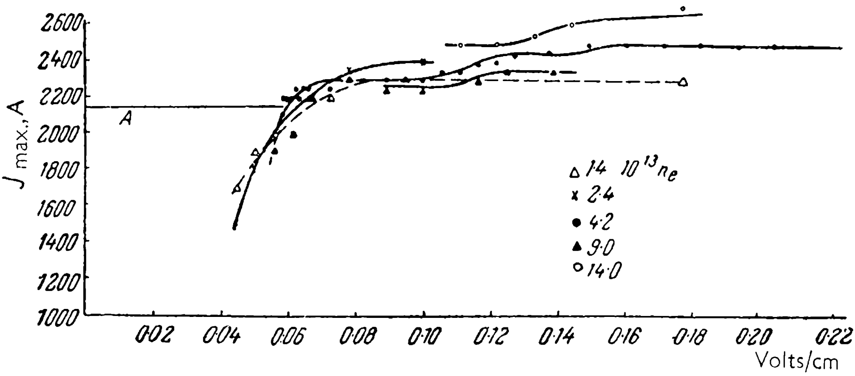

FIG. 111. Maximum longitudinal current as a function of the applied electric field in a Stellarator

of electron number density, and by recording the optical and ultra-violet spectrum and the hard X-rays radiated by the plasma.

With the electric field strengths mentioned above, the currents in the plasma are between some hundreds and some thousands of amperes. The maximum current for stable or, more accurately, quasi-stable operation, is limited by condition (*8.6*). If this condition is not fulfilled, there is marked instability of the plasma column; and this leads to intense interaction between the plasma and the wall, and to a sharp increase in the resistance of the column. In the installations so far studied, criterion (*8.6*) gives values for the critical current $J_{\text{crit}}$ which do not exceed a few kiloamperes.

One of the important results of experiments on the ohmic heating phase of plasma in a Stellarator, is the direct quantitative confirmation of the theoretical predictions on this point. Figure 111 shows the results obtained from oscillograms of the ohmic heating current on one of the first models of the Stellarator (model B-1). The applied voltage plotted as a function of time had in this case an almost rectangular form (constant-voltage heating mode). In Fig. 111 the maximum current during the pulse is plotted as a function of the strength of the applied electric field. The line *A* marks the limiting current for which the Kruskal-Shafranov condition is fulfilled. We see that in these experiments the peak value $J_{\max}$ of the current in a discharge pulse in practice ceases to increase with $E$ once the theoretical limit of stability has been reached. A change in the initial pressure of the gas (i.e. the plasma density) does not, in this range of electric field strengths, exert any notable influence on the value of $J_{\max}$. Observations of the effect of varying the longitudinal magnetic field strength, which were made in the same apparatus, show that $J_{\max}$ is proportional to $H$ and always remains close to the theoretical Kruskal-Shafranov limit.

Strictly speaking, there should be instability in the plasma column in a Stellarator only at current strengths close to $J_{\text{crit}}$, and stable conditions are also possible with $J > J_{\text{crit}}$. However, to reach such a state, one first has to pass through a region of strong instability. During the interval of time when $J$ is close to $J_{\text{crit}}$, the plasma column interacts strongly with the walls and undergoes marked cooling. Therefore its resistance will increase greatly and a very considerable increase in $E$ will be required to drive the current considerably higher than $J_{\text{crit}}$. During experiments on ohmic heating of plasma in the B-2 Stellarator, under conditions when the plasma conductivity was comparatively low, it proved possible to get currents considerably in excess of $J_{\text{crit}}$. When this was done, the moment when the current passed through the critical value could be seen clearly on the oscillograms: it was marked by the appearance of intense oscillations. At the same moment of time there was a flash of light due to an influx of impurities.

The processes that take place during the ohmic heating of plasma in a Stellarator are in many ways akin to those we encounter in quasi-stationary discharges in ordinary toroidal chambers with strong longitudinal fields. The usual conductivity of hydrogen and helium plasmas lies in the range $10^{14}$–$10^{15}$ e.s.u., corresponding to an electron temperature of some tens of electron-volts. The temperature of the ions does not, apparently, exceed a few electron volts, in agreement with theoretical estimates in which Coulomb collisions with electrons are regarded as the main cause of ion heating. Just as in experiments with ordinary toroidal chambers, experiments on the ohmic heating of plasma in Stellarators reveal that there is a gradual change in the spectral composition of the light during the discharge pulse. First of all, there are spectral lines corresponding to low energy levels, which later weaken and are largely replaced by lines showing evidence of higher degrees of ionisation and excitation.

The curves in Fig. 112 show the main observed parameters of ohmically heated hydrogen plasma as a function of time. These curves are typical of a mode of operation in which the applied voltage is maintained at a constant level. On correlating the changes in current and number density we see that by the time the current reaches its maximum the electron density has already dropped considerably. The current falls to zero well after the moment when $n_e$ falls below the level detectable by the interferometer. The variation of the intensity of line spectra also yields significant information. The intensity of the hydrogen line $H_\beta$ reaches its greatest value at the beginning of the discharge, and thereafter decreases rapidly. This indicates, apparently, that the hydrogen in the plasma column is, in effect, fully ionised well before the current reaches its maximum. The CIII line appears at the moment when the ionisation of the plasma is completed and the current starts building up rapidly. The intensity of all the spectral lines tends to zero before current disappears.

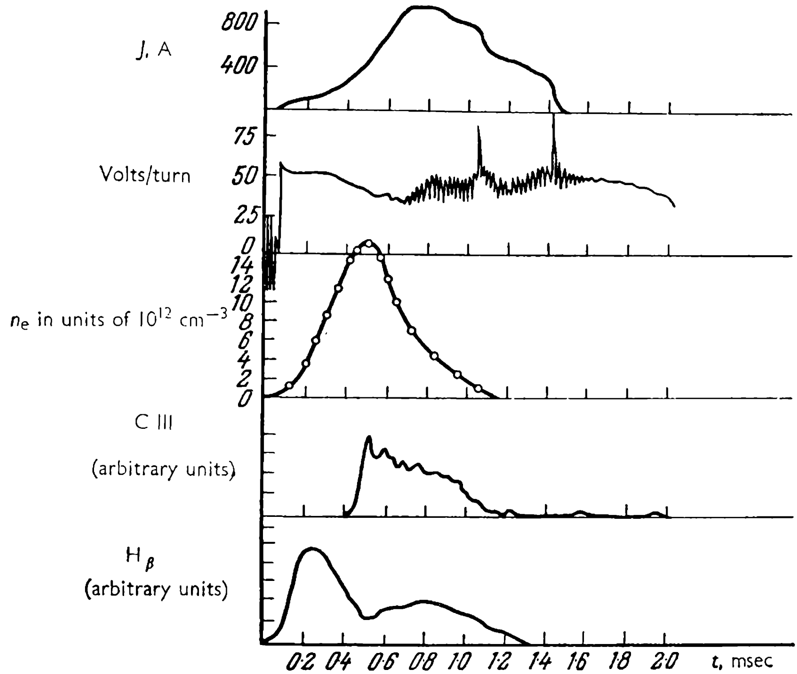

FIG. 112. The main characteristics of the state of plasma as a function of time in a Stellarator during ohmic heating

In their general character these results are very similar to those described in papers dealing with quasi-stationary discharges in toroidal chambers with strong stabilising fields. It can be considered, seemingly, that during the ohmic heating stage there is no qualitative difference between the behaviour of the plasma in these two types of device.

Amongst the main facts discovered during the experimental investigation of ohmic heating of plasma, particular interest attaches to the anomalous diffusion of plasma, which appears as a very rapid loss of charged particles from the plasma column. Painstaking experimental investigations of this phenomenon have been carried out at Princeton, using various devices of the Stellarator type. We shall indicate here the main conclusions that can be based on these investigations.

The variation of the density number $n_e$ with time should, seemingly, be regarded as resulting from the combined action of two processes: the loss of particles from the column to the wall as a result of anomalous diffusion; and the injection of fresh particles into the plasma column due to desorption of atoms from the walls. The second process is directly connected with the first and masks it. The measurements are consistent with the supposition that at a given time the flux of particles returning to the plasma is proportional to $n_e$ and to the original gas pressure in the chamber. If we suppose that the mean lifetime of a charged particle in the plasma column, while limited by anomalous diffusion, has one and the same value throughout the whole heating process, then we can write down the following expression for the change of electron density with time:

$$\frac{dn_e}{dt} = -\frac{n_e}{\tau}+\alpha n_e p_0. \qquad \text{.........}(8.12)$$

Here $\tau$ is the lifetime of the particle, $p_0$ is the initial gas pressure and $\alpha$ is a constant. This relationship is applicable only after all the hydrogen initially present has been fully ionised. From (*8.12*) it follows:

$$n = n_0 \exp(-t/\tau^*), \qquad 1/\tau^* = 1/\tau-\alpha p_0. \qquad \text{.........}(8.13)$$

Thus, in order to find the mean lifetime $\tau$, we have to plot $1/\tau^*$ (found from the measurements) as a function of initial pressure and extrapolate to zero pressure. Such measurements indicate that $\tau$ is nearly proportional to $\sqrt{H}$ where $H$ is the strength of the longitudinal field.† It further turns out that the presence or absence of currents in the helical windings does not in practice affect the particle loss rate, i.e. does not affect $\tau$; but reduction of the radius of the plasma column does reduce $\tau$. In the conditions of the experiments so far carried out, $\tau$ was usually about 50–100 microseconds. This short lifetime for particles in a plasma column is in marked disagreement with the values predicted by the classical theory of diffusion.

§ **8.6** In the present case the use of the term 'anomalous diffusion' is fully justified. The mechanism causing the rapid departure of particles from the plasma is at present unclear. Physicists working at Princeton have tried to associate this mechanism, if only phenomenologically, with Bohm's formula for the coefficient of 'turbulent diffusion' (see § **3.4**). According to this formula $D_\perp \propto T_i/H$. If we further assume that during ohmic heating the temperature of the ions is proportional to the interval of time they spend in the plasma, we arrive at the relationship $D_\perp \propto \tau/H$. On the other hand for a diffusion process one has the relationship $\tau \approx r^2/D_\perp$, where $r$ is the average distance to which particles are displaced in a time $\tau$. For particles in a plasma column, $r$ can be taken to be the column radius. From these relationships it follows that $\tau \propto r\sqrt{H}$. This dependence, which we obtained by starting from Bohm's formula, corresponds to the experimental data.† The magnitude of $\tau$, when calculated according to Bohm's formula, also agrees with the experimental data (if we take the energy of the ions in the column as being of the order of several electron-volts). However, this still leaves us very far from explaining the reasons for the anomalous diffusion.

---

† But see footnote on p. 309 and p. 75.

One of the attempts to provide such an explanation is based on the idea that the basic reason for the anomalous diffusion is the generation of plasma oscillations by runaway electrons in the plasma. It was indicated in Chapter III that if the ratio $E/E_c$ exceeds a certain minimum value, runaway electron acceleration will develop in the plasma. The streams of runaway electrons will, in turn, excite oscillations in the plasma; that is to say, they will cause oscillating electric fields which will produce particle drift. It is these drift movements brought on by the oscillating electric fields, that are the direct cause of particles leaving the inner regions of the plasma column and diffusing to its surface, i.e. this irregular drift motion constitutes the anomalous diffusion.

This hypothesis is supported by some of the results of experimental research into ohmic heating in Stellarators. Measurements show that $E/E_c$, at current maximum, undergoes only slight change over a very wide range of different initial experimental conditions. For current maximum it is always near to 0·16. When $E/E_c$ has this value, the runaway acceleration of the electrons should, according to theory, have quite an important effect. Therefore the acceleration can lead to anomalous diffusion, which cools the plasma through interaction between the plasma column and the walls; as a result of which the current starts to drop. The supposition that some proportion of the plasma electrons are accelerated during ohmic heating in a Stellarator is confirmed by the appearance of hard X-rays. Nevertheless the ideas put forward have one very serious shortcoming: the actual mechanism involved in the appearance of the fluctuating transverse electric fields remains wholly unclear, so that it is impossible to estimate the intensity of these fields or the effect they have on the diffusion rate.

We shall mention a number of other lines of approach to the explanation of anomalous diffusion in plasma columns stabilised by a strong longitudinal field. One can try to attribute anomalous diffusion to the generation of ion oscillations by the peculiarities of the directed speed of the electrons associated with the passing of current. Mention was made of such a process in the previous chapter, when various types of plasma instability were analysed. For intensive generation of ion oscillations, it is necessary that the mean value of the directed speed of the electrons $u = j/n_e e$ should be, in order of magnitude, not less than the speed of the ion acoustic waves. In practice this condition is nearly always satisfied during experiments. Although this way of explaining the anomalous diffusion is quite attractive, weighty objections can be advanced against it. It follows from theory that amplification of ion oscillations continues only as long as the ion temperature is considerably less than the electron temperature. However, if even at the very start of the process the ions are colder than the electrons, in a time of the order of $1/\nu$, where $\nu$ is the growth rate of the oscillations, the temperature of the ions becomes the same as that of the electrons. The growth rate $\nu$ in this case is about the frequency of the Langmuir ion oscillations. Therefore the reciprocal of $\nu$ is about $10^{-9}$ sec. This means that thermal contact between electrons and ions is established almost immediately during oscillations, and thereafter the mechanism causing the oscillations ceases to operate.

---

† However, according to the most recent information, measurements show that the variation of $\tau$ with $H$ is approximately linear.

In the previous chapter, the mechanism of anomalous diffusion put forward by Kadomtsev was considered. As has already been said, the conclusions from Kadomtsev's theory are in qualitative agreement with the experimental results. However, the question remains open whether one can use this theory for analysing the processes taking place in existing experimental installations where the electron temperature is above 10–20 eV. Finally, it cannot be excluded that the loss of particles from plasma columns in Stellarators and toroidal chambers is a consequence of the 'universal instability' of an inhomogeneous plasma, described by Sagdeev and Vedenov.

In theory, the Stellarator is the most nearly perfect of all the magnetic traps so far invented. Therefore results of research on heating and confinement of plasma in this magnetic system are of great interest.

The main question which should now determine the trend of this research can be formulated as follows: is it possible to create conditions in which the plasma in a Stellarator will have sufficient stability? Experiments so far carried out† show that during ohmic heating with a longitudinal current, we encounter well-marked anomalous diffusion, and this is a clear sign of instability. However, it is not known if it will be possible, by a simple modification of this mode of heating, to pass through the unstable state and then, at higher temperatures, to obtain a plasma column that conforms to the predictions of the classical theory. If this course does not succeed, there remains the hope of avoiding anomalous diffusion by going over to other methods of heating—cyclotron resonance or one of the forms of 'magnetic pumping'. If this road also leads nowhere, it will be necessary to try to produce hot plasma externally, and then inject it carefully into the Stellarator. This method is conceived of only in shadowy outline, and various ways of attempting it are still at the stage of preliminary and not very profound discussion. However, it is certain that, as new experimental installations of great power are brought into operation over the next few years, the prospects for using Stellarators to obtain high-temperature plasma and confine it for long periods will be clarified.

---

† Including those carried out with the Model C Stellarator in the period 1961–1963.

## *Magnetic Mirror Traps*

### *Basic Properties*

§ **8.7** This class of trap consists of all devices in which the confinement of particles depends on reflecting them from regions with a strong magnetic field. Out of this general class, a special group should be set aside consisting of magnetic configurations with a zero in the field strength at some point. This type of magnetic system with fields of opposite direction (cusp fields) will be considered in § **8.19**; but before reaching that section we shall be concerned with simpler systems in which the magnetic field strength nowhere falls to zero.

The simplest type of axially symmetric magnetic mirror trap is shown in Fig. 10. It contains all particles whose velocity vectors in the central zone are inclined to the lines of force at angles exceeding that determined by equation (*2.10*). The particle trajectories in traps of this type depend on initial conditions and are of a quite complicated form. If a particle moves only in that part of the field where the lines of force bulge outwards, it drifts round the axis the whole time in one and the same direction. When a particle penetrates into the region where the lines of force bulge inwards, the direction of this azimuthal drift changes. The speed of azimuthal drift is very sensitive to the distribution of the field in the mirror regions, and by changing this distribution one can increase or decrease the azimuthal drift over quite a broad range.

In the general case, the spatial distribution of particles enclosed in a magnetic mirror trap is far from being uniform. The number density changes in a direction both perpendicular and parallel to $\boldsymbol{H}$. To form an impression of the possible particle distributions in a trap, we shall consider a case in which the field has axial symmetry, and, for the sake of definiteness, we shall assume that the field strength changes on the axis between the centres of the mirrors according to a parabolic law, i.e. $H = H_0(1+h^2z^2)$. Let a group of particles having velocities similar in magnitude $v_0$ and direction be initially close to a point at a short distance $r$ from the axis in the plane $z = 0$ (i.e. in the region where the field strength is a minimum). Because of azimuthal drift, these particles—as they move—disperse to fill a region in space, having the form of a hollow envelope, formed by an annular bunch of force-lines symmetrically disposed round the axis of the system. The length of this region in the $z$-direction depends on the initial angle $\alpha_0$ between the velocity vector and the line of force.

We shall determine the probability that, at an arbitrary moment of time, any one of the particles we have chosen will be within the limits of a section of the magnetic system with a coordinate lying between $z$ and $z+dz$. This probability should be proportional to $dz$ and inversely proportional to the parallel velocity $v_{\parallel}$. It will therefore be given by the expression:

$$\frac{dz}{v_{\parallel}}\Big/\int\frac{dz}{v_{\parallel}}, \qquad \text{.........}(8.14)$$

where the integral is taken between the points at which $v_{\parallel}$ goes to zero. With the above assumed form of the function $H(z)$, we have

$$\int\frac{dz}{v_{\parallel}}=\frac{\pi}{v_0 h\sin\alpha_0}.$$

Consequently the probability of finding the particle in the section $dz$ is

$$dz\, h\sin\alpha_0/[1-(H/H_0)\sin^2\alpha_0]^{\frac{1}{2}}. \qquad \text{.........}(8.15)$$

The number density must be proportional to the ratio of the value given by (*8.15*) to the volume $d\Omega$ cut out of the particle-filled envelope by two plane sections with coordinates $z$ and $z+dz$. The volume of this ring is $2\pi r\Delta r\, dz$ ($\Delta r$ is the thickness of the envelope). Along the lines of force the product $Hr^2$ must be a constant (for simplicity we are considering a region close to the magnetic axis). Therefore $r\Delta r \propto 1/H$, and consequently the distribution of number density is determined by the expression

$$n \propto H\sin\alpha_0/[1-(H/H_0)\sin^2\alpha_0]^{\frac{1}{2}}. \qquad \text{.........}(8.16)$$

The graph of $n$ as a function of $z$ is shown in Fig. 113. At the mirror reflection point $n$ goes to infinity.

Now suppose that in the plane $z = 0$, the particle velocities have a certain angular distribution. In this more general case the number density at distance $z$ from the starting plane will be proportional to the quantity

$$H(z)\int_{\alpha_{\min}}^{\alpha_{\max}} f(\alpha_0)\sin\alpha_0[1-(H/H_0)\sin^2\alpha_0]^{-\frac{1}{2}}\,d\alpha_0. \qquad \text{.........}(8.17)$$

Here $f(\alpha_0)$ is the initial angular distribution function; $\alpha_{\max}$ is the angle at which the term in square brackets is zero; $\alpha_{\min}$ is the minimum value of $\alpha_0$ at which the particle is reflected at the mirrors, this value being determined from the condition $\sin\alpha_{\min} = (H_0/H_{\max})^{\frac{1}{2}}$. Figure 114 shows the number density as a function of $z$ for two different angular distribution functions: $f(\alpha_0) = \sin\alpha_0$ and $f(\alpha_0) = \cos\alpha_0$. The mirror ratio $H_{\max}/H_0$ is taken as equal to two. The first of these functions corresponds to the assumption that initially the particle velocities have an isotropic angular distribution and the only particles to leave the trap are those whose velocity vectors lie within the loss cone $\alpha_0 < \alpha_{\min}$. In this case the number density tends to infinity when $z = 0$. When $f(\alpha_0) = \cos\alpha_0$ the number density is proportional to $\sqrt{1-h^2z^2}$. The curves in Fig. 114 indicate that there can be a marked dependence of $n(z)$ on the form of the function $f(\alpha_0)$ which, in principle, can have an arbitrary character.

The above discussion of the spatial distribution of particles is valid only on condition that the interaction of the particles can be neglected. If $\beta \ll 1$, which in practice is almost always so, magnetic interaction due to the self-magnetic field of the plasma will not be important. However, even in rarefied plasma a strong electrostatic field can occur and change fundamentally the character of the particle motion and spatial distribution. If the dimensions of the plasma volume are considerably larger than the Debye shielding distance, the effect of the plasma electric field on the spatial distribution of particles in a fast ion plasma can be neglected only if one or other of the following two conditions is fulfilled:

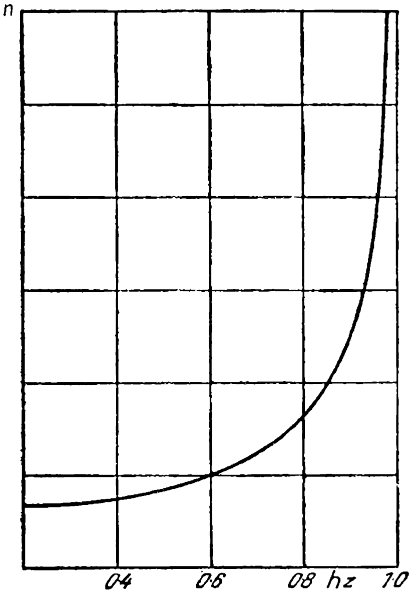

FIG. 113. Distribution of particles in a simple magnetic mirror trap when $\alpha_0 = 45°$

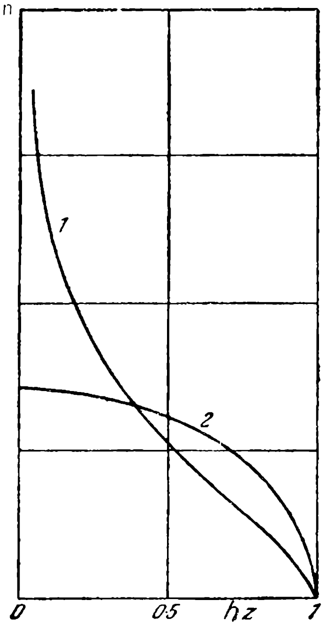

FIG. 114. Density of particles in the trap for two initial angular distributions

(1) $f(\alpha_0) = \sin \alpha_0$;
(2) $f(\alpha_0) = \cos \alpha_0$.

(1) the ions and the electrons have the same initial angular distribution. Given this condition, $n_e = n_i$ and therefore electric fields do not occur (for the moment we do not consider the loss of particles due to collisions);

(2) the energy of the electrons is many times less than that of the ions; in this case the electrons follow the ion distribution, thus compensating the space charge caused by the fact that $n_i$ is not constant.

This conception of the plasma as being wholly devoid of electric fields is, of course, highly simplified. It will be seen from what follows that, at least close to the surface of the plasma, there must be a strong electric field which equalises the flow of ions and electrons out of the trap arising from Coulomb collisions. This field is also bound to have an effect on the general character of the particle motion, because it induces rotation of the particles around the magnetic axis.

We now note that, in conditions where the effect of the plasma electric field can be neglected, the equilibrium distribution of particles along the lines of force can be of a quite different character at different distances from the magnetic axis of the trap. Consequently the form of the region occupied by the plasma in the magnetic field can vary widely. The variety of different forms is limited only by two obvious requirements: first, that the distribution of particles must be axially symmetric; and second, that along a given line of force the plasma number density cannot be zero where $H$ is a minimum if the density differs from zero in regions where $H$ is larger.

If the plasma density is so great that $\beta$ is comparable with unity, there is interaction between the particles primarily because the moving ions and electrons generate a strong diamagnetic field, as a consequence of which there is a significant change in the geometric form and the strength of the field in the trap. Clearly, a change in the form of the field will affect the spatial distribution of the particles. In the general case, the analysis of the distribution of the plasma in the trap is extremely complicated because of the need to obtain a self-consistent magnetic field. Up to the present, apparently, no one has succeeded in obtaining even particular solutions of this problem.

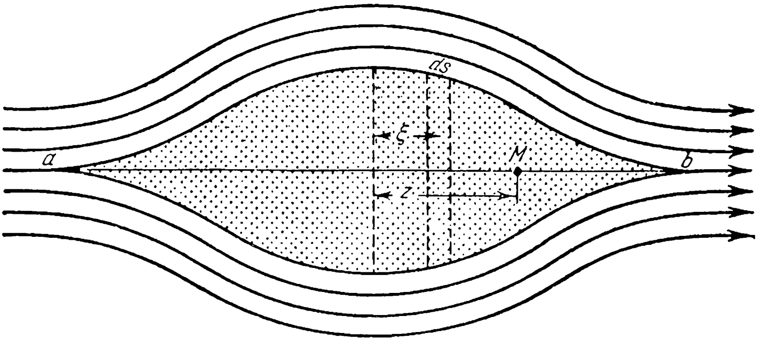

FIG. 115. Shape of a plasma blob in a magnetic mirror trap, when the plasma wholly excludes the magnetic field

Considerable simplification is obtained by assuming that the diamagnetic field exactly counteracts the initial field, so that the magnetic field is completely excluded from the plasma. In this limiting case, which probably does not have much practical interest, the plasma can be treated as an ideal gas; and, in particular, it can be supposed that the particle velocity distribution is isotropic. In the magnetic field of an axially symmetric mirror trap, an infinitely conducting isotropic plasma is calculated to occupy a spindle-shaped volume (Fig. 115).

The boundary of the plasma is formed by the lines of force. Because, in this case, the plasma pressure $p$ is everywhere the same, the field strength will have the same value $\sqrt{8\pi p}$ at all points on the boundary surface. The azimuthal current which must flow along the plasma surface to ensure that the field strength jumps from zero to $H$ at the surface, must also be the same everywhere and be equal to $c\sqrt{p/2\pi}$ per unit length. The condition for complete field exclusion is that the field created by the surface currents must, at each point within the plasma, cancel out the field which has been generated initially in the trap by the external coils. For this purpose, as can easily be seen, it is sufficient that this cancellation take place on the section of the axis lying between point *a* and point *b*.

The current $j\,ds$ which flows around the ring of width $ds$ (see Fig. 115) generates at the point $M$ on the axis a field

$$dH = \frac{2\pi r^2 j\,ds}{c\sqrt{[r^2+(z-\xi)^2]^3}}.$$

Therefore the condition for the fields to cancel can be written

$$\sqrt{2\pi p}\int \frac{r^2\,ds}{\sqrt{[r^2+(z-\xi)^2]^3}} = H_0(z). \qquad \text{.........}(8.18)$$

In this integral equation defining the form of the region occupied by the plasma, $H_0(z)$ represents the initial field strength on the axis. Analysis of equation (*8.18*) shows that the region occupied by the plasma must end at *a* and *b* in sharp points.

The fact that individual particles really can be contained in magnetic mirror traps for as long as is needed in practice, is demonstrated by the direct experiments referred to in Chapter II. However, the period of containment can change significantly if the trap is filled with high-density plasma. We shall first describe how Coulomb collisions between the particles affect the behaviour of the trapped plasma. We shall confine ourselves to the case when the two following conditions are fulfilled: (1) the plasma pressure is small compared with magnetic pressure and, because of this, the plasma does not significantly alter the field distribution in the trap; (2) the collision mean-free-path is large compared with the linear dimensions of the magnetic system, which is the case of most practical interest.

Let us suppose that, at some initial time, the plasma in the trap contains electrons and ions moving in all directions. It is clear that, within a very short time, the plasma loses all those particles whose initial velocity vectors lie within the loss cone. Thereafter, the only particles remaining on a given line of force are those for which $\sin\alpha_0 > \sqrt{H_1/H_2}$ at the moment when they pass through the region of minimum field strength; here $H_1$ and

$H_2$ are minimum and maximum values of field strengths along the given lines of force. In Fig. 116 the unbroken line shows the angular velocity distribution when the particles pass through the region with minimum $H$ (it is assumed that the initial distribution is isotropic and therefore that outside the loss cone $f(\alpha_0) = \sin \alpha_0$). Such a distribution can, however, be maintained only provided that there are no collisions at all. If there are collisions then particles for which $\alpha_0$ only slightly exceeds the loss cone angle will rapidly leave the trap (because, with Coulomb collisions, the probability of scattering through small angles is very high). Therefore, if

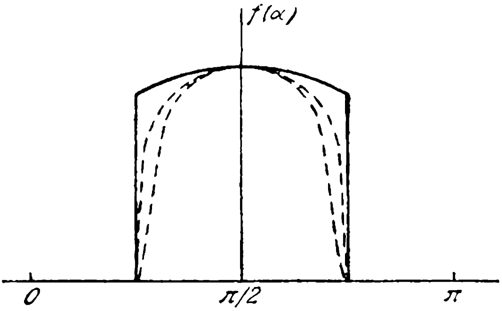

Fig. 116. The effect of Coulomb collisions on the angular distribution of particle velocities in a magnetic mirror trap

we leave all the conditions unchanged and do not introduce any new particles into the plasma from outside, the angular distribution will change with time as shown in Fig. 116 by the broken lines.

The lifetime of a particle in such a system depends on how greatly $\alpha_0$ differs from the critical value; it is greatest for those electrons and ions with angles $\alpha_0$ near to 90°. Such particles start by oscillating close to the minimum of the magnetic field. On undergoing successive collisions, the amplitude of their oscillations in the axial direction gradually increases until, eventually, they also leave the trap. If one compensates the loss of particles by a continuous injection of ions and electrons into the plasma, some sort of equilibrium angular distribution will be established and one could probably, by very complicated calculations, find its exact form.

What we have to concern ourselves with primarily is the determination of the mean lifetime of particles in a magnetic mirror trap. A rough estimate of this time can be obtained from simple considerations. If $H_2/H_1$ is not too large, the velocity directions available for free exit occupy a cone of solid angle comparable to that occupied by the directions of trapped motion. Therefore the mean lifetime of a charged particle is comparable to the time-interval between two Coulomb collisions, i.e. comparable with $\tau_{ie}$ for electrons and $\tau_{ii}$ for ions.

Due to the considerably greater speed of electrons, $\tau_{ei} \ll \tau_{ii}$ and, therefore, the loss of electrons from the trap predominates initially. But this initial loss produces an electric field at the boundary of the plasma, which hinders the subsequent departure of electrons and slightly facilitates that of the ions (i.e. the reverse of what happens when plasma diffuses across the lines of force). We shall not go far wrong if we assume that the mean lifetime of a particle will be comparable in order of magnitude with the larger of the two collision times $\tau_{ei}$ and $\tau_{ii}$, i.e. close to $\tau_{ii} = \tau_{ei}\sqrt{m_i/m_e}$ for $T_i = T_e$ and $Z = 1$. It follows from this that, for example, when $T = 10^9$ °K and $n = 10^{14}$ cm$^{-3}$ the ions of a deuterium-tritium mixture will be contained in the trap for a time of the order of one second.

If a plasma in a trap is stable, and if a sufficiently high vacuum is created in the space surrounding it, the loss of particles will be almost entirely determined by this scattering mechanism. The loss of particles by diffusion across the magnetic field will be negligibly small compared with that along the lines of force. The ratio of these two types of loss can serve as a characteristic of the qualitative difference between an ideal trap from which, in principle, particles can escape only across the field after undergoing a great number of collisions, and a trap with magnetic mirrors from which a particle can escape along the field after a single collision. In order of magnitude this ratio is

$$\left(\frac{R}{\rho_{Hi}}\right)^2 \sqrt{\frac{m_i}{m_e}},$$

where $R$ is the radius of the chamber. In cases of practical interest, the ratio is of the order of $10^3$–$10^4$.

If a magnetic mirror trap is to serve as a thermonuclear reactor, the nuclear energy generated in it must at least be able to make up for the energy losses brought about by the escape of fast particles and by other processes. If the energy losses are caused only by Coulomb collisions, this energy balance requires that

$$\sigma_n W_n \approx \sigma_s kT. \qquad \text{.........}(8.19)$$

Here $\sigma_n$ is the effective nuclear reaction cross-section, $\sigma_s$ is the Coulomb collision cross-section at a temperature $T$, and $W_n$ is the energy released by each nuclear reaction. From (*8.19*) we can estimate the minimum temperature at which a thermonuclear generator can begin to produce surplus energy. For a 50% mixture of deuterium and tritium, this minimum temperature proves to be of the order of 30–50 keV; for pure deuterium, it is about 1 MeV. From this it follows, seemingly, that the use of pure deuterium in this connection is wholly excluded. This conclusion is confirmed by more detailed calculations which take account of other types of loss. In actual fact it would appear that the fulfilment of condition (*8.19*) is far from adequate to ensure a promising future for magnetic mirror traps. Both theoretical calculations and experimental results show that, apart from Coulomb collisions, there are many other factors which cause the loss of fast particles from the trap.

One of these factors is the loss of fast ions through charge-exchange on neutral atoms and molecules which get into the plasma when the vacuum conditions are imperfect. It may be hoped that the rapid development of ultra-high vacuum technology will eliminate such losses (by raising available pumping speeds at very low pressures through the use of titanium and low-temperature gas-absorbers, and by carrying out prolonged outgassing of the chamber walls).

Losses which can be traced back to various kinds of plasma instability seem likely to be difficult to eliminate; and this applies in particular to those instabilities specifically associated with simple magnetic mirror machines. The cause of the most dangerous magnetohydrodynamic instabilities is the shape of the lines of force of the magnetic field which, over a great deal of their length within the trap, have a negative curvature. We shall return later to the part played by instabilities, when discussing the results of experimental research on various types of trap.

Plasma in a magnetic trap loses energy not only because the fast particles escape, but also because the plasma radiates electromagnetic energy. Because the temperature of plasma in a mirror trap must be very high to meet condition (*8.19*), particular importance attaches to the energy losses associated with betatron radiation of the fast electrons. For a given particle temperature, the relative importance of this radiation in the energy balance of the plasma increases as $\beta$ decreases, because the radiation intensity is proportional to the number density, whereas the energy released by nuclear reactions is proportional to the square of the number density (as also is the energy lost by collisional escape of particles through the mirrors). Moreover, a decrease in $\beta$ is also accompanied by a lessening of self-absorption of the radiation in the plasma.

From the formulae and graphs given in § **7.8**, the energy losses due to betatron radiation can be estimated for any trap designed to obtain high-temperature plasma. We shall not, however, give any examples of such calculations here, since they do not have much practical importance at the present state of development of mirror traps. We shall mention just one result that emerges from estimating the energy lost by betatron radiation. It is found that for a mirror trap working on pure deuterium, with condition (*8.19*) being observed, energy losses through betatron radiation will considerably exceed the release of energy by thermonuclear reactions (it is assumed that $\beta$ is considerably less than unity and that the field inside the plasma is thus not too different from the field on its boundary).

§ **8.8** A magnetic mirror trap in itself is merely a volume of vacuum in which a field of specific configuration has been generated. This volume must in some way be filled with plasma, and the plasma must either be heated to high temperature while it is in the trap, or must have been prepared in advance and then injected into the trap. Many different methods have been proposed for obtaining high-temperature plasma in mirror traps. We give here a very brief description of these methods, and after that we shall look in more detail at each of them separately and describe both the relevant experimental installations and the results obtained.

One category of methods comprises those in which high-temperature plasma is built up by injecting fast ions into a trap. The main problem here lies in developing the most rational way of trapping the injected particles. A particle introduced from outside into a magnetic field system can remain indefinitely within the field only if, during its motion, there is a marked, non-adiabatic change in its trajectory. This means that there has to be a change either in the properties of the particle (its speed or its mass) or in the magnetic field where the particle is moving.

FIG. 117

Scheme for injection and capture of ions in a trap, based on the dissociation of molecular ions

*1*, trajectory of molecular ion;

*2*, trajectory of atomic ion

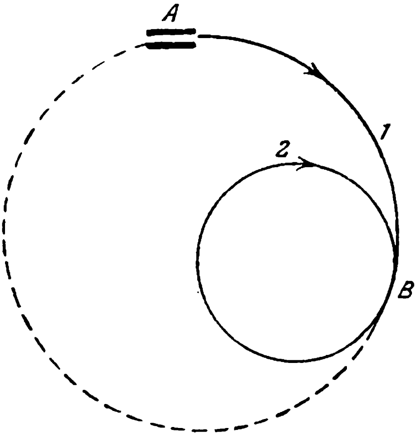

We first consider particle capture based on a sudden change in the particle's properties. Budker, in 1953, proposed the injection of molecular ions of deuterium into the space between the magnetic mirrors; the dissociation of these ions on the residual gas leads to the formation of atomic ions (deuterons) which are then trapped in the magnetic field. The capture mechanism is shown schematically in Fig. 117. A molecular ion, leaving the injector at *A*, dissociates at point *B*. The Larmor radius of the ion is thus halved (due to change in the ion mass) and therefore, during its subsequent motion in the trap, the ion will not return to the injector. This method of capture through dissociation of molecular ions on residual gas is used in the Ogra installation. In somewhat different form, the same method is used in the American DCX installation. Here the dissociation of $D_2^+$ ions occurs when they pass through an arc burning inside the magnetic system. Ogra and DCX are described below in §§ **8.13** and **8.14**.

Many other methods of injecting particles into a trap can also be mentioned. If, behind one of the mirrors, one puts an ion source which generates an ion beam at such an angle to the mirror axis that the particles pass through the maximum field region at an angle $\alpha_0$ very close to 90°, a small increase in field is sufficient to ensure that the particle passing through is captured. However, this increase in the field has to be sufficiently rapid. Particle capture will occur during the entire time that the field grows (and not merely during the time in which the ion makes one oscillation along the trap), provided that the entry angle $\alpha_0$ at the place where the lines of force are most tightly bunched remains practically unchanged over the whole period of field growth. For this condition to be fulfilled, it is necessary to adjust automatically those parameters of the ion source which determine the direction of the ion beam.

We shall estimate roughly the conditions that need to be fulfilled if this method of injection is to work. Let us assume that the field grows only where the magnetic mirrors are situated, and that elsewhere it is unchanged. From equation (*2.9*) it can be seen that to capture an ion, the field at the first mirror must grow by $\Delta H \approx H\cos^2\alpha_0$ before the ion returns. The time available is about $2l/v_0 \cos\alpha_1$, where $l$ is the trap length, and therefore the magnetic field must grow at a rate given by

$$\frac{1}{H}\frac{dH}{dt} = \frac{1}{2l}v_0\cos\alpha_1\cos^2\alpha_0. \qquad \text{.........}(8.20)$$

Let $v_0 = 10^8$ cm/sec, $\alpha_0 = 80°$, $\alpha_1 = 70°$ and $l = 10^3$ cm. Given these specific parameters, the value of the right-hand side is $5\times 10^2$ sec$^{-1}$. Thus, the magnetic field must increase with an *e*-folding time of about a millisecond. In practical circumstances, the conditions needed for good capture would probably be considerably less favourable.

An increase in the efficiency of the injection method under consideration can be achieved by modulating the density of the ion beam. If, instead of a continuous beam, one sends into the trap discrete blobs of ions, the blobs expand while moving, due to incomplete compensation of the space charge. It appears that this should lead to changes in the parallel velocity of the particles and should facilitate their capture. Up to the present time no experiments have been done to verify this method of injection (or, at least, no communication has appeared about such experiments).

The capture of particles in a magnetic field that increases with time can, in principle, also be effected by injecting particles across the magnetic field in the central section of the trap. In this case, the particle trajectory must be sufficiently displaced towards the magnetic axis in the time taken by the particle to return to the region of the injector. Because there is azimuthal drift, an ion is displaced by some angle $\psi$ during one transit along the trap. Therefore the total length of the trajectory back to the injector is $(2l)(2\pi/\psi)$, and the time of return is $4l\pi/v_{\parallel}\psi$, where $v_{\parallel}$ is the parallel velocity of the particles. During this time the particle, by (*2.21*), will be displaced a distance

$$\Delta r = -\frac{r_0}{2}\frac{1}{H}\frac{dH}{dt}\frac{4l\pi}{v_{\parallel}\psi}. \qquad \text{.........}(8.21)$$

If we take the distance from the injector to the axis as 50 cm and the angle $\psi$ as 30°, we find that, with $l = 10^3$ cm and $v_{\parallel} = 10^8$ cm/sec, the magnetic field must increase with an *e*-folding time of about one millisecond if the particle trajectory is to be moved inwards from the injector by a few centimetres. So far as the writer knows, no serious attempt has been made to use this method to capture particles in a magnetic mirror machine.

An interesting method of improving the conditions for capturing charged particles in a magnetic trap has been proposed by Fedorchenko, Rutkevich and Chernyi. In this method the particles traverse a section where the axial field varies periodically in space, with relatively small amplitude. If the speed of the particles is so chosen as to satisfy the condition

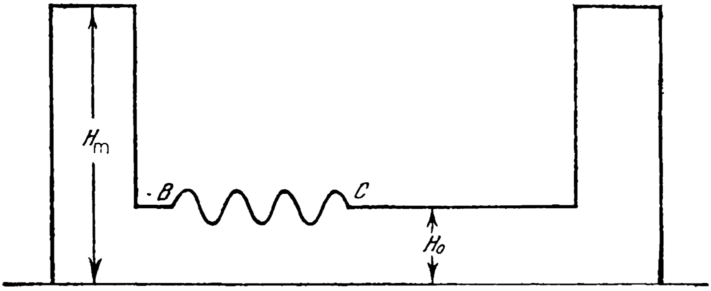

FIG. 118. Magnetic field strength in a trap with a corrugated field to improve the capture of charged particles

$$v_{\parallel} t_{H} \approx L, \qquad \text{.........}(8.22)$$

where $t_H$ is the Larmor period in the main field and $L$ is the wavelength of the spatial periodicity of the field, then resonance effects will alter the adiabatic invariant $W_{\perp}/H$ as the particles move along the field. In particular, if the initial motion of the particles is predominantly axial, the transverse velocity grows (at the expense of the axial velocity) as the particles move through the corrugated field.

To explain the origin of this effect we note that, in a coordinate system in which the axial velocity of the particles is zero, the magnetic field varies periodically with time. A solenoidal resonant electric field thus appears, which accelerates the particles in the plane perpendicular to the lines of force. To illustrate the effect, we shall consider the simple example of particle injection into a magnetic mirror machine. The form of the field is shown schematically in Fig. 118. If $H_m/H_0$ is very large, particles entering the trap at a large angle to the lines of force will move almost parallel to the field lines after passing through the mirror region. Given that the resonance condition (*8.22*) is fulfilled, the corrugated field in the region *BC* changes the direction of motion; the particles cannot then pass through the second mirror. As the particles return and again pass through the region of the periodic field, the resonance effects can either increase or decrease the inclination of the trajectory to the axis, depending on the exact initial conditions. These initial conditions are very sensitive to the length of time required to move from point $C$ to the second mirror and back again. When these initial conditions are correctly adjusted, a further increase in the transverse motion can be obtained as the particles return through the corrugated field from $C$ to $B$. In this particular case, particles cannot escape through the magnetic mirror through which they were injected. However, even in the most favourable case, the process does not represent a strictly irreversible capture; eventually the particles must escape. But their mean lifetime in a magnetic system can be increased many times by these means. This method can also be used to convert parallel motion of a plasma blob into transverse particle motion.

A number of suggestions have also been put forward for injecting fast neutral atoms, An atomic beam of this kind can be transformed into a beam of ions by interaction with cold plasma which could be generated inside the trap by some means; alternatively, ionisation could take place by collisions with the atoms of another beam moving in the opposite direction. Calculations show that both these methods are in principle practicable, and the first of them is in the stage of experimental development. The chief difficulty presented by these injection methods is that the time required to accumulate plasma in the traps is very long, and extremely stringent vacuum conditions are necessary to obviate particle losses through charge exchange on residual gas.

To establish the requirements for the vacuum, we shall estimate how rapidly the ion number density increases when one uses the method of two colliding neutral beams. Suppose that throughout a distance $L$ within the trap the beams pass through one another, moving in opposite directions. Let the cross-sectional area (assumed constant) of each beam be $S$. Then the atomic collisions occur uniformly throughout the volume $SL$. The total number of ions formed per unit time inside this volume is $2n_0^2 v\sigma SL$ where $n_0$ is the number density in an individual beam and $\sigma$ is the ionisation cross-section of the colliding atoms. The current $N_0$ of atoms in the beam (i.e. the number of atoms passing through the cross-section of the beam per unit time) is related to the density by $n_0 = N_0/Sv$. Let $\Omega$ be the effective volume of the magnetic trap. It follows that when there are no losses (this implies, in particular, that vacuum conditions are ideal) the ion number density at the start of injection is given by

$$n_i = 2\frac{N_0^2 \sigma L}{Sv\Omega}t. \qquad \text{.........}(8.23)$$

When $n_i$ becomes comparable with $n_0$, the plasma accumulates more rapidly than given by (*8.23*), because the neutral atoms also become ionised in collisions with the ions and electrons already trapped. This enhanced accumulation of ions begins after a time roughly equal to $\Omega/N_0\sigma L$. With $\Omega = 10^6$ cm$^3$, $N_0 \simeq 10^{19}$ sec$^{-1}$, $\sigma \simeq 10^{-16}$ cm$^2$ and $L = 50$ cm, this time is some tens of seconds. If we take $S$ to be 10 cm$^2$, and the speed of the atoms as $10^8$ cm/sec, then the number density of ions in the trap at this time is approximately $10^{10}$ cm$^{-3}$.

We can now specify the requirements that must be met by the vacuum system, using the specific assumptions given above. If we take it that, roughly, the charge-exchange cross-section for ions on molecules of residual gas is also equal to $10^{-16}$ cm$^2$, the density of gas atoms must be less than $10^7$ cm$^{-3}$ (corresponding to a vacuum of about $10^{-9}$ Torr) if significant loss of ions is to be avoided. Almost the same base pressure has to be achieved when trapping by dissociation of fast molecular ions is used. The accumulation of plasma by methods based on beam injection can be of practical importance only on the supposition that all kinds of particle loss due to plasma instability (particularly those instabilities which lead to anomalous diffusion) can be wholly eliminated.

It is worth noting a new and interesting method of accumulating plasma in a trap, which has recently emerged from the theoretical suggestion of Hiskes at Livermore and the experiments of Sweetman and Riviere at Aldermaston. These workers have discovered that when a beam of hydrogen molecular ions or neutral atoms passes through neutral gas, an unexpectedly large proportion of the hydrogen atoms prove to be in highly excited states. The lifetime of states with large quantum numbers $n$ and $l$ is comparatively long, and the particles can traverse quite long distances before decaying by radiative transitions to their ground state. If an excited atom of this kind moves with velocity $v$ into a magnetic field $H$, an electric field of strength $vH/c$ appears in the coordinate system of the moving atom. When $v$ and $H$ are large, this electric field can be strong enough to ionise the atom by the tunnel effect because, for states with high quantum numbers, the ionisation potential is very small (it varies roughly as $n^{-2}$). There is thus an enticing prospect of being able to accumulate fast ions together with electrons without the use of any collision process inside the magnetic trap itself. This is especially important during the very first phase of plasma formation.

§ **8.9** It is also possible to obtain high-temperature plasma in magnetic traps without injecting fast particles. Suppose that cold plasma of sufficiently high density is introduced into the trap. By compressing this plasma with a rising magnetic field, or by accelerating the plasma ions with an electric field, one can (at least in principle) raise the plasma to very high temperatures. Up to the present time the following methods for obtaining and heating plasma have been applied in various experiments.

1. *The ion magnetron.* In this method, which was proposed by Ioffe, fast ions are accumulated by extracting them from a cylindrical column of cold plasma on the axis of the magnetic system. A high voltage, applied between this column and the co-axial side wall of the chamber,

accelerates the ions to high energies. A method similar in concept was developed at Livermore and at Los Alamos, and installations based on it have been given the generic name of Ixion.

2. *Plasma injection.* In this method the plasma is injected into the trap from a plasma 'gun' source, and is then heated by compression in a rising magnetic field. This method has been the subject of a number of studies by Post and his colleagues as part of the so-called Pyrotron programme. The physical principles underlying plasma heating in this case have been given in Chapter II. As the strength of a field is increased, the kinetic energy of transverse motion of the particles increases in proportion to $H$. In a uniform field the number density is likewise proportional to $H$, so that the ratio of the gas-kinetic pressure to the magnetic pressure, i.e. the quantity $\beta$, does not change during compression (it is assumed that the plasma is compressed so rapidly that particle collisions have no effect). However, if the particles are in a magnetic mirror system, the increase of field over the whole region also produces an axial compression, which increases the parallel kinetic energy. To present more clearly the consequences of a simultaneous radial and axial compression, we shall assume that the plasma is enclosed in a uniform magnetic field bounded by two magnetic mirrors where the field strength is many times larger.

We shall suppose that initially the magnetic field is increased only in the region between the mirrors, and that its strength increases $q$ times. Then the density and transverse kinetic energy of the particles also increase $q$ times, and the radius of the region occupied by plasma decreases to $1/\sqrt{q}$ of its initial value. Suppose that the mirror regions are now moved towards one another, until the distance between them is diminished to $1/k$ of its initial value. The transverse particle velocity remains unchanged; but the parallel velocity increases, and the corresponding parallel kinetic energy increases as the inverse square of the distance between the mirrors; the particle density increases inversely as the first power of this distance. If $k = \sqrt{q}$, then, after compression of the plasma in the radial and axial directions, the ratio of the transverse to the parallel components of velocity for each particle is the same as it was before the start of the two processes, i.e. the angular distribution of velocities does not change. At the same time the total kinetic energy of the particles increases $q$-fold, the density of the plasma increases $q^{\frac{3}{2}}$-fold and $\beta$ increases $\sqrt{q}$-fold. However, all these effects occur only when the plasma compression takes place over an interval of time considerably shorter than the mean ion–ion collision time $\tau_{ii}$ because, in the opposite case, part of the plasma leaks out of the trap as a result of inter-particle collisions. Although this condition appears somewhat harsh, it is nonetheless realisable in practice—even when a large installation is involved. For example, if the trap contains a plasma with number density $n = 10^{12}$ cm$^{-3}$ at a temperature of 100 eV, $\tau_{ii}$ is about $2 \times 10^{-3}$ sec. Thus the rise-time of the magnetic field must not exceed about a millisecond if large leakage is to be avoided. As an elementary calculation shows, this requirement can be satisfied by comparatively simple means for an initial field strength of some thousands of oersteds and a chamber volume of some hundreds of litres.

While studying the heating of plasma by rising magnetic fields, we have in effect ignored up to now those specific properties of plasma which distinguish it from a simple collection of independent particles. A model consisting of independent particles situated in a given field configuration is clearly unsuitable for analysing the compression process if the plasma has high conductivity and such a high pressure that it squeezes the field out of the plasma-occupied region. In the limiting case, the plasma will behave like a gas bounded on all sides by an external magnetic field. The magnetic field, as it increases, acts on the plasma like an elastic envelope and compresses it. If the growth in field strength occurs slowly enough, one can say, neglecting radiation losses, that compression takes place adiabatically. If the field strength increases very rapidly there will be an imploding shock wave and an acceleration of ions; that is to say the compression process will display characteristics analogous to those found with the fast high-powered pulsed discharges described in Chapter V.

The heating of injected plasma by an increasing magnetic field has been experimentally confirmed at several research centres in the U.S.A. At the end of Chapter V we discussed the experiments on rapid compression of plasma carried out by Tuck and colleagues at Los Alamos and Kolb and colleagues at N.R.L. The following section will discuss the experiments on the compression of plasma by magnetic fields which increase comparatively slowly.

### *Experiments with compressional mirror traps*

§ **8.10** Almost all the experimental information on mirror traps with changing magnetic fields has come from the work done by Post and colleagues at Livermore. In this work, the deuterium plasma was injected from a pulsed arc source into a magnetic trap with a rapidly rising field. A typical device of this type, used by the Livermore group, is shown schematically in Fig. 119. The same figure also shows the variation of the magnetic field strength along the length of the trap. The rising magnetic field which grows to roughly 40 kOe in 0·5 msec is imposed on a weak steady field of up to 400 Oe. The arc source injects a blob of plasma along the axis, and after a certain lapse of time the growth of the compression field is initiated. The time between firing the arc source and switching on the compression field can be varied over wide limits.

The initial number density of particles in the injected blob of cold plasma amounts to roughly $10^{11}$–$10^{12}$ cm$^{-3}$ inside the trap, and the ion temperature will certainly not be more than a few eV. After compression, which in this case is both radial and axial, the plasma density will, in theory, go up by two or even three orders of magnitude and reach about $10^{14}$ cm$^{-3}$. Along with the increase in number density, there is also a rapid rise in the plasma temperature. The energy of the ions in these experiments was not established; however, the rapid rise in temperature could be demonstrated quite conclusively by direct measurement. X-rays, produced at the walls by collisions of fast electrons escaping from the plasma along the field lines, were detected with scintillation counters and photomultipliers. Study of this radiation made it possible first, to estimate the electron temperature of the plasma; second, to determine the radial dimensions of the region occupied by the hot plasma inside the trap; and third, to measure the containment time of the plasma.

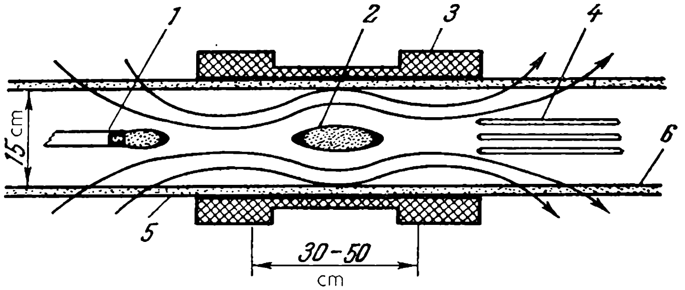

FIG. 119. Outline of apparatus for experiments on containing plasma in a compressional mirror trap

*1*, pulsed source of plasma; *2*, compressed plasma blob; *3*, field coils; *4*, scintillation counters for detection of fast electrons; *5*, steel wall of chamber; *6*, metallic layer sprayed on internal surface of glass

Measurement of the X-ray energy by absorption in filters shows that, in typical experimental conditions, the escaping electrons have an energy of from 10 to 100 keV. The electron temperature can be found from analysis of the absorption curves. Temperatures measured in this way come in the range 20–30 keV for individual experiments. Because electrons have small Larmor radii (in a field of 40 kOe the Larmor radius of a 30 keV electron is no more than about 0·1 mm) they are disposed almost exactly along the lines of force. Therefore, the intensity distribution of the X-rays produced when the electrons strike the inner wall of the chamber, is directly related to the radial density distribution of the hot plasma (it is assumed that the electrons leave the plasma as a result of Coulomb collisions and that the density of the electron stream is therefore proportional to $n_e^2$). By measurement of the X-ray intensity emitted at the walls as a function of position, it has been established that the radius of the region occupied by the hot plasma is about one-fifth the radius of the vacuum chamber.

The most interesting feature is the unexpectedly long time during which the hot plasma is preserved. Measurements, with a scintillation counter disposed along the magnetic axis, of the intensity of the X-rays show that the hard radiation lasts for several milliseconds after the time of maximum field strength. From this it follows that the convectional ('interchange') instability which—according to theoretical considerations—should occur in a system with convex lines of force, is suppressed by some effective stabilising mechanism in the experiments of Post and his colleagues.

The supposition of those responsible for this work is that the basic explanation lies in stabilisation caused by the free exchange of charges between the plasma and the chamber walls along the lines of force (see § 7.5). In the reported experiments with hot electron plasmas, the plasma occupies a small region in the centre of the trap and is, so to speak, immersed in a cold plasma which, apparently, has quite high density and occupies all the rest of the space. This cold plasma is in contact with the conducting walls of the chamber and ensures that charges of opposite sign, which occur when there are perturbations of the hot plasma blob, are shorted out.

This explanation can be regarded as likely enough. In particular, it has in its favour the fact that the containment time is markedly shortened if the internal walls of the chamber are made non-conducting. However, it is difficult at the present time (1961) to make a final assessment of the results obtained by the Livermore group in so far as the published data tend to be fragmentary and are not always adequately self-consistent. In this connection it should be noted that if we take the density of hot plasma as $10^{14}$ cm$^{-3}$, then, at an electron temperature of about 10 keV, the mean lifetime of the particles in the trap should not exceed about 100 $\mu$sec, if we take into account only collisional loss of electrons through the mirrors. The lifetime of the particles can reach a few milliseconds only if the density of the hot plasma is not more than $10^{12}$ cm$^{-3}$ in order of magnitude. It is also difficult to reconcile the claim of high plasma density with the estimated ion temperature. If deuterons in a compressed plasma blob were really at a temperature of several keV, as the authors of this work consider, then with a plasma number density of around $10^{14}$ relatively intense neutron radiation ought to be observed.

So long as we have at our disposal only the data so far published (1961), we cannot exclude the possibility that in Post's experiments a considerable part of the plasma leaks from the compression region while the magnetic field is rising, and that what remains inside the highly compressed region represents only a comparatively small part of the total number of particles that originally filled the trap.

The true value of the mean ion energy also remains unclear. It is entirely possible that, because of intense interaction between the plasma and the walls, a significant amount of impurities appears in the central space even during the very short time following the injection of the plasma blob. Charge exchange on these impurity atoms and also on neutral deuterium atoms and molecules will lead to a fall of ion temperature. From the quantitative point of view it is rather difficult to estimate the influence of this effect. Consequently it seems a pity that there are no direct measurements of the ion temperature in these experiments.

The method of multi-stage compression of plasma developed at the Livermore laboratory is of considerable interest. The idea underlying this method is that, by means of time-varying magnetic fields, a blob of plasma is transferred in several stages along the lines of force from one end of the vacuum chamber where it has large diameter and where consequently the magnetic field takes up considerable volume, to the other end of the chamber which has a small diameter so that the volume to be filled with high magnetic field is small. By this means, as the plasma blob is gradually compressed the ratio of the volume it fills to the volume occupied by the magnetic field is always quite large; that is to say the magnetic field energy is used relatively efficiently. Figure 120, which is taken from a paper by Coensgen, Cummins and Sherman, shows a sketch of an experimental device of this type. The lower part of the figure shows schematically an installation for three-stage compression of plasma. The vacuum chamber, the coils used to generate the constant field and the compression fields and the disposition of the plasma gun are shown. The upper part of the figure shows the distribution of field strength along the chamber. The unbroken line *I* corresponds to the initial constant field, and the broken lines to the changing fields used for successive compression and transfer of the plasma blob from right to left. The blob, once injected from

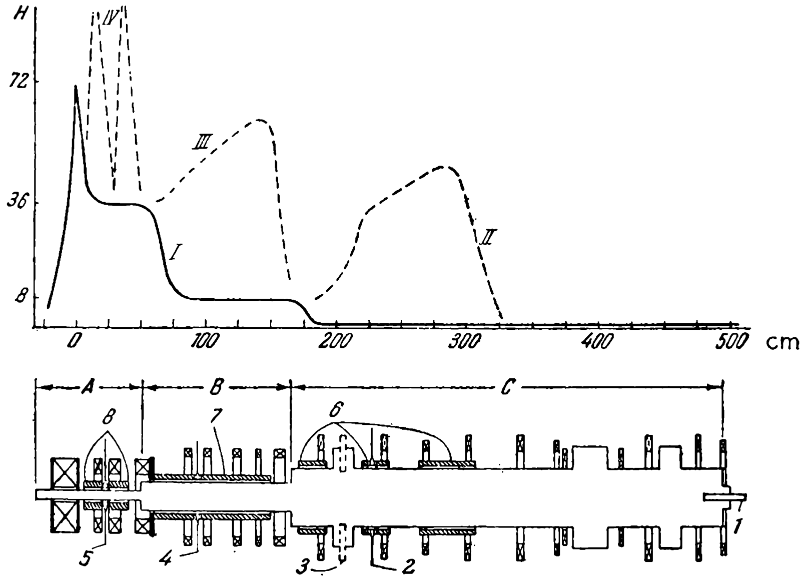

FIG. 120. Apparatus for the multi-stage compression of plasma

The upper figure shows the distribution along the chamber axis of the constant and the rising magnetic fields. The field strength is given in arbitrary units

*Lower figure:* *1*, pulsed source of cold plasma; *2*, *4*, *5*, microwave interferometers; *3*, source for radial injection of plasma; *6*, coils for first stage of compression; *7*, coils for second stage of compression; *8*, coils for third stage of compression the gun, first moves along the lines of force of the constant field and occupies the region *C* which is bounded on the left by the first constant magnetic mirror (the first rise on the unbroken curve, going from right to left). At a specific time after the discharge of the plasma gun, a rising magnetic field is switched on; the spatial distribution of this field is represented by the dotted curve *II*. As this field grows the plasma is heated and flows over into the region between the first constant magnetic mirror and the second. Having flowed over, the plasma cannot go back again because it is shut in on the right by the rising field. The second compression field (section *B*) now comes into action. Its effect is represented by curve *III*. The end result, after two-fold compression, is that the plasma blob is enclosed in the final trap region *A*. The field coils situated at the end of the chamber are responsible for the final stage of compression, during which the field has the form shown schematically by the dotted curve *IV*. One may hope that in devices of this kind it will be possible to compress the plasma by about 100 times or more.

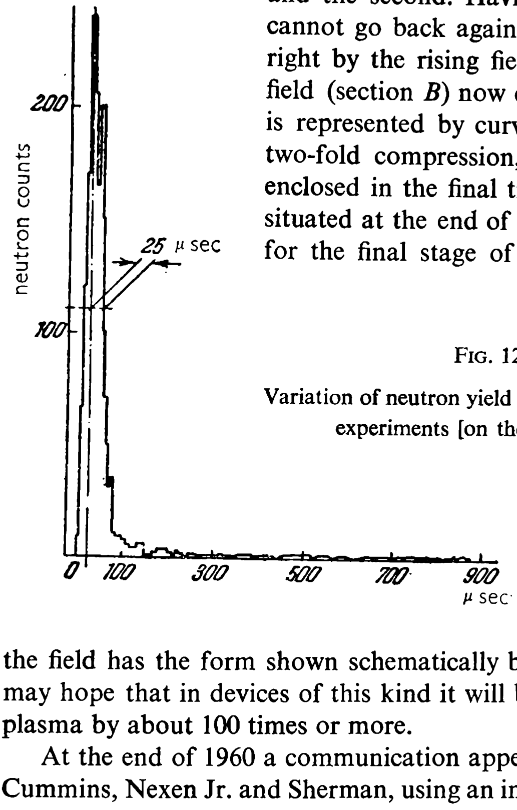

FIG. 121

Variation of neutron yield with time in Coensgen's experiments [on the diagram μ sec]

At the end of 1960 a communication appeared stating that Coensgen, Cummins, Nexen Jr. and Sherman, using an improved plasma injector and a two-fold compression system, had obtained a dense deuterium plasma with an ion temperature of about 3 keV, and had observed weak neutron radiation lasting some hundreds of microseconds. Unfortunately the account of the results obtained, which was given in a brief note, does not enable one to form any definite conclusions as to either the significance of the effect observed or the time-duration of the high-temperature plasma. The question remains open whether or not one can explain the curve showing the intensity of neutron radiation as a function of time, by postulating that the late neutrons are those delayed in an organic scintillator.† This explanation suggests itself because the observed intensity of neutron radiation first decreases very rapidly—by 10 times in 25 μsec—

---

† This supposition has been confirmed.

and then far more slowly; moreover, only a very small proportion of the neutrons falls on the scintillator during the time interval of about 0·5 msec. To illustrate the point, Fig. 121 shows neutron yield as a function of time. The curve has been taken from the published note of the authors mentioned. The curve differs from the original only in that the logarithmic scale on the vertical axis has been replaced by a linear scale.

### *The Ion Magnetron and other installations with rotating plasma*

§ **8.11** Research on a method of obtaining high-temperature plasma in an installation called the ion magnetron has been carried on for a number of years at the Kurchatov Institute of Atomic Energy by Ioffe and his

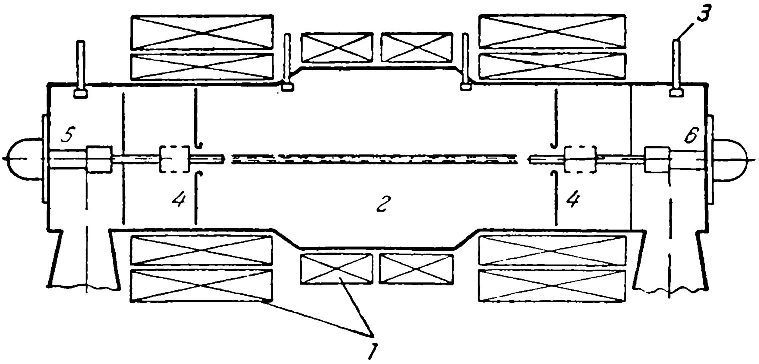

FIG. 122. Outline of the ion magnetron apparatus

*1*, coils generating magnetic field; *2*, vacuum chamber; *3*, titanium evaporators; *4*, diaphragms; *5*, plasma source; *6*, reflector

colleagues. Figure 122 shows schematically the design of an ion magnetron; Plate XVI is an external view of the actual installation on which, up to now, the main experiments have been done. The internal diameter of the central part of the vacuum chamber is 50 cm; the length of the chamber is 200 cm. The maximum field strength that can be generated is 8 kOe in the centre of the chamber and 12 kOe at the mirrors. By the use of high-vacuum diffusion pumps and four titanium evaporators, the base pressure in the chamber can be kept at $10^{-7}$ Torr during operation. Metal diaphragms with a hole diameter of 50 mm are fitted in the mirror regions. Their purpose is to produce a pressure drop between the centre of the chamber and the ends where the plasma source and the reflector are situated. The plasma source, which is shown separately in Fig. 123, is a cylinder containing a heated tungsten cathode. Hydrogen at an initial pressure of about $10^{-3}$ Torr is introduced into the source through the tube near the cathode. When a potential of about 300–400 V is applied between the cylinder and the heated cathode, an intense arc discharge occurs. Plasma fills the cylinder and flows out of it into the main chamber, spreading along the magnetic lines of force. As it flows from the arc discharge, the plasma forms a well-defined column with a diameter of 2 cm in the central part of the chamber. At the far end of the chamber the plasma column falls on to the reflector which is situated in a position equivalent to that of the plasma source. The potential of the reflector is that of the anode of the plasma source. The number density of the plasma in the column depends on the mode of operation of the arc source. In the experiments described, it was $10^{12}$–$10^{13}$ cm$^{-3}$.

To fill the trap with fast ions, a high potential is applied between the source and the chamber wall. The plasma column, because of its high parallel conductivity, assumes the potential of the source, and thus serves as the central anode in an ion magnetron. The applied potential thus creates a radial electric field between this plasma column and the side wall of the chamber. This field extracts ions from the column and out of the surrounding more rarefied plasma, and accelerates them. Acted on simultaneously by the radial electric field and the axial magnetic field, the ions move in a plane perpendicular to $H$ along trajectories which form something between a circle and a cycloid (they might be termed trochoidal trajectories). Each such trajectory can be regarded, roughly, as the result of combining two motions—the ordinary Larmor revolution, and the azimuthal drift in crossed fields. Consequently the particle trajectories encircle the magnetic axis of the system. The azimuthal drift speed is approximately equal to $cE/H$, where $E$ is the mean value of the radial electric fields at the extremities of one Larmor circle at a given time. The speed of Larmor rotation depends on the initial conditions of ion motion. If the ion was formed at a time and place when the electric field was $E_0$, this speed will be equal to the initial drift speed $cE_0/H$ (provided that the Larmor radius is considerably less than the distance over which the non-uniform electric field varies significantly). As the strength of the electric field increases or decreases in time, the drift speed varies as $E$. If the field does not change too quickly, the principle of adiabatic invariance must

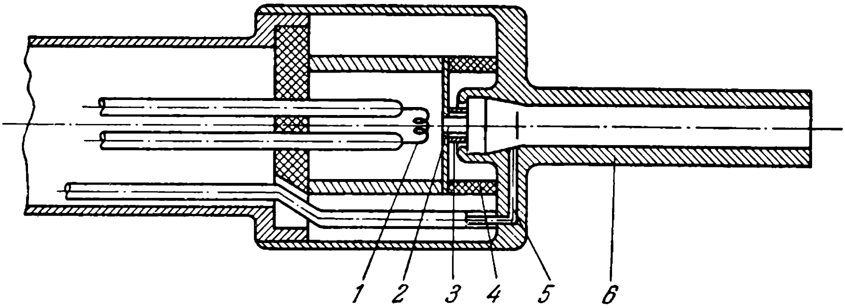

FIG. 123. Details of the plasma source used in Ioffe's installation

*1*, heating filament; *2*, hot tungsten cathode; *3*, molybdenum screen; *4*, insulator; *5*, channel for entry of gas; *6*, anode apply, that is, the ratio of the Larmor rotation energy to the magnetic field strength is constant. Therefore the speed of the Larmor rotation retains the initial value $cE_0/H$.

These arguments are not completely accurate. In particular, they take no account of the fact that the variation of $E$ with $r$ must introduce a correction into the relationship between the rotation speed and the drift speed. However, taken overall, it gives a correct picture of the character of the ion motion, and makes it possible to estimate the ion energy and explain how it changes with time. In the experiments now being described, the high voltage is fed to the ion magnetron as a single rectangular pulse of 10–24 kV lasting 30–40 $\mu$sec. If the electric field in the space between the plasma anode and the chamber wall changes with radius, as in an ordinary cylindrical condenser, the maximum ion energy at field strength 3000–5000 Oe would have to correspond roughly to the applied voltage (i.e. it would have to reach some tens of keV). However, once the voltage is removed, the ions retain only a part of their original energy; that is to say, in the region where $E$ is not too strongly dependent on $r$, the energy remaining after switching off the voltage amounts to roughly a quarter of the maximum initial value (since the drift component of the velocity becomes zero, and the maximum velocity is therefore halved).

Consequently, it may be expected that in the plasma which remains after the voltage has been switched off, the ions must have energies of roughly a few keV. The variation of the electric field with radius, as time elapses, is also bound to have an influence on the energy spectrum of the ions. After the voltage is switched on, the field changes initially under the influence of space charge; and then it changes as a result of formation of a relatively tenuous secondary plasma in the space between the plasma column and the chamber wall.

In explaining the properties of the plasma formed by the accelerated ions, it is of particular interest to consider the measurements of the flux of fast neutral atoms which appear as a result of charge exchange with fast ions in the volume of the chamber. To record these atoms, detectors were placed in nozzles close to the chamber wall. The detector consists of two electrodes between which a voltage is applied; when bombarded with fast neutral atoms, the negative electrode emits electrons. The strength of the current passing through the detector circuit is a measure of the flux of energetic neutral particles to the wall. The flux measured by the detector is proportional to $n_0 n_i v_i \sigma_c$ where $n_0$ is the number density of neutral atoms in the volume (in the conditions being considered these are essentially atoms of hydrogen combined into molecules), $n_i$ is the ion number density of the plasma, $v_i$ is the ion speed and $\sigma_c$ is the charge-exchange cross-section.

By recording the decay of the neutral flux after switching off the high voltage, one can determine the mean lifetime $\tau$ of fast ions in the plasma. Where the density of the neutral gas in the chamber is not too small, charge-exchange is the main loss mechanism. In this case the mean lifetime is given by:

$$\tau^{-1} = n_0 \overline{v_i \sigma_c}.$$

Given measurements of $\tau$ and $n_0$, one can find the mean value of $v_i\overline{\sigma_c}$; from this and the known variation of $\sigma_c$ with velocity, one can estimate the energy of the fast ions. Furthermore, from measurements of the absolute value of the neutral particle flux to the wall, one can make an estimate of the number density of fast ions. In the usual conditions of the present experiments, the estimated number density was $10^9$–$10^{10}$ cm$^{-3}$ immediately after switching off the high voltage.

The greatest interest attaches to the stability of the plasma in an ion magnetron. Light is thrown on this question by studying the variation of the lifetime of fast ions with experimental conditions. Because of the low density of plasma in an ion magnetron, Coulomb collisions cannot be responsible for escape of particles. Likewise, particle loss due to defects in the magnetic field configuration should not, apparently, occur. The plasma ions are accelerated by a radial electric field perpendicular to $H$, and therefore, even with a mirror ratio only slightly exceeding unity, they will be trapped by the magnetic field. It follows from all this that if the plasma is in a stable state, and if diffusion of particles across the field is almost wholly excluded (because $D_\perp$ is very small), then the sole factor limiting the lifetime of the ions can only be charge-exchange. If this supposition is correct, $\tau^{-1}$ as determined by the decay of the neutral particle flux will be proportional to $p_0$ (for a given value of $\overline{v_i \sigma_c}$ which depends solely on ion energy).

Figures 124 and 125 show the observed variation of $\tau^{-1}$ with $p_0$, when various applied voltages and magnetic field strengths were used. From the slope of the curves $\tau^{-1} = f(p_0)$ we can determine the value of $\overline{v_i \sigma_c}$, and hence the mean energy of the ions for different initial conditions. As was to be expected, these energies are of the order of a few kilo-electron-volts and increase with increasing applied potential, and decrease with $H$. The most important result which is obvious at first glance is that as $p_0$ decreases to zero, $\tau^{-1}$ tends towards a finite limit $\tau_0^{-1}$ depending on $H$ and the applied potential $V$. The limiting value of $\tau^{-1}$ for each experimental curve can be found by extrapolating it to $p_0 = 0$.

This result indicates plainly that fast ions disappear not only by charge-exchange but also by means of some other mechanism. In the conditions being considered, this mechanism can be connected only with instability of the plasma in the trap. From the experimental data given in Figs. 124 and 125, it follows that this instability, when judged by the magnitude of $\tau_0^{-1}$, appears more strongly as $H$ is made smaller and $V$ larger. With $H = 5$ kOe and $V = 30$ kV the mean lifetime of the ions, neglecting charge-exchange, is 200 $\mu$sec. It rises to 1500 $\mu$sec if $H$ is increased to 8 kOe.

To elucidate the nature of the anomalous particle loss, measurements

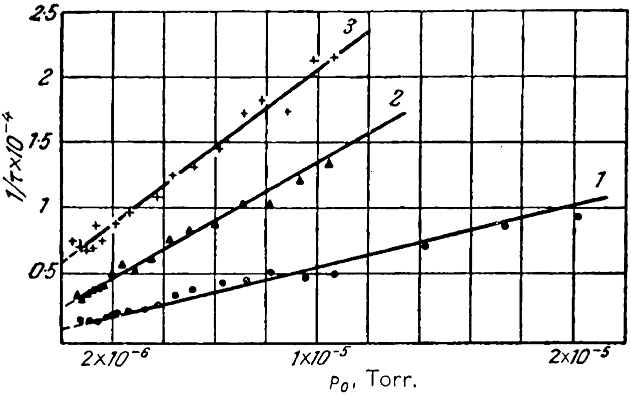

FIG. 124. Variation of the lifetime of fast ions with gas pressure, for different accelerating voltages when $H_0 = 5$ kOe and $H_m/H_0 = 1{\cdot}54$

*1*, $V_{acc} = 11$ kV, $\sigma_c v_i = 1{\cdot}3 \times 10^{-8}$; *2*, $V_{acc} = 20$ kV, $\sigma_c v_i = 3{\cdot}1 \times 10^{-8}$; *3*, $V_{acc} = 45$ kV, $\sigma_c v_i = 4{\cdot}2 \times 10^{-8}$

were first of all carried out to investigate the dependence of $\tau_0^{-1}$ on plasma density; and secondly, a study was made of the escape of fast ions along and across the lines of force. One might expect that, with a low enough number density of charged particles, when the Debye shielding distance corresponds roughly to the region occupied by the plasma, and when the plasma itself becomes a mere collection of mutually independent ions and electrons, the action of the various instability mechanisms will stop, and the value $\tau_0^{-1}$ will tend to zero. The dependence of $\tau_0$ on number density can be found by analysing curves of $n_i$ as a function of time $t$. The slope of this curve at each point gives $\tau^{-1}$ throughout the decay of plasma. Then

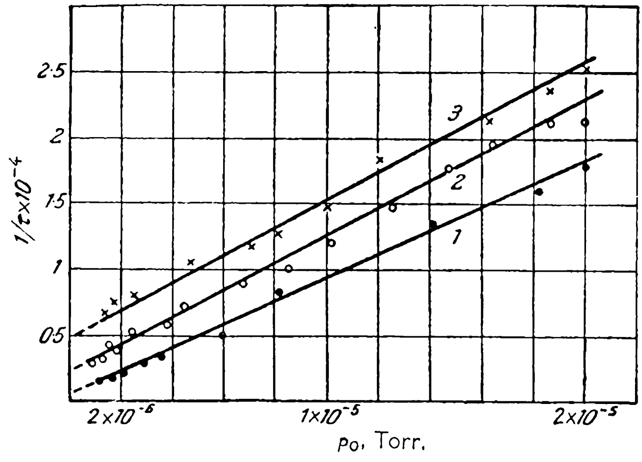

FIG. 125. Variation of lifetime of fast ions with gas pressure, for different values of $H_0$ when $H_m/H_0 = 1{\cdot}54$, and the initial accelerating voltage is 30 kV

*1*, $H_0 = 8$ kOe; *2*, $H_0 = 6$ kOe; *3*, $H_0 = 5$ kOe

$$\tau^{-1} = \tau_0^{-1} + \tau_c^{-1},$$

where $\tau_c$ is the mean lifetime determined by charge-exchange mechanism. In agreement with what has been said above, it is to be expected that for large values of $t$, when the plasma density becomes low enough, anomalous loss will stop, and therefore $\tau$ will become equal to $\tau_c$. This means that the function $n_i(t)$ will be different from a simple exponential, particularly when the pressure of neutral gas in the chamber is low, and when anomalous losses are of major importance during the first stage of plasma decay. Such analysis of the measurements does indeed show that when the plasma number density falls by two orders of magnitude and becomes about $10^7$ cm$^{-3}$, the lifetime of ions in the plasma increases and is in effect determined solely by charge-exchange; in other words $\tau_0$ tends to infinity.†

By means of electrodes placed in the mirrors and near the side wall, the way in which the particles disappear can be observed. Such observations show that fast ions escape from the trap mainly across the lines of force (as is only to be expected in view of the fact that they get their energy from the radial electric field and will therefore have small parallel velocities). Oscillograms of the ion current recorded by the electrodes show that the ion current is not a smooth function of time. Instead, large fluctuations are observed which are irregular in both amplitude and form. The range of characteristic frequencies lies between $10^4$–$10^6$ sec$^{-1}$. The amplitudes of the fluctuations are of the same order as the mean value of the ion current.

Oscillograms obtained simultaneously from electrodes placed at various points on the wall show that the fluctuations of ion current are in phase all along a given line of force. If one compares oscillograms for points displaced azimuthally relative to one another, the synchronisation of the fluctuations is seen only as long as the relative displacement is small; the correlation distance is smaller as the frequency becomes higher. Thus oscillations with frequencies of about $10^6$ sec$^{-1}$ are uncorrelated even at distances comparable with the ion Larmor radius (4–5 cm). It has also been noted that both the frequency of the oscillations and the degree of current modulation decrease when the plasma density decreases. These features of the oscillations of the ion flux to the wall are evidence that the escape of ions is due to some non-stationary mechanism, which may be classed under the broad category of 'anomalous diffusion' and may, in the last resort, be attributed to one of the forms of instability characteristic of a plasma in a trap of the ion magnetron type. It seems natural to suppose that instabilities begin to appear at the very earliest stage, a few microseconds after switching on the high voltage, and that they are associated, in the first place, with the rapid rotation of the plasma in the crossed fields and, in the second place, with the bulging magnetic field which is typical of a mirror trap. The consequence of all this is that the plasma (which formed initially at a comparatively short distance from the axis) undergoes a rapid radial diffusion and comes into contact with the side wall. After this the mechanism of convective diffusion examined by Kadomtsev comes into play, and the escape of particles is regulated by interaction between individual plasma threads and the wall. The fast ions, which have been formed somewhere inside the chamber, drift under the influence of fluctuating electric fields (only the azimuthal component of $E$ is involved here) towards the surface of the plasma. They reach the wall on the crests of the plasma tongues. It is very difficult to estimate the lifetime of an ion close to the plasma surface, because the nature of the electric field fluctuations is wholly obscure in this region (in the immediate proximity of the wall). If the lifetime near the wall is comparable with the time needed to diffuse to the plasma surface, an ion can approach the wall and then return to the central region of the plasma several times before it is lost to the walls.

---

† During the containment time of the plasma, the energy spectrum of the fast ions changes because $\sigma_c$ varies with energy. Consequently, the escaping flux $n(t)$ does not closely follow an exponential law. However, this complicating factor can be dealt with by carrying out measurements of $n(t)$ over a sufficiently wide range of background gas pressures.

As discussed in § **7.5**, Kadomtsev has investigated theoretically the mechanism of convectional diffusion in traps of the present type, and has derived a formula for the mean lifetime of fast ions. The results of calculations carried out according to formula (*7.36*) are in qualitative agreement with measurements made by Ioffe and his colleagues; or rather, to be more precise, they do not conflict with these measurements (the coefficient $C$ which comes into the theoretical expression for $\tau$ remains effectively an unknown quantity).

To get a clear picture of the true mechanism of the observed anomalous diffusion, further experiments will have to be carried out. In particular, the relation between the lifetime of ions in a trap and such geometrical factors as the radius of curvature of the lines of force and the form of the lateral surface of the chamber wall, will have to be investigated. Preliminary measurements show that the second factor mentioned can, apparently, have a marked influence on the rate of decay of a plasma in the ion magnetron. It is also of interest to investigate if the mean ion lifetime decreases when the number density of the plasma is increased. Further study of the energy spectrum of the ions, including the way in which it varies with time, must be made. Thanks to the method, developed by Tel'kovskii, for measuring the energies of neutral atoms by slowing them down in thin films, it is now possible to obtain data on the ion spectrum inside the chamber by determining the energy of neutral atoms produced by charge-exchange. This method enables us to determine the energies of comparatively slow ions (down to 500 eV). Finally the distribution of electric fields in the plasma remains to be determined. This can be done by using beams of electrons emerging from the chamber through the mirrors.

§ **8.12** The ion magnetron experiments described in the preceding

PLATE XVI

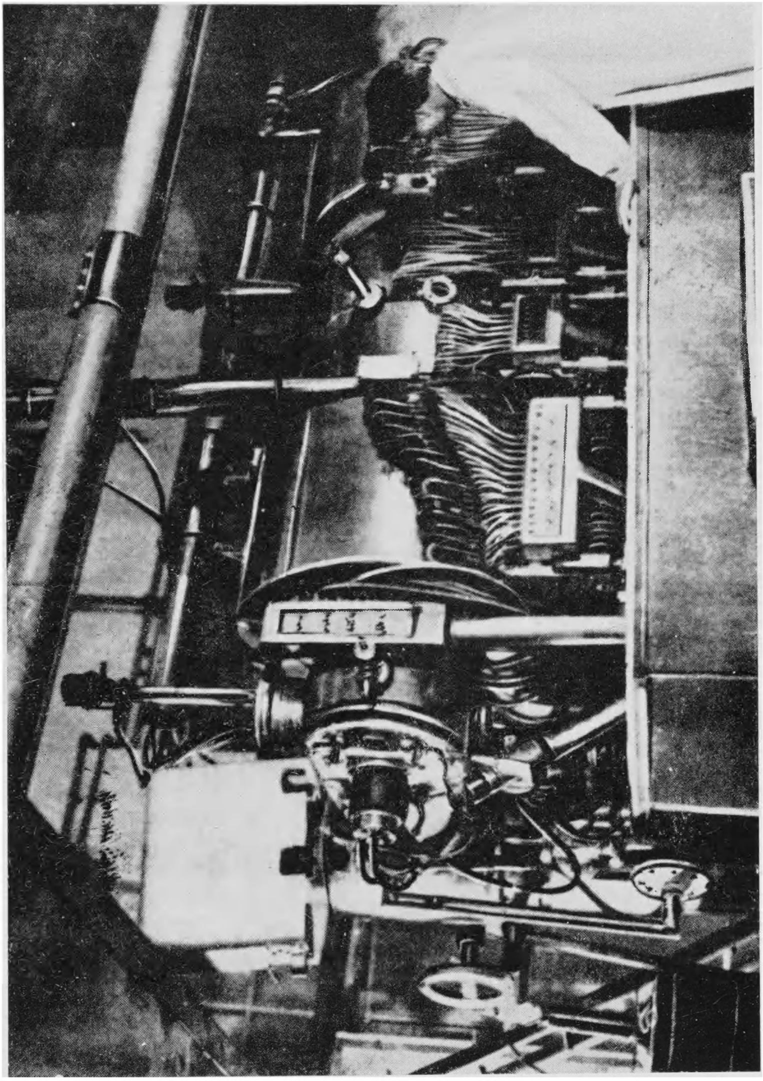

External view of Ioffe's installation.

section were mainly directed to studying the plasma after switching off the radial electric field. In the Ixion installation, however, the main phase of interest occurs when the plasma, formed after the breakdown of the gas in the chamber, revolves about the magnetic axis system under the influence of a sustained radial field (a radial $E$ and an axial $H$). The design of Ixion is reminiscent of Ioffe's installation. The wall of the chamber serves as the external electrode. The central electrode can be either a metallic rod placed along the magnetic axis or (as in the foregoing case) a column of cold dense plasma. However, unlike the ion magnetron, Ixion operates with a high initial gas pressure (about $10^{-3}$ Torr), and plasma is formed in it, not by emission of ions from the central column, but by the intense radial electric discharge in the gas filling the chamber. The magnetic system is an ordinary magnetic mirror trap. The behaviour of charged particles in 'Ixion' can be predicted from the elementary theory of drift motion (assuming, of course, that the process is stable). In crossed fields the particles drift round the axis at speeds close to $cE/H$. However, the ion and electron drift velocities will not be precisely equal.

To estimate the drift velocity, we shall assume that a particle of mass $m$ and charge $q$ rotates at a distance $r$ from the axis. In the stationary state, we must then have:

$$-\frac{mv_\theta^2}{r} = q\left(E_r + \frac{v_\theta H_z}{c}\right);$$

from this it follows that

$$v_\theta = -\frac{cE_r}{H_z} - \frac{mcv_\theta^2}{qrH_z}.$$

If we regard the second term on the right-hand side as a small correction (which is true when $E$ is not large) we can write

$$v_\theta = -\frac{cE_r}{H_z}\left(1 + \frac{mc^2E_r}{qH_z^2}\frac{1}{r}\right). \qquad \text{.........(8.24)}$$

Thus the magnitude of the additional term in the expression for $v_\theta$ depends on the relationship between the amplitude of the cycloid and the distance from the trajectory to the magnetic axis, and its sign depends on the sign of $q$. It follows that the drift speed of the ions differs from that of the electrons. Consequently, an azimuthal electric current appears. Neglecting $m_e$ in comparison with $m_i$, and taking $|q| = e$, we have

$${}_\theta = ne(v_{\theta i} - v_{\theta e}) = -\frac{nm_ic^3E_r^2}{H^3r}. \qquad \text{.........(8.25)}$$

With $n \simeq 10^{12}$ cm$^{-3}$, $E_r = 10$ (3000 V/cm), $r = 10$ cm and $H = 5000$ Oe, the current density will be about 1 A/cm$^2$. This current causes a diamagnetic effect which weakens the magnetic field in the plasma (this is additional to any weakening caused by the ordinary diamagnetism of the plasma), and counterbalances the centrifugal force of the rotating plasma.

We note two interesting peculiarities of systems of the 'Ixion' type. The first of these is that the confining effect of the magnetic mirrors is enhanced by the presence of a radial electric field. This is easy to understand if we note that, during drift motion, each particle has a certain additional angular momentum relative to the magnetic axis. When a particle moves towards one of the mirrors the distance from its trajectory to the axis decreases (because the lines of force converge) and therefore, to conserve angular momentum, the angular velocity must increase. Thus a sort of additional centrifugal potential arises which is associated with the drift motion and hinders the escape of the particle through the magnetic mirror. As has been shown by Longmire and others, all particles are contained in Ixion if they satisfy the following condition:

$$W_{\perp}\left(\frac{H_{\mathrm{m}}}{H_0}-1\right) > W_{\parallel} - \tfrac{1}{2}mv_{\mathrm{d}}^2\left(1-\frac{H_0}{H_{\mathrm{m}}}\right). \qquad \ldots\ldots\ldots(8.26)$$

Here $W_{\parallel}$ and $W_{\perp}$ are the parallel and perpendicular kinetic energy respectively in the central part of the trap where the field is $H_0$, $H_{\mathrm{m}}$ is the maximum field at the mirrors and $v_{\mathrm{d}}$ is the drift velocity. Condition (*8.26*) differs from the analogous relationship for a simple mirror trap by the presence of a term containing the kinetic energy of the drift rotation. Provided $H_{\mathrm{m}}/H_0$ is not too close to unity, this additional term for the ions in an Ixion-type system is usually about the same as that for the energy $W_{\perp}$ of Larmor rotation (for electrons, because of their small mass, $kT_{\mathrm{e}} \gg m_{\mathrm{e}}v_{\mathrm{d}}^2/2$).

The second feature of Ixion is that it is, in effect, a plasma capacitor in which the energy supplied from the high-voltage source is stored in the form of rotational energy of the plasma. Owing to the high value of the dielectric constant of the plasma in crossed fields, the capacity of the plasma capacitor can considerably exceed the value that would be associated with an ordinary air capacitor of the same dimensions. The energy stored in a plasma capacitor can in principle be returned to the circuit by switching the capacitor into an external load.

The comparatively sparse experimental data on the processes taking place in Ixion were presented by Boyer and others at the Geneva Conference. Figure 126 shows a schematic cross-section of the installation. The diameter of the chamber is 24 cm and its length 86 cm. The plasma column serving as the central electrode is obtained by using a pulsed injector. The plasma column passes inside two ring-shaped tungsten electrodes placed in the two magnetic mirrors at the point of maximum field strength. A potential of about 10 kV relative to the body of the chamber is applied to the column through these electrodes, which are in contact with the surface of the column. The magnetic field strength in the central part of the chamber is 5–10 kOe. The chamber is filled with deuterium at an initial pressure of about $10^{-3}$ Torr.

The discharge current lasts about 25 $\mu$sec and attains a maximum value of 10–20 kA. After that the current decays practically to zero. During a discharge pulse, the radial electric potential falls to approximately half its initial value, and subsequently falls more slowly to zero. These electrical characteristics are governed by the ionisation of the initial gas filling, and by the storage of the energy in the rotating plasma. Ideally, the discharge current would have a purely capacitive character; but because of the dissipative effects in the plasma it is partly ohmic.

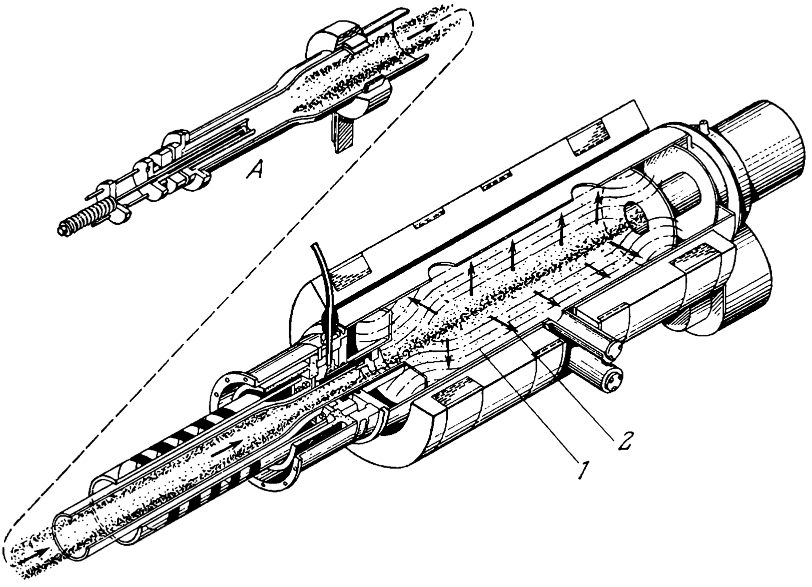

FIG. 126. The Ixion apparatus

*A*, pulsed source of plasma; *1*, the magnetic field lines; *2*, the electric field lines

To determine the capacity of the plasma capacitor, Ixion was short-circuited and the charge flowing in the circuit was measured. The measurements showed that the capacitor returns about 20% of the total charge passed through it during the charging pulse. This means that in these experiments the plasma impedance is predominantly ohmic. Because of the marked contamination of the deuterium by various impurities, the measured capacities were higher than the maximum values that had been calculated.

Measurements of Doppler shift of spectral lines confirmed the existence of a rotating plasma. During the passage of discharge current, it was sometimes possible to observe neutron radiation, the origin of which remains obscure. There is no ground for expecting that thermonuclear reactions occur in the conditions of these experiments, where the ions have a comparatively small average energy (not more than some tens of electron-volts).

The experiments performed on Ixion, despite their fragmentary nature and despite the insufficiently pure conditions in which they were done, do on the whole yield results of interest, if one regards them as a demonstration of the validity of physical ideas which flow from our basic concepts of plasma dynamics. In a programme of research into thermonuclear fusion, installations built on the Ixion principle will hardly acquire any great importance in their own right because it would be very difficult to use such installations to obtain fully ionised high-temperature plasma (due to the high initial pressure of the gas and the instability of the rotating plasma). However, the basic idea behind Ixion—a combination of the ion magnetron with the ionisation of a gas by a radial electric field—may find application as the first stage of obtaining hot plasma in magnetic mirror traps. If this happens, the main problem (apart from the stability question) will be to devise a mode of operation which will guarantee practically 100% ionisation of the gas in the chamber. At present one cannot see how this might be done.

### *Installations involving injection of fast particles*

§ **8.13** The largest existing magnetic mirror trap was built in 1958 under the guidance of I. N. Golovin at the Kurchatov Institute of Atomic Energy. It was given the name of 'Ogra'. The purpose of this installation was the experimental study of the build-up of high-temperature plasma by the injection of molecular ions which are then dissociated by collisions with atoms of the residual gas and the trapping of the resulting atomic ions. Calculations show that, with a favourable combination of circumstances, this method could yield plasma having not only a very high ion temperature but also a significant density. The high density can be obtained if one succeeds in achieving what has been termed 'burn-out' of the neutral gas. For this to be possible, there must be practically complete ionisation of the neutral gas in the chamber, so that charge-exchange of the fast ions—which otherwise represents the main cause of loss of the atomic ions—is eliminated. To get a picture of the 'burn-out' concept, we shall consider the accumulation of ions in the trap.

A molecular ion, when properly injected, will traverse a long path inside the trap, being reflected many times from the mirrors and drifting in the azimuthal direction. Ultimately, such a molecular ion is bound to strike the injector. If the residual gas pressure in the chamber is sufficiently low, almost all the molecular ions will reach the injector; only a small proportion will be dissociated by collisions with neutral gas molecules, thus forming atomic ions and fast neutral atoms. We start by assuming that the injected flux of molecular ions $N_{\mathrm{m}}^{+}$ has a small value, so that the number density of atomic ions $n_{\mathrm{a}}^{+}$ is small compared with the number density of neutral atoms, and one can therefore neglect dissociation of molecular ions by collisions with atomic ions. Consequently, the rate of formation of atomic ions by dissociative collisions is $N_{\mathrm{m}}^{+}n_0\sigma_{\mathrm{d}}L$, where

$n_0$ is the number density of neutral atoms, $\sigma_d$ is the dissociation cross-section and $L$ is the total distance traversed by a molecular ion from the point of injection to the point of loss on return to the injector. The value of $L$ is proportional to the product of the distance between the two magnetic mirrors and the chamber radius. The fast atomic ions formed by dissociation do not strike the injector. At this stage of the accumulation one can neglect the escape of particles through the magnetic mirrors as a result of Coulomb collisions. Therefore, in the absence of instabilities or irregular drift movements, the main loss of fast atomic ions is due to charge-exchange of the fast ions on collision with neutral atoms. In a unit of time the number of charge-exchange collisions in the trap is $n_a^+ n_0 v_i \sigma_c \Omega$, where $\Omega$ is the volume of the chamber. The accumulation of atomic ions is described by the equation

$$dn_a^+/dt = (N_m^+/\Omega) n_0 \sigma_d L - n_a^+ n_0 v_i \sigma_c. \qquad \text{.........}(8.27)$$

After reaching equilibrium

$$n_a^+ = (N_m^+ L/\Omega v_i)(\sigma_d/\sigma_c). \qquad \text{.........}(8.28)$$

The quantity $N_m^+ L/\Omega v_i$ represents the density of molecular ions in the volume of the trap. Therefore (*8.28*) could also be written

$$n_a^+/n_m^+ = \sigma_d/\sigma_c. \qquad \text{.........}(8.29)$$

Here $n_m^+$ is the number density of molecular ions. If the neutral gas in the chamber consists only of molecular hydrogen, then with an $H_2^+$ ion energy of 200 keV, the number density $n_a^+$ of protons will be approximately 10 times greater than $n_m^+$.

The density of the neutral gas in the chamber, in the absence of an injected beam of ions, depends on the amount of gas given off by the walls and on the pumping speed of the vacuum system. With the present state of vacuum technology, it is entirely feasible to achieve a vacuum of about $10^{-9}$ Torr in big installations of the Ogra type. When an ion beam is admitted into the chamber, a new source of gas emission appears—the neutralisation of molecular ions on their return to the injector. Simultaneously, processes lowering the density of the neutral gas begin to operate. These processes may be termed 'ion pumping'; neutral gas disappears from the volume as the result of collisions with fast atomic ions which have accumulated in the chamber. It is not only ionisation processes that are responsible for this, but also charge-exchange collisions, because the neutral atoms produced by charge-exchange move at a high speed, and embed themselves in the chamber walls.

Equation (*8.28*) for the equilibrium value of the atomic ion number density involves the assumption that $n_a^+$ remains considerably less than $n_0$. However, when the injected current is sufficiently large, this assumption is no longer valid. If $n_a^+$ is comparable with $n_0$, then the dissociation of molecular ions on atomic ions must be included; therefore the equilibrium number density of atomic ions becomes larger than the value determined by (*8.29*). Thus, as the strength of the injected current is raised, $n_a^+$ grows more rapidly than $N_m^+$, and at some critical value of the injected current there will be a marked change in operating conditions: it will no longer be possible for equilibrium to be established, and the number density of atomic ions will increase with time indefinitely (until the onset of other processes, not considered now, which limit the value of $n_a^+$). As a consequence of this big increase in the ion number density, the neutral gas inside the region occupied by the plasma becomes wholly ionised.

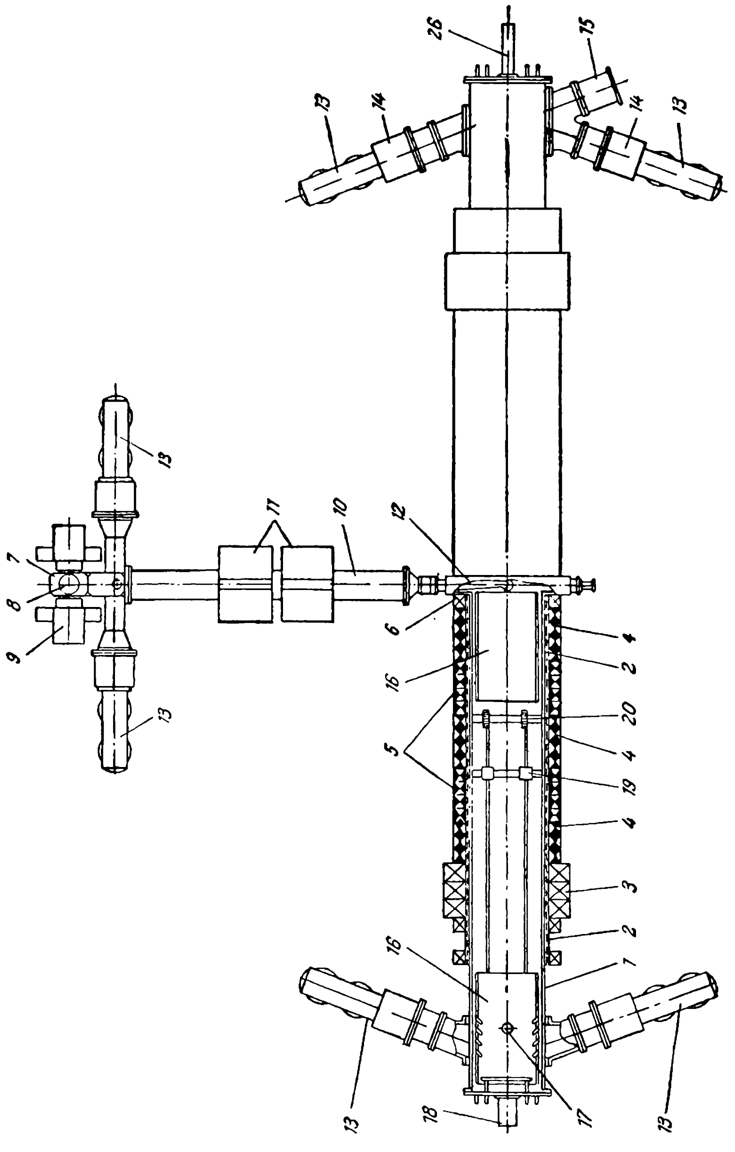

FIG. 127a

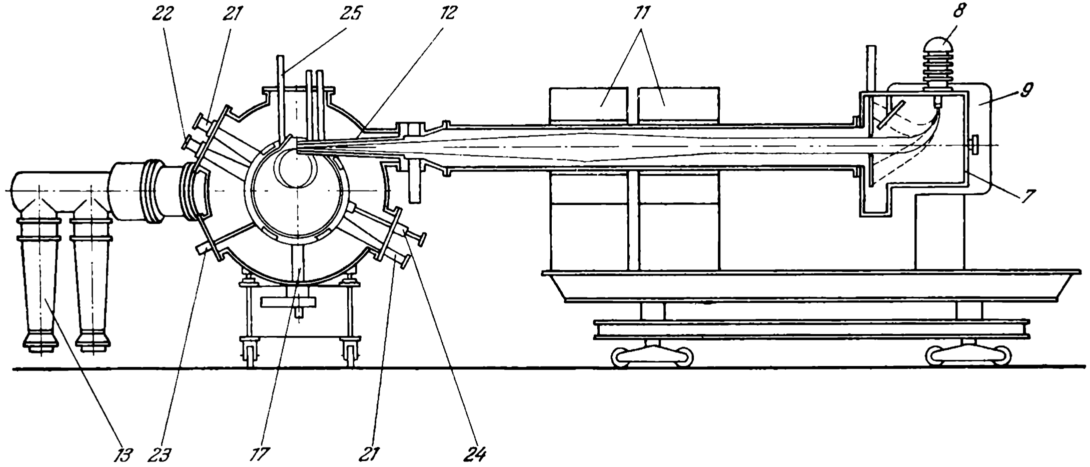

FIG. 127b

The Ogra apparatus: (a) in plan view; (b) cross-section of chamber and injector

*1*, vacuum chamber
*2*, heaters
*3*, mirror sections of the winding
*4*, main sections of winding
*5*, corrugated sections of winding
*6*, compensation section of winding
*7*, ion source chamber
*8*, ion source
*9*, ion source magnet
*10*, injector tube
*11*, magnetic quadrupole lenses
*12*, magnetic channel
*13*, mercury diffusion pumps
*14*, vacuum valves
*15*, access hatch to chamber
*16*, azotites (surfaces cooled by liquid nitrogen)
*17*, titanium evaporators
*18*, slow ion energy analyser
*19*, fast ion detectors
*20*, detectors of fast neutral atoms
*21*, microwave interferometer aerials
*22*, aerials for measuring thermal radiation of plasma
*23*, antenna for measuring ion cyclotron radiation
*24*, probe for measuring radial distribution of particle flux
*25*, beam monitor
*26*, chronotron (time-of-flight detector)

Let us suppose that the main source of neutral gas in the chamber is the neutralisation of molecular ions at the injector. In this case, to estimate the value of the critical current, we can use the condition

$$n_a^+ \sigma_d L \approx 1. \qquad \text{.........(8.30)}$$

When this condition is satisfied the dissociation of the molecular ions on the atomic ions accumulated in the chamber leads to a reduction of the beam reaching the injector, and this in turn leads to a corresponding fall in the density of the neutral gas and to a reduction of the charge-exchange losses. By combining equations (*8.30*) and (*8.28*) we obtain the following expression for the critical value of the injected flux $N_m^+$

$$N_m^+ \approx \frac{\sigma_c}{\sigma_d^2} \frac{\Omega v_i}{L^2}. \qquad \text{.........(8.31)}$$

To apply these formulae to Ogra, we take $\Omega = 10^7$ cm$^3$ and $L = 10^5$ cm; given further that the energy of the $H_2^+$ ions is 200 keV, the critical current obtained from (*8.31*) is about 100 mA. It must be borne in mind, however, that formula (*8.31*) represents only a very rough estimate because, in deriving it, no account was taken of a number of factors which influence the production and loss of fast ions.

The process of accumulating ions in Ogra type traps has been analysed in a number of papers by Golovin and his colleagues, and also by Simon of the Oak Ridge Laboratory. It emerges from these papers that the value of the critical (burn-out) current depends sensitively on the experimental conditions and can vary widely even for a given energy of the injected ions. Apparently, the only precise way of determining it is direct experiment.

Figure 127 shows schematically the design of the Ogra installation, and Plate XVII is a photograph of it. The vacuum chamber of Ogra is made of stainless steel. It has a length of 19 m and an internal diameter of 1·4 m. Batteries of vacuum pumps are connected to the ends of the chamber, and include both mercury diffusion pumps and ion getter pumps. Inside the chamber there are titanium evaporators. The average diameter of the magnetic field winding is 1·8 m. The winding consists of a large number of separate sections, so that magnetic fields of various configurations can be generated in the chamber. The maximum distance between the magnetic mirrors is 12 m. The field strength can be raised to 5000 Oe in the central part of the trap and to 8000 Oe in the mirror regions. An arc source with a transverse magnetic field, which was developed by Morozov and later improved by Semashko, is used to provide an intense beam of hydrogen molecular ions.† This source makes it possible to obtain molecular ions of 200 keV energy with a beam current of up to 300–400 mA. On leaving the source, the $H_2^+$ ion beam is bent through 90° in a sector

† So far all the main measurements on Ogra have been done with hydrogen, not deuterium.

magnet and is separated from $H^+$ and other unwanted ions. The ions then pass through a focusing-system consisting of two quadrupole magnetic lenses. The lenses change the diverging ion beam into a converging beam and direct it towards the entrance of the magnetic channel by which the ions are introduced into the trap. At the present time, about 50% of the total current of $H_2^+$ ions drawn from the source can be got into the trap. Thus the injected current can be up to 150 mA. The ions are introduced at an angle of about 70° to the direction of the magnetic field, and they can thus move only in that region of the trap where the field strength does not exceed that at the point of injection by more than 10–12%. The path length $L$ is a function of the geometry of the field in the chamber. Its maximum value, as measured experimentally, is about $1{\cdot}5 \times 10^5$ cm. When the ion beam is introduced, the vacuum in the chamber can be maintained at about $10^{-7}$ Torr.

The experimental research on Ogra has not yet passed the initial stage at which the main object of study is the behaviour of individual fast particles and of the directed beams which they form. In optimum conditions the number density of fast atomic ions is now $1\text{–}2 \times 10^7$. The number density of molecular ions is several times lower. In these conditions the Debye shielding distance for fast ions is comparable with the radius of the region within which the ions move. This means that the number density of fast particles is hardly sufficient for plasma formation, but is nevertheless sufficiently large for collective electrostatic interaction to have a big effect on the particle motion.

The behaviour of the assembly of fast particles formed in the chamber of Ogra depends on three main parameters: the strength of the injected ion current, the pressure of the neutral gas and the geometry of the magnetic field (this last governs the azimuthal drift speed of the particles and therefore has an influence on the value of $L$, and thus indirectly on the number density of molecular ions). The experimental results so far obtained do not give a sufficiently full picture of the effects of these parameters, and consequently some features of the ion accumulation process remain unclarified. One of the important results of the experimental research (though it is of qualitative, rather than quantitative, nature) is that the processes occurring in the chamber during the injection of ions are found to be non-stationary. The non-stationary character of these processes becomes more sharply pronounced as the pressure of the neutral gas is lowered and the injection current is increased. This non-stationary character is demonstrated by strong fluctuations of the signals from detectors recording the escape of fast particles from the volume. These fluctuations can have the character of irregular noise or can display well-marked periodicity. The frequencies of these oscillations cover a very wide range (from 2 to 100 kcs). The amplitude of the fluctuations depends not only on the magnitude of the injected current and the pressure of the residual gas, but also on the geometry of the magnetic field. In some modes of operation it approaches 100% of the mean value. It is obvious that a strong modulation of the flux of escaping charged particles is bound to be associated with marked fluctuations in the number density of the fast particles within the trap. It is also clear that, when there are non-stationary phenomena of this type, the mean lifetime of ions in the plasma will be shortened: that is to say, there will be additional particle losses. One of the main factors causing the occurrence of these non-stationary phenomena is, apparently, the space charge of the injected beam. At low pressure the compensation of this charge is made more imperfect because the accumulation of electrons in the volume is relatively slow.

Electrons can appear in the volume of the trap only through ionisation of the gas by fast ions. The corresponding ionisation cross-section of hydrogen in the energy region of interest is about $10^{-16}$ cm$^2$. Let us suppose that the pressure in the chamber is $10^{-7}$ Torr and the molecular ion path length is $10^5$ cm. Then, for every ten $H_2^+$ ions passing through the chamber only a single electron is formed. Therefore space charge neutralisation can occur only many ion transit times after the injector is switched on. In the actual case considered, neutralisation can be achieved some milliseconds after the start of injection. Therefore if the injected beam is very strong, there will be a time, before neutralisation occurs, during which electric fields can appear and deform the character of the drift movement and divert ions to the walls (they can also alter the path length $L$). Under these conditions various kinds of relaxation oscillation can easily occur, their periods being determined by the times necessary for sufficiently strong electric fields to arise. In particular, because of the azimuthal ion drift, any oscillations in density or in the angular divergence of the injected ion beam leads to the appearance of azimuthal electric fields which might easily drive plasma to the walls. We shall not dwell on the analysis of possible mechanisms by which oscillation processes might arise, because the available experimental material is inadequate and allows of many different interpretations; but we shall note that if we are to suppress oscillations and to achieve a quiescent accumulation of the ions, there must be an effective method of neutralising the ion space charge. What is necessary, apparently, is that even before the start of injection, the chamber should be filled with a dense cold plasma which will have to be formed by processes independent of the main method of accumulating fast ions.

Cold plasma formed by the ionisation of gas by fast ions has a very low number density at low pressures, and cannot therefore effectively damp the oscillations induced by fluctuations in the space charge of the injected ions. The best way to get rid of the difficulties due to the influence of the space charge will probably be to use other methods of accumulating fast particles: for instance, that based on injecting fast neutral atoms which are subsequently ionised inside the chamber.

With Ogra it was possible for the first time to observe ion cyclotron radiation. This radiation has a line spectrum, the lines being the harmonics of the fundamental ion Larmor frequency. The number density of particles in the chamber can be estimated from the intensity of this ion cyclotron radiation.

### *The DCX Experiment*

§ **8.14** An injection method based on dissociation of molecular ions is also used in the DCX installation at Oak Ridge. Fast molecular ions dissociate on passing through a plasma column which is formed inside the chamber by the action of a special type of arc discharge in an axial magnetic field. An arc discharge between two carbon electrodes was used in the first series of measurements, reported at the 1958 Geneva Conference. With discharge currents of 200 A an arc of this kind has a number density of about $10^{14}$ cm$^{-3}$ and is a very efficient dissociator; it has been studied in detail by Luce. The arc is struck when the initial pressure in the chamber is about $10^{-3}$ Torr and continues burning along the magnetic lines of force after a high vacuum has been established in the chamber. The central part of the arc plasma column is in the high vacuum region of the chamber; the electrodes of the arc are located outside the main chamber so that dust from electrode ablation does not get into the space where the high-temperature plasma is to be formed.

Molecular ions of 600 keV energy are injected into DCX. The direction of the ion beam on entry into the chamber is chosen so that the ion beam, after bending in the magnetic field through an angle close to 180°, passes through the arc column which is displaced off axis away from the injector snout (Fig. 128). The amount of displacement is chosen so that atomic ions formed by dissociation move in circular orbits centred on the symmetry axis. When injection is carried out in this way, the trajectories of fast atomic ions form a ring-shaped bundle in the centre of the trap. The ions will interact with the residual gas in the chamber and, as a consequence, ionisation of the gas will take place. In view of this there is ground for hope that, given a sufficiently large ion current, it will be possible to achieve total ionisation of the residual gas, that is to say a burn-out state analogous to that discussed in connection with Ogra. One can calculate that, if complete burn-out of the residual gas were achieved in DCX, a high-temperature plasma of significant density would be obtained some time after the start of injection. The plasma is formed by the gradual randomisation of the nearly coincident trajectories initially followed by the trapped ions. The first experiments carried out on the Oak Ridge installation showed that one could, by this method, accumulate atomic ions in a trap. If the current of $D_2^+$ ions admitted to the trap amounts to some tens of milliamps and the pressure is about $10^{-6}$ Torr, it is possible to accumulate up to $10^{12}$ deuterons in the system; these deuterons form a ring of trajectories with a total circulating ion current of several amperes. In these conditions the lifetime of the fast deuterons is about 0·01 sec.

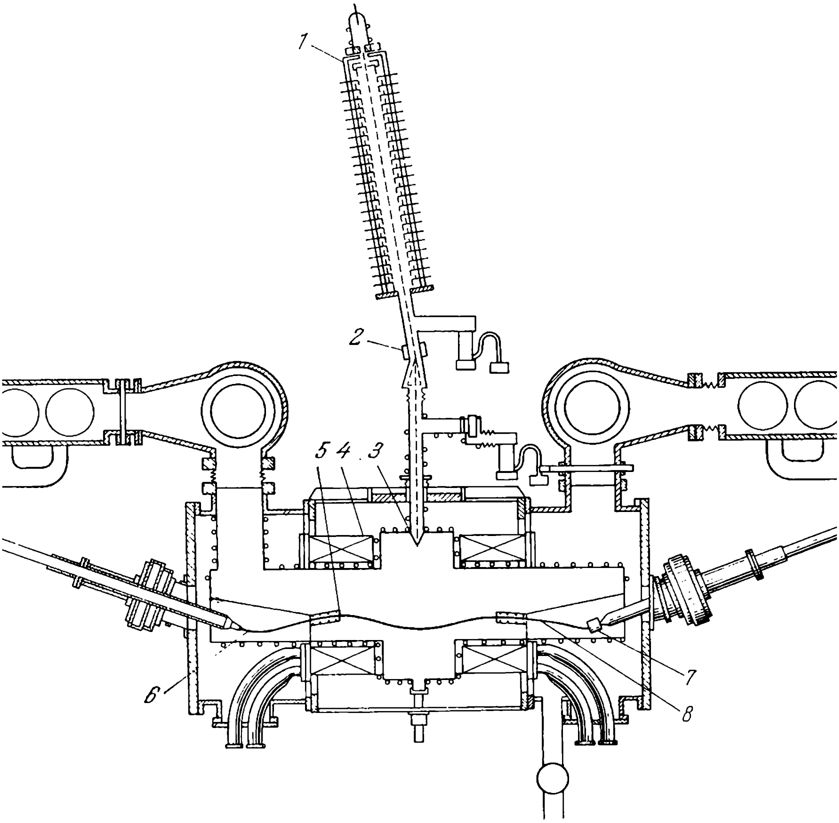

FIG. 128. The DCX apparatus

*1*, accelerator tube source of fast ions; *2*, deflection magnet; *3*, beam of ions entering chamber; *4*, coil; *5*, baffle; *6*, carbon arc cathode; *7*, carbon arc anode; *8*, arc

The next experiments, which were described in reports of the Oak Ridge Laboratory during 1958–9, provided interesting information on the behaviour of the atomic ions captured in the trap and of the plasma ring which they formed. In the first place it was discovered that the loss of fast ions from the trap was caused not only by charge-exchange on the background gas but also by charge-exchange on the incompletely ionised carbon atoms in the arc column. The attempts to eliminate this second loss mechanism by changing the geometry of the installation and the manner of operating the arc met with no success, not even a significant reduction of the effect. At present the only apparent way out of the difficulty is to change over from a carbon arc to a hydrogen arc. However, in order to make such a change worth while, efficient methods must be devised for pumping away the large quantity of hydrogen which enters the chamber from the hydrogen discharge.

Investigation of the form of the plasma ring made up of the $D^+$ ions has shown that when the strength of the magnetic field is high enough (10,000 Oe) the plasma fills a region in the chamber which has a hollow cylindrical shape. The outer diameter of this region is about 20 cm, and the inner diameter 10 cm. The plasma cylinder is centred on the symmetry axis, and is situated symmetrically about the central plane (the plane of injection of the molecular ions). The length of this plasma cylinder does not exceed 15 cm. The volume of the plasma in these conditions is approximately 3 litres. With an injection current of 5 mA and a field of 10 kOe, the number density of fast deuterons is $2 \times 10^9$ cm$^{-3}$, and their lifetime—determined entirely by charge-exchange processes—is about 4 msec.

The plasma in DCX should, apparently, have enhanced stability with respect to any deformations of its shape, because in this installation (particularly in the first phase of existence of the proton ring) none of the usual magnetohydrodynamic perturbations, for instance the flute instability, can occur. At this stage of the process we are essentially faced not with high-temperature plasma, but with an organised stream of monoenergetic fast ions. In each element of volume of the deuteron ring the speeds of all the ions are the same, and their directions are nearly so. The effective temperature of the ion constituent corresponds to that small proportion of the kinetic energy of the ions associated with the spread in velocity directions. In the experimental conditions being considered, this proportion probably amounts on average to less than 10% of the total energy of the ions. This, incidentally, is an indication of the low 'thermonuclear efficiency' of this method of injection.

### *Astron*

§ **8.15** A closed ring-shaped current-carrying conductor, which is freely levitated in space, generates an ideal magnetic trap for charged particles (see § 7.2). An original method for creating such a conductor—by using a beam of relativistic electrons—has been proposed by Christofilos and is being developed by him. The installation in which this idea is to find practical expression has been given the name of Astron. Only the basic principles of the Astron device will be presented here.

Suppose that a beam of relativistic electrons is injected at one end of a long straight solenoid with a uniform field in its central part and two magnetic mirrors at the ends; at the point of injection, the electron velocity is almost perpendicular to the magnetic field. Suppose also that the geometry of the injecting device and the ratio of the electron energy to the field strength are so chosen that the centre of the electron Larmor orbits lies on the axis of the magnetic system. In such a situation, the electrons will move inside the solenoid along a helical line passing symmetrically round the axis. If the strength of the field in the injection area is significantly increased during the time taken by an electron to pass along the solenoid and return to its starting point, then electrons are captured in the trap. As was said in § **8.8** it is possible, by slowly increasing the field strength in the injection area, to ensure that capture goes on for a period of time considerably longer than the time needed by an electron to get from one end of the trap to the other.

If the electron current injected into the trap is high enough, the magnetic field of this current will exceed the initial strength of the external field and therefore closed lines of force will appear inside the solenoid which enclose the cylindrical layer of electron trajectories. The magnetic field will then have a shape like that shown in Fig. 55. When the resulting magnetic field has this geometry it forms an ideal trap which can contain any particle that gets into it, provided the particle energy is not too great (it is, of course, assumed here that the space charge of the relativistic electrons is compensated by the ionisation of residual gas).

The conditions for creating a field of this type within the solenoid are easily derived. If we regard the length of the layer of relativistic electrons as large compared with its radius, the strength of the axial field generated by the rotation of the electrons is:

$$H_e = -\frac{4\pi}{c} j_e.$$

Here $j_e$ is the electron current per unit of length of the layer. The minus sign indicates that the direction of the field due to the electron layer is opposite to that generated by the external winding alone. The value of $j_e$ is $nec$, where $n$ is the number of electrons per unit area of the layer. Designating the number of electrons per unit length of trap by $N$, we can write

$$n = N/2\pi r,$$

where $r$ is the radius of the electron layer, which, for a small value of $N$, is the Larmor radius of the electrons in the initial field $H_0$, i.e. $r = pc/eH_0$ ($p$ is the momentum of the relativistic electrons). If closed lines of force are to appear, the field due to the electron layer must exceed $H_0$. From the above relationships, this occurs when the following inequality is fulfilled:

$$N > \frac{m_0 c^2}{2e^2} \Big/ [1 - v^2/c^2]^{\frac{1}{2}}. \qquad \text{.........}(8.32)$$

The electron speed $v$ is here taken as being close to $c$, which is certainly an adequate approximation at energies above 1 MeV.

When the field inside the layer changes sign, the motion of the relativistic electrons has a somewhat complicated character because their trajectories are squeezed between two regions where the directions of the vector $\boldsymbol{H}$ are opposite. In this case we are faced with the problem of how electrons behave in a self-consistent field; and this is itself determined by the character of the trajectories and the way the trajectories are distributed in space. This problem has been solved for the stationary case by Tonks.

The establishment of a stationary field geometry in Astron represents a physical process which is not very clear. As electrons are accumulated there is a continuing change in the magnetic flux inside the layer. Therefore, during the process of accumulation there is an azimuthal electric field formed by induction which slows down the electrons admitted to the trap. From equation (*8.32*) it follows that the number of electrons per centimetre length of layer must be about $10^{13}$ (if the electron energy is about a few MeV).

Besides generating a magnetic field of the required geometry, the relativistic electrons have two further important functions. First, they ionise neutral gas within the trap, to form a plasma; second, they heat up this plasma by means of Coulomb collisions. If the energy of the relativistic electrons is high enough, and if the energy losses from the heated plasma are not too great, one can, in principle, anticipate obtaining the temperatures needed for intense thermonuclear fusion.

Because there is no direct experimental data, it is at present extremely difficult to assess the prospects of using traps of the Astron type to obtain high-temperature plasma. One can merely note that there are very grave doubts as to whether such a system would be stable.

### *High-frequency confinement*

§ **8.16** The number of different methods that have been proposed to contain high-temperature plasma in a limited volume becomes very much greater if we include methods based on the use of high-frequency electromagnetic fields. The action of high-frequency fields on a plasma opens up a new range of possibilities of creating stable equilibrium plasma configurations, because the behaviour of a plasma in such fields differs markedly from its behaviour in a constant or quasi-stationary magnetic field. In the last resort, this difference arises from the difference between the motions of charged particles in constant and in rapidly alternating electromagnetic fields. The use of high-frequency fields to contain and thermally insulate a plasma can proceed along two main lines: the first is to devise new types of traps in which the plasma is contained on all sides by the pressure of a high-frequency field; the second line constitutes all those methods in which the main function of plasma containment is performed by a constant magnetic field, and the high-frequency fields play an auxiliary role by improving the thermal insulation and eliminating instabilities.

Even without detailed calculations it can be seen that, at the present state of technical development, it is apparently impossible to build a thermonuclear generator with a positive energy yield by the use of high-frequency fields alone. Because of the thinness of the skin layer in which the current generating the field is concentrated, much energy has to be expended on maintaining the field. Even if the plasma behaviour in a high-frequency trap is the most favourable possible, this expenditure of energy is so great that it cannot be compensated by the release of nuclear energy in the plasma. Given the same geometrical dimensions and mean field strength, the ratio of Joule losses in a high-frequency trap to Joule losses in a D.C. trap will be roughly equal to

$$\frac{d}{\delta} \approx d\sqrt{\frac{4\pi\sigma\omega}{c^2}},$$

where $d$ is the thickness of the current-carrying conductors which generate the constant field, and $\delta$ is the skin depth in the metallic wall of the equivalent high-frequency trap. Given $d \approx 10$ cm, $\sigma = 5\times 10^{17}$ e.s.u. and $\omega = 2\times 10^9$ cps ($\lambda \simeq 150$ cm), this ratio is about $4\times 10^4$. It should, however, be noted that in the most recent work on superconductivity, alloys have been found to exist in which the superconducting state can be maintained in very large magnetic fields (up to 70,000 Oe in an alloy of Nb and Ni). It would appear that the discovery of these properties opens up the possibility of considerably reducing the losses involved in producing powerful high-frequency fields. Nevertheless, the most interest is paid at present to those systems in which the high-frequency field is used only as an auxiliary means to correct those defects in the thermal insulation of the plasma that are characteristic, in one form or another, of magnetic traps with constant fields.

Before considering actual systems of the two types just described, we must describe in further detail the general characteristics of the action of a high-frequency field both on individual charged particles and on a plasma.

Let us start with the simplest case. Suppose that a particle of charge $q$ is in an electric field directed along the $x$ axis, whose strength is given by

$$E = E_0(x)\cos\omega t.$$

If the frequency $\omega$ is high enough, the particle will not have time to be displaced any significant distance during one high-frequency oscillation; the equation of motion of a particle then yields, to a first approximation,

$$\dot{x} = \frac{qE_0(x)}{m\omega}\sin\omega t + \dot{x}_0. \qquad \text{.........}(8.33)$$

The first term on the right-hand side of (*8.33*) describes the oscillatory motion due to the action of the alternating field, and the second term represents the mean velocity. The latter can be regarded as constant during one period of the oscillations. On averaging the value of $\dot{x}^2$ over the period of the high-frequency field, we find an expression for the mean value of the kinetic energy of a particle:

$$\overline{W} = \frac{m\dot{x}_0^2}{2} + \frac{q^2E_0^2(x)}{4m\omega^2}. \qquad \text{.........}(8.34)$$

We shall now explain what happens to the particle after a time considerably exceeding the period of the high-frequency field. For instance, let

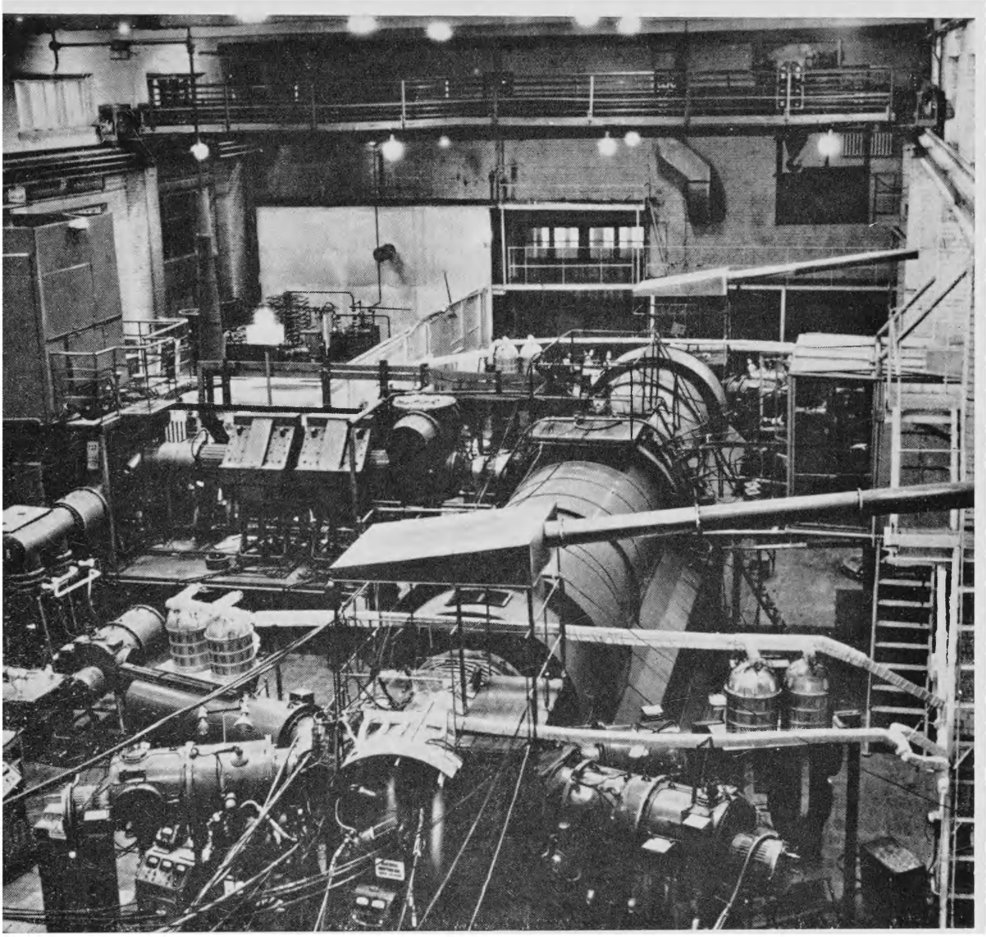

External view of Ogra.

PLATE XVIII

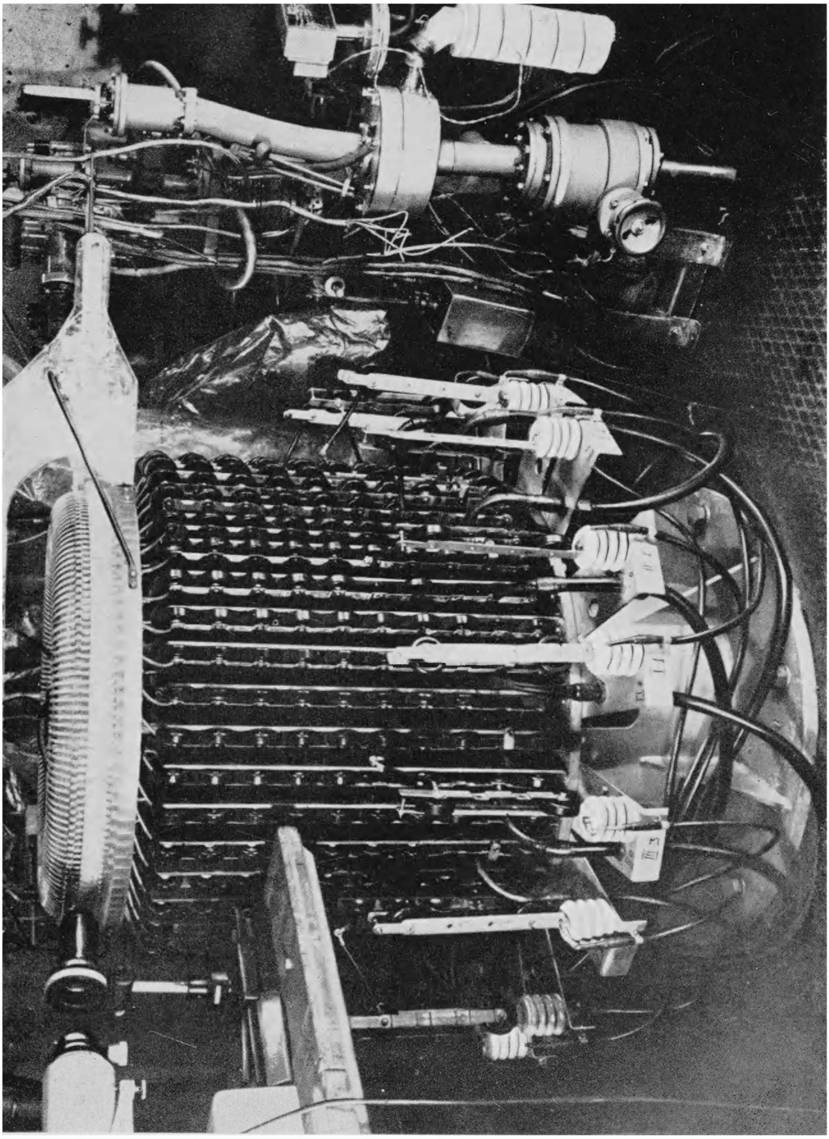

The experimental installation built to contain plasma by travelling wave fields.

a particle move from a point $x_0$ in the direction of increasing $E_0$. Then the kinetic energy of oscillatory motion increases during the time of motion. This increase will occur irrespective of the sign of the particle charge $q$. It cannot, therefore, be ascribed to a simple change of the electric potential (the mean value of this potential over a period is zero). Consequently a growth in the kinetic energy of the oscillatory motion can arise only at the expense of a corresponding decrease in the energy of directed motion. When a charged particle moves in a high-frequency field the sum of these energies can be regarded as constant.

Because the total mean energy $\overline{W}$ is constant, the second term in equation (*8.34*) affects the progressive motion of the particle in a way quite analogous to a potential field. The value of this potential is a function of $x$. In particular, if $E_0$ increases along the $x$-axis in both directions from some point, a potential well is formed which contains particles of either sign (the opposite of what happens in the case of a constant field). We can obtain an expression for the mean force acting on a charged particle due to the gradient of the alternating field strength. Differentiating (*8.34*) with respect to time, we find

$$m\ddot{x}_0 = -\frac{q^2}{2m\omega^2}E_0\frac{\partial E_0}{\partial x} = -\frac{q^2}{4m\omega^2}\operatorname{grad} E_0^2. \qquad \dots\dots\dots(8.35)$$

An expression for the mean force acting on a particle in a non-uniform high-frequency alternating electric field can be arrived at by another more obvious route. Suppose that a particle oscillates around a point $x_0$ in a field whose amplitude increases in the direction in which $x$ increases. In oscillatory motion, the oscillatory force is directed against the displacement. Therefore, when a particle is displaced to the right, the force acts to push it back and does so more strongly than when the displacement is to the left. Consequently, on the average, there is a net force directed towards decreasing $x$, whose magnitude is

$$F \approx -q\frac{\partial E_0}{\partial x}\delta x, \qquad \dots\dots\dots(8.36)$$

where $\delta x$ is the amplitude of oscillation, equal to $qE_0/m\omega^2$. Apart from the numerical coefficient, this expression agrees with equation (*8.35*).

This very simple example of motion of a charged particle in a high-frequency field is important only for illustration. Individual charged particles that do not interact with one another can be contained by the parallel gradient of a high-frequency electric field, but particles forming a plasma cannot be so contained. Considerably greater interest attaches to the motion of a particle in an alternating electric field whose amplitude is a function of distance in a direction perpendicular to the vector $\boldsymbol{E}$. Let us consider the motion of a particle in the field of a 'high-frequency plug'. Suppose that there is a constant uniform magnetic field $\boldsymbol{H}_0$ directed along the $z$ axis, and suppose that an alternating electric field is superimposed, this field being directed along the $x$-axis and varying according to the law

$$E_x = E_0(z) \cos \omega t.$$

An alternating magnetic field directed normal to the $x$-axis must be associated with such an electric field. We shall assume for simplicity that this alternating magnetic field is directed parallel to the $y$-axis.

From Maxwell's equations, we have

$$\frac{\partial E_x}{\partial z} = -\frac{1}{c}\frac{\partial H_y}{\partial t}. \qquad \ldots\ldots\ldots(8.37)$$

Thus the equations of particle motion are:

$$\ddot{x} = \frac{q}{m}E_x + \frac{q}{mc}(\dot{y}H_0 - \dot{z}H_y), \qquad \ldots\ldots\ldots(8.38)$$

$$\ddot{y} = -\frac{q}{mc}\dot{x}H_0, \qquad \ldots\ldots\ldots(8.39)$$

$$\ddot{z} = \frac{q}{mc}\dot{x}H_y. \qquad \ldots\ldots\ldots(8.40)$$

We note from these equations that if the gradient of $E_x$ is small enough, it has practically no effect on particle motion in the $xy$-plane, whereas it directly affects the motion along the $z$-axis (in a uniform electric field $H_y$ and $\ddot{z}$ are zero). Consequently, by discarding the quantity $\dot{z}H_y$ in equation (*8.38*) as a small term, we can solve the equations of motion to a first approximation for the $x$ and $y$ coordinates independently of the $z$ coordinate. Clearly, the quantities $x$ and $y$ must be periodic functions of time, with periods $\omega$ and $\omega_H = qH/mc$. The mean values of $x$ and $y$ and their derivatives, if taken over a sufficiently long time, must be zero.

With these approximations, equation (*8.39*) can be integrated to give:

$$\dot{y} = -\frac{q}{mc}xH_0.$$

Substituting this in equation (*8.38*) yields

$$\ddot{x} + \omega_H^2 x = \frac{q}{m}E_0(z) \cos \omega t.$$

In general, the solution of this equation is

$$x = \frac{q}{m}\frac{E_0 \cos \omega t}{\omega_H^2 - \omega^2} + \rho_H \cos(\omega_H t + \phi). \qquad \ldots\ldots\ldots(8.41)$$

We can now turn to equation (*8.40*) to elucidate the particle motion in the $z$ direction. Integrating (*8.37*) with respect to time

$$H_y = -\frac{c}{\omega}\frac{\partial E_0}{\partial z}\sin \omega t. \qquad \ldots\ldots\ldots(8.42)$$

From (*8.41*) and (*8.42*) it follows that

$$\ddot{z} = \frac{q^2}{m^2}\frac{E_0(\partial E_0/\partial z)}{\omega_H^2-\omega^2}\sin^2 \omega t + A \sin \omega t \sin(\omega_H t+\phi), \qquad \text{.........}(8.43)$$

where

$$A = \rho_H \frac{q}{m}\frac{\omega_H}{\omega}\frac{\partial E_0}{\partial z}.$$

The second term on the right-hand side of (*8.43*) describes oscillations with the combination frequencies $\omega_H+\omega$ and $\omega_H-\omega$; its mean value over a sufficiently long interval of time is zero. The first term corresponds to oscillations with a frequency of $2\omega$; in addition, it contains a constant component which defines the mean value of $\ddot{z}$. Multiplying it by the particle mass, we obtain the mean force acting on the particle along the $z$-direction:

$$\boldsymbol{F} = \frac{q^2}{4m}\frac{\text{grad } E_0^2}{(\omega_H^2-\omega^2)}. \qquad \text{.........}(8.44)$$

When $\omega \gg \omega_H$, equation (*8.44*) reduces to (*8.35*). However, this similarity does not mean that the factors responsible for the mean force $\boldsymbol{F}$ are the same in both the cases considered. In the case when the amplitude of the electric field changes in a direction normal to the vector $\boldsymbol{E}$, this force is simply the Lorentz force due to the associated magnetic field component $H_y$ whose magnitude is proportional to the gradient of $E$.

If $\omega_H > \omega$, the force changes sign and is directed towards the region of stronger electric field. As an illustration of the use of equation (*8.44*), consider the behaviour of a particle in the field of a plane standing wave. Let $E_0(z) = C \sin kz$, where $k = 2\pi/\lambda$. Such an electromagnetic field generates a periodic space potential, with the height of the potential barriers equal to

$$\frac{q^2C^2}{4m|\omega_H^2-\omega^2|}.$$

If $\omega_H > \omega$, the maxima of the potential barrier are at the nodes of the electric field; when $\omega > \omega_H$ they are at the antinodes of the field.

In the most general case, the vector $\boldsymbol{E}$ can be directed at an arbitrary angle to the constant field $\boldsymbol{H}_0$, and its gradient can also have an arbitrary direction. In these circumstances the particle motion averaged over many oscillations and Larmor periods is described by the following equation, the derivation of which we omit

$$m\dot{\boldsymbol{v}} = \frac{q}{c}\boldsymbol{v}\times\boldsymbol{H}_0 - \text{grad } \psi, \qquad \text{.........}(8.45)$$

where

$$\psi = \frac{q^2E_{\parallel}^2}{4m\omega^2} - \frac{q^2E_{\perp}^2}{4m(\omega_H^2-\omega^2)}. \qquad \text{.........}(8.46)$$

The quantities $E_{\parallel}$ and $E_{\perp}$ are the amplitudes of the components of $\boldsymbol{E}$ in directions parallel and perpendicular to $\boldsymbol{H}_0$. Equation (*8.45*) describes the mean trajectory of a particle; in other words, the trajectory of the guiding centre of the high-frequency rotation and oscillatory motion of the particle (see for comparison § **2.2**). From equations (*8.45*) and (*8.46*) it follows in particular that when grad $\psi$ has a component perpendicular to the static magnetic field $\boldsymbol{H}_0$, the particle drifts with a velocity

$$u = -\frac{c}{qH^2}\,[\mathrm{grad}\,\psi]\times \boldsymbol{H}. \qquad \text{.........}(8.47)$$

This result is interesting in that it suggests one possible method of compensating for toroidal drift in the simplest type of toroidal trap with a static longitudinal magnetic field. If, in such a trap, one generates a high-frequency field with an electric vector perpendicular to $\boldsymbol{H}_0$ and an amplitude which depends on the distance to the major axis of the torus (this type of oscillation is equivalent to $H_{01}$ waves in a straight cylindrical tube), then a drift motion occurs which is perpendicular to $\boldsymbol{H}_0$ and to grad $\psi$. This circular drift motion compensates the usual toroidal drift.

§ **8.17** The results of § **8.16** relate to the effect of high-frequency electromagnetic fields on individual charged particles. When we are faced with an assembly of particles having the characteristic properties of a plasma, the effect which these particles in turn have on the high-frequency field must be taken into account. A high-frequency alternating electromagnetic field at the boundary of a plasma is significantly distorted by currents due to particle movement. Therefore there is also a change in the force with which the field acts on the electrons and ions of the plasma. Interaction between the plasma and the high-frequency field requires special examination, and turns out to be far more complicated than the simple analysis of individual particle motion in given fields.

The equilibrium of a plasma confined by a high-frequency electromagnetic field has been the subject of a number of theoretical studies. Volkov established the equilibrium conditions for this case using a magnetohydrodynamic approximation. Sagdeev deduced the same conclusions after studying the kinetic equation and, furthermore, he analysed the structure of the boundary layer. Analysis of the interaction between a plasma and an external electromagnetic field shows that the condition for equilibrium at the plasma boundary is:

$$p_0 = \frac{1}{16\pi}(\tilde{E}_0^2+\tilde{H}_0^2), \qquad \text{........}(8.48)$$

where $p_0$ is the plasma pressure, and $\tilde{E}_0$ and $\tilde{H}_0$ are the amplitudes of the electric and magnetic field vectors (which we consider to be parallel to the plasma surface). Inside the plasma the alternating electromagnetic field is absent. The derivation of equation (*8.48*) in the magnetohydrodynamic approximation does not differ essentially from the derivation of the expression used in electrodynamics for the pressure of light. It is based on the fact that the mean force exerted on a unit volume of plasma by the electromagnetic field is $\boldsymbol{j}\times\boldsymbol{H}/c$, in conjunction with the mechanism of interaction between an electromagnetic wave and individual charged particles considered in § **8.16**. Incidentally, it should be noted in this connection that equilibrium is impossible in an alternating electric field when the vector $\boldsymbol{E}$ is directed normal to the plasma boundary.

The equilibrium condition (*8.48*) can be generalised by assuming that in addition to the alternating electromagnetic field, the plasma is also acted upon by a static magnetic field. In this case the plasma pressure is balanced by the sum of the pressures of the high-frequency field and the static field.

An intermediate boundary layer separates the region occupied by the high-frequency field from that occupied by plasma. In this layer, the number density of charged particles decreases along the normal to the plasma surface from $n_0$ to 0, and the amplitude of the electromagnetic field increases from zero to a maximum value corresponding to fulfilment of the equilibrium condition (*8.48*). The thickness of the intermediate layer is roughly equal to the skin-depth for the given frequency of the field. Sagdeev discovered that although the plasma as a whole is contained by the high-frequency field when condition (*8.48*) is satisfied, particles with energy considerably in excess of the mean thermal energy $\frac{3}{2}kT$ nevertheless escape from plasma through the boundary layer. The maximum energy of the particles contained by a high-frequency field is given approximately by the condition

$$\frac{W_{\max}}{kT} \approx \frac{\omega_0^2}{\omega^2}, \qquad \text{.........}(8.49)$$

where $\omega_0$ is the Langmuir frequency of the electron plasma oscillations (for ions a different value of $\omega_0$ would have to be used, but it is easy to understand that it is the electrons which will decide the loss rate). If $\omega \ll \omega_0$, only a negligible fraction of the particles, which will be proportional to $\exp(-\omega_0^2/\omega^2)$, will be able to trickle across the high-frequency barrier at the boundary of the plasma.

If, besides the high-frequency field, there is also a static magnetic field perpendicular to the plasma boundary, the expression for $W_{\max}$ is altered. In particular, when the high-frequency field can be regarded as a circularly polarised electromagnetic wave impinging on the plasma in the direction of the static field $\boldsymbol{H}_0$, the expression becomes

$$\frac{W_{\max}}{kT} \approx \frac{\omega_0^2}{\omega\omega_H}. \qquad \text{.........}(8.50)$$

It is not difficult to ensure, in this case, that the fraction of particles escaping across the barrier is acceptably small.

§ **8.18** At the present time, a number of specific methods are being developed to contain a high-temperature plasma in high-frequency fields. In one of these methods, which was first proposed by Thonemann, the plasma is enclosed in a toroidal chamber and is subjected to the action of an electromagnetic wave travelling along the surface of the plasma. This idea was further developed in the work of Osovets. The system which generates the field can consist of a number of conductors situated on the external surface of a dielectric chamber and supplied by high-frequency current with the appropriate phase shift. A diagram showing the principles of such a device is given in Fig. 129. The field strength at the boundary of the plasma alternates with frequency $\omega$, and during one period it passes through zero twice at every point.

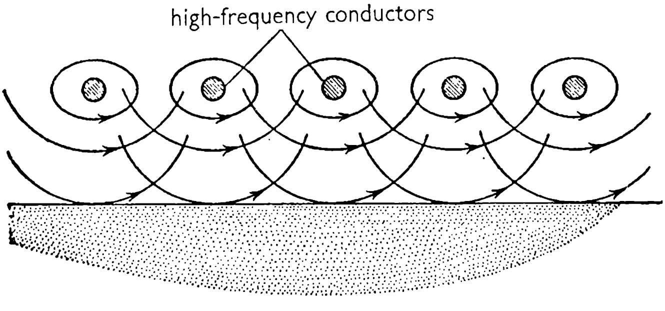

FIG. 129. Plasma in the field of a travelling wave

When the field is close to zero in some particular section, the plasma boundary is displaced outwards, the boundary moving at the ion thermal speed $v_i$. After a quarter period, the plasma boundary accelerates inwards under the action of a strong field. The travelling wave thus produces a moving ripple on the surface of the plasma, and at the same time ensures the constant mean pressure necessary to balance the plasma pressure. There will be efficient containment if the amplitude of the boundary oscillations is not too great, in particular the plasma must not come into contact with the insulating wall. It can be shown that the boundary displacements will be within acceptable limits if the condition $v_i < a\omega/2\pi$ is satisfied, where $a$ is the distance between two adjacent conductors generating the field. This relationship determines a lower limit for the frequency of the field. For plasma at a temperature of some tens of kilo-electron-volts, the minimum permissible frequency comes out to be about 10–20 Mc/s. There is one fairly obvious objection to this method in its simplest form. A wave travelling round a toroidal chamber is bound to exert a drag on the plasma; that is to say, it is bound to rotate the plasma at gradually increasing speed. After a time, the speed of the plasma becomes comparable with the speed of the travelling electromagnetic wave. The mechanism of high-frequency containment then ceases to operate, because the field becomes static relative to the moving plasma, and at those areas of the surface where the field is zero or small the plasma can expand without hindrance. This difficulty can be avoided by changing from a simple system with one travelling wave to a somewhat more complicated version which provides for the simultaneous action of two waves travelling in opposite directions. Plate XVIII shows one of the experimental installations built to study this method of high-frequency plasma containment. The major diameter of the toroidal quartz tube is 80 cm; and minor diameter is 7 cm. The total pulsed power of the high-frequency generators feeding the installation is 10–15 megawatts (at a wave length of 120 m).

Another system of high-frequency plasma containment, proposed by Trubnikov, is based on the principle that the plasma blob could be contained by the action of alternating magnetic fields rotating around three mutually perpendicular axes. Similar systems have been studied by Butler and others, whose results were reported at the Second Geneva Conference in 1958. A fundamental defect common to all such methods is that, in order to contain plasmas, they require high-frequency generating equipment of very high power.

Amongst the various combinations of static and high-frequency fields which can be used to confine plasma, the simplest is a static uniform magnetic field plugged at the ends with high-frequency alternating fields. This approach was proposed by Glagolev. A static axial magnetic field serves to prevent a long cylindrical column of plasma from expanding radially, and the high-frequency plugs confine the plasma in the axial direction. Such a system can be built by using 'resonant cavities' in which electromagnetic fields of adequate amplitude are excited (Fig. 130). If the plasma is to be contained, it is essential that the alternating electromagnetic field should not penetrate into it, and that the amplitudes of $\boldsymbol{E}$ and $\boldsymbol{H}$ should satisfy condition (*8.48*). Thus, the high-frequency field at the ends must withstand the full force of the plasma pressure. This feature cannot, of course, be regarded as a virtue of the method. Calculation shows that even with very long systems where the high-frequency field is responsible for the thermal insulation of only a relatively small part of the total plasma surface, there is no hope of achieving results of any practical importance. Nevertheless, like other methods of high-frequency containment, this method presents considerable interest for experimental studies of the properties of a fully-ionised plasma with a comparatively high electron temperature. The first crude experiments carried out with high-frequency plugs have shown that if the alternating electromagnetic fields are large enough, they can indeed repel plasma.

As mentioned in § **8.16**, a high-frequency field can in principle be used to establish an equilibrium plasma configuration in a toroidal chamber with a static longitudinal field. In this case, the pressure of the high-frequency field needed to contain the plasma is only a small part of the total plasma pressure which is mostly, though not entirely, balanced by the static magnetic field. For this purpose Glagolev proposed using a system of 'resonant cavities' situated along the surface of the toroidal chamber. We shall not consider this proposal in more detail because it does not at present appear to be especially promising.

In cases when a static magnetic field is sufficient to contain the plasma in equilibrium, a high-frequency electromagnetic field can in principle be useful to stabilise various modes of instability. Some particular problems involving the suppression of plasma instabilities by a high-frequency field have been analysed by Osovets, Glagolev and others. Osovets has studied the stability of a current-carrying plasma ring in an external magnetic field parallel to the major axis of the ring (Fig. 131). It can be proved that the stability requirements with respect to deformation of the ring parallel and perpendicular to the external field, impose contradictory demands on the geometric form of this field (i.e. on its radial distribution). If, however, this field distribution alternates sufficiently rapidly between the form which provides vertical stability of the ring (unbroken lines in Fig. 131) and that which provides horizontal stability (broken lines in the

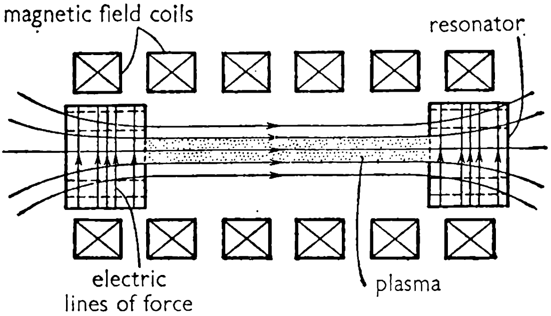

FIG. 130. Magnetic trap with high-frequency plugs

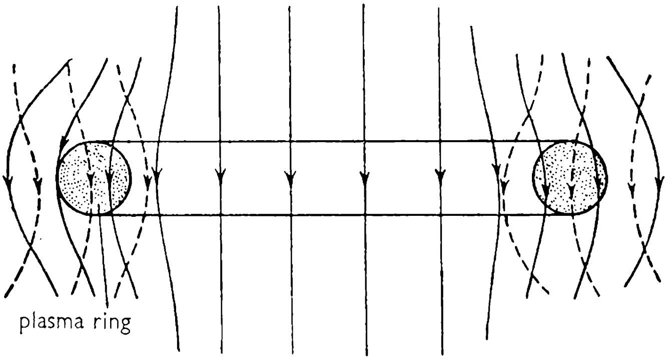

FIG. 131. The stabilisation of a plasma ring by using a high-frequency magnetic field

same figure), it is possible to ensure stability against both modes simultaneously. This method of stabilising plasma perturbations is to some extent analogous to the 'strong focusing' now used in the technology of accelerators. Calculation shows that to stabilise the perturbations of a plasma ring with longitudinal wave-length $\lambda$, the following conditions must be satisfied:

$$\omega > \frac{4\pi}{\lambda} v_i \sqrt{\ln \frac{\lambda}{\pi r_0}};$$

$$\frac{\partial \tilde{H}_0}{\partial r} > \frac{2J}{c}\left(\frac{2\pi}{\lambda}\right)^2 \ln (\lambda/\pi r_0),$$

where $r_0$ is the minor radius of the plasma ring and $J$ is the ring current. Further analysis based on these relationships shows that, by using high-frequency fields of no great amplitude ($\tilde{H}^2 \ll 8\pi p_0$), the long-wave deformations of the plasma can be effectively stabilised ('long-wave' deformations meaning those with a wave length $\lambda \gg 2\pi r_0$). Volkov has also shown that some of the most dangerous instabilities characteristic of a current-carrying plasma column can be suppressed by a rotating high-frequency field.

Glagolev has examined the suppression of magnetohydrodynamic plasma instabilities by using high-frequency fields in the decimetre range, the fields being generated by resonant cavities placed close to the surface of a plasma in equilibrium with a static field. He concluded that by the use of this technique, flute-type deformations due to non-uniformity of the main magnetic field can be effectively stabilised.

The experimental study of the use of high-frequency fields both to confine plasma and to suppress instabilities is still at the most elementary stage. At present there is nothing definite to be said about the results of such experiments. Probably they will acquire real significance only after several years. The use of strong high-frequency fields introduces an additional complication into the experimental techniques, and particularly into the interpretation of the observations—a matter which in any case is at present distinguished neither by unambiguity nor by simplicity.

### *Traps with Cusp-shaped Fields*

§ **8.19** Amongst traps based on the mirror reflection of particles from high-field regions, magnetic systems with cusp field geometry must be regarded as being in a special category. A typical example of a field of this form is shown in Fig. 132. The important characteristic of such field-geometries is that the magnetic field strength increases in all directions from a point at which the field strength is zero. To get a grasp of the geometry of these fields, we shall consider a field with axial symmetry, a case which is both the simplest and also of the greatest practical interest. Suppose that the field strength is zero on the symmetry axis at a point $A$

which we shall choose as the origin of our coordinate system. The field strength on the axis close to $A$ can be represented by the series

$$H_z = a_1 z + a_2 z^2 + \dots \qquad \dots\dots\dots(8.51)$$

At points not too far from the axis, both components of the field, $H_z$ and $H_r$, are defined by (*7.4*) and (*7.5*). Let us assume that the coefficient $a_1$ is not zero; then the field structure close to $A$ is given by:

$$H_z = a_1 z, \qquad H_r = -\frac{a_1}{2} r. \qquad \dots\dots\dots(8.52)$$

The shape of the lines of force is derived from the differential equation $\frac{dr}{dz} = \frac{H_r}{H_z}$. Substituting $H_r$ and $H_z$ from equation (*8.52*) into this equation, we can easily establish that in the region close to the point $A$ a line of force is defined by the equation

$$r^2 z = C^2, \qquad \dots\dots\dots(8.53)$$

where $C$ is a constant. In particular, if all but the first of the coefficients of the series (*8.51*) are zero, (*8.53*) defines the lines of force over the entire space. In practice, equations (*8.52*) and (*8.53*) describe the field only in a limited region, and the behaviour of $H_r$ and $H_z$ at large distances from $A$ depends on the dimensions, location and form of the coils or magnets generating the field.

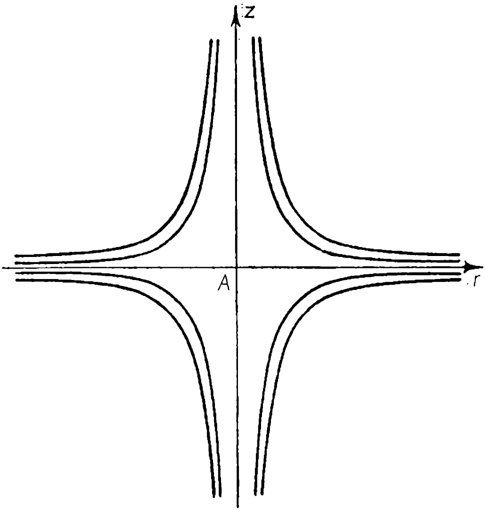

FIG. 132

Cusp-type magnetic field configuration

The simplest method of obtaining a field of the above type is to mount two identical coils (for instance, simply two single loops) parallel and coaxial to each other, and to pass currents through them in opposite directions so that the coils generate fields of opposite sign.

One could also have a case where, at a point on the $z$ axis, not only $H_z$ but a number of its derivatives are zero. This will occur if the coefficients

$a_1$, $a_2$ and so on are zero. In particular if $a_1 = 0$ but $a_2 \neq 0$, then $H_r$ and $H_z$ are given, close to the field zero, by

$$H_z = a_2(z^2 - r^2/2), \qquad H_r = -a_2 zr. \qquad \text{.........}(8.54)$$

With a suitable choice of the geometrical parameters of the magnetic system, it is possible to reduce even higher order terms to zero in (*8.51*), and thus to generate fields which weaken even more rapidly as one approaches the point $A$. However, we shall confine ourselves mainly to studying the properties of the very simple system in which the field near the point $A$ changes linearly.

The motion of particles in a magnetic field of this type has one important feature: if the trajectory of a particle passes close to the point $A$, the quantity $W_\perp/H$ can undergo marked change because in the weak field region the condition for adiabatic invariance is not fulfilled. This means that $W_\perp$ will not be so rigidly connected to $H$ as is the case in ordinary magnetic mirror traps where the ratio of the maximum to the minimum magnetic field is comparatively close to unity. Because of this, if a particle has a trajectory which passes through a region where the field is very small, the angle between the particle velocity and the line of force undergoes so large a change that even if the particle were trapped to start with, it would escape from the trap after a few oscillations. These qualitative ideas are confirmed by precise calculations, which show that a particle passing near to the point $A$ can 'forget' about the adiabatic invariant which initially governed its motion. For a particle of velocity $v$, the linear dimensions of the region 'where the past is forgotten' are roughly defined by

$$r_0 = (mvc/ea_1)^{\frac{1}{2}}, \qquad \text{.........}(8.55)$$

where $a_1$ is the coefficient of the first term in the expansion for $H_z$ in (*8.51*).

Breakdown of adiabatic invariance becomes still more obvious when we consider a trap filled with plasma. Even a very rarefied plasma with a low-pressure $p$ will reduce the magnetic field in the immediate vicinity of the point $A$ to zero; and as $p$ increases, the region from which the field is wholly excluded will also increase. A particle moving within the limits of such a region completely 'forgets about its previous history', and it acquires a new $W_\perp/H$ value every time it emerges into a strong field region. Consequently there is a rapid loss of particles from the trap without there being any collisions between the particles. We shall try to estimate the corresponding loss rate. Such an estimate is easy only when the field is assumed to be entirely excluded from the plasma. This simplified case is the one considered in the following paragraphs.

Let us assume that initially the field in the region of interest to us has the simple form described by equations (*8.52*). The value of the magnetic pressure in this case is proportional to $z^2 + r^2/4$. Now suppose plasma is put into the trap and that the field is wholly excluded from the neighbourhood of the initial field zero. Figure 133 shows the approximate form of the region occupied by the plasma. It may be noted, incidentally, that when a trap like this is filled, the plasma will spread further in the radial direction than in the axial direction (because the magnetic pressure increases more slowly with $r$ than with $z$). When the boundary surface has the form shown in Fig. 133, a particle can escape from the region occupied by the plasma only if it approaches the plasma boundary within a very short distance of the equatorial plane of symmetry of the trap.

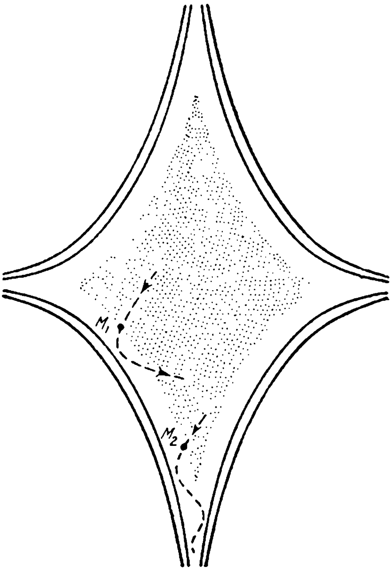

FIG. 133

Plasma blob in cusp magnetic fields

Figure 133 shows schematically the projection of the trajectories of two particles impinging onto the boundary surface between the plasma and the magnetic field. A particle impinging onto this surface at point $M_1$ penetrates a certain distance into the region of the external magnetic field and is then reflected back into the plasma. Therefore, this particle will not escape. On the other hand, a particle falling onto the surface at point $M_2$, close to the ring-shaped edge of the surface (the ring-cusp), can get round the edge and escape along the lines of force. The subsequent fate of such a particle will depend both on the angle $\alpha_0$ between its velocity and the lines of force near the surface and also on the ratio $H_0/H_m$, where $H_0$ is the field strength close to the plasma boundary and $H_m$ is the maximum field strength in the equatorial plane. If $\sin^2 \alpha_0 < H_0/H_m$, the particle will escape. In the opposite case, it will penetrate the magnetic field to some depth and then be reflected by the stronger field and return to the plasma.

A very rough estimate of the leak rate can be made by assuming $H_0 \approx H_m$, and that half the particles falling on that part of the boundary surface within a Larmor diameter of the ring cusp, are lost.† The area of surface from which particle leakage will take place is thus $2 \times 2\pi R \times 2\rho_H$, where $R$ is the radius of the ring cusp and $\rho_H$ is the Larmor radius. Taking the flux of particles falling on the surface to be $nv/4$, we find that the total leak rate will be $2nv_e\rho_{He}\pi R$ for electrons and $2nv_i\rho_{Hi}\pi R$ for ions. If $T_e$ and $T_i$ are equal, the loss rate will be the same for both ions and electrons.

---

† The particles lost will be those whose velocities are inclined at less than 90° to $H$.

However, a simple estimate like this gives far too high a value for the leak rate. The figure is too high, first because we took no account of the influence of the electric fields in the boundary layer, and second because we regarded the thickness of this layer as small compared with the Larmor radii of ions and electrons. The incorrectness of these assumptions is plain because they imply that the ions crossing the plasma surface penetrate far deeper into the external field than the electrons do. It follows that we must take account of the structure of the boundary layer. This structure has been analysed in Chapter IV; this analysis reveals that the thickness of the layer is roughly equal to the mean electron Larmor radius, and that a strong electric field is concentrated within the layer, giving total potential difference of $\approx kT/e$ which slows down ions approaching from within the plasma. When account is taken of this result, a simple kinematic calculation enables us to show that $\delta$ (the mean distance that they are displaced along the lines of force while in the boundary layer) is approximately the same for particles of either sign, and is roughly equal to double the thickness of the layer, i.e. to twice the electron Larmor radius. Consequently, the breadth of the region from which leakage of ions and electrons can occur is approximately equal to $2\rho_{He}$. Thus the leak rate for the ions is reduced by about $\rho_{He}/\rho_{Hi}$ compared with the original estimate, and is now estimated to be

$$-\frac{dN_i}{dt} = \gamma\frac{2\pi RN_iv_i\rho_{He}}{\Omega}, \qquad \text{.........}(8.56)$$

where $\gamma$ is a numerical coefficient of about unity, $\Omega$ is the volume occupied by the plasma and $N_i = n_i\Omega$.

This reduction of the estimated leak rate leads to a corresponding reduction in the electron loss. The mean lifetime of particles in the plasma is given by

$$\tau = \frac{1}{2\pi\gamma}\frac{\Omega}{Rv_i\rho_{He}}. \qquad \text{.........}(8.57)$$

This expression can be given in the following form which is more convenient for calculations†:

$$\tau = \frac{4\times10^{-4}H\Omega}{\gamma TR}. \qquad \text{.........}(8.57a)$$

Here $m_i/m_e$ is taken as equal to 3600. Since it is possible that particles escaping from the plasma will return to it again after being reflected by the strong field we must, when calculating $\tau$, take $H$ as the maximum field strength in the equatorial plane.

By a more profound and rigorous analysis of the behaviour of plasma in cusp-shaped magnetic fields, Firsov obtained a formula for $\tau$ quite similar to (*8.57a*) with the coefficient $\gamma$ equal to unity. Furthermore he tried to determine how the loss of particles is influenced by the gradual thickening of the boundary layer due to collisional diffusion of plasma across the magnetic field. According to Firsov's calculations the thickness of the boundary layer of the plasma will grow with time $t$ as $\sqrt{(1+\pi t/8\tau_{ei})}$, and therefore this quantity should also appear as a factor in the expression for the leak rate. However, it appears that this estimate of the thickness of the boundary layer is correct only when the linear dimensions of the region occupied by the plasma is many times greater than the ion mean-free-path; such cases are of comparatively little interest. Essentially, diffusion broadening of the boundary layer occurs mainly as a result of collisions between ions and electrons which trap these particles within the boundary layer. As a consequence of such collisions, however, these particles leave the trap comparatively rapidly along the lines of force; as a result the broadening of the boundary layer is considerably reduced. Nevertheless, the effect of diffusion broadening does not wholly disappear. Seemingly it can shorten the confinement time of the particle by roughly an order of magnitude compared to the value given by equation (*8.57*). It is apparent from this formula that, in ordinary experimental conditions, the confinement time is very short and, for a given field strength, decreases as the temperature increases.

---

† $\tau$ changes as particles escape from the trap, because particle loss involves a reduction of $\Omega$. Therefore formula (*8.57a*) is useful only for very rough estimates.

It thus turns out that the ring-cusp represents a leak through which particles escape, and that this is a very serious shortcoming of cusp geometry traps. Turning to the prospects of using this type of trap for generating intense thermonuclear reactions, we may recall that the energy efficiency of any thermonuclear device is proportional to $H^2\tau$. For these traps, we thus have

$$H^2\tau = \frac{4\times 10^{-4}H^3\Omega}{\gamma TR}. \qquad \ldots\ldots\ldots(8.58)$$

A thermonuclear generator working with a 50% mixture of deuterium and tritium will produce surplus energy provided $H^2\tau$ exceeds $10^8$ and the temperature of the mixture is $1{\cdot}5\times 10^8$ °K. If the reaction volume is assumed to be several litres and therefore $\Omega/R \simeq 10^2$, the field strength must exceed about $7\times 10^5$ Oe (when $\gamma = 1$) to achieve the minimum required value of $H^2\tau$. However, in this estimate, the effect of diffusion broadening of the equatorial leak has been neglected. If the requisite correction is made, the minimum value of $H$ for a positive energy yield is found to be $1\text{–}2\times 10^6$ Oe. Such field strengths in volumes measured in litres are beyond the present limits of technical feasibility. However, some small easement is provided by the fact that, in the general case, formula (*8.58*) should involve not $H^3$ but the product $H_0^2H_m$.

Everything that has been said here about leakage of particles relates only to the optimum case when there is no plasma outside the region where adiabatic invariance breaks down. If a considerable part of the plasma and field are mixed ($0 < \beta < 1$), the determination of the particle leak rate becomes a very difficult problem which still awaits solution. It can only be assumed that, because of the breakdown of adiabatic motion in the central zone, the lifetime of particles in a cusp magnetic field trap will be comparatively short in this general case as well. The following considerations can be advanced to support this assertion. If the plasma density decreases monotonically between the zero-field region and the high-field region, the lifetime of particles moving close to the point $A$ will be very short because, on the one hand, the adiabatic invariant is not maintained for them and, on the other, the 'leak' through which they can get out is very broad in this case. Therefore ions and electrons which are initially in the neighbourhood of the field zero will rapidly leave the trap. Let us suppose for a moment that all the particles leave this neighbourhood and a void is formed at the centre of the plasma blob. The plasma then acquires an internal boundary which is theoretically unstable because of the shape of the lines of force forming it. Therefore the plasma will spread inwards and the region of zero field will once again be filled. In this way, the leakage of particles through the equatorial leak will be continuously maintained by a flow of ions and electrons from the peripheral regions of the plasma towards the centre.

By way of counterbalancing the above defect, traps with cusp-shaped fields have an important advantage when compared with ordinary magnetic mirror systems. This advantage is that, because of the inward curvature of the lines of force, the plasma filling a cusp-shaped magnetic trap is magnetohydrodynamically stable. If this theoretically predicted virtue is confirmed by experiment, the type of magnetic trap described in this section will be very important in the future development of devices for containing hot plasma.

§ **8.20** In cusp systems, the most natural method of obtaining high-temperature plasma is to inject into the trap a plasma blob which is then compressed by a rising field. Concerning penetration of plasma into the trap and the formation of the captured plasma blob, one can at present express only the following rather general considerations.

A plasma jet injected along the axis of a magnetic system penetrates into the trap through a mirror region where the lines of force are most tightly bunched. Let us suppose that a plasma with high conductivity is formed in a region where the axial component of the magnetic field is small. In such a case, the plasma jet pushes aside the lines of force on entering the trap and in the process expends part of its directed kinetic energy. It is therefore natural to ask if the plasma jet can be reflected from the strong field region when the directed velocity is small. So far, neither theory nor experiment provides a satisfactory general answer to this question, largely because we have no very well defined picture of the phenomena that occur when plasma is forced into a magnetic field.

In ordinary experimental conditions the time taken by an element of plasma to pass through the high-field region is so small that we are faced with a typical 'rapid' process. Therefore the magnetic pressure exerted on the surface of the plasma will be balanced by the inertial forces (in other words, when the plasma enters the strong field a shock wave process will occur). In a coordinate system moving with the plasma, the penetration of the plasma jet into the high field is analogous to the process of compression leading to the formation of the $\theta$-pinch described in Chapter V.† Rough calculations based on this analogy yield an impression of the factors effecting the deceleration of plasma in the strong field region. We report here only some qualitative results, noting in advance that their persuasiveness is not very great since all the calculations are based on the special case of the deceleration of a small, infinitely-conducting plasma blob.

The behaviour of plasma entering a strong field depends in the first place on the ratio

$$\frac{H_{\mathrm{m}}^2}{8\pi}\Bigg/\frac{\rho_0 v_0^2}{2},$$

where $H_{\mathrm{m}}$ is the maximum strength of the magnetic field and $\rho_0 v_0^2/2$ is the kinetic energy per unit volume of the directed motion of the plasma before entry into the field. If this ratio is less than unity, the plasma jet passes freely through the high-field region, and is compressed in the regions where the lines of force are most tightly bunched. Of greater interest and practical importance is the case when this ratio is considerably more than unity. In this case the deceleration of the plasma depends markedly on the precise geometry of the magnetic field. The decisive geometrical parameter is the ratio of the initial radius $a_0$ of the plasma blob to the distance $L$ defining the length of the region of increasing magnetic field (the region of large grad $H$).

If $a_0/L$ is small enough, i.e. if the field increases very smoothly, the injected plasma undergoes strong radial contraction before it has time to lose any significant proportion of its directed energy in doing work against the magnetic pressure. Therefore, when $a_0/L \ll 1$, the plasma blob can pass through a high-field region even if $H_{\mathrm{m}}^2/8\pi$ is many times greater than $\rho_0 v_0^2/2$. A somewhat more precise formulation of the condition for this 'deep penetration' by a plasma blob is:

$$\frac{a_0}{L}\left(\frac{H_{\mathrm{m}}^2}{4\pi\rho_0 v_0^2}\right)^{\frac{1}{2}} \ll 1.$$

Other conditions are imposed when $a_0/L$ is not small, i.e. when the field changes very suddenly. In these circumstances the plasma blob is slowed down before its radial dimensions have had time to undergo any significant change. The extent to which plasma can be forced into a steep field gradient is determined by the condition $\frac{H_m^2}{8\pi} \simeq \frac{\rho_0 v_0^2}{2}$ and therefore when

---

† It follows that, in certain conditions, signs of instability should be observed during the penetration of plasma into a strong field.

$$\frac{H_m^2}{8\pi} \gg \frac{\rho_0 v_0^2}{2} \text{ and } \frac{a_0}{L} \approx 1$$

the plasma jet will be reflected. During penetration of plasma into a field with a very steep gradient, stratification of the plasma jet can, apparently, occur. If the lines of force at some small distance away from the axis are bent sharply to the side, the peripheral parts of the plasma jet can be reflected from the field (given that the directed energy is insufficiently large), but a thin inner thread of the jet can penetrate the field. We shall later meet an example of this phenomenon in discussing the experimental results.

It should be borne in mind that these results are valid only for an infinitely conducting plasma which wholly excludes the magnetic field as it moves. In reality the plasma is not infinitely conducting; therefore the field is not wholly excluded from the plasma during penetration, and they are at least partially intermingled. This makes it easier for the plasma jet to pass through the maximum field region, by reducing the compression of the jet. There is also one further effect due to the intermixing of the plasma with the field when the jet enters the trap: the plasma jet carries a part of the intermixed magnetic flux into the trap. Therefore, as the central region of the trap is filled, there is a deformation of the lines of force. Corresponding to this deformation, the position of the field zero is shifted along the $z$ axis (the plasma jet, so to speak, presses on the magnetic field generated by the opposite coil and pushes back the corresponding lines of force).

The length of the plasma blob fired from the injector can be very important in determining the general features of the deceleration of plasma penetrating into a magnetic field along the lines of force. It should be assumed that, for a given $\rho_0 v_0^2/2$, a long jet will penetrate the strong field more easily than a short plasma blob. This is because the first section of the jet forces apart the magnetic field lines and makes it easier for the following mass of matter to penetrate into the field.

Plasma, once it has penetrated into a trap, can be captured and contained through the action of various mechanisms; the comparative efficacy of these is very difficult to assess. When the plasma jet arrives in a space where the magnetic field strength is small, it expands rapidly. As it expands in all directions, the plasma is confronted everywhere by an increasing magnetic field† and is in part reflected by it. As a consequence the separate elements of the plasma blob can intermingle; these processes degrade part of the directed kinetic energy into energy of random motion, and, as a result, the plasma will not be able immediately to leave the trap.

---

† In particular, magnetic field is also encountered at the place where the plasma penetrated into the trap. Once the plasma jet has passed, the lines of force in this region squeeze together again and re-establish the original field configuration.

The breakdown of adiabatic invariance in the region close to the field zero—'where the past is forgotten'—is of fundamental importance in the capture processes. Particles in the neighbourhood of point $A$ can stay there for a time, but after the magnetic field has been completely excluded from the region of trapped plasma they escape through the 'leak' in the region of strong magnetic field. One should also include among the various irreversible processes leading to plasma capture, collisions between particles and various oscillatory processes. Plasma capture can also be assisted by producing conditions conducive to the development of certain non-dangerous forms of instability inside the plasma blob. Let us suppose, for example, that a plasma jet from an injector enters a cusp magnetic field through an annular diaphragm, coaxial with the coils; the plasma jet then disperses into a region bounded from without and from within by two hyperboloids formed by those magnetic field lines which intercept the edges of the diaphragm. Because the boundary formed by the inner hyperboloid is curved outwards from the plasma, it is unstable, and therefore the plasma will spread inwards and fill the region of weak field close to the point $A$. If the mechanisms that have been enumerated do not prove effective and do not make it possible to capture a sufficiently large proportion of the injected plasma in a static trap there remains the possibility of trapping the plasma by rapidly raising the magnetic field strength during injection. Given a very rapid increase in the field, the back streaming of particles out of the trap will be markedly reduced and there will be a corresponding increase in the number of trapped particles.

Heating plasma in a cusp-field trap is important if the initial energy of the ions arriving from the injector is small. To get an overall view of the main processes, we shall dwell on the simplest case of all. We assume that a blob has a well-marked boundary and, in addition, we shall assume that the velocity distribution of both the ions and electrons remains isotropic, due to collisions. Also we neglect the escape of particles through the 'leak'. All this being granted, the relation between pressure and volume conforms to the general law of adiabatic compression of a monatomic gas:

$$p\Omega^{5/3} = \text{const.} \qquad \text{.........}(8.59)$$

If the geometrical shape is preserved during compression, the volume of the blob varies as the cube of its linear dimensions. It thus follows from (*8.59*) that

$$pr^5 = \text{const.} \qquad \text{.........}(8.60)$$

where $r$ is a characteristic linear dimension.

The plasma pressure $p$ is balanced by the magnetic pressure which can be written

$$H^2/8\pi = k^2(t)r^2. \qquad \text{.........}(8.61)$$

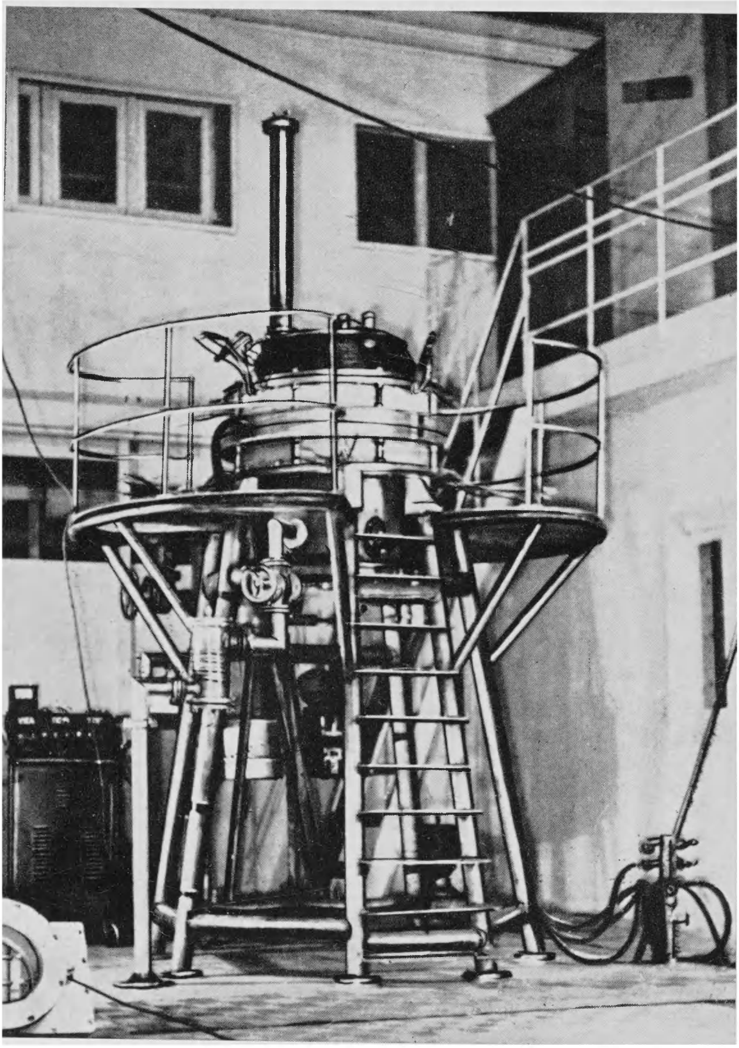

External view of one of the cusp field installations.

In this expression it is assumed that the field strength $H$ at any point is proportional to the length of the radius vector to the null point $A$.† The coefficient $k(t)$ describes the time dependence of $H$. By using equations *(8.60)* and *(8.61)* we obtain the following relation between $k$ and the characteristic linear dimension of the plasma boundary:

$$r \propto k^{-2/7}. \qquad \text{.........}(8.62)$$

The number density of particles is inversely proportional to $r^3$ and will therefore vary as $k^{6/7}$. The plasma pressure is proportional to $k^2 r^2$ and therefore changes as $k^{10/7}$, and the temperature is proportional to $k^{4/7}$. Consequently, if the field strength at a fixed geometrical point increases 10 times, i.e. if the total magnetic energy in the volume increases 100 times, the plasma temperature increases no more than 3·7 times and the number density of the particles 7·2 times. This slow increase of $T$ and $n$ is caused by the geometry of the field: the rising magnetic field squeezes the blob into regions where the magnitude of $H$ become relatively less and less. Heating by compression is even less effective if the plasma does not wholly exclude the magnetic field from the region it occupies, or if there is loss of plasma during compression.

Because compressional heating is not very effective in cusp-field traps, one has to try to ensure that the injected plasma is at the highest possible temperature; otherwise the ratio $k(t)/k(0)$, characterising the subsequent heating of the captured plasma during compression, has to be very large.

Experimental research on plasma injected into cusp-field traps has been carried out in the U.S.S.R. by Lukyanov and Podgorny. In the U.S.A. work of a similar nature has been done mainly at Los Alamos. The sum total of experimental information is still not very great, and is largely illustrative in nature. Figure 134 shows a typical scheme for a trap and plasma injector, and Plate XIX shows a photograph of one of these devices (the 'Orekh'‡ installation at the Kurchatov Institute of Atomic Energy).

To investigate the properties of plasma captured in cusp-field traps the following diagnostic methods have been used: (1) ultra-high-speed photography; (2) magnetic probes; (3) thermocouples for measuring the heat flux on the walls of the trap; (4) electric probes for measuring the number density, and also $T_e$ and $T_i$. Spectroscopic analysis of the plasma is still at the preliminary stage.

The use of electric probes to measure the flux of charged particles from the plasma as a function of the voltage between the probe and the chamber walls, calls for a few remarks. Starting with the early work of Langmuir, current-voltage characteristics of such probes have for 50 years been the main technique for determining the most important plasma characteristics. In research on the problem of controlled thermonuclear reactions, this technique has found only limited use, chiefly because the interpretation of the current-voltage characteristics becomes very complicated and gives ambiguous results when the plasma is in a strong magnetic field. This does not, however, apply to the study of plasma in cusp geometry because in the centre region the magnetic field is close to zero, and probe measurements made there can be interpreted with sufficient clarity.

---

† No account is taken of the influence of currents flowing in the plasma on the geometry of the field.

‡ Literally 'nut'.

Plate XX(*a*) shows framing camera photographs of a plasma blob formed by filling a trap with hydrogen plasma fired from a coaxial injector. The number density in this case is about $10^{14}$ cm$^{-3}$, the ion temperature is about 20 eV and the electron temperature is 5–10 eV. The maximum field strength on the axis is 6000 Oe. The time interval between successive frames is 4 microseconds. The dark horizontal lines crossing the pictures are due to the magnetic field coils. The gap between the coils is 8 cm and the diameter of the vacuum chamber is 20 cm. For comparison, Plate XX(*b*) shows photographs taken when the current in the two coils flowed in the same direction. All the other parameters injector voltage, number density and speed of the plasma jet, coil currents) are the same for both cases.

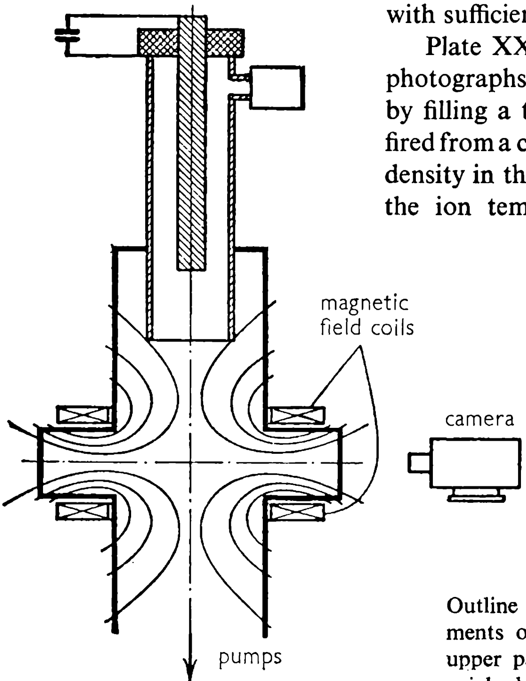

FIG. 134

Outline of an installation for experiments on cusp field confinement. The upper part of the installation is a coaxial plasma injector. The camera for high-speed photography of the plasma is to the side

The photographs give a clear picture of the penetration of a plasma jet into a trap and the formation of the blob of captured plasma. We shall note some of the most characteristic features of the picture. The plasma jet from the injector passes through a region of maximum field in the lower coil without undergoing any marked compression. This means that the field is not fully pushed aside when the plasma enters the magnetic system, and therefore, when the blob forms, the greater part of the plasma is intermingled with field. The same conclusion emerges from the measurements of the number density and the temperature, which show that the pressure in the blob is very small and therefore that the plasma excludes the field only from a small region close to the centre of the magnetic system. The processes shown in the successive framing camera photographs can be roughly divided into two main phases. In the first phase the trap is filled with plasma coming from the injector; in the second phase, the captured plasma gradually attenuates. In the pictures shown, the first phase lasts about 20 microseconds and is marked by the brighter luminosity.

By studying the shape of the plasma blob in the initial phase one interesting detail of the process can be discovered. Whereas the plasma goes through the lower coil looking like a broad band, the plasma emerging through the upper coil looks like a narrow thread. It is possible that what we see here is the reflection of the plasma jet by the strong and suddenly increasing field of the upper coil. The field of opposite sign, which the plasma jet carries with it, enhances this reflection process. This phenomenon may be of great importance for capturing plasma in the trap. When it encounters the lines of force in the upper part of the magnetic system, the plasma jet sprays out radially and is thereby caught in the trap.

The dissolution of the plasma blob takes place during some tens of microseconds. The plasma flows most quickly from the region close to the axis and the shape of the plasma blob thus gradually changes. In the final stage of its existence the plasma remaining in the trap occupies a flat lens-shaped region. However, there are often cases when the shape of the region occupied by the plasma at the end of the process is found to be asymmetrical with respect to the coils, and suggests on the photographs the shape of a small plate with a rim (see Plate XX).

Plate XXI shows synchronous oscillograms of the current flowing to a probe situated in the centre of a trap near point $A$, and of the discharge current in the injector. They were obtained on another installation. The probe potential was negative relative to the plasma, and so the probe measures the ion current which is proportional to the number density of charged particles in the plasma. Measurements of $n$ made in this way show that, for the same injector operating conditions, the number density of particles in the captured plasma blob increases with increasing magnetic field strength approximately as $\sqrt{H}$. The qualitative explanation of this increase of number density is quite obvious; while $N$ and $T$ remain unchanged, the plasma blob has to occupy a smaller region in the neighbourhood of point $A$ as the external magnetic pressure becomes greater. However, the quantitative interpretation of the observed variation of $n$ with $H$ is complicated because of the need to take into account a number of factors which are hard to determine. It should be noted that if the field were completely excluded from the plasma-occupied region, then, with $N$ and $T$ unchanged, the number density should vary roughly as $H^{6\ 5}$.

This conclusion is easily obtainable by arguments quite analogous to those used above in analysing the compression processes.

Probe oscillograms make it possible to determine the plasma lifetime as a function of different initial conditions. Such measurements show that for $n \simeq 10^{13}$ cm$^{-3}$, $H \simeq 10^3$ Oe and plasma temperature about 10–20 eV, the mean lifetime in a trap of the geometrical dimensions given on p. 372 is about 30 $\mu$sec and is weakly dependent on the strength of the magnetic field. On the basis of these results one can draw no conclusion as to the presence or absence of any specific mechanism causing leakage of plasma from cusp-field traps because, in the experimental conditions described, the high number density and the low temperature of the particles lead to very high Coulomb collision rates, which must destroy adiabatic invariance of the ion motion in no more than a few microseconds. Therefore the plasma can escape freely along the lines of force at a speed approximating to the mean thermal speed of the ions. Against such a general plasma loss, it is impossible to pick out that part due to non-adiabatic motion which is predicted by theory for the case when there are no Coulomb collisions. The justice of this comment is illustrated by a simple experiment. If a metal disc is placed on the axis of the cusp trap so that the zero-field point and the surrounding low-field region are shielded from the plasma flux, then this disc acts as a black body for all particles which would otherwise move into this region and lose adiabatic invariance. If such non-adiabatic motion were one of the main mechanisms determining the loss of the plasma from the trap, then by putting a disc into the centre of the magnetic system we should significantly influence the flow of particles and heat from the plasma to the outside. In the event, however, it turns out that a disc placed inside the trap has practically no effect either on the lifetime of the plasma or on the value of the thermal flux in the equatorial plane.

Magnetic probe observations confirm the assumption that the field is partly drawn along by the plasma jet. As it enters the trap, the plasma carries along with it a ring-shaped current of about 200–300 A. This current lasts for 10–20 $\mu$sec,† and displaces the position of the field zero. Thermocouples placed at various points on the chamber walls make it possible to find the distribution of heat flux in the trap. Unfortunately, however, the thermocouples measure the flux integrated over the whole duration of the process, so that it is not possible to distinguish between the leakage of energy from the captured plasma blob and the heat flow produced during the first phase by the passage of the plasma jet. Thus it is still not finally proved in these experiments that the particles leave the trap mainly in radial directions in the equatorial plane of symmetry.

From all that has been said above it follows that if the results of this type of experiment are to admit of clear and unambiguous interpretation, either the number density of the plasma must be considerably diminished or its temperature must be raised by many times. The first of these processes is far easier to achieve than the second. Therefore, without waiting for the development of injectors to provide high-temperature plasma jets, experiments were carried out at the Kurchatov Institute in 1962 in which the Orekh trap was filled with plasma of comparatively low density. It was thus established that reduction of number density from $10^{14}$ to $10^{12}$ cm$^{-3}$ increases the plasma's lifetime from some tens of microseconds to 150–200 microseconds. Even with this low number density, there is still no success in observing particle loss due to the field zero in the trap centre. With $n_e \simeq 10^{12}$ the lifetime of a plasma is determined by the Coulomb collisions which the particles undergo when they are trapped on the lines of force and oscillate along them. Apparently the hypothetical mechanism of internal instability which was discussed on p. 367 plays no significant part. It should, however, be noted that these results are still of a preliminary nature.

---

† i.e. for a time approximately equivalent to the duration of time in which the plasma jet moves across the trap.

Experiments on the compression of plasma in cusp fields are in an early stage, and we will not discuss the results in detail. In the work of Allen and co-workers,† by rapidly compressing plasma generated by the collisions of two shock waves, plasma with a density of about $10^{16}$ cm$^{-3}$ and temperatures of about 10–20 eV were obtained in a cusp-field trap. Because these densities are much higher than those obtained by injection into a static trap, it becomes possible to measure the spatial distribution of the outward flow of plasma momentum as a function of time, using piezo-electric pressure probes. These measurements, which have a resolution time of about 1 $\mu$sec, show that the equatorial cusp leak has a width of the order of 2–5 mm, and accounts for the great majority of the loss of particles and energy from the trap. The magnitude of the width corresponds to rough estimates of that expected from the Coulomb collision effects. Spectroscopically measured plasma confinement times in these experiments are about 10 $\mu$sec.

### *Hybrid Magnetic Field Traps*

§ **8.21** In considering the further outlook for research devoted to magnetic traps, both of the ordinary mirror machine type and of the cusp geometry type, we still cannot start from a fully established basis of experimental fact. It appears, however, from quite convincing theoretical arguments that both types of magnetic system suffer from fundamental defects making them unsuitable for the lengthy containment of high-temperature plasma. In ordinary magnetic mirror traps the defect is magnetohydrodynamic instability; in cusp-field traps it is the rapid escape of plasma due to breakdown of the adiabatic invariant in the region where the particles 'forget their past'. It is thus natural that the idea should arise of devising traps with magnetic fields of a combined type in which the virtues of the simple systems considered above would be united and their defects eliminated.

---

† Reported at Salzburg, 1961.

The basic requirements which such hybrid traps must satisfy are clear enough:

(1) to ensure magnetohydrodynamic stability, the field strength must increase in all directions from some particular region of space which is to be filled with plasma;

(2) to ensure the adiabatic motion of the particles, the field strength must not be zero at any point within the plasma.

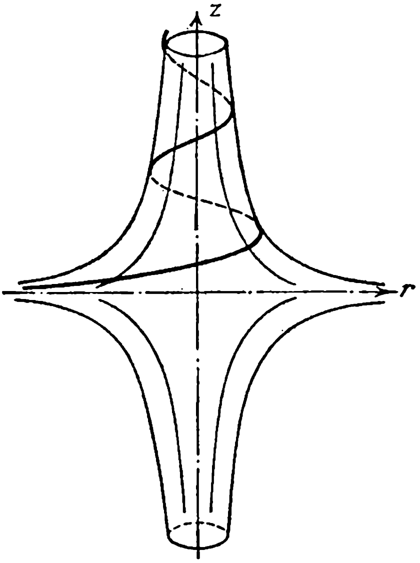

FIG. 135

Shape of magnetic field in a hybrid trap formed by combining a cusp field with that of an axial current

Figure 135 shows a very simple system of this type, a combination of a spindle cusp field and the field generated by a straight current-carrying conductor on the $z$-axis.† The lines of force take the form of spirals winding on the surface of the hyperboloid $zr^2 =$ const. The intensity of the field does not depend on the azimuthal angle $\theta$. At the point $z$, $r$, the magnetic pressure is proportional to $z^2 + r^2/4 + a^2/r^2$, where $a$ is a constant depending on the ratio of the axial current to the current in the coils generating the

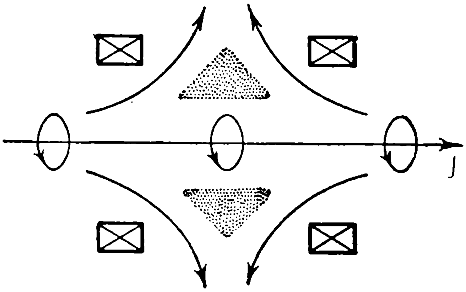

FIG. 136. Plasma in the hybrid configuration of Fig. 135

---

† Sometimes called a 'stuffed cusp'.

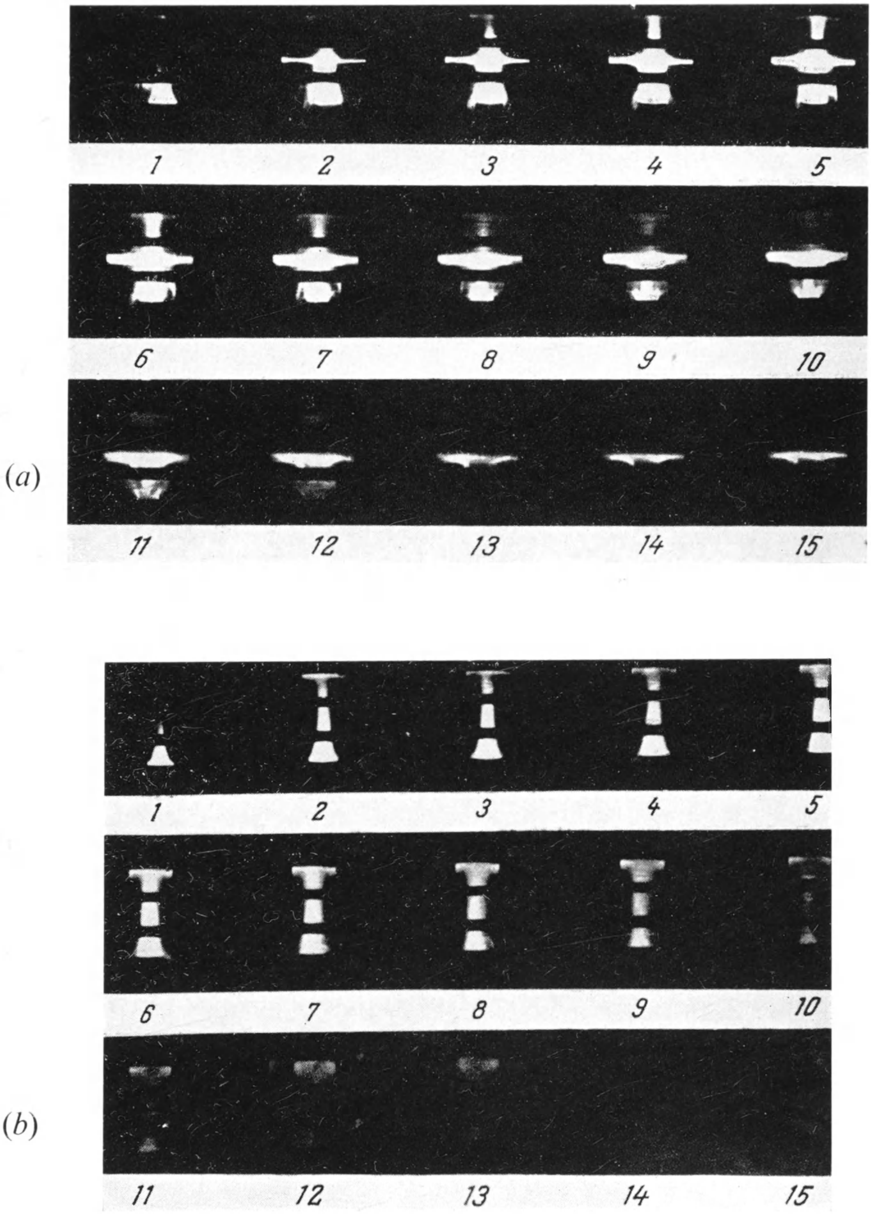

Successive photographs of the flow of plasma injected into (*a*), cusp geometry fields and (*b*), an ordinary magnetic mirror field configuration.

PLATE XXI

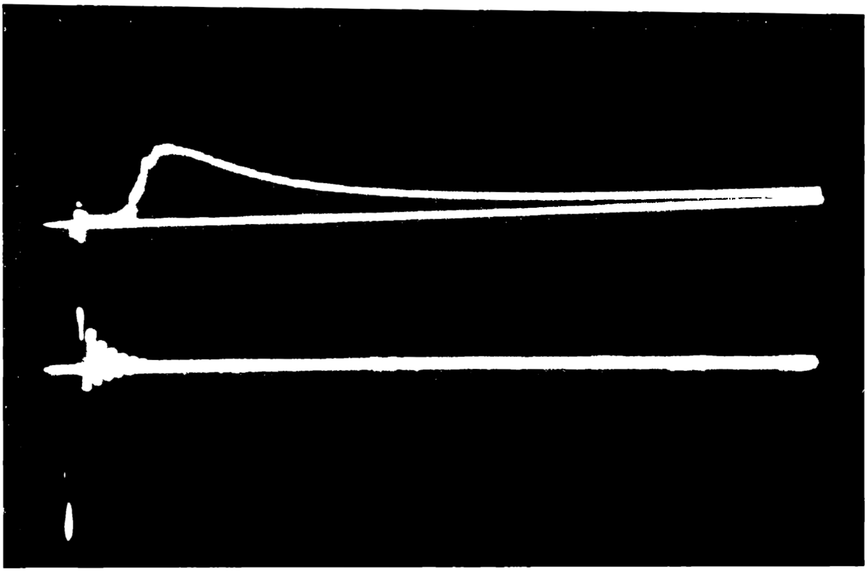

Oscillograms showing current on probe (upper) and current in the injector (lower).

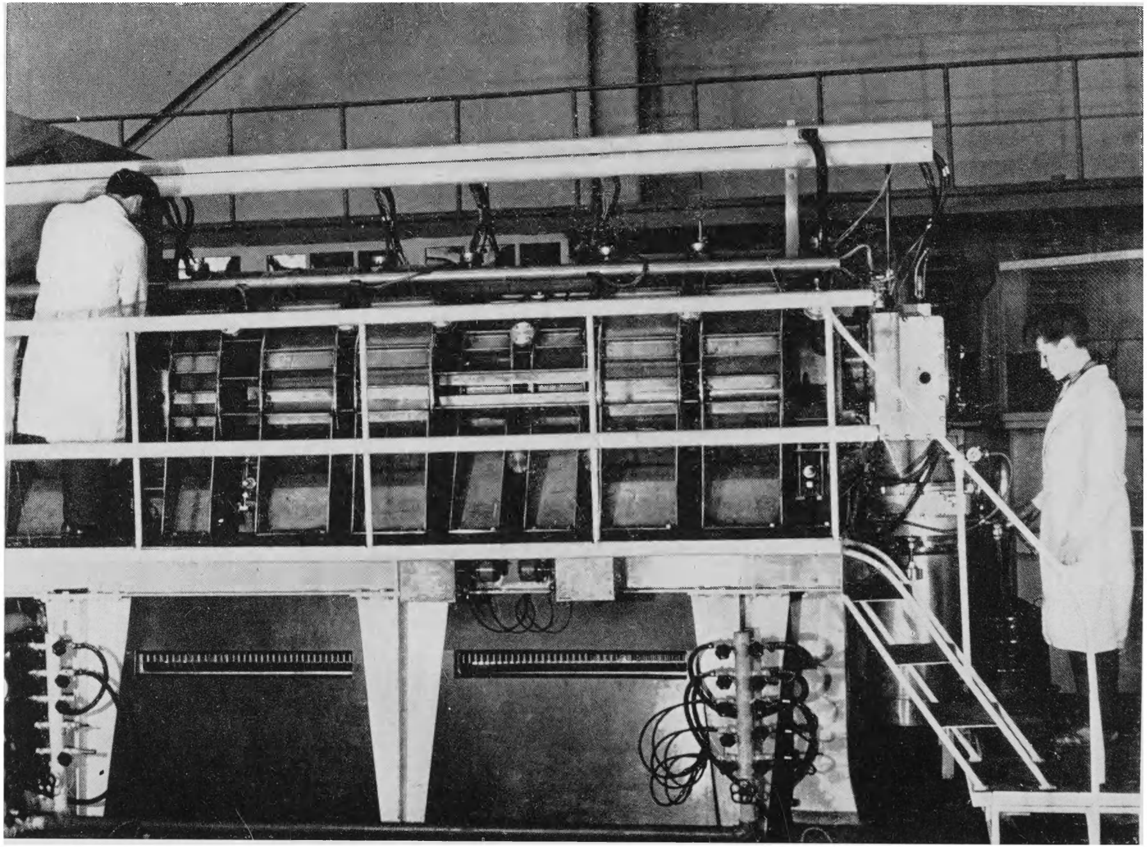

The PR-5 Installation for ion magnetron experiments on the hybrid

PLATE XXIII

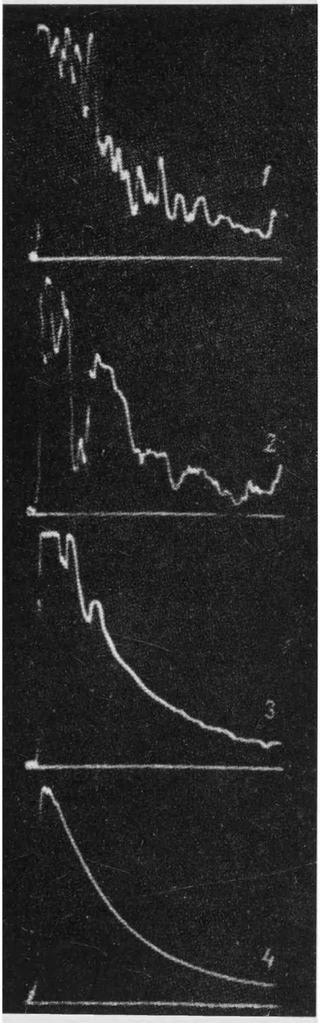

$H_\perp = 0$, $\alpha_\perp = 1\cdot00$.

$H_\perp = 900$ Oe, $\alpha_\perp = 1\cdot04$

$H_\perp = 1400$ Oe, $\alpha_\perp = 1\cdot09$.

$H_\perp = 2400$ Oe, $\alpha_\perp = 1\cdot21$.

Oscillograms of the current to the Langmuir probe, for four values of the stabilising field $H_\perp$ ($H_0 = 3{,}300$ Oe; base pressure, $1\cdot5 \times 10^{-7}$ Torr).

hyperbolic field. Plasma injected into the trap will occupy a ring-shaped region of roughly the shape shown by the dots in Fig. 136. If the plasma pressure is not too great the magnetic field will differ from zero at all points in this region, and therefore the conditions for adiabatic invariance will be satisfied. Thus, escape of particles from a magnetic system of this type can be caused only by collisions.† On the other hand, because the field strength everywhere grows with increasing distance from the plasma surface, magnetohydrodynamic stability of the confined plasma should, seemingly, be ensured.

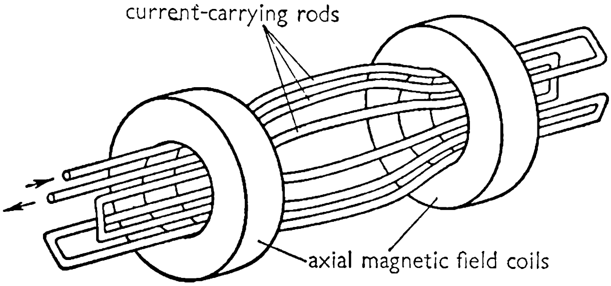

FIG. 137. Hybrid trap formed by a magnetic mirror field and axially-directed conductors

Figure 137 shows another possible type of hybrid field trap. In this case, an ordinary magnetic mirror trap is taken as the basis. To it is added a field generated by currents which flow in axially directed conductors arranged symmetrically round the $z$-axis. At a sufficiently great distance from the $z$-axis the field strength will everywhere increase outwards along the radius, and this will ensure that flute deformations of the confined plasma are stable. The lines of force of a hybrid system like this have a somewhat complicated structure; Fig. 138 gives an impression of it.

These very simple types of combined-field trap are now at the stage of

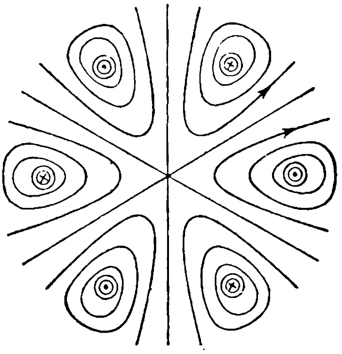

FIG. 138

Projection of the lines of force onto a plane perpendicular to the axis of the trap shown in Fig. 137

---

† However, there is some doubt about the behaviour of the plasma in the equatorial plane, where the lines of force are flat spirals which make a very small number of turns as they approach the axis.

experimental investigation. Gott, Ioffe and Tel'kovskii have supplemented the ion magnetron system described in § **8.11** by length-wise current-carrying conductors, and have thus built the device shown schematically in Fig. 137. The first experiments with this hybrid field system have yielded some very interesting results. It appears that by the use of these straight current-carrying conductors, the lifetime of fast ions in the trap can be increased many times and prolonged to a point which, within the limits of accuracy of measurement, is determined only by charge-exchange on the neutral gas. Along with this increase of the ion containment time, these authors reported a disappearance (or at any rate, a very marked diminution) of the high-frequency oscillations which are one of the most direct symptoms of instability.

Plate XXII is a photograph of a new hybrid-geometry installation which was built by Ioffe and co-workers at the Kurchatov Institute in 1962. This apparatus is intended to verify and amplify the results obtained in the preliminary experiments described above. At maximum power, the axial field strength in the centre of the chamber is 5000 Oe, rising to 8500 Oe at the mirrors. The straight conductors are placed in the gap between the vacuum chamber and the axial-field coils. These conductors, which are fed from a capacitor bank, produce a stabilising field whose strength at the wall can be anything up to 4500 Oe; the half-period is 55 msec. The vacuum chamber, 40 cm in diameter and 400 cm long, is evacuated with oil diffusion pumps baffled by liquid air traps. The trap region of the chamber is additionally pumped by titanium evaporated onto the wall. The distance between the axial-field magnetic mirrors is 120 cm. The plasma is produced in this apparatus by the ion-magnetron technique described in § **8.11.**

Results have been reported for the case of plasma with parameters $n \approx 10^9$ cm$^{-3}$, $T_i = 5$ keV and $T_e \approx 20$ eV. The decay time of the plasma, measured by detecting the flux of fast neutral atoms produced by charge-exchange, has been determined as a function of the current in the stabilising windings. Figure 139 shows that this time increases markedly when the stabilising field at the walls ($H_\perp$) is increased. In particular, the confinement time is about 35 times longer when $H_\perp = 1500$ Oe than when $H_\perp = 0$. The long confinement time of 3·5 msec can be accounted for by charge-exchange alone; indeed it has been extended first to 10–15 msec by lowering the base pressure and, more recently, to 50–70 msec by using the best vacuum conditions.

The diminution of fluctuation phenomena as the stabilising field increases, is demonstrated by the oscillograms of the current to a Langmuir probe placed 5 cm in from the chamber wall. The probe was biassed negatively to 40 V and measured the saturation ion current, i.e. a quantity proportional to the local plasma density. As shown in Plate XXIII, the amplitude of the fluctuations decreased from nearly 100% of the mean signal to an unnoticeable amount as the stabilising field was raised from zero to 2400 Oe. The gain of the oscillograph is the same for all four oscillograms; the sweep time is 1 msec for the top three traces, and is 3 msec for the bottom trace (the plasma decays more rapidly in the presence of the probe). The plasma density measured from the probe signal varies with radius: it is about $10^9$ $\mathrm{cm}^{-3}$ near the wall, and much exceeds $10^{10}$ $\mathrm{cm}^{-3}$ near the axis.

These new data entirely support the preliminary results reported in 1961, and give strong support to the view that, at least for a low-pressure plasma ($\beta \approx 10^{-5}$), this hybrid adiabatic trap provides a plasma confinement system free of magnetohydrodynamic instabilities.

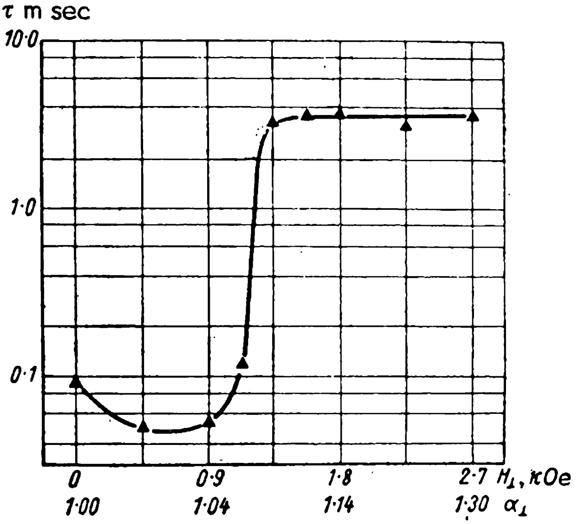

FIG. 139. Dependence of the plasma decay time $\tau$ on the strength of the stabilising field $H_\perp$ ($H_{0\parallel}$ = 3·3 kOe; $p$ = 1·5 × $10^{-7}$ Torr). The quantity $\alpha_\perp \equiv (1 + H_\perp^2/H_0^2)^{1/2}$ is the 'wall mirror ratio'.

For the present, these results are preliminary and have been obtained in only one form of hybrid trap with only one method of plasma production. However, if these results prove to be of general application, it will mean there is an effective method of suppressing that form of magnetohydrodynamic instability which hitherto has represented the main defect of magnetic mirror traps. It should be emphasised that the theory of stability indicated this method to us in advance of experiment.

The multifarious complex magnetic systems satisfying the main requirements described above are not exhausted, of course, by the two examples considered here. It is thus quite possible that future theoretical and experimental studies will lead to traps with quite different field configurations based on the principle that the magnetic field must everywhere increase outward from the plasma surface.

## CHAPTER IX

# CONCLUSION

The first impression one is left with after reviewing the present state of work on controlled thermonuclear fusion is a feeling of dissatisfaction: the results obtained after many years of intensive work do not measure up to the task before us. The first preliminary steps have been taken on the long road of research, and only now have we come squarely up against the main barrier obstructing our progress to the desired region of high temperatures.

Plasma heated to high temperature loses its accumulated thermal energy with extraordinary facility through various instability mechanisms. In the experiments done so far, dense plasma has been contained at relatively high temperature for times not greater than hundreds of microseconds. Up to the present, the intensity of 'real' thermonuclear reactions in plasma has been so insignificant that such reactions could be completely masked by various accelerating processes.

In a general view of the problem, one main feature is that experimental results lag far behind the results of theoretical analysis, particularly on questions involving the stability of plasma. This lag makes it difficult for us to enlarge our understanding of transport processes in plasma, and also makes it extremely hard to develop methods of suppressing plasma instabilities. One reason for this state of affairs is that many difficulties complicate the setting-up and conduct of experiments. It is in itself no mean task to produce hydrogen or deuterium plasma of adequate purity, because interaction with the walls of the vacuum chamber takes place, so that the plasma becomes contaminated very quickly by the atoms and ions of the substances adsorbed on the wall surface. To give an example, we may recall that in installations built to study toroidal discharges (Chapter VI) intense ultraviolet radiation due to impurity ions continues to occur even after many thousands of preliminary discharge pulses have been passed to de-gas the system. This radiation is one of the main factors impeding an increase in plasma temperature in this type of experiment.

Still greater difficulties arise when we try to investigate the properties of these toroidal plasmas, because we then encounter the singular principle of indefiniteness by which the need for cleanliness of experimental conditions is in direct conflict with the use of diagnostic procedures (particularly if local properties of the plasma are being studied). Hidden away as it is by a metal envelope and many layers of windings, inaccessible and extremely sensitive to any contact, a plasma column is an exceptionally awkward object to investigate. It is hardly surprising that we know so little about its properties.

In installations based on the principle of injecting fast particles into a magnetic trap, another difficulty faces us: the particle streams are very weak because of the low strength of existing ion sources, and therefore a very long time is needed to fill such traps. During this time even comparatively mild instabilities have time to cause the escape of particles from the volume, and it then becomes impossible to produce plasma of significant number density. It might be thought that the Stellarator would be free of these faults. But there is still no tried and proved method of obtaining hot plasma in this device; and, as regards the ordinary method of Joule heating the plasma, a Stellarator behaves no better than an ordinary toroidal system with a strong magnetic field. Incidentally, the fact that useful experimental knowledge accumulates only slowly in research on high-temperature plasma well illustrates one feature that characterises modern physics generally: new scientific results have begun to cost much more in terms of the sum of intellectual and material expenditure needed to obtain them.

The present state of experimental research should not give grounds for premature pessimism. When physicists made it their goal to achieve controlled thermonuclear fusion, they came to grips with a problem which surpasses in difficulty all the technical problems to which the scientific advances of the twentieth century have yet given rise. The difficulties involved stand out especially clearly in contrast with the limpidity and the appealing simplicity of the physical ideas which underlie the methods of confining and heating plasma so far proposed.

The assessment of future prospects largely depends on the answer to the question of how much progress can be made within the framework of existing ideas, without bringing in new fundamental principles of which as yet we have no conception. The following can be said on this point: despite the fact that theoretical studies are constantly revealing new mechanisms giving rise to instability, such studies by no means tend to demonstrate that plasma enclosed in a magnetic field is universally unstable. It must be borne in mind that the degree of conviction conveyed by theoretical forecasts of instability is not very great, in so much as theory is limited in the majority of cases to the linear approximation which is valid only for very small deformations.

It is still not clear how great a reduction can be made in the energy losses suffered by a confined plasma due to the various forms of instability; the reason is that methods of reducing these losses are only at the first stage of development.

Taking all this into account we have reason to suppose that, with further improvement of the already known methods of heating and thermally insulating plasma, it will be possible by using strong magnetic fields to produce high-temperature plasma stable to a first approximation and suitable for the generation of intense thermonuclear reactions. The question remains open, of course, whether the final goal will be achieved in this way.

It is an essential condition for further advances that experimental technique should be raised to a higher standard: vacuum technology must attain maximum cleanliness; magnetic configurations must be made to conform to precisely defined geometries; stray fields must be eliminated; electrical circuits must be programmed; and experimental procedures will have to be introduced that make it possible to obtain comprehensive information about the behaviour of the plasma without making contact with it. Rough survey-type estimates, like those underlying the majority of the papers on thermonuclear subjects presented at the 1958 Geneva Conference, have now reached the end of their usefulness and will not be of any real help in the future. In this respect work on thermonuclear fusion in plasma differs sharply from ordinary research in gas discharges—a field which has hitherto been distinguished neither by great precision nor by any special requirements for cleanliness.

One point, which now seems almost self-evident, must be specially emphasised: a plasma confined by a magnetic field is likely to be stable only within a very narrow range of parameters, and therefore plasma has to be handled very carefully if we are to get the parameters within these limits and keep them there.

It is difficult to prophesy which of the various methods that have been developed for heating and confining plasma will be the most successful; but this does not mean that all the methods must be regarded as being of equal worth. It is to be expected that, as our understanding of the nature of the various forms of plasma instability improves, more efficient means of combating these instabilities will be found. Along with this, the confinement times of high-temperature plasma must gradually improve.

Recent experimental data clearly indicate that a drastic method of suppressing strong rapidly growing instabilities is the use of hybrid field geometries in which the field strength increases in all directions from the regions occupied by the plasma blob. It is therefore necessary to concentrate research efforts in this direction. At the same time it is hardly possible to expect great advances in the development of devices in which it is proposed to obtain a plasma in a state $\beta \approx 1$ because in this case the magnetic system lacks the necessary degree of rigidity. An almost unexplored field of thermonuclear fusion research is the use of high-frequency electromagnetic fields.

It is hardly to be doubted that ultimately the problem of controlled thermonuclear fusion will be solved. Nature can put only a finite number of difficulties on the road to the solution; and when man has overcome them by unremitting creative activity, nature will not be able to invent new obstacles. All that is uncertain is how long the process will last.

# BIBLIOGRAPHY

References to English translations of Russian language papers are given immediately after the original Russian reference. The title of the four volumes 'Fizika Plazmy i Problema Ypravlyaemykh Termoyadernykh Reaktsiĭ' edited by Leontovich and published by the U.S.S.R. Academy of Sciences in 1958 has been abbreviated to 'Fizika Plazmy'; similarly the translation published by Pergamon Press with the title 'Plasma Physics and the Problem of Controlled Thermonuclear Reactions' has been abbreviated to 'Plasma Physics (Ed. Leontovich)'.

## CHAPTER I

L. A. ARTSIMOVICH: Research on controlled thermonuclear reactions in the USSR. *Proc. 2nd U.N. conf. on peaceful uses of atomic energy*, **31**, 6. U.N., Geneva, 1958.

R. F. POST: Controlled fusion research—an application of the physics of high-temperature plasmas. *Rev. Mod. Phys.*, **28**, 338 (1956).

J. D. LAWSON: Some criteria for a power-producing thermonuclear reactor. *Proc. Phys. Soc.* **B, 70**, 6 (1957).

## CHAPTER II

H. ALFVÉN: *Cosmical Electro-dynamics*. Oxford University Press, 1950 and 1963.

L. SPITZER: *Physics of Fully Ionised Gases*. Interscience, 1956 and 1962.

N. N. BOGOLYUBOV and N. N. MITROPOLSKI: *Asymptotic methods in the study of non-linear oscillations*. Gostekhizdat 1955; Office of Technical Services, U.S.A.E.C., Oak Ridge, NP-TR-233.

S. I. BRAGINSKII: On the theory of the motion of charged particles in a strong magnetic field. *Ukr. Matem. Zhurn.* (*Ukranian Mathematical Journal*), **8**, No. 2, 119 (1956).

S. N. RODIONOV: Experimental verification of the behaviour of charged particles in an adiabatic trap. *Atomnaya Energiya*, **6**, 623 (1959); *Journal of Nuclear Energy, Part C*, **1**, 247 (1960).

G. GIBSON, W. JORDAN and E. LAUER: Containment of positrons in a mirror machine. *Phys. Rev. Letters*, **5**, 141 (1960).

G. GIBSON, W. C. JORDAN and E. J. LAUER: Containment of positrons in an asymmetric mirror geometry. *Nuclear Fusion, 1962 Supplement, Part 1*, 151 (1962).

N. V. FEDORENKO, V. V. AFROSIMOV, R. N. IL'IN and D. M. KAMINKER: Dissociation of the molecular ion $H_2^+$ by collisions in gas. *Zh. Eksp. Teor. Fiz.*, **36**, 385 (1959); *Societ Physics, J.E.T.P.*, **9**, 267 (1959).

R. N. IL'IN: Ionisation and capture of electrons and dissociation of hydrogen ions of keV energies by collisions with gas atoms and gas molecules. Thesis. Leningrad State University 1959.

G. Knorr: Uber den Ionisationszustand und die Ausstrahlung von Fremdgasen in einem Wasserstoffplasma. *Zeitschrift f. Naturf.*, **13a**, 941 (1958).

V. I. Kogan: The role of radiation of impurities in the energy balance of a plasma column. *Doklady Acad. Nauk (USSR)*, **128**, 702 (1959); *Soviet Physics Doklady*, **4**, 1057 (1959).

A. P. Vasil'ev, G. G. Dolgov-Savel'ev and V. I. Kogan: Radiation by impurities in a rarefied hot hydrogen plasma. *Nuclear Fusion, 1962 Supplement, Part 2*, 655 (1962); *AEC-tr-5589*, **2**, 533 (1963).

W. Fite and R. Brackmann: Collisions of electrons with hydrogen atoms, I, ionisation. *Phys. Rev.*, **112**, 1141 (1958).

W. Fite, R. Brackmann and W. Snow: Charge exchange in proton-hydrogen-atom collisions. *Phys. Rev.*, **112**, 1161 (1958).

S. C. Brown: *Basic data of plasma physics.* New York, Wiley, 1959.

## CHAPTER III

S. Chapman and T. G. Cowling: *The Mathematical Theory of Non-uniform Gases.* Cambridge University Press, 1939.

H. Dreicer: On the theory of runaway electrons. *Proc. 2nd U.N. conf. on peaceful uses of atomic energy*, **31**, 57. U.N., Geneva, 1958.

D. Bohm in *The Characteristics of Electrical Discharges in Magnetic Fields*, by A. Gutherie and R. Wakerling, Ch. 2, §.5. McGraw-Hill, 1949.

B. Lehnert: Diffusion processes in the positive column in a longitudinal magnetic field. *Proc. 2nd U.N. conf. on peaceful uses of atomic energy*, **32**, 349. U.N., Geneva, 1958.

A. V. Nedospasov: Concerning ambipolar diffusion in a magnetic field. *Zh. Eksp. Teor. Fiz.*, **34**, 1338 (1957); *Soviet Physics, J.E.T.P.*, **7**, 923 (1958).

A. V. Zharinov: Intermittent increase of electron current to a probe during discharge in a magnetic field. *Atomnaya Energiya*, **7**, 215 (1959); *Soviet Journal of Atomic Energy*, **7**, 3, 710 (1961).

A. V. Zharinov: The diffusion of electrons in a magnetic field. *Atomnaya Energiya*, **7**, 224 (1959); *Soviet Journal of Atomic Energy*, **7**, 3, 715 (1961).

L. I. Elizarov and A. V. Zharinov: Transverse motion of a plasma in a magnetic field. *Nuclear Fusion, 1962 Supplement, Part 2*, 699 (1962); *AEC-tr-5589*, **1**, 283 (1963).

A. V. Zharinov: Rotating plasma jet in a discharge in a magnetic field. *Atomnaya Energiya* **10**, 368 (1961); *J. Nuclear Energy, Part C*, **4**, 63 (1962).

A. S. Syrgi and V. K. Granovskii: Speed of de-ionisation of rarefied helium in a magnetic field. *Part 1*, *Radiotekhnika i Elektronika*, **4**, 1854 (1959).

B. B. Kadomtsev and A. W. Nedospasov: Instability of the positive column in a magnetic field and the 'anomalous' diffusion effect. *J. Nuclear Energy, Part C*, **1**, 230 (1960).

B. E. Golant and A. P. Zhilinskii: Experimental investigation of decay of plasma in a magnetic field through diffusion. *Zh. Tech. Fiz.*, **30**, 745 (1960); *Soviet Physics Technical Physics*, **5**, 699 (1961).

G. A. Paulikas and R. V. Pyle: Macroscopic instability of the positive column in a magnetic field. *Physics of Fluids*, **5**, 348 (1962).

J. F. Bonnal, G. Briffod, M. Gregoire and C. Manus: Étude de la diffusion perpendiculaire au champ magnétique. *Nuclear Fusion, 1962 Supplement, Part 3*, 995 (1963).

## CHAPTER IV

V. D. Shafranov: On magnetohydrodynamical equilibrium configurations: *Zh. Eksp. Teor. Fiz.*, **33**, 710 (1957); *Soviet Physics, J.E.T.P.*, **6**, 545 (1958).

S. I. Braginskii and V. D. Shafranov: A plasma column with heat losses at electrodes. *Fizika Plazmy*, **2**, 26. Akad. Nauk SSSR, 1958; *Plasma Physics* (Ed. Leontovich), **2**, 1. Pergamon Press, 1959.

S. I. Braginskii and V. D. Shafranov: High-temperature pinches. *Proc. 2nd U.N. conf. on peaceful uses of atomic energy*, **31**, 43. U.N., Geneva, 1958.

V. D. Shafranov: Equilibrium of a toroidal plasma in a magnetic field. *Atomnaya Energiya*, **13**, 521 (1962); *J. Nuclear Energy, Part C*, **5**, 251 (1963).

V. D. Shafranov: On the equilibrium state of a ring pinch. *Zh. Tech. Fiz.*, **33**, 137 (1963); *Soviet Physics, Technical Physics*, **3** (2), 99 (1963).

V. C. A. Ferraro: On the theory of the first phase of a geomagnetic storm: a new illustrative calculation based on idealized (plane not cylindrical) model field distribution. *J. Geophys. Res.*, **57**, 15 (1952).

V. L. Ginzburg: *The propagation of electromagnetic waves in plasma*. Fizmatgiz, 1960. Gordon and Breach and North Holland, 1961.

T. E. Stringer: Low-frequency waves in an unbounded plasma. *J. Nuclear Energy, Part C*, **5**, 89 (1963).

## CHAPTER V

L. A. Artsimovich, A. M. Andrianov, O. A. Bazilevskaya, Yu. G. Prokhorov and N. V. Filippov: Investigation of pulse discharges at high currents. *Atomnaya Energiya*, **3**, 76 (1956); *Soviet Journal of Atomic Energy*, **1**, 367 (1956).

N. A. Borzunov, D. V. Orlinskii and S. M. Osovets: Investigations of intense pulsed discharges in gases by means of high-speed photography. *Atomnaya Energiya*, **4**, 149 (1958); *Soviet Journal of Atomic Energy*, **4** (2), 195 (1958).

V. S. Komelkov and G. N. Aretov: The production of large impulse currents. *Doklady Akad. Nauk SSSR*, **110**, 559 (1956).

S. Yu. Luk'yanov and V. N. Sinitsyn: Spectroscopic Investigation of intense pulsed discharges in Hydrogen II. *Zh. Eksp. Teor. Fiz.*, **34**, 849 (1958); *Soviet Physics. J.E.T.P.*, **7**, 587 (1958).

D. P. Petrov, N. V. Filippov, T. I. Filippova and V. A. Khrabrov: Powerful pulsed gas discharges in chambers with conducting walls. *Fizika Plazmy*, **4**, 170. Akad. Nauk SSSR, 1958; *Plasma Physics* (Ed. Leontovich), **4**, 198. Pergamon Press, 1959.

A. M. Andrianov, O. A. Bazilevskaya and Yu. G. Prokhorov: Study of a pulsed discharge in deuterium for current rates of rise up to $10^{12}$ A/sec and voltages up to 120 kV. *Fizika Plazmy*, **4**, 182. Akad. Nauk SSSR, 1958; *Plasma Physics* (Ed. Leontovich), **4**, 213. Pergamon Press, 1959.

N. V. Filippov: Investigation of pressures in a powerful pulsed gas discharge, using a piezoelectric measuring device. *Fizika Plazmy*, **3**, 231. Akad. Nauk SSSR, 1958; *Plasma Physics* (Ed. Leontovich), **3**, 280. Pergamon Press, 1959.

M. A. Leontovich and S. M. Osovets: On the mechanism by which the current contracts in fast and intense gas discharge. *Atomnaya Energiya*, **3**, 81 (1956); *Soviet Journal of Atomic Energy*, **1**, 371 (1956).

S. I. Braginskii, I. M. Gelfand and R. P. Fedorenko: Theory of the compression and oscillation of a plasma column in a powerful pulsed discharge. *Fizika Plazmy*, **4**, 201. Akad. Nauk SSSR, 1958; *Plasma Physics* (Ed. Leontovich), **4**, 236. Pergamon Press, 1959.

L. A. Artsimovich, A. M. Andrianov, E. I. Dobrokhotov, S. Yu. Luk'yanov, I. M. Podgornyi, V. I. Sinitsyn and N. V. Filippov; Penetrating radiation from pulse discharges. *Atomnaya Energiya*, **3**, 84 (1956); *Soviet Journal of Atomic Energy*, **1**, 375 (1956).

S. Yu. Luk'yanov and I. M. Podgornyi: Hard X-radiation accompanying a discharge in a gas. *Atomnaya Energiya*, **3**, 97 (1956); *Soviet Journal of Atomic Energy*, **1**, 389 (1956).

V. S. Komel'kov: Self-constricting discharge in deuterium at high rate of current growth. *Zh. Eksp. Teor. Fiz.*, **35**, 16 (1958); *Soviet Physics, J.E.T.P.*, **8**, 10 (1959).

O. A. Anderson, W. R. Baker, S. A. Colgate, J. Ise and R. V. Pyle: Neutron production in linear deuterium pinches. *III Int. Conf. on Ionisation Phenomena in Gases, Venice, 1957*, p. 62.

N. V. Filippov, T. I. Filippova and V. P. Vinogradov: Dense high-temperature plasma in a non-cylindrical *z*-pinch compression. *Nuclear Fusion, 1962 Supplement, Part 2*, 577 (1962); *AEC-tr-5589*, **1**, 311 (1963).

H. Fisser and J. Schluter: A comparison between numerical calculations of a linear *z*-pinch discharge, and measurements by magnetic probes. *Nuclear Fusion, 1962 Supplement, Part 2*, 571 (1962).

O. A. Anderson, W. R. Baker, J. Ise, Jr., W. B. Kunkel, R. V. Pyle and J. M. Stone: Sheet Pinch Devices. *Proc. 2nd U.N. conf. on peaceful uses of atomic energy*, **32**, 150. U.N., Geneva, 1958.

A. C. Kolb: Magnetic compression of shock preheated deuterium. *Proc. 2nd U.N. conf. on peaceful uses of atomic energy*, **31**, 328. U.N., Geneva, 1958.

W. C. Elmore, E. M. Little and W. E. Quinn: Neutrons from plasma compressed by an axial magnetic field (Scylla). *Proc. 2nd U.N. conf. on peaceful uses of atomic energy*, **32**, 337. U.N., Geneva, 1958.

K. Boyer, W. C. Elmore, E. M. Little, W. E. Quinn and J. L. Tuck: Studies of plasma heated in a fast rising axial magnetic field (Scylla). *Phys. Rev.*, **119**, 831 (1960).

F. C. Jahoda, E. M. Little, W. E. Quinn, G. A. Sawyer and T. F. Stratton: Continuum radiation in the X-ray and visible regions from a magnetically compressed plasma (Scylla). *Phys. Rev.*, **119**, 843 (1960).

G. A. Sawyer, F. G. Jahoda, F. L. Ribe and T. F. Stratton: X-ray spectroscopic measurements of a high-temperature plasma. *J. Quant. Spectrosc.*, **2**, 467 (1962).

H. R. Griem and A. C. Kolb: Radiation from high temperature collision-dominated plasmas. *J. Quant. Spectrosc.*, **2**, 503 (1962).

D. E. Nagle, W. E. Quinn, F. L. Ribe and W. B. Riesenfeld: Velocity spectrum of protons and tritons from the d-d reaction in Scylla. *Phys. Rev.*, **119**, 857 (1960).

T. S. Green and G. B. F. Niblett: Rayleigh-Taylor instabilities of a magnetically accelerated plasma. *Nuclear Fusion*, **1**, 42 (1960).

A. C. Kolb: Magnetic compression of plasma. *Rev. Mod. Phys.*, **32**, 748 (1960).

I. F. Kvartskhava, K. N. Kervalidze and Yu. S. Gvaladze. Magnetohydrodynamic effects observed in pulsed contraction of a plasma. *Zh. Tech. Fiz.*, **30**, 297 (1960); *Soviet Physics, Technical Physics*, **5**, 274 (1960).

I. F. Kvartskhava, K. N. Kervalidze, Yu. S. Gvaladze and B. K. Kapanadze: Some new data on self-compressed discharges. *Nuclear Fusion, 1962 Supplement, Part 2*, 533 (1962); *AEC-tr-5589*, **1**, 337 (1963).

G. B. F. Niblett: Rapid compression of plasma with azimuthal currents. *Proc. I.E.E.*, 106, Part A, Suppl. No. 2, 152 (1959).

G. N. Aretov, V. I. Vasil'ev, V. S. Komel'kov, M. I. Pergament and S. S. Tsereviti-

NOV: Compression of a plasma by a rapidly increasing magnetic field. *Nuclear Fusion, 1962 Supplement, Part 3,* 1226 (1962); *AEC-tr-5589,* **2**, 565 (1963).

E. M. LITTLE, W. E. QUINN, F. L. RIBE and G. A. SAWYER: Studies of stability and heating in the Scylla magnetic compression experiment. *Nuclear Fusion, 1962 Supplement, Part 2,* 497 (1962).

H. A. B. BODIN, T. S. GREEN, G. B. F. NIBLETT, N. J. PEACOCK, J. M. P. QUINN, J. A. REYNOLDS and J. B. TAYLOR: Rapid axial contraction of a high density deuterium plasma in a thetatron discharge. *Nuclear Fusion, 1962 Supplement, Part 2,* 511 (1962).

H. A. B. BODIN, T. S. GREEN, G. B. F. NIBLETT, N. J. PEACOCK, J. M. P. QUINN and J. A. REYNOLDS: The influence of trapped field on the characteristics of a magnetically compressed plasma (thetatron). *Nuclear Fusion, 1962 Supplement, Part 2,* 521 (1962).

H. R. GRIEM, A. C. KOLB, W. H. LUPTON and D. T. PHILLIPS: Measurements of electron densities and temperatures and other plasma parameters in magnetic compression experiment. *Nuclear Fusion, 1962 Supplement, Part 2,* 543 (1962).

A. C. KOLB, H. R. GRIEM, W. H. LUPTON, D. T. PHILLIPS, S. A. RAMSDEN, E. A. MCLEAN, W. R. FAUST and M. SWARTZ: A high energy magnetic compression experiment. *Nuclear Fusion, 1962 Supplement, Part 2,* 553 (1962).

K. HAIN and A. C. KOLB: Fast theta-pinch. *Nuclear Fusion, 1962 Supplement, Part 2,* 561 (1962).

H. L. JORDAN: Methods for the production of high density, high-temperature plasmas by magnetic compression under controlled initial conditions. *Nuclear Fusion, 1962 Supplement, Part 2,* 589 (1962).

H. BEERWALD, P. BOGEN, T. EL-KHALAFAWY, H. FAY, E. HINTZ and H. KEVER: Production of a highly ionised deuterium plasma of low impurity level, with and without magnetic bias fields, for magnetic compression experiments. *Nuclear Fusion, 1962 Supplement, Part 2,* 595 (1962).

E. HINTZ: Effects of amplitude and polarity of internal magnetic field on the fast magnetic compression of a fully ionised uniform plasma. *Nuclear Fusion, 1962 Supplement, Part 2,* 601 (1962).

P. BOGEN and E. HINTZ: Density distribution from radiation measurements during the fast magnetic compression of a plasma. *Nuclear Fusion, 1962 Supplement, Part 2,* 607 (1962).

H. KEVER: Theory of dynamical behaviour of plasmas with internal magnetic fields during magnetic compression: Comparison with experiments. *Nuclear Fusion, 1962 Supplement, Part 2,* 613 (1962).

J. E. ALLEN, M. U. MARTONE and S. E. SEGRE: Measurements on an orthogonal pinch discharge. *Nuclear Fusion, 1962 Supplement, Part 2,* 617 (1962).

J. E. ALLEN, C. BARTOLI, B. BRUNELLI, J. A. NATION, B. RUMI and R. TOSCHI: Observations on an orthogonal pinch discharge (Cariddi). *Nuclear Fusion, 1962 Supplement, Part 2,* 621 (1962).

S. M. OSOVETS, YU. F. PETROV and N. I. SHCHEDRIN. The study of a gas discharge in a simple connected region. *Fizika Plazmy,* **2**, 242. Akad. Nauk SSSR, 1958; *Plasma Physics* (Ed. Leontovich), **2**, 326. Pergamon Press, 1959.

S. M. OSOVETS, Y. F. NASEDKIN, E. I. PAVLOV, YU. F. PETROV and N. I. SHCHEDRIN: Plasma loop in a transverse magnetic field. *Proc. 2nd U.N. conf. on peaceful uses of atomic energy,* **32**, 311. U.N., Geneva, 1958.

S. M. OSOVETS, YU. F. NASEDKIN, E. I. PAVLOV and N. I. SHCHEDRIN: Investigation of various states of compression of a plasma loop in the Zh-O installation. *Nuclear Fusion, 1962 Supplement, Part 3,* 1229 (1962); *AEC-tr-5589,* **2**, 689 (1963).

L. A. ARTSIMOVICH, S. YU. LUK'YANOV, I. M. PODGORNYI and S. A. CHUVATIN: Electrodynamic acceleration of plasma bunches. *Zh. Eksp. Teor. Fiz.,* **33**, 3 (1957); *Soviet Physics, J.E.T.P.,* **6**, 1 (1958).

J. Marshall: Performance of a hydromagnetic plasma gun. *Phys. Fluids*, **3**, 134 (1960).

Yu. D. Klebanov and V. I. Sinitsyn: Injection of plasma into vacuum from a powerful pulse discharge. *Nuclear Fusion*, **1962** *Supplement, Part 3*, 1226 (1962); *AEC-tr-5589*, **2**, 585 (1963).

A. I. Morozov and L. S. Solov'ev: On the acceleration of plasma in a coaxial system. *Zh. Tech. Fiz.*, **30** (9), 1104 (1960); *Soviet Physics, Technical Physics*, **5**, 1033 (1961).

L. C. Burkardt and R. H. Lovberg: Current sheet in a co-axial plasma gun. *Physics of Fluids*, **5** (3), 341 (1962).

## CHAPTER VI

M. Kruskal and M. Schwarzschild: Some instabilities of a completely ionised plasma. *Proc. Roy. Soc.*, **223A**, 348 (1954).

M. A. Leontovich and V. D. Shafranov: The stability of a flexible conductor in a longitudinal magnetic field. *Fizika Plazmy*, **1**, 207. Akad. Nauk SSSR, 1958; *Plasma Physics* (Ed. Leontovich), **1**, 255. Pergamon Press, 1959.

V. D. Shafranov: The stability of a cylindrical gaseous conductor in a magnetic field. *Atonmaya Energiya*, **5**, 38 (1956); *Soviet Journal of Atomic Energy*, **1**, 709 (1956).

V. D. Shafranov: On the stability of a plasma column in the presence of a longitudinal magnetic field and a conducting casing. *Fizika Plazmy*, **2**, 130. Akad. Nauk SSSR, 1958; *Plasma Physics* (Ed. Leontovich), **2**, 197. Pergamon Press, 1959.

B. R. Suydam: Stability of a linear pinch. *Proc. 2nd U.N. conf. on peaceful uses of atomic energy*, **31**, 157. U.N., Geneva, 1958.

E. P. Butt, R. Carruthers, J. T. D. Mitchell, R. S. Pease, P. C. Thonemann, M. A. Bird, J. Blears and E. R. Hartill: The design and performance of Zeta. *Proc. 2nd U.N. conf. on peaceful uses of atomic energy*, **32**, 42. U.N., Geneva, 1958.

A. A. Ware: Sceptre IIIA. *Proc. I.E.E.*, Vol. 106, Part A, No. 2, 30 (1959).

V. V. Afrosimov, V. A. Glukhin, V. E. Golant, A. N. Zaidel, E. G. Komar, B. P. Konstantinov, G. M. Malyshev, I. F. Malyshev, N. A. Monoszon, A. M. Stolov and N. V. Fedorenko: Plasma investigations with the 'Alpha' system. *Zh. Tech. Fiz.*, **30**, 1381 (1960); *Soviet Physics, Technical Physics*, **5**, 1311 (1961).

A. N. Zaidel, G. M. Malyshev, E. Ya. Shreider, A. B. Berezin, V. A. Belyaeva, V. I. Gladushchak, V. V. Skidan and L. V. Sokolova: Spectroscopic investigations with 'Alpha'. I. Investigation of the ionic spectra and temperatures. *Zh. Tech. Fiz.*, **30**, 1422 (1960); *Soviet Physics, Technical Physics*, **5**, 1346 (1961).

A. N. Zaidel, G. M. Malyshev, E. I. Moskalev, E. A. Ptitsyna, L. V. Sokolova and G. I. Chaschina: Spectroscopic investigations with 'Alpha'. II. Directed ion motion. *Zh. Tech. Fiz.*, **30**, 1433 (1960); *Soviet Physics, Technical Physics*, **5**, 1356 (1961).

A. N. Zaidel, G. M. Malyshev, A. B. Berezin and G. T. Razobarin: Spectroscopic investigation with 'Alpha'. III. Time variation of plasma emission. *Zh. Tech. Fiz.*, **30**, 1437 (1960); *Soviet Physics, Technical Physics*, **5**, 1360 (1961).

V. A. Anoshkin, V. E. Golant, B. P. Konstantinov, B. P. Poloskin and O. N. Shcherbinin: Microwave investigation of plasma on the 'Alpha' device. *Zh. Tech. Fiz.*, **30**, 1447 (1960); *Soviet Physics, Technical Physics*, **5**, 1370 (1961).

V. V. Afrosimov, I. P. Gladkovskii, Yu. S. Gordeev, I. F. Kalinkevich and N. V. Fedorenko: Method of investigation of the flux of atoms emitted by a plasma.

*Zh. Tech. Fiz.*, **30**, 1456 (1960); *Soviet Physics, Technical Physics*, **5**, 1378 (1961).

V. V. Afrosimov, I. P. Gladkovskii, Yu. S. Gordeev, I. F. Kalinkevich, M. P. Petrov and N. V. Fedorenko: Investigation of the stream of neutral atomic particles emitted by the 'Alpha' plasma. *Zh. Tech. Fiz.*, **30**, 1469 (1960); *Soviet Physics, Technical Physics*, **5**, 1389 (1961).

V. V. Afrosimov, I. P. Gladkovskii, I. F. Kalinkevich, M. P. Petrov and N. V. Fedorenko: Investigation of a current of atomic particles emitted by a plasma. *Nuclear Fusion, 1962 Supplement, Part 3*, 921 (1962); *AEC-tr-5589*, **1**, 490 (1963).

A. B. Berezin, A. N. Zaidel, G. M. Malyshev, G. T. Razdobarin and V. V. Skidan: Spectral Investigations of plasma in the 'Alpha' device. *Nuclear Fusion, 1962 Supplement, Part 3*, 929 (1962); *AEC-tr-5589*, **2**, 506 (1963).

V. A. Burtsev, V. A. Glukhikh, D. E. Zavarin, E. G. Komar, B. A. Larionov, N. A. Monoszon, V. V. Skotnikov and A. M. Stolov: Experimental investigations of electric and magnetic characteristics of gas a discharge in the 'Alpha' apparatus. *Nuclear Fusion, 1962 Supplement, Part 3*, 1230 (1962); *AEC-tr-5589*, **2**, 773 (1963).

D. G. Bulyginskii, B. V. Galaktionov, K. A. Dolmatova and V. A. Ovsyannikov: Pulse method for the measurement of the energy distribution of particles leaving a plasma. *Nuclear Fusion, 1962 Supplement, Part 3*, 1231 (1962); *AEC-tr-5589*, **2**, 808 (1963).

A. L. Bezbatchenko, I. N. Golovin, D. P. Ivanov, V. D. Kirillov and N. A. Yavlinskii: Investigation of a high current gaseous discharge in a longitudinal magnetic field. *Atomnaya Energiya*, **5**, 26 (1956); *Soviet Journal of Atomic Energy*, **1**, 695 (1956).

A. L. Bezbatchenko, I. N. Golovin, P. N. Kozlov, V. S. Strelkov and N. A. Yavlinskii: A high-current electrodeless discharge in a toroidal chamber with a longitudinal magnetic field. *Fizika Plazmy*, **4**, 116. Akad. Nauk SSSR, 1958; *Plasma Physics* (Ed. Leontovich), **4**, 135. Pergamon Press, 1959.

I. N. Golovin, D. P. Ivanov, V. D. Kirillov, D. P. Petrov, K. A. Razumova and N. A. Yavlinskii: Stable plasma column in a longitudinal magnetic field. *Proc. 2nd U.N. conf. on peaceful uses of atomic energy*, **32**, 72. U.N., Geneva, 1958.

A. P. Babichev, A. I. Karchevskii, Yu. A. Muromkin and V. V. Sokol'skii: On the mechanism of the high-current gas discharge in a weak magnetic field. *Nuclear Fusion, 1962 Supplement, Part 2*, 635 (1962); *AEC-tr-5589*, **1**, 238 (1963).

A. P. Babichev, A. I. Karchevskii and Yu. A. Muromkin: Helical instability of a toroidal discharge in a varying magnetic field. *Zh. Eksp. Teor. Fiz.*, **43**, 881 (1962); *Soviet Physics, J.E.T.P.*, **16** (3), 625 (1963).

B. B. Kadomtsev: Turbulent discharge in a longitudinal magnetic field. *Nuclear Fusion, 1962 Supplement, Part 3*, 969 (1962); *AEC-tr-5589*, **1**, 438 (1963).

D. P. Ivanov and V. D. Kirillov: Investigations of a toroidal discharge in a rapidly varying longitudinal magnetic field. *Soviet Physics Doklady*, **5**, 820 (1961); *Doklady Akad. Nauk*, **133** (4), 793 (1960).

D. J. Lees and M. G. Rusbridge: Magnetic field diffusion in Zeta. *Phys. Fluids*, **4**, 653 (1961).

W. M. Burton, E. P. Butt, H. C. Cole, A. Gibson, D. Mason, R. S. Pease, K. Whiteman and R. Wilson: Plasma loss in Zeta. *Nuclear Fusion, 1963 Supplement, Part 3*, 903 (1963).

A. A. Ware: Comparison between theory and experiment for the stability of the toroidal pinch discharge. *Nuclear Fusion, 1962 Supplement, Part 3*, 869 (1963).

G. N. Harding and V. Roberts: Spectroscopic investigation of plasma in the wavelength range 0·1–2·0 mm. *Nuclear Fusion, 1962 Supplement, Part 3*, 883 (1963).

B. B. Jones and R. Wilson: Spectroscopic studies of ion energies in Zeta. *Nuclear Fusion, 1962 Supplement, Part 3*, 889 (1963).

M. G. Rusbridge, D. J. Lees and P. A. H. Saunders: Electric and magnetic field fluctuations in high-current toroidal discharges. *Nuclear Fusion, 1962 Supplement, Part 3,* 895 (1963).

D. H. Birdsall, S. A. Colgate, H. P. Furth, C. W. Hartman and R. L. Spoerlein: Particle motion on magnetic flux surfaces in stabilised and hard-core pinches. *Nuclear Fusion, 1962 Supplement, Part 3,* 955 (1963).

G. G. Dolgov-Saveliev, D. P. Ivanov, V. S. Mukhovatov, K. A. Razumova, V. S. Strelkov, M. N. Shepelyev and N. A. Yavlinskii: Investigations of the stability and heating of plasmas in toroidal chambers. *Proc. 2nd U.N. conf. on peaceful uses of atomic energy,* **32,** 82. U.N., Geneva, 1958.

V. D. Kirillov: Radiation energy losses in a plasma. *Zh. Tech. Fiz.,* **30,** 320 (1960); *Soviet Physics, Technical Physics,* **5,** 295 (1960).

G. G. Dolgov-Saveliev, V. S. Mukhovatov, V. S. Strelkov, M. N. Shepelev and N. A. Yavlinskii: Toroidal discharge in a strong magnetic field. *Zh. Eksp. Teor. Fiz.,* **38,** 394 (1960); *Soviet Physics, J.E.T.P.,* **11,** 287 (1960).

V. S. Vasil'evskii, V. S. Mukhovatov, V. S. Strelkov and N. A. Yavlinskii: Tokomak-2, A toroidal system with strong magnetic field. *Zh. Tech. Fiz.,* **30,** 1137 (1960); *Soviet Physics, Technical Physics,* **5,** 1075 (1961).

E. P. Gorbunov, G. G. Dolgov-Saveliev, V. S. Mukhovatov, V. S. Strelkov and N. A. Yavlinskii: Investigation of a toroidal discharge in a strong magnetic field. *Zh. Tech. Fiz.,* **30,** 1152 (1960); *Soviet Physics, Technical Physics,* **5,** 1089 (1961).

D. P. Ivanov and K. A. Razumova: Investigation of a toroidal discharge in a varying longitudinal magnetic field. *Nuclear Fusion, 1962 Supplement, Part 2,* 741 (1962); *AEC-tr-5589,* **1,** 295 (1963).

E. P. Gorbunov, G. G. Dolgov-Saveliev, K. B. Kartashev, V. S. Mukhovatov, V. S. Strelkov, M. N. Shepelev and N. A. Yavlinskii: Experimental investigation of Joule heating of plasma in a strong magnetic field. *Nuclear Fusion, 1962 Supplement, Part 3,* 941 (1962); *AEC-tr-5589,* **1,** 412 (1963).

V. G. Koloshnikov and S. L. Mandel'shtam: Spectroscopic measurement of ion temperature with the 'Tokomak' apparatus. *Nuclear Fusion, 1962 Supplement, Part 3,* 1232 (1962); *AEC-tr-5589,* **2,** 861 (1963).

L. A. Artsimovich and K. B. Kartashev: Effect of a transverse magnetic field on toroidal discharge. *Doklady Akad. Nauk SSSR,* **146,** 1305 (1962); *Soviet Physics Doklady,* **7,** 919 (1963).

S. A. Colgate and H. P. Furth: Stabilisation of pinch discharges. *Phys. Fluids,* **3,** 982 (1960).

W. A. Newcomb and A. N. Kaufman: Hydromagnetic stability of a tubular pinch. *Phys. Fluids,* **4,** 314 (1961).

P. H. Rebut: Instabilités non magnétohydrodynamiques dans les plasma à densité de courant élevé. *J. Nuclear Energy, Part C,* **4,** 159 (1962).

K. Aitken, R. Bickerton, R. Hardcastle, J. Jukes, P. Reynolds and I. Spalding: Pinch stability: theory and experiment. *Nuclear Fusion, 1962 Supplement, Part 3,* 979 (1963).

J. Adam, P. Ginot, P. H. Rebut and A. Torossian: Étude experimentale d'une décharge de striction tubulaire. *Nuclear Fusion, 1962 Supplement, Part 3,* 1001 (1963).

H. P. Furth, J. Killeen and M. N. Rosenbluth: Finite-resistivity instabilities of a sheet pinch. *Phys. Fluids,* **6,** 459 (1963).

M. Cotsaftis, M. Mercier and P. H. Rebut: Équilibres voisins et stabilités des plasmas cylindriques. *J. Nuclear Energy, Part C,* **5,** 1 (1963).

P. H. Rebut and A. Torossian: Plasma stability in an inverse pinch discharge. *Phys. Letters,* **2,** 52 (1962).

P. H. Rebut and A. Torossian: Plasmas stables dans une décharge du type 'striction inverse'. *J. Nuclear Energy, Part C,* **5,** 133 (1963).

## CHAPTER VII

M. N. ROSENBLUTH and C. L. LONGMIRE: Stability of plasmas confined by magnetic fields. *Annals of Physics*, **1**, 120 (1957).

B. B. KADOMTSEV: Magnetic traps with a 'corrugated' field. *Fizika Plazmy*, **3**, 285. Akad. Nauk SSSR, 1958; *Plasma Physics* (Ed. Leontovich), **3**, 340. Pergamon Press, 1959.

B. B. KADOMTSEV: Magnetic traps for plasma. *Fizika Plazmy*, **4**, 353. Akad. Nauk SSSR, 1958; *Plasma Physics* (Ed. Leontovich), **4**, 417. Pergamon Press, 1959.

L. SPITZER: Particle diffusion across a magnetic field. *Phys. Fluids*, **3**, 659 (1960).

B. B. KADOMTSEV: Plasma turbulence in a magnetic mirror system. *Zh. Eksp. Teor. Fiz.*, **40**, 328 (1961); *Soviet Physics, J.E.T.P.*, **13**, 223 (1961).

B. B. KADOMTSEV: Turbulent loss of particles from a discharge in a strong magnetic field. *Zh. Tech. Fiz.*, **31**, 1209 (1961); *Soviet Physics, Technical Physics*, **6**, 882 (1962).

L. I. RUDAKOV and R. Z. SAGDEEV: A quasi-hydrodynamic description of a rarefied plasma in a magnetic field. *Fizika Plazmy*, **3**, 268. Akad. Nauk SSSR, 1958; *Plasma Physics* (Ed. Leontovich), **3**, 321. Pergamon Press, 1959.

A. A. VEDENOV, E. P. VELIKHOV and R. Z. SAGDEEV: Stability of plasma. *Usp. Fiz. Nauk*, **73**, 701 (1961); *Sov. Phys. Usp.*, **4**, 332 (1961).

M. N. ROSENBLUTH, N. A. KRALL and N. ROSTOKER: Finite Larmor radius stabilisation of 'weakly' unstable confined plasmas. *Nuclear Fusion, 1962 Supplement, Part 1*, 143 (1962).

L. I. RUDAKOV and R. Z. SAGDEEV: Microscopic instabilities of spatially inhomogeneous plasma in a magnetic field. *Nuclear Fusion, 1962 Supplement, Part 2*, 481 (1962); *AEC-tr-5589*, **1**, 268 (1963).

I. F. KHARCHENKO, YA. B. FAINBERG, R. M. NIKOLAEV, E. A. KORNILOV, E. I. LUTSENKO and N. S. PEDENKO: Interaction of an electron beam with a plasma in a magnetic field. *Nuclear Fusion, 1962 Supplement, Part 3*, 1101 (1962); *AEC-tr-5589*, **1**, 463 (1963).

I. F. KHARCHENKO and J. B. FAINBERG: The interaction of an electron beam with plasma in a magnetic field. *Zh. Tech. Fiz.*, **31**, 761 (1961); *Soviet Physics, Technical Physics*, **6** (7), 551 (1962).

YA. B. FAINBERG: The interaction of charged particle beams with plasma. *Atomnaya Energiya*, **11**, 313 (1961); *J. Nuclear Energy, Part C*, **4**, 203 (1962).

A. B. MIKHAILOVSKII and L. I. RUDAKOV: On the stability of a spatially inhomogeneous plasma in a magnetic field. *Zh. Eksp. Teor. Fiz.*, **44**, 912 (1963); *Soviet Physics, J.E.T.P.*, **17** (3), 621 (1963).

I. B. BERNSTEIN and R. M. KULSRUD: Ion wave instabilities. *Phys. Fluids*, **3**, 937 (1960).

R. Z. SAGDEEV and V. D. SHAFRANOV: On the stability of plasma with an anisotropic distribution of velocities in a magnetic field. *Soviet Physics, J.E.T.P.*, **12**, 130 (1961); *Zh. Eksp. Teor. Fiz.*, **39**, 131 (1960).

A. I. AKHIEZER, G. YA. LYUBARSKII and R. V. POLOVIN: On the conditions of electron distribution functions in a plasma. *Zh. Eksp. Teor. Fiz.*, **40**, 963 (1961); *Soviet Physics, J.E.T.P.*, **13** (3), 673 (1963).

C. ETIEVANT: Expérience d'interaction faisceau-plasma en présence de champ magnétique. *Nuclear Fusion, 1962 Supplement, Part 3*, 1025 (1963).

W. E. DRUMMOND and D. PINES: Non-linear stability of plasma oscillations. *Nuclear Fusion, 1962 Supplement, Part 3*, 1049 (1963).

B. B. KADOMTSEV and A. V. TIMOFEEV: Drift fluctuations in nonhomogeneous plasma in a magnetic field. *Doklady Akad. Nauk SSSR*, **146**, 581 (1962); *Soviet Physics Doklady*, **7**, 826 (1963).

B. A. TRUBNIKOV: Plasma radiation in a magnetic field. *Doklady Akad. Nauk SSSR*, **118**, 913 (1958); *Soviet Physics Doklady*, **3**, 136 (1958).

B. A. TRUBNIKOV and A. E. BAZHANOVA: Magnetic radiation from a plasma layer. *Fizika Plazmy*, 3, 121. Akad. Nauk SSSR, 1958; *Plasma Physics* (Ed. Leontovich), 3, 141. Pergamon Press, 1959.

B. A. TRUBNIKOV and V. B. YAKUBOV: Cyclotron radiation of electrons having a two-dimensional Maxwellian distribution. *J. Nuclear Energy, Part C*, **5**, 7 (1963).

## CHAPTER VIII

L. SPITZER: The Stellarator Concept. *Proc. 2nd U.N. conf. on peaceful uses of atomic energy*, **32**, 181. U.N., Geneva, 1958.

A. I. MOROZOV and L. S. SOLOV'EV: The motion of particles in a helical toroidal magnetic field. *Zh. Tech. Fiz.*, **30**, 271 (1960); *Soviet Physics, Technical Physics*, **5**, 250 (1960).

C. R. BURNETT, D. J. GROVE, R. W. PALLADINO, T. H. STIX and K. E. WAKEFIELD: The divertor, a device for reducing the impurity level in a Stellarator. *Phys. Fluids*, **1**, 438 (1958).

J. M. BERGER, I. B. BERNSTEIN, E. A. FRIEMAN and R. M. KULSRUD: On the ionisation and ohmic heating of a helium plasma. *Phys. Fluids*, **1**, 297 (1958).

W. BERNSTEIN, F. F. CHEN, M. A. HEALD and A. Z. KRANZ: 'Runaway' electrons and co-operative phenomena in B-1 Stellarator discharges. *Phys. Fluids*, **1**, 430 (1958).

M. D. KRUSKAL, J. L. JOHNSON, M. B. GOTTLIEB and L. M. GOLDMAN: Hydromagnetic instability in a Stellarator. *Phys. Fluids*, **1**, 421 (1958).

T. COOR, S. P. CUNNINGHAM, R. A. ELLIS, M. A. HEALD and A. Z. KRANZ: Experiments on the ohmic heating and confinement of plasma in a Stellarator. *Proc. 2nd U.N. conf. on peaceful uses of atomic energy*, **32**, 201. U.N., Geneva, 1958.

T. H. STIX and R. W. PALLADINO: Ion cyclotron resonance. *Proc. 2nd U.N. conf. on peaceful uses of atomic energy*, **31**, 282. U.N., Geneva, 1958.

J. M. BERGER, W. A. NEWCOMB J. M. DAWSON, E. A. FRIEMAN, R. M. KULSRUD and A. LENARD: Heating of a confined plasma by oscillating electromagnetic fields. *Proc. 2nd U.N. conf. on peaceful uses of atomic energy*, **31**, 112. U.N., Geneva, 1958.

W. BERNSTEIN and A. Z. KRANZ: Ohmic heating in the B-1 Stellarator. *Phys. Fluids*, **2** 57 (1959).

R. A. ELLIS, L. P. GOLDBERG and J. G. GORMAN: Loss of charged particles in a Stellarator during ohmic heating. *Phys. Fluids*, **3**, 468 (1960).

R. A. ELLIS, L. P. GOLDBERG and J. G. GORMAN: Possibility of an electrostatic instability in a Stellarator. *Phys. Fluids*, **3**, 797 (1960).

W. STODIEK, R. A. ELLIS and J. G. GORMAN: Loss of charged particles during ionisation in Stellarator discharges. *Phys. Fluids*, **3**, 1035 (1960).

T. H. STIX: Absorption of plasma waves. *Phys. Fluids*, **3**, 19 (1960).

T. H. STIX and R. W. PALLADINO: Observation of ion cyclotron waves. *Phys. Fluids*, **3**, 641 (1960).

L. S. BOGDANKEVICH, A. A. RUKHADZE and V. P. SILIN: Cyclotron absorption of electromagnetic waves in a plasma. *Nuclear Fusion, 1962 Supplement, Part 2*, 755 (1962); *AEC-tr-5589*, **1**, 357 (1963).

A. V. BARTOV, E. K. ZAVOISKII, I. A. KOVAN, B. I. PATRUSHEV, V. D. RUSANOV and D. A. FRANK-KAMENETSKII: Experimental investigation of magnetic-acoustic resonance. *Nuclear Fusion, 1962 Supplement, Part 3*, 1067 (1962); *AEC-tr-5589*, **1**, 383 (1963).

M. V. Babykin, E. K. Zavoiskii, L. I. Rudakov and V. A. Skoryukin: Absorption of energy of alternating electromagnetic fields of large amplitude by a plasma. *Nuclear Fusion, 1962 Supplement, Part 3,* 1073 (1962); *AEC-tr-5589,* **1**, 399 (1963).

N. I. Nazarov, A. I. Ermakov, A. S. Lobko, V. A. Bondarev, V. T. Tolok and K. D. Sinel'nikov: Investigation of ion cyclotron waves. *Nuclear Fusion, 1962 Supplement, Part 3,* 1079 (1962); *AEC-tr-5589,* **1**, 479 (1963).

W. Stodiek, R. A. Ellis, Jr., and J. G. Gorman: Loss of charged particles in a Stellarator. *Nuclear Fusion, 1962 Supplement, Part 1,* 193 (1962).

R. W. Motley: Diffusion of plasma from the Stellarator. *Nuclear Fusion, 1962 Supplement, Part 1,* 199 (1962).

D. J. Grove, R. M. Sinclair, W. Stodiek, W. L. Harries and L. P. Goldberg: Some preliminary results on containment time in the Model C Stellarator. *Nuclear Fusion, 1962 Supplement, Part 1,* 203 (1962).

W. M. Hooke, P. Avivi, M. Brennan, M. A. Rothman and T. H. Stix: Experiments on ion cyclotron waves. *Nuclear Fusion, 1962 Supplement, Part 3,* 1083 (1963).

G. I. Budker: Thermonuclear reactions in a system with magnetic stoppers and the problem of direct transformation of thermonuclear energy into electrical energy. *Fizika Plazmy,* 3, 3. Akad. Nauk SSSR, 1958; *Plasma Physics* (Ed. Leontovich), 3, 1. Pergamon Press, 1959.

V. D. Fedorchenko, B. N. Rutkevich and B. M. Cherni: Motion of an electron in a spatially periodic magnetic field. *Zh. Tech. Fiz.,* **29**, 1212 (1959); *Soviet Physics, Technical Physics,* **4**, 1112 (1960).

K. D. Sinelnikov, B. N. Rutkevich and V. D. Fedorchenko: The motion of charged particles in a spatially periodic magnetic field. *Zh. Tech. Fiz.,* **30**, 249 (1960); *Soviet Physics, Technical Physics,* **5**, 229 (1960).

H. Dreicer, H. J. Karr, E. A. Knapp, J. A. Phillips, E. J. Stovall, Jr., and J. L. Tuck: Cyclotron resonance in the static magnetic field of a helix. *Nuclear Fusion, 1962 Supplement, Part 1,* 299 (1962).

R. F. Post: Summary of UCRL Pyrotron (Mirror Machine) Programme. *Proc. 2nd U.N. conf. on peaceful uses of atomic energy,* **32**, 245. U.N., Geneva, 1958.

F. H. Coensgen, W. F. Cummins and A. E. Sherman: Multistage magnetic compression of highly ionised plasma. *Phys. Fluids,* **2**, 350 (1959).

R. F. Post, R. E. Ellis, F. C. Ford and M. N. Rosenbluth: Stable confinement of a high temperature plasma. *Phys. Rev. Letters,* **4**, 166 (1960).

F. H. Coensgen, W. F. Cummins, W. E. Nexen, Jr., and A. E. Sherman: Evidence of containment of a 3-keV deuterium plasma. *Phys. Rev. Letters,* **5**, 459 (1960).

F. H. Coensgen, W. F. Cummins, W. E. Nexen, jr., and A. E. Sherman: Production and containment of hot deuterium plasmas in multistage magnetic compression experiments. *Nuclear Fusion, 1962 Supplement, Part 1,* 125 (1962).

M. S. Ioffe, R. I. Sobolev, V. G. Tel'kovskii and E. E. Yushmanov: Magnetic mirror confinement of a plasma. *Zh. Eksp. Teor. Fiz.,* **39**, 1602 (1960); *Soviet Physics, J.E.T.P.,* **12**, 1117 (1961).

M. S. Ioffe, R. I. Sobolev, V. G. Tel'kovskii and E. E. Yushmanov: Loss of plasma from a magnetic mirror system. *Zh. Eksp. Teor. Fiz.,* **40**, 40 (1961); *Soviet Physics, J.E.T.P.,* **13**, 27 (1961).

M. S. Ioffe and E. E. Yushmanov: Experimental investigation of plasma instability in a magnetic mirror trap. *Nuclear Fusion, 1962 Supplement, Part 1,* 177 (1962); *AEC-tr-5589,* **1**, 83 (1963).

Yu. V. Gott and V. G. Tel'kovskii: Measurement of the energy of ions in a trap with magnetic mirrors. *Nuclear Fusion, 1962 Supplement, Part 3,* 1227 (1962); *AEC-tr-5589,* **2**, 626 (1963).

Yu. V. Gott and V. G. Tel'kovskii: Determination of the lifetime of a high-temperature plasma by neutron radiation. *Zh. Eksp. Teor. Fiz.,* **43**, 831 (1962); *Soviet Physics, J.E.T.P.,* **16** (3), 588 (1963).

K. BOYER, J. E. HAMMEL, C. L. LONGMIRE, D. NAGLE, F. L. RIBE and W. B. RIESENFELD: Theoretical and experimental discussion of 'Ixion' a possible thermonuclear device. *Proc. 2nd U.N. conf. on peaceful uses of atomic energy*, **31**, 319. U.N., Geneva, 1958.

I. N. GOLOVIN: Studies of trapping fast charged particles in a constant magnetic field. *Proc. I.E.E., 106A, Supplement No. 2*, 95 (1959).

I. N. GOLOVIN, L. I. ARTEMENKOV, G. F. BOGDANOV, D. A. PANOV, V. I. PISTUNOVICH and N. N. SEMASHKO: Work with the experimental thermonuclear system OGRA. *Usp. Fiz. Nauk*, **73**, 685 (1961); *Sov. Phys. Usp.*, **4**, 323 (1961).

G. F. BOGDANOV, I. N. GOLOVIN, YU. A. KUCHERYAEV and D. A. PANOV: Properties of a plasma formed by the injection into Ogra of a beam of fast molecular hydrogen ions. *Nuclear Fusion, 1962 Supplement, Part 1*, 215 (1962); *AEC-tr-5589*, **1**, 29 (1963).

A. E. BAZHANOVA, V. T. KARPUKHIN, A. N. KHARKHOV and V. I. PISTUNOVICH: Cyclotron and thermal radiations of plasma in Ogra. *Nuclear Fusion, 1962 Supplement, Part 1*, 227 (1962); *AEC-tr-5589*, **1**, 65 (1963).

V. M. BALEBANOV, V. B. GLASKO, V. V. KUTNETSOV, Q. G. SVESHNIKOV, N. N. SEMASHKO and A. N. TIKHONOV: Motion of individual charged particles in a trap with magnetic mirrors of the Ogra type. *Nuclear Fusion, 1962 Supplement, Part 3*, 1227 (1962); *AEC-tr-5589*, **2**, 637 (1963).

YU. A. KUCHERIAEV and D. A. PANOV: On the cause of the anomalously fast loss of electrons from the plasma in 'Ogra'. *J. Nuclear Energy, Part C*, **5**, 145 (1963).

V. I. PISTUNOVICH: Cyclotron instability of plasma in Ogra. *Atomnaya Energiya*, **14**, 72 (1963); *Soviet Atomic Energy*, **14** (1), 63 (1963).

G. M. ANTROPOV, V. A. BELYAEV and M. K. ROMANOVSKII: The behaviour of fast electrons in the electron model of a trap with magnetic stoppers. *Fizika Plazmy*, **3**, 250. Akad. Nauk SSSR, 1958; *Plasma Physics* (Ed. Leontovich), **3**, 301. Pergamon Press, 1959.

N. N. BREVNOV and YU. F. TOMACHUK: The effect of local magnetic field perturbations on confinement of particles in an adiabatic magnetic trap. *Atomnaya Energiya*, **13**, 421 (1962); *Soviet Journal of Atomic Energy*, **13**, 1037 (1963).

N. N. BREVNOV, M. K. ROMANOVSKII and YU. F. TOMACHUK: Investigation of plasma in the adiabatic 'Ogrenok' trap. *Nuclear Fusion, 1962 Supplement, Part 1*, 289; *AEC-tr-5589*, **1**, 97 (1963).

C. F. BARNETT, P. R. BELL, J. S. LUCE, E. D. SHIPLEY and A. SIMON: The Oak Ridge thermonuclear experiment. *Proc. 2nd U.N. conf. on peaceful uses of atomic energy*, **31**, 298. U.N., Geneva, 1958.

J. S. LUCE: Intense gaseous discharges. *Proc. 2nd U.N. conf. on peaceful uses of atomic energy*, **31**, 305. U.N., Geneva, 1958.

J. L. DUNLAP, C. F. BARNETT, R. A. DANDL and H. POSTMA: Radiation and ion energy distributions of the DCX-1 plasma. *Nuclear Fusion, 1962 Supplement, Part 1*, 233 (1962).

P. R. BELL, G. G. KELLEY, N. H. LAZAR and R. J. MACKIN, JR.: The DCX-2 programme of plasma accumulation by high energy injection. *Nuclear Fusion, 1962 Supplement, Part 1*, 251 (1962).

J. R. HISKES: Dissociation of molecular ions by electric and magnetic fields. *Phys. Rev.*, **122**, 1207 (1961).

D. R. SWEETMAN: Mirror machine experiments and related atomic cross-section measurements at A.W.R.E. Aldermaston. *Nuclear Fusion, 1962 Supplement, Part 1*, 279 (1962).

N. C. CHRISTOFILOS: Astron Thermonuclear Reactor. *Proc. 2nd U.N. conf. on peaceful uses of atomic energy*, **32**, 279. U.N., Geneva, 1958.

L. TONKS: The structure of the Astron E-layer. *Nuclear Fusion*, **1**, 273 (1961).

S. M. OSOVETS: Containment of a plasma by a travelling magnetic field. *Fizika Plazmy*,

**4**, 3. Akad. Nauk SSSR, 1958; *Plasma Physics* (Ed. Leontovich), **4**, 1. Pergamon Press, 1959.

T. F. Volkov: Effect of a high-frequency electro-magnetic field on plasma oscillations. *Fizika Plazmy*, **4**, 98. Akad. Nauk SSSR, 1958; *Plasma Physics* (Ed. Leontovich), **4**, 114. Pergamon Press, 1959.

T. F. Volkov: Oscillations and stability of the surface of a plasma in the field of a travelling electromagnetic wave. *Fizika Plazmy*, **4**, 109. Akad. Nauk SSSR, 1958; *Plasma Physics* (Ed. Leontovich), **4**, 127. Pergamon Press, 1959.

A. A. Vedenov, T. F. Volkov, L. I. Rudakov, R. Z. Sagdeev, V. M. Glagolev, G. A. Yeliseyev and V. V. Khilil: Thermal insulation and confinement of plasma with a high-frequency electro-magnetic field. *Proc. 2nd U.N. conf. on peaceful uses of atomic energy*, **32**, 239. U.N., Geneva, 1958.

J. W. Butler, A. J. Hatch and A. J. Ulrich: Radio frequency thermonuclear machines. *Proc. 2nd U.N. conf. on peaceful uses of atomic energy*, **32**, 324. U.N., Geneva, 1958.

R. Z. Sagdeev: Containment of a plasma by the pressure of a standing electro-magnetic wave. *Fizika Plazmy*, **3**, 346. Akad. Nauk SSSR, 1958; *Plasma Physics* (Ed. Leontovich), **3**, 406. Pergamon Press, 1959.

Yu. I. Arsen'ev, V. M. Glagolev, G. A. Eliseev and N. S. Cheverev: Experiments on interaction of a plasma with an electro-magnetic field with a cavity resonator. *Nuclear Fusion, 1962 Supplement, Part 2*, 687 (1962); *AEC-tr-5589*, **1**, 253 (1963).

R. A. Demirkhanov, Yu. S. Khodyrev, N. I. Leont'ev and T. I. Gutkin: Interaction of high-frequency electromagnetic fields with a plasma. *Nuclear Fusion, 1962 Supplement, Part 1*, **259** (1962); *AEC-tr-5589*, **1**, 126 (1963).

V. G. Andreev, I. A. Borzunov, E. L. Burshtein, B. T. Zarubin, Yu. N. Knizhmikov, N. Ya. Kuz'mina, M. L. Levin, A. V. Mishchenko, I. A. Popov, I. Kh. Nevyazhskii, S. M. Osovets, Yr. F. Petrov, B. I. Polyakov, V. F. Trubetskoi, K. V. Khodataev and N. N. Yakovelev: System for the confinement of a plasma by the field of a travelling wave. *Nuclear Fusion, 1962 Supplement, Part 3*, 1233 (1962); *AEC-tr-5589*, **2**, 869 (1963).

M. L. Levin and M. S. Rabinovich: Method of strong focusing for stabilisation of straight and toroidal discharges. *Nuclear Fusion, 1962 Supplement, Part 3*, 1233 (1962); *AEC-tr-5589*, **2**, 888 (1963).

O. B. Kirsov: A plasma in a 'magnetic grid'. *Fizika Plazmy*, **3**, 327. Akad. Nauk SSSR, 1958; *Plasma Physics* (Ed. Leontovich), **3**, 386. Pergamon Press, 1959.

J. Berkowitz, K. O. Freidrichs, H. Goertzel, H. Grad, J. Killeen and E. Rubin: Cusped geometries. *Proc. 2nd U.N. conf. on peaceful uses of atomic energy*, **31**, 171. U.N., Geneva, 1958.

I. M. Podgornyi and V. N. Sumarokov: The injection of plasmoids into a magnetic trap with a field which increases towards the periphery. *Journal of Nuclear Energy, Part C*, **1**, 236 (1960).

H. Grad: Plasma trapping in cusped geometries. *Phys. Rev. Letters*, **4**, 222 (1960).

F. R. Scott and R. F. Wenzel: Experimental plasma flow into a vacuum magnetic cusp field. *Phys. Rev.*, **119**, 1187 (1960).

S. Yu. Lukyanov, I. M. Podgornyi and V. N. Sumarokov: Plasma confinement in a trap with a magnetic field that increases towards the periphery. *Zh. Eksp. Teor. Fiz.*, **40**, 448 (1961); *Soviet Physics, J.E.T.P.*, **3**, 308, 1961.

N. G. Koval'skii, S. Yu. Luk'yanov and I. M. Podgornyi: Investigation of behaviour of plasma in the Orekh magnetic trap. *Nuclear Fusion, 1962 Supplement, Part 1*, 81 (1962); *AEC-tr-5589*, **1**, 1 (1963).

I. M. Podgornyi and V. I. Sumarokov: Plasma trapping in a radially increasing magnetic field. *Nuclear Fusion, 1962 Supplement, Part 1*, 87 (1962); *AEC-tr-5589*, **1**, 15 (1963).

S. Yu. Luk'yanov and I. M. Podgornyi: Cusped geometry magnetic traps. *Atomnaya Energiya*, **11**, 336 (1961); *J. Nuclear Energy, Part C*, **4**, 135 (1962).

T. K. Allen and R. J. Bickerton: Experiments on the compression of plasma in cusp geometry. *Nature*, **191**, 794 (1961).

T. K. Allen, R. W. P. McWhirter and I. J. Spalding: Experiments on cusp compression. *Nuclear Fusion, 1962 Supplement, Part 1*, 67 (1962).

I. L. Gorelik, N. G. Koval'skii, I. M. Podgornyi and V. V. Sinitsyn: Investigation of plasma escape through magnetic gaps of traps with a field growing to the periphery. *Doklady Akad. Nauk SSSR*, **147**, 576 (1962); *Soviet Physics Doklady*, **7** (11), 1021 (1963).

D. C. Hagerman: Some experimental studies of plasma injected into a cusped magnetic field. *Nuclear Fusion, 1962 Supplement, Part 1*, 75 (1962).

Yu. V. Gott, M. S. Ioffe, V. G. Tel'kovskii: Some new results on confinement in magnetic traps. *Nuclear Fusion, 1962 Supplement, Part 3*, 1045 (1962).

V. M. Balebanov, B. I. Volkov, V. B. Glasko, A. L. Groshev, V. V. Kuznetsov, A. C. Sveshnikov and N. N. Semashko: Motion of the individual charged particles in a magnetic field which increases towards the periphery. *J. Nuclear Energy, Part C*, **5**, 205 (1963).

Yu. T. Baiborodov, M. S. Ioffe, V. M. Petrov and R. I. Sobolev: An adiabatic trap with combined magnetic fields. *Atomnaya Energiya*, **14** (5), 443 (1963); *J. Nuclear Energy, Part C*, **5**, 409 (1963).

## CHAPTER IX

L. A. Artsimovich: Controlled nuclear fusion research, September 1961: Review of experimental results. *Nuclear Fusion, 1962 Supplement, Part 1*, 15 (1962).

M. N. Rosenbluth: Controlled nuclear fusion research, September 1961: Review or theoretical results. *Nuclear Fusion, 1962 Supplement, Part 1*, 21 (1962).

# PRINCIPAL SYMBOLS

| | |
|---|---|
| $\boldsymbol{A}$, $A$ | magnetic vector potential |
| $A$ | a dimensionless plasma thickness ($4\pi nea/H$) (Ch. VII) |
| $\boldsymbol{a}$ | acceleration |
| $a$ | radius of a plasma cylinder; minor radius of a plasma ring |
| $B$ | magnetic induction |
| $b_o$ | coefficient of $T^{3/2}$ in formula for electrical conductivity |
| $C$ | capacitance; a constant (various) |
| $c$ | velocity of light |
| $D$ | coefficient of diffusion |
| $d$ | a displacement distance; an electrostatic shielding distance (Ch. II); total differential |
| $\boldsymbol{E}$, $E$ | electric field |
| $E_c$ | critical electric field for runaway electrons |
| $\Delta E$ | energy difference between two bound levels |
| $e$ | numerical value of the electron charge (in e.s.u.) |
| $\boldsymbol{F}$, $F$ | force |
| $F, f$ | function |
| $g$ | thermonuclear reaction rate per unit volume |
| $\boldsymbol{H}$, $H$ | magnetic field |
| $H_J$ | self-magnetic field at the boundary of a pinch |
| $\boldsymbol{h}$ | unit vector parallel to $\boldsymbol{H}$ |
| $h$ | Planck's constant; a magnetic field parameter (§ 8.7); |
| $h$ | height of a flute perturbation |
| $i$ | $\sqrt{-1}$ |
| $J$ | total current |
| $\boldsymbol{j}$, $j$ | current density |
| $k$ | Boltzmann's constant; wave number; a magnetic field parameter (§ 2.3): scaling factor (§ 8.20) |
| $L$ | Inductance; length (various) |
| $L_c$ | Coulomb logarithm |
| $l$ | length |
| $M$ | mass |
| $m$ | mass of a particle; azimuthal mode number |
| $m_e$ | electron mass |
| $m_i$ | ion mass |
| $m_o$ | rest mass of the electron (§ 7.8) |
| $N$ | number of particles of one sign per unit length |
| $n$ | number of particles of one sign per unit volume (number density); number of independent helical windings in the Stellarator |
| $P$ | electric polarization |
| $\boldsymbol{p}$, $p$ | momentum of a particle |
| $p$ | pressure |
| $Q$ | power; power per unit volume; surface charge on a side of a flute perturbation |
| $q$ | electric charge of a particle; generalized spatial co-ordinate; parameter in the stabilized pinch; a scaling parameter (§ 8.9) |
| $R$ | major radius; radius of curvature; power ratio (Ch. I) |
| $\boldsymbol{r}$, $r$ | radius |
| $r_o$ | radial distances (various); classical radius of electron (§ 7.8) |
| $r_D$ | Debye shielding distance $(kT/4\pi ne^2)^{1/2}$ |
| $S$, $s$ | cross-sectional area |
| $T$ | temperature in °K |
| $t$ | time |
| $t_H$ | cyclotron period ($\equiv 2\pi/\omega_H$) |
| $U$ | potential energy; $-\int dl/H$ (Ch. VII) |
| $\boldsymbol{u}$, $u$ | drift velocity |
| $V$ | electric potential; voltage |
| $\boldsymbol{v}$, $\mathrm{v}$ | velocity, speed |
| $\boldsymbol{v}_d$, $v_d$ | drift velocity of the guiding centre |
| $v_p$ | phase velocity of waves |

| | |
|---|---|
| $W$ | energy |
| $x, y, z$ | co-ordinates |
| $Z$ | (ionic charge)/$e$ |
| $\alpha$ | angle between particle velocity and $H$; angle; various coefficients; fractional amplitude of magnetic field variation (Ch. VIII) |
| $\alpha_0$ | semi-angle of loss cone in adiabatic traps |
| $\alpha_T$ | coefficient of $T^{5/2}$ in formula for thermal conductivity |
| $\beta$ | $8\pi p/H^2$; ratio of plasma pressure to self-magnetic pressure in a pinch |
| $\gamma$ | ratio of specific heats; various ratios |
| $\delta$ | resistive skin depth; displacement of plasma ring in a conducting torus |
| $\varepsilon$ | dielectric constant; energy density (Ch. VII); ratio of magnetic field strengths |
| $\varepsilon_m$ | dielectric constant of plasma in a magnetic field |
| $\zeta$ | a parameter of motion (Ch. VII) |
| $\zeta_0$ | relativistic correction to formula for bremsstrahlung power |
| $\eta$ | efficiency |
| $\theta$ | coordinate; temperature in electron volts; angle (various) |
| $\lambda$ | collision mean-free-path; wavelength |
| $\mu$ | magnetic moment ($\equiv W_\perp/H$); the quantity $H_\theta/rH_z$; an abbreviation (Ch. V) |
| $\nu$ | frequency of radiation; collision frequency; damping coefficient; growth rate |
| $\xi$ | inductance per unit length |
| $\rho$ | mass density |
| $\rho_H$ | Larmor radius ($mvc/qH$) |
| $\rho_{He}$ | electron Larmor radius |
| $\rho_{Hi}$ | ion Larmor radius |
| $\sigma$ | cross-section; electrical conductivity |
| $\sigma_T$ | thermal conductivity |
| $\tau$ | characteristic time; collision time |
| $\tau_p$ | confinement time for thermonuclear energy balance |
| $\tau_{ee}$, $\tau_{ei}$, $\tau_{ii}$ | collision time for electrons with electrons, electrons with ions, and ions with ions |
| $\tau_{eq}$ | characteristic time for collisional relaxation of ion-electron temperature differences |
| $\Phi$ | magnetic flux |
| $\phi$ | electrostatic potential; various functions |
| $\chi$ | thermal diffusivity |
| $\psi$ | rotational transform angle; azimuthal drift angle; an effective potential in high-frequency fields (§ 8.16) |
| $\Omega$ | volume; resistance |
| $\omega$ | angular frequency |
| $\omega_0$ | Langmuir frequency $(4\pi n_e e^2/m_e)^{\frac{1}{2}}$ |
| $\omega_H$ | cyclotron frequency ($qH/mc$) |
| $\omega_{He}$ | electron cyclotron frequency |
| $\omega_{Hi}$ | ion cyclotron frequency |

## SUBSCRIPT SYMBOLS

| | |
|---|---|
| $_e$ | pertaining to the electron(s) |
| $_i$ | pertaining to the ion(s) |
| $_\perp$ | perpendicular to (usually, the magnetic field) |
| | parallel to (usually, the magnetic field) |
| $_{\mathbf{o}}$ | outside the plasma |
| $_{\mathbf{i}}$ | inside the plasma |
| $_0$ | initial value, zero-order, etc. |

# INDEX

Absorption
  cyclotron, 106
  of radiation, 195, 282
Accelerators (plasma)
  coaxial plasma, 167
  pinch, 171
  rail, 165
  wire, 166
Adiabatic
  compression theory, 34–36
  compression experiments, 325 et seq.
  expansion, 16
  invariance, 30–32, 247
  invariant of parallel motion, 37
  invariant of transverse motion
    experiment, 31–33
    theory, 23–26
  linear pinch, 126
  motion in hybrid traps, 376
  $\theta$-pinch, 156
Alfvén waves, 105–106, 108
Alpha, 193, 196, 197, 201–204, 208, 224
  ion temperature, 201
Anisotropic plasma pressure, 253
Anisotropy
  diffusion, 71–72
  of electrical conductivity, 67, 71, 200, 225–228
  thermal conductivity, 75
Anomalous
  diffusion (see Diffusion)
  dispersion, 106
  resistance, 207
Apparatus effect, 211, 218
Astron, 241, 349–351
Axial compression, 36

'Barring', 198
Beam
  ion, 344, 347
  instability, 269–277
  interaction of neutral, 322
  randomisation (in DCX), 348
$\beta$-particles, 31–32
Betratron
  acceleration, 141
  condition, 163
  radiation from plasma, 9, 281–285, 318
Bohm diffusion, 75, 76, 308, 309
Boltzmann equation, 77
Boundary layer of plasma
  collisionless structure, 96–100
  diffusion broadening, 95–96
  in cusp geometry, 364–366
  in H.F. fields, 357
  pressure balance, 10, 83
Braginskii-Pease limiting current, 87
Branching ratio, 1
Bremsstrahlung, 6–7, 52, 86–87, 118, 121, 137
Bumpy torus, 242
Burn-out, 340–342
  DCX, 347–348
  of impurities, 228
  OGRA, 344

Cameras
  drum, 211
  framing, 112, 152, 371–372
  streak, 112, 151, 198, 213
Charge exchange
  energy loss, 217, 327
  fundamentals, 56–60
  in pinches, 128
  particle losses, 318, 327, 332, 341, 348, 378
Charged particles (see Motion of charged particles)
Circuit
  biasing, 187
  clamp, 187
Clamping, 187, 198
Collisions
  and electrical resistance, 61–63
  between like particles, 72
  Coulomb, 38–42, 64, 67
  in the plasma boundary, 100
  ionising collisions, 49–51
  ion-neutral, 51, 56–60
  mirror losses, 315–317
  scattering, 48–49
Collision mean free path, definition, 40
Collision times, 41–42
Compression of plasma
  in cusp geometry, 375
  in mirror geometry, 324–327
  in pinch, 231–233
  multi-stage, 328–329
Conducting metallic shell
  and toroidal equilibria, 90–92, 94
  stabilising effect, 174–177
Conductivity, electrical
  effect on stability, 234, 265–267
  experimental values, 160, 199, 201, 207, 213–214, 223–229, 306

Conductivity, electrical—*cont.*
  theory, 60–63, 70–71, 74, 79–81
  with impurities, 190
Conductivity, thermal, 5, 67, 74, 75
Containment time
  cusps, 374–375
  for thermonuclear energy balance, 11, 13, 15, 142, 366
  hybrid traps, 378–379
  in pinches, 142, 223
  in Stellarator, 308
  mirror machines, 326–327, 329, 333–335, 347–349
  theory, 268
Continuum intensity, 118
Corrugated magnetic field at entrance to trap, 321–322
Coulomb logarithm, 41
Coupling coefficient, 185–186
Criterion for positive thermonuclear energy yield, 13–15
Critical
  electric field, 65
  temperature, 9
  wave-length, 191
Cross-sections
  atomic hydrogen, 50
  molecular hydrogen, 50
  of charge exchange, 55–574
  of Coulomb collisions, 38–2
  of *d–d* reaction, 2
  of *d–t* reaction, 3
  of ionisation of atoms by electrons, 50
  of ionisation of atoms by fast ions, 51
Crossed-field drift, 33, 37–38, 68–70, 276, 331, 337
Currents
  Braginskii-Pease limiting, 87
  displacement, 79
  Foucault image, 90–91, 175–176
  in Ixion, 339
Cusp geometry, 251, 311
  compression experiments, 375
  injection experiments, 367–375
  theory of, 251, 311, 361–367
Cyclotron
  frequency (definition), 23
  radiation (see Betatron radiation)
  resonance, 106, 301–304
  wave heating, 304

DCX, 261, 319, 347–349
*d–d* reactions, 1–2
*d–t* reactions, 2
Debye shielding distance, 39, 82, 104–105, 313
Deformations
  flute, 251–257
  growth rate of, 258–262
  helical, 177–180
  kink, 173–176
  normal modes, 179–180
  sausage-type, 139, 173–175
Degassing, 210
Diamagnetism of plasma, 74, 83
Dielectric constant of plasma
  with magnetic field, 68–70, 105–106, 259
  without magnetic field, 63–64
Diffusion
  anomalous, 75–76, 219, 224–228, 231, 263–269, 275–277, 280, 297, 307–310, 336
  Bohm, 75, 308, 309
  broadening of leak in cusp geometry, 366, 374–375
  due to binary collisions, 10, 70–74
  relation to skin effect, 95–96
Direct conversion of thermonuclear energy into electrical energy, 15–17
Discharges, 'fast' and 'slow', 172
Divertor, 298
Doppler broadening
  of Betatron radiation, 283
  of spectral lines, 119–120, 194, 201–202, 206, 224
Drift of charged particles
  crossed-field, 33, 37–38, 68–70, 276, 331, 337
  in arbitrary force field, 38
  in axially symmetric fields, 238, 243–249
  in non-uniform magnetic field, 26–28
  in Stellarators, 291–294
  in toroidal chambers, 237, 241–242
Dynamic paramagnetism, 140
Dynamic pinch
  conducting walls, 141
  fast electrons, 141
  hard X-rays, 135 et seq.
  instabilities, 123
  thermonuclear prospects, 142
Dynamic stabilisation, 359–361
Dynamic systems, 19–20

Electrical conductivity (see Conductivity, electrical)
Electric fields, fluctuating, 191, 198, 205–206, 269, 276–277
Electrons
  acceleration in a plasma column, 63–67, 223–224
  acceleration of, 208
  cooling, 43
  mobility, 191
  relativistic, 281, 349
  runaway, 64–67, 194, 208, 211, 230, 274, 309
  temperature (spectroscopic), 194

Energy
  balance of a discharge, 122, 203–205, 215–216
  balance of thermonuclear generator, 5–15
  direct conversion, 15–17
  exchange, between electrons and ions, 42–46, 206
Equations
  continuity, 79
  energy, 85–87
  Maxwell's, 79
  momentum, 78
  of state, 82
Equilibrium
  breakdown, 281
  condition, 20, 172
  in H.F. fields, 356–357
  in hybrid geometry traps, 377
  in a linear pinch, 82–87
  in a magnetic mirror trap, 311–316
  in a plasma loop, 162–163
  in a Stellarator, 293–295
  in a $\theta$-pinch, 147–148
  in a toroidal pinch, 87–94
  in a tubular pinch, 144–145
  plasma (magnetic field configurations), 82–83

Fast ions
  reaction yield, 47
  scattering of, 48
  slowing down, 42–43
Fast particles
  in fast high-power discharges, 132–141, 160–161
  in sustained discharges, 203, 205
Fermi mechanism of acceleration of charged particles, 37, 140, 144, 205
Fields, multipole, 377
Force-free magnetic configuration, 19, 200, 224, 226–227
Foucault image current, 90, 175–176
Friction force, 62, 68, 77–78
'Frozen-in' magnetic field, 100–102
Fuel advantage, 17–18

Gas emission from walls, 49, 142, 208, 298, 308, 344
Gas valve, 167
Geomagnetic field (as a magnetic trap), 30
Gibson and Lauer experiments, 2–3
Gravitational drift, 281
Guiding centre, 27, 29, 30, 249

Hall effect, 80
Heat conduction, 5, 67, 74, 75
Heating of plasma
  by injection, 319
  compression (see Compression)
  crossed field (ion-magnetron), 323, 331–332, 337
  cyclotron, 106, 301–304
  Joule, 85–87, 229–231, 305–307
  magnetic pumping, 299–301
  mechanisms (pinch), 117, 231, 323
  ohmic, 305–307
  reversed field, 159
Helical
  magnetic field of Stellarator, 287–292
  perturbations, 141, 177–180, 200
High frequency confinement
  experiments, 358–359
  of plasma, 356–358
  of single particles, 352–356
  power losses, 351–352
  stabilisation, 360–361
Holtsmark effect, 121
Hot-cathode arc, 76
Hybrid geometry traps, 375–379
Hydromagnetic
  (see Magnetohydrodynamics)

Ideal
  gas law, 10, 81–82, 119
  trap, 238
Implosion
  time, 115–116, 126–127, 154–155
  velocity, 116–117
Impurities, 123, 327, 380
  burn-out, 228
  determination, 193
  effect on conductivity, 190
'Inertial' forces, 19
Infra-red radiation
  betatron, 284
  diagnostics, 192, 195–196
Injection
  accelerators (see Accelerators)
  across rising magnetic fields, 320
  electron, 349–350
  fast ion, 60, 319–323, 340–344, 346–349
  neutral, 322–333, 346
  of molecular ions, 340–347
  of plasmas, 324–325, 328, 367–369, 372–373
Instabilities
  beam, 269–276
  centrifugal, 263
  current convectional, 265–269
  due to anisotropic velocity distributions, 277–278
  effect of finite Larmor radius, 261
  growth rate of, 258
  helical, 141, 177–180, 200
  in mirror traps, 261–262, 318
  kinetic, 269–279
  kink, 173–177
  linear pinch, 123, 138

Instabilities—*cont.*
  magnetohydrodynamic, 207, 223, 250-264, 379
  of current-carrying plasma column, 139, 173–174
  of flute (or convectional) type, 252–264
  of slow pinches, 198
  Rayleigh-Taylor, 263-264
  sausage, 139, 160–161, 173, 175
  $\theta$-pinch, 152
  universal, 268-269, 310
  velocity space, 250, 277–278
Ion cyclotron radiation, 346–347
Ion magnetron, 323, 329–336, 378
Ion sound waves in plasma, 104–105 107–108, 274–276
Ion temperature, 194, (in Zeta and Alpha) 201, 203
Ionisation
  of atoms
    by electrons, 50
    by fast ions, 51
  rate of hydrogen in a hydrogen plasma, 51–52
Invariance (see Adiabatic)
Iron core, 185
Ixion, 324, 336–340

Joule heating, 85–87, 229–231, 305–307

Kerr cells, 113
Kinetic theory, 269–278
Kink instability, 173–177
Kruskal-Shafranov stability limit
  experiment, 212–213, 305–306
  theory, 178, 220, 228–229, 295–296

Landau damping, 104, 272
Langmuir
  electron oscillations, 102–104
  frequency, 64, 99, 104
  ion frequency, 105, 310
  probes, 371, 378
Larmor
  frequency (see Cyclotron frequency)
  radius (definition), 23
Leontovich and Osovets, theory of, 123–128
Levitron, 146, 233–235, 237, 240
Linear pinch, 109–144
  accelerating voltage, 138
  adiabatic compression, 126
  instability, 159
  snow plow model, 124
Line broadening (see Doppler broadening; Holtsmark effect)
Liner, 183
Longitudinal
  definition, ix
  waves, 103–105, 107
Lorentz ionisation, 323
Loss cone, 26, 34, 248–249, 315

Magnetic
  axis, 287
  beach, 304
  confinement, classification, 18–20
  field, earth's, 30
  field, stray, 186
  mirror, 26, 30
  moment, 25
  probes, 112, 116, 158, 190, 199–200, 371, 374
  pumping, 299, 301
  shielding (to reduce impurities), 123
  surfaces, 286–290
  thermo-insulation, 9–10
Magnetic traps
  general, 236–237, 318
  neutral injection, 322–333
  stability, 249 et seq.
  toroidal, 238, 241
  with cusp fields, 361–375
  with H.F. plugs, 359–360
  with hybrid fields, 375–379
  with ordinary magnetic mirrors, 311–349
Magneto-acoustic resonance, 301
Magnetohydrodynamic
  approximation, 19, 77, 82
  equations for plasma, 77–82
  instability, 173–182, 207, 223, 233, 250–265
  stability, 367, 376, 382
  waves, 106–108
Magnetosonic waves, 107
Magnetostatics, 82 et seq. (see Equilibrium)
Marshall gun, 167–168 (see Accelerators)
Maxwellian
  distribution and nuclear reaction rates, 4
  equation, 79
Mean-free path
  collision, 22, 40
  of charged particles in plasma, 40–41
Measurement methods
  in cusp geometry, 371
  in fast pulsed discharges, 111–112, 118–122
  in Stellarators, 305
  in sustained discharges, 189–197, 210–211
Metal screens, 186
Microwaves, density measurement, 191–192, 211, 305
'Minimum B' configurations (see Hybrid geometry traps)
Mirror
  magnetic, 26, 30

Mirror—*cont.*
  moving, 36
  ratio (enhanced) in rotating plasmas, 338
  reflection, 34
Mirror traps
  anisotropic pressure, 257
  azimuthal drift in, 311
  confinement time, 316, 326
  density distribution, 312
  diffusion losses, 317
  electron temperature, 326
  electrostatic fields, 313
  experiments with compressional traps, 325 et seq.
  ion temperature, 327
  minimum temperature, 317
  nonadiabatic trapping, 321
  plasma injection, 325
  rotation in, 314
  with $\beta = 1$, 314
  X-rays, 326
Molecular ion dissociation, 319, 340–342
Motion, disordered ('Turbulent'), 76, 191, 194, 202, 205–207, 268, 276–277, 335–336
Motion of charged particles, 23 et seq.
  in a high-frequency field, 352–355
  in a magnetic field increasing in time, 34–37
  in a Stellarator, 291–293
  in a trap with magnetic mirrors, 23–31
  in an axially symmetric magnetic field, 243–249

Neutral detector, 196–197, 332
Neutron
  binding energy, 9
  economy, 18
  emission, 112, 132–135, 140, 153, 161, 203
  energy spectrum, 133
  from Ixion, 339
  from magnetic mirror experiments, 329
  real thermonuclear, 162
  temperature, 120
Newton's second law, 77, 258
Nonadiabatic motion
  in cusp geometry, 363, 370, 374–375
  trapping, 321–322
Nuclear emulsions, 112, 134, 135

Ogra, 261, 319, 340–347
Ohm's law, 62, 64, 71, 79, (generalised) 80–81
Optical radiation of plasma, 52–56, 112, 119–122, 194–195
Orekh, 371
Oscillations
  see Waves
  Langmuir (electron plasma), 103, 107, 274, 310
  radial, 114

Paramagnetic pinch, 102, 177–178, 197–208
Pharos, 149, 152–153
Piezoelectric pressure probes, 112, 117, 375
Pinch
  dynamic, 109–142
  effect, 83–94
  linear (definition), 147
  'slow' and 'fast', 172
  stability theory, 173–182
  $\theta$- (definition), 147
  $\theta$-, 142–146
  toroidal, strong longitudinal field, 208–231
  toroidal, weak longitudinal field, 182–208
  tubular, 143–146, 233–235
Plasma
  capacitor, 70, 338
  definition of, 5
  injectors (see Accelerators)
  oscillations, 103–108, 268–281
Plasmoids, 165
Poisson's equation, 39
Polarisation, 39, 63 (see also Dielectric constant)
Potential divider, 112
Pressure
  anisotropic, 257, 278
  balance, 10, 83, 227
  isotropic, 78
  magnetic, 10, 83
  of plasma, 10, 82
  (see also Equilibrium)
Primary winding, 185
Probes
  electric, 112, 371
  (see also Langmuir probes; Magnetic probes; Piezo-electric pressure probes)
Pump-out, 218 (see Diffusion, anomalous)
Pyrotron programme, 324–329

Quantum
  theory of radiation, 6
  tunnel effect, 323
Quasi-neutrality, 77, 82, 96
Quasi-stationary pinch effect, formulae of, 84–87

Radiation
  black body, 6, 195, 283
  continuous, 118, 121

Radiation—*cont.*
  energy loss, 6, 7, 53, 194–196
  impurities, 7, 52–56
  infra-red, 195–196
  ion cyclotron, 246
  line, 7
  microwave, 121
  recombination, 7, 52–53, 118
  (see also Betatron radiation; Bremsstrahlung; Neutron; X-radiation)
Radio frequency (see High frequency confinement)
Radio-interferometric density measurements, 192–193
Rayleigh-Taylor instability, 152, 263–264
Recoil protons, 112, 134
Refractive index (see Dielectric constant)
Refractivity, 192
Relaxation time for ion-electron temperature differences, 43–44
Resonance, cyclotron, 106, 301, 321, 346
Resonator, 360
Reverse field
  in Astron, 350–351
  $\theta$-pinch, 158–161
  toroidal pinch, 199–200
Rodionov, experiments, 31–32
Rogovskii coils, 111
Rotational transform in a Stellarator, 241–242, 286–296

Scattering
  angle, 48
  cross-section, 38
  in mirror machines, 315–316
  while slowing down, 48–49
Sceptre, 197
Scylla, 148, 153, 154, 264
Separatrix, 289
Shear, 181
Shock-heating, 20, 142
Single particle motion, 23 et seq. (see Motion of charged particles)
Skin effect, 86, 95, 101, 199, 207, 264, 351–352
Snowplow model
  linear pinch, 124–128
  plasma gun, 167–170
  $\theta$-pinch, 154–155
Sound waves, 104, 107–108
Space-charge fields, 77
Spectrographs, 193
Spectroscopic techniques, 112, 118–122, 151, 192–194 (see Optical radiation)
Stability
  by internal conductors, 234
  diagram for plasma column in axial field, 177
  diffuse pinches, 181
  flutes in mirror geometries, 327
  influence of conducting walls, 261
  influence of diffuse boundaries, 257
  influence of finite conductivity, 262
  magnetic traps, 249
  of a plasma (general theory), 249–281
  of a plasma column (theory), 174–182
  shear, 290
  single-particle analysis, 253
Stark effect, 121–122
Stellarator, 219, 230, 241, 253, 267, 286–311
  advertisement, 310
  construction tolerances, 291
  diamagnetic currents, 293
  equilibrium, 292–295
  experimental results, 304–308
  limiting current, 305–306
  maximum $\beta$, 295
  mirror effects, 292
  ohmic heating, 295, 298, 305–307
  particle motion, 291
  race-track, 297
  runaway electrons and anomalous diffusion, 309
  shear stabilisation, 291, 295
  spectra, 306
  stability, 295
  transit-time heating, 301
  trend of future research, 310
  X-rays, 309
Strong focusing, 361
Superconductors, 352
Suydam stability criterion, 181–182, 207

Temperatures
  critical, 9
  electron, 193, 195, 201
  from conductivity, 190
  in compressional mirrors, 326–327, 328–329
  ion, 194, 201, 231, 327
  legitimate, 202
  measurement in pinches, 119, 130
  neutron, 120
  optimal, 13
  record values in U.S.S.R., 223
  X-ray, 120, 152
Thermal efficiency, 12
Thermonuclear efficiency, 11
Thermonuclear reaction rates, 2–5
$\theta$-pinch, 146–162
  acceleration mechanism, 161
  adiabatic compression, 156
  end losses, 156
  hard X-rays, 160
  instability, 152
  neutron radiation, 153, 161–162
  preheating, 150
  reverse field heating, 158

θ-pinch—*cont.*
  sausage instabilities, 160–161
  snowplow model, 154
  X-ray temperature, 152
Three-electrode spark gap, 111
Thompson parabola, 112
Tokomak, 208–231
  accelerated electrons, 219
  conductivity, 213
  current distribution, 212
  electron density, 218
  influence of degassing on, 213
  ion temperature, 224
  oscillations, 214
  paramagnetic pinch, 223
  radiation loss, 216
  stability, 214
  stray fields, 217
  streak photographs, 211
  TM
    conductivity in, 223
    electron temperature, 223
    energy balance, 223
    X-rays, 222
  T–1, T–2 parameters, 211
  T–3, 228, (conductivity in) 229
  transient processes, 214
  ultraviolet spectra, 216
  X-rays, 219
Toroidal
  chambers, 183
  coil (magnetic trap), 238
  discharges
    design, 185
    experimental techniques, 189
    preionisation, 188
  drift, 237–238, 294, (H.F. compensation) 356
  equilibria, 87–94
  systems with strong fields (see Tokomak)
Torus, inductance, 92, 190
Transition probabilities, 194
Trapping of stabilising field by a contracting pinch, 102
Triax (tubular pinch), 144–146
Turbulence, 205, 225, (see Diffusion; Motion, disordered)
Turns-ratio, 187

Ultra high-speed photography (see Cameras)

Vacuum requirements, 209, 323, 382
Velocity
  Alfvén, 106
  implosion, 116
  phase, 103, 105
  sound, 108

Wall effects, 49
Waves
  Alfvén, 105, 106
  cyclotron, 304
  excitation of, 265–281
  extraordinary, 106
  longitudinal electrostatic, 103–105
  magnetosonic, 107–108
  ordinary, 106
  shock, 128
  sound, 104, 107, 268, 275
  transverse electromagnetic, 105, 106
  travelling, for plasma confinement, 358

X-radiation (hard)
  in linear pulse discharges, 135–137
  in sustained discharges, 223–224
X-rays, 6, 219, 222, 231
  emission, 112
  energy spectrum, 151
  temperatures, 120, 152

Zeta, 178, 187–188, 197–200, 203–204, 206–207, 212, 223
  ion temperature, 201–202, 206
  magnetic field configuration, 199
  parameters, 197
Zharinov, experiments of, 76